

# Heteropolyacids as Highly Efficient and Green Catalysts Applied in Organic Transformations

# Heteropolyacids as Highly Efficient and Green Catalysts Applied in Organic Transformations

---

Advances in Green and Sustainable  
Chemistry

# Heteropolyacids as Highly Efficient and Green Catalysts Applied in Organic Transformations

---

Majid M. Heravi  
Fatemeh F. Bamoharram

Series Editors

Bela Torok  
Timothy Dransfield



ELSEVIER

Elsevier

Radarweg 29, PO Box 211, 1000 AE Amsterdam, Netherlands  
The Boulevard, Langford Lane, Kidlington, Oxford OX5 1GB, United Kingdom  
50 Hampshire Street, 5th Floor, Cambridge, MA 02139, United States

Copyright © 2022 Elsevier Inc. All rights reserved.

No part of this publication may be reproduced or transmitted in any form or by any means, electronic or mechanical, including photocopying, recording, or any information storage and retrieval system, without permission in writing from the publisher. Details on how to seek permission, further information about the Publisher's permissions policies and our arrangements with organizations such as the Copyright Clearance Center and the Copyright Licensing Agency, can be found at our website: [www.elsevier.com/permissions](http://www.elsevier.com/permissions).

This book and the individual contributions contained in it are protected under copyright by the Publisher (other than as may be noted herein).

### Notices

Knowledge and best practice in this field are constantly changing. As new research and experience broaden our understanding, changes in research methods, professional practices, or medical treatment may become necessary.

Practitioners and researchers must always rely on their own experience and knowledge in evaluating and using any information, methods, compounds, or experiments described herein. In using such information or methods they should be mindful of their own safety and the safety of others, including parties for whom they have a professional responsibility.

To the fullest extent of the law, neither the Publisher nor the authors, contributors, or editors, assume any liability for any injury and/or damage to persons or property as a matter of products liability, negligence or otherwise, or from any use or operation of any methods, products, instructions, or ideas contained in the material herein.

### Library of Congress Cataloging-in-Publication Data

A catalog record for this book is available from the Library of Congress

### British Library Cataloging-in-Publication Data

A catalogue record for this book is available from the British Library

ISBN: 978-0-323-88441-9

For information on all Elsevier publications  
visit our website at <https://www.elsevier.com/books-and-journals>

*Publisher:* Candice Janco  
*Acquisitions Editor:* Kathryn Eryilmaz  
*Editorial Project Manager:* Kyle Gravel  
*Production Project Manager:* Sruthi Satheesh  
*Cover Designer:* Matthew Limbert

Typeset by STRAIVE, India





# Chapter 1

## Introduction

### 1.1. Foreword

The term “catalysis” was coined by Swedish scientist Jons Jakob Berzelius in 1836 [1]; he described the process as adding a *catalytic power* to a chemical reaction to accelerate it while itself is not consumed.

Berzelius stated [1]:

*Many bodies have the property of exerting on other bodies an action which is very different from chemical affinity. By means of this action they produce decomposition in bodies, and form new compounds into the composition of which they do not enter. This new power, hitherto unknown, is common both in organic and inorganic nature; I shall call it catalytic power. I shall also call Catalysis the decomposition of bodies by this force.*

Currently, catalysis is more specifically defined as the acceleration of a chemical reaction assisted by a species known as a catalyst. A catalyst operates by providing a mechanism with a different transition state of a lower activation energy ( $E_a$ ) in comparison with those of the original mechanism. Through such an alternate pathway, more reactant molecules will have enough energy to reach the transition state and surmount the energy activation barrier, letting them react and transform into the product molecules (Fig. 1.1).

The process can be described by the Boltzmann distribution equation (Eq. 1.1):

$$N_i / N_j = e^{-(E_i - E_j / KT)} \quad (1.1)$$

where  $N_i$  and  $N_j$  are the numbers of particles corresponding to energy states  $E_i$  and  $E_j$ , respectively,  $k$  is the Boltzmann constant, and  $T$  is absolute temperature.

In addition, one can explain it based on the Arrhenius law (Eq. 1.2), which says lower activation energies lead to higher kinetic rate constants, which in turn result in faster reactions:

$$k = Ae^{-(E_a / RT)} \quad (1.2)$$

where  $k$  is the kinetic rate constant (not to be mistaken by the Boltzmann constant),  $A$  is a preexponential factor,  $E_a$  is the activation energy,  $R$  is the universal gas constant, and  $T$  is the absolute temperature.

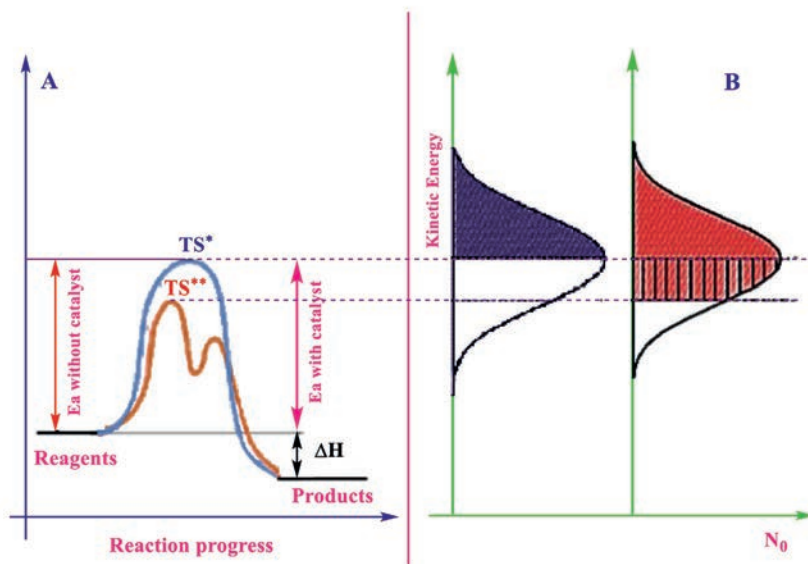


**FIG. 1.1** (A) The reaction potential energy diagram for an uncatalyzed reaction (blue line; black line in print versions) along with the catalyzed version (red line; dark gray in print versions). A decrease in the activation energy of the latter is evident. The peak with the highest energy demonstrates the transition state (TS) for a given reaction. (B) The Boltzmann distribution for the reactant energies. The violet area (black area in print versions) shows the number of molecules with enough energy to form the TS for the uncatalyzed reaction while the red (dark gray in print versions) area indicates the catalyzed reaction for which the transition state energy is lower [2].

Nowadays, catalysis is a pivotal factor in many chemical processes, representing a critical component in our everyday life. During one or more stages of the production of 90% or so of the chemicals industrially produced, a catalyst is necessary. In the fuel industry, catalysts are employed for the *cracking* and *reforming* of petroleum into petrol or diesel. The food industry employs catalysts for the hydrogenation of unsaturated oils. In polymer industries, different catalysts are used for the production of various polymeric products with a wide variety of chemical and physical properties. The global catalyst market size was valued at 33.9 billion USD in 2019 and is expected to grow at a compound annual growth rate of 4.4% from 2020 to 2027. Lots of chemical processes may be made faster, cleaner, and greener by appreciating and careful use of catalysis.

## 1.2. Catalysis

In chemistry, catalysis is to modify the rate of a chemical reaction, usually in an acceleration direction, by adding a substance, which is not consumed within the reaction. A chemical reaction rate, i.e., the velocity at which the reaction takes place, is dependent on several factors such as the chemical nature of the

reactants as well as the external conditions of the reaction. The study of catalysis is theoretically of interest as it reveals a plenty of information regarding the very nature of a chemical reaction; from a practical point of view, the study of catalysis is significant since many industrial processes rely on catalysts to be successful. The peculiar phenomenon of life would be absolutely impossible without the biological catalysts generally known as enzymes.

In general, a catalyst combines with the reactants but eventually is regenerated. Therefore, the amount of the catalyst remains intact. As the catalyst is not consumed in the course of the reaction, each catalyst molecule will be able to catalyze the transformation of many reactant molecules. For highly active catalysts, the number of the reactant molecules which are transformed by one molecule of the catalyst can be as large as several millions per minute.

When a certain substance or a combination of substances go through two or more parallel reactions to afford different products, it is possible to control the distribution of the products by applying a catalyst and selectively accelerating one reaction with respect to the other(s). One can make a particular reaction occur to such an extent that practically excludes another by selecting a suitable catalyst. Many important cases of catalysis applications are based on selectivity of this type.

Since a reverse reaction can take place by inversion of the steps comprising the mechanism of the forward reaction, the catalyst for a certain reaction is able to equally increase the reaction in both directions. In other words, catalysts do not influence the equilibrium position of a reaction; they only affect the rate at which an equilibrium is reached. Seemingly exceptions to this general rule are reactions in which one of the products is a catalyst as well. Such reactions are known as *autocatalytic*.

In addition, there are cases in which the addition of an extra substance, known as an *inhibitor*, reduces the rate of a reaction. This process, referred to as *inhibition* or *retardation*, is sometimes known as negative catalysis. Occasionally, concentrations of the inhibitor can be much lower than that of the reactant. Inhibition can be the result of:

- (1) a reduction in the concentration of one of the reactants due to the formation of complex between the reactant and the inhibitor;
- (2) a reduction in the concentration of an active catalyst (termed as the *poisoning* of the catalyst) due to the formation of complex between the catalyst and the inhibitor; or
- (3) termination of a chain of reactions upon the annihilation of the chain carriers by the inhibitor.

### 1.3. History

The word “catalysis” was taken from the Greek roots *kata-* (*down*) and *lyein* (*loosen*). It was coined by the great Swedish scientist Jöns Jacob Berzelius in

#### 4 Heteropolyacids as highly efficient and green catalysts

1835 in attempt to address a group of observations by other chemists in the late 18th and early 19th centuries. Among those observations were the improved conversion of starch into a sugar upon the addition of acids by Gottlieb Sigismund Constantin Kirchhoff; Sir Humphry Davy had observed that platinum accelerated the combustion of various gases; the stability of hydrogen peroxide in acid solution, while it decomposed in the presence of alkali and metals like manganese, platinum, silver, and gold; the oxidation of ethanol to acetic acid was accomplished in the presence of finely powdered platinum. The species that promoted such reactions were called catalysts. Berzelius supposed that a particular unknown *catalytic force* was behind these processes.

In 1834, Michael Faraday studied the capability of a platinum plate to achieve the recombination of gaseous oxygen and hydrogen (the products of water electrolysis) and deceleration of that recombination in the presence of other gases like carbon monoxide and ethylene. Faraday believed that an absolutely clean metallic surface (on which the decelerating gases could compete with the reacting gases to repress activity) was essential for activity; the concept was later shown to be generally important in catalytic processes.

Many of the primary techniques included unconscious applications of catalysis. Fermentation of wine into acetic acid and making soap from fats and alkalis were activities well-known to humans from the dawn of civilization. Sulfuric acid prepared by combustion of a mixture of sulfur and sodium nitrate was an early version of the lead chamber process for the manufacture of sulfuric acid, in which the oxidation of  $\text{SO}_2$  was accelerated by the nitric oxide produced.

In 1850, the concept of reaction rate was developed during the examination of sucrose hydrolysis, specifically known as *inversion*. The term inversion is related to the change observed in rotation of the monochromatic light when passed through the reaction system. The parameter could be readily measured, thus facilitating the study of the reaction progress. It was revealed that, at any moment, the inversion rate was proportional to the concentration of sucrose undergoing hydrolysis and the rate was accelerated when acids were present. Afterwards, it was demonstrated that the inversion rate was directly proportional to the acid strength.) This work paved the way for later studies of the reaction rates and the accelerating effect of higher temperatures on them by scientist such as Arrhenius, van't Hoff, and Ostwald, who played prominent roles in developing physical chemistry as a new discipline. Through his work on reaction rates, Ostwald came to define catalysts as species that changed the rate of a chemical reaction without altering the reaction energy factors.

This account of Ostwald was a breakthrough as it maintained that a catalyst did not change the equilibrium position in a reaction. In 1877, Lemoine proved that the decomposition of hydriodic acid to hydrogen and iodine reached the same equilibrium point at  $350^\circ\text{C}$ , 19% regardless of whether the reaction was conducted slowly in the gas phase or rapidly in the presence of platinum sponge. The observation had an important outcome: As noted before, *a catalyst for the forward process in a reaction is also a catalyst for the reverse reaction*. Berthelot, the eminent French chemist, verified this observation in 1879 with

liquid systems, when he found that the esterification of organic acids and alcohols was catalyzed by small quantities of a strong inorganic acid, just as was the reverse process, i.e., the hydrolysis of the ester.

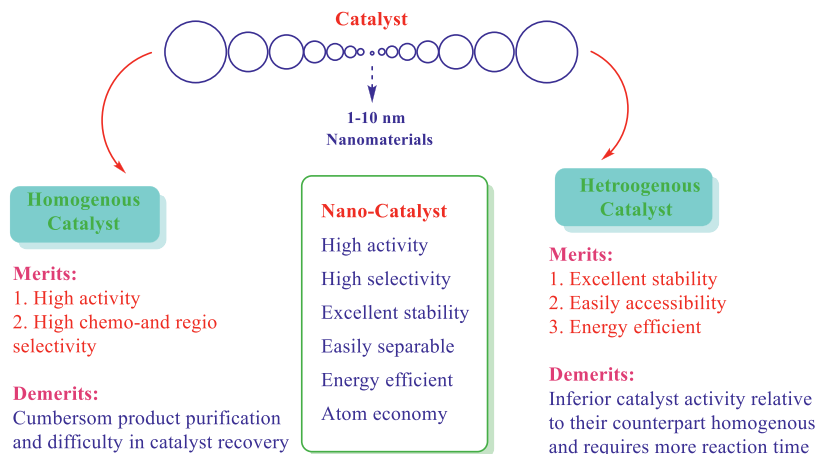
The purposeful application of catalysts to industrial processes commenced in the 19th century. Phillips, a British chemist, patented the use of platinum utilized in the oxidation of  $\text{SO}_2$  to  $\text{SO}_3$  with air. His process was used for a while, but it was discontinued since the platinum catalyst lost activity. In 1871, an industrial process was established for the oxidation of hydrochloric acid to chlorine in the presence of copper(II) salts impregnated in clay blocks. The afforded chlorine was utilized in the manufacture of a bleaching powder (a dry substance that released chlorine upon adding acid) in a reaction with lime. Once more, it was observed that the same equilibrium was reached in both directions. Moreover, it was revealed that the lower the temperature, the greater the equilibrium chlorine content; the maximum amount of chlorine was produced at a temperature of  $450^\circ\text{C}$  in a reasonable time.

By the end of the 19th century, the research by the distinguished French chemist, Paul Sabatier, on the interaction of hydrogen with a various organic compounds were conducted using a variety of metal catalysts; his studies led to a German patent for the hydrogenation of unsaturated liquid oils to solid saturated fats with nickel catalysts. Three important German catalytic industrial processes proved to be totally important by the end of the 19th century and in the early decades of the 20th century. The first one was the *contact process* for the production of  $\text{H}_2\text{SO}_4$  from  $\text{SO}_2$  by smelting. The second was the synthetic manufacture of the valuable dyestuff indigo. The last was the reaction of hydrogen and nitrogen gases to produce ammonia (known as the Haber-Bosch process for nitrogen fixation).

## 1.4. Nanocatalysis

Catalysis was among the very first applications of nanoparticles. A wide variety of elements and materials such as iron, aluminum, titanium dioxide, silica, and clay had been utilized as catalysts in nanoscale. However, an appropriate explanation of the outstanding catalytic behavior exhibited by nanoparticles has not been provided. The large surface area of nanoparticles has a forthright positive effect on the reaction rate also being a possible explanation for their catalytic activity. Structural properties of any substance at its nano size may also influence its catalytic activity. By fine-tuning of a nanocatalyst in terms of composition, size, and shape, greater selectivity is achievable. Therefore, one may ask what effects the physical properties of a nanoparticle have on its catalytic properties, and how the fabrication parameters may influence those properties. A better grasp of these factors allows a scientist to design highly active, highly selective, and highly resilient nanocatalysts. With all these advantages, industrial chemical reactions will be more efficient, consume much less energy, and generate less waste, thus alleviating the environmental impact arising from our reliance on chemical processes [3–7]. Nanoparticles are indisputably the most

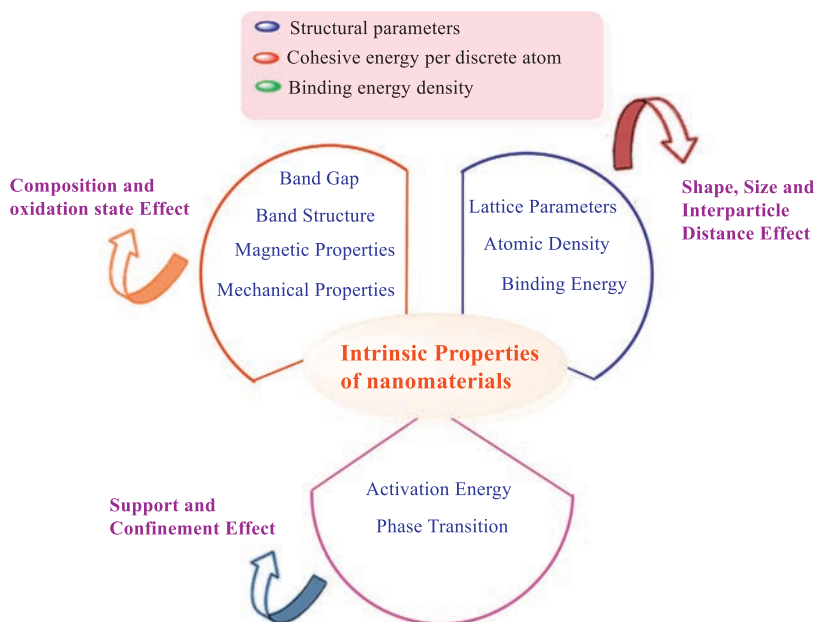
important industrial catalysts, with a wide array of applications from energy conversion and storage to chemical manufacturing. The versatile and particle-specific catalytic activity of nanoparticles is due to their heterogeneity and differences in size and shape. Scheme 1.1 represents basic differences in the bulk catalysis and the catalysis exhibited by nanoscale materials.



**SCHEME 1.1** A comparison between the efficiencies of homogeneous, heterogeneous, and nano-catalytic processes [8].

The concept behind nanocatalysis is conceivable by considering the effect of the inherent properties of nanomaterials on catalysis (Scheme 1.2) [9–13]. Inherent properties of nanomaterials with critical effects on their catalytic activity can be categorized into four different groups:

- (1) quantities that are directly connected to the bond lengths, e.g., the mean lattice constant, binding energy, and atomic density. Lattice contraction in a nano-solid causes densification and surface relaxation;
- (2) quantities that based on the cohesive energy per discrete atom, e.g., thermal stability. Self-organization growth, critical temperature for phase transitions, and evaporation in a nano-solid, coulomb blockade, as well as the activation energy for atomic dislocation, diffusion, and chemical reactions;
- (3) properties that vary with the binding energy density in the relaxed continuum region, e.g., the Hamiltonian that determines the entire band structure and related properties like core level energy, bandgap, photoabsorption, and photoemission; and
- (4) properties that from the joint effect of the binding energy density and atomic cohesive energy like the surface energy, mechanical strength Young's modulus, surface stress, the magnetic performance of a ferromagnetic nano-solid, and extensibility and compressibility of a nano-solid [14].



**SCHEME 1.2** Effect of intrinsic properties of materials on its catalytic activity [8].

Nanomaterials can be extensively utilized as catalysts with novel features and activity precise adjustment of their size, shape, electronic structure, and surface composition, as well as thermal and chemical stability. Lately, nanostructured catalysts have been considerably studied in both academic and industrial sectors due to their plentiful potential benefits (Scheme 1.3).

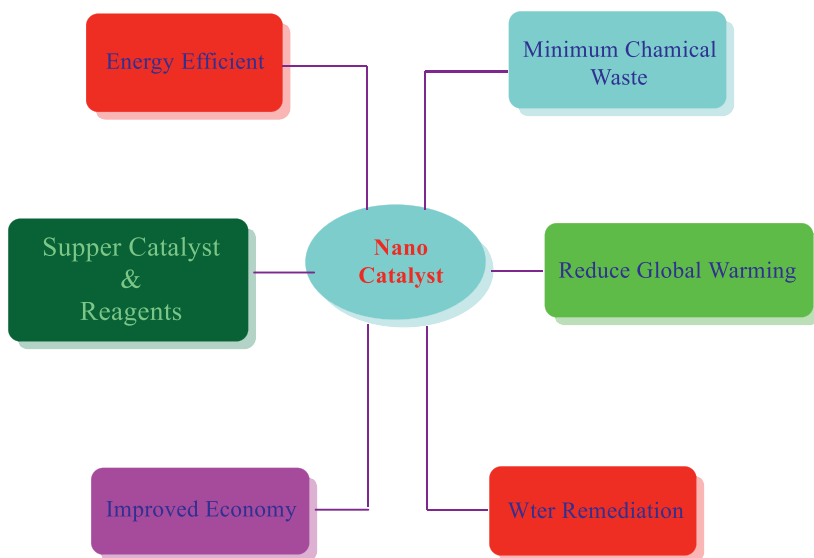
## 1.5. Classification of catalysis

Catalysis is dividable into three major classes: *biological*, *homogeneous*, and *heterogeneous*. Better known as *enzymes*, biological catalysts naturally occur in living organisms. In a reaction enzyme catalyzed by an enzyme, the reactant is called a *substrate*, which is converted into the desired product. Most enzymes are proteins and catalyze more than 5000 types of biochemical reactions. A number of important reactions, which are catalyzed by enzymes, are listed in Table 1.1.

In homogeneous catalysis, the catalyst exists in the same phase as the reactants are. Many commercially feasible processes have been devised in which homogeneous catalysis is utilized (Table 1.2).

A majority of homogeneous catalysts are expensive compounds of transition metals, and recovery of such catalysts from the workout solution is a challenge. In addition, many homogeneous catalysts can be used only at relatively low temperatures. Even under those conditions, they slowly decompose in solution.

## 8 Heteropolyacids as highly efficient and green catalysts



**SCHEME 1.3** Beneficial features of nanocatalysis [8].

**TABLE 1.1** A few chemical reactions catalyzed by enzymes.

Application	Enzyme	Use
Digestive system	Proteases, amylase, lipase	Used to digest protein, carbohydrates and fats
Molecular biology	Nucleases, DNA ligase, polymerase	Used in restriction digestion and Tire polymerase chain reaction to create recombinant DNA
Biological detergent	Proteases, amylases, lipase	Remove protein, starch, fat, and oil stains from laundry and dishware
Dairy industry	Rennin	Hydrolyze protein in the manufacture of cheese

**TABLE 1.2** A few chemical reactions in which homogeneous catalysts are utilized.

Commercial process	Catalyst	Application
Hydroformylation	Rh/PR <sub>3</sub> complexes	Production of aldehydes
Adiponitrile process	Ni/PR <sub>3</sub> complexes	Production of nylon
Olefin polymerization	(RC <sub>5</sub> H <sub>5</sub> ) <sub>2</sub> ZrCl <sub>2</sub>	Production of high-density polyethylene



In heterogeneous catalysis, the catalyst is in a different phase from that of the reactants. Fig. 1.2 shows a simplified energy diagram in which the steps involved in a heterogeneous catalyzed reaction are illustrated. A few reactions which utilize heterogeneous catalysts are listed in Table 1.3. In heterogeneous catalysis, the catalyst is usually a solid and the reactants are either a liquid or a gas. The reactants interact with the catalyst surface via a physical phenomenon known as adsorption. Upon such interaction, the chemical bonds in reactant A are loosened and break. Then, reactant B adsorbs to the catalyst surface. Reactant B reacts with the atoms of the adsorbed reactant A on the catalyst surface via a stepwise process, after which the product desorbs from the catalyst surface.

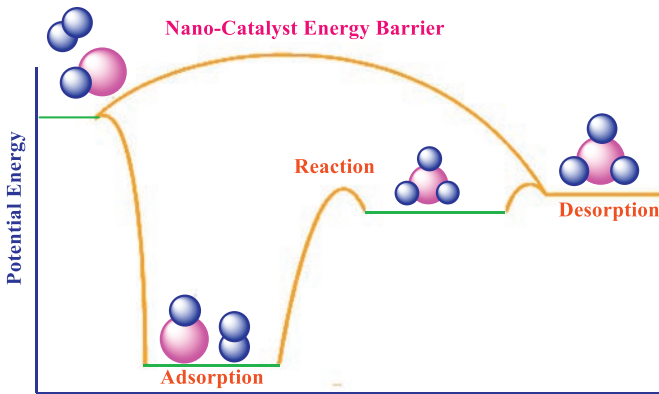


FIG. 1.2 A simplified energy diagram illustrating the steps involved in a heterogeneous reaction [15].

**TABLE 1.3** A few chemical reactions in which heterogeneous catalysts are utilized.

Commercial process	Catalyst	Final commercial product
Contact process	$V_2O_5$ or Pt	Sulfuric acid
Haber process	Fe, $K_2O$ , $Al_2O_3$	Ammonia
Ostwald process	Pt and Rh	Nitric acid
Water-gas shift reaction	Fe, $Cr_2O_3$ , or Cu	$H_2$ for ammonia, methanol, and other fuels
Catalytic hydrogenation	Ni, Pd, or Pt	Partially hydrogenated oils for margarine

## 1.6. Solid acid catalysts

According to their physical properties, solid acids can be classified into different categories. Examples are zeolites and zeotypes, mesoporous materials, mixed oxides, organic/inorganic composites, and heteropoly acids (HPAs).

- Zeolites are crystalline aluminosilicate compounds, with well-defined structures and pore sizes from 0.3 to 1.4 nm. Crystalline zeolites are formed of corner-sharing  $\text{SiO}_4$  and  $\text{AlO}_4$  units with different ratios of Al/Si. When Al or Si is substituted with other (transition) elements, e.g., Ga, Fe, Ge, Ti, V, Cr, Mn, and Co, they are called zeotypes. Substitution of  $\text{Si}^{4+}$  with  $\text{Al}^{3+}$  (or other trivalent ions) gives Brønsted acidity to these substances and leaves an oxygen atom with a negative charge, which is charge-balanced either by protons or by a counter cation like  $\text{K}^+$ ,  $\text{Na}^+$ ,  $\text{Mg}^{2+}$ ,  $\text{Ca}^{2+}$ , or  $\text{NH}_4^+$ . Heating results in dehydroxylation and leaves Lewis acid sites on the surface. The number of possible zeolites and zeotypes is immensely high, but only a few are actually utilized at industrial scales, among which are ZSM-5 (silicalite), MOR (mordenite), FAU (faujasite), BETA (beta), and LTA (Linde type A, or zeolite A).
- Mesoporous molecular sieves were originally utilized to increase the potential of zeolites in the processing of oil derivatives having larger molecules. These substances have pores (channels) of sizes between 2 and 50 nm. They are found in crystalline or amorphous forms in nature, generally having weaker acidities than zeolites. Mesoporous aluminosilicates, mesoporous silicas including SBA-15 and MCM-41, are examples of this wide category. Postsynthesis treatments, consisting of impregnation and grafting, improved their properties, which in turn enhanced their catalytic performances.
- Mixed oxides are species with more than one cations or just one cation in different oxidation states. There can be a wide variety of possible structures, pore sizes, and functional groups for these species, and they are found in crystalline or amorphous forms. Extensively studied examples are garnets and derivatives ( $\text{X}^{2+}_3\text{Y}^{3+}_2(\text{SiO}_4)_3$ ), perovskites and perovskite-like compounds ( $\text{CaTiO}_3$ ), magnetite with  $\text{Fe}^{3+}$  and  $\text{Fe}^{2+}$ , as well as sulfated and phosphated zirconia, which are widely used in acid-catalyzed reactions.
- Organic/inorganic materials are ordered inorganic structures functionalized with organic groups using coprecipitation or grafting. Periodic mesoporous organosilicas are instances of this category. The organic functional groups may be classified as either reactive participating in the reaction cycle, or passive and just improve the catalyst resistance to chemical and/or thermal degradation.
- Polyoxometalates are an important, special case of mixed oxides, used as acid catalysts. Polyoxometalate clusters are mainly anionic in nature and formed based on metal oxide building blocks having the general formula  $\{\text{MO}_x\}_n$ , where M is Mo, W, V, or (sometimes) Nb and  $x=4-7$  [16]. Different combinations and orientations of these basic building blocks results in thousands

of possible compounds polyoxometalate generally known as polyoxometalates (POMs). These materials can be classified into three broad subcategories [16]:

1. *Isopolyanions* contain the same metal oxygen framework as heteropolyanions but lacking the central heteroatom. Isopolyanions are mostly less stable in comparison with heteropolyanions and carry a large negative charge [16].
2. *Reduced polyoxometalate* clusters like molybdenum blue and molybdenum brown are among the very first discovered polyoxometalates; significant research has been dedicated to comprehending and controlling the formation of such materials [16,17]. These polyoxometalates are metal-oxygen anions with wheel-shaped structures.
3. *Heteropoly anions* are undoubtedly the most widely studied category of polyoxometalates. These species have been utilized in a wide variety of fields [18] such as catalysis [19–23], materials [24–26], and medicine [27]. They are composed of polyanion clusters and cations [28]. These compounds enjoy a structural diversity, in which the oxometal polyhedrons of  $MO_x$  ( $x=5, 6$ ) are the basic construction units. Here, M represents some of early transition metals in their high oxidation state centered by heteroatoms that considerably influence the properties of the species. Typically, the heteroatoms are main group elements, e.g., B, Si, P, S, As, Ga, Ge, Al, and Se. Late transition metals such as Co and Fe have also been observed as heteroatoms. Polyanions are bulky structures with highly negative charges on them. On the surface of the polyanions there are many oxygen atoms capable of donating one or more electrons to an electron acceptor. Polyanions can therefore be considered as soft bases. It is evident that the metal ions on the polyanions' skeleton have unoccupied orbitals that can accept electrons. In other words, polyanions can also serve as Lewis acids. Thus, polyanions can play the roles of a Lewis acid and Lewis base depending on different conditions. Furthermore, owing to their strong capacity to bear electrons and release electrons, polyanions are usually regarded as electron reservoirs; that is to say that these species possess redox properties as well [29]. Above all, these polyanions are designable. In order to achieve specific properties, their structures and components can be adjusted. Substitution of polyhedra, variation of the heteroatom, and pattern rearrangement of the basic construction units are among the most common methods to realize this. The most known structure of heteropoly acids is the Keggin structure. Keggin-type heteropoly acids have been investigated most of all in catalysis because of their unique stability. A Keggin heteropoly acid follows the general formula of  $[XM_{12}O_{40}]n^-$ , in which X is the heteroatom (typically  $P^{5+}$ ,  $Si^{4+}$ , or  $B^{3+}$ ), M is the addenda atom (usually molybdenum or tungsten), and O is oxygen.

The advantages of heteropoly anions as catalyst were summarized by Okuhara et al., and are listed in Table 1.4.

**TABLE 1.4 Advantages of heteropolyanion catalysts.**

1. Catalyst design at atomic/molecular levels based on the following
<ul style="list-style-type: none"> <li>• Acidic and redox properties</li> </ul> <p>These two important properties for catalysis can be controlled by choosing appropriate constituent elements, i.e.:</p> <ul style="list-style-type: none"> <li>• Type of poly anion</li> <li>• Addenda atom</li> <li>• Heteroatom</li> <li>• Counteranion, etc.</li> </ul>
<ul style="list-style-type: none"> <li>• Multifunctionality</li> </ul> <p>Acid-redox, acid base, multielectron transfer, photosensitivity, etc.</p>
<ul style="list-style-type: none"> <li>• Tertiary structure. Bulk-type behavior</li> </ul>
2. Molecularity-metal oxide cluster
<ul style="list-style-type: none"> <li>• Molecular design of catalysis</li> </ul>
<ul style="list-style-type: none"> <li>• Cluster models of mixed oxide catalyst and of relationships between solid and solution catalysts</li> </ul>
<ul style="list-style-type: none"> <li>• Description of catalytic processes at atomic molecular levels</li> <li>• Spectroscopic studies and stoichiometry are realistic</li> <li>• Model compounds of reaction intermediates</li> </ul>
3. Unique reaction field
<ul style="list-style-type: none"> <li>• Bulk-type catalysis</li> </ul> <p>“Pseudoliquid” and bulk-type II behavior provide unique three-dimensional reaction environment for catalysis</p>
<ul style="list-style-type: none"> <li>• Pseudoliquids behavior</li> </ul> <p>Spectroscopic and stoichiometric studies are feasible and realistic</p>
<ul style="list-style-type: none"> <li>• Phase-transfer catalysis</li> </ul>
<ul style="list-style-type: none"> <li>• Shape selectivity</li> </ul>
4. Unique basicity of polyanion
<ul style="list-style-type: none"> <li>• Selective coordination and stabilization of reaction intermediates in solution and in pseudoliquid phase</li> </ul>

The properties and applications of heteropoly acids will be discussed in the following sections.

### 1.7. Heteropoly acids as green catalysts

Over time, a number of different principles have been suggested that may be used when considering the design, development, and implementation of chemical processes. With these principles, scientists and engineers will be able enhance

and protect the economy, people, and the planet through devising new innovations and creative ways to save energy, diminish waste, and discover replacements for hazardous substances. Paul Anastas and John Warner [30] formulated 12 principles of green chemistry in 1998, which are outlined as follows:

1. *Prevention.* It is better to prevent the waste from being generation than to treat or clean it up after it has been generated.
2. *Atom Economy.* Synthetic procedures must be designed in which the incorporation of all the materials utilized in the process is maximized.
3. *Less Hazardous Chemical Synthesis.* Whenever possible, synthetic procedures must be designed to utilize and produce substances with little or no toxicity.
4. *Safer Chemical Design.* Chemical products must be designed in a way that the desired function is fulfilled while their toxicity is minimized.
5. *Safer Auxiliaries.* Using auxiliary substances, i.e., solvents, separation agents, etc. must be excluded whenever possible and/or the most innocuous ones are used.
6. *Designing for Energy Efficiency.* The energy needed for a chemical process must be considered for its environmental and economic impacts and minimized. Synthetic methods should be conducted at ambient temperature and pressure whenever possible.
7. *Use of Renewable Feedstock.* Whenever technically and economically possible, renewable rather than depleting raw materials must be used.
8. *Reduce Derivatives.* Unnecessary use of protection/deprotection, blocking groups, or temporary modification of physical/chemical processes must be minimized or avoided whenever possible, as these steps require more reagents and energy and result in more waste.
9. *Catalysis.* Catalytic reagents (as selective as possible) are preferred over stoichiometric reagents.
10. *Design and Degradation.* Chemical products must be designed in a way that eventually they break down into harmless degradation products that do not last for a long time in the environment.
11. *Real-Time Analysis for Pollution Prevention.* Analytical methodologies have to be developed more than before to enable real-time, in-process monitoring so that it is possible to control hazardous substances before they are formed.
12. *Inherently Safer Chemistry for Accident Prevention.* Substances and its various forms used in a chemical process must be chosen to minimize the potential for chemical accidents including explosions, releases, and fires.

Ryoji Noyori, a Chemistry Nobel Prize winner, pointed out to three important developments in green chemistry [31]. The first was to solve the solvent problem using supercritical carbon dioxide; the second was *green* oxidation with aqueous hydrogen peroxide; and the third one was the application of hydrogen in asymmetric syntheses.

Green catalytic processes and catalytic processes for green products play a significant role in green chemistry [30]. Meanwhile, since the entire life cycle of a product is considered in green chemistry, the priority of research and development cannot be determined unless the *greenness* of the process or product for the whole system is assessed. For this reason, it is necessary to establish the concept of greenness or a *green index*, which is applicable with a relatively easy procedure. The following factors must be regarded in order to assess quantitatively the greenness, or the reduction extent of undesirable environmental impact:

- (1) resource consumption.
- (2) energy consumption.
- (3) undesirable effects on human beings.
- (4) undesirable effects on ecosystems.
- (5) physical, chemical, and biological safety.
- (6) efficiency.

If we apply the principles suggested for green chemistry [30], the items listed in Table 1.5 may be the research and development targets for the development of green catalysts [33]. Moreover, development of green products (e.g., long-life products) is necessary.

Heteropoly acids can serve as useful acid and oxidation catalysts, which can be used in various reaction media, such as solid catalysts and in homogeneous solution, and in two-phase solution systems [34].

Heteropoly acids will find more sustainable/greener applications in the future. Owing to their noncorrosive nature, safety, low waste, and easy separation, they are green catalysts. Solid heteropoly acid catalysts have successfully resulted in the establishment of quite competitive green processes. These green catalysts have been effectively used for various reactions with high capability in practical uses [19,35] since their acidic and redox activities are tunable at atomic/molecular levels by changing the components wherever necessary.

**TABLE 1.5** Priority targets of research and development for the development of green catalysts [32].

1	Stoichiometric to catalyzed reactions, e.g., selective oxidation
2	Multistep routes to routes with fewer steps
3	Liquid acid or base catalysts to solid acid or base catalysts
4	Safer processes, e.g., by avoiding hazardous or toxic reagents and byproducts
5	Improving the reaction media, e.g., nonsolvent, water, solid-state, or supercritical media
6	Routes with increased atom economy

These solid acids are used in bulk or supported forms. They can serve as homogeneous and heterogeneous catalysts [36]. Several aspects of heteropoly acid as green/sustainable catalysts are described.

### 1.7.1 Water-tolerant solid acid catalysts

Acidic cesium salts of strongly acidic heteropoly acid are appropriate examples of useful active solid acid catalysts demonstrating a very good performance in many organic reactions because of their high surface acidity, and presumably due to their unique basic properties [37]. However, most of the times, the catalytic activities of solid acids are significantly suppressed in the presence of water; on the other hand, H-ZSM-5 with a high ratio Si:Al has been observed to have fair tolerance in aqueous solution [38]. Recently, it has been shown that the acidic cesium salts of heteropoly acids are catalysts high tolerance for water in hydration of olefins [39] and hydrolysis of esters [40]. This was attributed to the mild hydrophobicity of the catalysts [41]. Some examples of catalytic performances are provided in Table 1.6 [40].

### 1.7.2 Pseudoliquid phase

Having a flexible solid structure, in some heteropoly acids, reactants with polar molecules or basic properties are easily absorbed into the solid lattice (in the cavities between the polyanions of the lattice) sometimes expanding the lattice) and reacting therein. That is to say, the reaction field becomes a three-dimensional one as if it is in a solution but much more orderly.

Because of such a behavior, heteropoly acid catalysts usually demonstrate high catalytic activities as well as unique selectivities. A few examples are listed in Table 1.7 [42]. In this particular case, a heteropoly acid catalyst can be termed as a *catalytically active solid solvent*.

**TABLE 1.6** Water-tolerant catalytic activities of solid acids for the hydrolysis of cyclohexyl acetate.

Catalyst	Rate		
	Per weight	Per acid amount	Per volume
Cs <sub>2.5</sub> H <sub>0.5</sub> PW <sub>12</sub> O <sub>40</sub>	5.3	35.3	12.6
H-ZSM-5	1.5	3.8	0.5
SO <sub>4</sub> /ZrO <sub>2</sub>	1.1	5.8	2.5
H-Y zeolite	0.0	0.0	0.0
Nb <sub>2</sub> O <sub>5</sub>	0.0	0.0	0.0

**TABLE 1.7** A comparison of catalytic activities of heteropoly acids with silica-alumina.

Reaction	Catalyst	Temperature (°C)	Ratio
Dehydration of 2-propanol	PW <sub>12</sub> <sup>a</sup>	125–150	30–100
Isobutene + CH <sub>3</sub> OH → MTBE	PW <sub>12</sub> /SiO <sub>2</sub>	90	300
Dehydration of ethanol	PW <sub>12</sub>	200	> 300
Acetic acid + ethanol → ethyl acetate	PW <sub>12</sub> /carbon	150	> 4

<sup>a</sup> PW<sub>12</sub>: H<sub>3</sub>PW<sub>12</sub>O<sub>40</sub>.

## 1.8. Solid-solid phase catalysis

Very small particles of the acidic cesium salts of 12-tungstophosphoric acid effectively catalyze many organic reactions in the solid state, among which is solid *p*-toluenesulfonic acid [43]. In such cases, catalysts and reactants are both solids. The greenness of these reaction systems is probably dependent upon the workup process of the products after the reaction.

### 1.8.1 Combination of a heteropoly acid and noble metals (bi-functional catalysis)

Heteropoly acid catalysts promoted by platinum or palladium exhibit high catalytic activity and selectivity for the skeletal isomerization of *n*-alkanes (C<sub>4</sub>–C<sub>7</sub>) at low pressures of hydrogen and low temperatures. This is most likely because of the uniform and mildly strong acid strengths of heteropoly acid catalysts. An attractive example of heteropoly acid catalysts in combination with noble metals is Pd-H<sub>4</sub>SiW<sub>12</sub>O<sub>40</sub> promoted by Se or Te for the one-step oxidation of ethylene to acetic acid in the gas phase at about 150°C [44]. It was postulated that the reaction proceeded in two steps: first, hydration of ethylene to ethanol catalyzed by heteropoly acid (acid catalysis); and second, oxidation of ethanol to acetic acid on the palladium site. Presently, a plant annually producing 100,000 MT is operating in Japan (since 1997, by Showa Denko). The new process produced a much smaller amount of wastewater and by-products, and the system was not corrosive.

## 1.9. Green processes using heteropoly acid catalysts in two phases

Using heteropoly acid catalysts in solution, Asahi Chemical commercialized the selective hydration of isobutylene in a mixture of *n*-butenes and isobutylene



as well as the polymerization of tetrahydrofuran in the 1980s. Both of these reactions were conducted in two phases. Since the separation of product from the catalyst is very easy and the process is quite simple, energy and cost are tremendously reduced. The polymerization of THF is shown in Fig. 1.3 [46]. Polymerization to polyoxymethyleneglycol (PTMG) proceeds in the H<sub>2</sub>O-THF-HPA phase. Polyoxymethyleneglycol is recovered from its own phase and the phase containing the heteropoly acid and oligomer is just recycled to the reactor. It has been claimed that there is literally no waste. The molecular weight of the product polymer is controlled by its appropriate solubility in the THF-PTMG phase making the distribution narrow.

### 1.10. Types of catalytic activity of heteropoly acids

As illustrated in Figs. 1.4 and 1.5, Misono and coworkers [49] have defined the catalytic activity of heteropoly acids in two different types of reaction: reactants (R) and products (P) interact either at the surface (Fig. 1.4A) or in the depth of the three-dimensional bulk (Fig. 1.4B). The first type shows the common process in a heterogeneous system, in which the reaction is catalyzed on the external surface of the solid; the reactant is a nonpolar molecule only interacting with the external acid protons. Reaction rates are determined by the catalyst surface area and the number of protons accessible to the nonpolar substrate. In the second catalytic mechanism, catalysis takes place within a tertiary structure, in which the reactant diffuses, leading to an expanded interpolyanion distance occurring when the reactants are polar. After the formation, the products diffuse back to the external surface and then into the reactant phase (gas or liquid). This bulk-type catalytic mechanism may in turn be divided into two subcategories: *pseudoliquid catalysis* and *redox catalysis*. In pseudoliquid catalysis with the protons from the bulk are the active species. The title pseudoliquid comes from the fact that polar molecules like water, alcohols, or

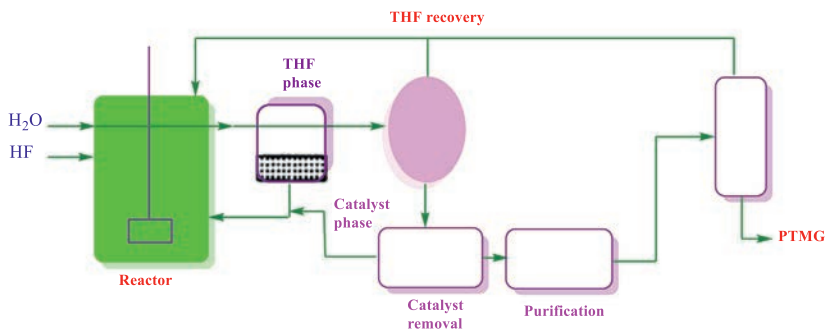


FIG. 1.3 Flow diagram for the polymerization of tetrahydrofuran to poly-oxytetramethyleneglycol (Asahi Chemical) [45].

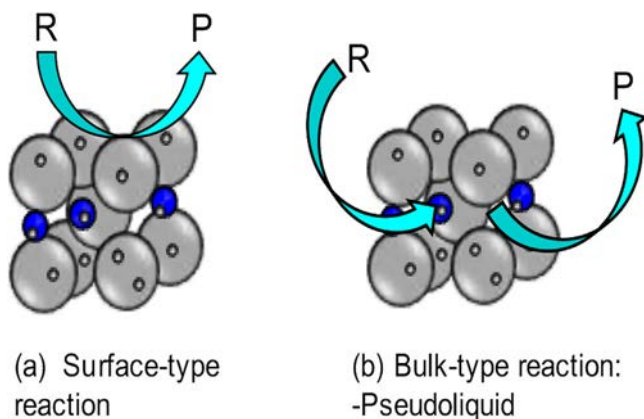


FIG. 1.4 Types of catalysis for heteropoly acids, where the K.U. are denoted in gray with an arbitrary number of hydrogens (*white*) and water molecules (*blue; light gray in print versions*). R stands for reactants and P for products [47].

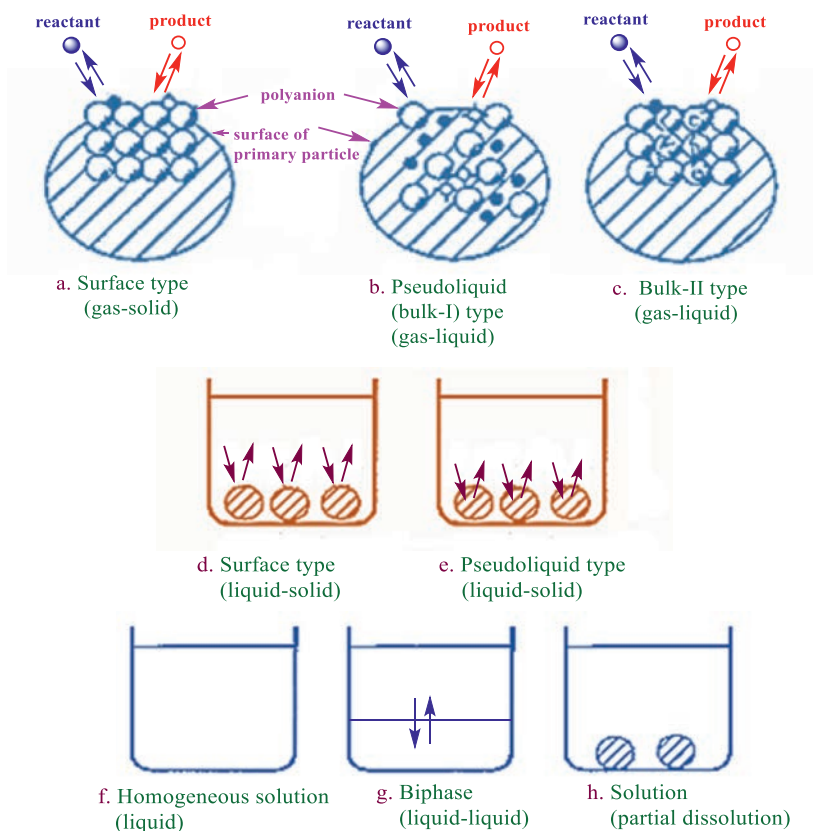


FIG. 1.5 Different types of catalysis by heteropoly acids [48].

small amines are able to diffuse into the bulk structure of the heteropoly acid to give a concentrated reaction solution in which conversion occurs [50]. Redox processes take place in reactions in which protons and electrons are rapidly diffused into the bulk.

## 1.11. Catalytic properties

The fascinating properties of heteropoly acids, such as tunable acidity and redox properties, high thermal stability, inherent resistance to oxidative decomposition, and striking sensitivity to light and electricity, have made them excellent candidates for catalytic purposes. There is a tight relationship between these remarkable properties and their structures and compositions. Their distinct atomic connectivity provides the compositional diversity necessary for a close assessment of the outcomes that result from composition change on catalytic reactivity.

With such tempting promises in industry, these powerful catalysts have been investigated for a long time. Presently, dozens of processes have been industrialized with heteropoly acids as the catalysts, among which are the hydration of propene [51], isobutene [52], and 2-butene [53] to their corresponding alcohols, oxidation of isobutyraldehyde with O<sub>2</sub> to isobutyric acid [52], polymerization of tetrahydrofuran [46,54], amination of ketones to imines [55], oxidation of ethylene with O<sub>2</sub> to acetic acid [44], and esterification of acetic acid with ethylene to ethyl acetate [56].

### 1.11.1 Active sites

Owing to their multiple active sites, which include protons, oxygen atoms, and metals, heteropoly acids are regarded as versatile catalysts. Protons are seemingly able to serve as Brønsted acids and promote acid-catalyzed reactions. Some oxygen atoms on the surface of these anions, especially those on the lacunary sites of lacunary anions with high negative charges, are basic enough to react with protons, to the extent of abstracting active protons from the organic substrates. In other words, the oxygen atoms on the surface of heteropoly acids can serve as active sites in base-catalyzed reactions. However, attention should be focused on the metal cores of a heteropoly acid catalyst since they are the active sites in all oxidative reactions, part of acid-catalyzed reactions, and a majority of other reactions. Thus far, plenty of heteropoly acid catalysts have been utilized in oxidative reactions, almost all of which are tungsten- or molybdenum-based compounds.

Additionally, some heteropoly acids work as catalyst precursors so that during the reaction, they may decompose to small active species. This is shown in a work by Ishii [19].

### 1.11.2 Stability

Stability is a critical concern for catalysts, which is in part due to the fact that it directly influences the activity and recyclability of the catalyst.

The stability in the case of heteropoly acid catalysts usually means thermal stability, oxidative stability, and hydrolytic stability. Depending upon the type of heteropoly acid catalyst, these stabilities change significantly. In general, heteropoly acid catalysts enjoy attractive thermal stabilities. The thermal stability in some of Keggin-type heteropoly acids is so high that they can be applied as catalysts in gas-phase reactions at high temperatures. The high thermal stabilities of heteropoly acids are relative. For instance,  $\text{H}_3\text{PW}_{12}\text{O}_{40}$  loses its protons at 450–470°C to form a new species of the formula  $\{\text{PW}_{12}\text{O}_{38.5}\}$ , and the structure is completely devastated at about 600°C [57]. Therefore, suitable reaction temperatures are essential for the systems using the Brønsted acid sites of a heteropoly acid catalyst, particularly for the gas-phase systems operated at high temperatures, since high temperatures will cause the molecule to lose its active protons. Moreover, the thermal stabilities are important for the regeneration process of the catalyst. High temperatures often result in coking on the catalyst during the reaction, which in turn deactivates the catalyst. Therefore, the catalyst regeneration involves decoking, which is typically done at high temperatures. The suitable decoking temperature must be less than the temperature at which the catalyst loses its active protons.

In addition to the heteroatoms, substituting metals and the counteranions may considerably influence the thermal stability of a heteropoly acid. Substituted heteropoly anions are generally more labile than their unsubstituted counterparts. For instance, vanadium atoms are released from the  $\text{H}_3+n\text{VnPMo}_{12-n}\text{O}_{40}$  skeleton at elevated temperatures to form monomeric vanadium species along with  $\text{PMo}_{12}\text{O}_{40}$  [58,59]. The detaching of substituting metals occurs for  $[\text{FePMo}_{11}\text{O}_{39}]^{4-}$  as well [60]. However, the detachment temperature is strongly related to its counteranion. If the ammonium ion is used as the counteranion, the release of iron from the Keggin anion occurs at 197°C due to the reaction of  $\text{Fe}^{3+}$  with  $\text{NH}_4^+$ . On the other hand, if cesium cation is used, iron is released at 297°C. Typically, heteropoly acids have a significant hydrolytic and oxidative stability owing to the absence of organic ligands. Even though it is possible that the polyhedral subunits of the anions are detached from the main skeleton in the presence of water, their stability in over a certain pH range is secured. A wide variety of reactions with heteropoly acid catalysts can be performed even in pure water [61–69]. In addition, heteropoly anions are intensely persistent against oxidizing agents. Therefore, this type of catalyst may be utilized in water- and oxygen-rich systems without the protection by inert gases, which is usually necessary for many organometallic catalysts. The strongest evidence is the oxidation of organic substrates by dilute hydrogen peroxide [70] and booming water oxidation with heteropoly acid catalysts [69].

In brief, all three kinds of catalyst stability—thermal, hydrolytic, and oxidative stability—are important, their relative importance being dependent on the type of catalysis and transformation.

## 1.12. Photocatalysis

It is possible to excite the heteropoly anions from their ground states can be by ultraviolet or near-visible radiation. The excitation is essentially a charge transfer from an oxygen atom to the  $d^0$  transition metal in the presence of radiation with enough energy. For instance, the excitation of  $[\text{PW}_{12}\text{O}_{40}]^{3-}$  corresponds to a charge transfer from  $\text{O}^{2-}$  to  $\text{W}^{6+}$ , which results in the formation of a pair consisting of a trapped electron center ( $\text{W}^{5+}$ ) and hole center ( $\text{O}^-$ ) [71]. Heteropoly anions in their excited states usually exhibit a better performance than in their ground states as both electron donors and electron acceptors [72]. Therefore, some of heteropoly acids, which are catalytically inactive even at high temperatures, but under dark conditions, may turn into robust reagents with the ability of oxidizing or reducing various substrates upon the irradiation of ultraviolet or near-visible light. In addition, the HOMO-LUMO bandgaps in heteropoly anions prevent the recombination of electrons and holes resulting from the irradiation of a light with an energy greater than or equal to their bandgap energy [71]. The photogenerated electrons and holes can therefore initiate the chemical reaction owing to the strong photoreductive ability of the electrons and photooxidative ability of the holes. Under moderate conditions, many photocatalytic reactions take place readily in the presence of heteropoly acids, among which are: the oxidation of alcohols [73–75], benzene [76], and phenol [77]; oxidative bromination of arenes and alkenes [78]; reduction of  $\text{CO}_2$ , [79,80], etc. More significantly, the photooxidation properties are eminently suitable for the degradation of a variety of aqueous organic pollutants [81–91] and their photoreduction properties can be utilized to remove transition metal ions from water [92].

Streb et al. [93] have reviewed new trends in the polyoxometalate photoredox chemistry of polyoxometalates. According to the review, in addition to the facile photoexcitation using ultraviolet or near-visible radiation, homogeneous heteropoly acid photocatalysts exhibit a number of advantages, e.g., intense absorption of radiation with high molecular absorption coefficients, high structural stability, high redox activity, multielectron redox capability, and easy reoxidation of reduced species. However, as an important problem, absorption of the radiation by heteropoly anions only takes places in the region of 200–500 nm. Therefore, photosensitization can be utilized as a strategy to allow for using visible light. Some photosensitizers, like fullerene, can be attached to heteropoly anions by forming covalent bonds; also, some cationic photosensitizers may be associated with heteropoly anions via electrostatic interactions.

For practical purposes, more emphasis has been put on heterogeneous photocatalysts in the field of photocatalysis by heteropoly acids. The original parent heteropoly acids are ordinarily supported on other substances to give composite heterogeneous photocatalysts. The most commonly used supports are  $\text{TiO}_2$  [94–98],  $\text{SiO}_2$  [99–103],  $\text{ZrO}_2$  [104,105], etc. Moreover, the solidification of heteropoly acids—i.e., their combination with supports—provides them with much larger specific surface areas, which in turn may lead to an increase in their

catalytic activities as large contact areas are provided between the catalysts and substrates for the surface-mediated, electron-transfer reactions. In addition, by using a semiconductor metal oxide as a support, the resulted combination can enhance photoactivities owing to the synergistic effect between the two components [104,106,107]. Another set of heterogeneous heteropoly acid photocatalysts is the acidic cesium salts  $\text{Cs}_x\text{H}_{3-x}\text{PW}_{12}$  ( $x \leq 3$ ), which have relatively high surface areas, porous structures, and strong acid sites.  $\text{Cs}_3\text{PW}_{12}\text{O}_{40}$  was the very first heterogeneous heteropoly acid photocatalyst utilized for photooxidation of propan-2-ol to acetone in aqueous solution [108].

### 1.13. Electrocatalysis

Heteropoly anions can go through several rapid one- and two-electron reversible reductions, and further irreversible multielectron reductions with concomitant decomposition, due to the high oxidation states of the M atoms in the peripheral metal-oxygen polyhedrons of  $\text{MO}_x$ . If all the M atoms are identical, the electrons will be delocalized on all  $\text{MO}_x$  polyhedrons at room temperature via rapid intramolecular electron transfers. The reduction raises the negative charge density on the heteropoly anions and therefore their basicity. Consequently, depending on the  $\text{p}K_a$  of the generated anions, the reduction can be accompanied by protonation. This is to say that pH has a significant influence on the potentials of the reversible redox pairs of heteropoly anions. In organic solution or neutral aqueous, in which no protonation can take place, both Keggin- and Dawson-type heteropoly anions can undergo successive one-electron reductions. Due to this particular property, a number of Keggin- and Dawson-type heteropoly acids have been utilized as oxidative and reductive electrocatalysts. It should be noted that each heteropoly acid demonstrates featured electrochemical behavior because of its particular redox potential,  $\text{p}K_a$ , and stability.

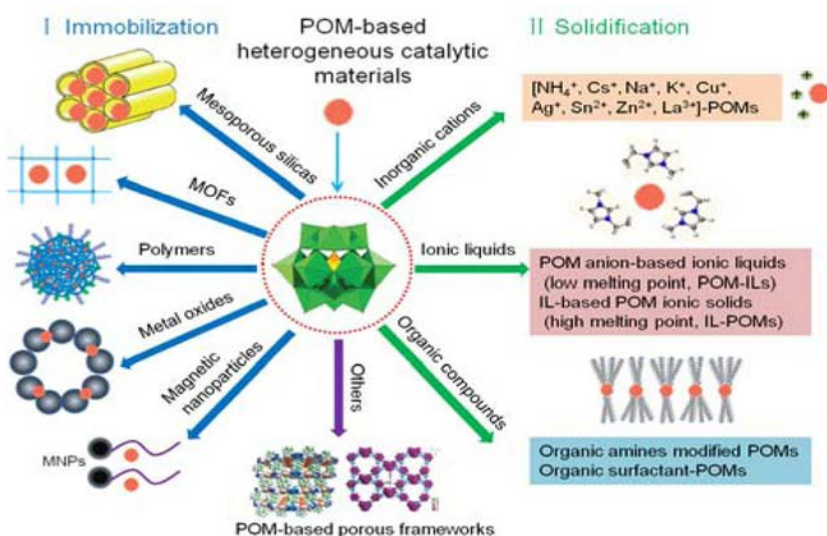
Steckhan et al. elegantly presented the electrochemical properties of heteropoly acids as electrocatalysts.

### 1.14. Homogeneous and heterogeneous catalysis

Heteropoly acids are often soluble in a wide range of polar solvents; this causes problems in their recovery, separation, and recycling when used as a catalyst, which in turn influences their use in systems that require green efficient transformations and sustainable development. Therefore, it is essential to develop heteropoly acid catalysts of high recoverability and recyclability for practical applications in industry. To realize this aim, heterogeneous catalysis is more desired owing to advantages such as facile separation of the catalyst from the product. However, heterogeneous HPA-based catalysts normally suffer from some disadvantages, e.g., the active site leaching as well as low activity [109,110].

It should be noted that HPA-based heterogeneous catalysts typically show lesser catalytic performance compared to their homogeneous counterparts,

which is largely attributed to the diffusion limitation of the active sites and the mass transfer resistance. In order to resolve the mentioned restrictions, many tactics have been suggested to enhance the stability and catalytic performance. Commonly, preparation of HPA-based heterogeneous catalysts is achievable mainly by two strategies, i.e., *solidification* and *immobilization* of the catalytically active heteropoly acids [111]. As presented in Scheme 1.4, the former involves preparing an insoluble salt of the heteropoly acid, while the latter involves supporting the active heteropoly acid on various porous substances. The preparation and application of HPA-based heterogeneous catalysts have been covered in many reviews, but very little attention has been paid to their homogeneous behavior.



SCHEME 1.4 Major strategies for the preparation of heterogeneous heteropoly acid catalysts [112].

It is also noteworthy that in heterogeneous catalysis with a heteropoly acid, in order to achieve high activity as well as sound recovery and recyclability, emphasis is placed on the solidification of heteropoly acid catalysts. A number of methods have been utilized in solidification of soluble active heteropoly acids among which are the introduction of large inorganic cations and dendritic organic cations, encapsulation by metal organic frameworks (MOFs), and blending with supporting materials, such as metal oxides, various C/Si-based substances, polymers, etc. There is another important difference between the heterogeneous and homogeneous systems in heteropoly acid catalysts, and that is their reaction fields. Homogeneous reactions take place in the solution since the heteropoly acid catalyst is evenly distributed in the solution. On the other hand, the case for a heterogeneous catalysis is extremely complicated. As illustrated in Fig. 1.6,



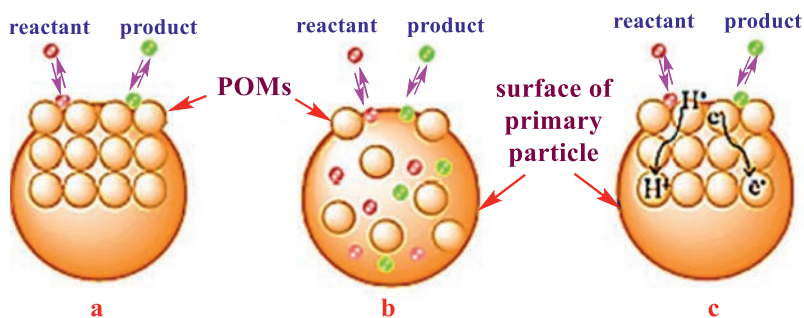


FIG. 1.6 Three catalysis models for solid POM catalysts: (A) surface type; (B) pseudoliquid bulk type; and (C) bulk type [49].

three different modes of catalysis exist for heteropoly acids as heterogeneous catalysts: *the surface-type catalysis*, *bulk-type I (pseudoliquid phase) catalysis*, and *bulk-type II catalysis in the presence of electrons or protons* [113].

### 1.14.1 Surface-type catalysis

The surface-type catalysis is the regular heterogeneous catalysis, in which the reactions occur on a 2D surface (outer surface and pore walls) of the solid catalyst. The rate of the reaction is principally proportional to the surface area. Reaction rates of olefins double-bond isomerization processes are proportional to the surface area of  $\text{H}_3\text{PMo}_{12}\text{O}_{40}$  [114]. Most of the reactions catalyzed over the acid  $\text{Cs}_x\text{H}_{3-x}\text{PW}_{12}\text{O}_{40}$  ( $2 < x < 3$ ) display the same correlation between the rate and surface acidity [115,116].

### 1.14.2 Bulk-type I catalysis

In the bulk-type I (pseudoliquid phase) catalysis, for example, reactions of polar molecules over the hydrogen and catalyzed by acid salts are formed at rather low temperatures, the reactant molecules are absorbed into the space between the heteropoly anions of the ionic lattice, and the reaction occurs inside that space. Next, the products desorb from the solid [117–119]. In this process, the solid behaves as if it is a solution and a three-dimensional reaction field is in operation. This is why it is also called the pseudoliquid phase. The reaction rate is proportional to the catalyst volume in the ideal case. From a different point of view, the rate of the acid-catalyzed reaction is governed by the bulk acidity. This sort of catalysis has been observed for both gas-solid and liquid-solid systems [120].

Using the transient response method with nondeuterated and deuterated alcohols, it was confirmed that under the reaction conditions of dehydration, a large number of alcohol molecules are absorbed into the catalyst bulk and the adsorption/desorption rate is faster than the dehydration rate [121].



### 1.14.3 Bulk-type II catalysis

Some oxidation reactions, such as oxidation of hydrogen and oxidative dehydrogenation at high temperatures, demonstrate bulk-type II catalysis [122]. In this sort of catalytic oxidation, the main reaction may proceed on the surface, but the whole solid bulk participates in the redox catalysis process due to rapid migration of redox carriers, i.e., protons and electrons. In such cases, the reaction rate is ideally proportional to the catalyst volume. The correlations between the catalytic activity for oxidation and the oxidizing ability of the catalysts are illustrated in Fig. 1.7A–C [123–126]. A monotonous correlation can be seen between the rates of catalytic oxidation of acetaldehyde and methacrolein (surface-type reaction) and the reduction rate of catalysts by CO (surface oxidizing ability) [124,125]. A similar correlation is evident for the oxidative dehydrogenation of cyclohexene (bulk-type II) and reduction rate of the catalysts by hydrogen (bulk oxidizing ability, Fig. 1.7C) [126]. For the catalytic oxidation of hydrogen (bulk-type II) and CO (surface-type) over alkali salts of  $\text{H}_3\text{PMo}_{12}\text{O}_{40}$ , a redox (Mars-van Krevelen) mechanism has been proposed. It is observed that the rates of catalytic oxidation, the rates of reduction, and reoxidation of catalysts coincide with each other at the stationary oxidation state of the catalyst [127].

Such correlations have not been observed for  $\text{H}_{3+x}[\text{PMo}_{12-x}\text{V}_x\text{O}_{40}]$  due to the thermal instability.

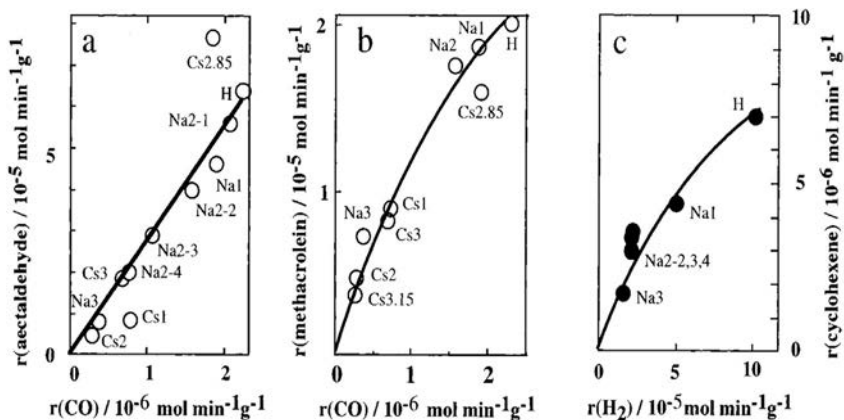


**FIG. 1.7** Correlations observed among the catalytic activity and oxidizing ability for the oxidation reactions of (A) acetaldehyde, (B) methacrolein (surface reactions), and (C) oxidative dehydrogenation of cyclohexene (bulk-type II reactions).  $r(\text{acetaldehyde})$ ,  $r(\text{methacrolein})$ , and  $r(\text{cyclohexene})$  are the rates of catalytic oxidations of acetaldehyde, methacrolein, and oxidative dehydrogenation of cyclohexene.  $r(\text{CO})$  is the rate of reduction of the catalysts by CO;  $r(\text{H}_2)$ , reduction rate of catalysts by hydrogen.  $\text{M}_x$  denotes  $\text{M}_x\text{H}_{3-x}\text{PMo}_{12}\text{O}_{40}$ . Na2-1, -2, -3, and -4 are  $\text{Na}_2\text{HPMo}_{12}\text{O}_{40}$  of different lots, for which surface areas are 2.8, 2.2, 1.7, and  $1.2 \text{ m}^2 \text{ g}^{-1}$ , respectively [20].

## 1.15. Nano polyoxometalates

In the last decade, the syntheses and applications of nanocompounds have been under the spotlight. In this regard, polyoxometalates are attracting a good deal of attention as building blocks for functional composite materials owing to their fascinating nano-sized structures. These species are ideal constructing hybrid systems, and are thus being considered as potential candidates for transforming into nanomaterials. The smaller the particle size, the higher the number of atoms per surface; therefore, the activity not only increases but also may exhibit unique properties for a number of applications. The nanostructure polyoxometalates are expected to show higher activities than any other micrometer-sized particles. This feature is crucial in catalyzed reactions.

Considerable efforts have been allocated to the design and meticulous fabrication of nanostructure polyoxometalates to be utilized in green reactions. This interest has ended up in the development of many various protocols for the synthesis of nanostructure materials over a wide range of sizes. Consequently, the idea of nano polyoxometalates and their applications remains attractive, and the number of publications and patents is increasingly growing as new researchers enter the field. This means that there is much scope for the exploration of opportunities for these polyoxometalate materials.

### 1.15.1 Nanocomposites

In the past few years, the design, manufacture, and functionalities of nanocomposite materials have been the focus of attention. This attention has its roots in the potential of the nano-sized building blocks of heterogeneous chemical species for being associated and generate new materials with enhanced properties [128]. Usually there are differences between the building blocks of a nanocomposite in terms of structures, compositions, and physical/chemical properties. This diversity among the components, together with potential synergies resulting from their combinations lead to multifunctional composites with extraordinary flexibility and a wide variety of applications.

Polyoxometalates have an unparalleled array of physical and chemical properties arising from their apparently boundless variety of molecular sizes and structures.

There are three forthright, efficient techniques for the manufacture of inorganic/organic polyoxometalate nanocomposites: chemisorption on carbon surfaces, immobilization in a polymer matrix, and layer-by-layer self-assembly.

#### 1.15.1.1 Chemisorption

Chemisorption of a polyoxometalate on a carbon substrate has been extensively investigated. It is frequently described as an irreversible strong bond formed between the carbon surface and polyoxometalate [129–131]. These strong interactions can be adjusted to provide potent carbon-POM composite materials.

The technique used for developing chemisorbed carbon-POM nanocomposites is commonly straightforward. First, the carbon substrate is oxidized with a strong acid to add surface functional groups, which act as binding sites and modify the polyoxometalate. Then the carbon material is dispersed in an organic or aqueous solution of the polyoxometalate and agitated by stirring or ultrasonication under ambient conditions. The solid product is finally washed with water many times to remove the excess loose species, dried, and the surface modified carbon-POM composite is produced [129–132]. This technique is extendable to a various carbon substrates, e.g., carbon nanofibers (CNFs) and multiwalled carbon nanotubes (MWCNTs) [129,132–138], mesoporous carbon [139], activated carbon [140], and graphene [141–144]. The chemisorption technique provides a simple, efficient means for the preparation of a wide range of nanostructured carbon-POM composites.

#### 1.15.1.2 Immobilization in a polymer matrix

The reversible redox chemistry and conductivity exhibited by conductive organic polymers (COPs) in combination with their relatively low cost and good handling capacity have rendered these materials excellent substrates for polyoxometalate integration with polyoxometalate. Various conductive organic polymers can be utilized to afford hybrid materials with polyoxometalates among which polypyrrole (PPy) [145–148], polyaniline (PANI) [149,150], polythiophene (PT) [151], and their derivatives are the most common. As illustrated in Fig. 1.8, the procedures for immobilizing polyoxometalates within a COP matrix are categorized into two broad groups. In the first type, after following a two-step approach, a polymer thin layer is deposited on a substrate through electro-polymerization or spin coating. Then the polymer film is dipped in a polyoxometalate solution so that the polyoxometalate is diffused and incorporated into the polymer matrix [145]. In the second type, which is a one-step method, a monomer molecule is chemically or electrochemically oxidized to form a polymer thin layer in the presence of a polyoxometalate solution. High ionic conductivity, strong oxidizing power, and acidic character of heteropoly acids deliver the best conditions for the polymerization of such monomers as thiophene, aniline, and pyrrole. In the electrochemical polymerization of a monomer, the polyoxometalate solution is frequently utilized as the electrolyte. A thin layer of polymer is deposited on the working electrode by applying a sufficient oxidation potential, which is doped with the polyoxometalate molecule. Polymerization techniques give rise to a nanostructured hybrid species in which the bulky polyoxometalate molecule is confined within a COP matrix [149,150]. The abovementioned approaches can be adapted to prepare a wide range of new POM-COP hybrids.

In comparison with chemisorption, immobilization within a COP matrix enjoys the advantage that it results in combined electrochemical activity. In addition to providing structural support, the substrate contributes reversible Faradaic reactions to improve the overall electrochemical performance of the

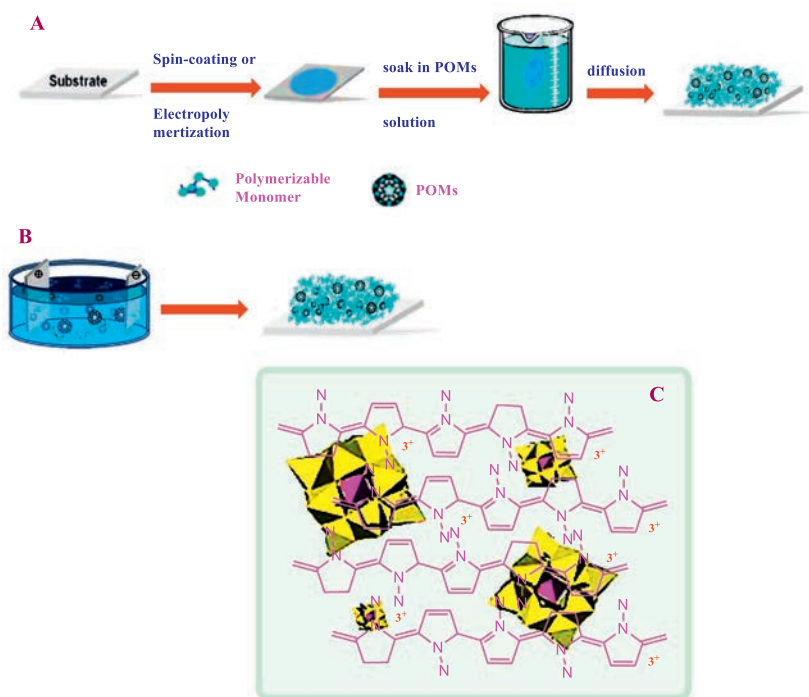


**FIG. 1.8** Preparation of a POM-COP matrix through (A) a two-step and (B) a one-step method. (C) The structure of hybrid PPy-PMO<sub>12</sub>O<sub>40</sub><sup>3-</sup> [152].

hybrid. Chemisorbed carbon-POM composites can be prepared by simple mixing, while more complex and potentially costly synthesis techniques are necessary for carbon-COP hybrids, particularly in the case of electropolymerization. Additionally, since inclusion within a COP matrix is not a technique for surface modification, the polyoxometalate is frequently embedded within the bulk of the polymer. Hence, additional preparation steps (such as the use of an external oxidant) are required to fabricate a true nanocomposite.

### 1.15.1.3 Layer-by-layer self-assembly

Developed by Decher in the 1990s [153], layer-by-layer (LbL) deposition is the alternate adsorption of positive and negative layers on a support surface using electrostatic forces. Aqueous solutions of two molecules with opposite charges are consecutively coated on the support surface. The surface charge is reversed after each dipping cycle to allow the deposition of the succeeding layer. With this method, multilayer structures are formed, which are predominantly stabilized by strong electrostatic forces; other interactions, e.g., hydrogen bonding may be present as well [154]. Layer-by-layer self-assembly is an excellent method for the preparation of carbon-POM films; since the groundbreaking

work by Ingersoll, Kulesza, and Faulkner [155], many more studies have been reported on electrostatically stabilized multilayer polyoxometalate composites [156–160]. Since polyoxometalates form anions (with negative charges) in solution, often a polyelectrolyte layer with positive charge is needed so that LbL deposition on carbon substrates is achieved. The procedure utilized for preparing carbon-POM composites by LbL assembly is depicted in Fig. 1.9. The carbon substrate (which is normally preoxidized to improve the negative charge on the surface) is dipped in a polycation solution and washed with water to remove the excess loose species. The substrate, which is now positively charged, is dipped in a solution of polyoxometalate and then washed again. Since there are strong electrostatic attractive forces, each step of deposition only takes a few minutes, which is much faster than the many hours necessary for chemisorption. The layer-by-layer procedure may be repeated many times so that electrostatically stabilized multilayer films are accumulated quickly and effectively. The ability to make thin multilayer films of polyoxometalate is among the most important advantages of the layer-by-layer procedure. The capability of depositing multiple polyoxometalate layers allows for the incorporation of different polyoxometalate molecules on the same substrate. Since the chemical and physical properties of polyoxometalates can vary significantly with their structure and chemical composition, incorporation of several different polyoxometalate chemistries on the same substrate may have apparent advantages for the design of composite materials with a wide variety of properties and potentials.

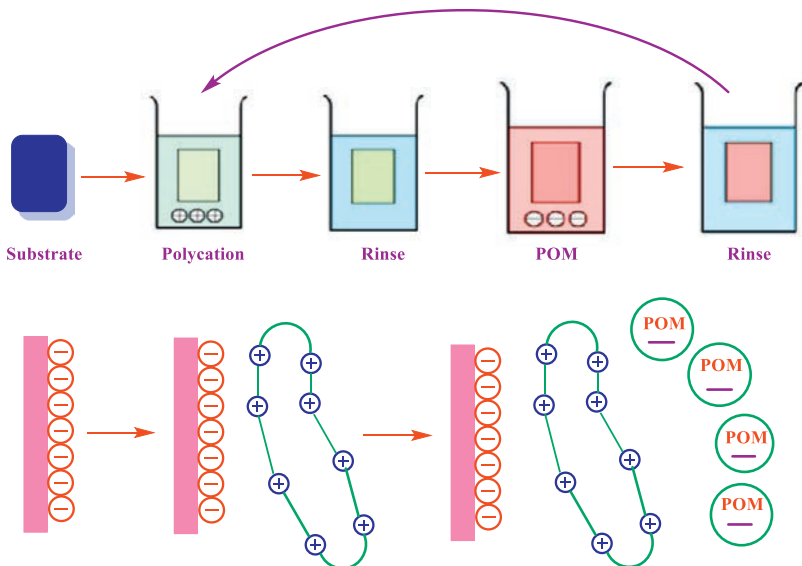


**FIG. 1.9** Layer-by-layer self-assembly of a polyoxometalate film composite via the alternate adsorption of polyoxometalate and polyelectrolyte layers [152].

Compared to polymer matrix immobilization and chemisorption, layer-by-layer self-assembly goes on by quick and simple deposition steps, yet allowing for a strict control over the structure, and accordingly functionality, of the resulting composite. Among the three procedures described, the layer-by-layer self-assembly is the most flexible since it may be applied to an extensive range of different substrates, which goes beyond organic materials; it can even be utilized in combination with the two other procedures [161,162]. The most important advantage of the layer-by-layer assembly is the capability of preparing multilayer nanostructured films, which results in composite materials in which numerous different chemistries are combined, thus exhibiting adjustable, various functionalities. One of the main present weaknesses of the layer-by-layer procedure is that many of the most common polyelectrolytes display restricted electrochemical activity and conductivity, which can diminish the activity of a composite electrode. Alternative highly conductive cation linkers, which exhibit their own redox functionality, can enhance layer-by-layer assembled polyoxometalate films even more.

### 1.15.2 Applications

Polyoxometalate-based composites and nanocarbons like carbon nanotubes (CNTs) or graphene have been the focus of much attention since they combine the exclusive chemical reactivity of polyoxometalates with the unique electronic properties of nanocarbons. The extraordinary properties of such composites have been utilized in catalysis, manufacture of molecular sensors, energy conversion and storage, and electronics. In this section, the latest advances in POM-CNT and POM-graphene nanocomposites will be addressed, with a focus on their applications in catalysis. The excessive redox-activity of polyoxometalates renders them ideal for the catalytic transfer of electrons from or to a substrate. This is mostly attractive for designing multielectron transfer reactions, which are usually troubled by high overpotentials that decrease the overall conversion yields. For dealing with this challenge, polyoxometalates are ideal candidates since they can be chemically modified with highly redox-active metals (such as Co, Mn, or Ru). Therefore, technologically relevant electrocatalysts will become accessible for splitting water into oxygen and hydrogen [163,164] and for oxidation/reduction reactions in fuel cells [165].

#### 1.15.2.1 Water oxidation

POM-based water oxidation catalysts (WOCs) functionalized with redox-active metals such as Co, Mn, or Ru have been developed [69,166]. Bonchio and coworkers [167] electrostatically assembled a prototype POM-WOC ( $M_{10}[Ru_4(H_2O)_4(\mu-O)_4(\mu-OH)_2(\gamma-SiW_{10}O_{36})_2]$ ;  $M_{10}Ru_4(SiW_{10})_2$ ,  $M=Cs^+$ ,  $Li^+$ ) on multiwalled carbon nanotubes (MWNTs) as a conductive substrate to form an electrocatalyst active enough for water oxidation (Fig. 1.10).

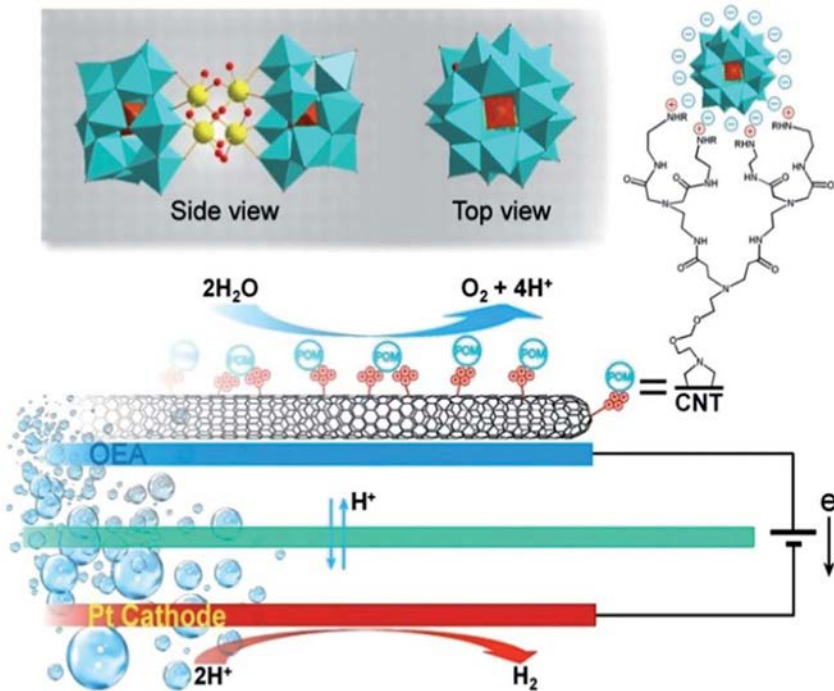


**FIG. 1.10** An electrocatalytic cell for water splitting with the integrated nanostructured oxygen-evolving anodes (OEAs) based on polyanionic ruthenium polyoxometalates. The polyoxometalate utilized is  $(M_{10}[Ru_4(H_2O)_4(\mu-O)_4(\mu-OH)_2(\gamma-SiW_{10}O_{36})_2])$ . Blue: tungsten, brown:  $SiO_4^{4-}$ , yellow: ruthenium, red: oxygen [167].

Following this initial development, Bonchio et al. [168] noticed that the attachment of the polyoxometalate to the carbon nanotube was still not optimal, and hence they developed new covalent and noncovalent approaches for the functionalization of the carbon nanotubes with cations (Fig. 1.11). The resulted cationic carbon nanotubes exhibited high binding affinity for the anionic POM-water oxidation catalysts to form a nanostructured composite surface upon dropcasting the composite on electrode surface, which provided high surface area electrocatalysts. Bonchio et al. [169] prepared a highly robust electrocatalyst for the oxidation of water by combining functionalized graphene with their ruthenium-based POM-WOC  $Ru_4(SiW_{10})_2$ . The obtained composite material exhibited oxygen evolution at overpotentials as low as 300 mV at neutral pH with insignificant loss of activity after 4 h of testing.

The authors attributed the observed high stability and catalytic activity to the highly dispersed and noninvasive surface modification of graphene, which enabled transportation and accumulation of electrons across the extended  $p$ -bond network. In addition, Hill and coworkers [170] investigated a similar ruthenium-based POM/rGO composite using electrochemical analyses. The composite displayed



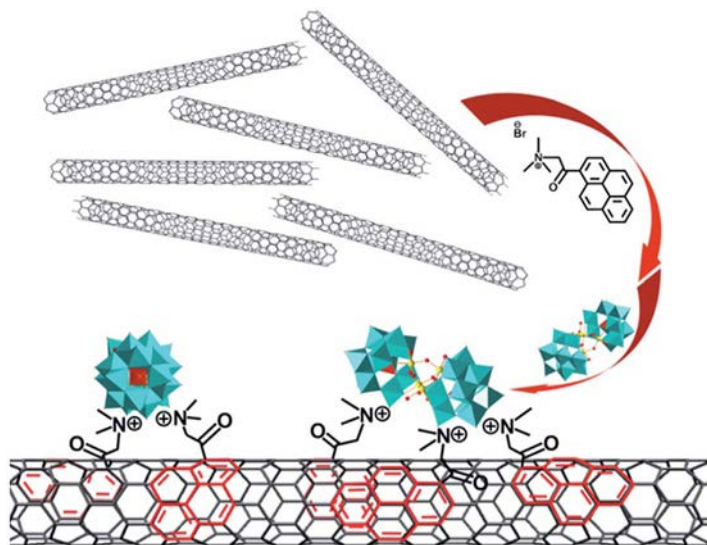


**FIG. 1.11** A CNT-bound polyoxometalate catalyst. The carbon nanotubes are functionalized with an amphiphilic cationic pyrene derivative via *p-p* stacking; the anionic  $\text{Ru}_4(\text{SiW}_{10})_2$  is then immobilized by means of electrostatic interactions [168].

high stability and excellent catalytic performance for the oxidation of water at neutral pH, especially in the presence of  $\text{Ca}(\text{NO}_3)_2$ , 1.0M, with a mild overpotential of 0.35 V. These preliminary results demonstrated the huge synergic potential of Ru-containing polyoxometalates as catalysts combined with graphene as a conductive support.

#### 1.15.2.2 Methanol oxidation

Chen et al. [171] reported a novel catalyst support based on carbon nanotubes altered with a Keggin-type polyoxometalate ( $\text{H}_3\text{PMo}_{12}\text{O}_{40}$ ) to observe spontaneous, robust chemisorption of the polyoxometalate on the carbon nanotubes. The composite was utilized as a redox-active support for highly dispersed platinum and platinum-ruthenium electrocatalysts, which were deposited using electro-deposition. Catalytic tests revealed that the combination of the unique electrical properties of the carbon nanotubes and the excellent redox properties as well as the high protonic conductivity of the polyoxometalates led to high specific activity, high current densities, and enhanced cycle stability in comparison with systems not modified by a polyoxometalate. These results were the first experimental evidence that carbon nanotubes modified by a polyoxometalate could serve as appropriate catalyst supports for DMFCs (Fig. 1.12).

An inventive approach to deposit small platinum nanoparticles on carbon nanotubes for the oxidation of methanol was reported by Zhang and coworkers [134]. They employed a photochemically reduced Keggin cluster  $\text{H}_3\text{PW}_{12}\text{O}_{40}$  in



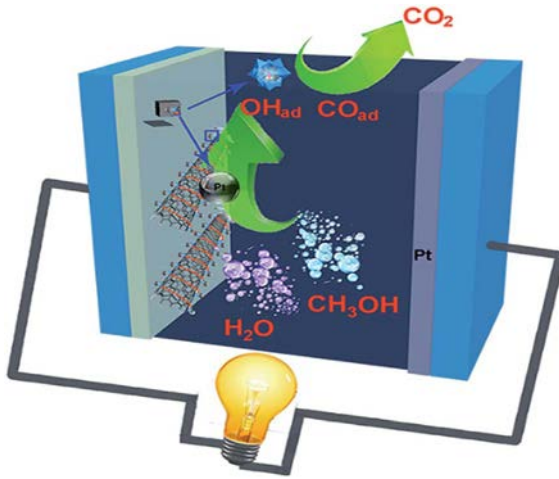


**FIG. 1.12** Electrochemical reactions in a direct methanol fuel cell functionalized with carbon nanotubes modified by  $\text{PMo}_{12}$ . The  $\text{PMo}_{12}$ /CNTs were utilized to support highly dispersed platinum and platinum-ruthenium electrocatalysts formed by electrodeposition. The presence of polyoxometalates was demonstrated to effectively decrease the catalyst poisoning and raise the catalytic activity [171].

situ as a redox facilitator to decrease the platinum (II) precursor; it also served as a linkage group to stabilize the nanoparticles on the carbon nanotube surface (Fig. 1.13). The composite exhibited a significantly higher electrocatalytic performance toward the oxidation of methanol in comparison with traditional Pt/C catalysts and other related Pt/CNT reference systems.

Current studies are revealing that POM-modified nanocarbon electrodes may provide many benefits to the manufacture of modern electrodes used in methanol oxidation, especially in the fields of metal nanoparticle stabilization and deposition, improved catalyst poison resistivity, and reduced usage of noble metals. A main challenge in this field is still designing low overpotential electrodes for the oxidation of methanol that do not employ noble metal catalysts. Consequently, access to extremely active POM-based methanol oxidation catalysts, which could act on a molecularly dispersed level, might provide an easy and promising route to earth-abundant materials with technological relevance.

### 1.15.2.3 Oxygen reduction

A sequence of POM/noble metal/nanocarbon composites have been critically reported to act as catalysts in the reduction of oxygen. Jiang et al. [172] introduced a Pd@POM-PDDA-MWNT electrocatalyst (Fig. 1.14) that was highly potent as an efficient nonplatinum catalyst for the reduction of oxygen in fuel cells.

Initial steps have been taken to replace the traditional noble metal particles for the reduction of oxygen by less expensive metals. Zhang et al. [173] showed

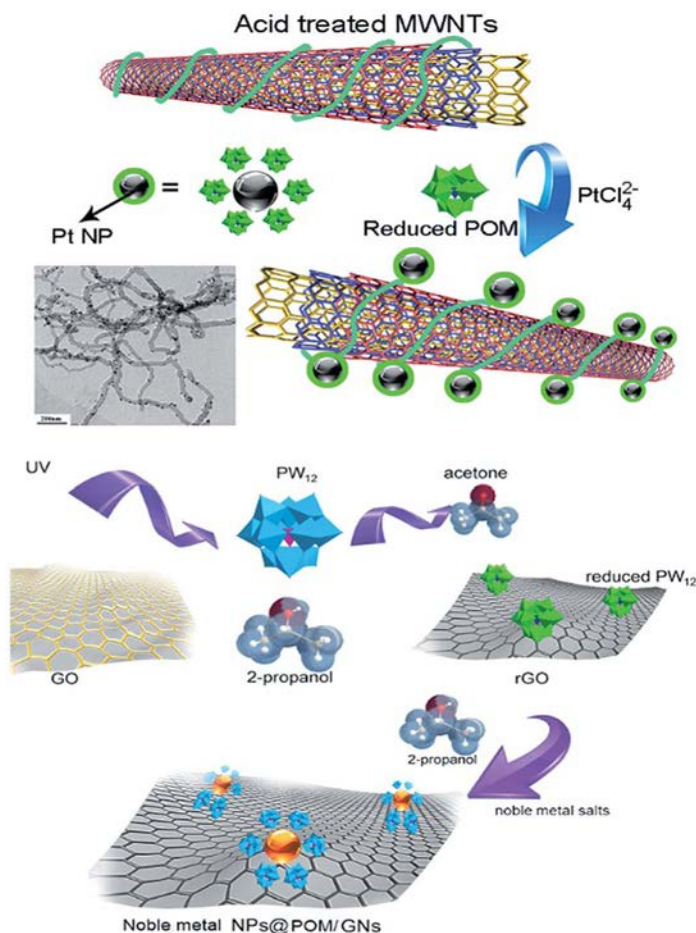


**FIG. 1.13** (Top) Formation of Pt@POM-CNT composite electrocatalysts. The polyoxometalate ( $\text{PW}_{12}$ ) is photochemically reduced by UV light with isopropyl alcohol as an electron donor; the reduced  $\text{PW}_{12}$  is combined with multiwalled carbon nanotubes and  $\text{H}_2\text{PtCl}_4$  to give the Pt@POM-CNT composite. Inset: The TEM image of Pt@POM-CNT composite. (Bottom) Preparation of the tricomponent metal NPs@POM/GNs composites. (1) Photoreduction of  $\text{PW}_{12}$  by isopropyl alcohol under UV light; (2) GO reduction by reduced  $\text{PW}_{12}$  to give  $\text{PW}_{12}$ /rGO composites; (3) photoreduction of the  $\text{PW}_{12}$ /rGO composites by isopropyl alcohol to give reduced  $\text{PW}_{12}$ /rGO; (4) reduction of noble metal salts by the reduced  $\text{PW}_{12}$ /rGO to give the noble metal NPs@POM/GNs [134].

that the less expensive silver nanoparticles may be employed as active reduction sites to reduce oxygen. They claimed to have found an easy, one-pot synthesis of silver nanoparticles-decorated carbon nanotubes by the reaction of acidized multiwalled carbon nanotubes with silver nitrate using in situ photoreduced Keggin anions as a reducing agent. The composites exhibited a high electrocatalytic activity for the reduction of oxygen owing to the synergic effect between the silver nanoparticles and carbon nanotubes. Significantly increased reduction

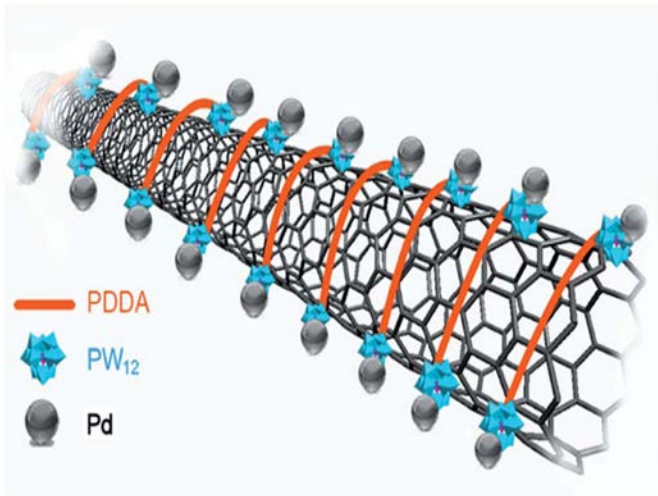


**FIG. 1.14** Self-assembly of Keggin-type polyoxometalates (PW<sub>12</sub>) on PDDA-functionalized multi-walled carbon nanotubes through electrostatic interactions and subsequent deposition of palladium nanoparticles on polyoxometalates assembled PDPA-MWNTs by reductive chemical deposition [172].

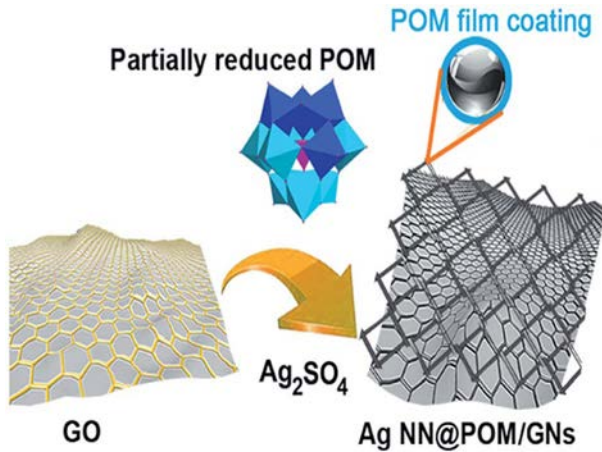


**FIG. 1.15** Polyoxometalate-mediated large-scale synthesis of 2D Ag NN@POM/GNs composites using the mixed-valent Keggin-type polyoxometalate H<sub>7</sub>[b-PMo<sub>4</sub><sup>V</sup>Mo<sub>8</sub><sup>VI</sup>O<sub>40</sub>] [174].

of oxygen current densities was observed in comparison with nonfunctionalized carbon nanotubes for the polyoxometalate functionalized system. The reduction of oxygen activity of Ag nanoparticles was substantiated in 2013, when a 2D-Ag nano-net (NN) functionalized graphene was reported as a substitution for Pt catalysts for the reduction of oxygen. The group used H<sub>7</sub>[b-PMo<sub>4</sub><sup>V</sup>Mo<sub>8</sub><sup>VI</sup>O<sub>40</sub>] as the reducing agent<sup>60</sup> (Fig. 1.15) to deposit an Ag nanostructure on graphene.

The prepared composites in this way displayed high electrocatalytic reduction of oxygen activity together with high catalytic activity of the Ag nano-nets.

### 1.15.3 Synthesis of nanomaterials

During the past decades, the synthesis of nanomaterials has been an important field of research, owing to their unique physical, chemical, and electrical properties [175,176]. They are therefore highly potent for applications in different fields, such as catalysis, semiconductors, electronics, imaging agents, drug delivery, etc. [177–181]. Polyoxometalates have recently found applications in the synthesis of nanomaterials as reducing and stabilizing agents. Polyoxometalates can be reduced photochemically [182], electrochemically [183], or radiochemically [184] or using suitable chemical reducing reagents [185] without undergoing decomposition or any change in their structures; then the reduced forms of the polyoxometalates are capable of reducing metal ions [186,187]. The synthesized nanomaterials provide negative charges owing to the existence of polyoxometalates on their surface. This can prevent the aggregation of the nanomaterials by electrostatic repulsive forces, which enables long-term stability [188]. In addition, polyoxometalates are appropriate candidates for the implementation of green chemistry, as they are recyclable and reusable during the redox process utilized for the green synthesis of nanomaterials in aqueous systems [174,189].

The nanomaterials synthesized in this manner are encircled with polyoxometalates, which have been demonstrated to influence the dispersion and stability of nanomaterials for a long time. Above all, POM-stabilized nanomaterials have exhibited improved catalytic activity in many works due to the synergic effects with polyoxometalates, showing properties of reversible multielectron redox transformations and high activity during the catalyzed reaction. Nonetheless, the shapes of the nanomaterials prepared by polyoxometalates are chiefly globular; therefore, investigating the shape control of such nanomaterials seems necessary.

### 1.15.4 Immobilized Polyoxometalates and their applications

The immobilization of polyoxometalates on a solid supports may be categorized into two groups. In the first group, the polyoxometalate species is supported on a material with no catalytic activity. In the second group, the polyoxometalate is supported on a catalytically active substance. The appropriate support materials are typically porous substances, preferably with nano-sized particles. The satisfaction of these two criteria provides a platform for the even distribution of active sites upon which the mass transfer resistance is lowered. Therefore, choosing appropriate supports for the effective design of efficient heterogeneous catalysts based on polyoxometalates is crucial. Additionally, controlling the polyoxometalate composition at the atomic and molecular levels provides the researchers with the ability to design green reagents to ensure sustainability.

### 1.15.4.1 Titanium dioxide-supported polyoxometalates

The polyoxometalate immobilization on  $\text{TiO}_2$  is of especial interest since the obtained combination represents the semiconductor-like properties exhibited by both components.  $\text{TiO}_2$  has been broadly examined as a photocatalyst since its chemical stability is relatively high, and it is nontoxic, inexpensive, and readily available. This means that the combination of polyoxometalates with  $\text{TiO}_2$  paves the way for designing green materials. Yang and coworkers [96] reported the preparation of a nanoporous anatase and  $\text{H}_3\text{PW}_{12}\text{O}_{40}$  composite following a sol-gel hydrothermal method that directly embedded the polyoxometalates within the lattice of anatase to form particles with sizes less than 10 nm (Fig. 1.16A). As illustrated in Fig. 1.16B, the formation of the nanocomposite led to a red-shift from the anatase support. The nanocomposite was found to have ability to degrade an array of dyes under visible light irradiation. Powder X-ray diffraction analysis could not reveal the presence of the polyoxometalates, which was perhaps because of the embedding of the polyoxometalates within the anatase, which did not allow the formation of polyoxometalates crystalline phase for detection.

Xie reported the preparation of an  $\text{H}_3\text{W}_{12}\text{O}_{40}$ -titania nanotubular array composite for photoelectrocatalysis and photocatalysis of bisphenol A, which is an

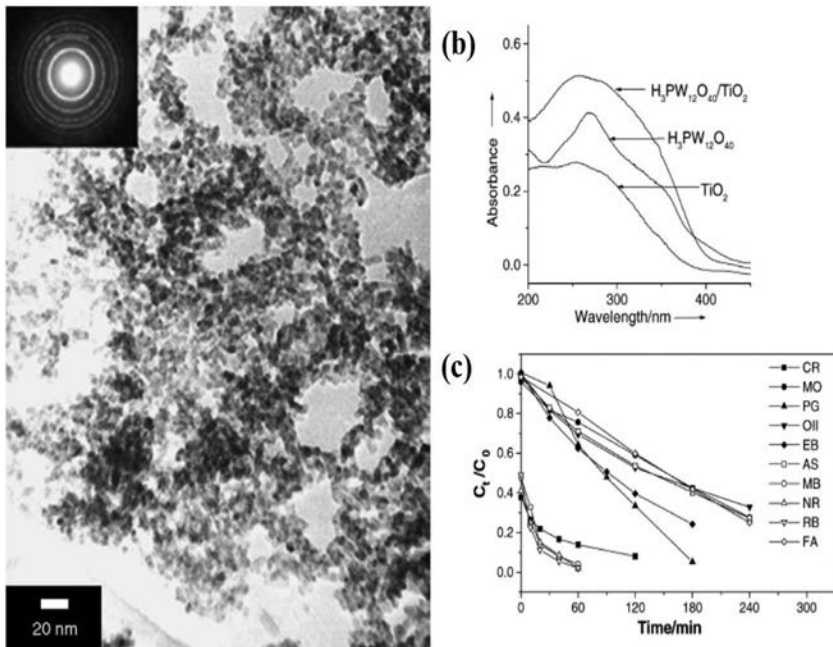


**FIG. 1.16** (A) TEM image and SAED pattern of the  $\text{H}_3\text{PW}_{12}\text{O}_{40}/\text{TiO}_2$  nanocomposite, (B) UV-vis diffuse reflectance spectra of  $\text{H}_3\text{PW}_{12}\text{O}_{40}$ ,  $\text{TiO}_2$ , and the  $\text{H}_3\text{PW}_{12}\text{O}_{40}/\text{TiO}_2$  composite. Photocatalytic degradation of various dyes using the nanocomposite is visible [96].



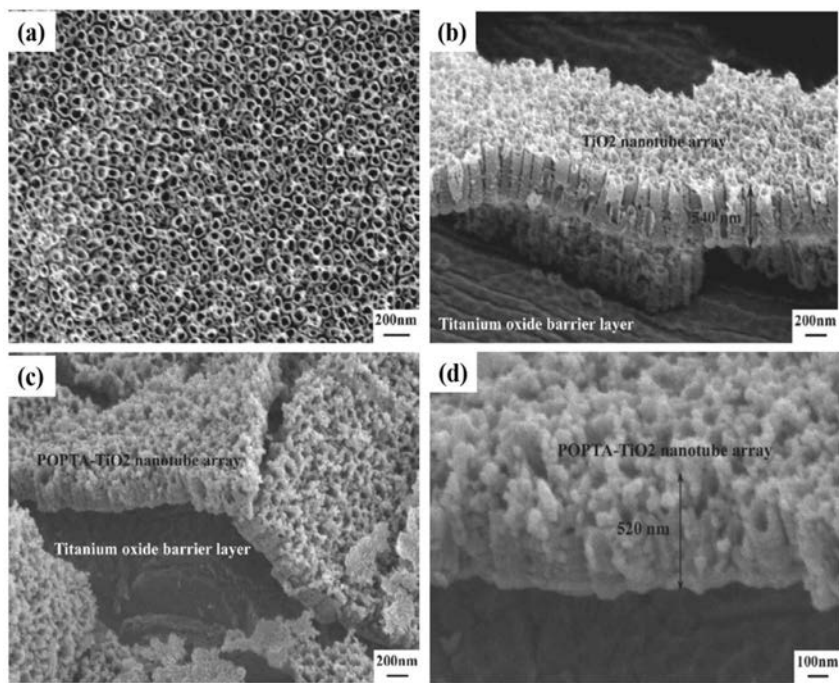


**FIG. 1.17** FESEM images of (A) TiO<sub>2</sub> nanotubular array, and cross-sectional SEM images of (B) TiO<sub>2</sub> tubules, (C) H<sub>3</sub>PW<sub>12</sub>O<sub>40</sub>-TiO<sub>2</sub> tubules, and (D) enlarged view of H<sub>3</sub>PW<sub>12</sub>O<sub>40</sub>/TiO<sub>2</sub> tubules [190].

endocrine disruptor. The mentioned nanotubular array was prepared through a low-voltage anodization process (Fig. 1.17A and B); H<sub>3</sub>PW<sub>12</sub>O<sub>40</sub> was then embedded into the nanotubular array (Fig. 1.17C and D). The composite was able to degrade bisphenol A entirely under ultraviolet light. Comparing these results with the ones by Yang and coworkers [96], the immobilization of H<sub>3</sub>PW<sub>12</sub>O<sub>40</sub> did not appear to achieve a similar synergic effect to that obtained by the composite formation. Moreover, the H<sub>3</sub>PW<sub>12</sub>O<sub>40</sub> embedding may not allow for appropriate interaction between the titania nanotubular array and the polyoxometalate. The solution was continuously purged by oxygen airflow, and the resulting solution displayed significant leaching of H<sub>3</sub>PW<sub>12</sub>O<sub>40</sub> in the UV-vis spectra. The necessity for supplying an external electrical potential in addition to the use of ultraviolet light decreased the viability of such a process for practical applications.

Lu et al. [191] prepared an amine-functionalized TiO<sub>2</sub>-based catalyst with three-dimensionally ordered macroporous (3DOM) to be able to immobilize K<sub>5</sub> [PW<sub>11</sub>Co(H<sub>2</sub>O)O<sub>39</sub>]. This strategy provided a new and efficient methodology for the preparation of a three-dimensional architecture for the polyoxometalate immobilization. Polystyrene spheres were used as a template for the formation of a three-dimensional TiO<sub>2</sub> structure (Fig. 1.18A–C). Then the resulted material was annealed in order to remove the template and eventually amine-functionalized

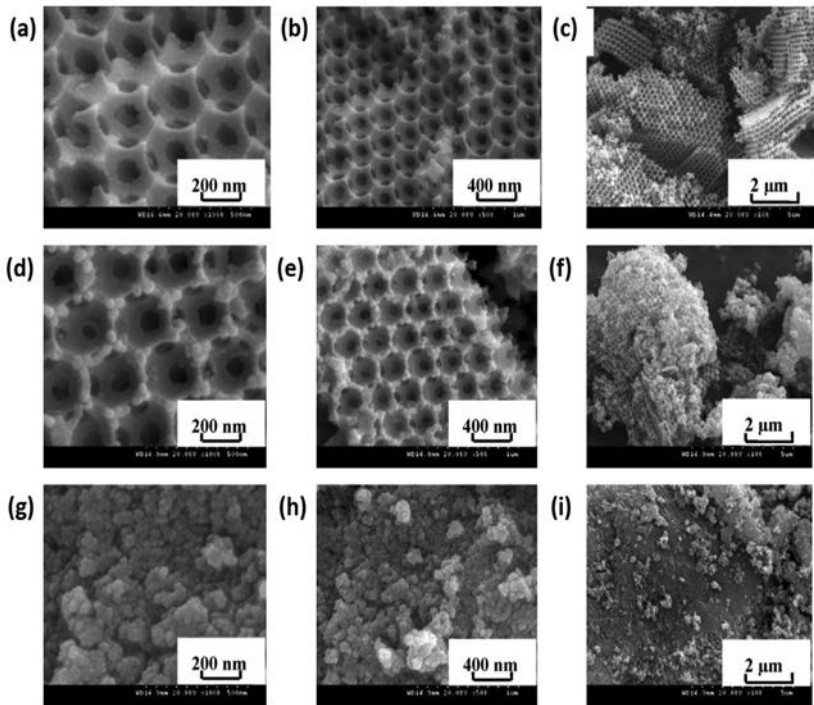


**FIG. 1.18** (A–C) SEM images of 3DOM-TiO<sub>2</sub>, (D–F) 3DOM-PW<sub>11</sub>Co-APS-TiO<sub>2</sub>, and (G–I) PW<sub>11</sub>Co-APS-TiO<sub>2</sub> [191].

with (3-aminopropyl) triethoxysilane. The K<sub>5</sub> [PW<sub>11</sub>Co(H<sub>2</sub>O)O<sub>39</sub>] was then immobilized by coordination of the amine group to the cobalt on the polyoxometalate (Fig. 1.18D–F). The authors prepared the same material without using polystyrene template as well. The result was a material with no distinct morphology, as illustrated in Fig. 1.18G–I. The prepared catalyst was able to degrade organic dyes efficiently under a combination of ultraviolet and microwave irradiations. The 3D structure was one of the chief strengths of the catalyst that provided an efficient mass transport of the pollutant to the surface of that catalyst. In spite of catalytic applications, the preparation might not be easy or robust due to the problem of partial filling of the template. On the other hand, the use of ultraviolet and microwave irradiations is rather energy consuming. Hence, it is important have a trade-off between the energy consumption and the efficiency of the material. In the prepared material, K<sub>5</sub> [PW<sub>11</sub>Co(H<sub>2</sub>O)O<sub>39</sub>] served as a mediator to retard the electron-hole pair recombination so that the catalytic capability of the polyoxometalate was not affected.

Reviewing the few studies on applying polyoxometalates immobilized on TiO<sub>2</sub> as a heterogeneous catalyst revealed that the role of polyoxometalates in the catalysis process was obscured by the catalytic activity of titanium dioxide.

Therefore, it is expected that researchers look into the catalytic and redox activity of the polyoxometalates for their environmental applications and for better understanding of their catalytic role. The robust design of the immobilized polyoxometalate catalysts could include the formation of *bulk* heteropoly acid phases to enhance the bulk-type II catalytic ability of polyoxometalates on the solid support. A one-pot synthesis is desired from the synthetic viewpoint, but under such conditions, it would be improbable to attain the formation of the crystalline acid phase of heteropoly acids. Direct embedding of the polyoxometalate may cause it to lose its catalytic sites. Therefore, the optimal conditions for the preparation of this type of supported catalyst must involve the use of a coupling agent with the capability of stabilizing and improving the growth and formation of polyoxometalates on the support surface.

#### 1.15.4.2 Polyoxometalates supported on carbon-based materials

Carbon-based materials have been used for the purpose of immobilization as well. Therefore, this section will provide a brief look into these materials, which includes carbon nanotubes [132,189], graphene oxide (GO), and carbon nitride [192]. The strategies employed for the immobilization of polyoxometalates on these supports are similar since all of these substances contain honeycomb hexagon aromatic networks. As an example, the case with graphene is depicted in Fig. 1.19. Because of their large surface area, presence of functional groups, and electronic properties, they are highly attractive substrates as solid supports.

Polyoxometalates are immobilized on carbon-based materials such as carbon nanotubes or graphene oxide mostly with the purpose of energy applications. They can be used as green components of rechargeable lithium batteries [193,194].

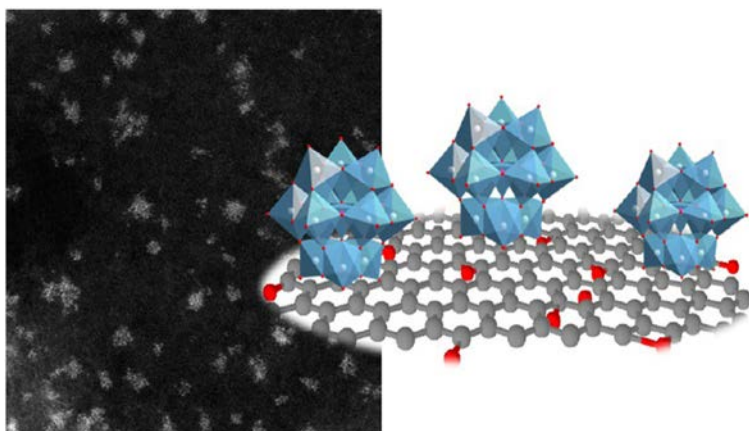


FIG. 1.19 Polyoxometalates immobilized on a functionalized graphene sheet [141].



However, even if the polyoxometalate is immobilized on the conducting polymer, the degradation of the polymer support damages the charge/discharge cycling [196–198]. This cycling process raises the solubility of the polyoxometalates [114], which in turn causes the fabricated devices lose their charges.

Fig. 1.20 illustrates a polyoxometalate immobilized on carbon nanotubes by Huang et al. In place of using covalent or electrostatic immobilization, the immobilization was accomplished by functionalizing an Anderson-type polyoxometalate with pyrene to form a Py-polyoxometalate species. In this way, a  $\pi$ - $\pi$  interaction is enabled between the pyrene group and the surface of the carbon nanotubes, which has a debundling effect on the carbon nanotubes. The fresh unchanged carbon nanotubes in Fig. 1.21 have regular and even features while the modified surface with Py-polyoxometalate species is highly uneven, showing the efficiency of this methodology in the modification of the carbon nanotube surface. The incorporation of the two materials electrochemically enhances the nanocomposite, which can serve as an anode material in a lithium battery.

He et al. reported the preparation of  $\text{H}_3\text{PW}_{12}\text{O}_{40}$  and  $\text{H}_3\text{PMo}_{12}\text{O}_{40}$  supported on  $\text{g-C}_3\text{N}_4$  to utilize them as hybrid photocatalysts for the degradation of methylene blue and phenol. One-pot hydrothermal synthesis of  $\text{g-C}_3\text{N}_4$  and polyoxometalates at different loadings was utilized to immobilize the heteropoly acids. The results revealed that at 6% loading, the obtained materials had the

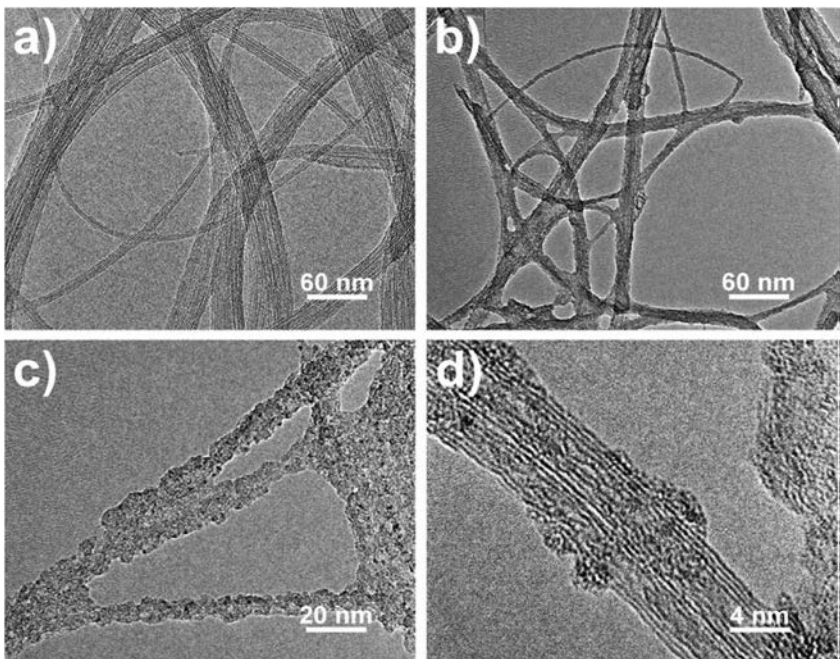


**FIG. 1.20** TEM micrograph of (A) fresh carbon nanotubes, and (B–D) Py-Anderson-CNTs nanocomposite [195].

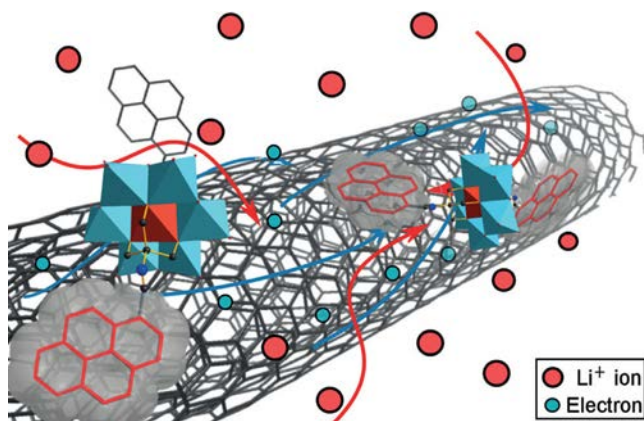


FIG. 1.21 Carbon nanotubes modified with Py-Anderson clusters through noncovalent functionalization [195].

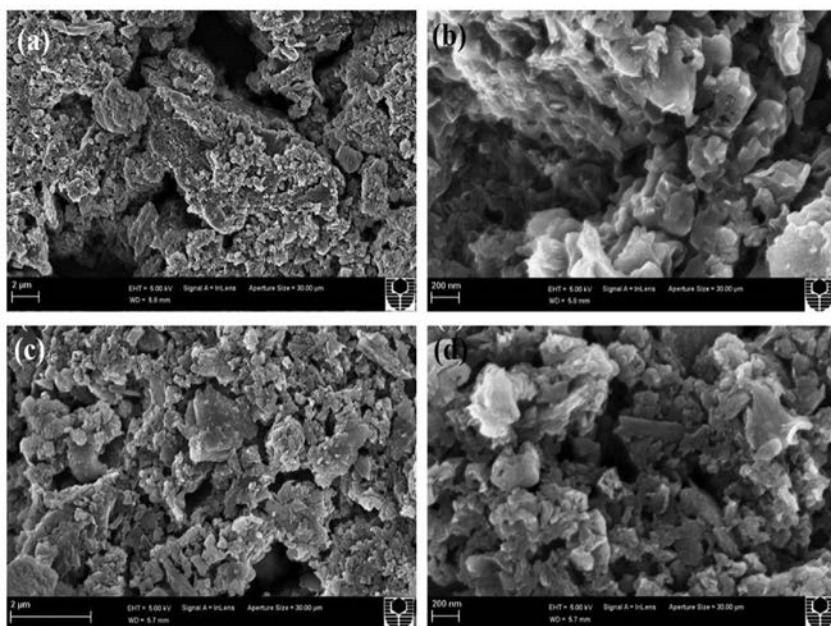


FIG. 1.22 SEM micrograph of  $C_3N_4$  modified with  $PMO_{12}O_{40}$  (A and B), and  $PW_{12}O_{40}$  (C and D) [199].

highest surface area and pore volume, which provided the best photocatalytic performance. The SEM images of the  $g-C_3N_4$  modified by polyoxometalates (Fig. 1.22) suggest that the prepared material lacks a well-defined morphology, which is probably attributable to the poor dispersion of  $g-C_3N_4$  and is challenging to control during the hydrothermal synthesis. Nonetheless, the X-ray

diffraction analysis indicated that the existent of the crystalline planes in the synthesized materials may explain their efficiency as photocatalysts.

## 1.16. Organic/inorganic hybrid materials

Solidification of a polyoxometalate simply with an inorganic countercation has been a conventional routine for obtaining a heterogeneous solid-oxide catalyst based on a heteropoly acid. However, in order to exploit the molecular character of a polyoxometalate in a more effective fashion in heterogeneous catalysis systems, it is extremely desirable to introduce a high-dimensional structure, e.g., a porous structure, into the polyoxometalate material. To satisfy this, the organic/inorganic hybridizing of a polyoxometalate is regarded as the most appropriate approach since currently a wide range of hybrid compounds of polyoxometalates can be created either by covalent bonding between the organic and inorganic components or through noncovalent electrostatic interactions between the two moieties. This approach not only works for the introduction of a high-dimensional organic structure around the polyoxometalate but also generates a synergetic effect between the organic and inorganic components on the heterogeneous catalyst. A basic classification of various organic/inorganic hybrid materials based on the organic/inorganic framework is given in Fig. 1.23 [200]. Moreover, according to this classification, a few examples of catalysts that can work heterogeneously are given in Table 1.8 [200]. In general, polyoxometalates can be versatile building blocks of supramolecular complexes since polyoxometalates display a wide variety of self-assembly properties [201]; therefore, controlling the formation of organic/inorganic hybrid networks in self-organization processes becomes possible. This means that the correct design of an organic component for the synthesis of hybrid materials is very important.

Hybrid materials prepared from a polyoxometalate in a three-dimensional crystalline structure (Type A) are, in most cases, a condensed packing structure and form a large group of organic/inorganic materials. However, they have been rarely used as heterogeneous catalysts. Pyridinium salt of  $\text{PMo}_{12}\text{O}_{40}$  is seemingly the first instance of this type [202]. This hybrid material, after heating for partial removal of pyridinium ions and reducing the polyoxometalate, exhibited particularly high catalytic performance for the selective oxidation of propane to acrylic acid in gas phase. This hybrid material is active only if the reduced polyoxometalate and remaining pyridinium ion are retained in the structure. Therefore, the electrostatic stabilizing effect of the pyridinium ion on the reduced polyoxometalate, where the catalytic oxidation occurs, is a critical point and maintained by the organic hybrid structure.

Type B is a hybrid material with a dendritic-type framework around the polyoxometalate. In the majority cases, each polyoxometalate is connected to organic polycations and surrounded by them; these polycations are tripods consisting of triammonium groups; alternatively, they may be encapsulated by cationic surfactants [203] or ionic liquids [204]. The dendritic isolated

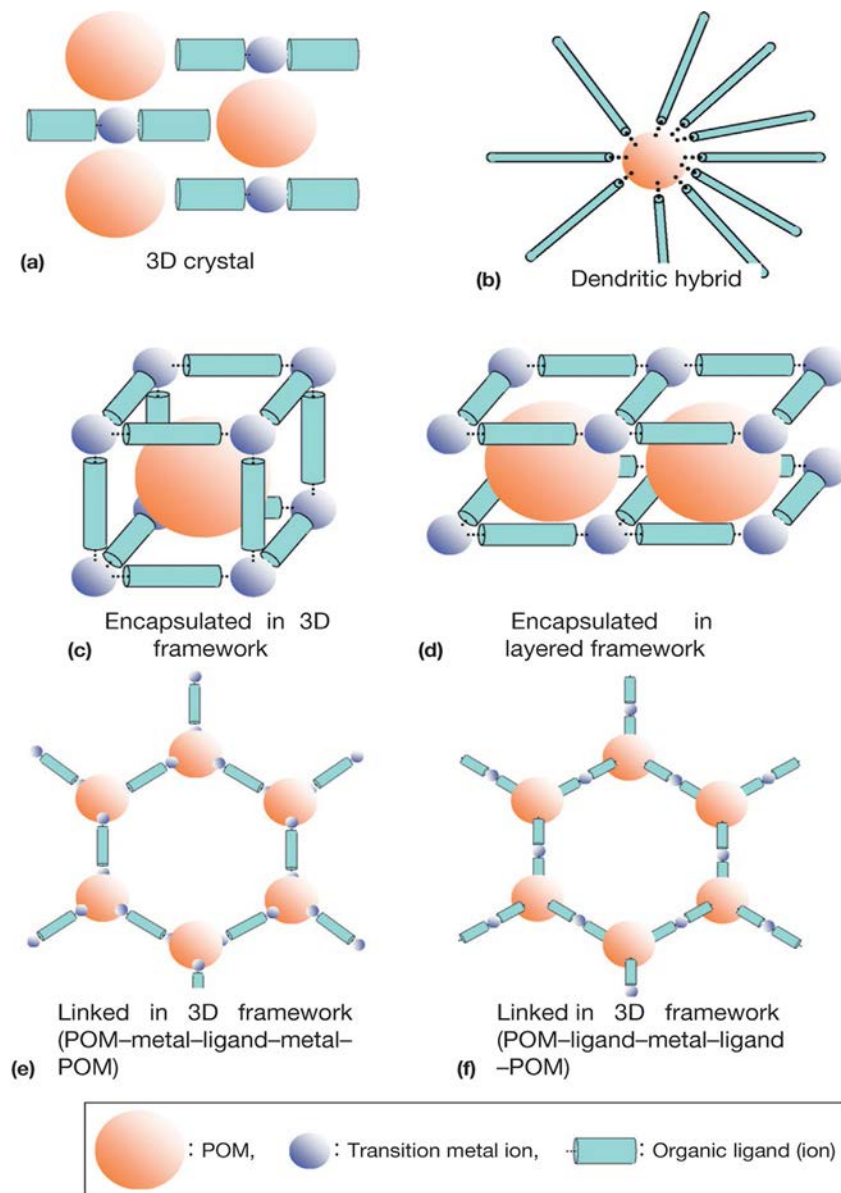


FIG. 1.23 Organic/inorganic hybrid of POM [200].

supramolecular structure possesses a hydrophilic polyoxometalate core and a hydrophobic shell with a precise composition [205,206]. The described situation raises the stability of the polyoxometalate core as well as its catalytic activity. The dendritic-type polyoxometalates have found many catalytic applications in homogeneous systems [207] in which dendritic-type catalysts exhibit better

**TABLE 1.8** A polyoxometalate with an organic/inorganic hybrid as a heterogeneous catalyst.

Classification	Example	Catalysis
3D crystal	$(\text{Pyridinium}) \times \text{PMo}_{12}\text{O}_{40}$	Selective oxidation of alkanes in gas phase
	$(\text{Pyridinium}) \times \text{NbPMo}_{11}\text{VO}_{40}$	Selective oxidation of alkanes in gas phase
	$[1, 1' - (\text{Butane} - 1, 4 - \text{diyl}) - \text{bis}(3 - \text{methylimidazolium})]_{2.5} \text{PMo}_{12}\text{O}_{40}$	Oxidation of benzene with hydrogen peroxide to phenol
	$[1 - \text{Butyl} - 3 - \text{methylimidazolium}]_3 \text{PW}_{12}\text{O}_{40}$	Azlactones Erlenmeyer synthesis
	$[\text{Cu}(\text{ethylenediamine})_2]_{1.5} [\text{Cu}(\text{ethylenediamine})(2, 2' - \text{bipyridine})(\text{H}_2\text{O})_n] \text{Ce}[(\alpha - \text{PW}_{11}\text{O}_{39})_2]$	Photocatalytic decomposition of rhodamine-B
Encapsulated	$\text{PW}_4\text{O}_{24}/[\text{Fe}_3\text{O}(\text{H}_2\text{O})_2(\text{F})\{\text{C}_6\text{H}_3(\text{CO}_2)_3\}_2 \cdot n\text{H}_2\text{O} (n = 14.5)]$	Epoxidation of olefins with hydrogen peroxide
	$\text{PW}_{11}\text{TiO}_{40}/[\text{Fe}_3\text{O}(\text{H}_2\text{O})_2(\text{F})\{\text{C}_6\text{H}_3(\text{CO}_2)_3\}_2 \cdot n\text{H}_2\text{O} (n = 14.5)]$	Oxidation of cyclohexane, $\alpha$ -pinene, and caryophyllene with oxygen gas and hydrogen peroxide in liquid-phase
	$\text{PW}_{12}\text{O}_{40}/[\text{Cr}_3\text{O}(\text{H}_2\text{O})_2(\text{F})\{\text{C}_6\text{H}_3(\text{CO}_2)_3\}_2 \cdot n\text{H}_2\text{O} (n = 14.5)]$	Selective dehydration of fructose and glucose to 5-hydroxymethylfurfural
	$\text{PW}_{12}\text{O}_{40}/[\text{Cr}_3\text{O}(\text{H}_2\text{O})_2(\text{F})\{\text{C}_6\text{H}_3(\text{CO}_2)_3\}_2 \cdot n\text{H}_2\text{O} (n = 14.5)]$	Knoevenagel condensation, esterification of acetic acid and <i>n</i> -butanol
	$\{[\text{Cu}_2(4, 4' - \text{bipy})_4(\text{H}_2\text{O})_4](\text{SiW}_{12}\text{O}_{40})(\text{H}_2\text{O})_{18}\}_n$	Selective oxidation of ethylbenzene with TBHP
	$\{[\text{Ho}_4(\text{dpdo})_8(\text{H}_2\text{O})_{16}\text{BW}_{12}\text{O}_{40}]_3 \cdot 2\text{H}_2\text{O}\}(\text{BW}_{12}\text{O}_{40})_2 \cdot (\text{H}_{1.5}\text{pz})_2 \cdot (\text{H}_2\text{O})_{11}$	Catalytic phosphodiester bond cleavage of bis(4-nitrophenyl) phosphate
	$[\text{Cu}_3(\text{C}_9\text{H}_3\text{O}_6)_2]_4 \{[(\text{CH}_3)_4\text{N}]_4\text{CuPW}_{11}\text{O}_{39}\text{H}\}_3 \cdot 40 - \text{H}_2\text{O}$	Aerobic oxidation of $\text{H}_2\text{S}$ to $\text{S}_8$
	$\text{H}_3\text{PW}_{12}\text{O}_{40}/\text{Cu}_3(\text{benzene tricarboxylic acid})_2$	Acid-catalyzed esterification

Continued

**TABLE 1.8** A polyoxometalate with an organic/inorganic hybrid as a heterogeneous catalyst—cont'd

Classification	Example	Catalysis
	$[\text{Cu}_2(1,3,5\text{-benzenetricarboxylate})_{4/3}(\text{H}_2\text{O})_2]_6[\text{H}_2\text{SiW}_{12}\text{O}_{40}] \cdot (\text{C}_4\text{H}_{12}\text{N})_2$	Dehydration of methanol to DME, formation of ethyl acetate from acetic acid and ethylene
	$\text{H}_3[(\text{Cu}_4\text{Cl})_3(1,3,5\text{-benzenetricarboxylate})_8]_2 - [\text{PW}_{12}\text{O}_{40}] \cdot (\text{C}_4\text{H}_{12}\text{N})_6 \cdot 3\text{H}_2\text{O}$	Adsorption and decomposition of dimethyl methylphosphonate
	$[\text{Cu}_2(1,3,5\text{-benzenetricarboxylate})_{4/3}(\text{H}_2\text{O})_2]_6[\text{HnXM}_{12}\text{O}_{40}] (\text{C}_4\text{H}_{12}\text{N})_2$ (X = Si, Ge, P, As; M = W, Mo)	Heterogeneous catalytic hydrolysis of esters in excess water
	$[\text{Cu}_5(\text{pyrazine})_6\text{Cl}][\text{HPMo}_{12}\text{O}_{40}]$	Photocatalytic decomposition of rhodamine-B
	$\text{H}\{\{\text{Ce}(\text{H}_2\text{O})_5\}_2\{\text{Ce}(\text{pyridine}-2,6\text{-dicarboxylate})_2(\text{H}_2\text{O})_4\}\{\text{Ce}(\text{pyridine}-2,6\text{-dicarboxylate})_3\}(\text{PW}_{12}\text{O}_{40})\}_2\text{H}_2\text{O}$	Photocatalytic $\text{H}_2$ evolution under UV irradiation
Linked	$(\text{Tetrabutylammonium})_3[\text{PMo}^{\text{V}}_8\text{Mo}^{\text{VI}}_4\text{O}_{36}(\text{OH})_4\text{Zn}_4][\text{C}_6\text{H}_3(\text{COO})_3]_{4/3} \cdot 36\text{H}_2\text{O}$	Electrocatalytic hydrogen evolution reaction
	$\text{Tb}[\text{V}_6\text{O}_{13}\{(\text{OCH}_2)_3\text{C}(\text{NH}_2\text{CH}_2\text{C}_6\text{H}_4-4-\text{CO}_2)\}\{(\text{OCH}_2)_3\text{C}-(\text{NHCH}_2\text{C}_6\text{H}_4-4-\text{CO}_2)\}_2]$	Aerobic oxidation of PrSH
Dendritic	$\text{Tris}[2\text{-(trimethylammonium)ethyl}]-1,3,5\text{-benzenetricarboxylate}-[\text{ZnWZn}_2(\text{H}_2\text{O})_2(\text{ZnW}_9\text{O}_{34})_2]$	Epoxidation of primary allylic alcohols with $\text{H}_2\text{O}_2$
	$\text{Benzene-1,3,5-[tris(phenyl-4-carboxylic acid)] tris(2-trimethyl-ammonium ethyl) ester}-[\text{PW}_{11}\text{O}_{39}]$	Epoxidation of olefins with hydrogen peroxide
	Dendritic polyammonium hexa $\text{PW}_{12}\text{O}_{40}$	Epoxidation of olefins with hydrogen peroxide



catalytic activity and reusability in comparison with simple organic ammonium polyoxometalate. When tripodal branched organic polyammonium salts were utilized for the synthesis of  $[(WZnZn_2(H_2O)_2)_2] \cdot [(ZnW_9O_{34})_2]$  catalysts, the obtained dendritic hybrid materials formed three-dimensional, amorphous, coral-shaped, perforated materials with mesopores, which were capable of catalyzing the epoxidation of allyl alcohol with hydrogen peroxide in a highly effective and selective manner [208].

Type C is related to the encapsulated polyoxometalate in a three-dimensional organic framework, while it is encapsulated in a layered framework in type D. The polyoxometalate can be introduced into the organic framework step by step [209] or else the polyoxometalate can be encapsulated via a one-step self-assembling procedure. In the latter, the polyoxometalate is sometimes considered as a template to shape the organic framework [210]. The host framework encapsulates a polyoxometalate must meet the following criteria to prove adequate in heterogeneous catalysis:

- (1) appropriate cavities with the suitable shape and size to encapsulate one polyoxometalate molecule in each cavity—this allows the dispersion of polyoxometalates at a molecular level;
- (2) appropriate openings that allow for the reactant and product diffusion;
- (3) a balance between the hydrophilicity and hydrophobicity for accessing the reactant and releasing the product during the catalysis process; and
- (4) a framework of enough stability and integrity capable of keeping the heterogeneous catalytic function [211].

By taking the above criteria into account in the design and synthesis of hybrid materials of this type, a wide variety of polyoxometalate-encapsulated hybrid materials have been synthesized among which metal-organic frameworks (MOFs) have been widely utilized and successfully offered a novel type of heterogeneous catalysts (Table 1.7). The most outstanding examples of this type would be  $[Cu_2(BTC)_{4/3}(H_2O)_2]_6[HnXM_{12}O_{40}] \cdot (C_4H_{12}N)_2$  ( $X = Si, Ge, P, As$ ;  $M = W, Mo$ ), which are achievable from a simple, one-step hydrothermal reaction, and exhibited proper heterogeneous acid catalysis with pore-size dependency as illustrated in Fig. 1.24 [211]. The catalyst is readily recovered from the aqueous solution by filtration. The metal-organic framework prevents from the conglomeration of  $H_3PW_{12}O_{40}$  so that was reusable without any significant loss of activity. Types E and F are the most advanced one given their high dimensionality in structure. The difference between Types C and D and Types E and F is in the location of the polyoxometalate within the framework; in the former types, the polyoxometalate is located inside the framework cavity while in the latter, the polyoxometalate is linked to linkers to form cavity. Therefore, these types of polyoxometalate hybrid form a new family of zeolitic MOF, denoted by Z-POMOFs. Two strategies have been proposed for the design and synthesis of Z-POMOFs. One is the POM-metal-ligand-metal-POM linkage, in which the polyoxometalate is first capped with a transition metal cation; then it is linked

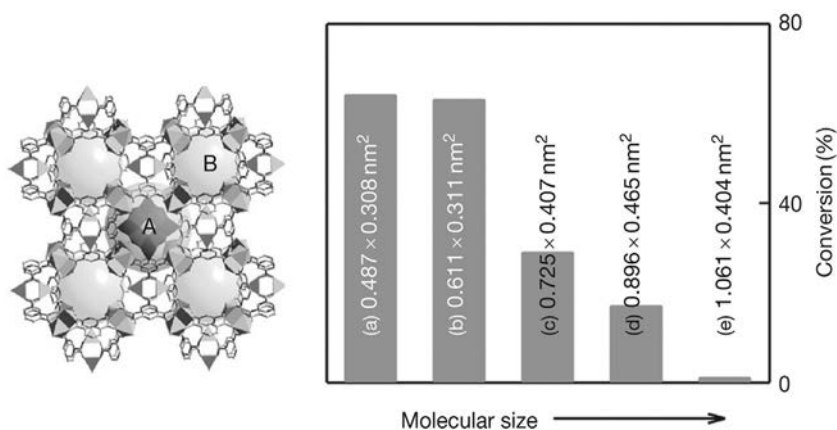


**FIG. 1.24** *Left:* crystalline structure of  $\text{H}_3\text{PW}_{12}\text{O}_{40}$ -copper-nitrate-benzene tricarboxylate complex with pore A that accommodates the Keggin polyanion and open pore B, and its size-selective catalysis for the hydrolysis of esters. *Right:* (a) methyl acetate, (b) ethyl acetate, (c) methyl benzoate, (d) ethyl benzoate, and (e) 4-methyl-phenyl propionate [200].

with an organic ligand through the metal cation. The second strategy is the POM-ligand-metal-ligand-POM linkage in which the polyoxometalate is first covalently bonded to an organic ligand and then they are linked to each other through transition metal cations [212]. The POM-ligand connection is achieved by replacing the terminal oxo ligands with ligands such as nitride, imido, hydrazido, etc. or by forming organosilyl, organotin, or organophosphoryl derivatives of lacunary polyoxometalate clusters. These species do not have many applications as heterogeneous catalysts. Nevertheless, a study evidently revealed the high electrocatalytic property of Z-POMOF for the of reaction hydrogen evolution which is attributable to the Z-POMOF structure and also to the confinement effect [213]. This exceptional feature is capable of promoting the synthesis of many more types of Z-POMOF for the creation of new efficient heterogeneous catalysts based on the Z-POMF structure.

### 1.17. Various morphological states

As noted earlier, supramolecular self-assembling into materials with three-dimensional hybrid structures is driven by covalent interactions between the polyoxometalate and other building blocks; however, noncovalent interactions (i.e., hydrogen bonding, p-p stacking, van der Waals forces, and electrostatic interactions) occur in a complicated fashion to create unanticipated shapes in the resulting solids. That is to say, organic substances, which are utilized for the synthesis of organic/inorganic hybrid materials, not only influence the structures at a molecular level but also affect the particle morphology of the obtained substances. The morphological shapes of the heterogeneous solid-state catalysts frequently influence the catalytic properties, mostly due to the



incoherence between the surface structure and bulk structure of the solid state catalyst. Morphological shapes of the POM-based hybrid materials principally have reduced effects on their catalytic activity as molecularity of polyoxometalate is retained even on the surface of the hybrid materials because of the supramolecular self-assembling. However, nanomorphology architecture in hybrid polyoxometalate systems is important in the construction of artificial cells, nano-sized compartments, nanomembranes, and nanoreactors, all of which result in an additional structural dimension [214].

## References

- [1] J.J. Berzelius, Considerations respecting a new power which acts in the formation of organic bodies, *Edinb. New Philos. J.* 21 (1836) 223–228.
- [2] G. Shaw, *The Direct Synthesis of Hydrogen Peroxide Using Bimetallic, Gold and Palladium, Supported Catalysts*, Doctoral dissertation, Cardiff University, 2013.
- [3] K. Yan, T. Lafleur, J. Liao, Facile synthesis of palladium nanoparticles supported on multi-walled carbon nanotube for efficient hydrogenation of biomass-derived levulinic acid, *J. Nanopart. Res.* 15 (9) (2013) 1–7.
- [4] Y. Qiao, H. Li, L. Hua, L. Orzechowski, K. Yan, B. Feng, Z. Hou, Peroxometalates immobilized on magnetically recoverable catalysts for epoxidation, *ChemPlusChem* 77 (12) (2012) 1128–1138.
- [5] K. Yan, C. Jarvis, T. Lafleur, Y. Qiao, X. Xie, Novel synthesis of Pd nanoparticles for hydrogenation of biomass-derived platform chemicals showing enhanced catalytic performance, *RSC Adv.* 3 (48) (2013) 25865–25871.
- [6] Z. Cao, H. Jiang, H. Luo, S. Baumann, W.A. Meulenberg, H. Voss, J. Caro, Simultaneous overcome of the equilibrium limitations in BSCF oxygen-permeable membrane reactors: water splitting and methane coupling, *Catal. Today* 193 (1) (2012) 2–7.
- [7] K. Yan, T. Lafleur, G. Wu, J. Liao, C. Ceng, X. Xie, Highly selective production of value-added  $\gamma$ -valerolactone from biomass-derived levulinic acid using the robust Pd nanoparticles, *Appl. Catal. A Gen.* 468 (2013) 52–58.
- [8] S.B. Singh, P.K. Tandon, Catalysis: a brief review on nano-catalyst, *J. Energy Chem. Eng.* 2 (3) (2014) 106–115.
- [9] K. Yan, G. Wu, J. Wen, A. Chen, One-step synthesis of mesoporous H<sub>4</sub>SiW<sub>12</sub>O<sub>40</sub>-SiO<sub>2</sub> catalysts for the production of methyl and ethyl levulinate biodiesel, *Catal. Commun.* 34 (2013) 58–63.
- [10] S.L. Candelaria, Y. Shao, W. Zhou, X. Li, J. Xiao, J.G. Zhang, G. Cao, Nanostructured carbon for energy storage and conversion, *Nano Energy* 1 (2) (2012) 195–220.
- [11] K. Yan, A. Chen, Efficient hydrogenation of biomass-derived furfural and levulinic acid on the facilely synthesized noble-metal-free Cu–Cr catalyst, *Energy* 58 (2013) 357–363.
- [12] H. Luo, T. Klimczuk, L. MÜchler, L. Schoop, D. Hirai, M.K. Fuccillo, R.J. Cava, Superconductivity in the Cu (Ir 1– x Pt x) 2 Se 4 spinel, *Phys. Rev. B* 87 (21) (2013), 214510.
- [13] K. Yan, T. Lafleur, C. Jarvis, G. Wu, Clean and selective production of  $\gamma$ -valerolactone from biomass-derived levulinic acid catalyzed by recyclable Pd nanoparticle catalyst, *J. Clean. Prod.* 72 (2014) 230–232.
- [14] B.R. Cuenya, Synthesis and catalytic properties of metal nanoparticles: size, shape, support, composition, and oxidation state effects, *Thin Solid Films* 518 (12) (2010) 3127–3150.
- [15] M. Bowker, *The basis and applications of heterogeneous catalysis*, *Oxf. Chem. Prim.* 53 (1) (1998). ALL-ALL.

- [16] D.L. Long, R. Tsunashima, L. Cronin, Polyoxometalates: building blocks for functional nanoscale systems, *Angew. Chem. Int. Ed.* 49 (10) (2010) 1736–1758.
- [17] S. Liu, Z. Tang, Polyoxometalate-based functional nanostructured films: current progress and future prospects, *Nano Today* 5 (4) (2010) 267–281.
- [18] C.L. Hill, Introduction: polyoxometalates multicomponent molecular vehicles to probe fundamental issues and practical problems, *Chem. Rev.* 98 (1) (1998) 1–2.
- [19] I.V. Kozhevnikov, Catalysis by heteropoly acids and multicomponent polyoxometalates in liquid-phase reactions, *Chem. Rev.* 98 (1) (1998) 171–198.
- [20] N. Mizuno, M. Misono, Heterogeneous catalysis, *Chem. Rev.* 98 (1) (1998) 199–218.
- [21] M. Sadakane, E. Steckhan, Electrochemical properties of polyoxometalates as electrocatalysts, *Chem. Rev.* 98 (1) (1998) 219–238.
- [22] I. Kozhevnikov, *Catalysts for Fine Chemical Synthesis, Catalysis by Polyoxometalates*, vol. 2, Wiley, 2002.
- [23] N. Mizuno (Ed.), *Modern Heterogeneous Oxidation Catalysis: Design, Reactions and Characterization*, John Wiley & Sons, 2009.
- [24] A. Müller, F. Peters, M.T. Pope, D. Gatteschi, Polyoxometalates: very large clusters-nanoscale magnets, *Chem. Rev.* 98 (1) (1998).
- [25] T. Yamase, Photo- and electrochromism of polyoxometalates and related materials, *Chem. Rev.* 98 (1) (1998) 307–325.
- [26] E. Coronado, C.J. Gómez-García, Polyoxometalate-based molecular materials, *Chem. Rev.* 98 (1) (1998) 273–296.
- [27] J.T. Rhule, C.L. Hill, D.A. Judd, R.F. Schinazi, Polyoxometalates in medicine, *Chem. Rev.* 98 (1) (1998) 327–358.
- [28] M.T. Pope, Heteropoly and isopoly oxometalates, in: *Inorganic Chemistry Concepts*, vol. 8, 1983.
- [29] B. Botar, A. Ellern, R. Hermann, P. Kögerler, Electronic control of spin coupling in keplerate-type polyoxomolybdates, *Angew. Chem. Int. Ed.* 48 (48) (2009) 9080–9083.
- [30] P.T. Anastas, J.C. Warner, Principles of green chemistry, in: *Green Chemistry: Theory and Practice*, 1998, pp. 29–56.
- [31] R. Noyori, Pursuing practical elegance in chemical synthesis, *Chem. Commun.* 14 (2005) 1807–1811.
- [32] M. Misono, 76th National Meeting of Chem. Soc. Japan, 1999.
- [33] J.H. Clark, Green chemistry: challenges and opportunities, *Green Chem.* 1 (1) (1999) 1–8.
- [34] (a) T. Okuhara, N. Mizuno, M. Misono, Catalytic chemistry of heteropoly compounds, *Adv. Catal.* 41 (1996) 113–252. (b) N. Mizuno, M. Misono, Heterogeneous catalysis, *Chem. Rev.* 98 (1) (1998) 199–218.
- [35] (a) M. Misono, N. Nojiri, Recent progress in catalytic technology in Japan, *Appl. Catal.* 64 (1990) 1–30. (b) M.N. Timofeeva, Acid catalysis by heteropoly acids, *Appl. Catal. A Gen.* 256 (1-2) (2003) 19–35.
- [36] Á. Molnár, T. Beregszászi, Mild and efficient tetrahydropyranlation and deprotection of alcohols catalyzed by heteropoly acids, *Tetrahedron Lett.* 37 (47) (1996) 8597–8600.
- [37] (a) T. Okuhara, N. Mizuno, M. Misono, Catalytic chemistry of heteropoly compounds, *Adv. Catal.* 41 (1996) 113–252. (b) N. Mizuno, M. Misono, Heterogeneous catalysis, *Chem. Rev.* 98 (1) (1998) 199–218.
- [38] S. Namba, N. Hosonuma, T. Yashima, Catalytic application of hydrophobic properties of high-silica zeolites: I. Hydrolysis of ethyl acetate in aqueous solution, *J. Catal.* 72 (1) (1981) 16–20.
- [39] S. Nakato, M. Kimura, T. Okuhara, Water-tolerant solid acid catalysis of  $\text{Cs}_{2.5}\text{H}_0.5\text{PW}_{12}\text{O}_{40}$  for hydration of olefins, *Chem. Lett.* (1997) 389.

- [40] M. Kimura, T. Nakato, T. Okuhara, Water-tolerant solid acid catalysis of Cs<sub>2</sub>. 5H<sub>2</sub>O. 5PW12O<sub>40</sub> for hydrolysis of esters in the presence of excess water, *Appl. Catal. A Gen.* 165 (1-2) (1997) 227–240.
- [41] T. Nakato, M. Kimura, S.I. Nakata, T. Okuhara, Changes of surface properties and water-tolerant catalytic activity of solid acid Cs<sub>2</sub>. 5H<sub>2</sub>O. 5PW12O<sub>40</sub> in water, *Langmuir* 14 (2) (1998) 319–325.
- [42] (a) M. Misono, Heterogeneous catalysis by heteropoly compounds of molybdenum and tungsten, *Catal. Rev. Sci. Eng.* 29 (2-3) (1987) 269–321. (b) M. Misono, Errata and Addenda, *Catal. Rev. Sci. Eng.* 30 (1988) 339–340.
- [43] Y. Toyoshi, T. Nakato, T. Okuhara, Zeolite, clay, and heteropolyacids in organic reactions zeolite, clay, and heteropolyacids in organic reactions, 1992, *Bull. Chem. Soc. Jpn.* 71 (12) (1998) 2817–2824.
- [44] K.I. Sano, H. Uchida, S. Wakabayashi, A new process for acetic acid production by direct oxidation of ethylene, *Catal. Surv. Jpn.* 3 (1) (1999) 55–60.
- [45] M. Misono, Acid catalysts for clean production. Green aspects of heteropolyacid catalysts, *C.R. Acad. Sci., Ser. IIC: Chim.* 3 (6) (2000) 471–475.
- [46] A. Aoshima, S. Tonomura, S. Yamamatsu, New synthetic route of polyoxytetramethyleneglycol by use of heteropolyacids as catalyst, *Polym. Adv. Technol.* 1 (2) (1990) 127–132.
- [47] L. Frattini, Polyoxometalates as Solid Acid Catalysts for Sustainable Chemistry, Doctoral dissertation, Aston University, 2017.
- [48] M. Misono, I. Ono, G. Koyano, A. Aoshima, Special Topic Issue on Green Chemistry, *Pure Appl. Chem.* 72 (7) (2000) 1305–1311.
- [49] M. Misono, Unique acid catalysis of heteropoly compounds (heteropolyoxometalates) in the solid state, *Chem. Commun.* 13 (2001) 1141–1152.
- [50] S. Shikata, T. Okuhara, M. Misono, Catalysis by heteropoly compounds. Part XXVI. Gas phase synthesis of methyl tert-butyl ether over heteropolyacids, *J. Mol. Catal. A Chem.* 100 (1-3) (1995) 49–59.
- [51] K. Weissmermel, H.J. Arpe, *Industrial Organic Chemistry*, John Wiley & Sons, 2008.
- [52] M. Misono, N. Nojiri, Recent progress in catalytic technology in Japan, *Appl. Catal.* 64 (1990) 1–30.
- [53] Y. Izumi, Hydration/hydrolysis by solid acids, *Catal. Today* 33 (4) (1997) 371–409.
- [54] Y. Izumi, K. Urabe, M. Onaka, Zeolite, Clay, and Heteropoly Acid in Organic Reactions, Kodansha/VCH, Tokyo, 1992.
- [55] J.N. Armor, New catalytic technology commercialized in the USA during the 1990s, *Appl. Catal. A Gen.* 222 (1-2) (2001) 407–426.
- [56] M.J. Howard, G.J. Sunley, A.D. Poole, R.J. Watt, B.K. Sharma, New acetyls technologies from BP chemicals, in: *Studies in Surface Science and Catalysis*, vol. 121, Elsevier, 1999, pp. 61–68.
- [57] I.V. Kozhevnikov, Sustainable heterogeneous acid catalysis by heteropoly acids, *J. Mol. Catal. A Chem.* 262 (1-2) (2007) 86–92.
- [58] S. Shinachi, M. Matsushita, K. Yamaguchi, N. Mizuno, Oxidation of adamantane with 1 atm molecular oxygen by vanadium-substituted polyoxometalates, *J. Catal.* 233 (1) (2005) 81–89.
- [59] J.E. Molinari, L. Nakka, T. Kim, I.E. Wachs, Dynamic surface structures and reactivity of vanadium-containing molybdophosphoric acid (H<sub>3</sub>+ x PMo<sub>12</sub>-x V x O<sub>40</sub>) keggin catalysts during methanol oxidation and dehydration, *ACS Catal.* 1 (11) (2011) 1536–1548.
- [60] C. Knapp, T. Ui, K. Nagai, N. Mizuno, Stability of iron in the Keggin anion of heteropoly acid catalysts for selective oxidation of isobutane, *Catal. Today* 71 (1-2) (2001) 111–119.

- [61] K. Kamata, K. Yamaguchi, S. Hikichi, N. Mizuno,  $[\{W(O)(O_2)_2(H_2O)\}_2(\mu-O)]_2$ -catalyzed epoxidation of allylic alcohols in water with high selectivity and utilization of hydrogen peroxide, *Adv. Synth. Catal.* 345 (11) (2003) 1193–1196.
- [62] D. Sloboda-Rozner, P. Witte, P.L. Alsters, R. Neumann, Aqueous biphasic oxidation: a water-soluble polyoxometalate catalyst for selective oxidation of various functional groups with hydrogen peroxide, *Adv. Synth. Catal.* 346 (2-3) (2004) 339–345.
- [63] B. Botar, Y.V. Geletii, P. Kögerler, D.G. Musaev, K. Morokuma, I.A. Weinstock, C.L. Hill, The true nature of the di-iron (III)  $\gamma$ -Keggin structure in water: catalytic aerobic oxidation and chemistry of an unsymmetrical trimer, *J. Am. Chem. Soc.* 128 (34) (2006) 11268–11277.
- [64] A. Haimov, R. Neumann, An example of Lipophilselectivity: the preferred oxidation, in water, of hydrophobic 2-alkanols catalyzed by a cross-linked polyethyleneimine-polyoxometalate catalyst assembly, *J. Am. Chem. Soc.* 128 (49) (2006) 15697–15700.
- [65] A. Rezaeifard, R. Haddad, M. Jafarpour, M. Hakimi, Catalytic epoxidation activity of keplerate polyoxomolybdate nanoball toward aqueous suspension of olefins under mild aerobic conditions, *J. Am. Chem. Soc.* 135 (27) (2013) 10036–10039.
- [66] M. Carraro, N. Nsouli, H. Oelrich, A. Sartorel, A. Sorarù, S.S. Mal, M. Bonchio, Reactive ZrIV and HfIV butterfly peroxides on polyoxometalate surfaces: bridging the gap between homogeneous and heterogeneous catalysis, *Chem. Eur. J.* 17 (30) (2011) 8371–8378.
- [67] S.S. Mal, N.H. Nsouli, M. Carraro, A. Sartorel, G. Scorrano, H. Oelrich, U. Kortz, Peroxo-Zr/Hf-containing undecatungstosilicates and-germanates, *Inorg. Chem.* 49 (1) (2010) 7–9.
- [68] Y. Ding, W. Zhao, W. Song, Z. Zhang, B. Ma, Mild and recyclable catalytic oxidation of pyridines to N-oxides with  $H_2O_2$  in water mediated by a vanadium-substituted polyoxometalate, *Green Chem.* 13 (6) (2011) 1486–1489.
- [69] H. Lv, Y.V. Geletii, C. Zhao, J.W. Vickers, G. Zhu, Z. Luo, C.L. Hill, Polyoxometalate water oxidation catalysts and the production of green fuel, *Chem. Soc. Rev.* 41 (22) (2012) 7572–7589.
- [70] N. Mizuno, K. Kamata, Catalytic oxidation of hydrocarbons with hydrogen peroxide by vanadium-based polyoxometalates, *Coord. Chem. Rev.* 255 (19–20) (2011) 2358–2370.
- [71] Y. Guo, C. Hu, Heterogeneous photocatalysis by solid polyoxometalates, *J. Mol. Catal. A Chem.* 262 (1-2) (2007) 136–148.
- [72] E. Papaconstantinou, Photochemistry of polyoxometallates of molybdenum and tungsten and/or vanadium, *Chem. Soc. Rev.* 18 (1989) 1–31.
- [73] M. Bonchio, M. Carraro, G. Scorrano, E. Fontananova, E. Drioli, Heterogeneous photooxidation of alcohols in water by photocatalytic membranes incorporating decatungstate, *Adv. Synth. Catal.* 345 (9-10) (2003) 1119–1126.
- [74] S. Farhadi, M. Afshari, M. Maleki, Z. Babazadeh, Photocatalytic oxidation of primary and secondary benzylic alcohols to carbonyl compounds catalyzed by H3PW12O40/SiO2 under an O2 atmosphere, *Tetrahedron Lett.* 46 (49) (2005) 8483–8486.
- [75] A. Troupis, A. Hiskia, E. Papaconstantinou, Synthesis of metal nanoparticles by using polyoxometalates as photocatalysts and stabilizers, *Angew. Chem. Int. Ed.* 41 (11) (2002) 1911–1914.
- [76] M. Schulz, C. Paulik, G. Knör, Studies on the selective two-electron photo-oxidation of benzene to phenol using polyoxometalates, water and simulated solar radiation, *J. Mol. Catal. A Chem.* 347 (1-2) (2011) 60–64.
- [77] M. Bonchio, M. Carraro, G. Scorrano, A. Bagno, Photooxidation in water by new hybrid molecular photocatalysts integrating an organic sensitizer with a polyoxometalate core, *Adv. Synth. Catal.* 346 (6) (2004) 648–654.
- [78] A. Molinari, G. Varani, E. Polo, S. Vaccari, A. Maldotti, Photocatalytic and catalytic activity of heterogenized W10O324– in the bromide-assisted bromination of arenes and alkenes in the presence of oxygen, *J. Mol. Catal. A Chem.* 262 (1-2) (2007) 156–163.

- [79] A.M. Khenkin, I. Efremenko, L. Weiner, J.M. Martin, R. Neumann, Photochemical reduction of carbon dioxide catalyzed by a ruthenium-substituted polyoxometalate, *Chem. Eur. J.* 16 (2010) 1356–1364.
- [80] J. Etedgui, Y. Diskin-Posner, L. Weiner, R. Neumann, Photoreduction of carbon dioxide to carbon monoxide with hydrogen catalyzed by a rhenium (I) phenanthroline– polyoxometalate hybrid complex, *J. Am. Chem. Soc.* 133 (2) (2011) 188–190.
- [81] R.R. Ozer, J.L. Ferry, Photocatalytic oxidation of aqueous 1, 2-dichlorobenzene by polyoxometalates supported on the NaY zeolite, *J. Phys. Chem. B* 106 (16) (2002) 4336–4342.
- [82] S. Gao, R. Cao, J. Lü, G. Li, Y. Li, H. Yang, Photocatalytic properties of polyoxometalate–thionine composite films immobilized onto microspheres under sunlight irradiation, *J. Mater. Chem.* 19 (24) (2009) 4157–4163.
- [83] Z. Fu, Y. Zeng, X. Liu, D. Song, S. Liao, J. Dai, Copper based metal–organic molecular ring with inserted Keggin-type polyoxometalate: a stable photofunctional host–guest molecular system, *Chem. Commun.* 48 (49) (2012) 6154–6156.
- [84] Y.H. Guo, Y.H. Wang, C.W. Hu, Y.H. Wang, E.B. Wang, Y.C. Zhou, S.H. Feng, Microporous polyoxometalates POMs/SiO<sub>2</sub>: synthesis and photocatalytic degradation of aqueous organochlorine pesticides, *Chem. Mater.* 12 (2000) 3501–3508.
- [85] H. Yang, T. Liu, M. Cao, H. Li, S. Gao, R. Cao, A water-insoluble and visible light induced polyoxometalate-based photocatalyst, *Chem. Commun.* 46 (14) (2010) 2429–2431.
- [86] R.N. Biboum, F. Doungmene, B. Keita, P. de Oliveira, L. Nadjo, B. Lepoittevin, R. Contant, Poly (ionic liquid) and macrocyclic polyoxometalate ionic self-assemblies: new water-insoluble and visible light photosensitive catalysts, *J. Mater. Chem.* 22 (2) (2012) 319–323.
- [87] P. Lei, C. Chen, J. Yang, W. Ma, J. Zhao, L. Zang, Degradation of dye pollutants by immobilized polyoxometalate with H<sub>2</sub>O<sub>2</sub> under visible-light irradiation, *Environ. Sci. Technol.* 39 (21) (2005) 8466–8474.
- [88] B. Yue, Y. Zhou, J. Xu, Z. Wu, X. Zhang, Y. Zou, S. Jin, Photocatalytic degradation of aqueous 4-chlorophenol by silica-immobilized polyoxometalates, *Environ. Sci. Technol.* 36 (6) (2002) 1325–1329.
- [89] A. Dolbecq, P. Mialane, B. Keita, L. Nadjo, Polyoxometalate-based materials for efficient solar and visible light harvesting: application to the photocatalytic degradation of azo dyes, *J. Mater. Chem.* 22 (47) (2012) 24509–24521.
- [90] J. Tucher, Y. Wu, L.C. Nye, I. Ivanovic-Burmazovic, M.M. Khusniyarov, C. Streb, Metal substitution in a Lindqvist polyoxometalate leads to improved photocatalytic performance, *Dalton Trans.* 41 (33) (2012) 9938–9943.
- [91] J.A. Rengifo-Herrera, M.N. Blanco, L.R. Pizzio, Photocatalytic bleaching of aqueous malachite green solutions by UV-A and blue-light-illuminated TiO<sub>2</sub> spherical nanoparticles modified with tungstophosphoric acid, *Appl. Catal. B Environ.* 110 (2011) 126–132.
- [92] A. Troupis, A. Hiskia, E. Papaconstantinou, Photocatalytic reduction and recovery of copper by polyoxometalates, *Environ. Sci. Technol.* 36 (24) (2002) 5355–5362.
- [93] C. Streb, New trends in polyoxometalate photoredox chemistry: from photosensitisation to water oxidation catalysis, *Dalton Trans.* 41 (6) (2012) 1651–1659.
- [94] K. Li, X. Yang, Y. Guo, F. Ma, H. Li, L. Chen, Y. Guo, Design of mesostructured H<sub>3</sub>PW<sub>12</sub>O<sub>40</sub>–titaniamaterials with controllable structural orderings and pore geometries and their simulated sunlight photocatalytic activity towards diethyl phthalate degradation, *Appl. Catal. B: Environ.* 99 (1–2) (2010) 364–375.
- [95] D. Li, Y. Guo, C. Hu, C. Jiang, E. Wang, Preparation, characterization and photocatalytic property of the PW11O397–TiO<sub>2</sub> composite film towards azo-dye degradation, *J. Mol. Catal. A Chem.* 207 (2) (2004) 183–193.

- [96] Y. Yang, Q. Wu, Y. Guo, C. Hu, E. Wang, Efficient degradation of dye pollutants on nanoporous polyoxotungstate–anatase composite under visible-light irradiation, *J. Mol. Catal. A Chem.* 225 (2) (2005) 203–212.
- [97] S. Zhang, L. Chen, H. Liu, W. Guo, Y. Yang, Y. Guo, M. Huo, Design of H3PW12O40/TiO2 and Ag/H3PW12O40/TiO2 film-coated optical fiber photoreactor for the degradation of aqueous rhodamine B and 4-nitrophenol under simulated sunlight irradiation, *Chem. Eng. J.* 200 (2012) 300–309.
- [98] L. Li, Q.Y. Wu, Y.H. Guo, C.W. Hu, Nanosize and bimodal porous polyoxotungstate–anatase TiO2 composites: preparation and photocatalytic degradation of organophosphorus pesticide using visible-light excitation, *Microporous Mesoporous Mater.* 87 (2005) 1.
- [99] D.F. Li, Y.H. Guo, C.W. Hu, L. Mao, E. Wang, *Appl. Catal. A Gen.* 235 (2002) 11.
- [100] Y. Guo, C. Hu, S. Jiang, C. Guo, Y. Yang, E. Wang, Heterogeneous photodegradation of aqueous hydroxy butanedioic acid by microporous polyoxometalates, *Appl. Catal. B Environ.* 36 (1) (2002) 9–17.
- [101] Y. Guo, C. Hu, X. Wang, Y. Wang, E. Wang, Y. Zou, S. Feng, Microporous decatungstates: synthesis and photochemical behavior, *Chem. Mater.* 13 (11) (2001) 4058–4064.
- [102] Y. Guo, C. Hu, C. Jiang, Y. Yang, S. Jiang, X. Li, E. Wang, Preparation and heterogeneous photocatalytic behaviors of the surface-modified porous silica materials impregnated with monosubstituted keggin units, *J. Catal.* 217 (1) (2003) 141–151.
- [103] Y. Guo, Y. Yang, C. Hu, C. Guo, E. Wang, Y. Zou, S. Feng, Preparation, characterization and photochemical properties of ordered macroporous hybrid silica materials based on monovalent Keggin-type polyoxometalates, *J. Mater. Chem.* 12 (10) (2002) 3046–3052.
- [104] S. Farhadi, M. Zaidi, Polyoxometalate–zirconia (POM/ZrO2) nanocomposite prepared by sol-gel process: a green and recyclable photocatalyst for efficient and selective aerobic oxidation of alcohols into aldehydes and ketones, *Appl. Catal. A Gen.* 354 (1-2) (2009) 119–126.
- [105] X. Qu, Y. Guo, C. Hu, Preparation and heterogeneous photocatalytic activity of mesoporous H3PW12O40/ZrO2 composites, *J. Mol. Catal. A Chem.* 262 (1-2) (2007) 128–135.
- [106] Y. Yang, Y. Guo, C. Hu, E. Wang, Lacunary Keggin-type polyoxometalates-based macroporous composite films: preparation and photocatalytic activity, *Appl. Catal. A Gen.* 252 (2) (2003) 305–314.
- [107] Y. Yang, Y. Guo, C. Hu, C. Jiang, E. Wang, Synergistic effect of Keggin-type [X n+ W 11 O 39](12– n)– and TiO 2 in macroporous hybrid materials [X n+ W 11 O 39](12– n)–TiO 2 for the photocatalytic degradation of textile dyes, *J. Mater. Chem.* 13 (7) (2003) 1686–1694.
- [108] D. Friesen, D. Gibson, Heterogeneous Cs 3 PW 12 O 40 Photocatalysts, *Chem. Commun.* 5 (1998) 543–544.
- [109] D.E. Katsoulis, A survey of applications of polyoxometalates, *Chem. Rev.* 98 (1) (1998) 359–388.
- [110] N. Mizuno, K. Yamaguchi, K. Kamata, Molecular design of polyoxometalate-based compounds for environmentally-friendly functional group transformations: from molecular catalysts to heterogeneous catalysts, *Catal. Surv. Jpn.* 15 (2) (2011) 68–79.
- [111] I.V. Kozhevnikov, Catalysts for fine chemical synthesis, in: *Catalysis by Polyoxometalates*, vol. 2, 2002, p. 216.
- [112] Y. Zhou, G. Chen, Z. Long, J. Wang, Recent advances in polyoxometalate-based heterogeneous catalytic materials for liquid-phase organic transformations, *RSC Adv.* 4 (79) (2014) 42092–42113.
- [113] G. Li, Y. Ding, J. Wang, X. Wang, J. Suo, New progress of Keggin and Wells–Dawson type polyoxometalates catalyze acid and oxidative reactions, *J. Mol. Catal. A Chem.* 262 (1-2) (2007) 67–76.

- [114] M. Misono, Y. Konishi, M. Furuta, Y. Yoneda, Surface properties of 12-molybdophosphoric acid catalyst, *Chem. Lett.* 7 (7) (1978) 709–712.
- [115] T. Okuhara, N. Mizuno, M. Misono, Catalytic chemistry of heteropoly compounds, *Adv. Catal.* 41 (1996) 113–252.
- [116] M. Misono, Proceedings of the 10th International Congress on Catalysis, 1992, pp. 69–103.
- [117] M. Misono, Heterogeneous catalysis by heteropoly compounds of molybdenum and tungsten, *Catal. Rev. Sci. Eng.* 29 (2-3) (1987) 269–321.
- [118] M. Misono, N. Mizuno, K. Katamura, A. Kasai, Y. Konishi, K. Sakata, Y. Yoneda, Catalysis by heteropoly compounds. III. The structure and properties of 12-heteropolyacids of molybdenum and tungsten ( $H_3PMo_{12-x}W_xO_{40}$ ) and their salts pertinent to heterogeneous catalysis, *Bull. Chem. Soc. Jpn.* 55 (2) (1982) 400–406.
- [119] T. Okuhara, S. Tatematsu, K.Y. Lee, M. Misono, Catalysis by heteropoly compounds. XII. Absorption properties of 12-tungstophosphoric acid and its salts, *Bull. Chem. Soc. Jpn.* 62 (3) (1989) 717–723.
- [120] T. Nishimura, T. Okuhara, M. Misono, High catalytic activities of pseudoliquid phase of dodecatungstophosphoric acid for reactions of polar molecules, *Chem. Lett.* 20 (10) (1991) 1695–1698.
- [121] (a) T. Okuhara, T. Hashimoto, M. Misono, Y. Yoneda, H. Nijiyama, Y. Saito, E. Echigoya, Evidence for “pseudo-liquid phase” in the dehydration of isopropanol over  $H_3PW_{12}O_{40}$ , *Chem. Lett.* 12 (4) (1983) 573–576. (b) T. Okuhara, T. Arai, T. Ichiki, K.Y. Lee, M. Misono, Dehydration mechanism of ethanol in the pseudoliquid phase of  $H_3-xCs_xPW_{12}O_{40}$ , *J. Mol. Catal.* 55 (1) (1989) 293–301.
- [122] (a) T. Komaya, M. Misono, Activity patterns of  $H_3PMo_{12}O_{40}$  and its alkali salts for oxidation reactions, *Chem. Lett.* 12 (8) (1983) 1177–1180. (b) M. Misono, N. Mizuno, T. Komaya, *Proc. 8th Int. Congr. Catal.*, Vol. 5, Verlag Chemie, Weinheim, 1984, p. 487.
- [123] M. Misono, N. Mizuno, H.O. Mori, K.Y. Lee, J. Jiao, T. Okuhara, Surface- and bulk-type catalysis of heteropolymolybdates. Importance of the concept in the structure-activity relationships for catalyst design, in: *Studies in Surface Science and Catalysis*, vol. 67, Elsevier, 1991, pp. 87–97.
- [124] H.O. Mori, N. Mizuno, M. Misono, Factors controlling the selectivity of the oxidation of acetaldehyde over heteropoly compounds, *J. Catal.* 131 (1) (1991) 133–142.
- [125] N. Mizuno, T. Watanabe, M. Misono, Catalysis by heteropoly compounds. XVIII. Oxidation of methacrylaldehyde over 12-molybdophosphoric acid and its alkali salts, *Bull. Chem. Soc. Jpn.* 64 (1) (1991) 243–247.
- [126] N. Mizuno, T. Watanabe, H. Mori, M. Misono, Surface-type and bulk-type (II) catalysis in catalytic oxidations over 12-molybdophosphoric acid and its alkali salts, *J. Catal.* 123 (1) (1990) 157–163.
- [127] N. Mizuno, T. Watanabe, M. Misono, Reduction-oxidation and catalytic properties of 12-molybdophosphoric acid and its alkali salts. The role of redox carriers in the bulk, *J. Phys. Chem.* 89 (1) (1985) 80–85. 1952.
- [128] P.M. Ajayan, L.S. Schadler, P.V. Braun, *Nanocomposite science and technology*, Wiley-VCH, Germany, 2003.
- [129] Z. Kang, Y. Wang, E. Wang, S. Lian, L. Gao, W. You, et al., Polyoxometalate nanoparticles: synthesis, characterization and carbon nanotube modification, *Solid State Commun.* 129 (2004) 559–564.
- [130] P. Garrigue, M.H. Delville, C. Labrugère, E. Cloutet, P.J. Kulesza, J.P. Morand, A. Kuhn, Top– down approach for the preparation of colloidal carbon nanoparticles, *Chem. Mater.* 16 (16) (2004) 2984–2986.



- [131] P.J. Kulesza, M. Skunik, B. Baranowska, K. Miecznikowski, M. Chojak, K. Karnicka, A. Ernst, Fabrication of network films of conducting polymer-linked polyoxometallate-stabilized carbon nanostructures, *Electrochim. Acta* 51 (11) (2006) 2373–2379.
- [132] A.K. Cuentas-Gallegos, R. Martínez-Rosales, M. Baibarac, P. Gomez-Romero, M.E. Rincón, Electrochemical supercapacitors based on novel hybrid materials made of carbon nanotubes and polyoxometalates, *Electrochem. Commun.* 9 (8) (2007) 2088–2092.
- [133] B. Fei, H. Lu, Z. Hu, J.H. Xin, Solubilization, purification and functionalization of carbon nanotubes using polyoxometalate, *Nanotechnology* 17 (6) (2006) 1589.
- [134] S. Li, X. Yu, G. Zhang, Y. Ma, J. Yao, P. De Oliveira, Green synthesis of a Pt nanoparticle/polyoxometalate/carbon nanotube tri-component hybrid and its activity in the electrocatalysis of methanol oxidation, *Carbon* 49 (6) (2011) 1906–1911.
- [135] N. Kawasaki, H. Wang, R. Nakanishi, S. Hamanaka, R. Kitaura, H. Shinohara, K. Awaga, Nanohybridization of polyoxometalate clusters and single-wall carbon nanotubes: applications in molecular cluster batteries, *Angew. Chem.* 123 (15) (2011) 3533–3536.
- [136] A.K. Cuentas-Gallegos, R. Martínez-Rosales, M.E. Rincón, G.A. Hirata, G. Orozco, Design of hybrid materials based on carbon nanotubes and polyoxometalates, *Opt. Mater.* 29 (1) (2006) 126–133.
- [137] A.K. Cuentas-Gallegos, M. Miranda-Hernández, A. Vargas-Ocampo, Dispersion effect of Cs-PW particles on multiwalled carbon nanotubes and their electrocatalytic activity on the reduction of bromate, *Electrochim. Acta* 54 (18) (2009) 4378–4383.
- [138] A.K. Cuentas-Gallegos, M. Gonzales-Toledo, M.E. Rincón, Nanocomposite hybrid material based on carbon nanofibers and polyoxometalates, *Rev. Mex. Fis.* 53 (5) (2007) 91–95.
- [139] M. Zhou, L.P. Guo, F.Y. Lin, H.X. Liu, Electrochemistry and electrocatalysis of polyoxometalate-ordered mesoporous carbon modified electrode, *Anal. Chim. Acta* 587 (1) (2007) 124–131.
- [140] J. Suárez-Guevara, V. Ruiz, P. Gomez-Romero, Hybrid energy storage: high voltage aqueous supercapacitors based on activated carbon–phosphotungstate hybrid materials, *J. Mater. Chem. A* 2 (4) (2014) 1014–1021.
- [141] J.P. Tessonnier, S. Goubert-Renaudin, S. Alia, Y. Yan, M.A. Barteau, Structure, stability, and electronic interactions of polyoxometalates on functionalized graphene sheets, *Langmuir* 29 (1) (2013) 393–402.
- [142] K. Kume, N. Kawasaki, H. Wang, T. Yamada, H. Yoshikawa, K. Awaga, Enhanced capacitor effects in polyoxometalate/graphene nanohybrid materials: a synergetic approach to high performance energy storage, *J. Mater. Chem. A* 2 (11) (2014) 3801–3807.
- [143] H. Li, S. Pang, X. Feng, K. Müllen, C. Bubeck, Polyoxometalate assisted photoreduction of graphene oxide and its nanocomposite formation, *Chem. Commun.* 46 (34) (2010) 6243–6245.
- [144] D. Zhou, B.H. Han, Graphene-based nanoporous materials assembled by mediation of polyoxometalate nanoparticles, *Adv. Funct. Mater.* 20 (16) (2010) 2717–2722.
- [145] D. Martel, H.N. Cong, M. Molinari, J. Ebothé, I.V. Kityk, Adsorption of polyanions on nanostructured polypyrrole submonolayer grafted on semiconducting transparent support, *J. Mater. Sci.* 43 (10) (2008) 3486–3490.
- [146] S. Dong, W. Jin, Study of a 1:12 phosphomolybdic anion doped polypyrrole film electrode and its catalysis, *J. Electroanal. Chem.* 354 (1-2) (1993) 87–97.
- [147] A. Balamurugan, S.M. Chen, Silicomolybdate doped polypyrrole film modified glassy carbon electrode for electrocatalytic reduction of Cr (VI), *J. Solid State Electrochem.* 11 (12) (2007) 1679–1687.



- [148] G.M. Suppes, B.A. Deore, M.S. Freund, Porous conducting polymer/heteropolyoxometalate hybrid material for electrochemical supercapacitor applications, *Langmuir* 24 (3) (2008) 1064–1069.
- [149] S. Subramanian, D.P. Padiyan, Investigation of pseudocapacitance effect and frequency dependence of ac impedance in polyaniline–polyoxometalate hybrids, *J. Mater. Sci.* 44 (22) (2009) 6040–6053.
- [150] J. Vaillant, M. Lira-Cantu, K. Cuentas-Gallegos, N. Casañ-Pastor, P. Gómez-Romero, Chemical synthesis of hybrid materials based on PANi and PEDOT with polyoxometalates for electrochemical supercapacitors, *Prog. Solid State Chem.* 34 (2-4) (2006) 147–159.
- [151] A. Balamurugan, S.M. Chen, Silicomolybdate-doped PEDOT modified electrode: electrocatalytic reduction of bromate and oxidation of ascorbic acid, *Electroanalysis* 19 (15) (2007) 1616–1622.
- [152] M. Genovese, K. Lian, Polyoxometalate modified inorganic–organic nanocomposite materials for energy storage applications: a review, *Curr. Opin. Solid State Mater. Sci.* 19 (2) (2015) 126–137.
- [153] G. Decher, Fuzzy nanoassemblies: toward layered polymeric multicomposites, *Science* 277 (5330) (1997) 1232–1237.
- [154] Y. Xiang, S. Lu, Layer-by-layer self-assembly in the development of electrochemical energy conversion and storage devices from fuel cells to supercapacitors, *Chem. Soc. Rev.* 41 (21) (2012) 7291–7321.
- [155] D. Ingersoll, P.J. Kulesza, L.R. Faulkner, Polyoxometallate-based layered composite films on electrodes: preparation through alternate immersions in modification solutions, *J. Electrochem. Soc.* 141 (1) (1994) 140.
- [156] Y. Song, E. Wang, Z. Kang, Y. Lan, C. Tian, Synthesis of polyoxometalates-functionalized carbon nanotubes composites and relevant electrochemical properties study, *Mater. Res. Bull.* 42 (8) (2007) 1485–1491.
- [157] M. Sosnowska, M. Goral-Kurbiel, M. Skunik-Nuckowska, R. Jurczakowski, P.J. Kulesza, Hybrid materials utilizing polyelectrolyte-derivatized carbon nanotubes and vanadium-mixed addenda heteropolytungstate for efficient electrochemical charging and electrocatalysis, *J. Solid State Electrochem.* 17 (6) (2013) 1631–1640.
- [158] A. Salimi, A. Korani, R. Hallaj, S. Soltanian, H. Hadadzadeh, Deposition of  $\alpha$ -SiMo12O4-40-[Ru (bipyridine)(terpyridine) Cl]<sup>+</sup> multilayer film on single wall carbon nanotube modified glassy carbon electrode: improvement of the electrochemical properties and chemical stability, *Thin Solid Films* 518 (18) (2010) 5304–5310.
- [159] J. Qu, X. Zou, B. Liu, S. Dong, Assembly of polyoxometalates on carbon nanotubes paste electrode and its catalytic behaviors, *Anal. Chim. Acta* 599 (1) (2007) 51–57.
- [160] T. Akter, K. Hu, K. Lian, Investigations of multilayer polyoxometalates-modified carbon nanotubes for electrochemical capacitors, *Electrochim. Acta* 56 (2011) 4966–4971.
- [161] D. Martel, M. Gross, Electrochemical study of multilayer films built on glassy carbon electrode with polyoxometalate anions and two multi-charged molecular cationic species, *J. Solid State Electrochem.* 11 (3) (2007) 421–429.
- [162] Y. Lan, E. Wang, Y. Song, Y. Song, Z. Kang, L. Xu, Z. Li, An effective layer-by-layer adsorption and polymerization method to the fabrication of polyoxometalate-polypyrrole nanoparticle ultrathin films, *Polymer* 47 (4) (2006) 1480–1485.
- [163] M.T. Koper, A basic solution, *Nat. Chem.* 5 (4) (2013) 255–256.
- [164] R. Subbaraman, D. Tripkovic, D. Strmcnik, K.C. Chang, M. Uchimura, A.P. Paulikas, N.M. Markovic, Enhancing hydrogen evolution activity in water splitting by tailoring Li<sup>+</sup>-Ni(OH) 2-Pt interfaces, *Science* 334 (6060) (2011) 1256–1260.

- [165] C. Bianchini, P.K. Shen, Palladium-based electrocatalysts for alcohol oxidation in half cells and in direct alcohol fuel cells, *Chem. Rev.* 109 (9) (2009) 4183–4206.
- [166] A. Sartorel, M. Bonchio, S. Campagna, F. Scandola, Tetrametallic molecular catalysts for photochemical water oxidation, *Chem. Soc. Rev.* 42 (6) (2013) 2262–2280.
- [167] F.M. Toma, A. Sartorel, M. Iurlo, M. Carraro, P. Parris, C. Maccato, M. Bonchio, Efficient water oxidation at carbon nanotube–polyoxometalate electrocatalytic interfaces, *Nat. Chem.* 2 (10) (2010) 826–831.
- [168] F.M. Toma, A. Sartorel, M. Iurlo, M. Carraro, S. Rapino, L. Hooper-Burkhardt, M. Prato, Tailored functionalization of carbon nanotubes for electrocatalytic water splitting and sustainable energy applications, *ChemSusChem* 4 (10) (2011) 1447–1451.
- [169] M. Quintana, A.M. Lopez, S. Rapino, F.M. Toma, M. Iurlo, M. Carraro, M. Bonchio, Knitting the catalytic pattern of artificial photosynthesis to a hybrid graphene nanotexture, *ACS Nano* 7 (1) (2013) 811–817.
- [170] S.X. Guo, Y. Liu, C.Y. Lee, A.M. Bond, J. Zhang, Y.V. Geletii, C.L. Hill, Graphene-supported  $[\{\text{Ru} 4 \text{ O} 4 (\text{OH}) 2 (\text{H} 2 \text{ O}) 4\}(\gamma\text{-SiW} 10 \text{ O} 36) 2] 10-$  for highly efficient electrocatalytic water oxidation, *Energy Environ. Sci.* 6 (9) (2013) 2654–2663.
- [171] D. Pan, J. Chen, W. Tao, L. Nie, S. Yao, Polyoxometalate-modified carbon nanotubes: new catalyst support for methanol electro-oxidation, *Langmuir* 22 (13) (2006) 5872–5876.
- [172] D. Wang, S. Lu, Pd/HPW-PDDA-MWCNTs as effective non-Pt electrocatalysts for oxygen reduction reaction of fuel cells, *Chem. Commun.* 46 (12) (2010) 2058–2060.
- [173] R. Liu, S. Li, X. Yu, G. Zhang, Y. Ma, J. Yao, Facile synthesis of a Ag nanoparticle/polyoxometalate/carbon nanotube tri-component hybrid and its activity in the electrocatalysis of oxygen reduction, *J. Mater. Chem.* 21 (38) (2011) 14917–14924.
- [174] R. Liu, X. Yu, G. Zhang, S. Zhang, H. Cao, A. Dolbecq, L. Zhi, Polyoxometalate-mediated green synthesis of a 2D silver nanonet/graphene nanohybrid as a synergistic catalyst for the oxygen reduction reaction, *J. Mater. Chem. A* 1 (38) (2013) 11961–11969.
- [175] A.P. Alivisatos, P.F. Barbara, A.W. Castleman, J. Chang, D.A. Dixon, M.L. Klein, G.L. McLendon, J.S. Miller, M.A. Ratner, P.J. Rossky, S.I. Stupp, M.E. Thompson, From molecules to materials: current trends and future directions, *Adv. Mater.* 10 (16) (1998) 1297–1336.
- [176] A.L. Efros, M. Rosen, The electronic structure of semiconductor nanocrystals, *Annu. Rev. Mater. Sci.* 30 (1) (2000) 475–521.
- [177] A.Z. Moshfegh, Nanoparticle catalysts, *J. Phys. D. Appl. Phys.* 42 (23) (2009), 233001.
- [178] B. Hvolbæk, T.V. Janssens, B.S. Clausen, H. Falsig, C.H. Christensen, J.K. Nørskov, Catalytic activity of Au nanoparticles, *Nano Today* 2 (4) (2007) 14–18.
- [179] X. Michalet, F.F. Pinaud, L.A. Bentolila, J.M. Tsay, S.J.J.L. Doose, J.J. Li, S. Weiss, Quantum dots for live cells, in vivo imaging, and diagnostics, *Science* 307 (5709) (2005) 538–544.
- [180] A.Z. Wang, R. Langer, O.C. Farokhzad, Nanoparticle delivery of cancer drugs, *Annu. Rev. Med.* 63 (2012) 185–198.
- [181] M.A. Hahn, A.K. Singh, P. Sharma, S.C. Brown, B.M. Moudgil, Nanoparticles as contrast agents for in-vivo bioimaging: current status and future perspectives, *Anal. Bioanal. Chem.* 399 (1) (2011) 3–27.
- [182] L. Chalkley, The extent of the photochemical reduction of phosphotungstic acid, *J. Phys. Chem.* 56 (9) (1952) 1084–1086.
- [183] T. Hsu-Yao, K.P. Browne, N. Honesty, Y.J. Tong, Polyoxometalate-stabilized Pt nanoparticles and their electrocatalytic activities, *Phys. Chem. Chem. Phys.* 13 (16) (2011) 7433–7438.

- [184] A.V. Gordeev, N.I. Kartashev, B.G. Ershov, Metal nanoparticles with PW11O397- and P2W17O6110-heteropoly anions as stabilizing agents: radiation-chemical preparation and properties, *High Energy Chem.* 36 (2) (2002) 75–79.
- [185] J. Yuan, Y. Chen, D. Han, Y. Zhang, Y. Shen, Z. Wang, L. Niu, Synthesis of highly faceted multiply twinned gold nanocrystals stabilized by polyoxometalates, *Nanotechnology* 17 (18) (2006) 4689.
- [186] M.T. Pope, Heteropoly and isopoly anions as oxo complexes and their reducibility to mixed-valence blues, *Inorg. Chem.* 11 (8) (1972) 1973–1974.
- [187] I.A. Weinstock, Homogeneous-phase electron-transfer reactions of polyoxometalates, *Chem. Rev.* 98 (1) (1998) 113–170.
- [188] J. Zhang, B. Keita, L. Nadjo, I.M. Mbomekalle, T. Liu, Self-assembly of polyoxometalate macroanion-capped Pd0 nanoparticles in aqueous solution, *Langmuir* 24 (10) (2008) 5277–5283.
- [189] S. Li, X. Yu, G. Zhang, Y. Ma, J. Yao, B. Keita, H. Zhao, Green chemical decoration of multiwalled carbon nanotubes with polyoxometalate-encapsulated gold nanoparticles: visible light photocatalytic activities, *J. Mater. Chem.* 21 (7) (2011) 2282–2287.
- [190] Y. Xie, Photoelectrochemical reactivity of polyoxophosphotungstates embedded in titania tubules, *Nanotechnology* 17 (14) (2006) 3340.
- [191] L. Lu, L. Li, T. Hu, W. Zhang, X. Huang, J. Zhang, X. Liu, Preparation, characterization, and photocatalytic activity of three-dimensionally ordered macroporous hybrid monosubstituted polyoxometalate K5 [Co (H2O) PW11O39] amine functionalized titanium catalysts, *J. Mol. Catal. A Chem.* 394 (2014) 283–294.
- [192] J. Wu, L. Liao, W. Yan, Y. Xue, Y. Sun, X. Yan, Y. Xie, Polyoxometalates immobilized in ordered mesoporous carbon nitride as highly efficient water oxidation catalysts, *ChemSusChem* 5 (7) (2012) 1207–1212.
- [193] T.F. Otero, S.A. Cheng, E. Coronado, E.M. Ferrero, C.J. Gómez-García, Functional hybrid materials containing polypyrrole and polyoxometalate clusters: searching for high conductivities and specific charges, *ChemPhysChem* 3 (9) (2002) 808–811.
- [194] S. Uematsu, Z. Quan, Y. Suganuma, N. Sonoyama, Reversible lithium charge–discharge property of bi-capped Keggin-type polyoxovanadates, *J. Power Sources* 217 (2012) 13–20.
- [195] L. Huang, J. Hu, Y. Ji, C. Streb, Y.F. Song, Pyrene-Anderson-modified CNTs as anode materials for lithium-ion batteries, *Chem. Eur. J.* 21 (51) (2015) 18799–18804.
- [196] P. Gomez-Romero, N. Casan-Pastor, Photoredox chemistry in oxide clusters. Photochromic and redox properties of polyoxometalates in connection with analog solid state colloidal systems, *J. Phys. Chem.* 100 (30) (1996) 12448–12454.
- [197] P. Gómez-Romero, M. Chojak, K. Cuentas-Gallegos, J.A. Asensio, P.J. Kulesza, N. Casañ-Pastor, M. Lira-Cantú, Hybrid organic–inorganic nanocomposite materials for application in solid state electrochemical supercapacitors, *Electrochem. Commun.* 5 (2) (2003) 149–153.
- [198] N. Benkirane-Jessel, P. Lavalle, E. HüBSCH, V. Holl, B. Senger, Y. Häikel, P. Schaaf, Short-time tuning of the biological activity of functionalized polyelectrolyte multilayers, *Adv. Funct. Mater.* 15 (4) (2005) 648–654.
- [199] J. He, H. Sun, S. Indrawirawan, X. Duan, M.O. Tade, S. Wang, Novel polyoxometalate@ g-C3N4 hybrid photocatalysts for degradation of dyes and phenolics, *J. Colloid Interface Sci.* 456 (2015) 15–21.
- [200] Y. Kamiya, M. Sadakane, W. Ueda, Heteropoly compounds, in: *Comprehensive Inorganic Chemistry II*, second ed., Elsevier Ltd, 2013.
- [201] R. Yu, X.F. Kuang, X.Y. Wu, C.Z. Lu, J.P. Donahue, Stabilization and immobilization of polyoxometalates in porous coordination polymers through host–guest interactions, *Coord. Chem. Rev.* 253 (23–24) (2009) 2872–2890.

- [202] W. Ueda, Y. Suzuki, Partial oxidation of propane to acrylic acid over reduced heteropolymolybdate catalysts, *Chem. Lett.* 24 (7) (1995) 541–542.
- [203] D.G. Kurth, P. Lehmann, D. Volkmer, H. Cölfen, M.J. Koop, A. Müller, A. Du Chesne, Surfactant-encapsulated clusters (SECs):(DODA) 20 (NH<sub>4</sub>)[H<sub>3</sub>Mo 57 V 6 (NO) 6 O 183 (H<sub>2</sub>O) 18], a case study, *Chem. Eur. J.* 6 (2) (2000) 385–393.
- [204] Y. Leng, J. Wang, D. Zhu, L. Shen, P. Zhao, M. Zhang, Heteropolyanion-based ionic hybrid solid: a green bulk-type catalyst for hydroxylation of benzene with hydrogen peroxide, *Chem. Eng. J.* 173 (2) (2011) 620–626.
- [205] S. Nlate, D. Astruc, R. Neumann, Synthesis, catalytic activity in oxidation reactions, and recyclability of stable polyoxometalate-centred dendrimers, *Adv. Synth. Catal.* 346 (12) (2004) 1445–1448.
- [206] Y. Yang, Y. Wang, H. Li, W. Li, L. Wu, Self-assembly and structural evolution of polyoxometalate-anchored dendron complexes, *Chem. Eur. J.* 16 (27) (2010) 8062–8071.
- [207] H. Zeng, G.R. Newkome, C.L. Hill, Poly (polyoxometalate) dendrimers: molecular prototypes of new catalytic materials, *Angew. Chem.* 112 (10) (2000) 1841–1844.
- [208] M.V. Vasylyev, R. Neumann, New heterogeneous polyoxometalate based mesoporous catalysts for hydrogen peroxide mediated oxidation reactions, *J. Am. Chem. Soc.* 126 (2004) 885–890.
- [209] O.A. Kholdeeva, N.V. Maksimchuk, G.M. Maksimov, Polyoxometalate-based heterogeneous catalysts for liquid phase selective oxidations: comparison of different strategies, *Catal. Today* 157 (1–4) (2010) 107–113.
- [210] C.H. Li, K.L. Huang, Y.N. Chi, X. Liu, Z.G. Han, L. Shen, C.W. Hu, Lanthanide–organic cation frameworks with zeolite gismondine topology and large cavities from intersected channels templated by polyoxometalate counterions, *Inorg. Chem.* 48 (5) (2009) 2010–2017.
- [211] C.Y. Sun, S.X. Liu, D.D. Liang, K.Z. Shao, Y.H. Ren, Z.M. Su, Highly stable crystalline catalysts based on a microporous metal–organic framework and polyoxometalates, *J. Am. Chem. Soc.* 131 (5) (2009) 1883–1888.
- [212] H.Y. Zang, Y.Q. Lan, S.L. Li, G.S. Yang, K.Z. Shao, X.L. Wang, Z.M. Su, Step-wise synthesis of inorganic–organic hybrid based on  $\gamma$ -octamolybdate-based tectons, *Dalton Trans.* 40 (13) (2011) 3176–3182.
- [213] B. Nohra, H. El Moll, L.M. Rodriguez Albelo, P. Mialane, J. Marrot, C. Mellot-Draznieks, A. Dolbecq, Polyoxometalate-based metal organic frameworks (POMOFs): structural trends, energetics, and high electrocatalytic efficiency for hydrogen evolution reaction, *J. Am. Chem. Soc.* 133 (34) (2011) 13363–13374.
- [214] S. Liu, Z. Tang, Polyoxometalate-based functional nanostructured films: current progress and future prospects, *Nano Today* 5 (2010) 267–281.

## Chapter 2

# Heteropoly acids: An overview

## 2.1 Polyoxometalates

### 2.1.1 Historical backgrounds

Polyoxometalates (POMs) have a history as early as 1826, when the first heteropoly salt, ammonium 12-molybdophosphate, was discovered by Berzelius. In 1848, Svanberg and Struve pioneered the determination of phosphorus based on this compound in analytical chemistry, which has been widely in use since then. About 750 heteropoly compounds had been reported by 1908. Nonetheless, the structures of POM species remained a challenge for more than a century after their discovery. Werner, Miolati, Rosenheim, and Pauling suggested structures based on metal-oxygen polyhedrons with shared edges and/or corners.

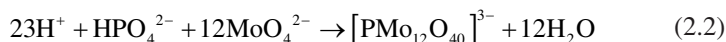
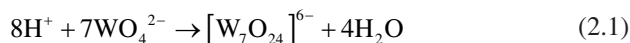
It was not until 1933 that Keggin solved the structure of the most important 12:1 type of heteropoly anions (HPAs), employing the powder diffraction study of  $\text{H}_3[\text{PW}_{12}\text{O}_{40}]$  [1]. The structure, which is now named after its discoverer, consisted of 12  $\text{WO}_6$  octahedrons bound by shared edges and corners, while the heteroatom occupied a tetrahedral hole in the core. Evans managed to determine the structure of another widespread type of POMs, i.e., the Anderson's 6:1 heteropoly anion, using the single-crystal X-ray analysis of  $[\text{TeMo}_6\text{O}_{24}]^{6-}$  salts in 1948. It is now known as the Anderson-Evan's structure [2]. The next new structure, i.e., 18:2 (or 9:1) heteropoly anion  $[\text{P}_2\text{W}_{18}\text{O}_{62}]^{6-}$ , was reported by Dawson in 1953, and is currently known as the Wells-Dawson's structure [3]. They demonstrated that the structure was closely related to the Keggin structure. Then, in 1968, Dexter and Silverton reported the X-ray structure of  $[\text{CeMo}_{12}\text{O}_{42}]^{8-}$  and proved that the large cerium heteroatom occupied a  $\text{CeO}_{12}$  central icosahedron [4].

In the early 1970s, the chemistry of POMs developed significantly. This period as well as the next 2 decades (1980s–1990s) witnessed extensive work by many groups from all around the world. Due to the growth of applications of heteropolyanions in various areas, the number of such groups further increased. The X-ray structures of approximately 180 POMs had been reported by 1995 [5], among which, salts of giant heteropoly anions such as  $[\text{La}_{16}\text{As}_{12}\text{W}_{148}\text{O}_{524}]^{76-}$  (ion mass about 40,000, diameter 40 Å) and others were prepared and characterized by Muller et al. [6]. Modern characterization techniques had

resulted in a much better grasp of the principles governing the structures of polyoxometalates and their properties. However, many essential problems with respect to the structural principles, mechanisms of syntheses, and reactivity of POMs remain unresolved.

### 2.1.2 A survey on Polyoxometalates

These compounds are members of a large group of nanosized metal-oxygen cluster anions [7] formed by a self-assembly process, typically in acidic aqueous solutions as illustrated by Eqs. (2.1) and (2.2). The oxoanions of molybdenum (VI), tungsten (VI), and vanadium (V) have the unique capability of going through condensation reactions under acidic conditions, which is an extraordinary feature of these compounds. This process results in the formation of polynuclear metal-oxide anions. The exceptional chemical and structural diversity of such anions has created a plethora of scientific research from principal studies [8–16] to applied industrial fields [17–22]. These oxoanions can be isolated in solid form if coupled with proper counteranions such as alkali metal cations, ammonium ions, etc. The structures of these species follows the general rule that the metal centers (M) coordinate to oxygen ligands and form coordination polyhedrons of the type  $[MO_y]$  (with  $y = 4–7$ ). The resulting structures may in turn go through further condensation reactions:



Octahedral structures  $[MO_6]$  (M = molybdenum, tungsten, vanadium, etc.) are by far the most common building blocks which are in turn linked to form larger clusters through shared edges and/or corners; that is to say each octahedron is linked by one (shared corners) or two bridging oxygen ligands (shared edges) to other octahedrons. Besides the important metal centers such as molybdenum (V/VI) and tungsten (V/VI), increasingly more structures of vanadium (IV/V), niobium (V), and tantalum (V) are being published. The abundance of polyoxometalate containing molybdenum and tungsten is due to several factors, which will be related as follows.

The molybdenum or tungsten center in a POM is typically found in its highest two oxidation states, which are fully oxidized (VI) or reduced by one electron (V). Consequently, they bestow empty d orbitals, which pave the way for the formation of strong metal oxide  $\pi$ -bonds besides the coordinative bond between the metal center and the oxygen atom as a ligand. Such  $\pi$ -bonding is possible between an occupied ligand orbital ( $p_x$  or  $p_y$ ) and a metal d-orbital of similar symmetry ( $d_{xy}$ ,  $d_{xz}$ , or  $d_{yz}$ ). This mode of bonding directly results in terminal double bonds between the metal center and oxygen atoms (M=O)

characterized by a drastic decrease in basicity (and accordingly nucleophilicity), which in turn restricts the growth of the metal-oxide structures and leads into the formation of separated clusters in place of infinite solid-state structures [23]. Curiously, the metal center polarizes the oxygen atoms, causing extremely weak bonding of protons by terminal oxygen ligands and explaining the high acidity of POMs [24]. In addition, the structural variety in both molybdenum- and tungsten-based polyoxometalates is their capability in accepting various numbers of oxygen atoms as ligands to form coordination polyhedrons that range from tetrahedral  $[\text{MO}_4]$  to pentagonal bipyramidal  $[\text{MO}_7]$  structures. The reason for this capability can be traced to the ratio of charge to ionic radius, which paves the way for effective bonding of oxygen ligands and hence the assembly of the usual building blocks as well as more condensation to larger fragments (Table 2.1). Conversely, elements such as chromium, tantalum, and niobium lack such versatility in coordination geometry and therefore they exhibit restrictions in the number of polyoxoanions they can form.

In general, two types of polyoxometalates can be distinguished based on their chemical compositions, i.e., isopoly anions and heteropoly anions, which may be represented by the general formulas  $[\text{M}_m\text{O}_y]^{p-}$  and  $[\text{X}_x\text{M}_m\text{O}_y]^{q-}$  ( $x < m$ ), respectively. In these general formulas, M is the addenda atom and X is the heteroatom, which is also called the central atom when located in the center of the polyanion.

**TABLE 2.1** Comparison of the ionic radii of some typical polyoxo anion-forming metals.

Element (oxidation state)	Coordination number	Ionic radius/Å [25]	Ratio oxidation state: ionic radius
MO(V)	6	0.61	8.20
MO(VI)	6	0.59	10.17
W(V)	6	0.62	8.06
W(VI)	6	0.60	10.00
V(IV)	5	0.53	7.55
V(IV)	6	0.58	6.90
V(V)	5	0.46	10.87
V(VI)	6	0.54	11.11
Cr(V)	6	0.49	10.20
Cr(VI)	6	0.44	13.64
Ta(V)	6	0.64	7.81
Nb(V)	6	0.64	7.81

Clusters only comprised of addenda atoms and oxygen ligands (with the ability of being protonated) are specifically called isopolyoxometalates, to emphasize the fact that there are no additional elements (other than H). On the other hand, a wide range of polyoxometalates includes an additional heteroatom X that often plays a crucial structural role. This category of polyoxometalates is known as heteropolyoxometalates. The heteroatoms observed so far approximately include the whole periodic table.

### 2.1.3 Applications

The numerous and varied applications of polyoxometalates are primarily pivoted around their ionic charge, redox properties, conductivity, photochemical response, and ionic weights. Therefore, the study of polyoxometalates continues to draw considerable attention and the number of publications and patents is still growing. The basic properties of a particular polyoxometalate that add value to these compounds are listed in [Table 2.2](#).

**TABLE 2.2** Valuable properties of polyoxometalates.

Entry	Property
1	Metal oxide like
2	Anionic (charge from $-3$ to $-14$ )
3	Stable ( $\text{H}_2\text{O}/\text{air}$ , T): processing advantage
4	Large size (diameter, $6\text{--}25 \text{ \AA}$ )
5	Discrete size/discrete structure (confined geometric factors)
6	High ionic weight ( $10^3\text{--}10^4$ )
7	Fully oxidized compounds/reducible
8	Variable oxidation numbers for the addenda atoms ( $E_{1/2}$ ) $0.5$ to $-1.0 \text{ V vs. SCE}$
9	Color of oxidized forms different from color of reduced forms
10	Photoreducible
11	Arrhenius acids ( $\text{p}K_{\text{a}} < 0$ )
12	Incorporate more than 70 elements and form large number of structures: processing advantage
13	Acid forms very soluble in $\text{H}_2\text{O}$ and other oxygen carrying solvents (ethers, alcohols, ketones); also soluble or transferable into nonpolar solvents: processing advantage
14	Hydrolyzable to form deficient structures: processing advantage



Given the abovementioned valuable properties, polyoxometalates are being welcomed by technologists and material scientists and evaluated from various application viewpoints. A majority of the applications of polyoxometalates falls in the field of catalysis. Between 80% and 85% of applied literature and patents investigate or claim polyoxometalates for their catalytic properties. Other categories listed in Table 2.3 entail the remaining 15%–20% of the applications [26].

Many systems, in both oxidized and reduced states, serve as powerful catalysts because they can be readily converted to reactive forms using light and

**TABLE 2.3** Categories of polyoxometalate applications.

Entry	Application
1	Catalysis
2	Medicine
3	Coatings
4	Analytical chemistry
5	Processing radioactive waste
6	Separations
7	Sorbents of gases
8	Membranes
9	Sensors
10	Dyes/pigments
11	Electro optics
12	Electrochemistry/electrodes
13	Capacitors
14	Dopants in nonconductive polymers
15	Dopants in conductive polymers
16	Dopants in sol-gel matrixes
17	Cation exchangers
18	Flammability control
19	Bleaching of paper pulp
20	Clinical analysis
21	Food chemistry

electricity, even though they are thermally and photochemically highly stable [27–30]. Instances from almost all categories of reduced polyoxometalates have been demonstrated to catalyze redox reactions. An important catalyst among polyoxometalates is the species decatung state  $[\text{HW}^{\text{v}}\text{W}_9^{\text{VI}}\text{O}_{32}]^{4-}$ , which is reduced by one electron. The species is a classic photocatalyst that catalyzes the dehydrogenation of alkanes to give alkenes [27].

These compounds are usually incorporated into multicomponent clusters to let them synergistically take advantage of their exclusive valuable properties along with the properties of the other components of the composites. Properties like electrochromicity, ion conductivity, redox activity, good thermal stability, and complex formation with a plethora of cations are employed in applications that include surface coating, membranes, thin films, electrochemical instruments, analytical reagents, pigments, etc. Of these properties, good thermal stability has been widely cited as an advantage in comparison to other similar materials.

As pointed out, polyoxometalates have also been used in surface coating, membranes, or films. Applications in these areas include corrosion-resistant coatings, surface modifiers of substrates (i.e., carbon electrodes), sol-gel matrices, conductive and nonconductive polymer membranes, pigments, wood pulp bleaching agents, toners, reagents for chemical/biochemical analysis, nuclear waste processing, etc.

As heteropoly compounds are extremely important for catalyzed reactions and other applications, this book is mainly focused on them. Heteropoly acids—strong acids composed of a heteropoly anion and protons as the counteranions—constitute a special case of heteropoly compounds which are particularly important for catalytic applications.

The most common addenda atoms are molybdenum or tungsten, vanadium and niobium (though less common), or mixtures of such in their highest oxidation states ( $d^0$ ,  $d^1$ ). A much broader range of elements serve as heteroatoms; therefore, almost all elements of the periodic table can be incorporated in heteropoly anions. However, the most typical of them are  $\text{P}^{5+}$ ,  $\text{As}^{5+}$ ,  $\text{Si}^{4+}$ ,  $\text{Ge}^{4+}$ ,  $\text{B}^{3+}$ , etc. Molybdenum(VI) and tungsten(VI) are the best transition metals to form polyoxometalate elements because of a favorable combination of ionic radius and charge as well as the accessibility of empty d-orbitals for metal-oxygen  $\pi$  bonding [31].

### 2.1.4 Structures

Scores of structural types and stoichiometries have been identified for heteropoly anions (HPAs). The lower limit of condensation degree for addenda atoms can be arbitrarily set in the range of 2–6 [5,31]. However, the upper limit may grow as large as a few hundred. For instance, a colossal heteropolytungstate like  $[\text{La}_{16}\text{Asi}_{12}\text{W}_{148}\text{O}_{524}]^{76-}$  contains 28 heteroatoms (La, As) as well as 148 addenda atoms (W) [6].

The structures follow two general rules [5,6,26–32]:

- (1) Addenda atoms are involved in metal-oxygen polyhedrons  $MO_x$ , which are usually octahedrons. Due to  $M-O$   $\pi$ -bonding, the metal atom is dislocated from the inversion center toward the peripheral vertices in such polyhedrons.
- (2) In general, structures with an  $MO_6$  octahedral containing more than two free vertices cannot be found amidst usual HPAs. This restriction, known as the Lipscomb principle, may be considered as a direct outcome of the strong trans effect of terminal  $M=O$  bonds, which works to facilitate the dissociation of  $MO_3$  from the polyanion [33].

As pointed out by Pope and Muller, the variety of HPAs structures can be easily discussed starting with a few parent polyanions of high symmetries. Then many other structures can be regarded as their derivatives [31,32]. Three of such parent structures, with a tetrahedron, an octahedron and an icosahedron as their central polyhedron  $XO_n$  ( $n = 4, 6,$  and  $12,$  respectively) specify the symmetry of all polyanions. The structures will be clarified in the following subsections.

## 2.2 Heteropoly acids

As an eminent group of polyoxometalates, heteropoly acids consist of hydrogen and oxygen atoms along with particular metals and nonmetals. To be considered a heteropoly acid, a species has to have a heteroatom (an element usually from the p-block of the periodic table, e.g., silicon, phosphorus, or arsenic), addenda atoms (i.e., a metal such as tungsten, molybdenum, or vanadium), oxygen atoms (to bridge the metal atoms), and acidic hydrogen atoms. The metal addenda atoms are linked by bridging oxygen atoms to construct a cluster inside which the heteroatom is bonded to oxygen atoms. It is noteworthy that species with more than one type of metal addenda atoms in the cluster are widely known. The conjugate anion of a heteropoly acid is referred to as a polyoxometalate.

Heteropoly acids typically are synthesized by acidification of the aqueous solution of the metaloxoanion and an appropriate heteroatom compound [34–40] in a suitable ratio. Acidification results in dehydration and polymerization of the metaloxoanion. Different structures may be formed depending on the conditions (i.e., temperature, pH, and counteranions). In addition to the pH, controlling the central atom to metal atom ratio ( $X/M$ ) is essential to afford the desired structure. Acidification is accomplished by adding a mineral acid. In order to isolate the heteropoly acid, extraction with ether (the etherate method) can be used. Shaking the aqueous acid solution with an excess of diethylether gives three separate phases: a lower aqueous layer, which is separately treated with more ether to recover the remaining heteropoly acid as much as possible; an upper layer of the excess ether; and a middle heavy oily etherate containing a complex between the ether molecules and the heteropoly acid. This complex may be hydrolyzed by adding a measured amount of water. After the ether is removed, the concentrated aqueous solution containing the heteropoly acid is evaporated

to crystallization [41]. In a different method, the excess ether of the etherate complex is first removed by evaporation; then the solid acid is obtained by drying and thermal decomposition of the ether complex at 80–100°C. However, the etherate method has the disadvantage that large amounts of the product are wasted and consequently the yield is diminished. The acid may be exchanged with other metal ions by solving in an aqueous solution and adding the proper metal salt. If the acquired salt or acid/salt mixture is soluble, it is recovered by evaporating the solvent.

Two types of protons have been determined to be present, i.e., strongly acidic protons that their number is related to the defined structures and weakly acidic protons that their number is varied. Heteropoly acids are usually represented as acid salts due the presence of the above-mentioned type of protons.

In fact, among HPAs, heteropolytungstates and heteropolymolybdates are much more known and prevalent than the other species. Their molecular weights are very high (some more than 4000) in comparison with those of other inorganic electrolytes; they are highly soluble in water and organic solvents, almost always existing in extensively hydrated forms, and highly colored. Some of them are strong oxidizing agents capable of being reduced to stable, profoundly dark blue species (called heteropoly blues), which in turn can serve as a reducing agent and reinstate the original color upon oxidation.

Heteropoly acids, like every other major solid acid catalyst, have a unique hexagonal cage-like structure so that there is a certain gap between heteropoly-anions in the bulk phase. This feature allow for smaller polar molecules to enter the bulk phase of the heteropoly acid forming a pseudoliquid phase, which is capable of showing homogeneous catalytic characteristics [42]. It is because of the presence of such surface-type and pseudoliquid phase catalysis that heteropoly acid catalysts are able to act not only on the surface of the catalysts but also from inside [43]. Therefore, heteropoly acids usually demonstrate more catalytic activity and selectivity compared to similar catalysts.

They have definite and stable structures, which have proven quite useful for the design and synthesis of novel catalysts at molecular and atomic levels. Furthermore, given their solubility in polar solvents and unique reaction field [44] (the pseudoliquid phase behavior mentioned previously), heteropoly acids may be used in both homogeneous or heterogeneous catalytic systems. Due to their acidity and oxidizing properties, heteropoly acids can be employed as acid-catalyzed oxidation catalysts or bifunctional catalysts. Their catalytic functionality is adjustable by changing the coordinative central atom and/or counter-cation without changing the very anion structure of the heteropoly acid. They are also transferrable into nonpolar solvents (e.g., benzene, toluene) through the action of a phase-transfer reagent (e.g., quaternary ammonium salts, halogenated hexadecyl pyridine). During phase transfer, they lose coordination water (acetone, pyridine, etc.) and inorganic molecules (sulfur dioxide, nitrogen dioxide, etc.) to form new complexes. Heteropoly acids can therefore exhibit sufficient catalytic activity in different processes. Nevertheless, because their

specific surface areas are quite small [45], their recycle and reuse are very difficult. Dispersing the heteropoly acid on an appropriate support or carrier of a large specific area can resolve such problems to a great extent [46].

## 2.3 Nomenclature

A systematic nomenclature has been developed for HPAs [31,47] that uses a labeling system for the metal atoms. In some cases, in order to avoid ambiguity the oxygen atoms are labeled as well. However, the names that resulted from this system are too lengthy and complicated. They are thus never used in practice. Usually, a simplified conventional nomenclature system suffices for reporting and retrieving information in the field. Sometimes even trivial names will do. In this book, we adopt the current nomenclature that regards polyoxometalates (also referred to as heteropoly compounds, heteropoly anions, polyoxoanions, or simply polyanions) as quasicoordination complexes [31]. The heteroatom, in the case of heteropoly compounds, is considered as the central atom of the complex and the addenda atoms are treated as ligands. In heteropoly anion formulas, the heteroatoms are mentioned before the addenda atoms; the whole heteropoly anion is surrounded by square brackets to be separated from the counteranions. The following examples help clarify the matter:

$[\text{SiW}_{12}\text{O}_{40}]^{4-}$ : 12-tungstosilicate or dodecatungstosilicate.

$\text{H}_3[\text{PMo}_{12}\text{O}_{40}]$ : 12-molybdophosphoric acid.

$\text{Na}_5[\text{PMo}_{10}\text{V}_2\text{O}_{40}]$ : sodium decamolybdodivanabdophosphate.

For simplification purposes, the counteranions, the polyanion charge, and even the oxygen atoms may be dropped. For instance,  $\text{Na}_6[\text{P}_2\text{Mo}_{18}\text{O}_{62}]$  is shortened to  $\{\text{P}_2\text{Mo}_{18}\text{O}_{62}\}$  or  $\text{P}_2\text{Mo}_{18}$ .

## 2.4 Classification of heteropoly acids

Heteropoly acids are categorized based on the relative numbers of the central atoms and the metal addenda atoms in the surrounding octahedral units. On this basis, four different major classes can be recognized.

- (1) *1:12 tetrahedral*: These are found with small heteroatoms such as  $\text{P}^{\text{V}}$ ,  $\text{As}^{\text{V}}$ ,  $\text{Si}^{\text{IV}}$ , and  $\text{Ti}^{\text{IV}}$  that yield tetrahedral oxoanions. Two important examples of this class are  $[\text{PW}_{12}\text{O}_{40}]^{3-}$  and  $\text{H}_3[\text{PMo}_{12}\text{O}_{40}]$ .
- (2) *2:18 tetrahedral*: If solutions of 1:12 anions  $[\text{X}^{\text{VM}}_{12}\text{O}_{40}]^{3-}$  are allowed to stand, generally 2:18  $[\text{X}_2\text{M}_{18}\text{O}_{62}]^{6-}$  ions are produced. The ion may be best considered to be formed from two 1:12 anions each losing three  $\text{MO}_6$  octahedral units before fusing the other one.
- (3) *1:6 octahedral*: This type is formed with larger heteroatoms, which are able to coordinate to six edge-sharing  $\text{MO}_6$  octahedrons. Examples are  $[\text{Te}^{\text{VI}}\text{Mo}_6\text{O}_{24}]^{6-}$  and  $[\text{X}^{\text{III}}\text{Mo}_6\text{O}_{24}]^{6-}$  that result from a ring of six octahedrons around the heteroatom.

(4) *1:9 octahedral*: These ions are structurally comprised of edge-sharing  $\text{MO}_6$  octahedrons. Examples are  $[\text{MnMo}_9\text{O}_{32}]^{6-}$  and  $[\text{Ni}^{4+}\text{Mo}_9\text{O}_{32}]^{6-}$ .

Heteropoly acids can therefore be classified as the Keggin structure (1:12), the Wells-Dawson structure (2:18), the Anderson-Evans structure (1:6), the Dexter-Silverton structure (1:9), and their derivatives, which include the transition metal substituted heteropoly anions, transition metal substituted sandwich-type heteropoly anions, lacunary structures, and the Preyssler structure.

### 2.4.1 The Keggin structure

When the Keggin structure was discovered less than a century ago, structural chemistry of polyoxometalates witnessed a turning point. During the last decades, a plethora of studies have been carried out to broaden the scope of their applications. More importantly, these studies have expanded our grasp of nanomolecular metal oxides. Table 2.4 shows the progress in the chemistry of Keggin polyoxometalates [48].

Structural similarities of molybdenum- and tungsten-based Keggin structures with many emerging metaloxo, hydroxo, and alkoxo clusters indicated the existence of common metaloxo frameworks, blurring the traditional borders of polyoxometalate chemistry.

Presently, most of the modern polyoxometalate chemistry pivots around the idea of the Keggin structure, which is representative of many heteropolymolybdates and heteropolytungstates. During 2 decades, a number of other common structures have been suggested and elucidated to provide a basis for this modern field.

The Keggin structure is the first characterized structure for HPAs which is assumed by many of them and is the best known [1]. Among a wide array of heteropoly compounds, the Keggin structures have the most stability and they are more easily available. These compounds, along with some of their derivatives, are of the most significance for catalysis purposes.

The general formula for the Keggin heteropolyanions is  $[\text{XM}_{12}\text{O}_{40}]^{n-8}$ . X is the heteroatom, n is its oxidation state, while M is an addenda atom, which is commonly  $\text{Mo}^{6+}$  or  $\text{W}^{6+}$ , but it can be many other metal ions such as  $\text{V}^{5+}$ ,  $\text{Co}^{2+}$ ,  $\text{Zn}^{2+}$ , etc. The diameter of the Keggin anion is about 1.2 nm and is located at the center of a tetrahedron  $\text{XO}_4$  enclosed by 12 edge- and corner-sharing octahedral  $\text{MO}_6$  species (Fig. 2.1). The octahedrons are positioned in four  $\text{M}_3\text{O}_{13}$  groups, each group formed by three edge-sharing octahedrons with a common oxygen atom, which also have a central tetrahedron  $\text{XO}_4$  in common. The total aggregation consists of 40 close-packed oxygen atoms. The oxygen atoms fall into four categories, i.e., 12 in terminal  $\text{M}=\text{O}$  bonds, 12 in edge-bridging angular  $\text{M}-\text{O}-\text{M}$  groups shared by the octahedron within an  $\text{M}_3\text{O}_{13}$  group, 12 in corner-bridging quasilinear  $\text{M}-\text{O}-\text{M}$  groups connecting two distinct  $\text{M}_3\text{O}_{13}$  groups, and four in internal  $\text{X}-\text{O}-\text{M}$  groups. These four types of oxygen atoms can be distinguished by the  $^{17}\text{O}$  NMR [31]. The related bonds show characteristic IR bands in the range of  $600\text{--}1100\text{ cm}^{-1}$  [31].

**TABLE 2.4** Chronology of progress in the Keggin chemistry [48].

Year 1820–1900	Year 1900–1930	Year 1930–1940	Year 1940–1980	Year 1980 till date
1826 Berzelius- Ammonium molybdate	1908 Miolati- heteroatom was octahedral coordination with $\text{MO}_4^{2-}$ or $\text{M}_2\text{O}_7^{2-}$ ligands	1933 Keggin powder X-ray diffraction of $[\text{H}_3\text{PW}_{12}\text{O}_{40}]\cdot 5\text{H}_2\text{O}$	Rigorous investigation over different types of POMs	Hundreds of POMs have been reported by different groups (especially by groups of Pope, Muller, Kortz, Hill, Newman, Cronin, Kholdeeva, Kozhevnikov, Misono, Okuhara, Moffat, Corma, Proust, Coronado, and many more)
1862 Marignac- $\alpha$ and $\beta$ isomers of tungstosilicic acid	1929 Pauling- Central $\text{PO}_4$ or $\text{SiO}_4$ tetrahedrons are surrounded by $\text{WO}_6$ octahedrons	1934 Singer and Gross- $\text{H}_4\text{SiW}_{12}\text{O}_{40}$ , $\text{H}_5\text{BW}_{12}\text{O}_{40}$ , and $\text{H}_6\text{H}_2\text{W}_{12}\text{O}_{40}$ isomorphous with Keggin structure	1977 Brown and co-workers supported results of Bradley and Illingworth by single crystal experiments	
		1936 Bradley and Illingworth- crystal structure of $\text{H}_3\text{PW}_{12}\text{O}_{40}\cdot 29\text{H}_2\text{O}$		



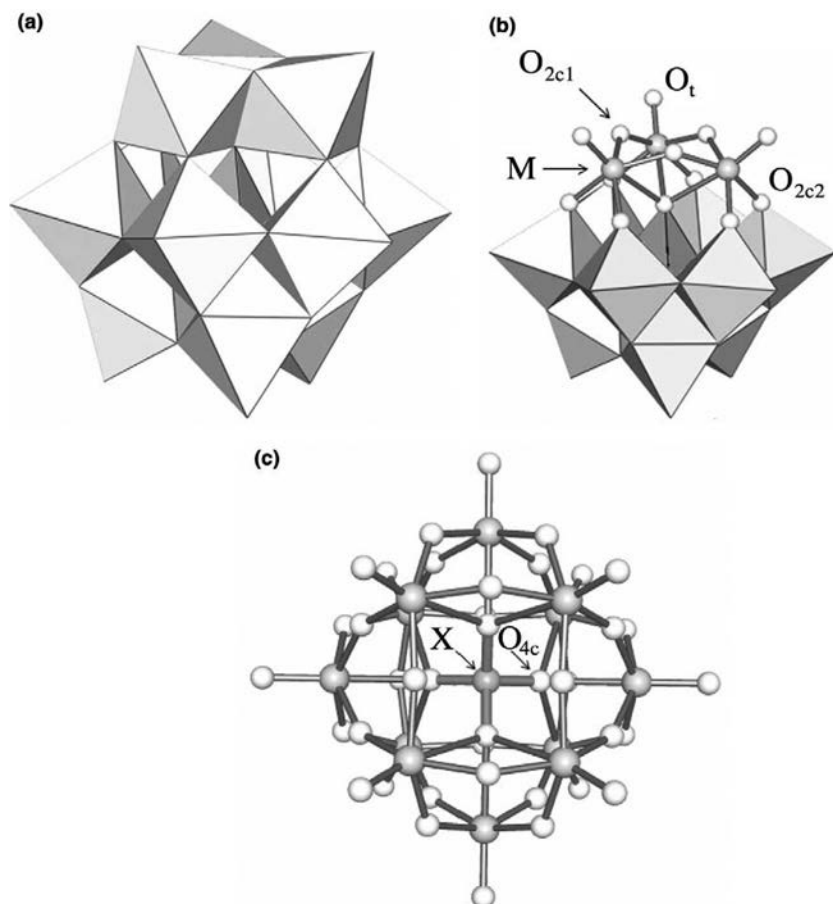
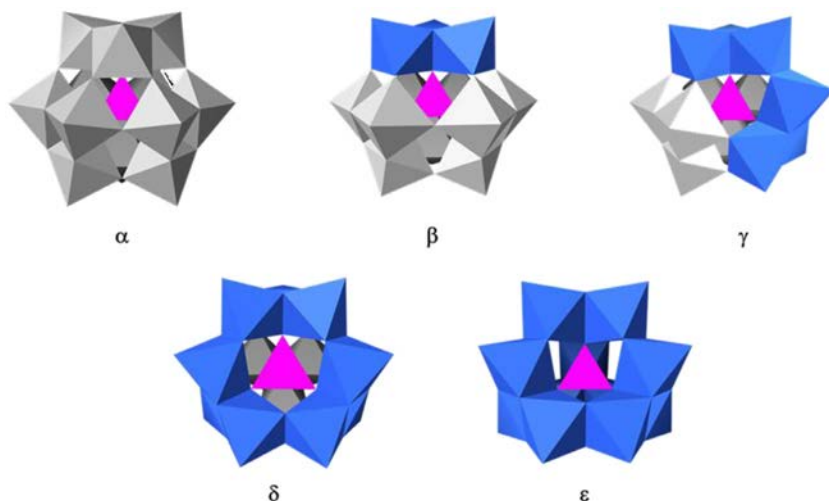


FIG. 2.1 The Keggin structure for the  $[XM_{12}O_{40}]^{n-8}$  anion (or  $\alpha$ -isomer) [49].

Rotation of each  $M_3O_{13}$  group by 60 degree about its  $C_3$  axis will result in geometrical isomers (Fig. 2.2). The structure in Fig. 2.1 is the most common  $\alpha$ -isomer of the Keggin structure. Due to rotation of one  $M_3O_{13}$  group, the  $\beta$ -isomer is created. Using methods such as fractional crystallization, these isomers can be separated in some cases.  $\gamma$ -,  $\delta$ -, or  $\epsilon$ -isomers can be produced by rotating two, three, or all four  $M_3O_{13}$ , respectively.

Measured treatment of Keggin species with a base can give rise to a lacunary species which is the result of removal of one or two MO units from the completely occupied Keggin.  $[XM_{12}O_{40}]^{n-8}$  result in mono- or di-lacunary polyoxometalates, i.e.,  $[XM_{11}O_{39}]^{(n+4)-}$  and  $[XM_{10}O_{36}]^{(n+5)-}$  [24].

Formation of such species mainly depends on pH, with each species having a particular reactivity and stability trend. Therefore, from a synthetic viewpoint, extraordinary attention is paid to even minor changes in reaction conditions



**FIG. 2.2** Polyhedral representation of the five different isomers of the Keggin anion [50].

such as pH, temperature, ionic strength, buffer capacity, and cation size, as each of the mentioned factors could potentially affect the polyanion equilibria and formation of a given product in a considerable manner [51,52].

A lacunary derivative of a Keggin anion is obtained by removing one or more M atoms, as shown in Fig. 2.3. This figure illustrates a few examples of lacunary derivatives (one monovacant and two trivacant species) of an  $\alpha$ -Keggin anion. The two trivacant species correspond to loss of a corner-shared group of the  $\text{MO}_6$  octahedron (an A-type  $[\text{XM}_9]$ ) or an edge-shared group (a B-type  $[\text{XM}_9]$ ). Such species can assemble into larger polyoxometalate structures, either directly or without incorporation of metal ion linkers.

They are also of broad applications in catalysis due to their exceptional adjustable properties at molecular levels through varying constituent elements [48].

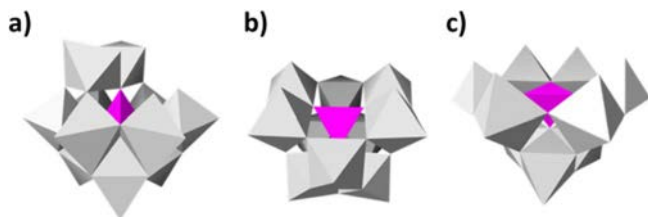


**FIG. 2.3** Polyhedral representation of different lacunary Keggin species: (A) monovacant, (B) divacant, and (C) trivacant. Color code: M, gray polyhedra and X, pink (light gray in print versions) polyhedra [50].

### 2.4.2 The Wells-Dawson structure

The Dawson anion,  $[X_2M_{18}O_{62}]^{6-}$ , consists of two truncated  $XM_9$  Keggin units [53] symmetrically assembled to form an  $X_2M_{18}$  cluster, as illustrated in Fig. 2.4. The most common compositions related to the Dawson structure are acquired from the phosphotungstate and molybdate anions ( $P_2W_{18}$ ,  $P_2Mo_{18}$ ). Species with sulfur or arsenic instead of phosphorus have been reported as well [55]. In  $P_2M_{18}$  species, like other derivatives of the Dawson structure, the 18 addenda atoms, in a local pseudo-octahedral environment, are organized in four parallel rings of three, six, six, and three metal ions each.

At variance to the highly symmetric Keggin anion, the structure presents two distinct positions: the  $M_3$  rings, located at the polar regions, are also called caps, and the two  $M_6$  rings are located at the equatorial region, forming the belt. These features result in some chemically different behaviors.

It is possible that metal addenda atoms are removed and/or substituted from the complete Dawson structure. The  $\alpha_1$  and  $\alpha_2$  isomers (the positional isomers, i.e., the shaded octahedrons in Fig. 2.5) are defined by the position at which the process takes place. In spite of high structural similarity, these isomers are chemically different in some aspects. For example, in both mono-vacant and metal substituted forms ( $P_2W_{17}$  and  $P_2W_{17}M$ , respectively),  $\alpha_1$  and  $\alpha_2$  exhibit different redox responses [56–61], basicities, and binding energies to M, which in turn result in different relative stabilities. It should be noted that the new properties of the compound are determined by the substituted atom, even though the position it takes in the final cluster is important as well.

In addition to positional isomers, Baker and Figgis postulated six rotational isomers for an  $[X_2M_{18}O_{62}]^{6-}$  anion ( $X = As^V, P^V$ ;  $M = Mo^{VI}, W^{VI}$ ) in 1970. Illustrated in Fig. 2.6, they are named as  $\alpha$ ,  $\beta$ ,  $\gamma$ , and  $\alpha^*$ ,  $\beta^*$ ,  $\gamma^*$  [62].

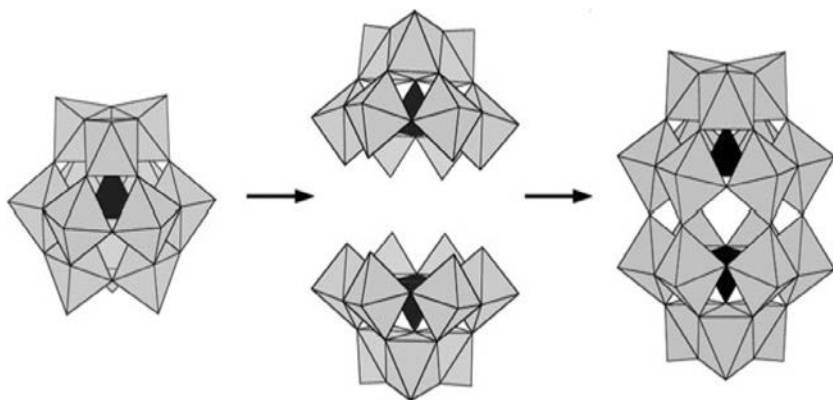
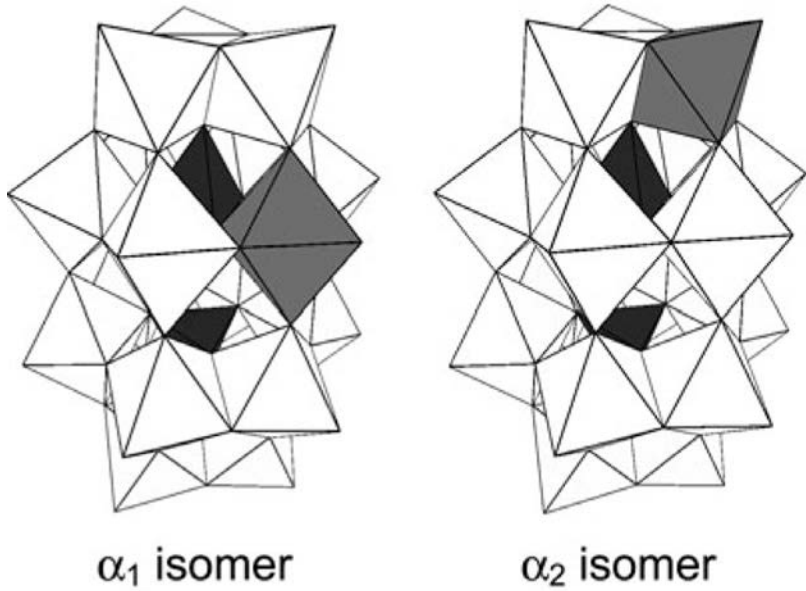
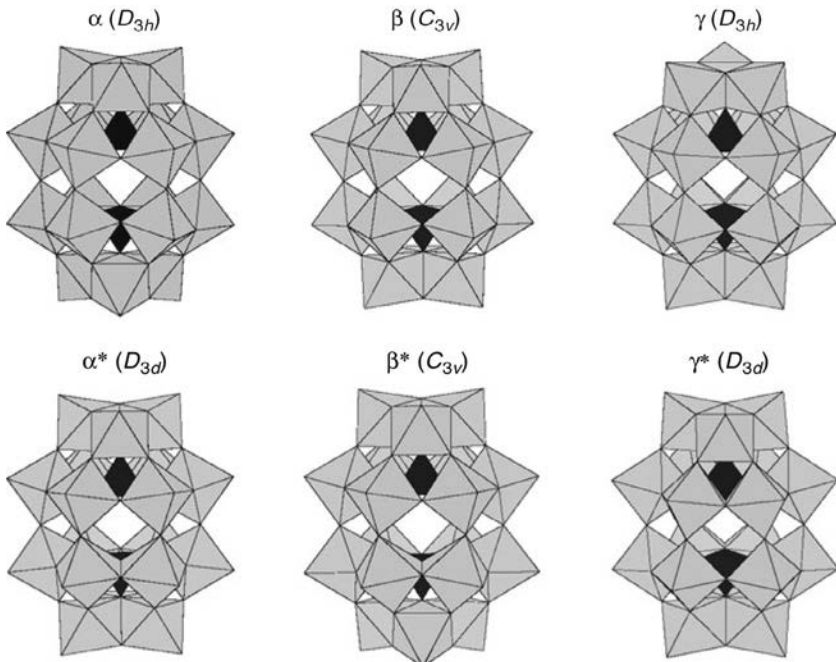


FIG. 2.4 Construction process from a  $\alpha$ -Keggin to an A- $\alpha$ -Dawson structure. Green octahedrons are  $MO_6$  units ( $M = W, Mo$ ), while black tetrahedrons represent the  $XO_4$  anions [54].



**FIG. 2.5** The two positional isomers derived from a monosubstituted Dawson anion. Substitution takes place in the belt or cap rings to yield the  $\alpha_1$  or  $\alpha_2$  isomers, respectively [54].



**FIG. 2.6** The six rotational isomers of the Dawson structure. *Top:*  $\alpha$ ,  $\beta$ ,  $\gamma$ . *Bottom:*  $\alpha^*$ ,  $\beta^*$ ,  $\gamma^*$  [54].

The  $\alpha$ - $[X_2M_{18}O_{62}]^{6-}$  anion is assembled from two A- $\alpha$ - $XM_9O_{34}$  half-units connected through six common oxygen atoms on a mirror plane. On the whole, the anion belongs to the  $D_{3h}$  symmetry group. The  $\beta$  anion is related to the  $\alpha$  isomer through the rotation of a polar  $M_3O_{13}$  group by  $\pi/3$ . The symmetry is then lowered to  $C_{3v}$ . The rotation of another polar  $M_3O_{13}$  group for a second  $\pi/3$  will restore the mirror plane and subsequently the  $D_{3h}$  symmetry for the  $\gamma$  isomer. In all cases, the hexagonal belts of the two  $XM_9$  fragments take the eclipsed conformation along the  $C_3$  axis. If an inversion center relates the two A- $\alpha$ - $PW_9O_{34}$  half-units as suggested by Wells for  $P_2W_{18}O_{62}$  in 1945 [63], the resulting anion, which is named  $\alpha^*$  will belong to the  $D_{3d}$  symmetry group. The two remaining isomers, i.e.,  $\beta^*$  ( $C_{3v}$ ) and  $\gamma^*$  ( $D_{3d}$ ), are generated due to the rotation of one or both polar  $M_3O_{13}$  groups of the  $\alpha^*$  isomer. In those cases, the hexagonal belts of both  $XM_9$  fragments are staggered along the  $C_3$  axis.

The polyoxometalate cluster  $[M_{18}O_{54}(SO_3)_2]^{3-}$  ( $M = Mo, W$ ) consisting of two embedded redox-active sulfite templates can be activated by a metallic surface and reversibly interconvert between two electronic states [64]. Both templates can be substituted by one single template located in the cluster center to give a Dawson-like  $\{W_{18}X\}$  polyoxometalate [65]. Indeed, the first discovered member of the family was an isopolyanion  $\{W_{19}\}$  with a Dawson-type cage. The 19th tungsten is situated in the center of the cluster instead of the two tetrahedral heteroatoms usually found within the usual Dawson clusters [66]. The structural analysis of this cluster reveals that the internal tungsten ion could be substituted by other elements, such as Pt(IV), Sb(V), Te(VI), or I(VII). The polyoxometalates  $\beta^*$ - $[H_3W_{18}O_{56}(IO_6)]^{6-}$  with an embedded high-valent iodine, and  $\gamma^*$ - $[H_3W_{18}O_{56}(TeO_6)]^{7-}$ , with a tellurium anion  $TeO_6^{6-}$ , were reported thereafter (Fig. 2.7) [67]. It is noteworthy that the  $[IO_6]$  unit inside the  $\{W_{18}\}$

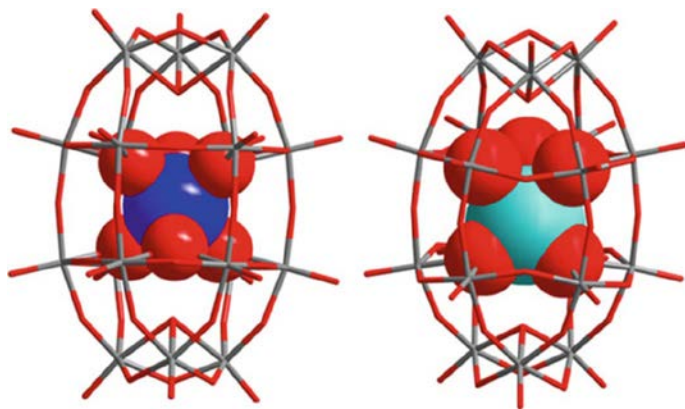


**FIG. 2.7** Structures of the new Dawson-like  $\{W_{18}X\}$  polyoxometalate. The  $\{W_{18}\}$  cages are depicted using sticks while the central  $[XO_6]$  group is shown using space-filling models. *Left:*  $\gamma^*$ - $[W_{18}O_{56}(XO_6)]^{10-}$   $X = W(VI)$  and  $Te(VI)$ . *Right:*  $\beta^*$ -  $[W_{18}O_{56}(IO_6)]^{9-}$ , which is the first example of  $\beta^*$  isomers [54].

cage has the ability to stabilize the  $\beta^*$  cage, which has been found to be rather high energy in a usual Dawson anion. The complete analysis of isomerism for these Dawson-like anions will be much more complicated when the presence of protons is considered.

### 2.4.3 The Anderson-Evans structure

An Anderson-Evans polyoxoanion consists of six edge-sharing  $\text{MoO}_6$  or  $\text{WO}_6$  octahedrons around a central, edge-sharing heteroatom of the  $\text{O}_h$  geometry ( $\text{XO}_6$ ), giving rise to a planar arrangement with an approximate final  $\text{D}_{3d}$  symmetry. The oxygen atoms have been found in three different coordination modes of such structures; six triple-bridged oxygen atoms ( $\mu_3\text{-O}$ ) link the heteroatom and two metal addenda atoms, six double-bridged oxygen atoms ( $\mu_2\text{-O}$ ) link two metal addenda atoms, and two terminal oxygen atoms ( $\text{O}_t$ ) are linked to each of the six metal addenda atoms (Fig. 2.8A, top). The general formula can be written as  $[\text{H}_y(\text{XO}_6)\text{M}_6\text{O}_{18}]^{n-}$ , where  $y = 0\text{--}6$ ,  $n = 2\text{--}8$ , M = addenda atoms (i.e., Mo(VI) or W(VI)), and X = central heteroatom [31,69,70]. In a first classification, the Anderson-Evans structures are divided into two categories: the nonprotonated species (A-type) with central heteroatoms in high oxidation states and the general formula  $[\text{X}^{n+}\text{M}_6\text{O}_{24}]^{(12-n)-}$  (e.g., X =  $\text{Te}^{\text{VI}}$  [71],  $\text{I}^{\text{VII}}$  [72]), and the protonated species (B-type) with heteroatoms in low oxidation states and the general formula  $[\text{X}^{n+}(\text{OH})_6\text{M}_6\text{O}_{18}]^{(6-n)-}$  (e.g., X = Cr(III) [73], Fe(III) [74]). The six protons in the B-type are located on the six  $\mu_3\text{-O}$  atoms around the heteroatom [31].

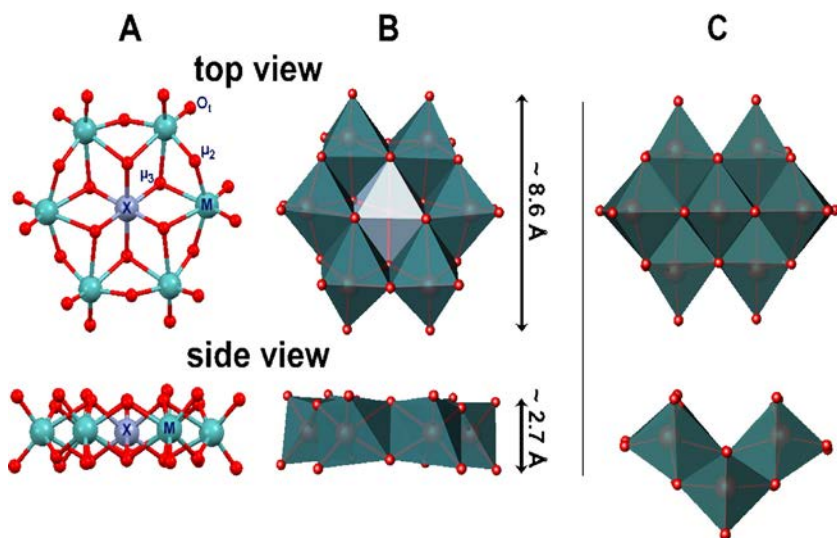


FIG. 2.8 (A) Ball-and-stick and (B) polyhedral representation of the Anderson-Evans polyoxometalates  $[\text{XM}_6\text{O}_{24}]^{n-}$  [68].



The average dimensions of the Anderson-Evans anion are about  $8.6 \times 8.6 \times 2.7 \text{ \AA}^3$  (Fig. 2.8B); an isomer of this species is heptamolybdate ( $[\text{Mo}_7\text{O}_{24}]^{6-}$ ) [68], which represents a bent structure (Fig. 2.8C). Heptamolybdate may be regarded as three edge-sharing octahedrons with two octahedrons located on each side of the cavity formed between the three octahedrons. The two octahedrons on each side are shifted by a half octahedron to furnish a bent structure (Fig. 2.8C, bottom). Structures similar to the Anderson-Evans ones have been reported with the central octahedral heteroatom substituted by trigonal pyramidal or tetrahedral atoms (such as  $\text{V}^{\text{V}}$  [75,76],  $\text{As}^{\text{V}}$ , and  $\text{Te}^{\text{IV}}$  [77,78] on each side of the planar structure, leaving the six-membered addenda ring unaffected. For color coding of the figures throughout this review, green/cyan octahedrons are used to illustrate addenda atoms that represent either Mo(VI) or W(VI) whereas red octahedrons represent Mo(VI) addenda octahedrons. Central heteroatoms are given a new color whenever a new  $\text{XM}_6$  system is discussed.

The elements found in the inorganic Anderson-Evans structures with oxidation states ranging from II to VII are highlighted in Fig. 2.9. The element X in  $\text{XM}_6$  systems (highlighted in red) involves a wider variety of heteroatoms compared to the one in  $\text{XW}_6$  systems (highlighted in green). All transition metals in the first row except Sc and Ti have been reported to serve as a heteroatom in  $\text{XM}_6$  systems. The  $\text{XW}_6$  systems exist with  $\text{Mn}^{\text{II/IV}}$  and  $\text{Ni}^{\text{II}}$  forming the B-type Anderson-Evans polyoxometalates including six hydrogen atoms, which is relatively unusual when tungsten serves as addenda atoms [80]. Surprisingly, in view of the plethora of the hybrid structures in the  $\text{Mn}^{\text{III}}\text{Mo}_6$  systems, no inorganic crystal structure exists, even though the synthesis and spectroscopic characterization have been reported [81]. Thus far, among the heavier transition metals, only noble metals have been able to enter in both

1 H																	2 He	
3 Li	4 Be											5 B	6 C	7 N	8 O	9 F	10 Ne	
11 Na	12 Mg											13 Al	14 Si	15 P	16 S	17 Cl	18 Ar	
19 K	20 Ca	21 Sc	22 Ti	23 V	24 Cr	25 Mn	26 Fe	27 Co	28 Ni	29 Cu	30 Zn	31 Ga	32 Ge	33 As	34 Se	35 Br	36 Kr	
37 Rb	38 Sr	39 Y	40 Zr	41 Nb	42 Mo	43 Tc	44 Ru	45 Rh	46 Pd	47 Ag	48 Cd	49 In	50 Sn	51 Sb	52 Te	53 I	54 Xe	
55 Cs	56 Ba	57-70 *	71 Lu	72 Hf	73 Ta	74 W	75 Re	76 Os	77 Ir	78 Pt	79 Au	80 Hg	81 Tl	82 Pb	83 Bi	84 Po	85 At	86 Rn
87 Fr	88 Ra	89-102 **	103 Lr	104 Rf	105 Db	106 Sg	107 Bh	108 Hs	109 Mt	110 Uun	111 Uuu	112 Uub	114 Uuq	*Lanthanide series **Actinide series				

FIG. 2.9 Periodic table illustrating heteroatoms in  $\text{XM}_6$  and  $\text{XW}_6$  systems and the different cation linkers successfully applied [79].



$\text{XMo}_6$  and  $\text{XW}_6$  systems (Fig. 2.9). Posttransition metals and metalloids such as  $\text{Al}^{\text{III}}$ ,  $\text{Ga}^{\text{III}}$ ,  $\text{Sb}^{\text{V}}$ ,  $\text{Te}^{\text{VI}}$ , and  $\text{I}^{\text{VII}}$  are observed in  $\text{XMo}_6$  systems while  $\text{Sb}^{\text{V}}$  and  $\text{Te}^{\text{VI}}$  are observed in  $\text{XW}_6$  systems. However, in both systems still many atoms are missing as heteroatoms while they are theoretically accessible based on their ionic radius. Noble metals such as  $\text{Ru}(\text{II/III})$  and  $\text{Rh}(\text{II})$  are not observed in either system, and many of the transition metals from the first row such as chromium, iron, cobalt, and copper are not found in the  $\text{XW}_6$  systems. Inorganic counteranions (highlighted in orange) have instead been widely explored. Most of the alkali metals and alkaline earth metals as well as the entire lanthanide series are among them.

The Anderson-Evans structures demonstrate physical and chemical properties of high versatility. However, these properties are heavily dependent on the heteroatom, counteranion, and any organic functionalization.

#### 2.4.4 The Dexter-Silverton structure

A type of 12-heteropoly anions which is less common is  $[\text{XM}_{12}\text{O}_{42}]^{n-12}$ , where M is molybdenum(VI) and X is cerium(IV), uranium(IV), or thorium(IV). It takes the arrangement illustrated in Fig. 2.10, which is known as the Dexter-Silverton structure. The molecular formula is very similar to that of the Keggin type except that it has two more oxygen atoms. In such anions, 12 oxygen atoms surround the central atom to form an icosahedron as the central polyhedron. The  $\text{MO}_6$  octahedrons are arranged in face-sharing pairs so that the anion is comprised of six  $\text{M}_2\text{O}_9$  units, each formed by two octahedrons sharing a face. The  $\text{M}_2\text{O}_9$  units in turn share corners with four adjacent  $\text{M}_2\text{O}_9$  units to construct the whole anion [4,31].

#### 2.4.5 Heteropoly anions with substituted transition metals

Modification of the precursors of parent polyoxometalates may result in the development of a new group of compounds with unparalleled structural and

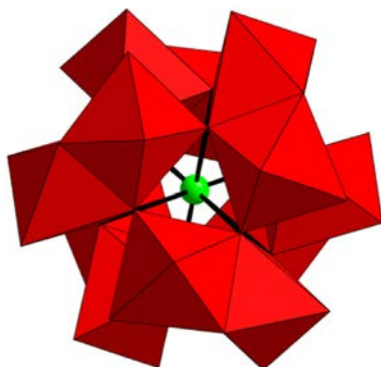


FIG. 2.10 The Dexter-Silverton structure for  $[\text{XM}_{12}\text{O}_{42}]^{n-12}$  anions [82].

electronic properties through incorporation of transition metal ions into flawed structures. The oxo ligands on the vacant sites are basic enough to react with metal cations to form a new group of compounds more commonly referred to as transition metal substituted polyoxometalates (TMSPOMs) or mixed addenda polyoxometalates. In the field of polyoxometalate chemistry, they have continuously gone through profound development and attracted growing attention [83–88] because they are rationally modifiable at a molecular level. The modification includes many aspects, e.g., size, shape, charge density, acidity, redox states, stability, and solubility, giving rise to prominent chemical properties and their ability to serve as stabilizing agents. They provide suitable platforms to stabilize unusually metal-oxo species of high oxidation states. In comparison with organometallic complexes, TMSPOMs have advantages such as: (a) robustness under oxidation conditions, while most organic ligands decompose under such conditions; (b) adjustable solubility by changing the counteranions; and (c) adjustable redox properties by changing the central heteroatom and the addenda transition metal [89]. Furthermore, the oxometalate clusters in this unique group are prominent inorganic building blocks thanks to their irrefutable structural beauty and adjustable sizes, shapes, and high negative charges [32,86,90]. They demonstrate a wide variety of structures resulting in intriguing, unexpected properties that lead to a plethora of applications.

The addenda atoms were first substituted between the late 1950s and early 1960s when different tungstocobaltates were being studied [24]. In 1966, Baker et al. proved that it was possible to form several different mixed-addenda heteropolyanions with the general formula  $[(\text{XO}_4)_m\text{M}_x\text{M}_{12-x}\text{O}_{36}]^{n-}$  [91]. In 1973, Pope et al. reported the formation of mixed-addenda  $[(\text{XO}_4)_v\text{W}_x\text{W}_{12-x}\text{O}_{36}]^{n-}$  polyanions by reaction of tungstate and vanadate precursors in aqueous media [92]. The presence of various isomeric forms was proved based on the multiple chemical shifts observed in the  $^{31}\text{P}$  NMR spectra, which could be traced to the encapsulation of phosphate groups in different configurations of shell environments of mixed oxometalates. Based on these observations, Pope et al. came to the conclusion that formation of different positional or (as it is more commonly known now) configurational isomers is quite possible. In 1975, Scully and Pope reported the unique isomer set existing for  $\alpha$ - $[(\text{XO}_4)_m\text{M}_x\text{M}_{12-x}\text{O}_{36}]^{n-}$  [93]. Afterward, Pope also reported the number of possible isomers for  $\beta$ - $[(\text{XO}_4)_m\text{M}_x\text{M}_{12-x}\text{O}_{36}]^{n-}$  in his book, *Hetero and Isopoly Oxometalates* [31].

A number of two-metal (e.g., V/W, V/Nb, V/Mo, Nb/W, Mo/W) mixed-addenda polyoxometalates with Keggin, Wells-Dawson, or Lindqvist structures have been reported as well [94–107]. For instance, the occurrence of one or more vanadium(V) centers in the W(VI) or Mo(VI) polyoxometalate framework has been demonstrated to result in extensively improved catalytic performance.  $[\text{PV}_2\text{MoO}_{40}]^{5-}$  serves as a powerful oxidation catalyst for a group of organic reactions [99,101]. The anion  $[\text{W}_6\text{O}_{19}]^{2-}$  is a rather poor nucleophile. In  $[\text{NbW}_5\text{O}_{19}]^{3-}$ , substitution of one W(VI) atom by Nb(V) to give  $[\text{Nb}_2\text{W}_4\text{O}_{19}]^{4-}$  significantly increases the reactivity, allowing the formation of POM-supported

organometallic derivatives. In recent years, the orbital engineering for Ta/W [103], Nb/W [104,105], V/Mo [106,108], and V/W [107] mixed-addenda polyoxometalates to modify the electronic structure, light absorption, and photocatalytic activity has been reported as well. The design and synthesis of novel mixed-addenda polyoxometalates with new structures and extraordinary performances remain challenges.

The Dawson type mixed-addenda (Ta/W) polyoxometalate  $\{P_2W_{15}Ta_3\}$  may be used as a nucleophilic structural building block [109]. In addition, incorporation of molybdates into  $\{P_2W_{15}Ta_3\}$  affords a ternary mixed-addenda polyoxometalate  $(NH_4)_{41}H_7[K_3(H_2O)_3(P_2W_{15}Ta_3O_{62})^6-(Mo_2O_4CH_3CO_2)_3(MoO_3)_2] \cdot 85 H_2O$  [110] prepared by reducing a mixture of  $K_5Na_4[P_2W_{15}O_{59}(TaO_2)_3] \cdot 17H_2O$  and  $(NH_4)_6Mo_7O_{24} \cdot 4H_2O$  (or  $Na_2MoO_4 \cdot 2H_2O$ ) with  $N_2H_4$  (Fig. 2.11).

Fine-tuning of the electronic [15], electrochemical [111], photochemical [112], and catalytic properties [113] of mixed-addenda polyoxometalates is

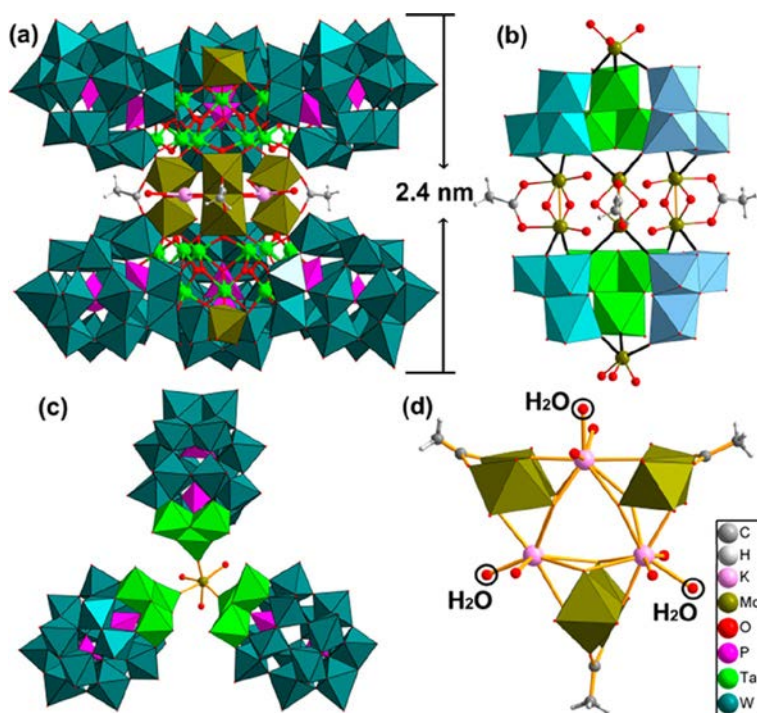


**FIG. 2.11** Combined polyhedral/ball-and-stick representation (A, the teal and pink (gray and light gray in print versions) polyhedrons represent  $WO_6$  and  $PO_4$ , respectively) polyhedrons represent  $WO_6$  and  $PO_4$ , respectively); the coordination models of  $\{MoV_2O_4(OOCH_3)_3\}^+$  and  $\{MoVIO_3\}$  with six  $\{Ta_3\}$  clusters (B, the  $\{Ta_3\}$  clusters are shown in different colors, three  $K^+$  cations are omitted for clarity); the triangular  $\{[P_2W_{15}Ta_3]Mo\}$  subunits (C) and the connection of three  $[K(H_2O)]^+$  and three  $\{Mo_2Ac\}$  (D) [110].

achieved by changing the type and ratios of the addenda atoms. This makes them attractive in designing new compounds with a wide array of applications.

### 2.4.6 Transition metal substituted sandwich-type polyoxometalate

A very common approach in the synthesis of novel polyoxoanions has been the treatment of lacunary heteropolyanions with transition metals. The approach requires the production of highly negatively charged (accordingly soluble) intermediate fragments, which can subsequently be stabilized by electrophilic groups or linked together through polycondensation reactions (Fig. 2.12) [117–119].

Polyoxoanions with heteroatoms having an unshared pair of electrons, e.g.,  $\text{As}^{\text{III}}$ ,  $\text{Sb}^{\text{III}}$ ,  $\text{Bi}^{\text{III}}$ ,  $\text{Se}^{\text{IV}}$ , and  $\text{Te}^{\text{IV}}$ , are particularly interesting. The lone pair of electrons impedes the formation of the closed Keggin heteroanion, resulting in the formation of polymeric polyoxoanions. For instance,  $\text{Na}_2\text{WO}_4$  and  $\text{Sb}_2\text{O}_3$  react in aqueous solution at pH 7.5 to form the trivacant Keggin anion  $[\text{SbW}_9\text{O}_{33}]^{9-}$ . Because of its charge, the  $[\text{SbW}_9\text{O}_{33}]^{9-}$  can either be stabilized by a counteranions or go through further condensation upon protonation to form huge inorganic clusters like the  $[\text{Na}_2\text{Sb}_8\text{W}_{36}\text{O}_{132}(\text{H}_2\text{O})_4]^{22-}$  anion which is a combination of four  $[\text{SbW}_9\text{O}_{33}]^{9-}$  fragments with  $\text{Na}^+$  and  $\text{Sb}^{3+}$  as counteranions between them. Besides, upon the addition of more electrophilic groups to the reaction mixture of  $\text{WO}_4^{2-}$  and/or  $\text{M}^{n+}$  ( $\text{M} = \text{Fe}^{3+}$ ,  $\text{Co}^{2+}$ ,  $\text{Mn}^{2+}$ ,  $\text{Ni}^{2+}$ ), novel heteroanions of the general formula  $[\text{Sb}_2\text{W}_{20}\text{M}_2\text{O}_{70}(\text{H}_2\text{O})_6]^{(14-2n)-}$  are afforded in which two  $[\text{SbW}_9\text{O}_{33}]^{9-}$  fragments are connected by two  $\text{M}^{n+}(\text{H}_2\text{O})$  as well as two  $\text{WO}_2\text{OH}$  groups [114]. More examples of dimeric polyanions made of two

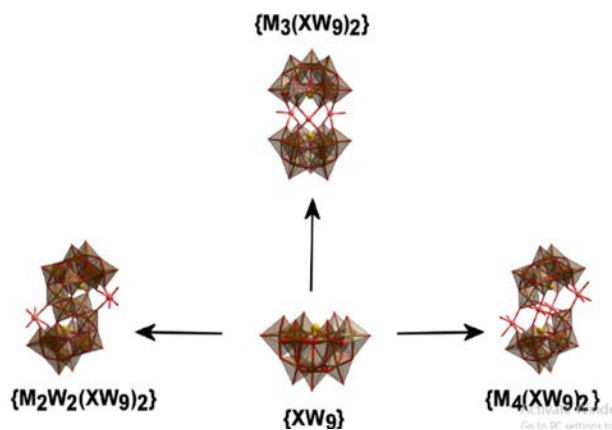


FIG. 2.12 Summaries of the different heteropolyanions derived from the reaction of a trivacant lacunary precursor  $\{\text{XW}_9\}$  with different transition metal ions and lanthanides. The interaction of the lacunary  $\{\text{XW}_9\}$  Keggin anion with transition metals results in the formation of polyanions of sandwich type, e.g.,  $\{\text{M}_2\text{W}_2(\text{XW}_9)_2\}$ ,  $\{\text{M}_3(\text{XW}_9)_2\}$ , and  $\{\text{M}_4(\text{XW}_9)_2\}$  in which the two  $\{\text{XW}_9\}$  fragments are linked via two, three, or four metal atoms [114–116].

$\{XMo_9O_{33}\}^{n-}$  lacunary building units ( $X = As^{III}, Sb^{III}, Bi^{II}, Se^{IV},$  and  $Te^{IV}$ ) with analogous archetypes may be found in the literature [115,116,120].

Formal metal addenda substitution in the matrix of a bulk metal oxide has been a powerful approach to produce a plenty (non)stoichiometric all-inorganic species with adjustable electronic and magnetic properties, and extensive technological applications for decades. These mixed-addenda oxometalate clusters are crucial among the classical heteropoly anions archetypes (i.e., those without vacant metal sites), which have growing applications in homogeneous catalysis as well as materials science (e.g., in generation of open frameworks). They have also been studied extensively in heterogeneous metal organic framework (MOF) catalysts and the synthesis of sandwich-type polyoxometalates.

Tourne et al. reported a sandwich-type polyoxometalate in 1973 for the first time to open a new chapter in the field of polyoxometalates [121]. As illustrated in Fig. 2.13, the new polyoxometalate was formulated as  $[P_2Co_4(H_2O)_2W_{18}O_{68}]^{10-}$ . The four cobalt atoms were observed to be actually sandwiched between two lacunary trivacant Keggin units composed of  $(PW_9O_{34})^9-$  fragments.

Shortly after the introduction of this heteropoly anion, a wide range of other sandwich-type POMs with similar structures, with different central atoms and transition metal ions, were reported. Some of the eminent examples are:  $[M_4(H_2O)_2(XW_9O_{34})_2]^{n-}$  ( $n = 6, X = P^V, As^V, M = Fe^{3+}; n = 10, X = P^V, As^V,$

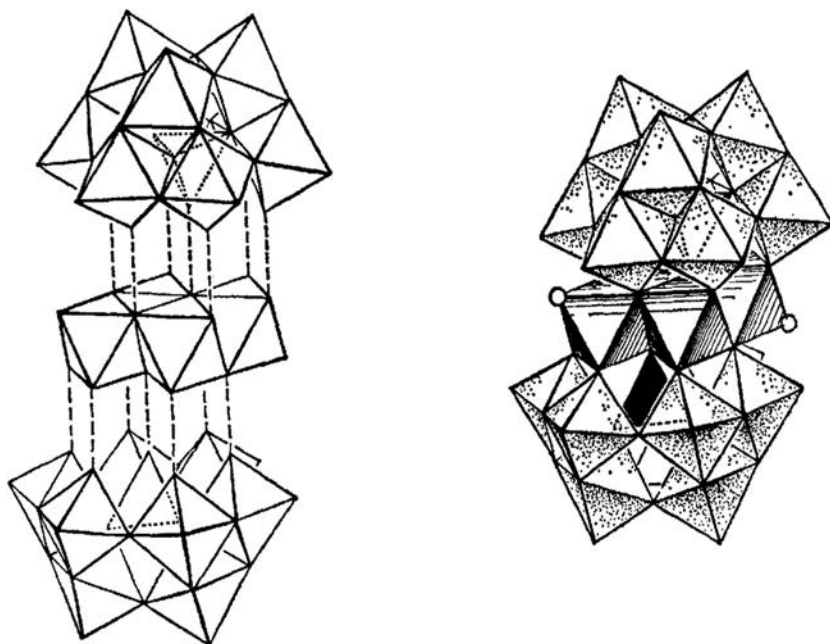


**FIG. 2.13** The  $[P_2Co_4(H_2O)_2W_{18}O_{68}]^{10-}$  anion in which Co atoms occupy the central octahedrons with circles representing water molecules [121].

$M = \text{Mn}^{2+}, \text{Co}^{2+}, \text{Ni}^{2+}, \text{Cu}^{2+}, \text{Cd}^{2+}$ ;  $n = 12$ ,  $X = \text{Ge}^{\text{IV}}, \text{Si}^{\text{IV}}$ ,  $M = \text{Mn}^{2+}, \text{Cu}^{2+}, \text{Zn}^{2+}, \text{Cd}^{2+}$ ; and  $n = 14$ ,  $X = \text{Ga}^{\text{III}}$ ,  $M = \text{Cu}^{2+}, \text{Zn}^{2+}$ ) [122–141]. In every case, the central atom adopts a tetrahedral geometry.

As shall be seen further, more sandwich-type heteropoly anions similar to the abovementioned heteropoly anions with different structures were reported as well. As a substantial difference between these HPAs and the above sandwich-type HPAs, the central atom geometry was pyramidal. Furthermore, in these POMs, depending on the central atom and the transition metal atoms, three or four transition metal ions may be sandwiched between the two lacunary trivalent Keggin fragments. Fig. 2.14 represents the structures for these two kinds of HPAs. Examples of three transition metal ions sandwiched between two lacunary trivalent Keggin fragments are  $[\text{M}_3(\text{H}_2\text{O})_3(\text{XW}_9\text{O}_{33})_2]^{n-}$  ( $n = 10$ ,  $X = \text{Se}^{\text{IV}}, \text{Te}^{\text{IV}}$ ,  $M = \text{Cu}^{2+}$ ;  $n = 12$ ,  $X = \text{As}^{\text{III}}, \text{Sb}^{\text{III}}$ ,  $M = \text{Mn}^{2+}, \text{Co}^{2+}, \text{Ni}^{2+}, \text{Cu}^{2+}, \text{Zn}^{2+}$ ) and  $[(\text{VO})_3(\text{XW}_9\text{O}_{33})_2]^{n-}$  ( $n = 11$ ,  $X = \text{As}^{\text{III}}$ ;  $n = 12$ ,  $X = \text{As}^{\text{III}}, \text{Sb}^{\text{III}}, \text{Bi}^{\text{III}}$ ) [142–149].

The sandwich-type anion  $[\text{Ni}_4\text{V}_{10}\text{O}_{30}(\text{OH})_2(\text{H}_2\text{O})_6]^{4-}$  consists of a central  $\text{Ni}^{2+}$  tetramer of four  $\text{NiO}_6$  octahedral units surrounded by 10  $\text{VO}_4$  tetrahedrons linked to each other via shared corners [150]. Recently, cyclic sandwich polyoxovanadates  $[\text{Co}_2(\text{H}_2\text{O})_2\text{V}_{10}\text{O}_{30}]^{6-}$  and  $[\text{Mn}_2\text{V}_{10}\text{O}_{30}]^{6-}$  have been reported (Fig. 2.15) [152]. In the former, a decavanadate ring is connected to two  $\text{CoO}_6$  octahedral units that occupy the center of the ring and are linked to each other

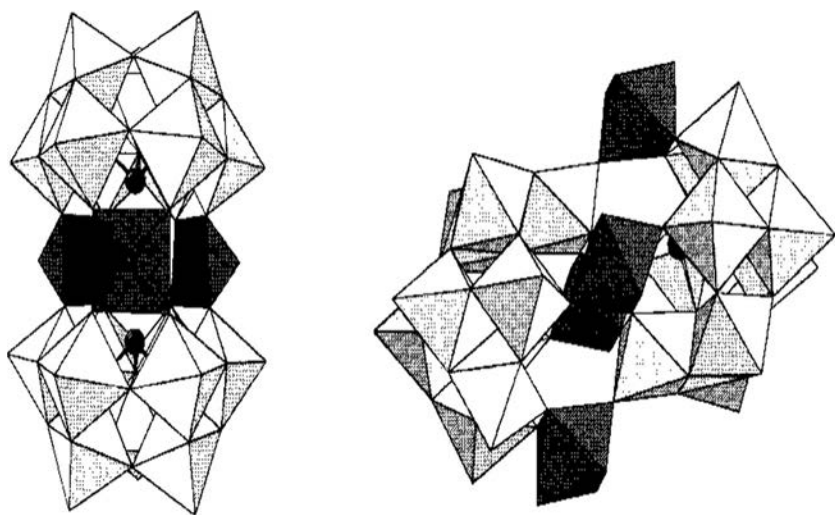


**FIG. 2.14** Structures of sandwich-type heteropoly anions with three (*left*) and four (*right*) transition metal atoms sandwiched between two lacunary trivalent Keggin fragments, with pyramidal central atoms (denoted by *black circles* in the lacunary trivalent Keggin fragment). The *black polyhedrons* illustrate the transition metal polyhedrons, which are square pyramidal in the case of “left,” and octahedral in the case of “right” [142].



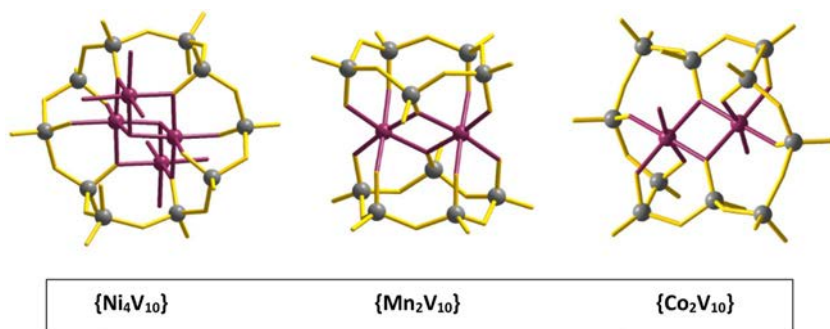


**FIG. 2.15** Ball-and-stick models for three cyclic polyoxovanadates with octahedral addendas. (A)  $[\text{Ni}_4\text{V}_{10}\text{O}_{30}(\text{OH})_2(\text{H}_2\text{O})_6]^{4-}$ , (B)  $[\text{Mn}_2\text{V}_{10}\text{O}_{30}]^{6-}$ , (C)  $[\text{Co}_2(\text{H}_2\text{O})_2\text{V}_{10}\text{O}_{30}]^{6-}$  (right). The  $\text{XO}_6$  octahedrons are represented by *purple* (light gray in print versions) spheres while *gray* spheres denote the  $\text{VO}_4$  tetrahedrons. For clarity, the oxygen atoms have been eliminated [151].

via shared edges, whereas the latter is made of two  $\text{V}_5$  rings linked together via bridging oxygen atoms from two  $\text{MnO}_6$  octahedral units. In both cases, all the vanadate units take tetrahedral geometries linking to each other via shared corners.

The inclusion of sulfur atoms into the polyoxoanionic framework leads to the isolation of unusual polyoxometalates archetypes, which are called thiometalates. These species exhibit unique chemical properties. The first thiometalate was isolated by sulfurization of a Keggin unit formed previously. However, modern synthetic strategies for the preparation of such compounds are based on the self-condensation of  $[\text{M}_2\text{S}_2\text{O}_2]^{2+}$  fragments in the presence or absence of guest species [153].

The acid-base self-condensation of the  $[\text{M}_2\text{S}_2\text{O}_2]^{2+}$  building units leads to the formation of cyclic molecules such as  $[\text{Mo}_{10}\text{S}_{10}\text{O}_{10}(\text{OH})_{10}(\text{H}_2\text{O})_{10}]$  and  $[\text{Mo}_{12}\text{S}_{12}\text{O}_{12}(\text{OH})_{12}(\text{H}_2\text{O})_6]$  (Fig. 2.16, left) [154]. These clusters provide a cationic cavity that may be filled with anions like phosphates or carboxylates (Fig. 2.16, right). These species have been demonstrated to be capable of being used as templates to tune the nuclearity of the inorganic host [155].

On the other hand, polyoxometalates containing lanthanide atoms of high nuclearity have been studied as well. Because of their oxophilicity and multiple coordination prerequisites, lanthanide cations are appropriate for connection of polyoxometalates together and forming new compounds with larger metal-oxygen frameworks. For instance, by the addition of stoichiometric amounts of tungstate, arsenite, and cerium in acidified aqueous solution, the largest heteropolytungstate anion is afforded, which contains a cyclic  $[\text{As}_{12}\text{Ce}_{16}(\text{H}_2\text{O})_{36}\text{W}_{148}\text{O}_{524}]^{76-}$  anion [156], while the addition of  $\text{Yb}^{3+}$  and  $\text{Gd}^{3+}$  gives the polyoxoanions  $[\text{Yb}_{10}\text{As}_{10}\text{W}_{88}\text{O}_{308}(\text{OH})_8(\text{H}_2\text{O})_{28}(\text{OAc})_4]^{40-}$  and  $[\text{Gd}_6\text{As}_6\text{W}_{65}\text{O}_{229}(\text{OH})_4(\text{H}_2\text{O})_{12}(\text{OAc})_2]^{38-}$ , respectively [157].



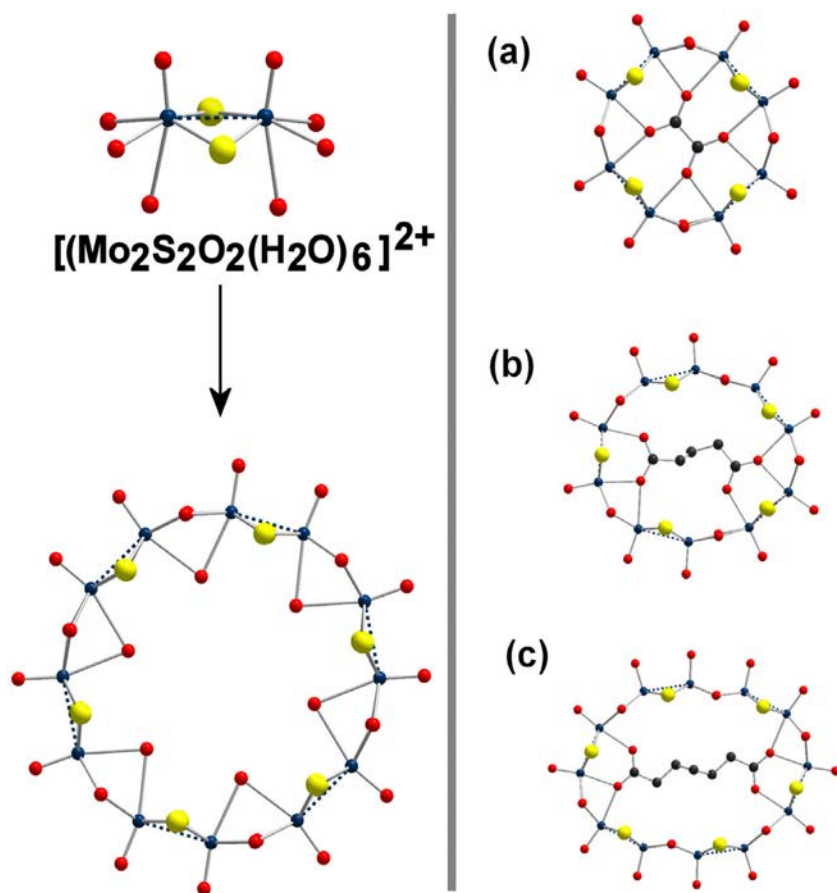


**FIG. 2.16** Ball-and-stick representation for the self-assembly of the  $[\text{Mo}_{12}\text{S}_{12}\text{O}_{12}(\text{OH})_{12}(\text{H}_2\text{O})_6]$  ring (left) from the building blocks of  $[(\text{Mo}_2\text{S}_2\text{O}_2(\text{H}_2\text{O})_6)]^{2+}$ . Rings containing polycarboxylate units (right). (A)  $[\text{Mo}_8\text{S}_8\text{O}_8(\text{OH})_8(\text{C}_2\text{O}_4)]^{2-}$ , (B)  $[\text{Mo}_{10}\text{S}_{10}\text{O}_{10}(\text{OH})_{10}(\text{H}_6\text{C}_5\text{O}_4)]^{2-}$ , and (C)  $[\text{Mo}_{12}\text{S}_{12}\text{O}_{12}(\text{OH})_{12}(\text{H}_{10}\text{C}_7\text{O}_4)]^{2-}$  [151].

### 2.4.7 The Preyssler structure

As a pioneering instance of polyoxometalates with an internal cavity,  $[\text{NaP}_5\text{W}_{30}\text{O}_{110}]^{14-}$  was first reported in 1970 by Preyssler [158] and structurally resolved using X-ray diffraction by Pope et al. 15 years later [159]. However, while a wide array of unusual anion clusters have been reported [160], only three species— $[\text{NaSb}_9\text{W}_{21}\text{O}_{86}]^-$  [161],  $[\text{NaAs}_4\text{W}_{40}\text{O}_{140}]^{25-}$  [162], and  $[\text{NaP}_5\text{W}_{30}\text{O}_{110}]^{14-}$  [163]—have been reported to encapsulate a rare-earth ion. In the latter case,  $[\text{NaP}_5\text{W}_{30}\text{O}_{110}]^{14-}$ ,  $\text{Na}^+$  is encapsulated inside a central cavity formed by five  $\text{PW}_6\text{O}_{22}$  fragments configured in a crown shape [163]. A schematic is depicted in Fig. 2.17.

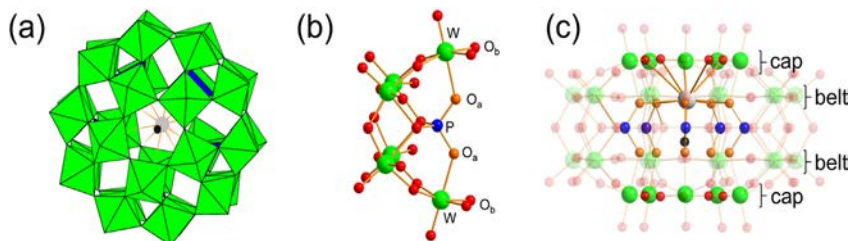


**FIG. 2.17** (A) Polyhedral representation of a Preyssler-type phosphotungstate molecule with one encapsulated cation. (B) Ball-and-stick representation of one-fifth of the Preyssler-type phosphotungstate [PW<sub>6</sub>O<sub>22</sub>] unit. Ball-and-stick representation of a (C) mono-cation-encapsulated Preyssler-type molecule [164].

The anions look like ellipsoids (prolate spheres), each made of five PW<sub>6</sub> units arranged in a crown shape in a way that the anion has an internal C<sub>5</sub> symmetry axis (Fig. 2.18). A mirror plane perpendicular to this axis entails the five phosphorus atoms. The tungsten atoms are distributed among four parallel planes perpendicular to this axis so that each outer plane entails five tungsten atoms while each inner plane entails 10 tungsten atoms. Each PW<sub>6</sub> contains two groups of three corner-shared WO<sub>6</sub> octahedrons. Two pairs of octahedrons of

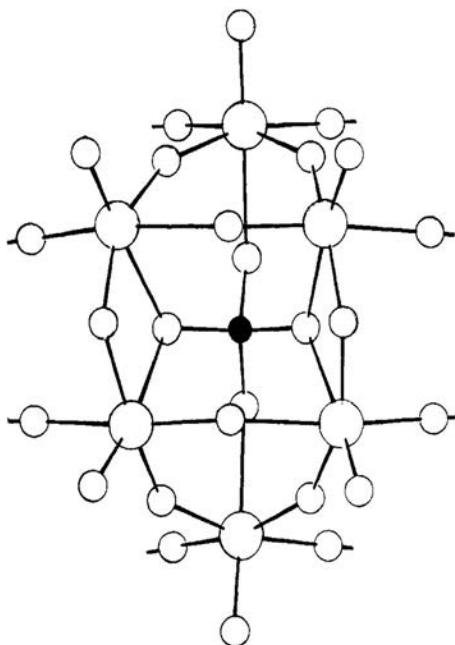


**FIG. 2.18** The PW<sub>6</sub>O<sub>22</sub> unit viewed perpendicular to the anion's virtual C<sub>5</sub> axis. Oxygen and tungsten atoms are represented by the large and small open circles, respectively, and the phosphorus atom by the closed circle [159].

each group are linked through one shared edge settled in the mirror plane. As depicted in Fig. 2.18, each  $\text{WO}_6$  octahedron shares an apex with the core  $\text{PO}_4$  tetrahedron. The  $\text{PW}_6$  unit has the well-known Keggin structure. Upon removing a corner-shared  $\text{W}_3\text{O}_{13}$  fragment from the latter, the structure of the  $\text{PW}_9$  fragment of the  $\text{P}_2\text{W}_{18}$  is (a Dawson anion) created. Removing a second such  $\text{W}_3$  group results in the formation of the  $\text{PW}_6$  unit in  $\text{P}_5\text{W}_{30}$  (Fig. 2.19). Each  $\text{PW}_6$  unit is linked to two more such fragments by eight oxygen atoms making only corner-shared octahedrons. As in the Keggin and Dawson structures, all tungsten atoms are enclosed by oxygen atoms in an octahedral geometry. Each octahedron has only one  $\text{W}=\text{O}$  double bond pointing to the exterior of the anion.

The 30 tungsten atoms may be categorized as axial and equatorial (labeled as 1 and 2 in Fig. 2.20A, respectively). There are ten axial and twenty equatorial centers distributed among four parallel rings. The doughnut-like structure of this anion provides a cavity wide enough to encapsulate an  $\text{Na}^+$  cation (Fig. 2.20B). After that, it was demonstrated that a water molecule was linked to the internal metal ion [166]. Nevertheless, this feature is not very important because for most of Preyssler's properties, the internal water molecule only slightly changes the orbital energies of the polyoxometalate framework. Also, the synthesis and structure of  $\{[\text{Sn}(\text{CH}_3)_2]_4(\text{H}_2\text{P}_4\text{W}_{24}\text{O}_{92})_2\}^{28-}$  have been reported [167]. This molecule can be regarded as a lacunary derivative of the Preyssler anion with an empty hydrophobic cavity in the center of the cluster. The central  $\text{Na}^+$  may be substituted by other cations of similar size under hydrothermal conditions [168]. The anion has shown to be quite helpful in nuclear waste treatment as it has the ability to capture lanthanide/actinide cations from neutral aqueous solutions of high salt content in a selective manner [168d]. Cations already incorporated into the internal cavity are trivalent lanthanides like  $\text{La}^{3+}$ ,  $\text{Ce}^{3+}$ ,  $\text{Nd}^{3+}$ ,  $\text{Eu}^{3+}$ , etc., as well as tetravalent actinides like  $\text{U}^{4+}$  [169]. Preyssler anions have

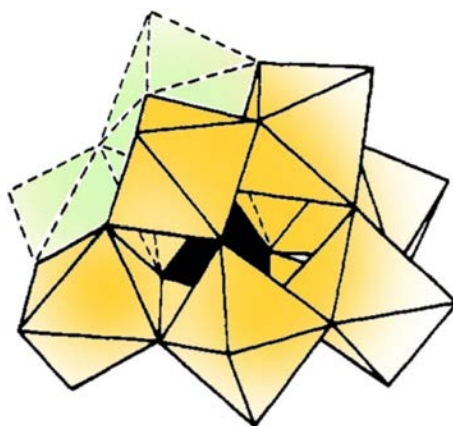
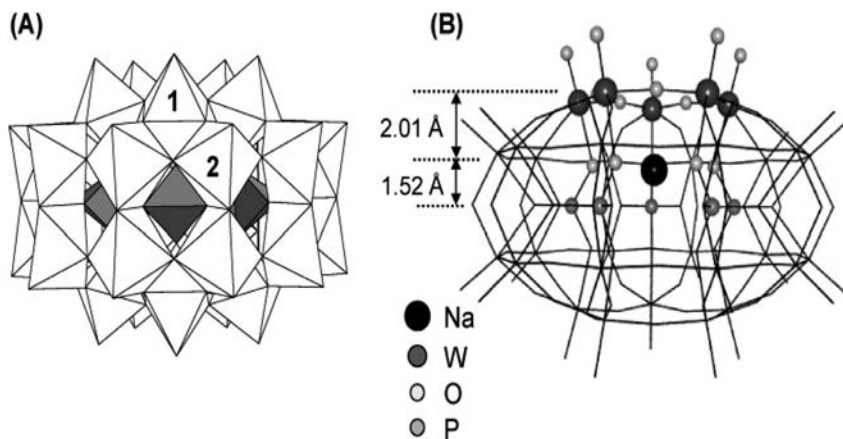


FIG. 2.19 Polyhedral representation showing the relationship of the  $\text{PW}_6$  unit to the  $\text{PW}_9$ , half-Dawson anion [159].



**FIG. 2.20** Polyhedral (A) and ball-and-stick (B) representations of the Preyssler anion  $[\text{NaP}_5\text{W}_{30}\text{O}_{110}]^{14-}$ . The internal cavity in which the  $\text{Na}^+$  ion is shifted off the center toward a five-fold coordination of oxygen atoms is apparent in the latter. The values, in angstroms, indicate the distances from the sodium atom to the planes constituted by five phosphorous atoms and five axial tungsten atoms [165].

also been tested in catalysis processes [170]. Many authors have predicted a brilliant future for the Preyssler anion as a green catalyst [171], based on its ability to replace the existing corrosive mineral acids, which are environmentally hazardous as well.

## 2.5 General properties

Given the large possibilities of sizes, structures, and elemental compositions in which polyoxometalates can be produced, they may demonstrate a wide variety of properties, with a molecular identity maintained both in solutions and in the solid state.

### 2.5.1 Solubility

Chemistry of HPAs is a prominent field in modern inorganic chemistry with extensive applications in catalysis, photochemistry, oxidation chemistry, and biochemistry. They have also found value as inorganic drugs [172,173]. While the chemistry of metal oxides in solution is generally limited given their limited solubility, HPAs are important exceptions that form an unparalleled class of compounds with particular properties. While the insoluble metal oxides crystallize in close-packed arrangements of oxide ions to form infinite chains, sheets, or three-dimensional lattices, the HPAs form discrete anions with high symmetries [174]. The potential analogy between the solid-state chemistry of the metal oxides and the solution chemistry of large polyoxoanions has given the latter the title pseudoliquid phase [175]. These isolated anions are water-soluble

species with charges ranging from  $-3$  to  $-14$ . In general, their surface basicity is believed to be rather weak so that most of the charge is concentrated on the oxygen atoms below the surface [176]. In harmony with the low surface charge density, in the presence of an appropriate counteranion, HPAs are soluble in organic solvents of various polarities spanning a range from dimethyl sulfoxide to benzene [177].

The acid properties of heteropoly acids in solution have been well documented based on dissociation constants and Hammett acidity function [178]. HPAs are highly soluble in polar solvents such as water, and lower alcohols, ketones, ethers, etc. However, they are not soluble in nonpolar solvents. Heteropoly acids such as  $\text{H}_3\text{PW}_{12}\text{O}_{40}$ ,  $\text{H}_4\text{SiW}_{12}\text{O}_{40}$ , and  $\text{H}_3\text{PMo}_{12}\text{O}_{40}$  are totally dissociated aqueous solutions. As a result of the leveling influence of the solvent, a stepwise dissociation is not observable.

As listed in Table 2.5, heteropoly acids in solution are stronger than the usual mineral acids such as  $\text{H}_2\text{SO}_4$ ,  $\text{HCl}$ , or  $\text{HNO}_3$ . The acidity of the Keggin heteropoly acids weakly depends on their compositions. Tungsten acids are remarkably stronger than molybdenum acids. The acidities of concentrated solutions of HPAs based on the Hammett acidity function also weakly depends on their compositions being stronger than that of equimolar solutions of  $\text{H}_2\text{SO}_4$ .

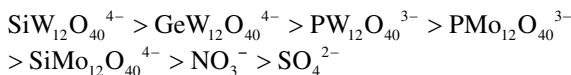
The acid strength and catalytic activity of a Brønsted acid is best quantified in terms of its dissociation constants as well as the Hammett acidity function. However, other characteristics, e.g., the hardness of the acid or the softness of its corresponding base, are among the significant parameters in the hard/soft acid/base theory, and related to the polarizability of the species. Therefore, they are generally applied to Lewis acids and bases [179].

**TABLE 2.5** Dissociation constants for heteropoly acids in acetone at 25°C [178].

	$\text{p}K_1^a$	$\text{p}K_2$	$\text{p}K_3$
$\text{H}_3\text{PW}_{12}\text{O}_{40}$	1.6	3	4
$\text{H}_4\text{PW}_{11}\text{VO}_{40}$	1.8	3.2	4.4
$\text{H}_4\text{SiW}_{12}\text{O}_{40}$	2	3.6	5.3
$\text{H}_3\text{PMo}_{12}\text{O}_{40}$	2	3.6	5.3
$\text{H}_4\text{SiMo}_{12}\text{O}_{40}$	2.1	3.9	5.9
$\text{H}_2\text{SO}_4$	6.6		
$\text{HCl}$	4.3		
$\text{HNO}_3$	9.4		

<sup>a</sup> $\text{p}K_1 = -\log K_1$ ,  $\text{p}K_2 = -\log K_2$ ,  $\text{p}K_3 = -\log K_3$ .

The characteristics of Keggin anions are their weak basicity and great softness [180]. The softness of HPAs is believed to play a key role in stabilizing organic intermediates. The following order of softness was estimated for a number of heteropoly anions in aqueous solution:



### 2.5.1.1 Solubility in water

In general, most free acids are excessively (up to 85% by weight of solution) soluble in water. In addition, heteropoly salts with small cations, including the ones containing many heavy metals, are generally quite soluble. Heteropoly anions with larger countercations are less soluble. Therefore,  $\text{Cs}^+$ ,  $\text{Ag}^+$ ,  $\text{Tl}^+$ ,  $\text{Hg}^{2+}$ ,  $\text{Pb}^{2+}$ , and larger alkaline earth metal salts are mostly insoluble. The  $\text{NH}_4^+$ ,  $\text{K}^+$ , and  $\text{Rb}^+$  salts of several important series of HPAs are insoluble. Salts of heteropolymolybdates and heteropolytungstates with cationic coordination complexes, alkaloids, or organic amines are usually insoluble. Solubility of heteropoly compounds in water is attributed to the very low lattice energies and strong solvation of the cations. Solubility is governed by the packing patterns in the crystals. The countercations occupy the cavities between large anions. When there are huge cations such as  $\text{Rb}^+$  or  $\text{Cs}^+$ , they allow stable packing in large interstices, decreasing the lattice energy enough to produce insolubility.

One of the most basic roles of the countercations in the chemistry of HPAs is solubility tuning. While many applications rely on solubility of the species in various solvents, others require insolubility, say, to prevent leaching from a material or device. Therefore, knowing solubility trends is an important aspect of HPA chemistry, which is useful in crystallization, purification, or colloid stabilization.

Based on the effects of HPAs on the solution stability of macromolecules, one can conclude that these anions enjoy a colossal hydration shell showing high polarizability and low charge density [15,181]. Consider the Keggin anion  $[\text{SiW}_{12}\text{O}_{40}]^{4-}$ . Whereas the total charge is relatively high (4-), the charge density, i.e., charge divided by number of atoms, is rather low ( $-4/53 = -0.075$ ). In comparison, for conventional anions such as sulfate and chloride, charge density is  $-2/5$  ( $-0.4$ ) and  $-1$ . Furthermore, in comparison of the charge density trends for different classes of polyoxometalates, recently the ratio charge to number of metal atoms ( $q/M$ ) has been introduced as an important reactivity criterion [182,183]. For instance, tungstates with W(VI) feature low  $q/M$  ratios (e.g.,  $[\text{PW}_{12}\text{O}_{40}]^{3-}$ ,  $q/M = 0.25$ ;  $[\text{P}_2\text{W}_{18}\text{O}_{62}]^{6-}$ ,  $q/M = 0.33$ ), while the Nb(V) species like  $[\text{Nb}_6\text{O}_{19}]^{8-}$  feature  $q/M = 1.33$ . In brief, these properties cause the polyoxometalates to be chaotropic anions [184], meaning disrupting hydrogen bonding in aqueous solvents [181,185,186], so that they facilitate the precipitation of macromolecules like neutral surfactants, polymers, and proteins from water. Since HPAs are employed with a broad range of solvents, the solvation

energies of the polyoxometalate anion as well as the corresponding cation must be carefully taken into account, since it is essentially the interplay between solvation energies and lattice energies of the respective salt that tunes the solubility of the species in question.

Solubility is determined by cation-anion interactions and specific natures of such interactions in solution. Interestingly, solubility trends from various polyoxometalate-cation pairs are significantly varied depending on the polyoxometalate type. Polyoxometalates of Group 5/6 which are formed in acid (V, Mo, and W) show high aqueous solubility when paired with small alkali metal cations (e.g.,  $\text{Li}^+$  and  $\text{Na}^+$ ), while their salts with larger alkali metal cations (e.g.,  $\text{Cs}^+$ ) often exhibit poor solubility in water (Fig. 2.21).

This alleged normal solubility trend is predictable, because small cations (such as  $\text{Li}^+$ ) have a large hydration shell which is strongly bound and cannot be in close contact with polyoxometalates that have low charge densities. Precipitation initiated by ion-pairing is therefore prohibited. Furthermore, lack of enough contacts and poor packing in the solid state results in a low lattice stabilization energy, rendering precipitation energetically less preferred. This is while large cation like  $\text{Cs}^+$  can readily have electrostatic interactions with polyoxometalates and form insoluble aggregates. This very feature of polyoxometalates is employed in heterogeneous catalysis [188]. Such polyoxometalates may be soluble in organic solvents (aromatic, chlorinated, polar or nonpolar) if large organic cations such as alkylammonium or alkylphosphonium are used [189,190]. Contrary to the solubility behavior exhibited by the classic

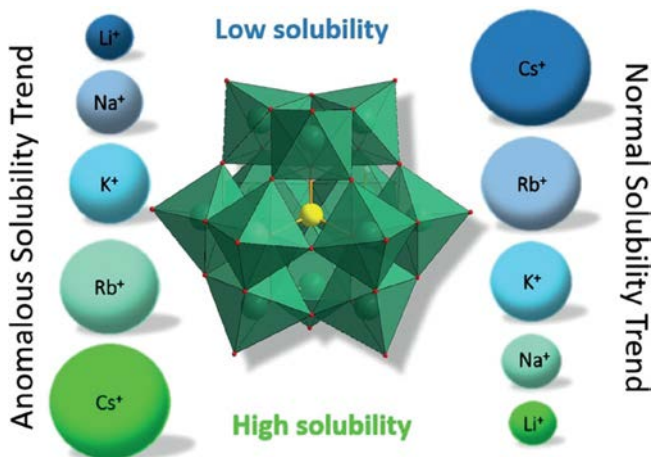


**FIG. 2.21** General solubility trends observed for the salts of polyoxometalates with alkali metal cations. For illustrative purposes, a Keggin ion heteropolyanion  $[\text{XM}_{12}\text{O}_{40}]^{n-}$  (with X usually being P, Si, M = Mo, W) is used. The normal solubility trend is observed for most polyoxometalate salts including Mo, V, and W, whereas the anomalous trend is mostly exhibited by Nb and Ta polyoxometalates. (Blue (dark gray in print versions) represents the least soluble, while green (light gray in print versions) shows the most soluble agents [187].)



polyoxometalates (formed under acidic conditions), polyoxometalates formed under basic conditions (with Nb or Ta) show more solubility with larger alkali metal cations (such as  $\text{Cs}^+$ ), even though they form contact ion-pairs in solution [191]. This unusual solubility course is referred to as inverse or anomalous solubility [192,193]. One may be tempted to relate this behavior to the pH-stability of the polyoxometalates. On the other hand, the alkaline-stable uranyl peroxide polyoxometalates demonstrate a usual solubility behavior [194,195]. The Nb/Ta polyoxometalates also have high solubility in water as salts of tetramethylammonium (TMA) [196]. Determination of solubility behavior and ion-pairing trends within a group (i.e., Nb compared to Ta, Mo compared to W) is more difficult as there are few isostructural analogues. However, Pfitzner et al. [181] suggested stronger adsorption of the phosphotungstate Keggin ion to nonionic micelles in comparison with the similar phosphomolybdate Keggin because of its lower charge density. Nyman et al. noticed different patterns of ion-pairing between Nb and Ta Lindqvist ions, and suggested a covalent character for the Cs–O bond in a Cs–Lindqvist ion-pair [191,197].

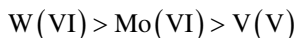
While there is still no clear account of both the normal and anomalous solubility trends, they may be summarized as follows:

- (a) A cation of low charge density paired with a polyoxometalate of high density charge is soluble.
- (b) A cation of high charge density paired with a polyoxometalate of low density charge is soluble.

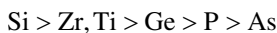
These somewhat predictable solubility trends exhibited by polyoxometalate salts may be utilized in manipulation of polyoxometalates including crystallization, rapid dissolution, or precipitation.

According to many studies, typical Keggin heteropoly acids completely—or at least at with a relatively high concentration—maintain their polyanion structure in aqueous solution [31]. X-ray diffraction (XRD), infrared (IR), and Raman spectroscopy as well as  $^{17}\text{O}$  NMR data support this [198]. On the other hand, in dilute solutions ( $< 10^{-2} \text{ mol}^{-1}$ ), degradation of the polyanion may take place.

In general, the stability of 12-heteropoly anions with different addenda atoms toward hydrolysis in aqueous solution decreases in the following order [31,199]:



Stabilities of 12-heteropolymolybdates with different central atoms toward degradation in water solution vary notably in the following order [31,199]:



The crystals of free acids and salts of heteropolymolybdates and heteropolytungstates nearly always occur in highly hydrated forms. Each acid or salt is often found in several solid hydrated forms. Most of the heteropolymolybdates

form isomorphous 30-hydrates that, upon heating between 40°C and 100°C, melt in their own hydration water. In dry air, these species begin to give up water and over sulfuric acid, in vacuum, they lose most of their water molecules.

### 2.5.1.2 Solubility in organic solvents

Many free heteropoly acids and a few of their salts are highly soluble in organic solvents, particularly in oxygen-containing ones. As a rule, ethers, alcohols, and ketones (in that order) are the best solvents. Free acids are not soluble in non-oxygen solvents such as benzene, chloroform, and carbon disulfide. While the dehydrated salts are sometimes readily soluble in organic solvents, the hydrated ones do not dissolve.

## 2.5.2 Stability

Generally speaking, salts of heteropoly acids are more stable than their corresponding acids because as the first step in a decomposition sequence, the lattice oxygen atom is to be removed by two protons. The influence of the central heteroatom is minor; however, heteropoly acids with arsenic or phosphorus as their heteroatom are more stable than their silicon, germanium, or boron counterparts [34,200,201].

### 2.5.2.1 Stability in solution

As mentioned in the earlier section, in general, the solubility of a heteropoly anion is usually governed by the solvation energy of the countercation because of the low lattice and solvation energies [202]. Heteropolyanions are extremely soluble in aqueous solutions so that a weight percentage of 88 has been reported for water, and it remains high for other polar solvents like ethyl acetate (86 wt%) or diethyl ether (85 wt%) [199]. Those salts of heteropolyanions with small cations maintain a high solubility. However, the salts become insoluble when small cations are replaced by large cations or organic species [202]. Therefore, huge cations are usually employed to separate stable heteropolyanions from solution [202].

Compared to the chemistry of polyoxometalates in aqueous media, which has been studied extensively, it is somehow under development in nonaqueous media. Their stability in aqueous or nonaqueous solvents is generally measured by how much they maintain their structural identities and resist degradation or transformation to other configurations. Nonetheless, the Keggin anions with their quasispherical structures, shown to have a very low negative charge density on peripheral and exterior (i.e., bridging and terminal) oxygen atoms, are able to form merely weak hydrogen bonds. This obviously results in heteropoly anions only weakly solvated in solution.

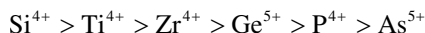
In solution, transformation of a polyoxometalate ion into multiple derivative species existing in dynamic equilibrium is quite complicated and the equilibrium position strongly depends on the final pH [203]. Pettersson et al. studied

the process for the hydrogen molybdate-phosphate system over extended ranges of pH and concentration using  $^{31}\text{P}$  NMR [204]. The system was much more complicated than was previously thought, and demonstrated that solutions with  $[\text{MoO}_4]^{2-}$  and  $[\text{HPO}_4]^{2-}$  in a ratio of 12:1 had more than one species at a certain pH. At low pH (i.e., less than 1.5), the 12:1 species dominates the solution, even though a considerable amount of the 9:1 species is present. At higher pH values (between 1.5 and 5), the monovacant lacunary species dominates, which is a result of the Keggin structure partial hydrolysis. Above pH 5, the Keggin structure is completely hydrolyzed so that the single oxoanion species is present. Pettersson and Grate extended this study to include a ternary Keggin system containing protons, molybdates, phosphates, and vanadates [204].

The stability of Keggin heteropoly anions in aqueous solution drastically depends on the addenda atom(s) that construct the structure [199,203]. Based on the three main addenda atom types, i.e., tungsten, molybdenum, and vanadium, the stability of the related POMs toward hydrolysis decreases in the following order:



The stability of the heteropoly anions of molybdenum in turn depends on the heteroatom and follows the order:



Tsigdinos pointed that at pH values less than 1.5, 12-molybdophosphate is stable in solution. However, when pH is increased, it undergoes alkaline hydrolysis [199]. At concentrations less than 1 mM, hydrolysis takes place though the formation of the monovacant lacunary species, which in turn undergoes further hydrolysis to give much smaller molybdophosphate species. The initial Keggin structure will continue to decompose as the pH increases until the structure is completely hydrolyzed into its simple oxoanion components. The alkaline hydrolysis of the Keggin structure is also observed at higher concentrations, but it proceeds through the formation of a Wells-Dawson derivative (i.e.,  $[\text{P}_2\text{Mo}_{18}\text{O}_{62}]$ ) as an intermediate. In spite of the presence of a trivacant lacunary species (i.e.,  $\{\text{PMo}_9\}$ ) in solution and its stability above pH 1.5, the of the dimeric Wells-Dawson derivative is formed slowly [204]. As a result of this slow formation, the trivacant lacunary species are used as building blocks for polyoxometalate structures with mixed addenda atoms [202]. Higher solution stabilities may be attained in organic solvents with polyoxometalates stable toward solvolysis at concentrations as low as  $10^{-6}$  M [202]. Keggin structures with mixed addenda atoms have been studied and show a minor increase in stability when one single molybdenum(VI) is replaced by vanadium(V) [203]. This is likely because of a decrease in the overall steric strain on the Keggin structure. Further replacements of molybdenum atoms by vanadium decrease its stability in solution even more. The stability order is  $\{\text{PMo}_{11}\text{V}\} > \{\text{PMo}_{10}\text{V}_2\} > \{\text{PMo}_9\text{V}_3\}$  [202,203]. Mixed addenda systems not only show an increased vulvar ability to alkaline

hydrolysis because of incorporation of vanadium, but also are easily hydrolyzed in dilute (0.8 M) HCl [202,205]. Courtin showed that increases in acidity result in the anions  $\{\text{PMo}_{12-n}\text{V}_n\text{O}_{40}\}$  with  $n > 1$  to lose vanadiums, resulting in lower substituted heteropoly anions [206].

At pH values between 1 and 3, the  $\{\text{PMo}_{12-n}\text{V}_n\text{O}_{40}\}$  anions undergo disproportionation. A similar process has been observed for the tungsten derivative as well [207].

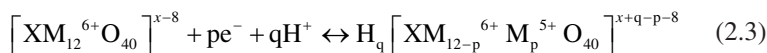
### 2.5.2.2 Thermal stability

The heteropolytungstates and their free acids are thermally quite stable and of great significance as heterogeneous catalysts [44,208]. Thermal stability is dependent on the nature of the central atom as well as addenda atoms. In general, species with phosphorous as the central atom are more stable than compounds with silicon as the central atom. The thermal stability of heteropoly compounds with tungsten as the addenda is more than that of molybdenum species. Decomposition at high temperatures results in loss of acidity. The phosphomolybdic acid decomposes into  $\text{MoO}_3$  and  $\text{P}_2\text{O}_5$  [208]. As soon as a complex is exposed to a humid atmosphere, its Keggin structure is reconstructed. On the other hand, in labile polyoxotungstates, such a reconstruction is less likely. Heteropoly acids are usually used as solid acid catalysts for reactions carried out in vapor phase at high temperatures. In these complexes, if the transition metals in the anionic framework are substituted, thermal stability is generally reduced. The substitution of addenda atoms of molybdenum in phosphomolybdic acid by other transition metals such as vanadium decreases the thermal stability of the resultant phosphomolybdovanadates. The presence of vanadium atom(s) in the polyanion framework reduces the thermal stability. At higher temperatures, vanadium atoms are expelled from the primary structural framework, and subsequently it degrades into simple oxides, i.e.,  $\text{MoO}_3$  and  $\text{V}_2\text{O}_5$ . The formation of such species is detectable by X-ray diffraction technique that clearly differentiate between the heteropoly and the metal oxide phases. The structure of such complexes may be reconstructed upon exposure to a humid atmosphere.

### 2.5.3 Redox properties

Many heteropoly compounds, particularly heteropolymolybdates, are powerful oxidizing agents, which can be very easily changed to relatively stable, reduced heteropolymolybdates. The reduced species are known as heteropoly blues. Extreme diversity is observed in the redox chemistry of polyoxometalates [31,209], and as the subject of a huge body of studies, it has found various applications in analytical chemistry and selective oxidation reactions [199]. Pope suggests that HPAs may be categorized into two groups according to redox abilities, i.e., mono-oxo (type I) and cis-dioxo (type II) [32,209]. This categorization is based on the number of terminal oxygen atoms bonded to each addenda atom. Keggin anions, Wells-Dawson anions, and their derivatives with one

terminal M=O per each addenda atom are examples of type I. Type II may be exemplified by Dexter-Silverton anions with two terminal oxygen atoms in *cis* positions on each addenda atom. In type I, the LUMO of the MO<sub>6</sub> octahedron is a nonbonding metal-centered orbital, whereas in type II, the LUMO of the MO<sub>6</sub> octahedron is antibonding in regard with the terminal M=O bonds. Therefore, anions of type I are readily reduced (frequently in a reversible manner) to form a mixed-valence anions (heteropoly blues), which goes back to the structure of the parent oxidized species. Conversely, anions of type II are reduced with more difficulty and irreversibly to species with structures not determined yet [32,209]. Accordingly, only heteropoly compounds of type I, generally the Keggin anions, have proved interesting for oxidation catalysis purposes. The total number of electrons that type I HPAs can accept during the reduction can be quite high. As the anion structure is maintained upon this process, the additional negative charge is balanced by protonation from the solvent. Therefore, the reduction process frequently depends on pH, which is represented by Eq. (2.3).



where  $q < p$  [32,209].

When reduced in acidic solution (pH 1), a Keggin tungsten anion, such as [SiW<sub>12</sub>O<sub>40</sub>]<sup>4-</sup>, can add two electrons without being protonated—that is, the anion charge becomes –6. In more neutral solutions, a pH-independent reduction can raise the anion charge to up to –9. The reduced Wells-Dawson anions {X<sub>2</sub>W<sub>18</sub>O<sub>62</sub>} can bear up to –12 without protonation [31].

### 2.5.3.1 Heteropoly blues

Heteropoly blues are a group of mixed-valence complexes obtained by reduction of isopoly- and heteropoly vanadates, molybdates, and tungstates. Some of these polyoxoanions give colloidal or insoluble mixed valence oxides, called molybdenum and tungsten blues. However, we limit the term heteropoly blue to well-defined crystalline, molecular, or ionic species. Even with this limitation, heteropoly blues entail several hundred complexes because a single polyanion may result in more than 10 mixed valence species. Most—but of course not all—anions in their reduced forms are intensely blue.

Heteropoly blues were first isolated and analyzed in crystalline form in 1920, 14 years before the structure of a heteropoly complex was determined by Keggin with the X-ray method [1].

There is physical evidence supporting the idea that the first added electrons in a heteropoly blue are weakly trapped by the individual metal atoms with each metal atom in the reducible polyanion occupying a site with C<sub>4v</sub> symmetry and the extra electron occupying an orbital with b<sub>2</sub> symmetry (i.e., dx<sub>xy</sub>) (Fig. 2.22). Consequently, electron delocalization in heteropoly blues may be regarded as a combination of two different factors, i.e., a thermally-activated jumping process from one metal atom to the other, as well as ground-state delocalization (GSD)

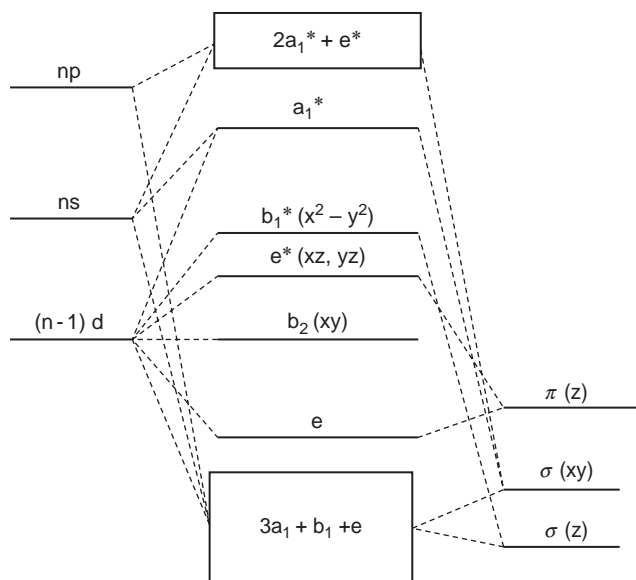


**FIG. 2.22** Simplified molecular orbital scheme, neglecting equatorial TI-bonding, for  $\text{MOL}_5$  complexes of  $C_{4v}$  symmetry. For  $d^1$  metals, the unpaired electron occupies the  $b_2$  orbital [210].

[211], which probably involves  $\pi$ -bonding through the bridging oxygens from the reduced metal atom to its neighbors. Although the GSD extent is relatively low, its occurrence is essential to justify the nonzero intensities optical absorption bands in intervalence charge transfer (IVCT).

### 2.5.3.2 General electrochemical properties

Before extensive investigation of the electrochemical behavior of HPAs can take place, aspects remain to be cleared. From the electrochemical point of view, the reduced sites on a HPA, when the anion has two and more electrons, the detailed redox mechanism coupled with protons are still unclear.

The electrochemistry of Keggin anions has been extensively studied in both aqueous and nonaqueous media. Since the redox potentials of heteropoly anions are pH-sensitive and also protons contained as counteranions affect these potentials, the conditions of the solution in which the voltammetry of heteropoly anions is carried out must be controlled carefully. The redox potentials in nonaqueous media and ionic liquids under neutral conditions are provided in Tables 2.6 and 2.7 [212].

In general, under neutral conditions, the redox potentials of heteropolymolybdates are more positive than those of the corresponding heteropolytungstates. For example,  $\text{PMo}_{12} > \text{PW}_{12}$  and  $\text{SiMo}_{12} > \text{SiW}_{12}$ . Furthermore, there is a linear correlation between the first redox potentials of heteropoly anions of the same framework and the anion charge in any solvent. For example,

**TABLE 2.6** Potentials ( $E_1$ ,  $E_2$ , mV vs.  $F_c/F_c^+$ ) due to the first and second redox of MoVI/V in Keggin-type V(V)-POMs.

POMs	Solvents	$E_1/E_2$
	AC	+84/−409
$\alpha$ -SMo <sub>12</sub>	1,2-DCE	+61/−329
	NB	+83/−345
	AC	−468/−902
	ACN	−260/−675
$\alpha$ -PMo <sub>12</sub>	1,2-DCE	−378/−777
	DMSO	−225/−684
	NB	−389/−825
	PC	−140/−556
$\beta$ -PMo <sub>12</sub>	ACN	−179/−615
	AC	−447/−874
	ACN	−236/−653
$\alpha$ -AsMo <sub>12</sub>	1,2-DCE	−357/−750
	DMSO	−206/−657
	NB	−367/−805
	PC	−120/−528
$\beta$ -AsMo <sub>12</sub>	ACN	−164/−587
	AC	−962/
	ACN	−744/−1149
$\alpha$ -SiMo <sub>12</sub>	1,2-DCE	−842/−1234
	DMSO	−749/−1183
	NB	−888/
	PC	−616/
$\beta$ -SiMo <sub>12</sub>	ACN	−671/−1082
	AC	−943
	ACN	−721/−1123
$\alpha$ -GeMo <sub>12</sub>	1,2-DCE	−825/−1217
	DMSO	−728/−1165

*Continued*



**Table 2.6** Potentials ( $E_1$ ,  $E_2$ , mV vs.  $F_c/F_c^+$ ) due to the first and second redox of MoVI/V in Keggin-type V(V)-POMs—cont'd

POMs	Solvents	$E_1/E_2$
	NB	– 864/
	PC	– 591/
$\beta$ -GeMo <sub>12</sub>	ACN	– 680/–1088
$\alpha$ -GaMo <sub>12</sub> <sup>a</sup>	ACN	– 1118/–1550

<sup>a</sup> Measured after the addition of *n*-Bu<sub>4</sub>NOH to neutralize the protons present as a counteranion. AC, acetone; ACN, acetonitrile; 1,2-DCE, 1,2-dichloroethane; DMSO, dimethyl sulfoxide; NB, nitrobenzene; PC, propylene carbonate.

**TABLE 2.7** Potentials ( $E_1$ ,  $E_2$ , mV vs.  $F_c/F_c^+$ ) due to the first and second redox of WVI/V in Keggin-type V(V)-POMs.

POMs	Solvents	$E_1/E_2$
$\alpha$ -SW <sub>12</sub>	AC	– 530 <sup>a</sup> /–1110 <sup>a</sup>
	AC	– 895/–1435
	ACN	– 691/1205
$\alpha$ -PW <sub>12</sub>	1,2-DCE	– 823/–1319
	DMSO	– 657/–1216
	PC	– 586/–1090
	AC	– 1376/–1894
	ACN	– 1143/–1653
	1,2-DCE	– 1261/–1772
$\alpha$ -SiW <sub>12</sub>	DMSO	– 1154/–1705
	PC	– 1022/
	DIMCARB	310 <sup>b</sup> /147 <sup>b</sup>
	BMIMPF <sub>6</sub>	614 <sup>b</sup> /263 <sup>b</sup>
$\alpha$ -BW <sub>12</sub> <sup>c</sup>	ACN	– 1650/
$\alpha$ -AlW <sub>12</sub> <sup>c</sup>	AAN	– 1560/
$\alpha$ -GaW <sub>12</sub> <sup>c</sup>	AAN	– 1540/
$\alpha$ -H <sub>2</sub> W <sub>12</sub> <sup>c</sup>	AAN	– 2020/
$\alpha$ -ZnW <sub>12</sub> <sup>c</sup>	ACN	– 1920/
$\alpha$ -CoW <sub>12</sub> <sup>c</sup>	ACN	– 1900/

<sup>a</sup> vs. Ag/Ag<sup>+</sup>.

<sup>b</sup> vs. CoCp2/CoCp2<sup>+</sup>.

<sup>c</sup> Measured after the addition of *n*-Bu<sub>4</sub>NOH to neutralize the protons present as a counteranion.

$SMo_{12} > PMo_{12} > SiMo_{12}$  [212b]. Keita et al. found that the redox potentials of  $SiW_{12}$  and  $P_2W_{18}$ , were linearly correlated with the number of acceptors on the organic solvent [213]. Himeno et al. found that the first redox potentials of  $PW_{12}$ ,  $PMo_{12}$ , and  $GeMo_{12}$  in various organic solvents were correlated with both the number of donors and permittivity [214]. The ion-transfer voltammetric behavior of heteropoly anions has been studied to find the correlation between the ion-transfer potentials and their size and charge [215].

Keggin and Wells-Dawson heteropolytungstates can partially decompose upon the addition of weak bases, such as  $KHCO_3$ . Refined pH control may lead to the formation of lacunary species, such as  $[XW_{11}O_{39}]^{n-}$  and  $[X_2W_{17}O_{61}]^{n-}$ . Different metal ions can be introduced into the defective sites of lacunary heteropoly anions to form metal-substituted anions. Depending on the introduced metal ions, they demonstrate intriguing chemical properties. The electrochemical properties of the metal-substituted heteropoly anions are also different from those of the parent anions. In the case of metal ion- metal-substituted heteropoly anions with the most redox activity, redox waves due to redox of the introduced ions were observed at more positive potentials than those due to the reduction of  $W(VI/V)$  [61].

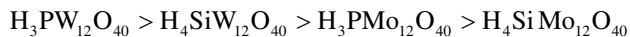
Small cations and protons can influence the voltammetric behavior of a heteropoly anion in organic solvents. The influence of  $Li^+$  and  $Na^+$  on the voltammetric behavior of Keggin anions has been studied in various solvents. The results of  $^7Li$  NMR studies revealed the selective solvation of the  $Li^+$  cation in binary solvents [216]. The electrochemical properties of  $S_2Mo_{18}$  (A Wells-Dawson heteropoly anion) were investigated in  $CH_3CN$  in the presence of  $LiClO_4$  and  $H_2O$  to explain the  $Li^+$ -coupled redox process and hydration of  $Li^+$  [217].

## 2.5.4 Acidic properties

Heteropolytungstates and molybdates are among strong acids. In general, the acidity is determined by dissociation constants as well as the Hammett acidity function [178]. Most of the free acids have several replaceable protons. In aqueous solution, they are completely dissociated from the main structure. This is because in heteropoly acids, the negative charges of similar values are spread over much larger anions compared those from mineral acids, and the electrostatic interactions between the protons and the anion is much less for heteropoly acids compared to those for mineral acids. Another important factor is probably the ability of the charge or electron for dynamic delocalization. Any change in the electronic charge due to proton removal may distribute over the whole polyanion unit. The strengths and the number of acid centers along with the related properties of heteropoly acids may be adjusted by the structure and composition of heteropoly anions, the degree of hydration, the support type, the thermal conditions, etc. Solid heteropoly acids such as  $H_3PW_{12}O_{40} \cdot xH_2O$  and  $H_3PMo_{12}O_{40} \cdot xH_2O$  are pure Brønsted acids and stronger than conventional solid acids like  $SiO_2-Al_2O_3$  or  $H-X$  and  $H-Y$  zeolites [44,218,219].

There are two differing outer oxygen sites on a Keggin anion structure potentially capable of being protonated: terminal oxygen (M=O) present on each addenda atom and bridging oxygens (both corner- and edge-sharing). Kozhevnikov et al. [220–222] extensively studied the specific oxygen site that undergoes protonation and their findings have been supported by a more recent computational study by Neumann [223], who investigated both vanadium-substituted and nonsubstituted phosphomolybdates. It was demonstrated that the terminal oxygen sites had a lower electron density compared to the bridging oxygen atoms. This means that the bridging oxygen atoms are protonated more favorably. In addition, MO calculations demonstrated that the bridging oxygens were more basic, again meaning they are protonated more favorably. A 12-heteropoly anion comprising  $[\text{MoO}_4]^{2-}$  and  $[\text{HPO}_4]^{2-}$  in a 12:1 ratio undergoes protonation at the bridging oxygen atoms farthest from the metal addenda centers. On the other hand, in the substituted vanadium heteropoly anion, the bridging oxygens bound to a vanadium atom show higher proton affinity, which in turn leads to protons bound to the nucleophilic sites surrounding the vanadium atom [223]. This protonation destabilizes the oxovanadium bonding within the Keggin fragment. However, these findings were based on calculations in which a free Keggin was assumed to be in the gas phase. In the solid phase, the protonation sites will vary. In the latter mode, the solid crystal lattice energy and the basicity of available oxygens are considered. The terminal oxygens may therefore undergo protonation as well [202].

Acidic properties are also reflected in thermal desorption of basic molecules. The pyridine, which is adsorbed by SiOAlO, is completely desorbed at 573 K. However, the pyridine sorbed by  $\text{H}_3\text{PW}_{12}\text{O}_{40}$  largely remains at 573 K, which indicates that  $\text{H}_3\text{PW}_{12}\text{O}_{40}$  is an extremely strong acid. The acidity may also be illustrated by temperature programmed desorption (TPD) with  $\text{NH}_3$ . The acid strengths of common heteropoly acids follow the general trend below [180]:



The appreciable number of investigations made during the last three decades has made it possible to formulate selection rules for effective catalysts from among the Keggin heteropoly acids. However, attention is increasingly being focused on acquiring more quantitative data for acid-catalytic properties of heteropoly acids with different structures and compositions. Their significantly higher Brønsted acidity, in comparison with the acidity of the traditional mineral acid catalysts, is extremely important for catalysis purposes. There is no doubt that in the future, the number of such processes will increase as the activity of heteropoly acid catalysts is higher than that of traditional ones. Frequently, the use of heteropoly acids as catalysts allows higher selectivity and solves ecological problems more successfully.

### 2.5.4.1 In solution

From a Brønsted point of view, heteropoly acids are strong acids. Their acidities have been quantitatively characterized and compared with the acidities of the usual mineral acids.

The increasingly growing number of heteropoly acid applications in solution, particularly their catalytic [224] and biological applications [225–228], requires a profounder apprehension and analysis of the fundamental relationship between their structural behavior in the solid state and in solution.

A compound isolated in crystalline form may not necessarily be the most abundant species. In solution, they form species capable of being protonated and undergoing redox processes that contribute to the extreme importance of the speciation characterization. Regarding the application and/or investigation of their complexes in aqueous solution, a thorough perception of the solution chemistry is necessary to get a grasp of the reaction mechanism and adjust the application conditions.

To provide the briefest definition for chemical speciation, it is the composition, concentration, and oxidation state of each chemical form of an element in a particular sample [229,230]. In addition, the term “speciation” is used to describe the distribution of the species present in a sample, in which case it is synonymous with the term “species distribution” [231]. This concept is widely used in fields as diverse as geochemistry, toxicology, clinical chemistry, biochemistry, environmental chemistry, and inorganic chemistry.

There are many factors that influence speciation of heteropoly acids and the mechanism of heteropoly anion formation, among which are the added acid and metal concentrations, types of interactions, and the range of chemical conditions (ionic strength, buffer type, presence of potential heteroatoms, type of the counteractions, etc.) under which the dissolution occurs.

Distribution curves, as the main outcomes of speciation studies, represent the percentages, partial mole fractions ( $\alpha$ ), or equilibrium concentrations of different species in a solution under certain conditions [232]. In general, concentration distribution curves are plotted as a function of a single variable, e.g., pH. For distribution curves of heteropoly acids,  $Z$ , i.e., the degree of protonation is usually used as one single variable. The equilibrium concentrations of different species are calculated by solving the mathematical system of mass balance equations set up for each species. Then these equations are solved for the concentrations of the free species [233]. It is noteworthy that the thermodynamic equilibrium constants are calculated based on activities which are dependent on temperature and pressure. The majority of the stability constants reported for heteropoly acids are regarded as stoichiometric constants, being expressed as equilibrium concentration quotients. They are therefore valid only at a certain ionic strength ( $\mu$ , M) in a certain solvent.

Kozhevnikov [218,220] scrutinized the properties of the heteropoly acids in solution. In more recent works, Okyakov [234–236] focused on the mixed addenda (Mo and V) heteropoly acids. Kozhevnikov characterized the

acidic properties of a series of heteropoly acids based on their Hammett acidity functions and dissociation constants. Kozhevnikov managed to show that  $\text{H}_3[\text{PW}_{12}\text{O}_{40}]$ ,  $\text{H}_3[\text{SiW}_{12}\text{O}_{40}]$ , and  $\text{H}_3[\text{PMo}_{12}\text{O}_{40}]$  are fully dissociated in aqueous media and such behavior is similar to that of strong acids. In addition, Pope reported that the heteropoly acids of  $[\text{SiW}_{12}\text{O}_{40}]^{4-}$  and  $[\text{PW}_{12}\text{O}_{40}]^{3-}$  remain fully dissociated even when they are reduced by two and three electrons, respectively [237].

It is noteworthy that the heteropoly acids  $\text{H}_3[\text{PW}_{12}\text{O}_{40}]$ ,  $\text{H}_3[\text{SiW}_{12}\text{O}_{40}]$  and  $\text{H}_3[\text{PMo}_{12}\text{O}_{40}]$  are not fully dissociated in organic solvents and therefore they no longer behave as strong acids [178].

In spite of the fact that the respective acids of the individual heteroatoms can differ significantly, the effect of the heteroatom upon the acidities is basically very weak. However, heteropoly acids are much stronger than the corresponding individual acids of the heteroatoms [202]. This is probably due to the fact that the heteropoly anion contains more external oxygen atoms capable of sufficiently delocalization of the increased charge than the anion receives in the dissociation process [178].

#### 2.5.4.2 The dissociation constants

Plenty of works have been dedicated to the study of acidities of heteropoly acids in solutions. However, the dissociation constant data for heteropoly acids are very limited, chiefly because the polyanions are labile in solution. In aqueous solution, heteropoly acids are completely dissociated in the first three steps, normally rendering the consecutive dissociation unnoticeable due to leveling effect of the solvent. As electroconductivity data suggest,  $\text{H}_4\text{PMo}_{11}\text{VO}_{40}$  and  $\text{H}_5\text{PMo}_{10}\text{V}_2\text{O}_{40}$  are respectively strong 1–4 and 1–5 electrolytes in aqueous solution.

The dissociation constants in aqueous solution (starting from  $K_4$ ) were measured for  $\text{H}_5\text{PMo}_{10}\text{V}_2\text{O}_{40}$ ,  $\text{H}_6\text{PMo}_9\text{V}_3\text{O}_{40}$ , and  $\text{H}_7\text{PV}_{12}\text{O}_{36}$  using potentiometric methods. In these acids, the first three protons are completely dissociated and the others undergo stepwise dissociation upon increasing pH. The dissociation constants are listed in Table 2.8. Note that the variation in the values of dissociation constants for heteropoly acids is not very appreciable, while the differences between the dissociation constants of inorganic acids are more noticeable. For comparison,  $\text{p}K_i$  values for  $\text{H}_3\text{PO}_4$  are listed in Table 2.8. As is evident from the data, the studied heteropoly acids are much stronger than  $\text{H}_3\text{PO}_4$ . This can be attributed to the large size, low surface density of the polyanion charge, and the peculiarity of the proton position with respect to the heteropoly acid structure. Nonaqueous and mixed solvents show differentiating influences on the dissociation constants of heteropoly acids. Furthermore, stabilities of heteropoly acids are noticeably higher in organic solutions. The acidity of heteropoly acids in organic solvents has been systematically studied in a few works [238,239]. Table 2.9 provides the values of dissociation constants in a few organic solvents, e.g., acetonitrile, acetone, ethanol, and acetic acid in the form of  $\text{p}K_i$ . In addition,

**TABLE 2.8** Dissociation constants for heteropoly acids and phosphoric acid in aqueous solution at 25°C.

	$\text{H}_5\text{PMo}_{10}\text{V}_2\text{O}_{40}$	$\text{H}_6\text{PMo}_9\text{V}_3\text{O}_{40}$	$\text{H}_7\text{PV}_{12}\text{O}_{36}$	$\text{H}_8\text{NbMo}_{12}\text{O}_{42}$	$\text{H}_8\text{CeMo}_{12}\text{O}_{42}$	$\text{H}_8\text{UMo}_{12}\text{O}_{42}$	$\text{H}_3\text{PO}_4$
$\text{p}K_4$	1.16	1.25	3.4	3.24	–	–	2.12 ( $\text{p}K_1$ )
$\text{p}K_5$	2.14	1.62	4.9	3.43	2.12	–	7.20 ( $\text{p}K_2$ )
$\text{p}K_6$	–	2.00	6.4	3.64	1.98	2.13	11.9 ( $\text{p}K_3$ )
$\text{p}K_7$	–	–	7.9	4.28	2.99	3.02	–
$\text{p}K_8$	–	–	–	5.73	4.16	4.31	–

**TABLE 2.9** Dissociation constant values of heteropoly acids in different solvents at 25°C.

Acid	HOAc	CH <sub>3</sub> CN			(CH <sub>3</sub> ) <sub>2</sub> CO			CH <sub>2</sub> H <sub>5</sub> OH		
	pK <sub>1</sub>	pK <sub>1</sub>	pK <sub>2</sub>	pK <sub>3</sub>	pK <sub>1</sub>	pK <sub>2</sub>	pK <sub>3</sub>	pK <sub>1</sub>	pK <sub>2</sub>	pK <sub>3</sub>
H <sub>6</sub> P <sub>2</sub> W <sub>21</sub> O <sub>71</sub> (H <sub>2</sub> O) <sub>3</sub>	4.66	1.8	5.6	7.6	–	–	–	–	–	–
H <sub>6</sub> P <sub>2</sub> W <sub>18</sub> O <sub>62</sub>	4.39	1.8	5.7	7.7	–	–	–	–	–	–
H <sub>6</sub> P <sub>2</sub> Mo <sub>18</sub> O <sub>62</sub>	4.36	2.0	6.0	8.0	–	–	–	–	–	–
H <sub>3</sub> PMo <sub>12</sub> O <sub>40</sub>	4.68	–	–	–	2.0	3.6	5.3	1.8	3.4	5.3
H <sub>4</sub> SiW <sub>12</sub> O <sub>40</sub>	4.87	1.9	5.9	7.9	2.0	3.6	5.3	2.0	4.0	6.3
H <sub>3</sub> PW <sub>12</sub> O <sub>40</sub>	4.70	1.7	5.3	7.2	1.6	3.0	4.1	1.6	3.0	4.1
H <sub>5</sub> PW <sub>11</sub> TiO <sub>40</sub>	5.32	2.00	6.0	7.9	1.7	3.2	4.2	–	–	–
H <sub>5</sub> PW <sub>11</sub> ZrO <sub>40</sub>	5.45	1.8	5.5	7.5	2.0	3.4	5.2	–	–	–
H <sub>3</sub> PW <sub>11</sub> ThO <sub>39</sub>	5.48	–	–	–	–	–	–	–	–	–
CF <sub>2</sub> SO <sub>3</sub> H	4.97	5.5	–	–	2.7	–	–	–	–	–
HNO <sub>3</sub>	–	–	–	–	3.6	–	–	3.6	–	–
HClO <sub>4</sub>	4.84	–	–	–	–	–	–	–	–	–
HBr	5.6	–	–	–	–	–	–	–	–	–
H <sub>2</sub> SO <sub>4</sub>	7.00	–	–	–	–	–	–	–	–	–
HCl	8.40	–	–	–	4.0	–	–	–	–	–



the dissociation constants for a few traditional acids are provided for comparison. First, it is clear that all the heteropoly acids are stronger than the traditional acids (e.g., HCl, H<sub>2</sub>SO<sub>4</sub>, HNO<sub>3</sub>, HBr) and even strong acids like HClO<sub>4</sub> and CF<sub>3</sub>SO<sub>3</sub>H. This is of essential significance for the application of heteropoly acids in acid catalysis. It is noticeable that sulfuric acid, used as a traditional acid catalyst, falls by 2–5 units of pK below heteropoly acids. According to the data in Table 2.9, the variation in acidic properties of heteropoly acids in CH<sub>3</sub>CN, C<sub>2</sub>H<sub>5</sub>OH, and (CH<sub>3</sub>)<sub>2</sub>CO is not so remarkable depending on the heteropoly acid composition and structure. For each solvent, the acidity series is different.

Even though the composition of a heteropoly acid has a minor influence on its acidity, it is quite observable. The acidity values decrease upon the reduction of heteropoly acids and replacement of W<sup>6+</sup> or Mo<sup>6+</sup> by V<sup>5+</sup> and/or the replacement of the central P<sup>V</sup> by Si<sup>IV</sup>. In every case, this decrease in acidity must be accompanied with an increase in basicity of the species (i.e., the number of equivalent protons connected to the heteropoly anion). The dependence of acidity on the composition and structure of heteropoly acids is observed more pronouncedly in acetic acid solution [238]. The basicity of the solvent has a significant effect on the acidity and the extent of acidic dissociation. Therefore, in HOAc, which is less polar, all heteropoly acids are relatively weak monobasic acids. In polar solvents like acetonitrile, ethanol, and acetone, the Keggin heteropoly acids are completely dissociated in the first step and partially in the second step. In acetone, heteropoly acids such as H<sub>3</sub>PW<sub>12</sub>O<sub>40</sub> and H<sub>5</sub>PW<sub>11</sub>TiO<sub>40</sub> are totally dissociated in the first and second steps, but partially in the third step. For heteropoly acids of other structures, data acquisition in a polar solvent is not achievable because of the complicated dependence of electroconductivity on the concentration of the acid in solution. Nevertheless, one can suppose that their acidities are close to those of H<sub>3</sub>PW<sub>12</sub>O<sub>40</sub>.

#### 2.5.4.3 The Hammett acidity

In solution, the acidity of heteropoly acids may be defined the Hammett acidity function, H<sub>0</sub> [240,241]. It has been demonstrated that the series of the strengths of heteropoly acids in diluted and concentrated aqueous solutions are not the same. This may be attributed to the fact that the acidity of a concentrated solution is determined not only by the values of the acid dissociation constants (as it occurs for diluted acids) but also by the salt effects, which are dependent on the composition and structure of the heteropoly acid [240]. The difference in the acidities of aqueous solutions of heteropoly acids disappears at the same weight concentrations (Table 2.10). The differences in acidity become more evident in aqueous-organic solutions. The acidic series in aqueous-organic solutions does not correlate with the thermodynamic dissociation constants in nonaqueous organic solutions. One can conclude that heteropoly acids in aqueous-organic solutions become polyelectrolytes essentially different from other acids [241]. The acid strength is lessened when W<sup>6+</sup> is replaced by Mo<sup>6+</sup> or V<sup>5+</sup> and/or when the central P<sup>V</sup> is replaced by Si<sup>IV</sup>. The central atom role has been investigated for

**TABLE 2.10** The Hammett acidity function  $H_0$  values for heteropoly acids in different solutions.

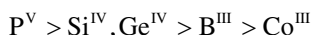
Acid	H <sub>2</sub> O			(CH <sub>3</sub> ) <sub>2</sub> CO (90%)		CH <sub>3</sub> CN (90%)		HOAc (85%)	
	$H_0^a$ (0.1 mol/L)	$H_0^b$ (0.3 mol/L)	$H_0^c$ (288.2 g/L)	$H_0^a$ (0.05 mol/L)	$H_0^b$ (0.15 mol/L)	$H_0^a$ (0.05 mol/L)	$H_0^b$ (0.15 mol/L)	$H_0^a$ (0.05 mol/L)	$H_0^b$ (0.20 mol/L)
H <sub>21</sub> B <sub>3</sub> W <sub>39</sub> O <sub>132</sub>	- 0.52	+ 0.21	+ 0.11	+ 0.21	+ 1.55	- 0.55	+ 0.35	-	-
H <sub>4</sub> P <sub>2</sub> W <sub>21</sub> O <sub>71</sub>	- 0.40	+ 0.15	+ 0.04	+ 0.11	+ 0.38	- 0.58	- 0.36	- 0.27	- 0.20
H <sub>5</sub> PW <sub>11</sub> TiO <sub>40</sub>	- 0.18	+ 0.01	- 0.06	+ 1.31	+ 1.77	+ 0.06	+ 0.17	+ 0.19	+ 0.40
H <sub>3</sub> PW <sub>12</sub> O <sub>40</sub>	- 0.05	- 0.05	- 0.05	+ 2.17	+ 2.17	+ 0.14	+ 0.14	+ 0.10	- 0.17
H <sub>5</sub> PW <sub>11</sub> ZrO <sub>40</sub>	- 0.07	+ 0.03	- 0.05	+ 1.43	+ 2.02	- 0.03	+ 0.20	+ 0.79	+ 1.06
H <sub>4</sub> SiW <sub>12</sub> O <sub>40</sub>	- 0.03	+ 0.06	- 0.03	+ 1.36	+ 2.13	+ 0.46	+ 0.60	- 0.07	- 0.04
HClO <sub>4</sub>	+ 0.81	+ 0.36	- 0.71	+ 2.32	+ 1.80	+ 0.86	+ 0.66	-	-
CF <sub>3</sub> SO <sub>3</sub> H	+ 0.56	+ 0.25	- 0.83	+ 2.00	+ 1.66	+ 0.77	+ 0.62	-	-
H <sub>2</sub> SO <sub>4</sub>	-	-	-	-	-	-	-	-	+ 0.75

<sup>a</sup>The molar concentration of acid.

<sup>b</sup>The proton concentration of acid.

<sup>c</sup>The weight concentration of acid.

the Keggin heteropolytungstates in acetonitrile solutions [242,243]. It has been demonstrated that the acidity generally increases as the negative charge on the heteropoly anion decreases and the charge of the central atom increases:



A study [241] showed that the acidity of aqueous-organic solutions of Keggin heteropoly acids was inversely dependent on the basicity of the organic solvent. The decrease in the solvent basicity follows the order of acetone > acetonitrile > water.

The effect of the water content on the acidity of an aqueous-organic solution assumes an extreme pattern, which is quite common for mixed solutions. Addition of water sharply decreases the acidity. Then it passes through a minimum to increase with further addition of water [240]. Such a type of dependence is attributed to the solvent effect on the activity coefficient of reagents [239].

## 2.6 Basic properties

A variety of polyoxometalate catalysts have been developed for acid-catalyzed, photocatalytic, or oxidation reactions. On the other hand, base catalysis has been scarcely studied [19,44,99,224,244–254]. Quite recently, the use of polyoxometalates as base catalysts has drawn much attention as a target for detailed studies. Based on their structures, polyoxometalate base catalysts are categorized into four groups: (i) monomeric metalates, (ii) isopolyoxometalates, (iii) heteropolyoxometalates, and (iv) transition metal substituted polyoxometalates (Fig. 2.23). The advantages of polyoxometalate base catalysts are: (i) in contrast with solid bases, electrically and structurally adjusted uniform basic sites can be designed; (ii) polyoxometalates are thermally and oxidatively more stable than organic bases such as amines, phosphines, guanidines, amidines, phosphazenes, etc.; and (iii) the metal-oxo fragment (i.e.,  $M=O$  and  $M-O-M$ ) activates nucleophilic substrates in a specific manner.

The basic sites of a polyoxometalate are usually its constituent oxygen atoms, and the basicity is correlated with the anion charge, size, molecular structure, and the nature of its constituent elements. The oxygen atoms on the surface of a polyoxometalate ion with the highest negative charges are likely to be active sites for base catalysis. Normally, the negative charge densities on the oxygen atoms cannot be measured experimentally. Therefore, most of the basic oxygen atoms have been analyzed by X-ray crystallography [22,101,256–265] and/or multinuclear magnetic resonance (NMR) [266–274] spectra of the protonated forms of the polyoxometalates. In addition, the basic oxygen atoms have been computationally analyzed using molecular electrostatic potential maps, relative energies of the various protonated forms, and the anion charge [15,223,275–277].

For heteropolyoxometalates (the acid form) in the solid state, the protons have a key role in the structure of the crystal as they link the neighboring

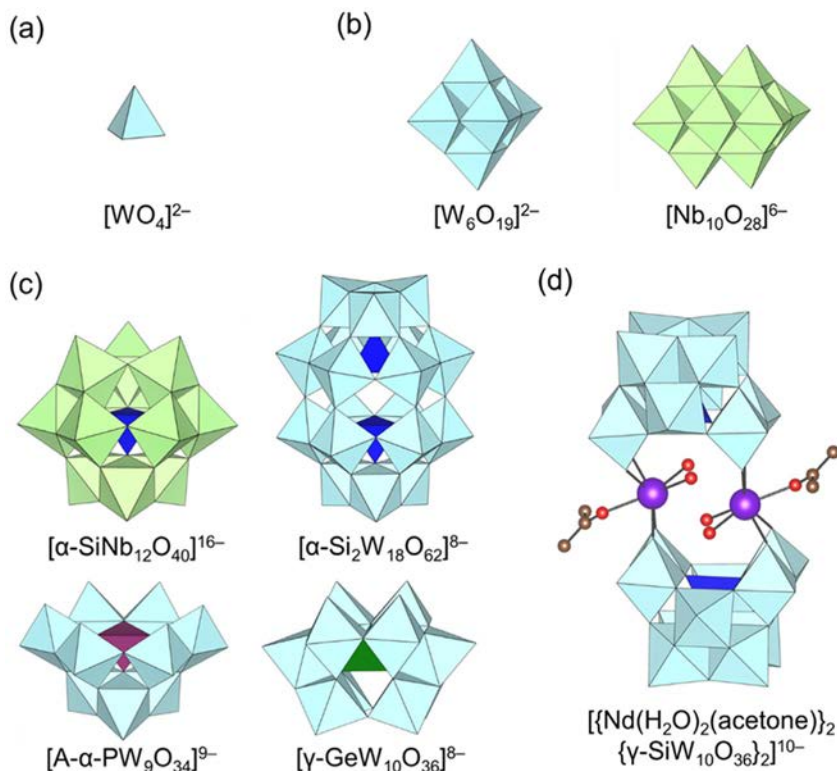
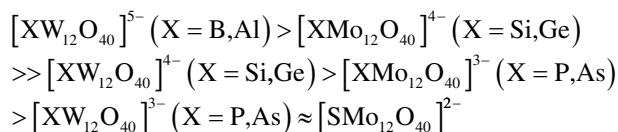
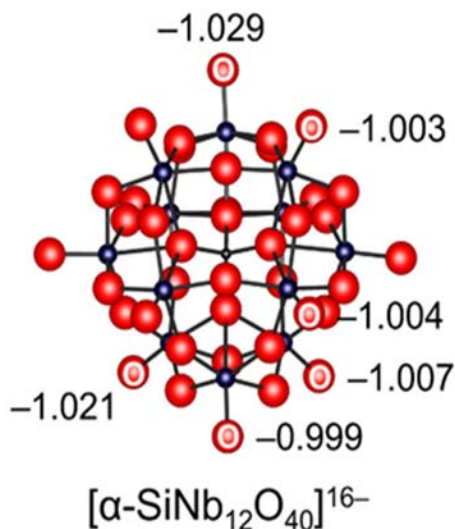


FIG. 2.23 Molecular structures of the different types of polyoxometalate anions used base catalysts. (A) Monomeric metalates, (B) isopolyoxometalates, (C) heteropolyoxometalates, and (D) transition metal substituted polyoxometalates [255].

heteropoly anions. Protons of the crystalline  $H_3PW_{12}O_{40} \cdot 6H_2O$  are present as an oxonium hydrate ( $H_5O_2^+$ ), with each one linking four neighboring heteropoly anions through hydrogen bonding to terminal W–O oxygen atoms [44]. Based on the results from infrared (IR) and  $^{17}O$  NMR spectroscopies [44], it has been suggested that the protons of the anhydrous form of  $H_3PW_{12}O_{40}$ , are attached to the most basic bridging oxygen atoms. According to Himeno et al., the potential difference between the first one- and two-electron redox waves of cyclic voltammograms may be used as a functional measure for the basicity of Keggin anions [212e,214]. On this measure, the basicity of the Keggin anions declines in the following order:





**FIG. 2.24** Ball-and-stick representations of the anion parts of  $[\text{SiNb}_{12}\text{O}_{40}]^{16-}$  base catalyst and natural bond orbital (NBO) charges of oxygen atoms [255].

which is in good agreement with the order of the anion charges. Wang et al. suggested that the NBO charges on the terminal oxygens in  $[\text{SiNb}_{12}\text{O}_{40}]^{16-}$  are much lower than those of other polyoxometalates (Fig. 2.24). However, the difference between the basic properties of various oxygen atoms is yet to be elucidated. The sodium salt of  $[\text{SiNb}_{12}\text{O}_{40}]^{16-}$ ,  $\text{Na}_{16}[\text{SiNb}_{12}\text{O}_{40}]$ , can serve as an efficient heterogeneous catalyst for reactions like the Knoevenagel condensation and  $\text{CO}_2$  cycloaddition [278].

Mizuno et al. suggested that the catalytic activity of a divacant silicododecatungstate,  $[\gamma\text{-SiW}_{10}\text{O}_{36}]^{8-}$ , for the epoxidation of alkenes with hydrogen peroxide drastically depends on the protonation state of the polyoxometalates [22]. A tetra-protonated silicododecatungstate with two aquo ligands at the vacant sites, i.e.,  $[\gamma\text{-SiW}_{10}\text{O}_{34}(\text{H}_2\text{O})_2]^{4-}$ , can efficiently catalyze the selective oxidation of alkenes by hydrogen peroxide. Following this, experimental and theoretical works on the catalytic properties of lacunary polyoxometalates (particularly  $[\gamma\text{-SiW}_{10}\text{O}_{34}(\text{H}_2\text{O})_2]^{4-}$ ) were carried out by a number of research groups (Fig. 2.25) [276,277,279–282]. Although the formula  $[\gamma\text{-SiW}_{10}\text{O}_{34}(\text{H}_2\text{O})_2]^{4-}$  has been proposed based on the X-ray crystallographic structure analysis, the precise assignment of the four protons on the lacunary sites remains unclear and needs more investigations.

Formation of several deprotonated species was revealed during the potentiometric titration of  $[\gamma\text{-SiW}_{10}\text{O}_{34}(\text{H}_2\text{O})_2]^{4-}$  with TBAOH. The reversibility and structures, however, remain blurred [277]. Mizuno and coworkers reported the in situ formation of tri-, di-, and mono-protonated silicododecatungstates,  $[\gamma\text{-SiW}_{10}\text{O}_{34}(\text{OH})(\text{OH}_2)]^{5-}$ ,  $[\gamma\text{-SiW}_{10}\text{O}_{34}(\text{OH})_2]^{6-}$ , and  $[\gamma\text{-SiW}_{10}\text{O}_{35}(\text{OH})]^{7-}$ , respectively with  $C_1$ ,  $C_{2v}$ , and  $C_2$  symmetries based on the  $^1\text{H}$ ,  $^{29}\text{Si}$ , and  $^{183}\text{W}$  NMR data (Fig. 2.26) [283].

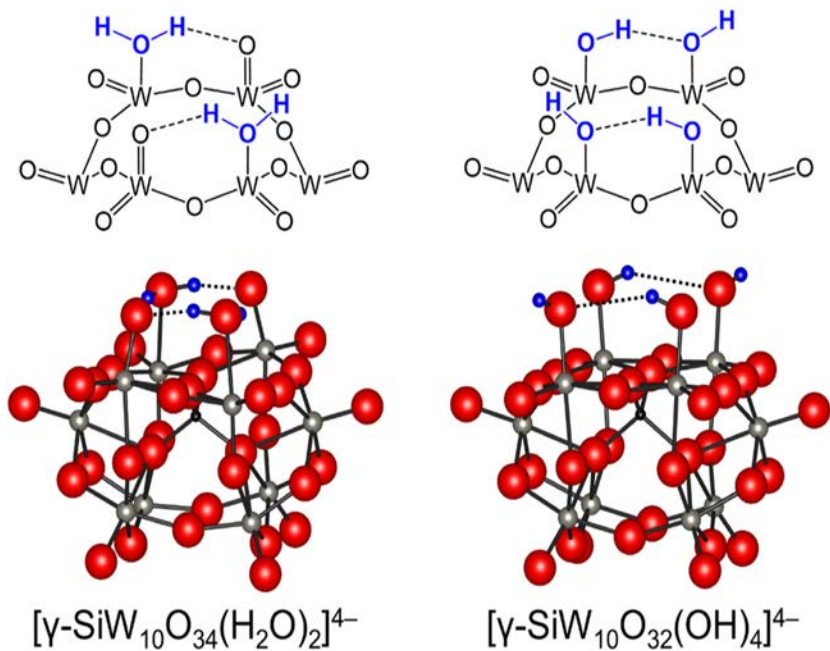


FIG. 2.25 Representations of lacunary sites of  $[\gamma\text{-SiW}_{10}\text{O}_{34}(\text{H}_2\text{O})_2]^{4-}$  and  $[\gamma\text{-SiW}_{10}\text{O}_{32}(\text{OH})_4]^{4-}$  [276,277].

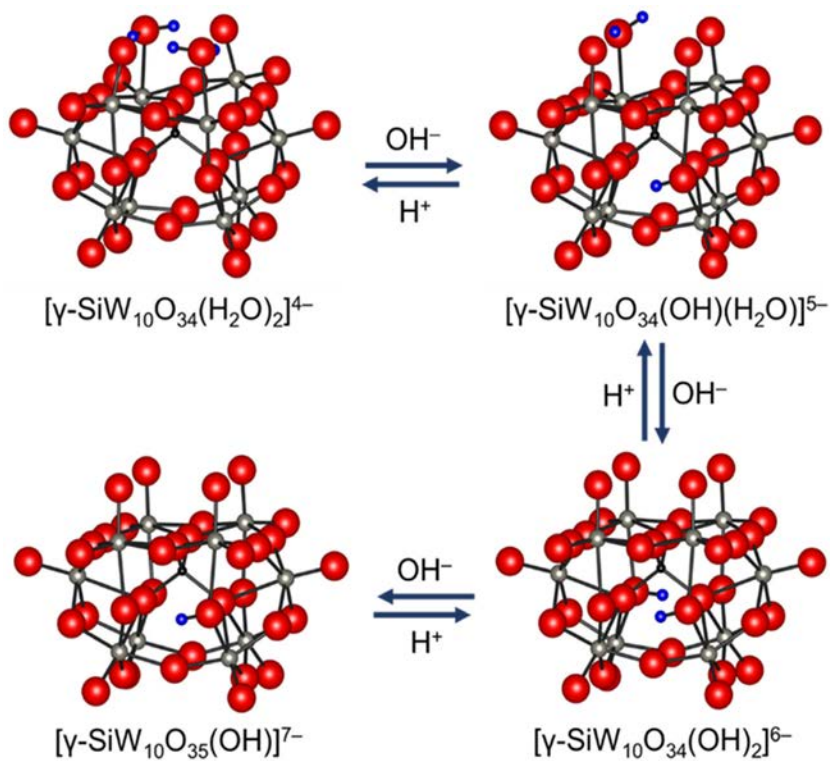


FIG. 2.26 Reversibility of changes among  $[\gamma\text{-SiW}_{10}\text{O}_{34}(\text{OH})(\text{H}_2\text{O})]^{5-}$ ,  $[\gamma\text{-SiW}_{10}\text{O}_{34}(\text{OH})_2]^{6-}$ , and  $[\gamma\text{-SiW}_{10}\text{O}_{35}(\text{OH})]^{7-}$  upon protonation/deprotonation [283].



Single crystals of TBA<sub>6</sub> [ $\gamma$ -SiW<sub>10</sub>O<sub>34</sub>(OH)<sub>2</sub>] appropriate for X-ray structure analysis were prepared successfully. The anion part was a monomeric  $\gamma$ -Keggin divacant silicodecatungstate containing two protonated bridging oxygens. Similar reversible deprotonation/protonation behaviors were observed for germanodecatungstates. Therefore, bridging oxygens could be possible active sites for [ $\gamma$ -XW<sub>10</sub>O<sub>35</sub>(OH)]<sup>7-</sup> (X = Si and Ge), while the terminal lacunary oxygens may serve as active sites for [ $\gamma$ -XW<sub>10</sub>O<sub>34</sub>(OH)<sub>2</sub>]<sup>6-</sup> (X = Si and Ge) (Fig. 2.27). The di-protonated germanodecatungstate, [ $\gamma$ -GeW<sub>10</sub>O<sub>34</sub>(OH)<sub>2</sub>]<sup>6-</sup>, could act as a homogeneous catalyst for the Knoevenagel condensation and the mono-protonated germanodecatungstate [ $\gamma$ -GeW<sub>10</sub>O<sub>35</sub>(OH)]<sup>7-</sup> could play the same role for the chemoselective acylation of alcohols [284,285].

The  $\alpha$ -Dawson silicotungstate, TBA<sub>8</sub> [ $\alpha$ -Si<sub>2</sub>W<sub>18</sub>O<sub>62</sub>], synthesized by dimerization of a trivacant lacunary  $\alpha$ -Keggin silicotungstate TBA<sub>4</sub>H<sub>6</sub> [ $\alpha$ -SiW<sub>9</sub>O<sub>34</sub>] in an organic solvent can capture protons inside its aperture in a reversible manner. The process occurs through intramolecular hydrogen bonds [286]. Compared to the starting material, which was the trivacant TBA<sub>4</sub>H<sub>6</sub> [ $\alpha$ -SiW<sub>9</sub>O<sub>34</sub>], this compound exhibits much higher catalytic activity for the Knoevenagel condensation of ethyl cyanoacetate with benzaldehyde.

## 2.7 Characterization

Heteropoly acids are identified by a wide array of analytical techniques. Each of these methods adds one more piece of information to determine the final structural model.

A majority of heteropoly acids have been prepared and studied in aqueous solutions. Therefore, this book focuses on speciation of HPAs in aqueous solutions, in which many applications such as catalysis and biological processes are carried out.

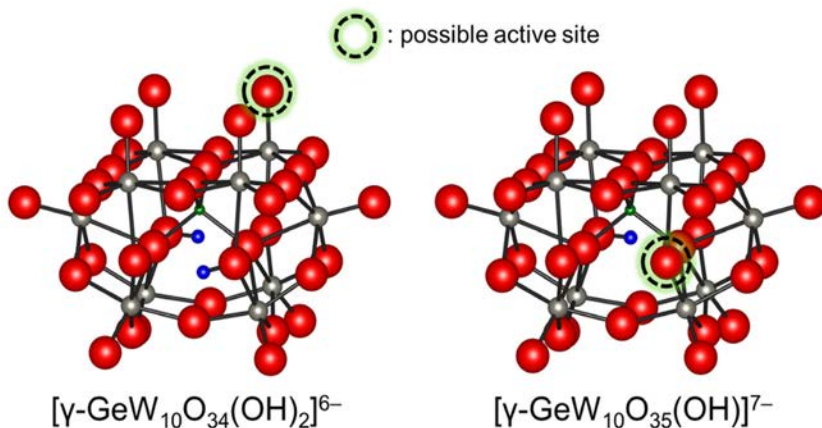


FIG. 2.27 The ball-and-stick representations of [ $\gamma$ -GeW<sub>10</sub>O<sub>34</sub>(OH)<sub>2</sub>]<sup>6-</sup> and [ $\gamma$ -GeW<sub>10</sub>O<sub>35</sub>(OH)]<sup>7-</sup> and their possible active sites for base-catalyzed reactions [284].



Adequate experimental techniques and careful interpretation of the results are necessary to resolve the ambiguities in heteropoly acid equilibria in solution. Under ideal conditions, many different complementary experimental techniques are needed to realize the distribution of the species. To acquire a spectrum as a fingerprint and assign it to a certain species, it must be either homogeneous in solution or solid. The polyoxometalate solution under question requires monitoring over a pH range, time range, and, if possible, temperature and concentration ranges. Presently, for studies in solution the exclusive use of potentiometry and vibration spectroscopy for characterizing metal oxide systems is not suggested any more, but a wide variety of advanced complementary methods such as multinuclear NMR spectroscopy, small angle X-ray scattering (SAXS), X-ray absorption spectroscopy (XAS comprising of extended X-ray absorption fine structure (EXAFS) and X-ray absorption near edge structure (XANES)), and mass-spectrometry are used as well. The characterization methods in the context of their application in HPA systems will be briefly summarized. An elaborate description of the fundamentals of each method, as well as the recording, evaluation, and interpretation of the data collected, may be found in the related literature.

In the following subsections, the methods widely used for the examination of heteropoly acids in solutions and solid state will be presented in the chronological order of appearance.

### 2.7.1 Potentiometry

Potentiometric titration was among the first methods employed to investigate the speciation of heteropoly acids [31]. Principally, this method involves measuring the concentration of hydrogen ions in polyanion solutions as a function of the added acid or base (Fig. 2.28A) and the concentration of the total metal ion [233,287,288]. The values for the formation constants and stoichiometric

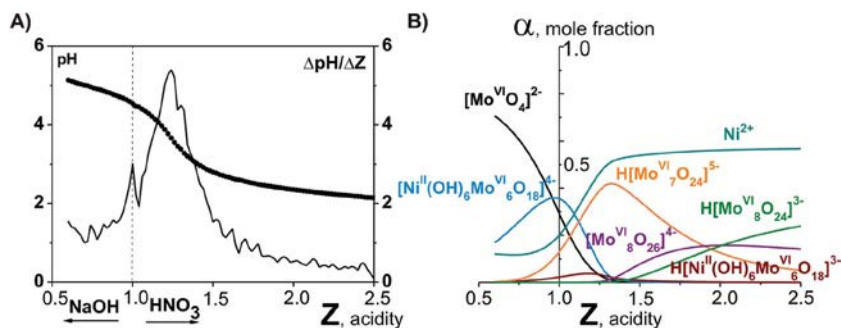
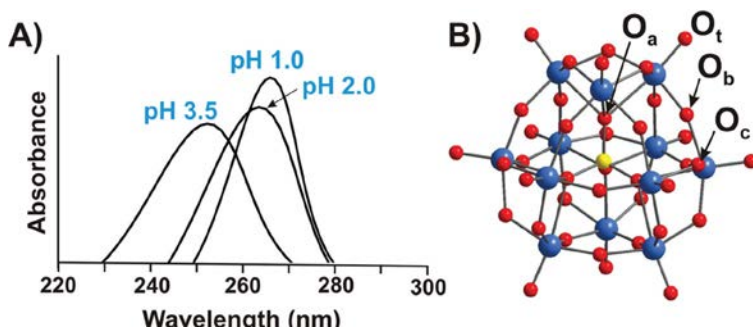


FIG. 2.28 pH-potentiometry and mathematical modeling for the system  $\text{Ni}^{2+}-[\text{Mo}^{\text{VI}}\text{O}_4]^{2-}-\text{H}^+-\text{H}_2\text{O}$  acidified to the mole ratio  $Z = n(\text{H}^+)/n([\text{Mo}^{\text{VI}}\text{O}_4]^{2-}) = 1.00$  [287]. (A) Integral (points,  $\text{pH} = f(Z)$ ) and differential (line,  $\Delta\text{pH}/\Delta Z = f'(Z)$ ) titration curves. (B) Distribution diagrams of the ions presented in solution after 60 days aging of the initial  $\text{Ni}^{2+}-[\text{Mo}^{\text{VI}}\text{O}_4]^{2-}-\text{H}^+-\text{H}_2\text{O}$  solution.

coefficients are then determined by titration, followed by the iterative computation of the constants of one species in the presence of another. The entire system will be computationally described in an iterative process. The formation constants  $KC$  provide a basis for species distribution diagrams (Fig. 2.28B) demonstrating various types of polyoxometalates which are present at different pH values. To ensure that for each measurement, the equilibrium has been truly reached, that the activity coefficient quotients are constant enough (by using a supporting electrolyte), and that the potentials of the liquid transitions are adjustable, great care must be taken. Presently, potentiometry is obsolete as other advanced methods are available that provide more details about the processes in solution.

## 2.7.2 Electronic and vibrational spectroscopy

The addenda ions in polyoxometalates usually have the electronic configuration  $d^0$ , and consequently just one absorption band occurs in their UV-vis spectra between 190 and 400 nm, which is due to an oxygen-to-metal charge transfer transition [289,290]. The spectra of the reduced heteropoly blue complexes demonstrate intervalence charge-transfer transitions, e.g., Mo(V)-Mo(VI) at  $\sim 700$  nm [291]. In practice, electronic spectroscopy does not provide any structural information. However, it is among the easiest ways to check the stability of a polyoxometalate in solution [292,293]. As an example, at pH 1, the Keggin polyanion  $[P^V W_{12} O_{40}]^{3-}$  ( $\{PW_{12}\}$ ) (Fig. 2.29B) gives two intense absorption bands in the UV range, with maxima approximately at 200 and 263 nm, which are attributed to  $p_\pi-d_\pi$  charge-transfer transitions of the  $O_t$ -W(VI) ( $O_t$ : terminal oxygen atom) and  $p_\pi-d_\pi$  charge transfer transitions of the  $O_{b,c}$ -W(VI) ( $O_{b,c}$ : bridge oxygen atoms), respectively (Fig. 2.29A) [293]. The absorption band



**FIG. 2.29** (A) UV-vis spectra of  $H_3[P^V W^VI_{12} O_{40}]$  in aqueous solutions recorded at pH values of 1.0, 2.0, and 3.5 [293]. The Keggin anion decomposition is clearly seen to have commenced already at pH 3.5 by shifting of the maximum absorption from 263 nm to 252.5 nm. (B) The ball-and-stick model of a Keggin type anion  $[P^V W^VI_{12} O_{40}]^{3-}$  in which types of oxygen atoms are indicated as  $\mu_3$ - $O_a$  (the oxygen atoms linked to the heteroatom  $P^V$ ),  $\mu_2$ - $O_b$  and  $\mu_2$ - $O_c$  (two types of bridging oxygen atoms), and  $O_t$  (the terminal oxygen atom).

maximum at 263 nm is assigned to the electron transition  $O_{b,c}\text{-W(VI)}$  of the intact Keggin which is shifted to 252.5 nm at pH 3.5 corresponding to the monolacunary form  $[\text{P}^{\text{V}}\text{W}_{11}^{\text{VI}}\text{O}_{39}]^{7-}$  ( $\{\text{PW}_{11}\}$ ), which indicates the decomposition of  $[\text{P}^{\text{V}}\text{W}_{12}^{\text{VI}}\text{O}_{40}]^{3-}$  (Fig. 2.29) [293].

Infrared, Raman, and resonance Raman spectroscopies are widely used in the chemistry of heteropoly acids as diagnostic fingerprints. If the positions, shapes, and relative intensities of spectral bands for two compounds are similar, one may decisively conclude that both have identical structures. The characteristic range for the POMs is between 1000 and 400  $\text{cm}^{-1}$ , in which absorptions due to metal-oxygen stretching vibrations occur. Raman spectroscopy is usually used for aqueous solution studies of heteropoly acids [294–297] while the IR spectroscopy is employed for studies in both aqueous and nonaqueous solvents [298].

### 2.7.3 Nuclear magnetic resonance (NMR)

Nuclear magnetic resonance spectroscopy has been carried out on heteropoly acids containing NMR-active nuclei of various natural abundances (NA) to study their structures and dynamics in solution since the 1970s. The examples are  $^{31}\text{P}$  (NA = 100%;  $I = 1/2$ ),  $^{51}\text{V}$  (NA = 99.75%;  $I = 7/2$ ),  $^{17}\text{O}$  (NA = 0.04%;  $I = 5/2$ ),  $^1\text{H}$  (NA = 99.98%;  $I = 1/2$ ),  $^{29}\text{Si}$  (NA = 4.7%;  $I = 1/2$ ), and, later,  $^{95}\text{Mo}$  (NA = 15.87%;  $I = 5/2$ ) and  $^{183}\text{W}$  (NA = 14.32%,  $I = 1/2$ ) [299,300]. For reliable identification of a heteropoly acid in solution, it is desirable to take the NMR spectra of all NMR-active nuclei whenever possible.

#### 2.7.3.1 *Addenda nuclei*

*$^{51}\text{V}$  NMR.* Thus far, the most of measurements for heteropoly acids have been made at  $^{51}\text{V}$ , a nucleus of relatively high sensitivity that provides spectra with line widths between  $\sim 10$  and  $\sim 800$  Hz for diamagnetic polyanions. The chemical shifts (with  $\text{VOCl}_3$  as a reference) in isopoly- and heteropolyvanadates fall in a range between  $-400$  and  $-600$  ppm. Even relatively small structural variations give rise to separable peaks because of a broad range of chemical shift [301].

*$^{95}\text{Mo}$  NMR.* Although there are two NMR-active isotopes, i.e.,  $^{95}\text{Mo}$  (NA = 15.87%;  $I = 5/2$ ) and  $^{97}\text{Mo}$  (NA = 9.46%,  $I = 5/2$ ), Mo NMR is not frequently used because of the low natural abundance and low gyromagnetic ratios of these isotopes:  $\gamma(^{95}\text{Mo}) = -1.751 \times 10^7 \text{ rad s}^{-1} \text{ T}^{-1}$  and  $\gamma(^{97}\text{Mo}) = -1.788 \times 10^7 \text{ rad s}^{-1} \text{ T}^{-1}$ . In general, the  $^{95}\text{Mo}$  nucleus is preferred over  $^{97}\text{Mo}$  because it has a lower quadrupolar moment. In comparison with  $^{183}\text{W}$  NMR, the  $^{95}\text{Mo}$  NMR signals from a typical asymmetric HPA-Mo environment are drastically broadened due to this quadrupole moment, which complicates spectral measurements and their interpretation.

*$^{183}\text{W}$  NMR.* The  $^{183}\text{W}$  NMR is uniquely important in studying polyoxotungstates (POTs) even though its sensitivity is not very high. Narrow NMR lines of  $^{183}\text{W}$  with  $I = 1/2$  allow us to observe constants of indirect spin-spin coupling,

i.e.,  ${}^2J$  (W-P),  ${}^2J$  (W-W), that carry structural information. The sensitivity limitations are significantly resolvable by using high field spectrometers, even though a concentrated solution of the sample ( $\sim 1$  mol/L) and a long acquisition time are still necessary. A saturated solution of sodium tungstate is recommended as a reference [300]. For polyoxotungstates, the range of  ${}^{183}\text{W}$ -chemical shifts falls between + 260 and – 300 ppm, and even down to – 670 ppm provided that the polyoxotungstate peroxocomplexes are taken into account as well [300]. For the reduced polyoxotungstates or polyoxotungstates with incorporated paramagnetic ions, even larger chemical shifts from + 2500 to – 4000 ppm may be observed.

${}^{93}\text{Nb}$  (NA = 100%;  $I = 9/2$ ) and  ${}^{181}\text{Ta}$  (NA = 99.98%;  $I = 7/2$ ) NMR spectroscopies are hardly used for heteropoly acid investigations because of excessive line widths, which are in turn a result of a large quadrupole coupling.

### 2.7.3.2 Other nuclei ( ${}^1\text{H}$ , ${}^{17}\text{O}$ , ${}^{31}\text{P}$ , ${}^{19}\text{F}$ , ${}^{11}\text{B}$ , ${}^{27}\text{Al}$ )

**${}^1\text{H}$  NMR.** Rapid exchange with solvent protons restricts the use of high resolution  ${}^1\text{H}$  NMR for fully inorganic polyoxometalates. On the other hand, integrated resonances of nonlabile protons from organic units of hybrid polyoxoanions and counteranions are routinely used for analytical purposes [31]. However, separate signals have been observed for solvent and polyanions in some cases. One of the earlier successful instances was published in 1966. Pope and Varga showed the presence of two central protons in the metatungstate anion,  $[\text{H}_2\text{W}_{12}\text{O}_{40}]^{6-}$ , using  ${}^1\text{H}$  NMR [302].

**${}^{17}\text{O}$  NMR.** It is more universal since presence of oxygen in all HPA clusters is inevitable. As we know, there are two main structural types of oxygen atoms in a polyanion: terminal oxygens with coordination number one ( $\text{O}=\text{M}$ ) and bridging oxygens ( $\text{M}-\text{O}-\text{M}$ ) with coordination numbers ranging between two and six. NMR lines for different types of oxygen atoms are fully resolved and their shape is characteristic for a structural type of oxygen atom [299].

Although it is difficult to observe  ${}^{17}\text{O}$  because of low natural abundance (0.04%) and negative quadrupole moment  $Q({}^{17}\text{O}) = -26$  mB, its large chemical shift ranging from 1200 to – 100 ppm makes up for those drawbacks [31,299]. To overcome the low natural abundance of  ${}^{17}\text{O}$  (0.04%), the target polyoxometalates may be enriched with  $\text{H}_2{}^{17}\text{O}$ . In this way, studying the rates of oxygen-isotope exchange between solvent and HPA molecule sites becomes possible and has been demonstrated to be useful in understanding the equilibria of polyoxometalates [268,303].

**${}^{31}\text{P}$  NMR.** The large number and wide variety of heteropoly compounds with phosphorus as a heteroatom have led to the significant development of  ${}^{31}\text{P}$  NMR that indicates the high sensitivity of its chemical shift based on the polyoxometalates composition. In the  ${}^{31}\text{P}$  NMR spectra of a Keggin type species, i.e.,  $\text{H}_3[\text{P}^{\text{V}}\text{W}_{12}\text{O}_{40}]$  and most of its derivatives, each form is represented only by one signal in a chemical shift ranging from – 15 to – 2.5 ppm (relative to 85%  $\text{H}_3\text{PO}_4$ ), which permits direct detection of several coexisting species and determination of their concentrations [304].

*Other nuclei.*  $^{11}\text{B}$  (NA = 80.42%,  $I = 3/2$ ) [305],  $^{19}\text{F}$  (NA = 100%,  $I = 1/2$ ) [306],  $^{27}\text{Al}$  (NA = 100%,  $I = 5/2$ ) [307], and  $^{195}\text{Pt}$  (NA = 33.7%,  $I = 1/2$ ) [308] NMR spectroscopies are not used very frequently. However, they may be of equal importance for investigation of polyoxometalates in solution. When appropriate NMR-active cations are present, the NMR measurements can also be used in the analysis of cation-POM interactions in solution, which can influence the transformation between polyoxometalates [187]. The Nyman group managed to study the cationic association with various polyoxometalates in solution using  $^7\text{Li}$  [309],  $^{23}\text{Na}$  [310], and  $^{133}\text{Cs}$  [197] NMR spectroscopies.

### 2.7.4 Mass-spectrometry (MS)

Electrospray-ionization mass-spectrometry (ESI-MS) is appropriate to account for solution phase equilibria of stable upon ionization anions, as it allows semi-quantitative detection of both cationic and anionic species in aqueous solutions with excellent detection boundaries. Mass spectrometry is an ideal candidate for heteropoly acid studies since it shows complex isotopic envelopes resulting from the high number of stable isotopes as for tungsten ( $^{182}\text{W}$ , 26.5%;  $^{183}\text{W}$ , 14.3%;  $^{184}\text{W}$ , 30.6%;  $^{186}\text{W}$ , 28.4%) or molybdenum ( $^{92}\text{Mo}$ , 14.8%;  $^{94}\text{Mo}$ , 9.3%;  $^{95}\text{Mo}$ , 15.9%;  $^{96}\text{Mo}$ , 16.7%;  $^{97}\text{Mo}$ , 9.6%;  $^{98}\text{Mo}$ , 24.1%;  $^{100}\text{Mo}$ , 9.6%), and are basically charged [311,312]. However, the experiments must be designed carefully to obtain reliable data without misinterpretation of gas phase data for the solution phase [313]. While ESI-MS is not providing any information beyond the mass-to-charge ratio of the analyte, it enjoys a high sensitivity and does not necessitate too many requirements for the system under analysis. In addition, time-resolved data can be collected on very dilute solutions. ESI-MS has been used for comprehensive speciation of HPAs with all kinds of addenda atoms contributing significantly to the speciation analysis.

### 2.7.5 Small angle X-ray scattering (SAXS)

SAXS is a nondestructive method used in the determination of the size, shape, reactivity, and interactions of dissolved species [314]. As a well-established method, it is quite powerful. However, it has not been utilized very extensively to obtain speciation information on HPA solutions thus far. In principle, SAXS is similar to X-ray crystallography, in which the sample is subjected to the radiation of a collimated monochromatic X-ray beam [315]. Similar to nanoparticles and quantum dots, many heteropoly acids exhibit high net charges, and contain elements with high electron densities (W, Mo, and other metals). Therefore, they drastically scatter X-rays. Because heteropoly acids are molecular by nature, solutions in which the clusters are stable must be totally monodisperse, and their X-ray scattering data may be simulated with high accuracy using data sets from solid-state crystal structures. Thus far, many groups of polyoxometalates have been thoroughly investigated using SAXS, among which are the polyoxometalates of group V ( $\text{Nb}^{\text{V}}$  and  $\text{Ta}^{\text{V}}$ ) [314,315], POTs [98] and their

actinide complexes [316], large reduced polyoxometalates [317], and polyoxometalate supramolecular assemblies [318]. SAXS can also be applied in the speciation of POMs in catalytic systems. As one example, the speciation process for cobalt containing POTs as a function of pH, buffer salts, and addition of a chemical oxidant during water oxidation catalysis has been studied with excellent results [319].

### 2.7.6 Other methods

A rich electrochemistry has been observed for heteropoly acids, which is assigned to the reduction of tungsten or molybdenum [320] and redox reactions of heterometals (i.e., incorporated cobalt, ruthenium, iridium, or nickel). These characteristic redox wave peaks may be used for identification of the number of terminal oxygen atoms, new isomers and reduced anions, and metastable hydrolysis fragments [111,321].

Extended X-ray absorption fine structure (EXAFS) and X-ray absorption near edge structure (XANES) are invaluable methods to determine both the local coordination environment and the oxidation state of the atoms of a heteropoly acid either in solution or in solid state. Each type of atom in a heteropoly acid cluster can be individually accessed and an average spectrum for each element is recorded [322]. Even though XAS (X-ray absorption spectroscopy) is a powerful technique, there are a limited number of examples for its usage in structure analysis of polyoxometalates [323,324]. Since heteropoly acids are generally crystalline solids, determination of their structures using single-crystal X-ray diffraction is quite possible. For this reason, it has been the most important tool in the investigation of their structures in solid state. Determination of structures based on single-crystal diffraction data is a routine and one of the oldest methods used in studying the structures of these compounds. Single crystal X-ray diffraction is the only reliable method for determination of the structures of paramagnetic or multidimensional heteropoly acids. Powder X-ray diffraction (PXRD) has not been regularly used in heteropoly acids chemistry, even though it is of reasonable importance in providing evidence for phase pure products.

Dynamic light scattering (DLS) is employed to determine if particles are formed in solutions and, if so, to examine their sizes [325]. DLS has found its broadest application in monitoring the stability of heteropoly acids in the course of a catalytic reaction (e.g., water-splitting systems [326]).

Thermogravimetric analysis (TGA) is another technique routinely applied to determine the number of crystal water molecules present in the structure of a heteropoly acid. No common definition has been accepted of whether crystal water molecules coordinating to the TM-cores are part of the crystal water content that is supposed to evaporate or not. Crystal water molecules may evaporate already upon sample preparation. The accuracy of this technique is not high enough to decide if the origin of the remaining electron density in a crystal structure is arising from the disturbed crystal water molecules or if it is just a background noise. Routinely, samples should be dried under high vacuum prior to analysis.

Cyclic voltammetry (CV) techniques have been widely employed in the study of heteropoly acids properties [111], mostly in measuring the redox potentials of the dissolved molecular species. Given this information, the kinetics of electron transfer and subsequent reactions can be studied [327]. To facilitate the electron transfer between the dissolved species and the electrodes, an electrolyte is used. Electron transfers from the working electrode to the dissolved molecular species and vice versa are examined by applying a potential between the two electrodes, i.e., the working and the counter electrode. The current observed during the electron transfers is plotted against the potential. The result is a characteristic plot known as a cyclic voltammogram (Fig. 2.30). Launay et al. [329,330] and others [111,331,332] have presented elaborate studies of cyclic polyanion voltammograms. They have tested electrochemical properties of polyanions and assigned the observed waves in cyclic voltammograms to certain electron-transfer processes. Under specific conditions (pH, additives, buffers), the potential at which an electron transfer occurs can be determined and used to predict if a reaction may occur.

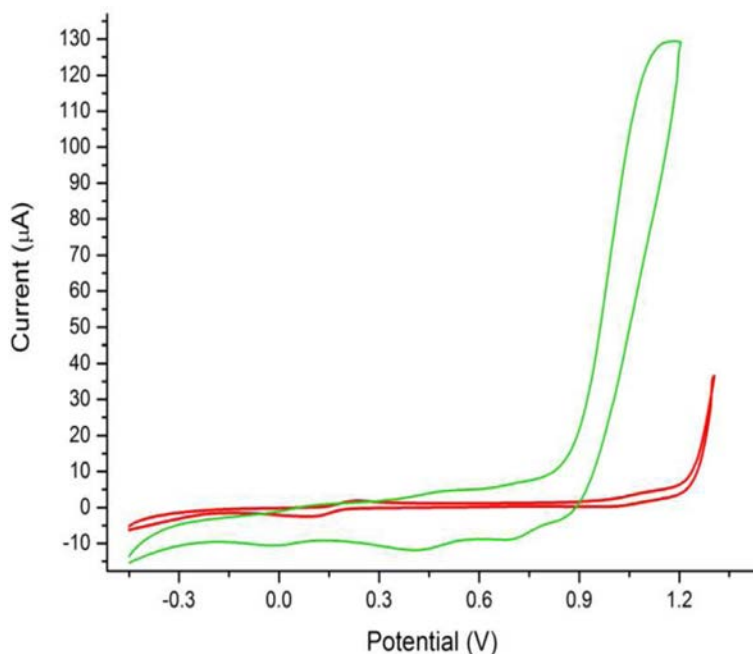


**FIG. 2.30** CVs measured with POM-PS complex functionalized carbon paste electrodes vs. Ag/AgCl, in acetate buffer (pH 4.75, 0.1 M), 50 mV/s; *red* (dark gray in print versions):  $\text{Na}_n[\text{Ru}(\text{bpy})_3]^{10-2n} [\text{Co}_4(\text{H}_2\text{O})_2(\text{PW}_9\text{O}_{34})_2]$ ; *green* (light gray in print versions):  $[\text{Ru}(\text{bpy})_3]_2\text{K}_3 [ \{ \text{Ru}_3\text{O}_3(\text{H}_2\text{O})\text{Cl}_2 \} (\alpha\text{-SiW}_9\text{O}_{34}) ]$  [328].



## References

- [1] J.F. Keggin, The structure and formula of 12-phosphotungstic acid, *Proc. R. Soc. Lond.* 144 (851) (1934) 75–100.
- [2] B. Dawson, The structure of the 9 (18)-heteropoly anion in potassium 9 (18)-tungstophosphate,  $K_6(P_2W_{18}O_{62}) \cdot 14H_2O$ , *Acta Crystallogr.* 6 (2) (1953) 113–126.
- [3] H.T. Evans Jr., The crystal structures of ammonium and potassium molybdatellurates, *J. Am. Chem. Soc.* 70 (3) (1948) 1291–1292.
- [4] D.D. Dexter, J.V. Silverton, A new structural type for heteropoly anions. The crystal structure of  $(NH_4)_2H_6(CeMo_{12}O_{42}) \cdot 12H_2O$ , *J. Am. Chem. Soc.* 90 (13) (1968) 3589–3590.
- [5] G.M. Maksimov, Advances in the synthesis of polyoxometalates and in the study of heteropolyacids, *Russ. Chem. Rev.* 64 (5) (1995) 445.
- [6] A. Müller, W. Plass, E. Krickemeyer, S. Dillinger, H. Bögge, A. Armatage, U. Bergmann,  $[Mo_{57}Fe_6(NO)_6O_{174}(OH)_3(H_2O)_{24}]^{15-}$ : a highly symmetrical giant cluster with an unusual cavity and the possibility of positioning paramagnetic centers on extremely large cluster surfaces, *Angew. Chem. Int. Ed. Engl.* 33 (8) (1994) 849–851.
- [7] M.T. Pope, A. Müller, Introduction to polyoxometalate chemistry: from topology via self-assembly to applications, in: *Polyoxometalate Chemistry From Topology via Self-Assembly to Applications*, Springer, Dordrecht, 2001, pp. 1–6.
- [8] D.L. Long, C. Streb, P. Kögerler, L. Cronin, Observation and theoretical analysis of the “sensitive coordination sites” in the isopolyoxomolybdate cluster  $[Mo_{36}O_{112}(H_2O)_{14}]^{8-}$ , *J. Clust. Sci.* 17 (2) (2006) 257–266.
- [9] A. Rodríguez-Forteza, C. de Graaf, J.M. Poblet, Ab initio and DFT study of the exchange coupling in the highly reduced polyoxoanion  $[PMo_{12}O_{40}(VO)_2]^{5-}$ , *Chem. Phys. Lett.* 428 (1-3) (2006) 88–92.
- [10] X. López, C. de Graaf, J.M. Maestre, M. Bénard, M.M. Rohmer, C. Bo, J.M. Poblet, Highly reduced polyoxometalates: ab initio and DFT study of  $[PMo_8V_4O_{40}(VO)_4]^{5-}$ , *J. Chem. Theory Comput.* 1 (5) (2005) 856–861.
- [11] L. Yan, G. Yang, W. Guan, Z. Su, R. Wang, Density functional theory study on the first hyperpolarizabilities of organoimido derivatives of hexamolybdates, *J. Phys. Chem. B.* 109 (47) (2005) 22332–22336.
- [12] S.P. de Visser, D. Kumar, R. Neumann, S. Shaik, Computer-generated high-valent iron–oxo and manganese–oxo species with polyoxometalate ligands: how do they compare with the iron–oxo active species of heme enzymes? *Angew. Chem. Int. Ed.* 43 (42) (2004) 5661–5665.
- [13] J.M. Poblet, X. López, C. Bo, Ab initio and DFT modelling of complex materials: towards the understanding of electronic and magnetic properties of polyoxometalates, *Chem. Soc. Rev.* 32 (5) (2003) 297–308.
- [14] D. Volkmer, B. Bredenkötter, J. Tellenbröker, P. Kögerler, D.G. Kurth, P. Lehmann, B. Krebs, Structure and properties of the dendron-encapsulated polyoxometalate  $(C_{52}H_{60}NO_{12})_{12}[(Mn(H_2O))_3(SbW_9O_{33})_2]$ , a first generation dendrzyme, *J. Am. Chem. Soc.* 124 (35) (2002) 10489–10496.
- [15] X. López, C. Bo, J.M. Poblet, Electronic properties of polyoxometalates: electron and proton affinity of mixed-Addenda Keggin and Wells-Dawson anions, *J. Am. Chem. Soc.* 124 (42) (2002) 12574–12582.
- [16] M.M. Rohmer, M. Bénard, J.P. Blaudeau, J.M. Maestre, J.M. Poblet, From Lindqvist and Keggin ions to electronically inverse hosts: ab initio modelling of the structure and reactivity of polyoxometalates, *Coord. Chem. Rev.* 178 (1998) 1019–1049.

- [17] C. Yangying, H. Xiuwen, Progress in catalytic epoxidation of olefins with hydrogen peroxide, *Prog. Chem.* 18 (04) (2006) 399.
- [18] V. Nardello, J.M. Aubry, D.E. De Vos, R. Neumann, W. Adam, R. Zhang, P.L. Alsters, Inorganic compounds and materials as catalysts for oxidations with aqueous hydrogen peroxide, *J. Mol. Catal. A Chem.* 251 (1-2) (2006) 185–193.
- [19] N. Mizuno, K. Yamaguchi, K. Kamata, Epoxidation of olefins with hydrogen peroxide catalyzed by polyoxometalates, *Coord. Chem. Rev.* 249 (17-18) (2005) 1944–1956.
- [20] A.R. Gaspar, D.V. Evtuguin, C.P. Neto, Polyoxometalate-catalyzed oxygen delignification of kraft pulp: a pilot-plant experience, *Ind. Eng. Chem. Res.* 43 (24) (2004) 7754–7761.
- [21] J.H. Holles, C.J. Dillon, J.A. Labinger, M.E. Davis, A substrate-versatile catalyst for the selective oxidation of light alkanes: I. Reactivity, *J. Catal.* 218 (1) (2003) 42–53.
- [22] K. Kamata, K. Yonehara, Y. Sumida, K. Yamaguchi, S. Hikichi, N. Mizuno, Efficient epoxidation of olefins with  $\geq 99\%$  selectivity and use of hydrogen peroxide, *Science* 300 (5621) (2003) 964–966.
- [23] A. Müller, S. Roy, En route from the mystery of molybdenum blue via related manipulatable building blocks to aspects of materials science, *Coord. Chem. Rev.* 245 (1-2) (2003) 153–166.
- [24] L.C. Baker, D.C. Glick, Present general status of understanding of heteropoly electrolytes and a tracing of some major highlights in the history of their elucidation, *Chem. Rev.* 98 (1) (1998) 3–50.
- [25] R.D. Shannon, Revised effective ionic radii and systematic studies of interatomic distances in halides and chalcogenides, *Acta Crystallogr., Sect. A: Cryst. Phys., Diffr., Theor. Gen. Crystallogr.* 32 (5) (1976) 751–767.
- [26] D.E. Katsoulis, A survey of applications of polyoxometalates, *Chem. Rev.* 98 (1) (1998) 359–388.
- [27] R.F. Renneke, M. Pasquali, C.L. Hill, Polyoxometalate systems for the catalytic selective production of nonthermodynamic alkenes from alkanes. Nature of excited-state deactivation processes and control of subsequent thermal processes in polyoxometalate photoredox chemistry, *J. Am. Chem. Soc.* 112 (18) (1990) 6585–6594.
- [28] E. Haviv, L.J. Shimon, R. Neumann, Photochemical reduction of CO<sub>2</sub> with visible light using a polyoxometalate as photoreductant, *Chem. A Eur. J.* 23 (1) (2017) 92–95.
- [29] B. Yang, J.J. Pignatello, D. Qu, B. Xing, Reoxidation of photoreduced polyoxotungstate ( $(PW_{12}O_{40})^{4-}$ ) by different oxidants in the presence of a model pollutant. Kinetics and reaction mechanism, *Chem. A Eur. J.* 119 (6) (2015) 1055–1065.
- [30] G. Cao, J. Xiong, Q. Xue, S. Min, H. Hu, G. Xue, Organic–inorganic heteropoly blue based on Dawson-type molybdosulfate and organic dye and its characterization and application in electrocatalysis, *Electrochim. Acta* 106 (2013) 465–471.
- [31] M.T. Pope, *Heteropoly and Isopoly Oxometalates*, Springer, Berlin, 1983.
- [32] M.T. Pope, A. Müller, Polyoxometalate chemistry: an old field with new dimensions in several disciplines, *Angew. Chem. Int. Ed. Engl.* 30 (1) (1991) 34–48.
- [33] W.N. Lipscomb, Paratungstate ion, *Inorg. Chem.* 4 (1) (1965) 132–134.
- [34] G.A. Tsigdinos, Preparation and characterization of 12-molybdophosphoric and 12-molybdosilicic acids and their metal salts, *Ind. Eng. Chem. Prod. Res. Dev.* 13 (4) (1974) 267–274.
- [35] K. Nomiya, R. Kobayashi, M. Miwa, An improved preparation and characterization of tetrahedral Co<sup>II</sup> and Co<sup>III</sup> complexes with dodecatungstate as the tetrahedral ligand, *Bull. Chem. Soc. Jpn.* 56 (8) (1983) 2272–2275.
- [36] L.C. Baker, V.E. Simmons, Heteropoly tungstocobaltate anions containing respectively Co (II) and Co (III) in CoO<sub>4</sub> Tetrahedra. I. 12-tungstocobaltoate and 12-tungstocobaltate1, *J. Am. Chem. Soc.* 81 (17) (1959) 4744–4745.

- [37] D.H. Brown, J.A. Mair, 774. The preparation, properties, and structure of 12-tungstocupric (II) acid, *J. Chem. Soc.* (1962) 3946–3948.
- [38] K. Nomiya, M. Miwa, R. Kobayashi, M. Aiso, Tetrahedral transition metal complexes of [MW<sub>12</sub>O<sub>40</sub>]-type (M = Cu<sup>II</sup>, Fe<sup>III</sup>, Co<sup>II</sup>) with dodecatungstate as tetrahedral ligand, *Bull. Chem. Soc. Jpn.* 54 (10) (1981) 2983–2987.
- [39] W.H. Knoch, R.L. Harlow, New tungstophosphates: Cs<sub>6</sub>W<sub>5</sub>P<sub>2</sub>O<sub>23</sub>, Cs<sub>7</sub>W<sub>10</sub>PO<sub>36</sub>, and Cs<sub>7</sub>Na<sub>2</sub>W<sub>10</sub>PO<sub>37</sub>, *J. Am. Chem. Soc.* 103 (7) (1981) 1865–1867.
- [40] Y. Jeannin, J. Martin-Frère, Tungsten-183 NMR and x-ray study of a heteropolyanion [As<sub>2</sub>W<sub>21</sub>O<sub>69</sub> (H<sub>2</sub>O)]<sup>6-</sup> exhibiting a rare square-pyramidal environment for some tungsten (VI), *J. Am. Chem. Soc.* 103 (7) (1981) 1664–1667.
- [41] F. Cavani, Heteropolycompound-based catalysts: a blend of acid and oxidizing properties, *Catal. Today* 41 (1-3) (1998) 73–86.
- [42] I.V. Kozhevnikov, K.I. Matveev, Homogeneous catalysts based on heteropoly acids, *Appl. Catal.* 5 (2) (1983) 135–150.
- [43] G.D. Yadav, C.K. Mistry, Oxidation of benzyl alcohol under a synergism of phase transfer catalysis and heteropolyacids, *J. Mol. Catal. A Chem.* 172 (1-2) (2001) 135–149.
- [44] T. Okuhara, N. Mizuno, M. Misono, Catalytic chemistry of heteropoly compounds, in: *Advances in Catalysis*, vol. 41, Academic Press, 1996, pp. 113–252.
- [45] A. Nisar, Y. Lu, J. Zhuang, X. Wang, Polyoxometalate nanocone nanoreactors: magnetic manipulation and enhanced catalytic performance, *Angew. Chem. Int. Ed.* 50 (14) (2011) 3187–3192.
- [46] W. Guangjian, L. Guangqing, Y. Zhenxing, X. Mingxia, W. Lei, Catalysts loaded with Keggin heteropolyacids and their application to organic synthesis, *Chin. J. Org. Chem.* 29 (7) (2009) 1039–1047.
- [47] Y. Jeannin, M. Fournier, Nomenclature of polyanions, *Pure Appl. Chem.* 59 (1987) 1529–1548.
- [48] A. Patel, N. Narkhede, S. Singh, S. Pathan, Keggin-type lacunary and transition metal substituted polyoxometalates as heterogeneous catalysts: a recent progress, *Catal. Rev.* 58 (3) (2016) 337–370.
- [49] A.J. Bridgeman, Density functional study of the vibrational frequencies of  $\alpha$ -Keggin heteropolyanions, *Chem. Phys.* 287 (1-2) (2003) 55–69.
- [50] aly Moussawi, M., Assemblages à base de polyoxométallates: des interactions fondamentales aux matériaux hybrides supramoléculaires, Doctoral dissertation, Université Paris-Saclay (ComUE), 2017.
- [51] N.H. Nsouli, A.H. Ismail, I.S. Helgadottir, M.H. Dickman, J.M. Clemente-Juan, U. Kortz, Copper-, cobalt-, and manganese-containing 17-tungsto-2-germanates, *Inorg. Chem.* 48 (13) (2009) 5884–5890.
- [52] S.G. Mitchell, H.N. Miras, D.L. Long, L. Cronin, A dimeric polyoxometalate sandwich motif containing a truncated {Mn<sub>3</sub>O<sub>4</sub>} cubane core, *Inorg. Chim. Acta* 363 (15) (2010) 4240–4246.
- [53] (a) B. Dawson, The structure of the 9 (18)-heteropoly anion in potassium 9 (18)-tungstophosphate, K<sub>6</sub>(P<sub>2</sub>W<sub>18</sub>O<sub>62</sub>)·14H<sub>2</sub>O, *Acta Crystallogr.* 6 (2) (1953) 113–126. (b) H. d'Amour, Vergleich der heteropolyanionen [PMo<sub>9</sub>O<sub>31</sub> (H<sub>2</sub>O)<sub>3</sub>]<sup>3-</sup>, [P<sub>2</sub>Mo<sub>18</sub>O<sub>62</sub>]<sup>6-</sup> und [P<sub>2</sub>W<sub>18</sub>O<sub>62</sub>]<sup>6-</sup>, *Acta Crystallogr. Sect. B: Struct. Crystallogr. Cryst. Chem.* 32 (3) (1976) 729–740.
- [54] L. Vilà-Nadal, S. Romo, X. López, J.M. Poblet, Structural and electronic features of Wells-Dawson polyoxometalates, in: *Complexity in Chemistry and Beyond: Interplay Theory and Experiment*, Springer, Dordrecht, 2012, pp. 171–183.
- [55] (a) A.F. Wells, *Structural Inorganic Chemistry*, first ed., Clarendon Press, Oxford, 1947. (b) T. Hori, O. Tamada, S. Himeno, The structure of 18-molybdodisulphate (VI)(4-) ion in (NEt<sub>4</sub>)<sub>4</sub>S<sub>2</sub>

- Mo<sub>18</sub>O<sub>62</sub>·CH<sub>3</sub>CN, *J. Chem. Soc. Dalton Trans.* 8 (1989) 1491–1497. (c) R. Contant, R. Thouvenot, Hétéropolyanions de type Dawson. 2. Synthèses de polyoxotungstoarsénates lacunaires dérivant de l'octadécatingstodiarsénate. Étude structurale par RMN du tungstène-183 des octadéca (molybdotungstovanado) diarsénates apparentés, *Canadian J. Chem.* 69 (10) (1991) 1498–1506.
- (d) R. Contant, R. Thouvenot, A reinvestigation of isomerism in the Dawson structure: syntheses and <sup>183</sup>W NMR structural characterization of three new polyoxotungstates [X<sub>2</sub>W<sub>18</sub>O<sub>62</sub>]<sup>6-</sup> (X = P<sup>V</sup>, As<sup>V</sup>), *Inorg. Chim. Acta* 212 (1-2) (1993) 41–50. (e) S. Himeno, H. Tatewaki, M. Hashimoto, Synthesis, structure, and characterization of an α-Dawson-type [S<sub>2</sub>W<sub>18</sub>O<sub>62</sub>]<sup>4-</sup> complex, *Bull. Chem. Soc. Jpn.* 74 (9) (2001) 1623–1628. (f) R. Contant, J.-M. Fruchart, Investigation, in solution, of reduced 18-molybdo-2-arsenates and 18-molybdo-2-phosphates (alpha and beta), *Rev. Chim. Miner.* 11 (1974) 123–140. (g) P.J. Richardt, R.W. Gable, A.M. Bond, A.G. Wedd, Synthesis and redox characterization of the polyoxo anion, γ<sup>\*</sup>-[S<sub>2</sub>W<sub>18</sub>O<sub>62</sub>]<sup>4-</sup>: a unique fast oxidation pathway determines the characteristic reversible electrochemical behavior of polyoxometalate anions in acidic media, *Inorg. Chem.* 40 (4) (2001) 703–709.
- [56] M. Kozik, C.F. Hammer, L.C. Baker, Direct determination by tungsten-183 NMR of the locations of added electrons in ESR-silent heteropoly blues. Chemical shifts and relaxation times in polysite mixed-valence transition metal species, *J. Am. Chem. Soc.* 108 (10) (1986) 2748–2749.
- [57] M. Kozik, L.C. Baker, Electron exchange reactions between heteropoly anions: comparison of experimental rate constants with theoretically predicted values, *J. Am. Chem. Soc.* 112 (21) (1990) 7604–7611.
- [58] R. Acerete, S. Harmalker, C.F. Hammer, M.T. Pope, L.C. Baker, Concerning isomerisms and interconversions of 2:18 and 2:17 heteropoly complexes and their derivatives, *J. Chem. Soc. Chem. Commun.* 17 (1979) 777–779.
- [59] J.P. Ciabrini, R. Contant, J.M. Fruchart, Heteropolyblues: relationship between metal-oxygen-metal bridges and reduction behaviour of octadeca (molybdotungsto) diphosphate anions, *Polyhedron* 2 (11) (1983) 1229–1233.
- [60] (a) R. Contant, M. Abbessi, J. Canny, A. Belhouari, B. Keita, L. Nadjo, Iron-substituted Dawson-type tungstodiphosphates: synthesis, characterization, and single or multiple initial electronation due to the substituent nature or position, *Inorg. Chem.* 36 (22) (1997) 4961–4967. (b) B. Keita, L. Nadjo, R. Contant, New electroactive metal oxides electrodeposited from selected Keggin and Dawson-type heteropolyanions, *J. Electroanal. Chem.* 443 (2) (1998) 168–174. (c) R. Contant, M. Richet, Y.W. Lu, B. Keita, L. Nadjo, Isomerically pure α1-monosubstituted tungstodiphosphates: synthesis, characterization and stability in aqueous solutions, *Eur. J. Inorg. Chem.* 2002 (10) (2002) 2587–2593.
- [61] B. Keita, F. Girard, L. Nadjo, R. Contant, J. Canny, M. Richet, Metal ion complexes derived from the α1 isomer of (P<sub>2</sub>W<sub>17</sub>O<sub>61</sub>)<sup>10-</sup>: comparison with the corresponding α2 species, *J. Electroanal. Chem.* 478 (1-2) (1999) 76–82.
- [62] L.C. Baker, J.S. Figgis, New fundamental type of inorganic complex: hybrid between heteropoly and conventional coordination complexes. Possibilities for geometrical isomerisms in 11-, 12-, 17-, and 18-heteropoly derivatives, *J. Am. Chem. Soc.* 92 (12) (1970) 3794–3797.
- [63] A.F. Wells, *Structural Inorganic Chemistry*, Oxford university press, 2012.
- [64] (a) C. Fleming, D.L. Long, N. McMillan, J. Johnston, N. Bovet, V. Dhanak, M. Kadodwala, Reversible electron-transfer reactions within a nanoscale metal oxide cage mediated by metallic substrates, *Nat. Nanotechnol.* 3 (4) (2008) 229–233. (b) N. Fay, A.M. Bond, C. Baffert, J.F. Boas, J.R. Pilbrow, D.L. Long, L. Cronin, Structural, electrochemical, and spectroscopic characterization of a redox pair of sulfite-based polyoxotungstates: α-[W<sub>18</sub>O<sub>54</sub>(SO<sub>3</sub>)<sub>2</sub>]<sup>4+</sup> and α-[W<sub>18</sub>O<sub>54</sub>(SO<sub>3</sub>)<sub>2</sub>]<sup>5-</sup>, *Inorg. Chem.* 46 (9) (2007) 3502–3510.
- [65] D.L. Long, Y.F. Song, E.F. Wilson, P. Kögerler, S.X. Guo, A.M. Bond, L. Cronin, Capture of periodate in a {W<sub>18</sub>O<sub>54</sub>} cluster cage yielding a catalytically active polyoxometalate

- [H<sub>3</sub>W<sub>18</sub>O<sub>56</sub> (IO<sub>6</sub>)<sup>6-</sup> embedded with high-valent iodine, *Angew. Chem.* 120 (23) (2008) 4456–4459.
- [66] D.L. Long, P. Kögerler, A.D. Parenty, J. Fielden, L. Cronin, Discovery of a family of isopolyoxotungstates [H<sub>4</sub>W<sub>19</sub>O<sub>62</sub>] 6- encapsulating a {WO<sub>6</sub>} moiety within a {W<sub>18</sub>} Dawson-like cluster cage, *Angew. Chem.* 118 (29) (2006) 4916–4921.
- [67] J. Yan, D.L. Long, E.F. Wilson, L. Cronin, Discovery of heteroatom-“Embedded” Te ⊂ {W<sub>18</sub>O<sub>54</sub>} nanofunctional polyoxometalates by use of cryospray mass spectrometry, *Angew. Chem.* 121 (24) (2009) 4440–4444.
- [68] I. Lindqvist, Structure of the paramolybdate ion, *Acta Crystallogr.* 3 (2) (1950) 159–160.
- [69] P.A. Lorenzo-Luis, P. Gili, Polyoxometalates with an Anderson-Evans structure, in: *Recent Research Developments in Inorganic Chemistry*, 2000, pp. 185–196.
- [70] J.A. McCleverty, T.J. Meyer (Eds.), *Comprehensive Coordination Chemistry II: From Biology to Nanotechnology*, vol. 1, Elsevier Pergamon, Amsterdam, Boston, 2004, pp. 635–678, p. 25.
- [71] K.J. Schmidt, G.J. Schrobilgen, J.F. Sawyer, Hexasodium hexatungstotellurate (VI) 22-hydrate, *Acta Crystallogr., Sect. C: Cryst. Struct. Commun.* 42 (9) (1986) 1115–1118.
- [72] H.I.D.E.T.A.K.A. Kondo, A.K.I.K.O. Kobayashi, Y.U.K.I.Y.O.S.H.I. Sasaki, The structure of the hexamolybdoperiodate anion in its potassium salt, *Acta Crystallogr. B Struct. Crystallogr. Cryst. Chem.* 36 (3) (1980) 661–664.
- [73] A. Perloff, Crystal structure of sodium hexamolybdochromate (III) octahydrate, Na<sub>3</sub>(CrMo<sub>6</sub>O<sub>24</sub>H<sub>6</sub>)·8H<sub>2</sub>O, *Inorg. Chem.* 9 (10) (1970) 2228–2239.
- [74] C. Wu, X. Lin, R. Yu, W. Yang, C. Lu, H. Zhuang, [Na<sub>4</sub>(H<sub>2</sub>O)<sub>7</sub>][Fe(OH)<sub>6</sub>Mo<sub>6</sub>O<sub>18</sub>]: a new [12] metallacrown-6 structure with an octahedrally coordinated iron at the center, *Sci. China, Ser. B: Chem.* 44 (1) (2001) 49–54.
- [75] A. Björnberg, Multicomponent polyanions. 26. The crystal structure of Na<sub>6</sub>Mo<sub>6</sub>V<sub>2</sub>O<sub>26</sub>(H<sub>2</sub>O)<sub>16</sub>, a compound containing sodium-coordinated hexamolybdodivanadate anions, *Acta Crystallogr. B Struct. Crystallogr. Cryst. Chem.* 35 (9) (1979) 1995–1999.
- [76] A.M. Nenner, Multicomponent Polyanions. 38. Structure of K/sub 5/NaMo/sub 6/V/sub 2/O/sub 26/. 4H/sub 2/O, a Compound Containing a new Configuration of the Hexamolybdodivanadate Anion, 1985.
- [77] V. Balraj, K. Vidyasagar, Hydrothermal synthesis and characterization of novel one-dimensional tellurites of molybdenum (VI), A<sub>4</sub>Mo<sub>6</sub>TeO<sub>22</sub>·2H<sub>2</sub>O (A = NH<sub>4</sub>, Rb), *Inorg. Chem.* 38 (7) (1999) 1394–1400.
- [78] V. Balraj, K. Vidyasagar, Low-temperature syntheses and characterization of novel layered tellurites, A<sub>2</sub>Mo<sub>3</sub>TeO<sub>12</sub> (A = NH<sub>4</sub>, Cs), and “zero-dimensional” tellurites, A<sub>4</sub>Mo<sub>6</sub>Te<sub>2</sub>O<sub>24</sub>·6H<sub>2</sub>O (A = Rb, K), *Inorg. Chem.* 37 (19) (1998) 4764–4774.
- [79] A. Blazevic, A. Rompel, The Anderson-Evans polyoxometalate: from inorganic building blocks via hybrid organic-inorganic structures to tomorrow’s “Bio-POM”, *Coord. Chem. Rev.* 307 (2016) 42–64.
- [80] A.V. Oreshkina, G.Z. Kaziev, S.H. Quinones, A.I. Stash, P.A. Shipilova, Synthesis, thermogravimetric analysis, IR spectrum, and the crystal structure of sodium hexatungstomanganate [Na<sub>2</sub>(H<sub>2</sub>O)<sub>10</sub>][Na(H<sub>2</sub>O)<sub>3</sub>]<sub>2</sub>[MnW<sub>6</sub>O<sub>18</sub>(OH)<sub>6</sub>]·6H<sub>2</sub>O, *Russ. J. Coord. Chem.* 37 (11) (2011) 845.
- [81] K. Nomiya, T. Takahashi, T. Shirai, M. Miwa, Anderson-type heteropolyanions of molybdenum (VI) and tungsten (VI), *Polyhedron* 6 (2) (1987) 213–218.
- [82] M. Alsufyani, *Host-Guest Chemistry of Inorganic Porous Platforms*, 2018. Doctoral dissertation.
- [83] G. Iaccarino, E.D. Tomhave, R.J. Lefkowitz, W.J. Koch, Reciprocal in vivo regulation of myocardial G protein-coupled receptor kinase expression by β-adrenergic receptor stimulation and blockade, *Circulation* 98 (17) (1998) 1783–1789.

- [84] L.H. Bi, U. Kortz, B. Keita, L. Nadjo, The ruthenium (ii)-supported heteropolytungstates [Ru(dmsO)<sub>3</sub>(H<sub>2</sub>O)XW<sub>11</sub>O<sub>39</sub>]<sup>6-</sup>(X = Ge, Si), *Dalton Trans.* 20 (2004) 3184–3190.
- [85] N. Vankova, T. Heine, U. Kortz, NMR chemical shifts of metal centres in polyoxometalates: relativistic DFT predictions, *Eur. J. Inorg. Chem.* 2009 (34) (2009) 5102–5108.
- [86] D. Rehder, in: M.T. Pope, A. Müller (Eds.), *Polyoxometalates: From Platonic Solids to Anti-Retroviral Activity*, 1994.
- [87] T. Yamase, M.T. Pope (Eds.), *Polyoxometalate Chemistry for Nano-Composite Design*, Springer Science & Business Media, 2006.
- [88] J.J. Borrás-Almenar, E. Coronado, A. Müller, M. Pope, *Polyoxometalate Molecular Science*, vol. 98, Springer Science & Business Media, 2003.
- [89] M. Sadakane, D. Tsukuma, M.H. Dickman, B. Bassil, U. Kortz, M. Higashijima, W. Ueda, Structural characterization of mono-ruthenium substituted Keggin-type silicotungstates, *Dalton Trans.* 35 (2006) 4271–4276.
- [90] P.J. Hagrman, D. Hagrman, J. Zubieta, Organic-inorganic hybrid materials: from “Simple” coordination polymers to organodiamine-templated molybdenum oxides, *Angew. Chem. Int. Ed.* 38 (18) (1999) 2638–2684.
- [91] L.C. Baker, V.S. Baker, K. Eriks, M.T. Pope, M.S. Orville, W. Rollins, L.L. Koh, A new general structural category of heteropolyelectrolytes. Unusual magnetic and thermal contraction phenomena, *J. Am. Chem. Soc.* 88 (10) (1966) 2329–2331.
- [92] D.P. Smith, M.T. Pope, Heteropoly 12-metallophosphates containing tungsten and vanadium. Preparation, voltammetry, and properties of mono-, di-, tetra-, and hexavanado complexes, *Inorg. Chem.* 12 (2) (1973) 331–336.
- [93] M.T. Pope, T.F. Scully, Geometrical isomerism arising from partial substitution of metal atoms in isopoly and heteropoly complexes. Possibilities for the Keggin structure, *Inorg. Chem.* 14 (4) (1975) 953–954.
- [94] J. Marrot, M.A. Pilette, M. Haouas, S. Floquet, F. Taulelle, X. López, E. Cadot, Polyoxometalates paneling through {Mo<sub>2</sub>O<sub>2</sub>S<sub>2</sub>} coordination: cation-directed conformations and chemistry of a supramolecular hexameric scaffold, *J. Am. Chem. Soc.* 134 (3) (2012) 1724–1737.
- [95] J.H. Son, Y.U. Kwon, Crystal engineering through face interactions between tetrahedral and octahedral building blocks: crystal structure of [e-Al<sub>13</sub>O<sub>4</sub>(OH)<sub>24</sub>(H<sub>2</sub>O)<sub>12</sub>]<sub>2</sub>[V<sub>2</sub>W<sub>4</sub>O<sub>19</sub>]<sub>3</sub>(OH)<sub>2</sub>·27H<sub>2</sub>O, *Inorg. Chem.* 43 (6) (2004) 1929–1932.
- [96] G. Guo, Y. Xu, J. Cao, C. Hu, An unprecedented vanadoniobate cluster with ‘trans-vanadium’biccapped Keggin-type {VNb<sub>12</sub>O<sub>40</sub>(VO)<sub>2</sub>}, *Chem. Commun.* 47 (33) (2011) 9411–9413.
- [97] Y. Huang, J. Zhang, J. Ge, C. Sui, J. Hao, Y. Wei, [V<sub>4</sub>Mo<sub>3</sub>O<sub>14</sub>(NAr)<sub>3</sub>(μ<sub>2</sub>-NAr)<sub>3</sub>]<sup>2-</sup>: the first polyarylimido-stabilized molybdovanadate cluster, *Chem. Commun.* 53 (17) (2017) 2551–2554.
- [98] A.A. Shmakova, V.V. Volchek, V. Yanshole, N.B. Kompankov, N.P. Martin, M. Nyman, M.N. Sokolov, Niobium uptake by a [P8W<sub>48</sub>O<sub>184</sub>]<sup>40-</sup> macrocyclic polyanion, *New J. Chem.* 43 (25) (2019) 9943–9952.
- [99] N. Mizuno, K. Kamata, Catalytic oxidation of hydrocarbons with hydrogen peroxide by vanadium-based polyoxometalates, *Coord. Chem. Rev.* 255 (19–20) (2011) 2358–2370.
- [100] B.B. Sarma, I. Efremenko, R. Neumann, Oxygenation of methylarenes to benzaldehyde derivatives by a polyoxometalate mediated electron transfer–oxygen transfer reaction in aqueous sulfuric acid, *J. Am. Chem. Soc.* 137 (18) (2015) 5916–5922.
- [101] V.W. Day, W.G. Klemperer, C. Schwartz, Synthesis, characterization, and interconversion of the niobotungstic acid Nb<sub>2</sub>W<sub>4</sub>O<sub>19</sub>H<sub>3</sub> and its anhydride and alkyl/silyl esters, *J. Am. Chem. Soc.* 109 (20) (1987) 6030–6044.

- [102] H. Driss, K. Boubekeur, M. Debbabi, R. Thouvenot, Synthesis and spectroscopic characterization of organophosphono derivatives of lindqvist niobotungstates—X-ray crystal structures of  $(n\text{-Bu}_4\text{N})_3 [\text{NbW}_{10}\text{O}_{38} (\text{RP})_2]$  ( $\text{R} = n\text{-Bu, Hep and Ph}$ ), *Eur. J. Inorg. Chem.* 2008 (23) (2008) 3678–3686.
- [103] S. Li, S. Liu, S. Liu, Y. Liu, Q. Tang, Z. Shi, J. Ye,  $\{\text{Ta}_{12}\}/\{\text{Ta}_{16}\}$  cluster-containing polyantatungstates with remarkable photocatalytic H<sub>2</sub> evolution activity, *J. Am. Chem. Soc.* 134 (48) (2012) 19716–19721.
- [104] P. Huang, C. Qin, X.L. Wang, C.Y. Sun, Y.Q. Jiao, Y. Xing, K.Z. Shao, Self-assembly and visible-light photocatalytic properties of W/Nb mixed-addendum polyoxometalate and transition-metal cations, *ChemPlusChem* 78 (8) (2013) 775.
- [105] P.I. Molina, D.J. Sures, P. Miró, L.N. Zakharov, M. Nyman, Bridging the opposite chemistries of tantalum and tungsten polyoxometalates, *Dalton Trans.* 44 (36) (2015) 15813–15822.
- [106] J. Tucher, S. Schlicht, F. Kollhoff, C. Streb, Photocatalytic reactivity tuning by heterometal and addenda metal variation in Lindqvist polyoxometalates, *Dalton Trans.* 43 (45) (2014) 17029–17033.
- [107] C. Li, K. Suzuki, N. Mizuno, K. Yamaguchi, Polyoxometalate LUMO engineering: a strategy for visible-light-responsive aerobic oxygenation photocatalysts, *Chem. Commun.* 54 (52) (2018) 7127–7130.
- [108] J. Tucher, Y. Wu, L.C. Nye, I. Ivanovic-Burmazovic, M.M. Khusniyarov, C. Streb, Metal substitution in a Lindqvist polyoxometalate leads to improved photocatalytic performance, *Dalton Trans.* 41 (33) (2012) 9938–9943.
- [109] S. Li, Y. Zhou, Q. Peng, R. Wang, X. Feng, S. Liu, Z. Zheng, Controllable synthesis and catalytic performance of nanocrystals of rare-earth-polyoxometalates, *Inorg. Chem.* 57 (11) (2018) 6624–6631.
- [110] S. Li, G. Li, P. Ji, J. Zhang, S. Liu, J. Zhang, X. Chen, A giant Mo/Ta/W ternary mixed-addenda polyoxometalate with efficient photocatalytic activity for primary amine coupling, *ACS Appl. Mater. Interfaces* 11 (46) (2019) 43287–43293.
- [111] M. Sadakane, E. Steckhan, Electrochemical properties of polyoxometalates as electrocatalysts, *Chem. Rev.* 98 (1) (1998) 219–238.
- [112] K. Suzuki, N. Mizuno, K. Yamaguchi, Polyoxometalate photocatalysis for liquid-phase selective organic functional group transformations, *ACS Catal.* 8 (11) (2018) 10809–10825.
- [113] N. Mizuno, M. Misono, Heterogeneous catalysis, *Chem. Rev.* 98 (1) (1998) 199–218.
- [114] M. Bösing, I. Loose, H. Pohlmann, B. Krebs, New strategies for the generation of large heteropolymetalate clusters: the  $\beta\text{-B-SbW}_9$  fragment as a multifunctional unit, *Chem. A Eur. J.* 3 (8) (1997) 1232–1237.
- [115] A. Müller, E. Krickemeyer, S. Dillinger, J. Meyer, H. Bögge, A. Stammler,  $[(\text{AsOH})_3 (\text{MoO}_3)_3 (\text{AsMo}_9\text{O}_{33})]^{7-}$  and  $[(\text{AsOH})_6 (\text{MoO}_3)_2 (\text{O}_2\text{Mo-O-MoO}_2)^2 (\text{AsMo}_9\text{O}_{33})_2]^{10-}$ : coupling of highly negatively charged building blocks, *Angew. Chem. Int. Ed. Engl.* 35 (2) (1996) 171–173.
- [116] U. Kortz, M.G. Savelieff, B.S. Bassil, B. Keita, L. Nadjjo, Synthesis and characterization of iron (III)-substituted, dimeric polyoxotungstates,  $[\text{Fe}_4 (\text{H}_2\text{O})_{10} (\beta\text{-XW}_9\text{O}_{33})_2]^{n-}$  ( $n = 6, \text{X} = \text{As}^{\text{III}}, \text{Sb}^{\text{III}}, n = 4, \text{X} = \text{Se}^{\text{IV}}, \text{Te}^{\text{IV}}$ ), *Inorg. Chem.* 41 (4) (2002) 783–789.
- [117] B. Krebs, E. Droste, M. Piepenbrink, Syntheses and crystal structure studies of novel selenium- and tellurium-substituted lacunary polyoxometalates, in: *Polyoxometalate Chemistry From Topology via Self-Assembly to Applications*, Springer, Dordrecht, 2001, pp. 89–99.
- [118] K. Wassermann, M.T. Pope, Large cluster formation through multiple substitution with lanthanide cations (La, Ce, Nd, Sm, Eu, and Gd) of the polyoxoanion  $[(\text{B-}\alpha\text{-AsO}_3\text{W}_9\text{O}_{30})_4$



- (WO<sub>2</sub>)<sub>4</sub>] 28-. Synthesis and structural characterization, *Inorg. Chem.* 40 (12) (2001) 2763–2768.
- [119] P. Mialane, L. Lisnard, A. Mallard, J. Marrot, E. Antic-Fidancev, P. Aschehoug, F. Sécheresse, Solid-state and solution studies of {Ln<sub>n</sub> (SiW<sub>11</sub>O<sub>39</sub>)} polyoxoanions: an example of building block condensation dependent on the nature of the rare earth, *Inorg. Chem.* 42 (6) (2003) 2102–2108.
- [120] D. Drewes, M. Piepenbrink, B. Krebs, The first structurally characterized Mn (III) substituted sandwich-type polyoxotungstates, *J. Clust. Sci.* 17 (2) (2006) 361–374.
- [121] T.J. Weakley, H.T. Evans, J.S. Showell, G.F. Tourné, C.M. Tourné, 18-Tungstotetracobalto (II) diphosphate and related anions: a novel structural class of heteropolyanions, *J. Chem. Soc. Chem. Commun.* 4 (1973) 139–140.
- [122] R.G. Finke, M. Droege, J.R. Hutchinson, O. Gansow, Trivalent heteropolytungstate derivatives: the rational synthesis, characterization, and tungsten-183 NMR spectra of P<sub>2</sub>W<sub>18</sub>M<sub>4</sub> (H<sub>2</sub>O)<sub>2</sub>O<sub>68</sub><sup>10-</sup> (M=cobalt, copper, zinc), *J. Am. Chem. Soc.* 103 (6) (1981) 1587–1589.
- [123] R.G. Finke, M.W. Droege, Trivalent heteropolytungstate derivatives. 2. Synthesis, characterization, and tungsten-183 NMR of P<sub>4</sub>W<sub>30</sub>M<sub>4</sub> (H<sub>2</sub>O)<sub>2</sub>O<sub>112</sub><sup>16-</sup> (M= Co, Cu, Zn), *Inorg. Chem.* 22 (6) (1983) 1006–1008.
- [124] H.T. Evans, C.M. Tourné, G.F. Tourné, T.J. Weakley, X-Ray crystallographic and tungsten-183 nuclear magnetic resonance structural studies of the [M<sub>4</sub> (H<sub>2</sub>O)<sub>2</sub> (XW<sub>9</sub>O<sub>34</sub>)<sub>2</sub>]<sup>10-</sup> heteropolyanions (M= CO<sup>II</sup> or Zn, X= P or As), *J. Chem. Soc. Dalton Trans.* 12 (1986) 2699–2705.
- [125] R.G. Finke, M.W. Droege, P.J. Domaille, Trivalent heteropolytungstate derivatives. 3. Rational syntheses, characterization, two-dimensional tungsten-183 NMR, and properties of tungstometallophosphates P<sub>2</sub>W<sub>18</sub>M<sub>4</sub> (H<sub>2</sub>O)<sub>2</sub>O<sub>68</sub><sup>10-</sup> and P<sub>4</sub>W<sub>30</sub>M<sub>4</sub> (H<sub>2</sub>O)<sub>2</sub>O<sub>112</sub><sup>16-</sup> (M= cobalt, copper, zinc), *Inorg. Chem.* 26 (23) (1987) 3886–3896.
- [126] S.H. Wasfi, A.L. Rheingold, G.F. Kokoszka, A.S. Goldstein, Preparation, structure, and magnetic properties of Na<sub>10</sub>Fe<sub>4</sub>Cu<sub>2</sub>W<sub>18</sub>O<sub>70</sub>H<sub>6</sub>·29H<sub>2</sub>O, containing the double Keggin anion [Fe<sub>4</sub>Cu<sub>2</sub>W<sub>18</sub>O<sub>70</sub>H<sub>6</sub>]<sup>10-</sup>, *Inorg. Chem.* 26 (18) (1987) 2934–2939.
- [127] T.J. Weakley, R.G. Finke, Single-crystal x-ray structures of the polyoxotungstate salts K<sub>8</sub>Na<sub>17</sub>[Cu<sub>4</sub>(H<sub>2</sub>O)<sub>2</sub>(PW<sub>9</sub>O<sub>34</sub>)<sub>2</sub>].24H<sub>2</sub>O and Na<sub>14</sub>Cu[Cu<sub>4</sub>(H<sub>2</sub>O)<sub>2</sub>(P<sub>2</sub>W<sub>15</sub>O<sub>56</sub>)<sub>2</sub>].53H<sub>2</sub>O, *Inorg. Chem.* 29 (6) (1990) 1235–1241.
- [128] C.J. Gomez-Garcia, E. Coronado, J.J. Borrás-Almenar, Magnetic characterization of tetranuclear copper (II) and cobalt (II) exchange-coupled clusters encapsulated in heteropolyoxotungstate complexes. Study of the nature of the ground states, *Inorg. Chem.* 31 (9) (1992) 1667–1673.
- [129] N. Casan-Pastor, J. Bas-Serra, E. Coronado, G. Pourroy, L.C. Baker, First ferromagnetic interaction in a heteropoly complex: [Co<sub>4</sub>O<sub>14</sub> (H<sub>2</sub>O)<sub>2</sub> (PW<sub>9</sub>O<sub>27</sub>)<sub>2</sub>]<sup>10-</sup>. Experiment and theory for intramolecular anisotropic exchange involving the four Co (II) atoms, *J. Am. Chem. Soc.* 114 (26) (1992) 10380–10383.
- [130] C.J. Gómez-García, E. Coronado, P. Gómez-Romero, N. Casan-Pastor, A tetranuclear rhomb-like cluster of manganese (II). Crystal structure and magnetic properties of the heteropoly complex K<sub>10</sub> [Mn<sub>4</sub> (H<sub>2</sub>O)<sub>2</sub> (PW<sub>9</sub>O<sub>34</sub>)<sub>2</sub>].20H<sub>2</sub>O, *Inorg. Chem.* 32 (15) (1993) 3378–3381.
- [131] C.J. Gómez-García, J.J. Borrás-Almenar, E. Coronado, L. Ouahab, Single-crystal X-ray structure and magnetic properties of the polyoxotungstate complexes Na<sub>16</sub> [M<sub>4</sub> (H<sub>2</sub>O)<sub>2</sub> (P<sub>2</sub>W<sub>15</sub>O<sub>56</sub>)<sub>2</sub>].nH<sub>2</sub>O (M=Mn<sup>II</sup>, n=53; M=Ni<sup>II</sup>, n=52): an antiferromagnetic Mn<sup>II</sup> tetramer and a ferromagnetic Ni<sup>II</sup> tetramer, *Inorg. Chem.* 33 (18) (1994) 4016–4022.

- [132] X.Y. Zhang, G.B. Jameson, C.J. O'Connor, M.T. Pope, High-valent manganese in polyoxotungstates—II. Oxidation of the tetramanganese heteropolyanion  $[\text{Mn}_4(\text{H}_2\text{O})_2(\text{PW}_9\text{O}_{34})_2]^{10-}$ , *Polyhedron* 15 (5-6) (1996) 917–922.
- [133] X. Zhang, Q. Chen, D.C. Duncan, C.F. Campana, C.L. Hill, Multiiron polyoxoanions. syntheses, characterization, X-ray crystal structures, and catalysis of  $\text{H}_2\text{O}_2$ -based hydrocarbon oxidations by  $[\text{Fe}_4^{\text{III}}(\text{H}_2\text{O})_2(\text{P}_2\text{W}_{15}\text{O}_{56})_2]^{12-}$ , *Inorg. Chem.* 36 (19) (1997) 4208–4215.
- [134] X. Zhang, Q. Chen, D.C. Duncan, R.J. Lachicotte, C.L. Hill, Multiiron polyoxoanions. Synthesis, characterization, X-ray crystal structure, and catalytic  $\text{H}_2\text{O}_2$ -based alkene oxidation by  $[(n\text{-C}_4\text{H}_9)_4\text{N}]_6[\text{Fe}_4^{\text{III}}(\text{H}_2\text{O})_2(\text{PW}_9\text{O}_{34})_2]$ , *Inorg. Chem.* 36 (20) (1997) 4381–4386.
- [135] J.M. Clemente-Juan, E. Coronado, J.R. Galán-Mascarós, C.J. Gómez-García, Increasing the nuclearity of magnetic polyoxometalates. Syntheses, structures, and magnetic properties of salts of the heteropoly complexes  $[\text{Ni}_3(\text{H}_2\text{O})_3(\text{PW}_{10}\text{O}_{39})\text{H}_2\text{O}]^7-$ ,  $[\text{Ni}_4(\text{H}_2\text{O})_2(\text{PW}_9\text{O}_{34})_2]^{10-}$ , and  $[\text{Ni}_9(\text{OH})_3(\text{H}_2\text{O})_6(\text{HPO}_4)_2(\text{PW}_9\text{O}_{34})_3]^{16-}$ , *Inorg. Chem.* 38 (1) (1999) 55–63.
- [136] L.H. Bi, E.B. Wang, J. Peng, R.D. Huang, L. Xu, C.W. Hu, Crystal structure and replacement reaction of coordinated water molecules of the heteropoly compounds of sandwich-type tungstoarsenates, *Inorg. Chem.* 39 (4) (2000) 671–679.
- [137] L.H. Bi, R.D. Huang, J. Peng, E.B. Wang, Y.H. Wang, C.W. Hu, Rational syntheses, characterization, crystal structure, and replacement reactions of coordinated water molecules of  $[\text{As}_2\text{W}_{18}\text{M}_4(\text{H}_2\text{O})_2\text{O}_{68}]^{10-}$  ( $\text{M}=\text{Cd}, \text{Co}, \text{Cu}, \text{Fe}, \text{Mn}, \text{Ni}$  or  $\text{Zn}$ ), *J. Chem. Soc. Dalton Trans.* (2) (2001) 121–129.
- [138] U. Kortz, S. Isber, M.H. Dickman, D. Ravot, Sandwich-type silicotungstates: structure and magnetic properties of the dimeric polyoxoanions  $\{[\text{SiM}_2\text{W}_9\text{O}_{34}(\text{H}_2\text{O})_2]^{12-}$  ( $\text{M}=\text{Mn}^{2+}, \text{Cu}^{2+}, \text{Zn}^{2+}$ ), *Inorg. Chem.* 39 (13) (2000) 2915–2922.
- [139] E.M. Limanski, M. Piepenbrink, E. Droste, K. Burgemeister, B. Krebs, Syntheses and X-ray characterization of novel  $[\text{M}_4(\text{H}_2\text{O})_2(\text{XW}_9\text{O}_{34})_2]^{n-}$  ( $\text{M}=\text{Cu}^{\text{II}}, \text{X}=\text{Cu}^{\text{II}}$ ; and  $\text{M}=\text{Fe}^{\text{III}}, \text{X}=\text{Fe}^{\text{III}}$ ) polyoxotungstates, *J. Clust. Sci.* 13 (3) (2002) 369–379.
- [140] C. Rosu, D.C. Crans, T.J. Weakley, Rational synthesis and X-ray structure of  $[\text{Mn}_4^{\text{II}}(\text{H}_2\text{O})_2(\text{AsVW}_9\text{O}_{34})_2]^{10-}$  from  $[\text{AsIII}_4\text{W}_{40}\text{O}_{140}]^{28-}$ ,  $\text{MnO}_4^-$  and  $\text{Mn}^{2+}$ , *Polyhedron* 21 (9-10) (2002) 959–962.
- [141] U. Kortz, S. Nellutla, A.C. Stowe, N.S. Dalal, U. Rauwald, W. Danquah, D. Ravot, Sandwich-type germanotungstates: structure and magnetic properties of the dimeric polyoxoanions  $[\text{M}_4(\text{H}_2\text{O})_2(\text{GeW}_9\text{O}_{34})_2]^{12-}$  ( $\text{M}=\text{Mn}^{2+}, \text{Cu}^{2+}, \text{Zn}^{2+}, \text{Cd}^{2+}$ ), *Inorg. Chem.* 43 (7) (2004) 2308–2317.
- [142] M. Bösing, A. Nöh, I. Loose, B. Krebs, Highly efficient catalysts in directed oxygen-transfer processes: synthesis, structures of novel manganese-containing heteropolyanions, and applications in regioselective epoxidation of dienes with hydrogen peroxide, *J. Am. Chem. Soc.* 120 (29) (1998) 7252–7259.
- [143] F.R.A.N.C.I.S. Robert, M. Leyrie, G. Hervé, Structure of potassium diaquatricuprooctadecatungstodiarсенate (III)(12-) undecahydrate, *Acta Crystallogr. B Struct. Crystallogr. Cryst. Chem.* 38 (2) (1982) 358–362.
- [144] U. Kortz, N.K. Al-Kassem, M.G. Savelieff, N.A. Al Kadi, M. Sadakane, Synthesis and characterization of copper-, zinc-, manganese-, and cobalt-substituted dimeric heteropolyanions,  $[(\alpha\text{-XW}_9\text{O}_{33})_2\text{M}_3(\text{H}_2\text{O})_3]^{n-}$  ( $n=12, \text{X}=\text{As}^{\text{III}}, \text{Sb}^{\text{III}}, \text{M}=\text{Cu}^{2+}, \text{Zn}^{2+}$ ;  $n=10, \text{X}=\text{Se}^{\text{IV}}, \text{Te}^{\text{IV}}, \text{M}=\text{Cu}^{2+}$ ) and  $[(\alpha\text{-AsW}_9\text{O}_{33})_2\text{WO}(\text{H}_2\text{O})\text{M}_2(\text{H}_2\text{O})_2]^{10-}$  ( $\text{M}=\text{Zn}^{2+}, \text{Mn}^{2+}, \text{Co}^{2+}$ ), *Inorg. Chem.* 40 (18) (2001) 4742–4749.
- [145] B. Botar, T. Yamase, E. Ishikawa, Synthesis and crystal structure of a novel vanadium-containing tungstobismutate (III)  $\text{K}_{12}[(\text{VO})_3(\text{BiW}_9\text{O}_{33})_2]\cdot 30\text{H}_2\text{O}$ , *Inorg. Chem. Commun.* 4 (10) (2001) 551–554.

- [146] T. Yamase, B. Botar, E. Ishikawa, K. Fukaya, Chemical structure and intramolecular spin-exchange interaction of  $[(VO)_3(SbW_9O_{33})_2]^{12-}$ , *Chem. Lett.* 30 (1) (2001) 56–57.
- [147] P. Mialane, J. Marrot, E. Riviere, J. Nebout, G. Herve, Structural characterization and magnetic properties of sandwich-type tungstoarsenate complexes. Study of a mixed-valent  $V_2^{IV}V^V$  heteropolyanion, *Inorg. Chem.* 40 (1) (2001) 44–48.
- [148] U. Kortz, S. Nellutla, A.C. Stowe, N.S. Dalal, J. van Tol, B.S. Bassil, Structure and magnetism of the tetra-copper (II)-substituted heteropolyanion  $[Cu_4K_2(H_2O)_8(\alpha-AsW_9O_{33})_2]^{8-}$ , *Inorg. Chem.* 43 (1) (2004) 144–154.
- [149] D. Drewes, E.M. Limanski, M. Piepenbrink, B. Krebs, Neue heteropolyanionen des Wolframs mit vanadium (IV) als heteroatom, *Z. Anorg. Allg. Chem.* 630 (1) (2004) 58–62.
- [150] T. Kurata, A. Uehara, Y. Hayashi, K. Isobe, Cyclic polyvanadates incorporating template transition metal cationic species: synthesis and structures of hexavanadate  $[PdV_6O_{18}]^{4+}$ , octavanadate  $[Cu_2V_8O_{24}]^{4+}$ , and decavanadate  $[Ni_4V_{10}O_{30}(OH)_2(H_2O)_6]^{4-}$ , *Inorg. Chem.* 44 (7) (2005) 2524–2530.
- [151] M.D.L. Nieves Corella Ochoa, Incorporation of Pyramidal Heteroanions in Mixed-Metal Polyoxometalate Based Cages, Doctoral dissertation, University of Glasgow, 2011.
- [152] S. Inami, M. Nishio, Y. Hayashi, K. Isobe, H. Kameda, T. Shimoda, Dinuclear manganese and cobalt complexes with cyclic polyoxovanadate ligands: synthesis and characterization of  $[Mn_2V_{10}O_{30}]^{6-}$  and  $[Co_2(H_2O)_2V_{10}O_{30}]^{6-}$ , *Eur. J. Inorg. Chem.* 2009 (34) (2009) 5253–5258.
- [153] E. Cadot, B. Salignac, A. Dolbecq, F. Secheresse, From the first sulfurated Keggin anion to a new class of compounds based on the  $[M_2O_2S_2]^{2+}$  building block  $M=Mo, W$ , in: *Polyoxometalate Chemistry From Topology via Self-Assembly to Applications*, Springer, Dordrecht, 2001, pp. 39–53.
- [154] E. Cadot, B. Salignac, S. Halut, F. Sécheresse,  $[Mo_{12}S_{12}O_{12}(OH)_{12}(H_2O)_6]$ : a cyclic molecular cluster based on the  $[Mo_2S_2O_2]^{2+}$  building block, *Angew. Chem. Int. Ed.* 37 (5) (1998) 611–613.
- [155] J.F. Lemonnier, S. Duval, S. Floquet, E. Cadot, A decade of oxothiomolybdenum wheels: synthesis, behavior in solution, and electrocatalytic properties, *Isr. J. Chem.* 51 (2) (2011) 290–302.
- [156] K. Wassermann, M.H. Dickman, M.T. Pope, Self-assembly of supramolecular polyoxometalates: the compact, water-soluble heteropolytungstate anion  $[As Ce (H_2O)_{36}W_{148}O_{524}]^{76-}$ , *Angew. Chem. Int. Ed. Engl.* 36 (13-14) (1997) 1445–1448.
- [157] F. Hussain, R.W. Gable, M. Speldrich, P. Kögerler, C. Boskovic, Polyoxotungstate-encapsulated  $Gd_6$  and  $Yb_{10}$  complexes, *Chem. Commun.* 3 (2009) 328–330.
- [158] C. Preyssler, Existence of 18-tungsto-3-phosphate, *Bull. Soc. Chim. Fr.* 1 (1970) 30–36.
- [159] M.H. Alizadeh, S.P. Harmalker, Y. Jeannin, J. Martin-Frere, M.T. Pope, A heteropolyanion with fivefold molecular symmetry that contains a nonlabile encapsulated sodium ion. The structure and chemistry of  $[NaP_5W_{30}O_{110}]^{14-}$ , *J. Am. Chem. Soc.* 107 (9) (1985) 2662–2669.
- [160] A. Müller, F. Peters, M.T. Pope, D. Gatteschi, Polyoxometalates: very large clusters nanoscale magnets, *Chem. Rev.* 98 (1) (1998) 239–272.
- [161] J. Liu, S. Liu, L. Qu, M.T. Pope, C. Rong, Derivatives of the 21-tungsto-9-antimonate heteropolyanion. Part 1. Inclusion of lanthanide cations, *Transit. Met. Chem.* 17 (4) (1992) 311–313.
- [162] J.F. Liu, Y.G. Chen, L. Meng, J. Guo, Y. Liu, M.T. Pope, Synthesis and characterization of novel heteropoly-tungstoarsenates containing lanthanides  $[LnAs_4W_{40}O_{140}]^{25-}$  and their biological activity, *Polyhedron* 17 (9) (1998) 1541–1546.
- [163] A. Haider, K. Zarschler, S.A. Joshi, R.M. Smith, Z. Lin, A.S. Mougharbel, U. Kortz, Preyssler-pope-jeannin polyanions  $[NaP_5W_{30}O_{110}]^{14-}$  and  $[AgP_5W_{30}O_{110}]^{14-}$ : microwave-assisted synthesis, structure, and biological activity, *Z. Anorg. Allg. Chem.* 644 (14) (2018) 752–758.

- [164] A. Hayashi, M.N.K. Wihadi, H. Ota, X. López, K. Ichihashi, S. Nishihara, M. Sadakane, Preparation of Preyssler-type phosphotungstate with one central potassium cation and potassium cation migration into the Preyssler molecule to form di-potassium-encapsulated derivative, *ACS Omega* 3 (2) (2018) 2363–2373.
- [165] J.A. Fernández, X. López, C. Bo, C. de Graaf, E.J. Baerends, J.M. Poblet, Polyoxometalates with internal cavities: redox activity, basicity, and cation encapsulation in  $[X^{n+}P_5W_{30}O_{110}]^{(15-n)-}$  Preyssler complexes, with  $X=Na^+$ ,  $Ca^{2+}$ ,  $Y^{3+}$ ,  $La^{3+}$ ,  $Ce^{3+}$ , and  $Th^{4+}$ , *J. Am. Chem. Soc.* 129 (40) (2007) 12244–12253.
- [166] K.C. Kim, M.T. Pope, G.J. Gama, M.H. Dickman, Slow proton exchange in aqueous solution. Consequences of protonation and hydration within the central cavity of preyssler anion derivatives,  $[M(H_2O)_6P_5W_{30}O_{110}]^{n-}$ , *J. Am. Chem. Soc.* 121 (48) (1999) 11164–11170.
- [167] F. Hussain, U. Kortz, B. Keita, L. Nadjo, M.T. Pope, Tetrakis (dimethyltin)-containing tungstophosphate  $[\{Sn(CH_3)_2\}_4(H_2P_4W_{24}O_{92})_2]^{28-}$ : first evidence for a lacunary preyssler ion, *Inorg. Chem.* 45 (2) (2006) 761–766.
- [168] (a) M.R. Antonio, L. Soderholm, Cerium valence in cerium-exchanged preyssler's heteropolyanion through X-ray absorption near-edge structure, *Inorg. Chem.* 33 (26) (1994) 5988–5993. (b) S. Lis, M. Elbanowski, S. But, Synthesis and spectroscopic study of Europium (III) in heteropolyanion  $[EuP_5W_{30}O_{110}]^{12-}$ , *Acta Phys. Polon. A* 2 (90) (1996) 361–366. (c) A. Szczyzewski, S. Lis, Z. Kruczynski, J. Pietrzak, S. But, M. Elbanowski, EPR study of Gadolinium (III) complexes with heteropolyanions:  $(Gd(SiW_{11}O_{39})_2)^{13-}$  and  $(GdP_5W_{30}O_{110})^{12-}$ , *Acta Phys. Polon.-Ser. A Gen. Phys.* 90 (2) (1996) 345–352. (d) M.R. Antonio, C.W. Williams, L. Soderholm, Synthesis and characterization of actinide-exchanged Preyssler heteropolyanions  $[AnP_5W_{30}O_{110}]^{n-}$  ( $An \equiv Th, Am, Cm$ ), *J. Alloys Compd.* 271 (1998) 846–849.
- [169] M.H. Dickman, G.J. Gama, K.C. Kim, M.T. Pope, The structures of europium (III)-and uranium (IV) derivatives of  $[P_5W_{30}O_{110}]^{15-}$ : evidence for “cryptohydration”, *J. Clust. Sci.* 7 (4) (1996) 567–583.
- [170] M.H. Alizadeh, H. Razavi, F.F. Bamoharram, M.K. Hassanzadeh, R. Khoshnavazi, F.M. Zonoz, Novel catalytic acetylation of alcohols with preyssler's anion,  $[NaP_5W_{30}O_{110}]^{14-}$ , *Kinet. Catal.* 44 (4) (2003) 524–528.
- [171] (a) F.F. Bamoharram, M. Roshani, M.H. Alizadeh, H. Razavi, M. Moghayadi, Novel oxidation of aromatic aldehydes catalyzed by Preyssler's anion,  $[NaP_5W_{30}O_{110}]^{14-}$ , *J. Braz. Chem. Soc.* 17 (3) (2006) 505–509. (b) F.F. Bamoharram, M.M. Heravi, M. Roshani, N. Tavakoli, N-oxidation of pyridine carboxylic acids using hydrogen peroxide catalyzed by a green heteropolyacid catalyst: Preyssler's anion,  $[NaP_5W_{30}O_{110}]^{14-}$ , *J. Mol. Catal. A: Chem.* 252 (1-2) (2006) 219–225.
- [172] M.T. Pope, *Heteropoly and Isopoly Oxometalates*, Springer-Verlag, New York, 1983.
- [173] A.D. Kirk, W. Riske, R.G. Finke, D.K. Lyon, B. Rapko, Rapid, high-resolution, reversed-phase HPLC separation of highly charged polyoxometalates using ion-interaction reagents and competing ions, *Inorg. Chem.* 28 (4) (1989) 792–797.
- [174] M.T. Pope, B.W. Dale, Isopoly-vanadates, -niobates, and-tantalates, *Q. Rev. Chem. Soc.* 22 (4) (1968) 527–548.
- [175] V.W. Day, W.G. Klemperer, Metal oxide chemistry in solution: the early transition metal polyoxoanions, *Science* 228 (4699) (1985) 533–541.
- [176] L.C. Baker, L. Lebioda, J. Grochowski, H.G. Mukherjee, Heteropoly periodates: structure of  $[Co_4^{3+}I_3^{7+}O_{24}H_{12}]^{3-}$  ion and principles pertinent to a separate potentially important category of heteropoly complexes, *J. Am. Chem. Soc.* 102 (9) (1980) 3274–3276.

- [177] D.E. Katsoulis, M.T. Pope, New chemistry for heteropolyanions in anhydrous nonpolar solvents. Coordinative unsaturation of surface atoms. Polyanion oxygen carriers, *J. Am. Chem. Soc.* 106 (9) (1984) 2737–2738.
- [178] I.V.E. Kozhevnikov, Advances in catalysis by heteropolyacids, *Russ. Chem. Rev.* 56 (9) (1987) 811.
- [179] I.V. Kozhevnikov, Catalysis by heteropoly acids and multicomponent polyoxometalates in liquid-phase reactions, *Chem. Rev.* 98 (1) (1998) 171–198.
- [180] Y. Izumi, R. Hasebe, K. Urabe, Catalysis by heterogeneous supported heteropoly acid, *J. Catal.* 84 (2) (1983) 402–409.
- [181] T. Buchecker, P. Schmid, S. Renaudineau, O. Diat, A. Proust, A. Pflitzner, P. Bauduin, Polyoxometalates in the Hofmeister series, *Chem. Commun.* 54 (15) (2018) 1833–1836.
- [182] X. López, J.A. Fernández, J.M. Poblet, Redox properties of polyoxometalates: new insights on the anion charge effect, *Dalton Trans.* 9 (2006) 1162–1167.
- [183] A. Solé-Daura, V. Goovaerts, K. Stroobants, G. Absillis, P. Jiménez-Lozano, J.M. Poblet, J.J. Carbó, Probing polyoxometalate-protein interactions using molecular dynamics simulations, *Chem Eur J* 22 (43) (2016).
- [184] K.I. Assaf, W.M. Nau, Der chaotrope Effekt als Aufbaumotiv in der Chemie, *Angew. Chem.* 130 (43) (2018) 14164–14177.
- [185] B. Naskar, O. Diat, V. Nardello-Rataj, P. Bauduin, Nanometer-size polyoxometalate anions adsorb strongly on neutral soft surfaces, *J. Phys. Chem. C* 119 (36) (2015) 20985–20992.
- [186] A. Malinenko, A. Jonchére, L. Girard, S. Parrés-Maynadié, O. Diat, P. Bauduin, Are Keggin's POMs charged nanocolloids or multicharged anions? *Langmuir* 34 (5) (2018) 2026–2038.
- [187] A. Misra, K. Kozma, C. Streb, M. Nyman, Beyond charge balance: counter-cations in polyoxometalate chemistry, *Angew. Chem. Int. Ed.* 59 (2) (2020) 596–612.
- [188] M. Blasco-Ahicart, J. Soriano-López, J.J. Carbó, J.M. Poblet, J.R. Galan-Mascaros, Polyoxometalate electrocatalysts based on earth-abundant metals for efficient water oxidation in acidic media, *Nat. Chem.* 10 (1) (2018) 24–30.
- [189] S. Herrmann, A. Seliverstov, C. Streb, Polyoxometalate-ionic liquids (POM-ILs)—the ultimate soft polyoxometalates: a critical perspective, *J. Mol. Eng. Mater.* 2 (01) (2014) 1440001.
- [190] S. Herrmann, M. Kostrzewa, A. Wierschem, C. Streb, Polyoxometallat-basierte ionische Flüssigkeiten als selbstreparierender Säure-Korrosionsschutz, *Angew. Chem.* 126 (49) (2014) 13814–13817.
- [191] L.B. Fullmer, P.I. Molina, M.R. Antonio, M. Nyman, Contrasting ion-association behaviour of Ta and Nb polyoxometalates, *Dalton Trans.* 43 (41) (2014) 15295–15299.
- [192] M. Nyman, Polyoxoniobate chemistry in the 21st century, *Dalton Trans.* 40 (32) (2011) 8049–8058.
- [193] Y. Hou, M. Nyman, M.A. Rodriguez, Soluble heteropolyniobates from the bottom of group IA, *Angew. Chem.* 123 (52) (2011) 12722–12725.
- [194] M. Nyman, P.C. Burns, A comprehensive comparison of transition-metal and actinyl polyoxometalates, *Chem. Soc. Rev.* 41 (22) (2012) 7354–7367.
- [195] P.C. Burns, M. Nyman, Captivation with encapsulation: a dozen years of exploring uranyl peroxide capsules, *Dalton Trans.* 47 (17) (2018) 5916–5927.
- [196] L.B. Fullmer, R.H. Mansergh, L.N. Zakharov, D.A. Keszler, M. Nyman, Nb<sub>2</sub>O<sub>5</sub> and Ta<sub>2</sub>O<sub>5</sub> thin films from polyoxometalate precursors: a single proton makes a difference, *Cryst. Growth Des.* 15 (8) (2015) 3885–3892.
- [197] D.J. Sures, S.A. Serapian, K. Kozma, P.I. Molina, C. Bo, M. Nyman, Electronic and relativistic contributions to ion-pairing in polyoxometalate model systems, *Phys. Chem. Chem. Phys.* 19 (13) (2017) 8715–8725.

- [198] I.V.E. Kozhevnikov, K.I. Matveev, Heteropolyacids in catalysis, *Russ. Chem. Rev.* 51 (11) (1982) 1075.
- [199] G.A. Tsigdinos, Heteropoly compounds of molybdenum and tungsten, in: *Topics in Current Chemistry*, Springer, Berlin, Heidelberg, 1978, pp. 1–64.
- [200] J.G. Highfield, J.B. Moffat, Characterization of 12-tungstophosphoric acid and related salts using photoacoustic spectroscopy in the infrared region: I. Thermal stability and interactions with ammonia, *J. Catal.* 88 (1) (1984) 177–187.
- [201] K. Brückman, J. Haber, E. Lalik, E.M. Serwicka, Heteropolysalt-supported heteropolyacids as a new class of acid-base and redox catalysts, *Catal. Lett.* 1 (1-3) (1988) 35–40.
- [202] I.V. Kozhevnikov, Catalysts for fine chemical synthesis, in: *Catalysis by Polyoxometalates*, vol. 2, Wiley, 2002.
- [203] P. Souchay, Polyanions et polycations; Monographies de chimie mineerale, Gaithier-Villars, Paris, 1963.
- [204] L. Pettersson, I. Andersson, L.O. Oehman, Multicomponent polyanions. 39. Speciation in the aqueous hydrogen ion-molybdate ( $\text{MoO}_4^{2-}$ )-hydrogenphosphate ( $\text{HPO}_4^{2-}$ ) system as deduced from a combined Emf-phosphorus-31 NMR study, *Inorg. Chem.* 25 (26) (1986) 4726–4733.
- [205] M. Ammam, Polyoxometalates: formation, structures, principal properties, main deposition methods and application in sensing, *J. Mater. Chem. A* 1 (21) (2013) 6291–6312.
- [206] P. Courtin, Molybdenum and tungsten heteropolyanions substituted by vanadium(-v). 2. Compounds with high vanadium content, *Revue De Chimie Minerale* 8 (2) (1971) 221.
- [207] D.P. Smith, M.T. Pope, Heteropoly 12-metallophosphates containingtungsten and vanadium. Preparation, voltammetry, and properties of mono-, di-, tetra-, andhexavanado complexes, *Inorg. Chem.* 12 (2) (1973) 331–336.
- [208] J.B. Moffat, *Metal-Oxygen Clusters: The Surface and Catalytic Properties of Heteropoly Oxometalates*, Springer Science & Business Media, 2006.
- [209] P. Souchay, *Ions minéraux condensés*, Masson et Cie, 1969.
- [210] M.T. Pope, Heteropoly Blues, in: *Mixed-Valence Compounds*, Springer, Dordrecht, 1980, pp. 365–386.
- [211] J.J. Altenau, M.T. Pope, R.A. Prados, H. So, Models for heteropoly blues. Degrees of valence trapping in vanadium (IV)-and molybdenum (V)-substituted Keggin anions, *Inorg. Chem.* 14 (2) (1975) 417–421.
- [212] (a) S. Himeno, M. Takamoto, M. Hoshiba, A. Higuchi, M. Hashimoto, Preparation and characterization of an  $\alpha$ -Keggin-type  $[\text{SW}_{12}\text{O}_{40}]^{2-}$  complex, *Bull. Chem. Soc. Jpn.* 77 (3) (2004) 519–524. (b) K. Maeda, H. Katano, T. Osakai, S. Himeno, A. Saito, Charge dependence of one-electron redox potentials of Keggin-type heteropolyoxometalate anions, *J. Electroanalyt. Chem.* 389 (1-2) (1995) 167–173. (c) S. Himeno, S. Murata, K. Eda, A route to a Keggin-type  $\alpha$ - $[\text{X}^{\text{III}}\text{O}_4] \text{Mo}_{12} \text{O}_{35} (\text{OH})^{4-}$  anion through an Anderson-type  $[\text{X}^{\text{III}} (\text{OH})_6 \text{Mo}_6 \text{O}_{18}]^{3-}$  anion: X=Ga, *Dalton Trans.* 31 (2009) 6114–6119. (d) J. Zhang, A.I. Bhatt, A.M. Bond, A.G. Wedd, J.L. Scott, C.R. Strauss, Voltammetric studies of polyoxometalate microparticles in contact with the reactive distillable ionic liquid DIM-CARB, *Electrochem. Commun.* 7 (12) (2005) 1283–1290. (e) K. Nakajima, K. Eda, S. Himeno, Effect of the central oxoanion size on the voltammetric properties of Keggin-type  $[\text{XW}_{12}\text{O}_{40}]^n$  ( $n=2-6$ ) complexes, *Inorg. Chem.* 49 (11) (2010) 5212–5215.
- [213] B. Keita, D. Bouaziz, L. Nadjo, Solvent effects on the redox potentials of potassium 12-tungstosilicate and 18-tungstodiphosphate, *J. Electrochem. Soc.* 135 (1) (1988) 87.
- [214] S. Himeno, M. Takamoto, R. Santo, A. Ichimura, Redox properties and basicity of Keggin-type polyoxometalate complexes, *Bull. Chem. Soc. Jpn.* 78 (1) (2005) 95–100.

- [215] (a) J. Ding, H. Hotta, T. Osakai, Ion transfer of heteropolytungstate anions at the nitrobenzene| water interface and its relevance to their antiviral activities, *J. Electroanal. Chem.* 505 (1-2) (2001) 133–141. (b) J. Ding, T. Osakai, Ion transfer of reduced Keggin-type heteropolymolybdate anions at the nitrobenzene/water interface and its relevance to their antitumoral activities, *Electroanalysis* 13 (5) (2001) 384–391. (c) T. Osakai, H. Katano, K. Maeda, S. Himeno, A. Saito, A hydrophobicity scale of heteropoly- and isopolyanions based on voltammetric studies of their transfer at the nitrobenzene/water interface, *Bull. Chem. Soc. Jpn.* 66 (4) (1993) 1111–1115. (d) T. Osakai, S. Himeno, A. Saito, Voltammetric study of the transfer of kegggin-type heteropolyanions across the nitrobenzene/water interface, *J. Electroanal. Chem. Interf. Electrochem.* 302 (1-2) (1991) 145–156.
- [216] (a) S. Himeno, M. Takamoto, T. Ueda, R. Santo, A. Ichimura, Solvation effect of Li<sup>+</sup> on the voltammetric properties of [PMo<sub>12</sub>O<sub>40</sub>]<sup>3-</sup>. Part 2: comparative studies on the preferential solvation in acetonitrile and acetone mixtures, *Electroanalysis* 16 (8) (2004) 656–660. (b) M. Takamoto, T. Ueda, S. Himeno, Solvation effect of Li<sup>+</sup> on the voltammetric properties of [PMo<sub>12</sub>O<sub>40</sub>]<sup>3-</sup> in binary solvent mixtures, *J. Electroanal. Chem.* 521 (1-2) (2002) 132–136.
- [217] A.M. Bond, T. Vu, A.G. Wedd, Voltammetric studies of the interaction of the lithium cation with reduced forms of the Dawson [S<sub>2</sub>Mo<sub>18</sub>O<sub>62</sub>]<sup>4-</sup> polyoxometalate anion, *J. Electroanal. Chem.* 494 (2) (2000) 96–104.
- [218] M. Misono, Heterogeneous catalysis by heteropoly compounds of molybdenum and tungsten, *Catal. Rev. Sci. Eng.* 29 (2-3) (1987) 269–321.
- [219] M. Misono, *Catal. Rev. Sci. Eng.* 30 (1988) 339.
- [220] I.V. Kozhevnikov, A. Sinnema, H. Van Bekkum, M. Fournier, <sup>17</sup>O MAS NMR study of 12-molybdophosphoric acid, *Catal. Lett.* 41 (3-4) (1996) 153–157.
- [221] I.V. Kozhevnikov, A. Sinnema, R.J.J. Jansen, H. Van Bekkum, <sup>17</sup>O NMR determination of proton sites in solid heteropoly acid H<sub>3</sub>PW<sub>12</sub>O<sub>40</sub>. <sup>31</sup>P, <sup>29</sup>Si and <sup>17</sup>O NMR, FT-IR and XRD study of H<sub>3</sub>PW<sub>12</sub>O<sub>40</sub> and H<sub>4</sub>SiW<sub>12</sub>O<sub>40</sub> supported on carbon, *Catal. Lett.* 27 (1-2) (1994) 187–197.
- [222] I.V. Kozhevnikov, A. Sinnema, H. Van Bekkum, Proton sites in Keggin heteropoly acids from <sup>17</sup>O NMR, *Catal. Lett.* 34 (1-2) (1995) 213–221.
- [223] I. Efremenko, R. Neumann, Protonation of phosphovanadomolybdates H<sub>3+x</sub>V<sub>x</sub>Mo<sub>12-x</sub>O<sub>40</sub>: computational insight into reactivity, *Chem. A Eur. J.* 115 (18) (2011) 4811–4826.
- [224] S.S. Wang, G.Y. Yang, Recent advances in polyoxometalate-catalyzed reactions, *Chem. Rev.* 115 (11) (2015) 4893–4962.
- [225] A. Bijelic, A. Rompel, Ten good reasons for the use of the tellurium-centered Anderson–Evans polyoxotungstate in protein crystallography, *Acc. Chem. Res.* 50 (6) (2017) 1441–1448.
- [226] A. Bijelic, A. Rompel, Polyoxometalates: more than a phasing tool in protein crystallography, *Chem Texts* 4 (3) (2018) 10.
- [227] A. Bijelic, M. Aureliano, A. Rompel, The antibacterial activity of polyoxometalates: structures, antibiotic effects and future perspectives, *Chem. Commun.* 54 (10) (2018) 1153–1169.
- [228] A. Bijelic, M. Aureliano, A. Rompel, Polyoxometalates as potential next-generation metal-odrugs in the combat against cancer, *Angew. Chem. Int. Ed.* 58 (10) (2019) 2980–2999.
- [229] T. Kiss, A. Odani, Demonstration of the importance of metal ion speciation in bioactive systems, *Bull. Chem. Soc. Jpn.* 80 (9) (2007) 1691–1702.
- [230] A. Levina, D.C. Crans, P.A. Lay, Speciation of metal drugs, supplements and toxins in media and bodily fluids controls in vitro activities, *Coord. Chem. Rev.* 352 (2017) 473–498.
- [231] S.A.O. Speciation, Guidelines for terms related to chemical speciation and fractionation of elements. Definitions, structural aspects, and methodological approaches, *Pure Appl. Chem.* 72 (8) (2000) 1453–1470.



- [232] T. Kiss, É.A. Enyedy, T. Jakusch, Development of the application of speciation in chemistry, *Coord. Chem. Rev.* 352 (2017) 401–423.
- [233] I. Ali, H.Y. Aboul-Enein, *Instrumental Methods in Metal Ion Speciation*, CRC Press, 2006.
- [234] E.G. Zhizhina, V.F. Odyakov, Physicochemical properties of catalysts based on aqueous solutions of Mo–V–phosphoric heteropoly acids, *Appl. Catal. Gen.* 358 (2) (2009) 254–258.
- [235] E.G. Zhizhina, V.F. Odyakov, Physicochemical and corrosive properties of oxidation catalysts based on solutions of Mo–V–phosphoric heteropoly acids, *Catal. Ind.* 2 (3) (2010) 217–224.
- [236] E.G. Zhizhina, V.F. Odyakov, Corrosivity of catalysts based on aqueous solutions of Mo–V–P heteropoly acids, *React. Kinet. Catal. Lett.* 98 (1) (2009) 51–58.
- [237] M.T. Pope, E. Papaconstantinou, Heteropoly blues. II. Reduction of 2: 18-tungstates, *Inorg. Chem.* 6 (6) (1967) 1147–1152.
- [238] M.N. Timofeeva, M.M. Matrosova, G.M. Maksimov, V.A. Likholobov, A study of the acid properties of structurally and compositionally different heteropoly acids in acetic acid, *Kinet. Catal.* 42 (6) (2001) 785–790.
- [239] В.А. Захаров, Г.Д. Букатов, Ю.И. Ермаков, Механизм каталитической полимеризации олефинов на основе данных о числе активных центров и константах скоростей отдельных стадий, *Успехи химии* 49 (11) (1980) 2213–2240.
- [240] I.V. Kozhevnikov, S.T. Khankhasaeva, S.M. Kulikov, Acidity of concentrated solutions of heteropolyacids, *Kinet. Katal.* 29 (1) (1988) 76–80.
- [241] M.N. Timofeeva, G.M. Maksimov, V.A. Likholobov, Acidity of solutions of heteropoly acids with various structures and compositions, *Kinet. Catal.* 42 (1) (2001) 30–34.
- [242] C.W. Hu, M. Hashimoto, T. Okuhara, M. Misono, Catalysis by heteropoly compounds. XXII. Reactions of esters and esterification catalyzed by heteropolyacids in a homogeneous liquid-phase effects of the central atom of heteropolyanions having tungsten as the addenda atom, *J. Catal.* 143 (2) (1993) 437–448.
- [243] T. Okuhara, C. Hu, M. Hashimoto, M. Misono, Acid strength of heteropolyacids and its correlation with catalytic activity, *Bull. Chem. Soc. Jpn.* 67 (4) (1994) 1186–1188.
- [244] C.L. Hill, C.M. Prosser-McCartha, Homogeneous catalysis by transition metal oxygen anion clusters, *Coord. Chem. Rev.* 143 (1995) 407–455.
- [245] I.V. Kozhevnikov, *Catalysts for Fine Chemical Synthesis*, in: *Catalysis by Polyoxometalates*, vol. 2, John Wiley & Sons, Chichester, UK, 2002.
- [246] R. Neumann, A.M. Khenkin, Molecular oxygen and oxidation catalysis by phosphovanadomolybdates, *Chem. Commun.* 24 (2006) 2529–2538.
- [247] N. Mizuno, K. Kamata, K. Yamaguchi, Liquid-phase selective oxidation by multimetallic active sites of polyoxometalate-based molecular catalysts, in: *Bifunctional Molecular Catalysis*, Springer, Berlin, Heidelberg, 2011, pp. 127–160.
- [248] H. Lv, Y.V. Geletii, C. Zhao, J.W. Vickers, G. Zhu, Z. Luo, C.L. Hill, Polyoxometalate water oxidation catalysts and the production of green fuel, *Chem. Soc. Rev.* 41 (22) (2012) 7572–7589.
- [249] M. Sun, J. Zhang, P. Putaj, V. Caps, F. Lefebvre, J. Pelletier, J.M. Basset, Catalytic oxidation of light alkanes (C1–C4) by heteropoly compounds, *Chem. Rev.* 114 (2) (2014) 981–1019.
- [250] K. Kamata, Design of highly functionalized polyoxometalate-based catalysts, *Bull. Chem. Soc. Jpn.* 88 (8) (2015) 1017–1028.
- [251] Y. Zhou, Z. Guo, W. Hou, Q. Wang, J. Wang, Polyoxometalate-based phase transfer catalysis for liquid–solid organic reactions: a review, *Cat. Sci. Technol.* 5 (9) (2015) 4324–4335.
- [252] N. Narkhede, S. Singh, A. Patel, Recent progress on supported polyoxometalates for biodiesel synthesis via esterification and transesterification, *Green Chem.* 17 (1) (2015) 89–107.

- [253] L.M. Sanchez, H.J. Thomas, M.J. Climent, G.P. Romanelli, S. Iborra, Heteropolycompounds as catalysts for biomass product transformations, *Catal. Rev.* 58 (4) (2016) 497–586.
- [254] D. Ravelli, S. Protti, M. Fagnoni, Decatungstate anion for photocatalyzed “window ledge” reactions, *Acc. Chem. Res.* 49 (10) (2016) 2232–2242.
- [255] K. Kamata, K. Sugahara, Base catalysis by mono-and polyoxometalates, *Catalysts* 7 (11) (2017) 345.
- [256] B.R.I.T.T. Hedman, Multicomponent polyanions. 18. A neutron diffraction study of Na<sub>3</sub>Mo<sub>9</sub>PO<sub>31</sub>(OH)<sub>2</sub> · 12<sup>-13</sup>H<sub>2</sub>O, a compound containing 9-molybdomonophosphate anions with molybdenum-coordinated water molecules, *Acta Chem. Scand. A* 32 (5) (1978).
- [257] T.M. Che, V.W. Day, L.C. Francesconi, M.F. Fredrich, W.G. Klemperer, W. Shum, Synthesis and structure of the [(*n*-<sup>5</sup>-C<sub>3</sub>H<sub>5</sub>)Ti(Mo<sub>5</sub>O<sub>18</sub>)]<sup>3-</sup> and [(*n*-<sup>5</sup>-C<sub>3</sub>H<sub>5</sub>)Ti(W<sub>5</sub>O<sub>18</sub>)]<sup>3-</sup> anions, *Inorg. Chem.* 24 (24) (1985) 4055–4062.
- [258] V.W. Day, W.G. Klemperer, D.J. Maltbie, Where are the protons in H<sub>3</sub>V<sub>10</sub>O<sub>28</sub><sup>3-</sup>? *J. Am. Chem. Soc.* 109 (10) (1987) 2991–3002.
- [259] T.M. Che, V.W. Day, L.C. Francesconi, W.G. Klemperer, D.J. Main, A. Yagasaki, O.M. Yaghi, Mono-and diprotonation of the [(η<sup>5</sup>-C<sub>5</sub>H<sub>5</sub>)Ti(W<sub>5</sub>O<sub>18</sub>)]<sup>3-</sup> and [(η<sup>5</sup>-C<sub>5</sub>Me<sub>5</sub>)Ti(W<sub>5</sub>O<sub>18</sub>)]<sup>3-</sup> anions, *Inorg. Chem.* 31 (13) (1992) 2920–2928.
- [260] T. Ozeki, T. Yamase, H. Naruke, Y. Sasaki, X-ray structural characterization of the protonation sites in the dihydrogenhexaniobate anion, *Bull. Chem. Soc. Jpn.* 67 (12) (1994) 3249–3253.
- [261] S. Nakamura, T. Ozeki, Hydrogen-bonded aggregates of protonated decavanadate anions in their tetraalkylammonium salts, *J. Chem. Soc. Dalton Trans.* 4 (2001) 472–480.
- [262] N. Leclerc-Laronze, M. Haouas, J. Marrot, F. Taulelle, G. Hervé, Step-by-step assembly of trivacant tungstosilicates: synthesis and characterization of tetrameric anions, *Angew. Chem. Int. Ed.* 45 (1) (2006) 139–142.
- [263] A. Yoshida, M. Yoshimura, K. Uehara, S. Hikichi, N. Mizuno, Formation of S-shaped disilicoicosatungstate and efficient baeyer–villiger oxidation with hydrogen peroxide, *Angew. Chem.* 118 (12) (2006) 1990–1994.
- [264] X. Fang, C.L. Hill, Multiple reversible protonation of polyoxoanion surfaces: direct observation of dynamic structural effects from proton transfer, *Angew. Chem.* 119 (21) (2007) 3951–3954.
- [265] S. Nakamura, T. Ozeki, Guest driven rearrangements of protonation and hydrogen bonding in decavanadate anions as their tetraalkylammonium salts, *Dalton Trans.* 44 (2008) 6135–6140.
- [266] W.G. Klemperer, W. Shum, Charge distribution in large polyoxoanions: determination of protonation sites in vanadate (V<sub>10</sub>O<sub>28</sub><sup>6-</sup>) by oxygen-17 nuclear magnetic resonance, *J. Am. Chem. Soc.* 99 (10) (1977) 3544–3545.
- [267] W.G. Klemperer, W. Shum, Isomerism and charge distribution in mixed-metal polyoxoanion clusters: oxygen-17 nuclear magnetic resonance structure determinations of cis-V<sub>2</sub>W<sub>4</sub>O<sub>19</sub><sup>4-</sup> and cis-HV<sub>2</sub>W<sub>4</sub>O<sub>19</sub><sup>3-</sup>, *J. Am. Chem. Soc.* 100 (15) (1978) 4891–4893.
- [268] M. Filowitz, R.K.C. Ho, W.G. Klemperer, W. Shum, Oxygen-17 nuclear magnetic resonance spectroscopy of polyoxometalates. 1. Sensitivity and resolution, *Inorg. Chem.* 18 (1) (1979) 93–103.
- [269] A.T. Harrison, O.W. Howarth, Oxygen exchange and protonation of polyanions: a multi-nuclear magnetic resonance study of tetradecavanadophosphate (9-) and decavanadate (6-), *J. Chem. Soc. Dalton Trans.* 9 (1985) 1953–1957.
- [270] R.G. Finke, B. Rapko, R.J. Saxton, P.J. Domaille, Trisubstituted heteropolytungstates as soluble metal oxide analogs. III. Synthesis, characterization, phosphorus-31, silicon-29, vanadium-51, and 1- and 2-D tungsten-183 NMR, deprotonation, and proton mobility studies of organic solvent solute forms of H<sub>x</sub>SiW<sub>9</sub>V<sub>3</sub>O<sub>40</sub><sup>x-7</sup> and H<sub>x</sub>P<sub>2</sub>W<sub>15</sub>V<sub>5</sub>O<sub>62</sub><sup>x-9</sup>, *J. Am. Chem. Soc.* 108 (11) (1986) 2947–2960.

- [271] M. Pohl, R.G. Finke, Polyoxoanion-supported, atomically dispersed transition-metal precatalyst [(1, 5-COD) Ir P<sub>2</sub>W<sub>15</sub>Nb<sub>3</sub>O<sub>62</sub>]<sup>8-</sup>: direct oxygen-17 NMR evidence for Ir-ONb<sub>2</sub> bonding and for a C<sub>3v</sub> average symmetry, iridium-to-polyoxoanion support interaction, *Organometallics* 12 (4) (1993) 1453–1457.
- [272] H. Weiner, J.D. Aiken, R.G. Finke, Polyoxometalate catalyst precursors. Improved synthesis, H<sup>+</sup>-titration procedure, and evidence for <sup>31</sup>P NMR as a highly sensitive support-site indicator for the prototype polyoxoanion – organometallic-support system [(n-C<sub>4</sub>H<sub>9</sub>)<sub>4</sub>N] <sub>9</sub>P<sub>2</sub>W<sub>15</sub>Nb<sub>3</sub>O<sub>62</sub>, *Inorg. Chem.* 35 (26) (1996) 7905–7913.
- [273] C.R. Sprangers, J.K. Marmon, D.C. Duncan, Where are the protons in α-[H<sub>x</sub>W<sub>12</sub>O<sub>40</sub>]<sup>(8-x)-</sup> (x = 2 – 4), *Inorg. Chem.* 45 (24) (2006) 9628–9630.
- [274] E. Balogh, T.M. Anderson, J.R. Rustad, M. Nyman, W.H. Casey, Rates of oxygen-isotope exchange between sites in the [H<sub>x</sub>Ta<sub>6</sub>O<sub>19</sub>]<sup>(8-x)-</sup>(aq) Lindqvist ion and aqueous solutions: comparisons to [H<sub>x</sub>Nb<sub>6</sub>O<sub>19</sub>]<sup>(8-x)-</sup>(aq), *Inorg. Chem.* 46 (17) (2007) 7032–7039.
- [275] A. Dolbecq, A. Guirauden, M. Fourmigué, K. Boubekeur, P. Batail, M.M. Rohmer, P. Blanchard, Relative basicities of the oxygen atoms of the Linquist polyoxometalate [Mo<sub>6</sub>O<sub>19</sub>]<sup>2-</sup> and their recognition by hydroxyl groups in radical cation salts based on functionalized tetrathiafulvalene π donors, *J. Chem. Soc. Dalton Trans.* 8 (1999) 1241–1248.
- [276] D.G. Musaev, K. Morokuma, Y.V. Geletii, C.L. Hill, Computational modeling of di-transition-metal-substituted γ-Keggin polyoxometalate anions. Structural refinement of the protonated divacant lacunary silicodecatungstate, *Inorg. Chem.* 43 (24) (2004) 7702–7708.
- [277] A. Sartorel, M. Carraro, A. Bagno, G. Scorrano, M. Bonchio, Asymmetric tetraprotonation of γ-[(SiO<sub>4</sub>)W<sub>10</sub>O<sub>32</sub>]<sup>8-</sup> triggers a catalytic epoxidation reaction: perspectives in the assignment of the active catalyst, *Angew. Chem. Int. Ed.* 46 (18) (2007) 3255–3258.
- [278] W. Ge, X. Wang, L. Zhang, L. Du, Y. Zhou, J. Wang, Fully-occupied Keggin type polyoxometalate as solid base for catalyzing CO<sub>2</sub> cycloaddition and Knoevenagel condensation, *Cat. Sci. Technol.* 6 (2) (2016) 460–467.
- [279] M. Carraro, L. Sandei, A. Sartorel, G. Scorrano, M. Bonchio, Hybrid polyoxotungstates as second-generation POM-based catalysts for microwave-assisted H<sub>2</sub>O<sub>2</sub> activation, *Org. Lett.* 8 (17) (2006) 3671–3674.
- [280] A. Sartorel, M. Carraro, A. Bagno, G. Scorrano, M. Bonchio, H<sub>2</sub>O<sub>2</sub> activation by heteropolyacids with defect structures: the case of γ-[(XO<sub>4</sub>)W<sub>10</sub>O<sub>32</sub>]<sup>n-</sup> (X=Si, Ge, n=8; X=P, n=7), *J. Phys. Org. Chem.* 21 (7-8) (2008) 596–602.
- [281] T.D. Phan, M.A. Kinch, J.E. Barker, T. Ren, Highly efficient utilization of H<sub>2</sub>O<sub>2</sub> for oxygenation of organic sulfides catalyzed by [γ-SiW<sub>10</sub>O<sub>34</sub>(H<sub>2</sub>O)<sub>2</sub>]<sup>4-</sup>, *Tetrahedron Lett.* 46 (3) (2005) 397–400.
- [282] S. Berardi, M. Bonchio, M. Carraro, V. Conte, A. Sartorel, G. Scorrano, Fast catalytic epoxidation with H<sub>2</sub>O<sub>2</sub> and [γ-SiW<sub>10</sub>O<sub>36</sub>(PhPO)<sub>2</sub>]<sup>4-</sup> in ionic liquids under microwave irradiation, *J. Org. Chem.* 72 (23) (2007) 8954–8957.
- [283] K. Sugahara, S. Kuzuya, T. Hirano, K. Kamata, N. Mizuno, Reversible deprotonation and protonation behaviors of a tetra-protonated γ-Keggin silicodecatungstate, *Inorg. Chem.* 51 (14) (2012) 7932–7939.
- [284] K. Sugahara, N. Satake, K. Kamata, T. Nakajima, N. Mizuno, A basic germanodecatungstate with a –7 charge: efficient chemoselective acylation of primary alcohols, *Angew. Chem.* 126 (48) (2014) 13464–13468.
- [285] K. Sugahara, T. Kimura, K. Kamata, K. Yamaguchi, N. Mizuno, A highly negatively charged γ-Keggin germanodecatungstate efficient for Knoevenagel condensation, *Chem. Commun.* 48 (67) (2012) 8422–8424.

- [286] T. Minato, K. Suzuki, K. Kamata, N. Mizuno, Synthesis of  $\alpha$ -Dawson-type silicotungstate [ $\alpha$ -Si<sub>2</sub>W<sub>18</sub>O<sub>62</sub>]<sup>8-</sup> and protonation and deprotonation inside the aperture through intramolecular hydrogen bonds, *Chem. A Eur. J.* 20 (20) (2014) 5946–5952.
- [287] N.I. Gumerova, A.V. Notich, G.M. Rozantsev, S.V. Radio, pH-metric studies on the interaction of Ni-containing anderson type heteropolyanions in aqueous solution, *J. Solution Chem.* 45 (6) (2016) 849–860.
- [288] D.C. Crans, K.A. Woll, K. Prusinskas, M.D. Johnson, E. Norkus, Metal speciation in health and medicine represented by iron and vanadium, *Inorg. Chem.* 52 (21) (2013) 12262–12275.
- [289] T. Yamase, Photo- and electrochromism of polyoxometalates and related materials, *Chem. Rev.* 98 (1) (1998) 307–326.
- [290] H. So, M.T. Pope, Origin of some charge-transfer spectra. Oxo compounds of vanadium, molybdenum, tungsten, and niobium including heteropoly anions and heteropoly blues, *Inorg. Chem.* 11 (6) (1972) 1441–1443.
- [291] G.M. Varga Jr., E. Papaconstantinou, M.T. Pope, Heteropoly blues. IV. Spectroscopic and magnetic properties of some reduced polytungstates, *Inorg. Chem.* 9 (3) (1970) 662–667.
- [292] P. Yang, Z. Lin, G. Alfaro-Espinoza, M.S. Ullrich, C.I. Raț, C. Silvestru, U. Kortz, 19-Tungstodiarсенate (III) functionalized by organoantimony (III) groups: tuning the structure–bioactivity relationship, *Inorg. Chem.* 55 (1) (2016) 251–258.
- [293] I. Holclajtner-Antunović, D. Bajuk-Bogdanović, M. Todorović, U.B. Mioč, J. Zakrzewska, S. Uskoković-Marković, Spectroscopic study of stability and molecular species of 12-tungstophosphoric acid in aqueous solution, *Can. J. Chem.* 86 (10) (2008) 996–1004.
- [294] P. Häufe, Raman-spectrophotometric determination of the tungstate anion and its isopolyanions in aqueous systems, *Fresenius Z. Anal. Chem.* 310 (5) (1982) 388–391.
- [295] R.Q. Cabrera, S. Firth, C.S. Blackman, D.L. Long, L. Cronin, P.F. McMillan, Spectroscopic studies of sulfite-based polyoxometalates at high temperature and high pressure, *J. Solid State Chem.* 186 (2012) 171–176.
- [296] A.F. Redkin, G.V. Bondarenko, Raman spectra of tungsten-bearing solutions, *J. Solution Chem.* 39 (10) (2010) 1549–1561.
- [297] M. Aureliano, C.A. Ohlin, M.O. Vieira, M.P.M. Marques, W.H. Casey, L.A.B. De Carvalho, Characterization of decavanadate and decaniobate solutions by Raman spectroscopy, *Dalton Trans.* 45 (17) (2016) 7391–7399.
- [298] W.G. Klemperer, W. Shum, Synthesis and interconversion of the isomeric  $\alpha$ - and  $\beta$ -Mo<sub>8</sub>O<sub>26</sub><sup>4-</sup> ions, *J. Am. Chem. Soc.* 98 (25) (1976) 8291–8293.
- [299] M.A. Fedotov, R.I. Maksimovskaya, NMR structural aspects of the chemistry of V, Mo, W polyoxometalates, *J. Struct. Chem.* 47 (5) (2006) 952–978.
- [300] Y.G. Chen, J. Gong, L.Y. Qu, Tungsten-183 nuclear magnetic resonance spectroscopy in the study of polyoxometalates, *Coord. Chem. Rev.* 248 (1-2) (2004) 245–260.
- [301] A.S. Tracey, G.R. Willsky, E.S. Takeuchi, Vanadium: Chemistry, Biochemistry, Pharmacology and Practical Applications, CRC press, 2007.
- [302] M.T. Pope, G.M. Varga, Proton magnetic resonance of aqueous metatungstate ion: evidence for two central hydrogen atoms, *Chem. Commun. (Camb)* 18 (1966) 653–654.
- [303] C.A. Ohlin, W.H. Casey, <sup>17</sup>O NMR as a tool in discrete metal oxide cluster chemistry, in: *Annual Reports on NMR Spectroscopy*, vol. 94, Academic Press, 2018, pp. 187–248.
- [304] R.I. Maksimovskaya, G.M. Maksimov, <sup>31</sup>P NMR studies of hydrolytic conversions of 12-tungstophosphoric heteropolyacid, *Coord. Chem. Rev.* 385 (2019) 81–99.
- [305] R.I. Maksimovskaya, G.M. Maksimov, Borotungstate polyoxometalates: multinuclear NMR structural characterization and conversions in solutions, *Inorg. Chem.* 50 (11) (2011) 4725–4731.

- [306] M. Bugnola, R.E. Schreiber, Y. Kaufman, G. Leitus, L.J. Shimon, R. Neumann, Reversible temperature dependent dimerization of transition metal substituted quasi wells–dawson polyfluoroxometalates, *Eur. J. Inorg. Chem.* 2019 (3-4) (2019) 482–485.
- [307] J.J. Cowan, A.J. Bailey, R.A. Heintz, B.T. Do, K.I. Hardcastle, C.L. Hill, I.A. Weinstock, Formation, isomerization, and derivatization of Keggin tungstoaluminates, *Inorg. Chem.* 40 (26) (2001) 6666–6675.
- [308] P. Klonowski, J.C. Goloboy, F.J. Uribe-Romo, F. Sun, L. Zhu, F. Gándara, W.G. Klemperer, Synthesis and characterization of the platinum-substituted Keggin anion  $\alpha\text{-H}_2\text{SiPtW}_{11}\text{O}_{40}^{4-}$ , *Inorg. Chem.* 53 (24) (2014) 13239–13246.
- [309] J. Xie, H.A. Neal, J. Szymanowski, P.C. Burns, T.M. Alam, M. Nyman, L. Gagliardi, Resolving confined  $^7\text{Li}$  dynamics of uranyl peroxide capsule U24, *Inorg. Chem.* 57 (9) (2018) 5514–5525.
- [310] M. Nyman, F. Bonhomme, T.M. Alam, J.B. Parise, G.M. Vaughan,  $[\text{SiNb}_{12}\text{O}_{40}]^{16-}$  and  $[\text{GeNb}_{12}\text{O}_{40}]^{16-}$ : highly charged Keggin ions with sticky surfaces, *Angew. Chem.* 116 (21) (2004) 2847–2852.
- [311] H.N. Miras, E.F. Wilson, L. Cronin, Unravelling the complexities of inorganic and supramolecular self-assembly in solution with electrospray and cryospray mass spectrometry, *Chem. Commun.* 11 (2009) 1297–1311.
- [312] C.S. Truebenbach, M. Houalla, D.M. Hercules, Characterization of isopoly metal oxyanions using electrospray time-of-flight mass spectrometry, *J. Mass Spectrom.* 35 (9) (2000) 1121–1127.
- [313] C.A. Ohlin, Reaction dynamics and solution chemistry of polyoxometalates by electrospray ionization mass spectrometry, *Chem. Asian J.* 7 (2) (2012) 262–270.
- [314] M. Nyman, Small-angle X-ray scattering to determine solution speciation of metal-oxo clusters, *Coord. Chem. Rev.* 352 (2017) 461–472.
- [315] M. Nyman, L. Fullmer, Small angle x-ray scattering of group vpolyoxometalates, in: *Trends in Polyoxometalates Research*, 2015, pp. 151–170.
- [316] M. Dufaye, S. Duval, G. Stoclet, T. Loiseau, Crystal chemistry and SAXS studies of an octahedral polyoxoarsenotungstate nanocluster encapsulating four unprecedented thorium arsenate fragments ( $\{\text{Th}_3\text{As}_2\text{O}_n\}^{n-}$  = 25 or 26), *Eur. J. Inorg. Chem.* 2019 (42) (2019) 4500–4505.
- [317] P. Yin, B. Wu, E. Mamontov, L.L. Daemen, Y. Cheng, T. Li, A.J. Ramirez-Cuesta, X-ray and neutron scattering study of the formation of core–shell-type polyoxometalates, *J. Am. Chem. Soc.* 138 (8) (2016) 2638–2643.
- [318] P. Yin, T. Li, R.S. Forgan, C. Lydon, X. Zuo, Z.N. Zheng, T. Liu, Exploring the programmable assembly of a polyoxometalate–organic hybrid via metal ion coordination, *J. Am. Chem. Soc.* 135 (36) (2013) 13425–13432.
- [319] S. Goberna-Ferrón, J. Soriano-López, J.R. Galán-Mascarós, M. Nyman, Solution speciation and stability of cobalt-polyoxometalate water oxidation catalysts by X-ray scattering, *Eur. J. Inorg. Chem.* 2015 (2015) 2833–2840.
- [320] N.I. Gumerova, A. Rompel, Synthesis, structures and applications of electron-rich polyoxometalates, *Nat. Rev. Chem.* 2 (2) (2018) 1–20.
- [321] T. Ueda, Electrochemistry of polyoxometalates: from fundamental aspects to applications, *ChemElectroChem* 5 (6) (2018) 823–838.
- [322] G. Bunker, *Introduction to XAFS: A Practical Guide to X-Ray Absorption Fine Structure Spectroscopy*, Cambridge University Press, 2010.
- [323] M.P.M. Marques, D. Gianolio, S. Ramos, L.A. Batista de Carvalho, M. Aureliano, An EXAFS approach to the study of polyoxometalate–protein interactions: the case of decavanadate–Actin, *Inorg. Chem.* 56 (18) (2017) 10893–10903.

- [324] B.C. Bostick, J. Sun, J.D. Landis, J.L. Clausen, Tungsten speciation and solubility in munitions-impacted soils, *Environ. Sci. Technol.* 52 (3) (2018) 1045–1053.
- [325] S. Bhattacharjee, DLS and zeta potential—what they are and what they are not? *J. Control. Release* 235 (2016) 337–351.
- [326] J.J. Stracke, R.G. Finke, Distinguishing homogeneous from heterogeneous water oxidation catalysis when beginning with polyoxometalates, *ACS Catal.* 4 (3) (2014) 909–933.
- [327] J. Heinze, Cyclic voltammetry—“electrochemical spectroscopy”. *New analytical methods* (25), *Angew. Chem. Int. Ed. Engl.* 23 (11) (1984) 831–847.
- [328] K.D. von Allmen, *Synthetic and Structural Studies of Polyoxometalates as Versatile All-Inorganic Catalysts*, Doctoral dissertation, University of Zurich, 2016.
- [329] J.P. Launay, Reduction de l'ion metatungstate: stades elevés de reduction de  $\text{H}_2\text{W}_{12}\text{O}_{40}^{6-}$ , derives de l'ion  $\text{HW}_{12}\text{O}_{40}^{7-}$  et discussion generale, *J. Inorg. Nucl. Chem.* 38 (4) (1976) 807–816.
- [330] J.J. Stracke, R.G. Finke, Electrochemical water oxidation beginning with the cobalt polyoxometalate  $[\text{Co}_4(\text{H}_2\text{O})_2(\text{PW}_9\text{O}_{34})_2]^{10-}$ : identification of heterogeneous CoOx as the dominant catalyst, *J. Am. Chem. Soc.* 133 (38) (2011) 14872–14875.
- [331] H. El Moll, W. Zhu, E. Oldfield, L.M. Rodriguez-Albelo, P. Mialane, J. Marrot, A. Dolbecq, Polyoxometalates functionalized by bisphosphonate ligands: synthesis, structural, magnetic, and spectroscopic characterizations and activity on tumor cell lines, *Inorg. Chem.* 51 (14) (2012) 7921–7931.
- [332] B. Keita, I.M. Mbomekalle, L. Nadjó, R. Contant,  $[\text{H}_4\text{AsW}_{18}\text{O}_{62}]^{7-}$ , A novel Dawson heteropolyanion and two of its sandwich-type derivatives  $[\text{Zn}_4(\text{H}_2\text{O})_2(\text{H}_4\text{AsW}_{15}\text{O}_{56})_2]^{18-}$ ,  $[\text{Cu}_4(\text{H}_2\text{O})_2(\text{H}_4\text{AsW}_{15}\text{O}_{56})_2]^{18-}$ : cyclic voltammetry and electrocatalytic properties towards nitrite and nitrate, *Electrochem. Commun.* 3 (6) (2001) 267–273.

## Chapter 3

# Applications of heteropoly acids as heterogeneous catalysts

### 3.1. Introduction

Supported materials are usually solids with huge surface areas on which a catalyst could be attached. Supported catalysts consist of three major components: a promoter, an active phase, and a support [1]. From an economic viewpoint, applying a support for a catalyst seems quite appropriate as the preparation costs are very low. Due to the electronic interaction between the support and active phase of the catalyst, the former can also affect the activity of the catalyst. The porosity in the support provides high catalytic activity because it allows the substances (reactants/product) to diffuse (in/out) more easily. Therefore, the catalytic activity depends on the nature, size, and number of the pores in the catalyst support. Owing to the pores present in the structure of the support, the surface area of the supportive material expands in the acidic sites of the anchored desired catalyst. During the preparation of a catalyst, the support is modified to anchor the catalytic species. The active phase of the acid catalyst is extensively concentrated and dispersed on the surface of the support. The catalyst stability, selectivity, and activity are evaluated by the precise dispersion of the catalyst active phase. Due to certain properties such as high porosity, high mechanical stability, high thermal stability, and large specific surface area, metal oxides such as aluminum oxides, silica gel, titanium oxide, aluminosilicates, magnesium oxide, and zirconium dioxide are among the most widely used catalyst supports. Other supportive materials such as activated carbon, zeolites, and ceramics are used as well [2,3].

Heteropoly compounds have been quite versatile and useful in organic transformations owing to their super acidic and redox properties [4]. Among these compounds, heteropoly acids can serve as catalysts with more activities than those of conventional mineral acids. Using heteropoly acids as catalysts has been recently studied with more interest. Apart from the environmental concerns, potential hazards of mineral acids as well as their handling and disposal, the attention of the chemist has been attracted to alternative processes using solid acid catalysts [5]. Since heteropoly acids have numerous advantages over conventional inorganic acids and they are economically and environmentally



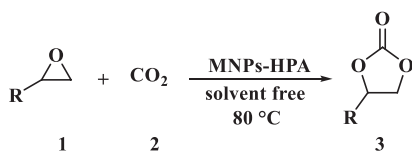
attractive in both academic and industrial arenas, they provide green alternatives to homogeneous catalysts in organic reactions and in the manufacture of chemical compounds [6]. In addition, these compounds have many advantages in comparison with homogeneous liquid acid catalysts, i.e., higher acid strengths and thermal stabilities. They are noncorrosive, cheap, reusable, and environmentally friendly, and require less waste disposal [7]. On the other hand, low surface area, high solubility in water, and constant leakage during operation are among the main disadvantages of heteropoly acids, restricting the scope of their practical applications. To resolve these restrictions, it is recommended to heterogenize the heteropoly acid via immobilization onto a support of high surface area.

Equipped with this strategy, scientists were able to resolve the restrictions encountered when separating and recycling the homogeneous catalysts.

### 3.2. Synthesis of heterocycles

Organic compounds may be classified as aliphatic and aromatic; some are heterocycles. Heterocycles chemistry form by far the largest of the classical divisions of organic chemistry. The widely held of pharmaceutical products with biological activity are heterocycles showing antimalarial, vasodilator, anticonvulsant, fungicidal, pesticidal, and herbicidal potencies. Heterocycles are also broadly present in several naturally occurring compounds. Due to their wide range of biological activity in synthetic and industrial applications, the synthesis of these compounds has recently received a great deal of attention for the discovery of improved strategies toward clean, milder, and high yielding approaches.

Sadeghzadeh et al. [8] reported the preparation of magnetite-polyoxometalate hybrid nanomaterials,  $\text{Fe}_3\text{O}_4/\text{SiO}_2/\text{Salen}/\text{Mn}/\text{IL}/\text{HPW}$  (MNPs HPW) by grafting of  $\text{H}_3\text{PW}_{12}\text{O}_{40}$  (HPW) on the ionic liquid-functionalized  $\text{Fe}_3\text{O}_4$  magnetite nanoparticles. This species could be used as a recoverable catalyst in the one-pot synthesis of cyclic carbonate derivatives with high to excellent yields without a solvent. The MNPs-HPW catalyst was analyzed by FT-IR spectroscopy, XRD, transmission electron microscopy, thermogravimetric analysis, and a vibrating sample magnetometer. The prepared system catalyzed the synthesis cyclic carbonate **3** from epoxides **1** and carbon dioxide **2** under solvent-free conditions (Scheme 3.1).

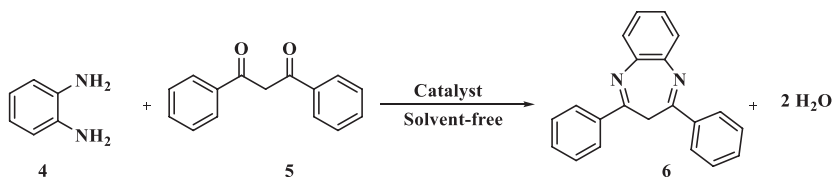


R= Me, Ph, 4-ClC<sub>6</sub>H<sub>4</sub>, 4-BrC<sub>6</sub>H<sub>4</sub>, HOCH<sub>2</sub>, ClCH<sub>2</sub>, PhOCH<sub>2</sub>, Bu<sup>n</sup>, Oct<sup>n</sup>, 4-MeC<sub>6</sub>H<sub>4</sub>, 4-MeSC<sub>6</sub>H<sub>4</sub>, Et

**SCHEME 3.1** Synthesis of cyclic carbonate catalyzed by MNPs-HPW.

The catalyst was readily recoverable using magnetic separation and it was recycled 10 times without any considerable loss in catalytic activity.

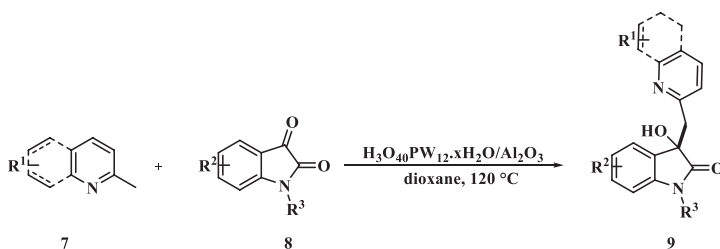
Morales and coworkers [9] successfully prepared solid acid catalysts using mesoporous silica (MESOSI) as a support and tungstophosphoric acid (KTPA) as an active phase, which was incorporated by impregnation (MESOSI#KTPA) and inclusion (MESOSI@KTPA). Transmission electron microscopy images of the MESOSI samples showed the presence of mesopores and specific pore channels. The XRD patterns of the MESOSI#KTPA samples revealed small crystals of  $\text{H}_3\text{PW}_{12}\text{O}_{40} \cdot 6\text{H}_2\text{O}$ , which did not exist in the MESOSI@KTPA materials. The specific surface area of the MESOSI modified with KTPA diminished as the heteropoly acid content increase.  $^{31}\text{P}$  NMR and FT-IR data confirmed the existence of undegraded  $[\text{PW}_{12}\text{O}_{40}]^{3-}$  and  $\text{H}_{3-x}[\text{PW}_{12}\text{O}_{40}]^x-$  anions interacting with the  $\equiv\text{Si}-\text{OH}_2^+$  groups of MESOSI. Potentiometric titration demonstrated that acid strength and number of acid sites would increase with the KTPA loading in MESOSI#KTPA and MESOSI@KTPA samples. In addition, the acidic properties of the MESOSI#KTPA materials were observed to be considerably higher than those of MESOSI@KTPA. The activity, selectivity, and reusability of the prepared catalysts were very high in the one-pot solvent-free reaction between 1,2-phenylenediamine **4** and 1,3-diphenyl-1,3-propanedione **5** to obtain the corresponding 3H-1,5-benzodiazepine **6** (Scheme 3.2).



**SCHEME 3.2** Condensation reaction between 1,2-phenylenediamine and 1,3-diphenyl-1,3-propanedione to obtain 3H-1,5-benzodiazepine.

While the total acidity strongly depended on the method used to incorporate the heteropoly acid, it was almost independent from the KTPA content. Although both series of the catalysts (MESOSI@KTPA and MESOSI#KTPA) demonstrated high activity and selectivity in the synthesis of 3H-1,5-benzodiazepines, the better catalytic performance of the latter could be assigned to its higher acidity.

Hao et al. [10] developed a method for  $\text{C}(sp^3)\text{-H}$  bond functionalization of methyl azaarenes catalyzed by an alumina-supported heteropoly acid-catalyzed reactions of 2-alkyl azaarenes **7** with isatins **8** to afford 3-hydroxy-2-oxindole derivatives **9** (Scheme 3.3). This method could be applied for the synthesis of biologically important derivatives of 3-hydroxy-2-oxindole with good to excellent yields while the catalyst is reusable for six runs without any significant loss of activity. The use of a heteropoly acid supported by alumina allowed the easy separation of the product from the catalyst.



R<sup>1</sup>= 2-methylpyridine, 2,6-dimethylpyridine, 2,4,6-trimethylpyridine, 2-methylquinoline, 6-bromo-2-methylquinoline, 2,6-dimethylquinoline

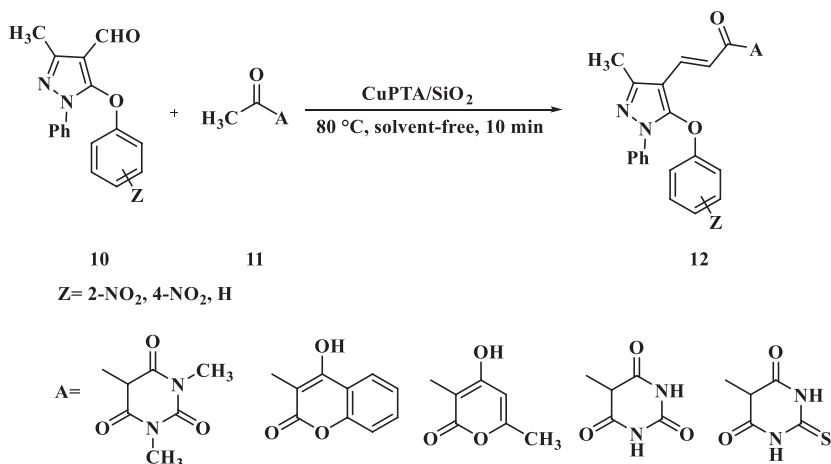
R<sup>2</sup>= 5-NO<sub>2</sub>, 5-Br, 5-Me, 5-OMe, 8-Br

R<sup>3</sup>= H, Me, Ph

**SCHEME 3.3** Synthesis of azaarene-substituted 3-hydroxy-2-oxindoles via C(sp<sup>3</sup>)-H functionalization of 2-methyl azaarenes with isatins.

Siddiqui and coworkers [11] synthesized an efficient, new, and recyclable silica-supported, copper-doped phosphotungstic acid (CuPTA/SiO<sub>2</sub>) by the impregnation method. The catalyst was analyzed by different methods such as FT-IR, XRD, SEM/EDX, ICP-AES, EPR, XPS, and NH<sub>3</sub>-TPD. The catalytic applications of the species were studied for Claisen-Schmidt condensation. The catalyst was recyclable for six runs without any considerable decrease in its activity. The sustained catalytic activity of the recovered catalyst after six runs was confirmed by FT-IR, XRD, SEM/EDX, ICP-AES, and EPR methods. The Claisen-Schmidt yields were excellent in shorter time periods.

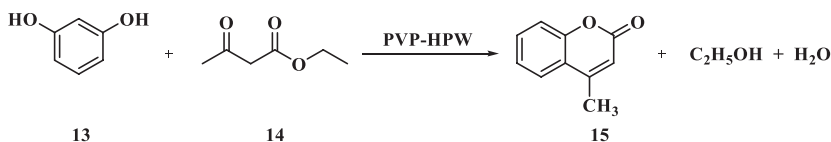
The CuPTA/SiO<sub>2</sub> catalyst was used in the synthesis of phenoxy pyrazolyl chalcones **12** via heating a mixture of different active methyl compounds **10** and 5-aryloxy-3-methyl-1 phenylpyrazole-4-carbaldehydes **11** at 80 °C under solvent-free conditions for 10–12 min (Scheme 3.4). A widespread scope, clean



**SCHEME 3.4** Synthesis of phenoxy pyrazolyl chalcones catalyzed by CuPTA/SiO<sub>2</sub>.

reaction profile, reusability of the catalyst, enhanced rate of reaction, and product yield were among the advantages of the proposed protocol.

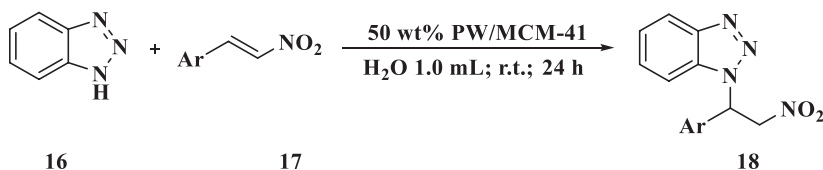
Li and coworkers [12] developed a new protocol for the synthesis of 7-hydroxy-4-methylcoumarin **15** from resorcinol **13** and ethyl acetoacetate **14** using the Pechmann reaction with polyvinylpyrrolidone-supported phosphotungstic acid (PVP-HPW) as a catalyst (Scheme 3.5). The catalyst was characterized by FT-IR, TGA, UV-vis, elemental analysis, and a Hammett acidity function test. Upon protonation by phosphotungstic acid, polyvinylpyrrolidone formed polymeric cations. The polymeric cations strongly interacted with phosphotungstic anions to give an ionic liquid structure. The performance of the PVP-HPW was compared with that of other catalysts like HPW and NMP-H<sub>2</sub>SO<sub>4</sub> as well as PVP-H<sub>2</sub>SO<sub>4</sub>. For a PVP-HPW dosage of 9% based on the weight of resorcinol, the yield of 7-hydroxy-4-methylcoumarin reached 96.73% within 2 h of reflux at 110°C, which proved to be much more valuable than other catalysts. The PVP-HPW could be readily separated from the reaction mixture retaining its activity during the recycling process.



**SCHEME 3.5** Synthesis of 7-hydroxy-4-methylcoumarin from resorcinol and ethyl acetoacetate.

Multiple characterization methods demonstrated that the content of PVP significantly influenced the acidity of PVP-HPW. Apart from high catalytic activity, the Brønsted acidic organic heteropoly acid hybrid catalyst PVP-HPW showed simple preparation.

Xie et al. [13] synthesized heteropoly acid catalysts supported by MCM-41. Their catalytic activity was explored in an aza-Michael addition reaction between nitro olefins **16** and benzotriazole **17** in aqueous solution at ambient temperature (Scheme 3.6). The highest activity (up to 96% yield) was demonstrated



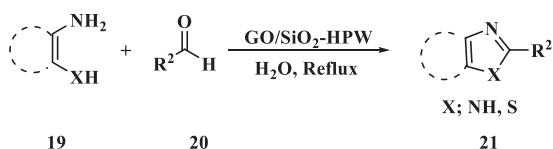
Ar=C<sub>6</sub>H<sub>5</sub>, 4-CH<sub>3</sub>C<sub>6</sub>H<sub>4</sub>, 4-CH<sub>3</sub>OC<sub>6</sub>H<sub>4</sub>, 4-FC<sub>6</sub>H<sub>4</sub>, 4-ClC<sub>6</sub>H<sub>4</sub>, 4-BrC<sub>6</sub>H<sub>4</sub>, 4-NO<sub>2</sub>C<sub>6</sub>H<sub>4</sub>, 2-NO<sub>2</sub>C<sub>6</sub>H<sub>4</sub>, 2,4-Cl<sub>2</sub>C<sub>6</sub>H<sub>3</sub>, 2-furyl

**SCHEME 3.6** Aza-Michael addition reaction nitro olefins derivatives and benzotriazole catalyzed by H<sub>3</sub>PW<sub>12</sub>O<sub>40</sub>/MCM-41.

to occur at 50 wt%  $\text{H}_3\text{PW}_{12}\text{O}_{40}/\text{MCM-41}$  (PW/MCM-41). Being employed in six consecutive experiments, the catalyst showed no obvious loss of activity, verifying the success of the anchoring process and the catalyst stability.

The authors characterized the supported catalysts using power XRD, FT-IR, TEM, and SEM techniques.

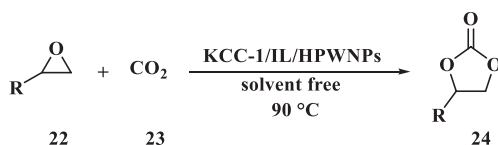
Habibzadeh and coworkers [14] developed a new supported solid acid catalyst comprising of 12-phosphotungstic acid (HPW) on graphene oxide/silica nanocomposite ( $\text{GO@SiO}_2$ ) via immobilizing it onto an amine-functionalized  $\text{GO/SiO}_2$  surface through coordination interaction ( $\text{GO@SiO}_2\text{-HPW}$ ). The  $\text{GO@SiO}_2\text{-HPW}$  nanocomposite was characterized by FT-IR spectroscopy, TGA, powder XRD, and scanning electron microscopy (SEM). The novel nanocomposite could be homogeneously dispersed in water and used as a heterogeneous, efficient, and reusable catalyst for the synthesis of benzimidazoles and benzothiazoles **21** through the reaction of 1,2-phenylenediamine or 2-aminothiophenol **19** with different aldehydes **20** (Scheme 3.7). The catalyst could be readily separated from the workup mixture using centrifugation and reused for several runs without any appreciable degradation in its activity.



$\text{R}^2 =$  4- $\text{ClC}_6\text{H}_4$ , 2- $\text{ClC}_6\text{H}_4$ , 4- $\text{OMeC}_6\text{H}_4$ , 4- $\text{CNC}_6\text{H}_4$ , 2- $\text{OHC}_6\text{H}_4$ , 2-naphthyl, 4- $\text{NO}_2\text{C}_6\text{H}_4$ , 4- $\text{OHC}_6\text{H}_4$ , 4- $(\text{CH}_3)_2\text{NC}_6\text{H}_4$ , 3- $\text{OMe-2-OHC}_6\text{H}_3$ , 2-furyl, 2-thienyl,  $\text{C}_2\text{H}_5$ ,  $\text{C}_4\text{H}_9$ , 3- $\text{OMeC}_6\text{H}_4$ , 4-Me, 4- $\text{CHOC}_6\text{H}_4$ , 4- $\text{FC}_6\text{H}_4$ , 4- $\text{BrC}_6\text{H}_4$ , 2-pyridyl, 3,4- $(\text{OMe})_2\text{C}_6\text{H}_3$

**SCHEME 3.7** One-pot synthesis of benzazoles catalyzed by  $\text{GO/SiO}_2\text{-HPW}$ .

Sadeghzadeh and coworkers [15] synthesized a heteropoly acid-based ionic liquid supported by fibrous nanosilica ( $\text{KCC1/IL/HPW}$ ) via a simple, inexpensive procedure. The species featured easy accessibility of active sites as well as high catalytic activity. The  $\text{KCC-1/IL/HPW}$  nanocatalyst was found to be quite active in the synthesis of the cyclic carbonate **24** from epoxides **22** and carbon dioxide **23** under moderate conditions (Scheme 3.8). The nanocatalyst

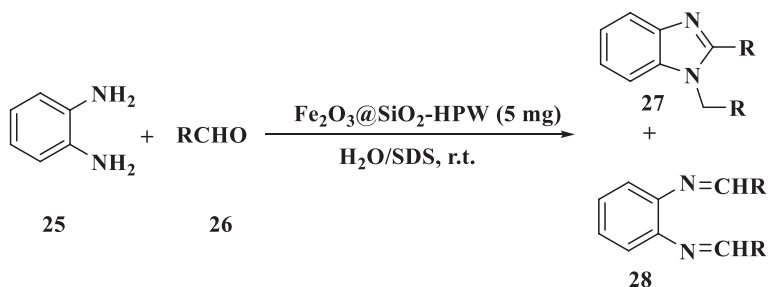


$\text{R} =$  Me, Ph, 4- $\text{ClC}_6\text{H}_4$ , 4- $\text{BrC}_6\text{H}_4$ ,  $\text{HOCH}_2$ ,  $\text{ClCH}_2$ ,  $\text{PhOCH}_2$ ,  $\text{Bu}^n$ ,  $\text{Oct}^n$ , 4- $\text{MeC}_6\text{H}_4$ , 4- $\text{MeSC}_6\text{H}_4$ , Et

**SCHEME 3.8** Synthesis of cyclic carbonate in the presence of  $\text{KCC-1/IL/HPW}$  NPs.

was characterized by FT-IR, TGA, XRD, scanning electron microscopy (SEM), and transmission electron microscopy (TEM). High catalytic activity and easy recovery from the workup mixture with filtration as well as several reuses without any appreciable degradation in performance were among other eco-friendly features of this novel catalytic system.

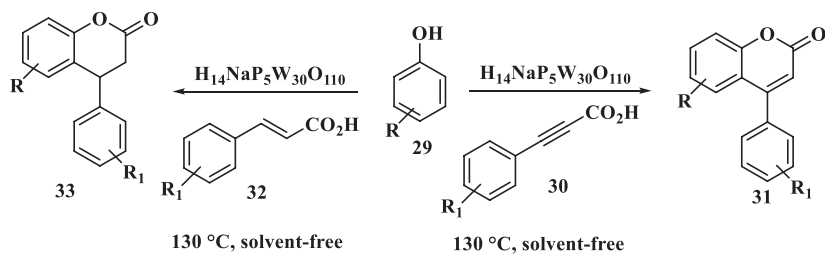
Rafiee and others [16] reported an improved methodology for the preparation of 12-tungstophosphoric acid (HPW) supported on magnetic silica-coated nanoparticles and characterized it using various techniques such as scanning electron microscopy, transmission electron microscopy, powder XRD, and inductively coupled plasma atomic emission spectroscopy. The acidity of the prepared catalyst was measured by potentiometric titration with *n*-butylamine. The catalytic activity was determined in the synthesis of 1,2-disubstituted benzimidazole derivatives **27** in aqueous solution as a model (Scheme 3.9). The catalyst demonstrated excellent activity and the products were afforded in good to excellent yields under moderate conditions. Moreover, the catalyst could be readily recovered using an external magnet and reused for several more runs. The use of water as the solvent, low catalyst loading, and simple workup were among other advantages of this catalytic system, making this new methodology practical for the synthesis of benzimidazole derivatives.



**SCHEME 3.9**  $\gamma$ -Fe<sub>2</sub>O<sub>3</sub>@SiO<sub>2</sub>-HPW catalyzed synthesis of 1,2-disubstituted benzimidazoles in water.

Escobar et al. [17] prepared 4-phenyl **31** and 3,4-dihydro-4-phenylcoumarins **33** via direct esterification of phenols **29** with phenylpropionic **30** and cinnamic acids **32**, respectively. In their new method, they used a compound with Preyssler structure (H<sub>14</sub>NaP<sub>5</sub>W<sub>30</sub>O<sub>110</sub>) as a heterogeneous catalyst with no solvent included at 130°C, in a short reaction time of 2 h (Scheme 3.10). Good to excellent yields (11 examples: 61%–90%) without secondary products were obtained under such conditions. The catalyst was nontoxic, recyclable, neither air- nor moisture-sensitive, and easy to operate.

Xiao and coworkers [18] designed and prepared 13 novel amine or quaternary ammonium functionalized polyacrylonitrile fiber (PANF) supported

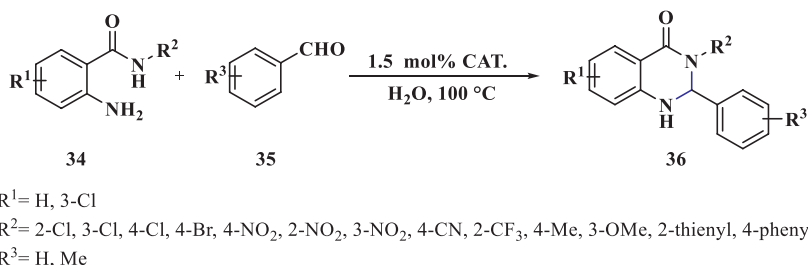


R= 3-OH, 3-OMe, 4-CH<sub>3</sub>, 4-OMe, 3-Me, 2-Me,

R<sub>1</sub>= 4-OMe, 4-Me

**SCHEME 3.10** Synthesis of 4-phenylcoumarins and 4-phenyl-3,4-dihydro-4-phenylcoumarins.

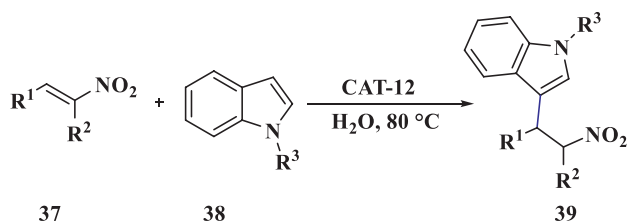
phosphotungstic acid catalysts. They managed to screen the activities of these catalysts using the condensation/annulation tandem synthesis of 2,3-dihydroquinazolin-4(1H)-one compounds **36** via C–N bond formation between 2-aminobenzamide **34** and benzaldehyde **35** (Scheme 3.11). By tuning the functionality and hydrophobic/hydrophilic properties of the amine/ammonium structure as well as the density of phosphotungstic acid sites, the fiber catalyst CAT-12, which was prepared from quaternary ammonium functionalized PANF with a benzyl group of high PTA loading, afforded the best catalytic activity for most reactions in aqueous solution. The CAT-12 could be easily separated from the workup and recycled for seven runs without any considerable loss in catalytic activity. In addition, the reaction progressed mildly in gram scale to afford nearly quantitative yields using this effective, eco-friendly and easily recyclable catalyst with great industrial potential. Its activity was also demonstrated in Friedel-Crafts alkylation of indoles **37** with *b*-nitrostyrene **38** (Scheme 3.12).



**SCHEME 3.11** CAT-12 catalyzed synthesis of 2,3-dihydroquinazolin-4(1H)-ones with hydrophilic 2-aminobenzamide and hydrophobic benzaldehyde.

Liu et al. [19] prepared a heteropoly acid-based organic hybrid heterogeneous catalyst, by combining 8-hydroxy-2-methylquinoline (HMQ) with Keggin-structured H<sub>4</sub>SiW<sub>12</sub>O<sub>40</sub>(STW). The catalyst (HMQ-STW) was characterized using elemental analysis, XRD, FT-IR, TGA, scanning electron





$\text{R}^1 = \text{C}_6\text{H}_5, 4\text{-OHC}_6\text{H}_4, 4\text{-CNC}_6\text{H}_4, 4\text{-NO}_2, 2\text{-naphtyl}, 2\text{-thienyl}$

$\text{R}^2 = \text{H}$

$\text{R}^3 = \text{H}, \text{CH}_3,$

**SCHEME 3.12** CAT-12 catalyzed Friedel-Crafts alkylation of indoles.

microscopy (SEM), and potentiometric titration methods. The catalyst performance was evaluated in the ketalization of ketones with glycol or 1,2-propylene glycol (Table 3.1). A variety of reaction parameters, such as the molar ratio of glycol to cyclohexanone, reaction temperature and time, as well as catalyst dosage, were explored systematically. HMQ-STW demonstrated a relatively high yield of the corresponding ketal, with 100% selectivity under the optimized reaction conditions. Furthermore, catalytic recycling tests showed that the heterogeneous catalyst had a high potential for reusability. It was also revealed that the organic modifier HMQ had a significant effect on the formation of a heterogeneous system as well as enhancing the structural stability.

These findings demonstrated that the HMQ-STW catalyst was a new promising heterogeneous acid catalyst for the ketalization of ketones.

Mozafari and others [20] synthesized a novel acid nanocatalyst,  $\text{MnFe}_2\text{O}_4/\text{chitosan/phosphotungstic acid}$  ( $\text{MnFe}_2\text{O}_4@\text{CS@PTA}$ ). As a magnetically recoverable nanoparticle, the synthesized species was studied as a heterogeneous nanocatalyst to prepare the functionalized oxazolidin-2-ones **42** as flexible chiral synthons in the asymmetric synthesis of biologically active compounds through the reaction of  $\alpha$ -epoxyketones **40** with urea and thiourea **41** (Scheme 3.13). Excellent yields, green reaction conditions, and short reaction time were among the considerable features of this new protocol. Moreover, excellent catalytic activity in protic solvent as well as easy preparation, thermal stability, and separation of the catalyst rendered it a satisfactory heterogeneous system as a useful alternative to the other heterogeneous catalysts. The synthesized  $\text{MnFe}_2\text{O}_4@\text{CS@PTA}$  may prove a promising catalytic species for production of mass fine chemicals. The composition and structure of the nanocomposite were analyzed by different methods such as FT-IR, field emission scanning electron microscopy (FESEM), XRD, TGA, vibrating sample magnetometer (VSM), transmission electron microscopy (TEM), and Brunauere-Emmette Teller (BET).

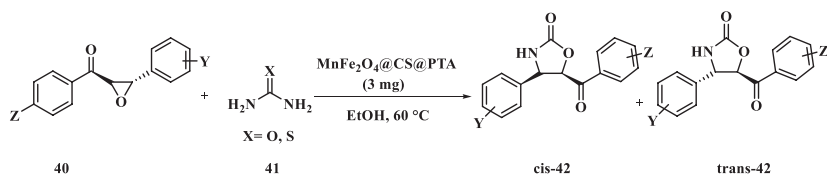
Kumaresan et al. [21] developed a green Keggin-type heteropoly-12-tungstophosphoric acid (HPW) supported on graphitic carbon nitride  $\text{g-C}_3\text{N}_4$

**TABLE 3.1** Ketalization of carbonyl compounds with diols catalyzed with HMQ-STW.

Entry	Ketone/aldehyde	Diol	Product
1	Benzaldehyde	Glycol	
2	Acetophenone	Glycol	
3	<i>p</i> -Nitrobenzaldehyde	Glycol	
4	<i>m</i> -Nitrobenzaldehyde	Glycol	
5	<i>p</i> -Chlorobenzaldehyde	Glycol	
6	<i>p</i> -Nitroacetophenone	Glycol	
7	Benzaldehyde	1,2-Propylene glycol	
8	Acetophenone	1,2-Propylene glycol	
9	Cyclohexanone	1,2-Propylene glycol	
10	<i>p</i> -Chlorobenzaldehyde	1,2-Propylene glycol	
11	<i>p</i> -Nitrobenzaldehyde	1,2-Propylene glycol	
12	<i>p</i> -Nitroacetophenone	1,2-Propylene glycol	

**TABLE 3.1** Ketalization of carbonyl compounds with diols catalyzed with HMQ-STW—cont'd

Entry	Ketone/aldehyde	Diol	Product
13	Acetone	1,2-Propylene glycol	
14	Benzaldehyde	Glycol	
15	Benzaldehyde	Pentaerythritol	
16	Benzaldehyde	Neopentyl glycol	



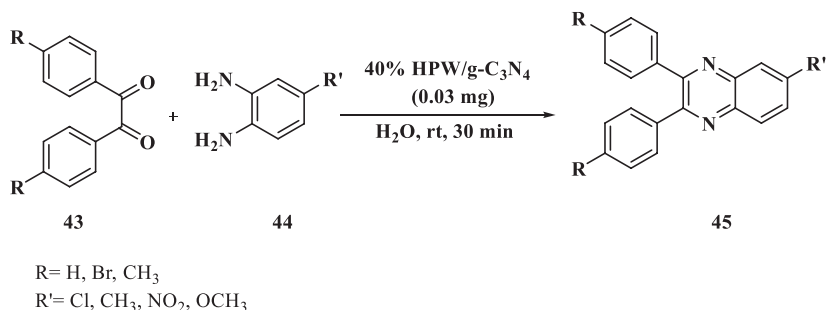
Z = H, 4-Me, 4-OMe,

Y = H, 4-Me, 4-OMe, 2-OMe, 4-Cl, 4-NO<sub>2</sub>, 2-Cl, 3-NO<sub>2</sub>

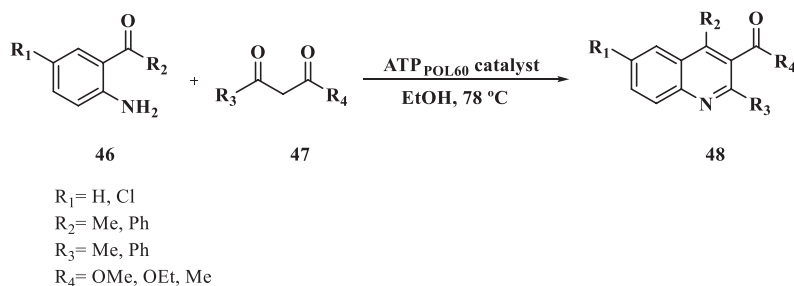
**SCHEME 3.13** The preparation of 5-Benzoyl-4-phenyloxazolidin-2-one derivatives in the presence MnFe<sub>2</sub>O<sub>4</sub>@CS@PTA.

(40% HPW/g-C<sub>3</sub>N<sub>4</sub>). It was used to catalyze a one-pot synthesis of quinoxaline derivatives **45** from 1,2-diketone **43** and 1,2-diamines **44** (Scheme 3.14). Using green solvents, heterogeneous reaction conditions, operational simplicity, short reaction times, and catalyst reusability were the advantages of this protocol.

Bennardi and coworkers [22] proposed a new, effective, and green protocol to afford quinolines based on employing tungstophosphoric acid in a polymeric matrix of polyacrylamide (APT<sub>POL60</sub>). The protocol consisted of the formation of polysubstituted quinoline compounds **48** using various 2-aminoaryl ketones **46** and -dicarbonyl compounds **47**, in absolute ethanol at a temperature of 78°C (Scheme 3.15). The efficiency of the catalyst remained intact after successive uses with no leaching observed. Seven different quinolone derivatives were synthesized in excellent yields (89%–99%).



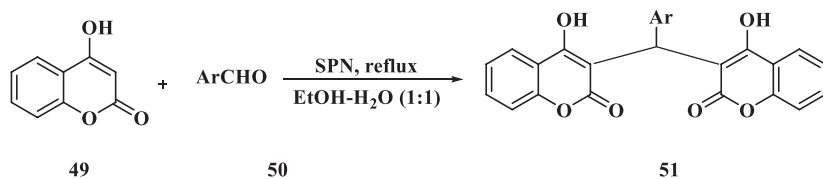
**SCHEME 3.14** Synthesis of quinoxaline derivatives using HPW/g-C<sub>3</sub>N<sub>4</sub> as a catalyst.



**SCHEME 3.15** Preparation of quinoline derivatives by the reaction 2-amino-ketones and -dicarbonyl compounds using APTPOL60 catalyst.

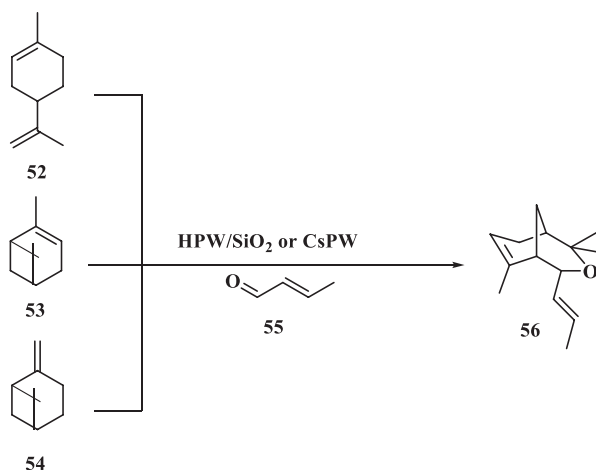
Gharib and others [23] reported a new methodology efficient in the synthesis of dicoumarol (3,3'-methylene-bis-4-hydroxycoumarin) **51** catalyzed by silica-supported Preyssler nanoparticles (SPN) (Scheme 3.16). Compared to the other heteropoly acid catalysts, the catalyst performed quite well. A significant advantage of the catalyst was the ease of separating from the workup mixture. In addition, it could be recycled several times.

Costa and coworkers [24] reported that the interaction of monoterpenes such as limonene **52**,  $\alpha$ -pinene **53**, and  $\alpha$ -pinene **54** with crotonaldehyde **55** using silica-supported H<sub>3</sub>PW<sub>12</sub>O<sub>40</sub> and its acidic cesium salt Cs<sub>2.5</sub>H<sub>0.5</sub>PW<sub>12</sub>O<sub>40</sub> as solid



Ar= C<sub>6</sub>H<sub>5</sub>, 4-ClC<sub>6</sub>H<sub>4</sub>, 2-NO<sub>2</sub>C<sub>6</sub>H<sub>4</sub>, 4-OMeC<sub>6</sub>H<sub>4</sub>, 4-BrC<sub>6</sub>H<sub>4</sub>, 4-NO<sub>2</sub>C<sub>6</sub>H<sub>4</sub>, 2-OH-3-MeOC<sub>6</sub>H<sub>3</sub>

**SCHEME 3.16** Synthesis of dicoumarols **51** from 4-hydroxycoumarin **49** and benzaldehydes **50** catalyzed by silica-supported Preyssler nanoparticles (SPN).

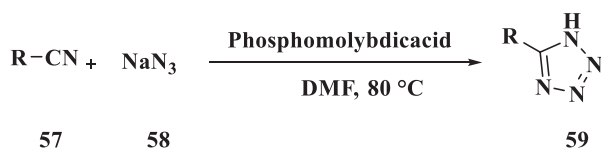


**SCHEME 3.17** Acid-catalyzed reaction of limonene, α-pinene, and α-pinene with crotonaldehyde.

acid catalysts in dichloroethane solutions resulted in cycloaddition reactions to give the same fragrant oxabicyclo[3.3.1] nonene product **56** with a very good yield (Scheme 3.17). The product was probably formed via an α-terpenyl carbenium ion intermediate, generated from monoterpene protonation to undergo a nucleophilic attack by crotonaldehyde. H<sub>3</sub>PW<sub>12</sub>O<sub>40</sub> and Cs<sub>2.5</sub>H<sub>0.5</sub>PW<sub>12</sub>O<sub>40</sub> were both found to be efficient as heterogeneous cycloaddition catalysts.

Takale et al. [25] reported an effective and practical method for the preparation of 5-substituted 1H-tetrazole derivatives **59** from a wide variety of nitriles **57** with phosphomolybdic acid as an efficient heterogeneous catalyst (Scheme 3.18). Good yields, simplicity of operation, and easy workup, plus elimination of hazardous and harmful hydrazoic acid, rendered the method more attractive for the diversity-oriented synthesis of the mentioned heterocycles. The catalyst was recyclable for three times with satisfactory yields.

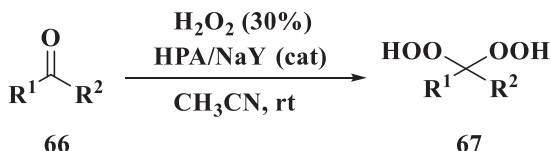
Hosseini and coworkers [26] prepared a new sulfonic-phosphotungstic dual-acid hybrid catalyst based on silica coated magnetite nanoparticles (SCMNPs), which contained two types of Brønsted acidic sites that is sulfonic acid (-SO<sub>3</sub>H)



R = C<sub>6</sub>H<sub>5</sub>, 4-CH<sub>3</sub>C<sub>6</sub>H<sub>4</sub>, 4-OMeC<sub>6</sub>H<sub>4</sub>, 4-OHC<sub>6</sub>H<sub>4</sub>, 4-NO<sub>2</sub>C<sub>6</sub>H<sub>4</sub>, 4-BrC<sub>6</sub>H<sub>4</sub>, 2-BrC<sub>6</sub>H<sub>4</sub>, 2-naphtyl, C<sub>6</sub>H<sub>5</sub>CH<sub>2</sub>, C<sub>5</sub>H<sub>11</sub>, C<sub>4</sub>H<sub>9</sub>, Ts

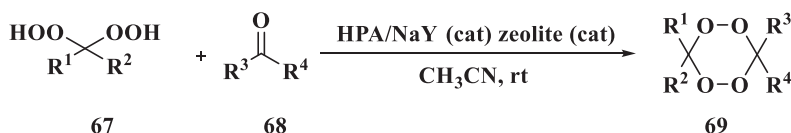
**SCHEME 3.18** Preparation of 5-substituted 1H-tetrazoles catalyzed by phosphomolybdic acid.





$\text{R}^1, \text{R}^2 = \text{H}, \text{alkyl}, \text{cycloalkyl}, \text{and aryl}$

**SCHEME 3.21** Peroxidation of aldehydes and ketones in the presence of heteropoly acid/NaY.



$\text{R}^1-\text{R}^4 = \text{H}, \text{alkyl}, \text{cycloalkyl}, \text{and aryl}$

**SCHEME 3.22** Synthesis of different 1,2,4,5-tetraoxanes in the presence of heteropoly acid/NaY.

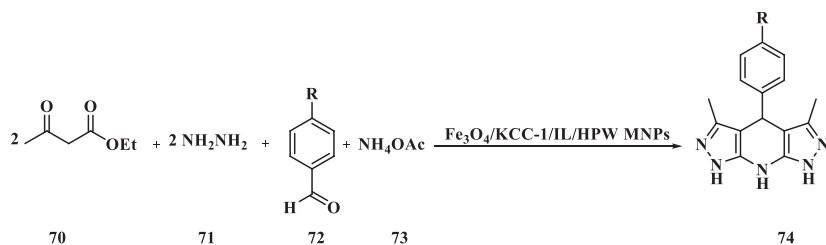
progressed with high rates and very good yields. In addition, the hybrid catalyst was successfully used to facilitate the synthesis of 1,2,4,5-tetraoxanes **69** by the direct condensation of *gem*-dihydroperoxides obtained from different ketones (Scheme 3.22). Consequently, the heteropoly acid/NaY system was proved to be an inexpensive, recoverable, and environmentally friendly solid catalyst. Mild reaction conditions, shorter reaction times, and higher yields were among the notable features of this method.

### 3.3. Multicomponent reactions (MCRs)

Multicomponent reactions (MCRs) are convergent reactions, in which three or more commercially available or easily accessible starting materials react to generate a product, where essentially all or most of the atoms subsidize to the newly formed product. In an MCR, a product is assembled according to a cascade of elementary chemical reactions.

Sadeghzadeh et al. [29] demonstrated the application of a catalyst containing phosphotungstic acid and an ionic liquid based organosilica ( $\text{Fe}_3\text{O}_4/\text{KCC-1}/\text{IL}/\text{HPW}$ ) for the synthesis of tetrahydrodipyrzolopyridines **74** (Scheme 3.23). High loading capacities were achieved for the heteropoly acid due to the amplification effect of the ionic liquid. The catalyst system could be successfully reused several times without any appreciable loss in activity or selectivity. The  $\text{Fe}_3\text{O}_4/\text{KCC-1}/\text{IL}/\text{HPW}$  nanocatalyst synthesized in this work showed excellent catalytic activity in multicomponent reactions under moderate conditions, which was assigned to the accessibility of the active sites. Based on these results, the



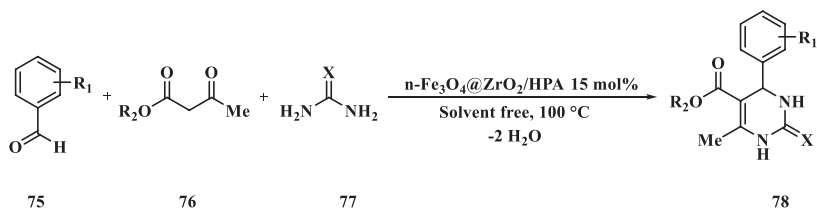


R = H, Cl, F, NO<sub>2</sub>, MeO, Me, HO, NC, Me<sub>2</sub>N

**SCHEME 3.23** Synthesis of tetrahydropyrazolo pyridines catalyzed by Fe<sub>3</sub>O<sub>4</sub>/KCC-1/IL/HPW in water.

author concluded that although the Fe<sub>3</sub>O<sub>4</sub>/KCC-1/IL nanostructure acted as a for the soluble phosphotungstic acid, it could also operate as a nanoscaffold to retake the phosphotungstic acid into the *meso* fibers. The result was prevention of wide agglomeration of phosphotungstic acid.

Zolfagarinia et al. [30] developed a novel highly effective catalyst via the immobilization of phosphotungstic acid (20–60 wt%) on the surface of zirconia-encapsulated Fe<sub>3</sub>O<sub>4</sub> nanoparticles, which were magnetically retrievable. The prepared heterogeneous acid catalyst, i.e., phosphotungstic acid supported on nano Fe<sub>3</sub>O<sub>4</sub>@ZrO<sub>2</sub>(n-Fe<sub>3</sub>O<sub>4</sub>@ZrO<sub>2</sub>/HPW) was completely characterized using a number of techniques, such as FT-IR, transmission electron microscopy, field emission scanning electron microscopy, XRD, energy-dispersive X-ray spectroscopy, vibrating sample magnetometry, and TGA. The FT-IR data showed that the phosphotungstic acid molecules on the nano-Fe<sub>3</sub>O<sub>4</sub>@ZrO<sub>2</sub> support existed in the Keggin structure. The acidity of the catalyst was determined by potentiometric titration with *n*-butylamine. The catalytic activity of the prepared new nano Fe<sub>3</sub>O<sub>4</sub>@ZrO<sub>2</sub>/HPW was examined over the one-pot, three-component synthesis of different 3,4-dihydropyrimidin-2(1*H*)-ones **78** (i.e., Biginelli reaction) (Scheme 3.24) and 1,4-dihydropyridines **80** (i.e., Hantzsh reaction) (Scheme 3.25) in the absence of any solvent. The sample of 40 wt% exhibited

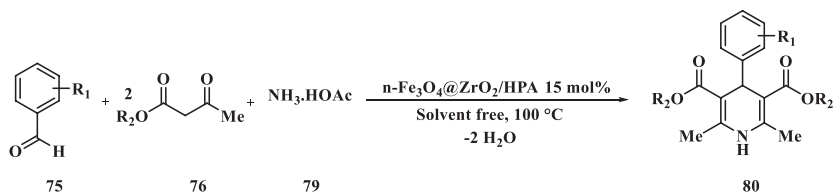


R<sub>1</sub> = H, 2-Cl, 4-Cl, 3-NO<sub>2</sub>, 4-NO<sub>2</sub>, 2-OCH<sub>3</sub>, 4-OCH<sub>3</sub>, 4-OH, 4-CH<sub>3</sub>, 3-OEt, 4-OH, 3,4-(OMe)<sub>2</sub>, 4-N(CH<sub>3</sub>)<sub>2</sub>, 3-OEt, 4-OH

R<sub>2</sub> = Me, Et

X = O, S

**SCHEME 3.24** Synthesis of 3,4-dihydropyrimidin-2(1*H*)-ones.

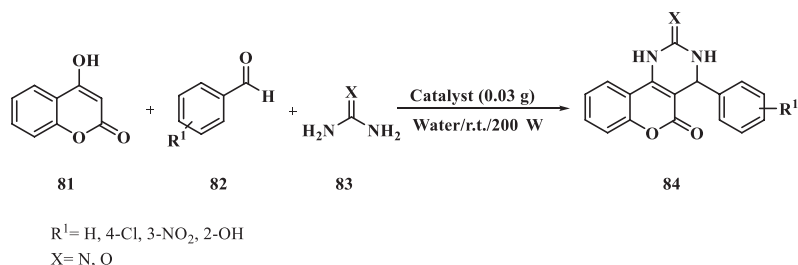


**SCHEME 3.25** Synthesis of 1,4-dihydropyridines.

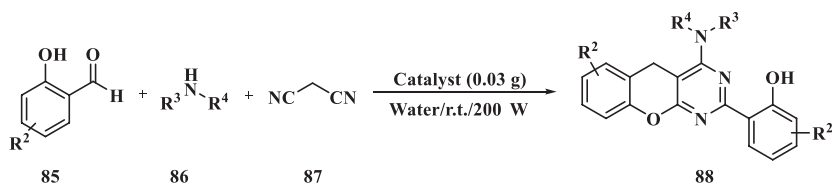
higher acidity and activity in the catalytic transformation. When the reaction was complete, the catalyst/product separation was easily achievable with an external magnetic field and the separated catalyst was easily recycled for at least five runs without any considerable loss in its catalytic activity. The excellent recyclability was ascribed to the strong interaction between the hydroxyl groups of the nano- $\text{Fe}_3\text{O}_4\text{/ZrO}_2$  support and the phosphotungstic acid.

Sadjadi and coworkers [31] designed and synthesized a novel hybrid catalyst via incorporation of a heteropoly acid into creatin-functionalized halloysite clay. Characterized by different methods such as SEM/EDS, XRD, FT-IR, BET, ICP-AES, thermogravimetric analysis, and DTGA, the resulted catalysts were successfully applied in promoting the synthesis of two series of benzopyranopyrimidines under ultrasonic irradiation in aqueous solution of two series of benzopyranopyrimidines **84** and **88** from the reaction of 4-hydroxycoumarin **81**, aldehydes **82**, and urea/thiourea **83** (Scheme 3.26) and the reaction of 2-hydroxy benzaldehydes **85**, amine **86**, and malononitrile **87** (Scheme 3.27). The results demonstrated the effectiveness of the proposed method in terms of the yield, reaction time, the green nature of the process, and simplicity of the workup procedure. In addition, immobilization of the heteropoly acid on creatin-functionalized halloysite retarded the heteropoly acid leaching and made the catalyst entirely reusable.

Sadeghzadeh and coworkers [32] prepared magnetite-polyoxometalate hybrid nanomaterials ( $\text{Fe}_3\text{O}_4\text{/SiO}_2\text{/salen/Mn/IL/HPW}$ ). For this purpose, they grafted phosphotungstic acid on  $\text{Fe}_3\text{O}_4$  magnetite nanoparticles functionalized by an ionic liquid. The prepared catalyst was absolutely recoverable when used



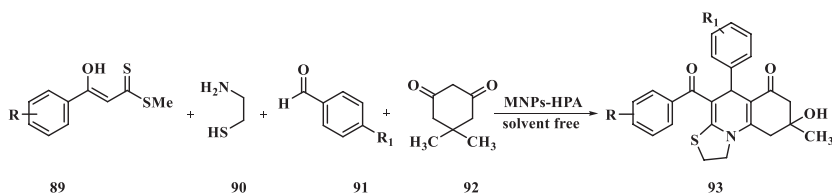
**SCHEME 3.26** Synthesis of benzopyranopyrimidines using 4-hydroxycoumarin under ultrasonic irradiation.



$\text{R}^2 = \text{H}, 3\text{-MeO}, 5\text{-Br}$

$\text{R}^3, \text{R}^4 = -(\text{CH}_2)_2\text{-O}-(\text{CH}_2)_2-, -(\text{CH}_2)_5-, \text{CH}_3, \text{CH}_3$

**SCHEME 3.27** Synthesis of benzopyranopyrimidines using salicylaldehydes under ultrasonic irradiation.



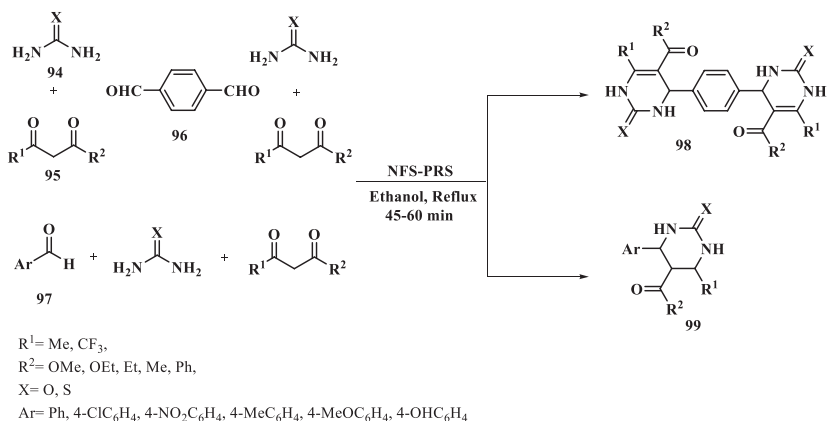
$\text{R} = \text{H}, 4\text{-Me}, 3\text{-OMe}, 2\text{-Cl}$

$\text{R}_1 = \text{H}, 4\text{-Me}, 4\text{-NO}_2, 4\text{-Me}, 2\text{-NO}_2$

**SCHEME 3.28** Synthesis of thiazoloquinolines in the presence of MNPs-HPW.

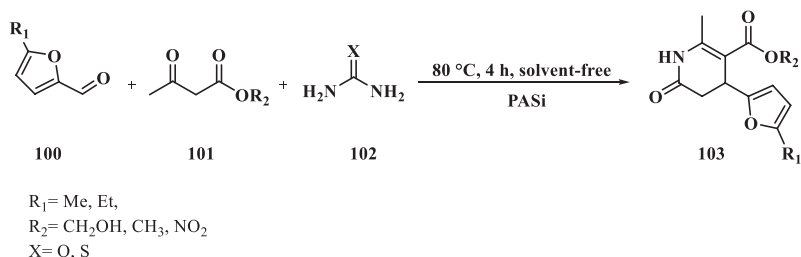
for the one-pot synthesis of thiazoloquinolines **93** from the reaction of  $\alpha$ -enolic dithioesters **89**, cysteamine **90**, aldehyde **91**, and cyclohexane-1,3-dione **92** with high to excellent yield in the absence of a solvent (Scheme 3.28). The catalyst was characterized using FT-IR, TGA, XRD, vibrating sample magnetometry (VSM), and transmission electron microscopy (TEM). In addition, the catalyst was readily recoverable by magnetic separation and recycled for 10 runs without any appreciable degradation in its activity.

Eshghi et al. [33] prepared a new magnetic acidic catalyst containing a Preyssler heteropoly acid, i.e.,  $\text{H}_{14}[\text{NaP}_5\text{W}_{30}\text{O}_{110}]$  supported on nickel ferrite nanoparticles coated with silica ( $\text{NiFe}_2\text{O}_4@\text{SiO}_2$ ). The prepared catalyst was characterized by FT-IR, scanning electron microscopy (SEM), transmission electron microscopy (TEM), XRD, energy dispersive spectrum, vibrating sample magnetometer (VSM), as well as particle size measurement. Its catalytic activity was studied over the synthesis of bis(dihydropyrimidinone)benzene **98** and 3,4-dihydropyrimidin-2(1*H*)-ones and -thiones derivatives **99** by the Biginelli reaction. With the prepared catalyst, the reactions occurred in less than 1 h in good to excellent yields. The catalyst was readily separated from the workup mixture using an external magnetic field and reused for at least five runs without any loss in activity. This proposed protocol was simple, green, and efficient (Scheme 3.29).



**SCHEME 3.29** Synthesis of bis(dihydropyrimidinone)benzene and 3,4-dihydropyrimidin-2(1*H*)-ones and -thiones derivatives.

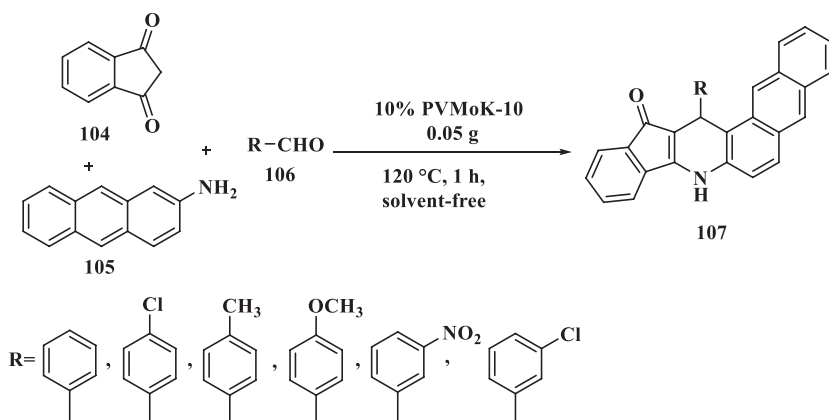
Portilla-Zuñiga and others [34] developed an effective method with high yields using the renewable platform molecule furfural for the synthesis of Biginelli derivatives **103** via a three-component, domino reaction via a combination of aldehydes (furfural) **100**,  $\beta$ -ketoesters **101**, and urea or thiourea **102** catalyzed by a Preyssler heteropoly acid, i.e.,  $\text{H}_{14}\text{NaP}_5\text{W}_{29}\text{MoO}_{110}$ , encapsulated in a silica framework (Scheme 3.30). The reaction was carried out without any solvent with high yields using thermal and microwave heating. Atom economy, environmental friendliness, reusability of the catalysts, and short reaction times were among the significant features of the protocol. The Preyssler catalyst embedded in the silica matrix ( $\text{PCSiO}_2$ ) was not soluble in polar and nonpolar media, allowing easy separation of the reaction products without any influence on its catalytic activity. The proposed catalytic strategy exhibited the benefits of the Preyssler acid ( $\text{H}_{14}\text{NaP}_5\text{MoW}_{29}\text{O}_{110}$ ) as a Brønsted acid catalyst in the Biginelli multicomponent reaction. On the other hand, it was evident that the acid strength of the active phase was too high for the reaction to proceed with the bulk catalyst. Nonetheless, the inclusion of the catalyst in the silica framework made it suitable for the reaction as a catalyst that is easy to recover and reuse.



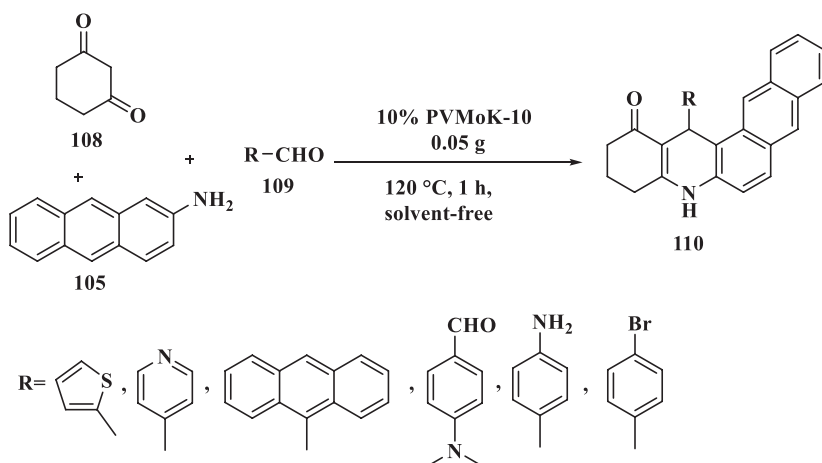
**SCHEME 3.30** Synthesis of dihydropyrimidinones (thiones).

Kumaresan et al. [35] reported the condensation of 1,3-indanedione **104**, 2-aminoanthracene **105** and substituted aromatic aldehydes **106** catalyzed by 10% PVMoK-10 to yield naphtho[2,3-*f*]quinolin-13-one **107** (Scheme 3.31) as well as condensation of 1,3-cyclohexanedione **108**, 2-aminoanthracene **105**, and substituted aromatic aldehydes **109** catalyzed by 10% PVMoK-10 catalyst to yield naphtho[2,3-*a*]acridin-1(2H)-one **110** (Scheme 3.32). The significant features of the protocol were simple operation, evading toxic solvents, shorter reaction time, good yields, as well as recovery and reusability of the catalyst.

Sadjadi and coworkers [36] designed and synthesized a novel heterogeneous catalyst, HPA@HNTs-IMI-SO<sub>3</sub>H, based on functionalization of halloysite nanotubes with an ionic liquid followed by incorporation of the heteropoly acid. The structure of the catalyst was determined with SEM/EDX, FT-IR,

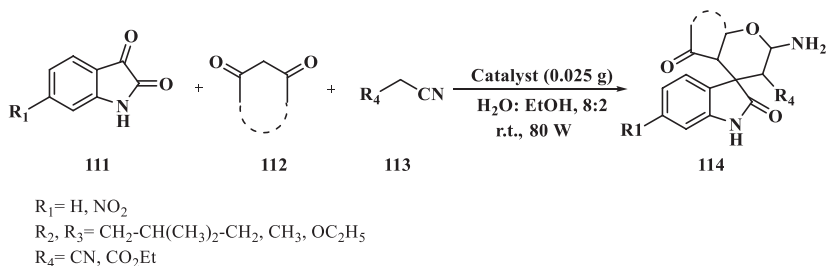


**SCHEME 3.31** Synthesis of naphtho[2,3-*f*]quinolin-13-one derivatives catalyzed by 10% PVMoK-10.



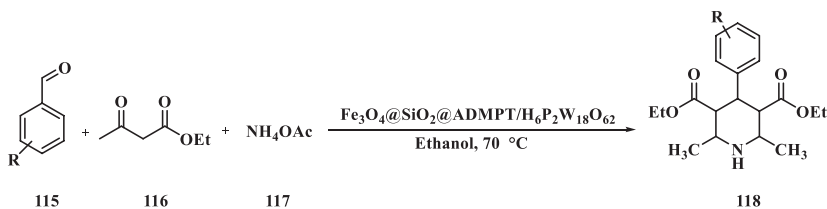
**SCHEME 3.32** Synthesis of naphtho[2,3-*a*]acridin-1(2H)-one catalyzed by 10% PVMoK-10.

XRD, ICP-AES, thermogravimetric analysis, DTGA, and BET. In addition, the catalytic activity of HPA@HNTs-IMI-SO<sub>3</sub>H was examined in promotion of the ultrasonic-assisted, three-component reaction of isatins **111**, 1,3-dicarbonyl compounds **112**, and malononitrile or cyanoacetic esters **113** to give the corresponding spirooxindole **114** with high yields and short reaction times (Scheme 3.33). The reusability of the catalyst was also investigated. It is noteworthy that the catalyst could be recovered and reused for three successive runs. Given the leaching test results, that observation was attributed to the leaching of heteropoly acids, which in turn could be induced by ultrasonic irradiation.



**SCHEME 3.33** Three-component reaction catalyzed by HPA@HNTs-IMI-SO<sub>3</sub>H under ultrasonic irradiation.

Ghanbari and others [37] designed a novel magnetic Wells-Dawson heteropoly acid-based inorganic/organic nanohybrid, (Fe<sub>3</sub>O<sub>4</sub>@SiO<sub>2</sub>@ADMPT/H<sub>6</sub>P<sub>2</sub>W<sub>18</sub>O<sub>62</sub>) and used it as a green, efficient, and totally recyclable catalyst for the one-pot, multicomponent synthesis of 1,4-Dihydropyridine (1,4-DHP) derivatives **118** from the reaction of a variety of aromatic aldehydes **115** with ethyl acetoacetate **116** and ammonium acetate **117** with satisfactory to excellent yields and in short reaction times (Scheme 3.34). The mentioned nanohybrid catalyst was synthesized by the chemical anchoring of the Wells-Dawson heteropoly acid H<sub>6</sub>P<sub>2</sub>W<sub>18</sub>O<sub>62</sub> onto the surface of functionalized Fe<sub>3</sub>O<sub>4</sub> nanoparticles using 2,4-bis(3,5-dimethylpyrazol)-triazine (ADMPT) as a linker. These nanohybrid catalysts were analyzed using different techniques such as scanning

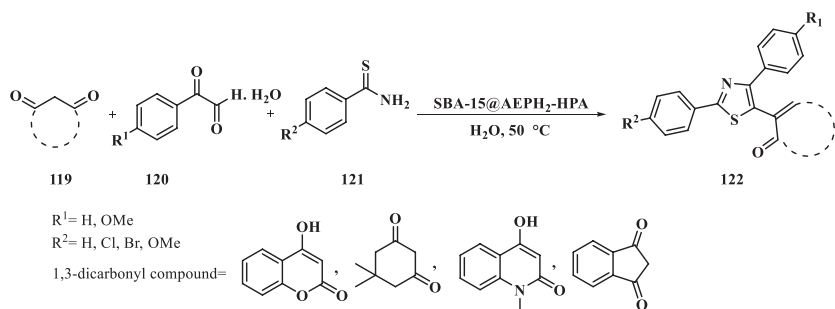


R = H, 4-Br, 4-Cl, 3-OMe, 2-Me, 2-F, 4-F, 3-Cl, 2,3-(Cl)<sub>2</sub>, 4-OMe, 2-Cl, 4-NO<sub>2</sub>, 3-NO<sub>2</sub>, 4-N(Me)<sub>2</sub>

**SCHEME 3.34** Synthesis of 1,4-DHP derivatives catalyzed by Fe<sub>3</sub>O<sub>4</sub>@SiO<sub>2</sub>@ADMPT/H<sub>6</sub>P<sub>2</sub>W<sub>18</sub>O<sub>62</sub>.

electron microscopy (SEM), transmission electron microscopy (TEM), XRD, IR spectroscopy, and vibrating sample magnetometer (VSM). The protocol was developed as a safe, inexpensive, and convenient alternative to the synthesis of 1,4-DHP derivatives employing a green, highly reusable catalyst.

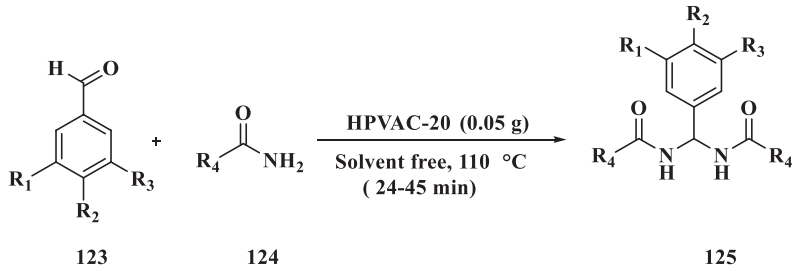
Jahanshahi and coworkers [38] anchored a heteropoly acid on SBA-15 functionalized with 2-aminoethyl dihydrogen phosphate (SBA-15@AEPH<sub>2</sub>-HPA) to synthesize a novel and extensively efficient heterogeneous mesoporous catalyst. The synthesized catalyst was successfully characterized using many techniques such as FT-IR, BET, small-angle XRD, EDX, SEM, TGA, TEM, ICP-OES, and elemental analysis. The novel catalyst exhibited a high catalytic activity over the one-pot synthesis of a wide variety of trisubstituted 1,3-thiazole derivatives **122**. The protocol involved the three-component reactions of arylglyoxals **119**, cyclic 1,3-dicarbonyls **120**, and thioamides **121** under moderate reaction conditions (Scheme 3.35). The proposed methodology was far better than the only method found in the literature. The most promising advantages of the presented method were affording a very important class of pharmaceutically and biologically active 1,3-thiazoles in excellent yields in short reaction times, mild reaction conditions, using water as the solvent, and easy reusability of the catalyst for at least nine runs without any considerable loss in its activity. Importantly, the small-angle XRD analysis and TEM images of the ninth recovered catalyst clearly proved the privileged durability and stability of the introduced catalytic system, under the reaction condition.



**SCHEME 3.35** Synthesis of trisubstituted 1,3-thiazoles in the presence of SBA-15@AEPH<sub>2</sub>-HPA, under mild aqueous media.

Selvakumar et al. [39] achieved a one-pot, multicomponent synthesis of *N,N'*-alkylidene bisamides **125** (Scheme 3.36), 2,4,5-trisubstituted imidazoles **129** (Scheme 3.37), and 1,2,4,5-tetrasubstituted imidazoles **134** (Scheme 3.38) catalyzed by heteropoly 11-tungsto-1-vanadophosphoric acid (HPV) supported on activated natural clay for about 20% (HPVAC-20) in the absence of a solvent. Green reaction conditions, simple workup, short reaction times, high yields, and reusability of the catalyst were among the advantages of the proposed method.

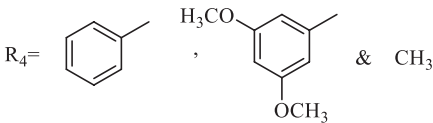




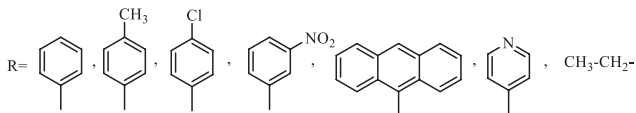
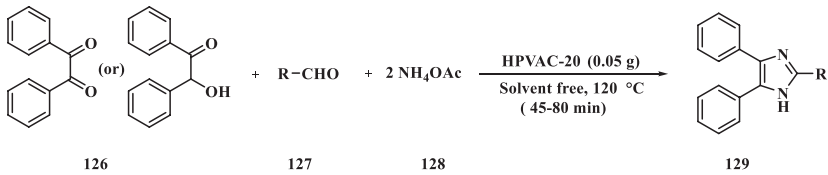
$R_1$  &  $R_3 = -\text{OCH}_3$

$R_3 = -\text{NO}_2$

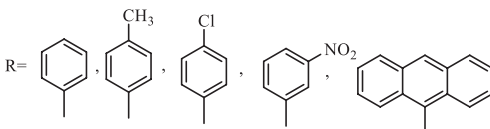
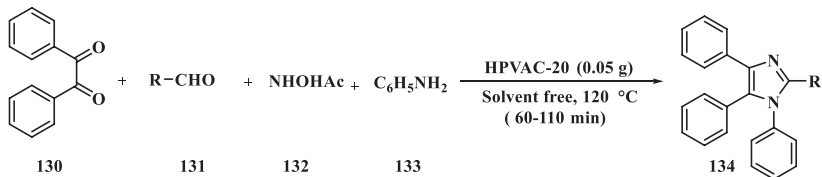
$R_2 = -\text{H}, -\text{Cl}, -\text{Br}, -\text{CH}_3$  &  $-\text{OCH}_3$



**SCHEME 3.36** Synthesis of *N, N'*-alkylidene bisamides in the presence of HPVAC-20 as a catalyst.

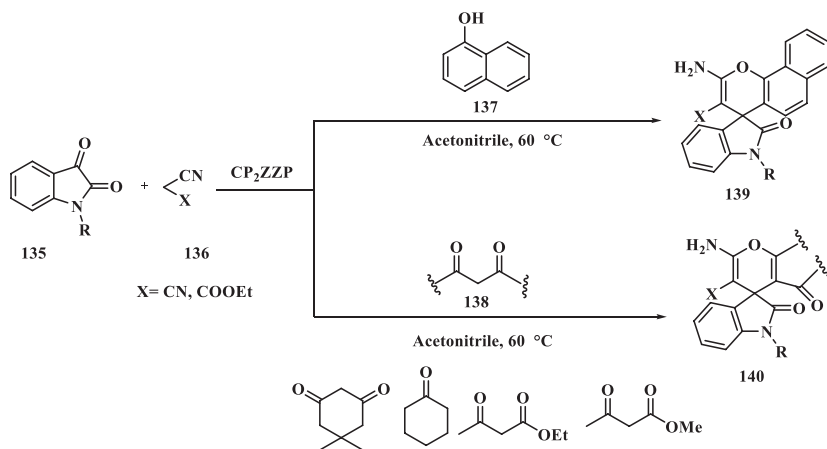


**SCHEME 3.37** Synthesis of 2,4,5-trisubstituted imidazoles in the presence of HPVAC-20 as a catalyst.



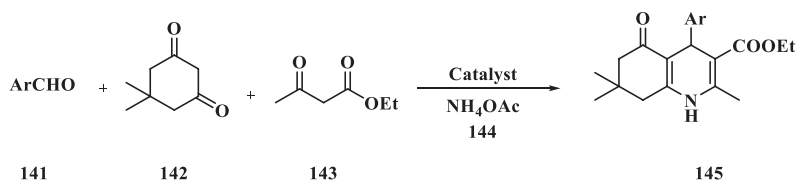
**SCHEME 3.38** Synthesis of 1,2,4,5-tetrasubstituted imidazoles in the presence of HPVAC-20 as a catalyst.

Pradhan and coworkers [40] prepared a layered  $\alpha$ -zirconium phosphate ( $\alpha$ -ZrP) by reflux with  $\text{ZrOCl}_2 \cdot 8\text{H}_2\text{O}$  and  $\text{H}_3\text{PO}_4$  as precursor. The  $\alpha$ -ZrP material was pillared with Zr-oxyhydroxy nanoclusters to afford the Zr-pillared  $\alpha$ -zirconium phosphate (ZZP). As a result of Zr-pillaring, improvements in the interlayer spacing, surface area, and porosity were observed. The cesium exchanged phosphotungstic acid ( $\text{Cs}_x\text{H}_{3-x}\text{PW}_{12}\text{O}_{40}$ ) nanoparticles were dispersed in the porous matrix of ZZP material to give a  $\text{Cs}_x\text{H}_{3-x}\text{PW}_{12}\text{O}_{40}$ -ZZP nanocomposite system. The resulted nanocomposites were characterized with various techniques such as XRD, FT-IR, UV-vis-DRS, XPS, TGA-DTA,  $\text{N}_2$  sorption, TPD, FESEM, and HRTEM. The expansion in layer structure of  $\alpha$ -ZrP upon pillaring and its subsequent retention in the composite material was observed from XRD. UV-vis and FT-IR examinations indicated the structural integrity of the  $\text{Cs}_x\text{H}_{3-x}\text{PW}_{12}\text{O}_{40}$  nanoclusters in the ZZP interlayer. The nanocomposite materials were employed as effective heterogeneous catalysts in the synthesis of spirooxindoles **139** and **140** via the one-pot, multicomponent condensation of isatin **135**, malononitrile **136**, and naphthol/1,3-diketones **137** and **138** (Scheme 3.39). Spirooxindole derivatives with structural diversity were synthesized with high yield and purity in short reaction times using the  $\text{Cs}_x\text{H}_{3-x}\text{PW}_{12}\text{O}_{40}$ -ZZP nanocomposites as a catalyst under moderate and mild conditions.



**SCHEME 3.39** One-pot, multicomponent synthesis of spirooxindoles catalyzed by  $\text{CP}_2$  ZZP.

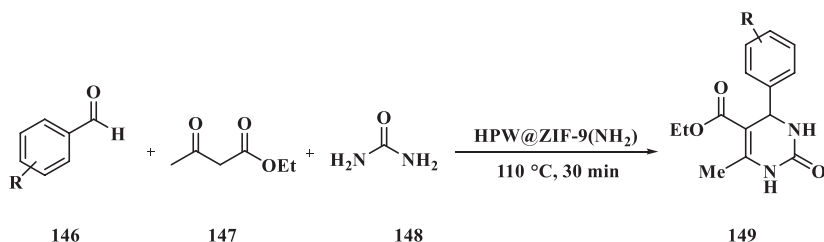
Sabaghian and others [41] prepared a novel magnetic acidic catalyst consisting of a Preyssler heteropoly acid ( $\text{H}_{14}[\text{NaP}_5\text{W}_{30}\text{O}_{110}]$ ) supported on silica-coated nickel zinc ferrite nanoparticles ( $\text{Ni}_{0.5}\text{Zn}_{0.5}\text{Fe}_2\text{O}_4 @ \text{SiO}_2$ ). The characterization of the catalyst was done by FT-IR, TEM, and particle size measurements. To investigate the catalytic activity of the prepared catalyst, the synthesis of polyhydroquinoline derivatives **145** via the Hantzsch reaction was chosen. The products were synthesized from the condensation of aldehydes **141**, dimed one **142**, ethyl acetoacetate **143**, ammonium acetate **144**, and catalyst in ethanol (Scheme 3.40).



**SCHEME 3.40** Synthesis of polyhydroquinolines using  $\text{Ni}_{0.5}\text{Zn}_{0.5}\text{Fe}_2\text{O}_4@\text{SiO}_2$  as a nano magnetic catalyst.

With the catalyst, the reactions progressed within less than 1 h in good to excellent yields. As a more important feature, the catalyst was readily separated from the workup mixture using an external magnet and reused for at least four runs without any loss in activity.

Tayebe and coworkers [42] supported phosphotungstic acid (HPW) on ZIF-9( $\text{NH}_2$ ) for the first time and used it as an efficient, green catalyst in the one-pot, three-component Biginelli condensation of a variety of substituted benzaldehydes **146** with ethyl acetoacetate **147** and urea **148** to give the related 3,4-dihydropyrimidin-2-(1H)-ones **149** under solvent-free conditions (Scheme 3.41). The structures of ZIF-9( $\text{NH}_2$ ) and the prepared nanocatalyst, i.e., HPW@ZIF-9( $\text{NH}_2$ ) were determined by FT-IR, XRD, TEM, BET, FESEM, AAS, TGA, EDX, and UV-vis. After the reaction was complete, the nanocatalyst was easily separated from the workup mixture using a centrifuge and the recovered catalyst was reusable for at least five runs with only 14% reduction in yield after the fifth run. The authors concluded that the ZIF-9( $\text{NH}_2$ ) can be utilized as a promising support for HPW to develop a highly active, nontoxic, stable, and reusable heterogeneous catalyst under easy reaction conditions in multicomponent organic syntheses.

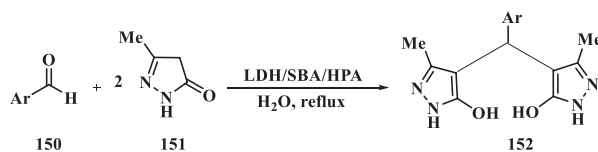


R = H, 4-Cl, 4- $\text{NO}_2$ , 3- $\text{NO}_2$ , 2,6-(Cl) $_2$ , 2-OH, 4-Me, 4-OMe

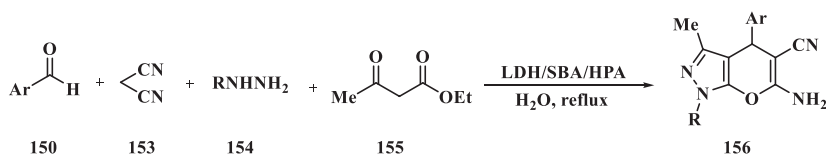
**SCHEME 3.41** Three-component condensation of ethyl acetoacetate, urea and different aldehydes in the presence of PTA@ZIF-9( $\text{NH}_2$ ) as a catalyst.

Sadjadi and coworkers [43] synthesized SBA/hydrotalcite/heteropoly acid nanocomposite using a novel method in which SBA-15 loaded with a heteropoly acid (HPA) was impregnated with calcined hydrotalcite (LDH). The resulting ternary hybrid system (SBA/LDH/HPA) was characterized using various techniques

such as FT-IR, XRD, BET, SEM/EDS, TPD, TGA, and ICP-AES. It was used as an efficient catalyst for the synthesis of 2,4-dihydro-3H-pyrazol-3-one derivatives via the reaction of aryl aldehydes and 5-methyl-1H-pyrazol-3(2H)-one under reflux condition. The catalytic activity of this catalyst was investigated for the development of 4,4'-alkylmethylene-bis(3-methyl-5-pyrazolones) **152** via the treatment of aldehyde **150** and 5-methyl-1H-pyrazol-3(2H)-one **151** in aqueous solution under reflux condition (Scheme 3.42). The authors also studied the catalytic activity of the novel catalyst in promotion of the four-component reaction of aromatic aldehydes **150**, malononitrile **153**, hydrazine hydrate/phenylhydrazine **154**, and ethylacetoacetate **155** for the synthesis of pyranopyrazoles **156** (Scheme 3.43). A few advantageous of the above procedure were cleaner reaction profiles, moderate reaction conditions, excellent product yields, wide substrate scope, recyclability of the catalyst, and easy operation. Notably, water has been considered as a green solvent for these reactions.



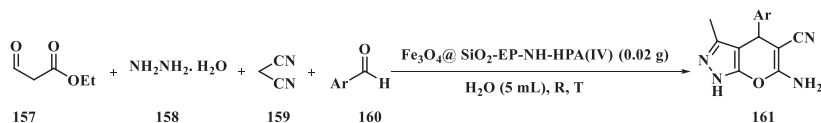
**SCHEME 3.42** Synthesis of 4,4'-alkylmethylene-bis(3-methyl-5-pyrazolones) derivatives in the presence of LDH/SBA/HPA as an efficient catalyst.



**SCHEME 3.43** Synthesis of pyranopyrazoles in the presence of LDH/SBA/HPA as an extremely effective catalyst.

Mohtasham et al. [44] prepared nanomesoporous silica from a medicinal plant, i.e., horsetail (*Equisetum arvense*) with a high surface area. They used this natural silica as a support to immobilize phosphotungstic acid on aminated epibromohydrin-functionalized Fe<sub>3</sub>O<sub>4</sub>@SiO<sub>2</sub> nanoparticles (Fe<sub>3</sub>O<sub>4</sub>@SiO<sub>2</sub>-EP-NH-HPA) as a highly powerful magnetic solid acid catalyst. The nanocatalyst was characterized by several different techniques such as XRD, FT-IR, N<sub>2</sub> adsorption-desorption, TEM, VSM, SEM-EDX, TGA, ICP-OES, and elemental analysis. This magnetic solid acid nanocatalyst was successfully used for the

one-pot, green synthesis of pyrano[2,3-*c*]pyrazole derivatives **161** in an aqueous medium at ambient temperature (Scheme 3.44). The procedure resulted in structurally different pyrano[2,3-*c*]pyrazoles in excellent yields in very low reaction times. In addition, the magnetic solid acid nanocatalyst could be readily recovered using an external magnetic field and reused for seven consecutive runs without any considerable loss in activity.

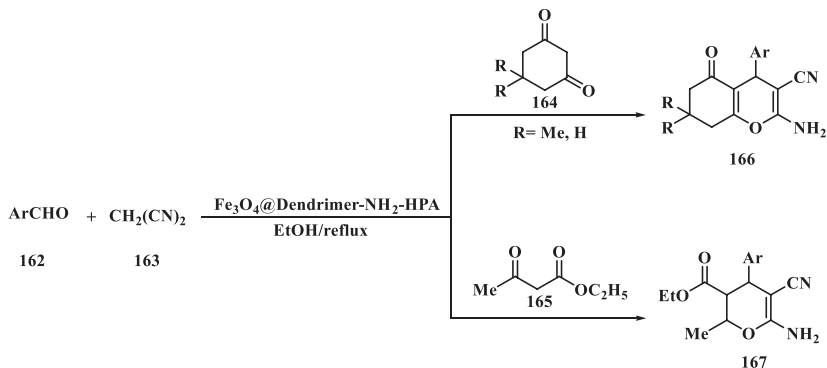


Ar = C<sub>6</sub>H<sub>5</sub>, 4-ClC<sub>6</sub>H<sub>4</sub>, 2-ClC<sub>6</sub>H<sub>4</sub>, 4-NO<sub>2</sub>C<sub>6</sub>H<sub>4</sub>, 3-NO<sub>2</sub>C<sub>6</sub>H<sub>4</sub>, 4-MeC<sub>6</sub>H<sub>4</sub>, 3-MeC<sub>6</sub>H<sub>4</sub>, 4-OHC<sub>6</sub>H<sub>4</sub>, 3-OHC<sub>6</sub>H<sub>4</sub>, 2-OHC<sub>6</sub>H<sub>4</sub>, 4-BrC<sub>6</sub>H<sub>4</sub>, 3-BrC<sub>6</sub>H<sub>4</sub>

**SCHEME 3.44** Synthesis of pyrano[2,3-*c*]pyrazole derivatives in the presence of Fe<sub>3</sub>O<sub>4</sub>@ SiO<sub>2</sub>-EP-NH-HPA(IV) as a catalyst.

Notably, the present study aimed to improve the catalytic properties of heteropoly acid using natural silica as a support to show the high performance of Fe<sub>3</sub>O<sub>4</sub>@SiO<sub>2</sub>-EP-NH-HPA as a reusable solid acid nanocatalyst that provided a green protocol for the synthesis of pyrano[2,3-*c*]pyrazole derivatives in short reaction times.

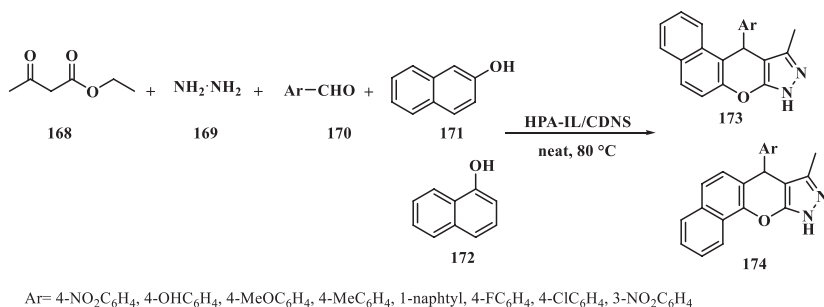
Jamshidi and coworkers [45] successfully prepared an environmentally friendly heteropoly acids-dendrimer functionalized magnetic nanoparticle (Fe<sub>3</sub>O<sub>4</sub>@D-NH<sub>2</sub>-HPA) and assessed it for the first time as a novel nanocatalyst efficient in the one-pot synthesis of highly substituted pyran derivatives **166** and **167** (Scheme 3.45). The prepared nano-magnetic catalyst was analyzed by FT-IR, TGA, powder XRD, scanning electron microscopy (SEM), and vibrating sample magnetometry (VSM). Furthermore, the catalyst could be easily recovered and reused without any appreciable loss in activity. Heterogeneous nature,



**SCHEME 3.45** One-pot synthesis of highly substituted pyran derivatives.

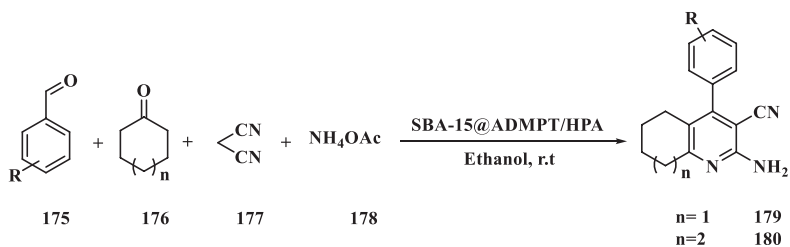
thermal stability, clean and simple procedure, excellent yields, short reaction time, easy product separation and purification, and low amount of catalyst were among the notable advantages of this procedure.

Sadjadi et al. [46] developed an efficient hybrid catalyst via immobilization of a Keggin-type heteropoly acid, i.e., phosphomolybdic acid, in the nanocavities of cyclodextrin nanosponges (CDNS) modified by an ionic liquid. The immobilized species was characterized by FT-IR, SEM/EDX, TGA, ICP-AES, and XRD. The activity of the hybrid catalyst was confirmed over the synthesis of benzochromenopyrazole derivatives **173** and **174** via the cascade reaction of ethyl acetoacetate **168**, hydrazine hydrate **169**, benzaldehyde **170**, and  $\alpha$ - or  $\beta$ -naphthols **171** and **172** (Scheme 3.46). The catalytic activity of the hybrid catalyst was compared to that of the bare ionic liquid-modified cyclodextrin nanosponges in order to determine the synergetic effects of the conjugation of heteropoly acid and ionic liquid. The results revealed the superior activity of the former, from different aspects. The catalyst was recoverable and reusable for several runs.



**SCHEME 3.46** Synthesis of benzochromeno-pyrazole derivatives in the presence of the hybrid catalyst.

Ghanbari and coworkers [47] prepared a novel inorganic/organic nanohybrid material SBA-15@triazine/H<sub>5</sub>PW<sub>10</sub>V<sub>2</sub>O<sub>40</sub> (SBA15@ADMPT/H<sub>5</sub>PW<sub>10</sub>V<sub>2</sub>O<sub>40</sub>) and used it as a green, efficient, and totally recyclable catalyst for the one-pot, multicomponent synthesis of multisubstituted pyridines **179** or **180** from the reaction of aldehydes **175**, cyclic ketones **176**, malononitrile **177**, and ammonium acetate **178** in satisfactory good to excellent yields (77%–97%) at room temperature in ethanol (Scheme 3.47). The mentioned catalyst was prepared by the chemical anchoring of Keggin heteropoly acid H<sub>5</sub>PW<sub>10</sub>V<sub>2</sub>O<sub>40</sub> onto the surface of SBA-15 mesoporous silica modified with 2-APTS-4,6-bis(3,5-dimethyl-1H-pyrazol-1-yl)-1,3,5-triazine (ADMPT) as a linker. Standard data such as FT-IR, SEM, TEM, XRD, BET, EDX, as well as DTA-TGA spectroscopy confirmed that the heteropoly acid H<sub>5</sub>PW<sub>10</sub>V<sub>2</sub>O<sub>40</sub> was well dispersed on the surface of the solid support and its structure was preserved after being immobilized on the SBA-15 mesoporous silica modified with ADMPT. Additionally, the

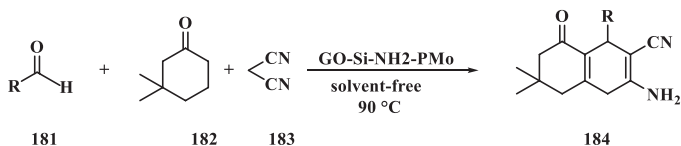


R = 4-Me, 4-OMe, 2,4-(Cl)<sub>2</sub>, 2-Cl, 4-NO<sub>2</sub>, 4-Cl, 4-Br, H, 2,3-(OMe)<sub>2</sub>

**SCHEME 3.47** Synthesis of 2-amino-3-cyanopyridine derivatives.

nanocatalyst was readily recoverable and reusable for five cycles without any significant loss of catalytic activity.

Ataie and coauthors [48] prepared a graphene oxide (GO) functionalized organic-inorganic hybrid via covalently immobilization of organic (3-aminopropyltrimethoxysilane) and inorganic (H<sub>3</sub>PMo<sub>12</sub>O<sub>40</sub>) groups on the basal plane of GO. The structure of this a new, green catalyst was characterized with various analytical methods such as FT-IR, TEM, SEM, EDS, XRD, WDX, and TGA. The activity of catalyst was tested over the synthesis of tetrahydrobenzo[*b*]pyran derivatives **184** in short reaction times, under solvent-free condition with good to excellent yields (Scheme 3.48).

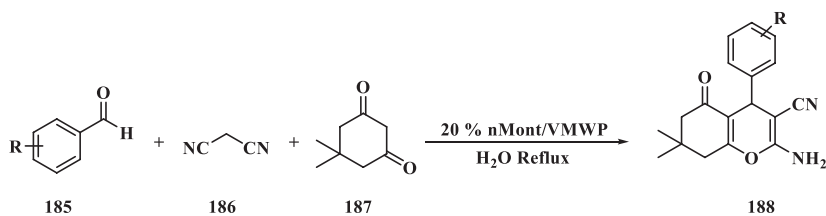


R = C<sub>6</sub>H<sub>5</sub>, 4-ClC<sub>6</sub>H<sub>4</sub>, 4-MeC<sub>6</sub>H<sub>4</sub>, 4-HOC<sub>6</sub>H<sub>4</sub>, 4-NO<sub>2</sub>, 3-BrC<sub>6</sub>H<sub>4</sub>, 2-ClC<sub>6</sub>H<sub>4</sub>, 2-CIC<sub>6</sub>H<sub>4</sub>, 2-NO<sub>2</sub>C<sub>6</sub>H<sub>4</sub>, 3-NO<sub>2</sub>C<sub>6</sub>H<sub>4</sub>

**SCHEME 3.48** Synthesis of tetrahydrobenzo[*b*]pyran derivatives in the presence of GO-Si-NH<sub>2</sub>-PMo.

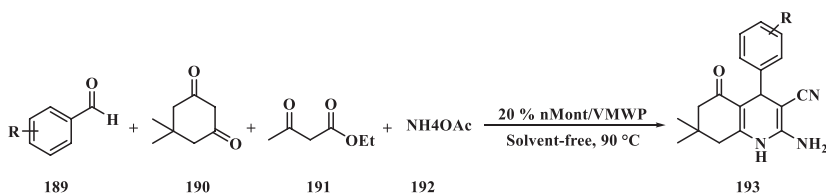
Aher et al. [49] synthesized an efficient and novel vanadium substituted molybdotungstophosphoric acid, H<sub>5</sub>PW<sub>6</sub>Mo<sub>4</sub>V<sub>2</sub>O<sub>40</sub>·14H<sub>2</sub>O (VMWP) supported on montmorillonite (nMont) clay via an incipient wetness impregnation technique. Inductively coupled plasma atomic emission spectroscopy (ICPAES), FT-IR, scanning electron microscopy (SEM), powder XRD, energy dispersive X-ray analysis (EDX), transmission electron microscopy (TEM), and thermogravimetric-differential thermal analysis (TG-DTA) were employed to characterize the support and the resulting catalyst. The authors showed that the newly synthesized VMWP well incorporated on nMont with good performance and activity. The catalytic usage was evaluated over a one-pot, multicomponent synthesis of tetrahydrobenzo[*b*]pyrans (4HPyran) **188** and polyhydroquinolines **193** in excellent yields (Schemes 3.49 and 3.50). High yields, shorter reaction





R= H, 4-Cl, 4-NO<sub>2</sub>, 4-Me, 3-Cl, 4-F, 2-OH, 4-Br, 3-NO<sub>2</sub>, 4-OH, 4-OMe

**SCHEME 3.49** The one-pot, three-component synthesis of tetrahydrobenzo[*b*]pyran derivatives.

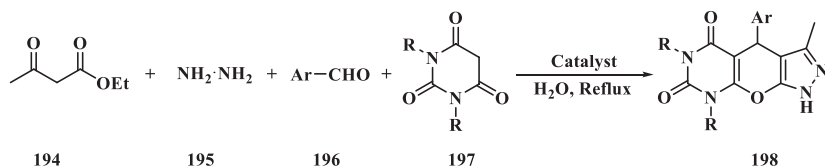


R= H, 4-Cl, 4-NO<sub>2</sub>, 4-OH, 4-OMe, 2-OH, 3-NO<sub>2</sub>, 4-CH<sub>3</sub>, 4-F, 4-Br, 3-Cl

**SCHEME 3.50** The one-pot, multicomponent synthesis of polyhydroquinoline.

times, use of a green solvent, easy experimental and work procedure, and re-usability of the catalyst were among the important features of the proposed synthetic route.

Sadjadi and coworkers [50] developed an efficient heterogeneous hybrid catalyst by functionalization of halloysite clay nanotubes by  $\gamma$ -aminopropyltriethoxysilane and then immobilization of a Keggin-type heteropoly acid, i.e., phosphotungstic acid. The developed hybrid catalyst was characterized by FT-IR, SEM/EDX, and XRD. Its catalytic activity for the synthesis of pyrazolopyranopyrimidine derivatives **198** via the four-component, domino reaction of ethyl acetoacetate **194**, hydrazine hydrate **195**, benzaldehyde **196**, and barbituric acid **197** was studied (Scheme 3.51). The results revealed that the hybrid catalyst was able to promote the reaction to give the desired products in short reaction times and high yields. The superior catalytic activity of this novel system was established in comparison



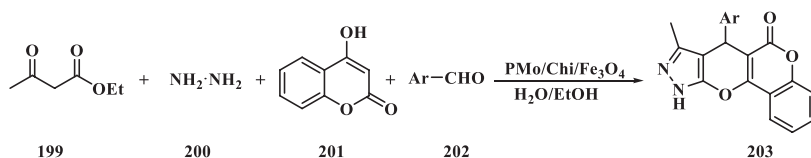
Ar= C<sub>6</sub>H<sub>5</sub>, 4-ClC<sub>6</sub>H<sub>4</sub>, 4-MeC<sub>6</sub>H<sub>4</sub>, 4-NO<sub>2</sub>C<sub>6</sub>H<sub>4</sub>, 3-NO<sub>2</sub>C<sub>6</sub>H<sub>4</sub>, 2-MeOC<sub>6</sub>H<sub>4</sub>

R= H, CH<sub>3</sub>

**SCHEME 3.51** Synthesis of pyrazolopyranopyrimidines.

with those of previously reported species. In addition, it was found to be readily separable and recyclable for at least three runs without any appreciable loss of activity. Notably, the protocol could be extended to nonconventional green heating sources such as microwave or ultrasonic irradiations.

Ayati et al. [51] reported a simple protocol for the preparation of pyranopyrazole derivatives **203** with high yields from the reaction of ethyl acetoacetate **199**, hydrazine hydrate **200**, 4-hydroxy coumarin **201**, and aldehydes **202** in the presence of PMo/Chit/Fe<sub>3</sub>O<sub>4</sub> (Scheme 3.52). In this regard, they prepared a novel nanocomposite consisting of H<sub>3</sub>PMo<sub>12</sub>O<sub>40</sub> immobilized on chitosan/Fe<sub>3</sub>O<sub>4</sub> (PMo/Chit/Fe<sub>3</sub>O<sub>4</sub>) via a facile one-pot synthetic approach. The method proved eco-friendly, with a simple isolation procedure.

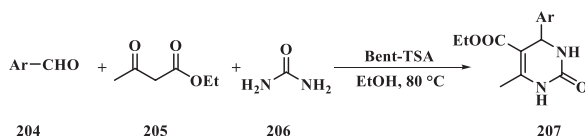


Ar = C<sub>6</sub>H<sub>5</sub>, 4-NO<sub>2</sub>C<sub>6</sub>H<sub>4</sub>, 4-MeC<sub>6</sub>H<sub>4</sub>, 4-OHC<sub>6</sub>H<sub>4</sub>, 3-NO<sub>2</sub>C<sub>6</sub>H<sub>4</sub>, 4-FC<sub>6</sub>H<sub>4</sub>, 1-naphthyl, 2-furyl

**SCHEME 3.52** Synthesis of pyranopyrazole derivatives.

Chopda and others [52] modified available bentonite using 12-tungstosilicic acid H<sub>4</sub>[SiW<sub>12</sub>O<sub>40</sub>] (TSA). The prepared catalysts (TSA/bent) were characterized using FT-IR, XRD, FESEM, and EDS. The catalytic activity of three samples (10%, 20%, and 30%) was investigated on the classical Biginelli reaction. Among all, the 30% sample displayed the highest catalytic activity and reusability. The solvent effect was also taken into account to find the best possible media for the reaction. The procedure was extended to a variety of aldehydes **204** for the synthesis of different dihydropyrimidones (DHPMs) **207** in high yields in ethanol (Scheme 3.53). Loss of activity was negligible after the fifth cycle.

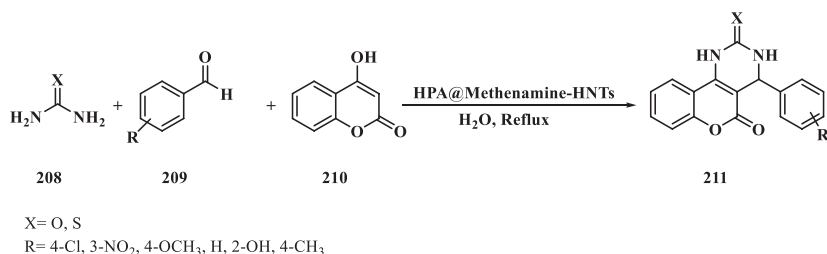
Sadjadi and coworkers [53] prepared a novel catalyst through functionalization of halloysite nanoclay (HNTs) with methenamine followed by incorporation of Keggin-type heteropoly acid (HPA). The catalyst was



Ar = 4-OHC<sub>6</sub>H<sub>4</sub>, 4-ClC<sub>6</sub>H<sub>4</sub>, 3ClC<sub>6</sub>H<sub>4</sub>, 4-MeOC<sub>6</sub>H<sub>4</sub>, 3,4-(OMe)<sub>2</sub>C<sub>6</sub>H<sub>3</sub>, 4-N(CH<sub>3</sub>)<sub>2</sub>C<sub>6</sub>H<sub>4</sub>, 4-NO<sub>2</sub>C<sub>6</sub>H<sub>4</sub>, 3-NO<sub>2</sub>C<sub>6</sub>H<sub>4</sub>, 4-BrC<sub>6</sub>H<sub>4</sub>, 4-FC<sub>6</sub>H<sub>4</sub>, 3-MeC<sub>6</sub>H<sub>4</sub>, 3-MeOC<sub>6</sub>H<sub>4</sub>, 2-furyl, 2-thienyl

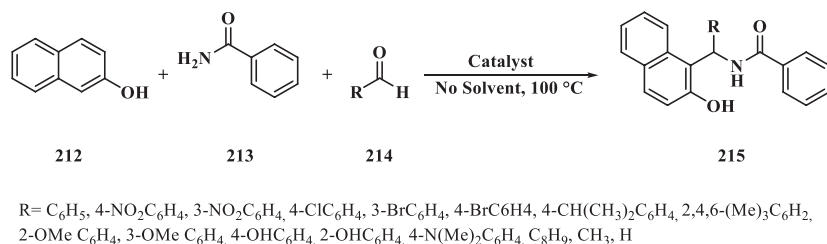
**SCHEME 3.53** Synthesis of dihydropyrimidones.

used to promote the synthesis of chromenopyrimidine-2,5-diones and thioxochromenopyrimidin-5-ones **211** via the one-pot reaction of urea/thiourea **208**, aldehydes **209**, and 4-hydroxycoumarin **210** under moderate reaction conditions (Scheme 3.54). The results established that the catalyst could effectively catalyze the reaction to afford the corresponding products in short reaction times and high yields. Furthermore, the catalyst was reusable up to three cycles with negligible heteropoly acid leaching. The comparison of the efficiency of the proposed protocol with those in the literature confirmed the merits of using this novel catalyst in terms of yield and heterogeneity of the catalyst.



**SCHEME 3.54** Synthesis of chromenopyrimidine-2,5-diones and thioxochromenopyrimidin-5-ones **4** via multicomponent reaction.

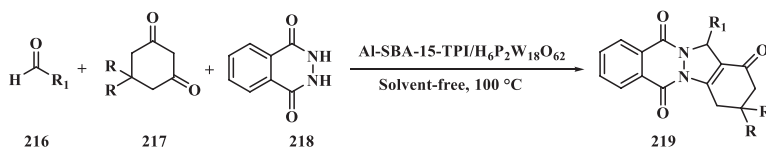
Tayebbe and coworkers [54] prepared a new inorganic/organic nanohybrid material H<sub>4</sub>SiW<sub>12</sub>O<sub>40</sub>/pyridino-MCM-41 and used it as an efficient, green, and extremely recyclable catalyst for the one-pot, multicomponent synthesis of different substituted 1-amidoalkyl-2-naphthols **215** with no solvent present (Scheme 3.55). The nanohybrid catalyst was provided by electrostatic anchoring of the Keggin heteropoly acid H<sub>4</sub>SiW<sub>12</sub>O<sub>40</sub> on the surface of MCM-41 nanoparticles modified by N-[3(triethoxysilyl)propyl]isonicotinamide. The prepared composite was characterized by FT-IR spectroscopy, XRD, SEM, EDX, DTA-TGA, DLS, and UV-vis, and the data confirmed that the heteropoly acid was well dispersed on the surface of the solid support and its structure was preserved after immobilization on the TPI-modified MCM-41 nanoparticles.



**SCHEME 3.55** Synthesis of different  $\alpha$ -amidoalkyl- $\beta$ -naphthol derivatives in the presence of HPA/TPI-MCM-41 under solvent-free conditions.

The recovered catalyst was easily recycled for at least seven runs without any significant loss of activity.

Tayebbe et al. [55] prepared a new inorganic/organic hybrid material Al-SBA-15-TPI/H<sub>6</sub>P<sub>2</sub>W<sub>18</sub>O<sub>62</sub> and fully characterized it using FT-IR, SEM, TGA-DTA, XRD, and UV-vis spectroscopic techniques. The prepared nanomaterial was then used as a simple, inexpensive, and reusable heterogeneous catalyst for the a one-pot, three-component synthesis of 2H-indazolo[2,1-*b*]phthalazine-1,6,11(13H)-trione derivatives **219** via the condensation of aromatic aldehydes **216**, cyclic diones **217**, and phthalhydrazide **218** under solvent-free conditions at 100°C in short times (Scheme 3.56). The method proved to be efficient and green with high yields and low reaction times, offering significant improvements in respect with the simplicity in operation and workup as well as the scope of transformation by avoiding expensive or corrosive catalysts.



R= H, Me

R<sub>1</sub>= Ph, 4-FC<sub>6</sub>H<sub>4</sub>, 2-OHC<sub>6</sub>H<sub>4</sub>, 3-NO<sub>2</sub>C<sub>6</sub>H<sub>4</sub>, 4-NO<sub>2</sub>C<sub>6</sub>H<sub>4</sub>, 2-ClC<sub>6</sub>H<sub>4</sub>, 4-ClC<sub>6</sub>H<sub>4</sub>, 2,6-Cl<sub>2</sub>C<sub>6</sub>H<sub>4</sub>, 2-OMeC<sub>6</sub>H<sub>4</sub>, 3-OMeC<sub>6</sub>H<sub>4</sub>, 3,4-(OMe)<sub>2</sub>C<sub>6</sub>H<sub>4</sub>, 3-BrC<sub>6</sub>H<sub>4</sub>, 4-BrC<sub>6</sub>H<sub>4</sub>, 4-isopropyl, 4-MeC<sub>6</sub>H<sub>4</sub>, (CH<sub>3</sub>)<sub>2</sub>CHCH<sub>2</sub>-, (CH<sub>3</sub>)<sub>2</sub>CH-, CH<sub>3</sub>-CH<sub>2</sub>-

**SCHEME 3.56** Synthesis of different phthalhydrazide-triones.

### 3.4. Oxidation

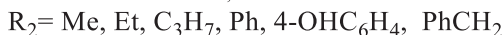
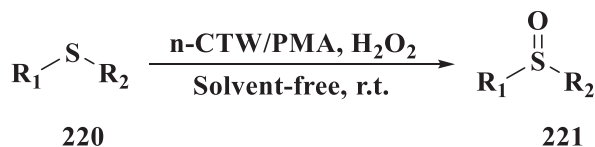
In general, oxidation is any chemical reaction that involves the moving of electrons. Specifically, it means the substance that gives away electrons is oxidized. Normally, this is a reaction between oxygen and a substance such as iron. IUPAC provides many other different definitions of oxidation: loss of electrons, increase in oxidation state, loss of hydrogen, or gain of oxygen. Most introductory or general chemistry textbooks use all of these definitions at one time or another.

Rožić et al. [56] established the correlation between the catalytic activity and selectivity of a series of catalysts with different loadings of tungsten heteropoly acids (HPW) over bentonite has been for vapor-phase oxidation of 2-propanol. The catalysts were characterized by various methods such as energy dispersive spectroscopy, ammonia temperature programmed desorption (NH<sub>3</sub>-TPD), differential scanning calorimeter, IR spectroscopy, and nitrogen adsorption/desorption. Energy dispersive spectroscopy results demonstrated good agreement regarding the chemical composition corresponding to the desired content of heteropoly acids on bentonite. Thermal analysis proved the thermal stability of catalysts under the investigated conditions of the oxidation reaction.

The NH<sub>3</sub>-TPD spectra revealed that each catalyst had two types of acidic sites: weak adsorption centers being active up to 390 K and a broad distribution of stronger acidic sites active at higher temperatures. The catalysts were active in the vapor-phase conversion of 2-propanol to acetone in the temperature interval of 343–553 K. An increase of in the heteropoly acid loading improved selectivity toward the formation of acetone.

The oxidation of 2-propanol over a bentonite support with no additive afforded propene and diisopropyl ether as organic derivatives, while reaction over the prepared catalysts created acetone as an additional organic product at temperatures over 425 K. Increasing the HPW content raised of acetone yield and selectivity, while lowering selectivity toward propene.

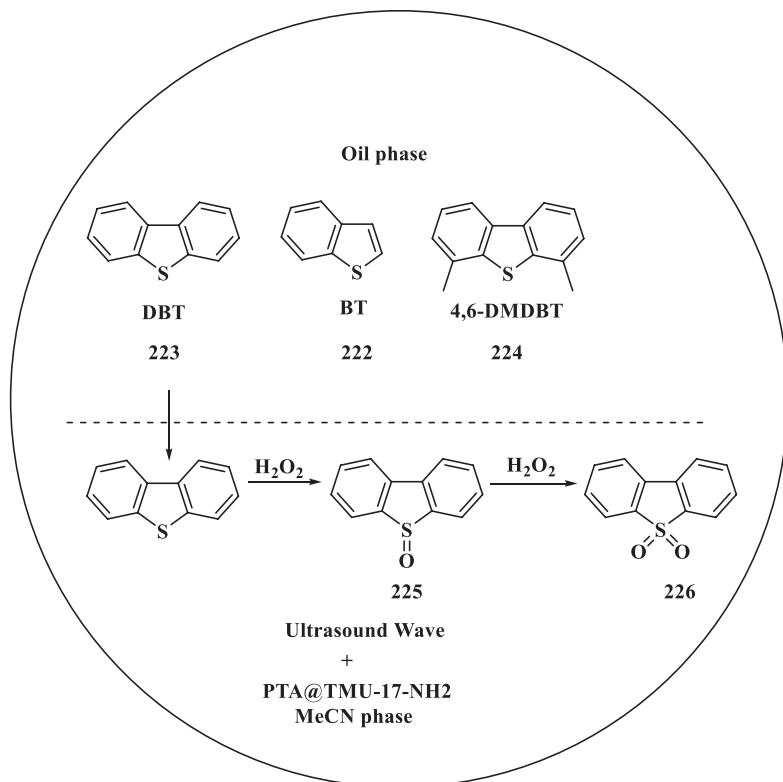
Zolfagarinia and others [57] used nano-ceramic tile wastes as nontoxic, inexpensive support materials to immobilize phosphomolybdic acid (PMA) in 1–20 wt% employing an impregnation method. The new active heterogeneous solid acid nanocatalyst, called nano-ceramic tile waste, supported phosphomolybdic acid. The resulted system (n-CTW/PMA) was well characterized using FT-IR, XRD, FE-SEM, EDX, and TGA methods. The activity of the prepared catalyst was over the chemoselective oxidation of sulfides **220** to sulfoxides **221** using 30% hydrogen peroxide as a green oxidant at ambient temperature with no solvent present (Scheme 3.57). The reaction conditions were optimized with central composite design as one of the most useful response surface methodologies. The results revealed that the catalyst with PMA loading of 11 wt% led to high yields (up to 97%). High activity and selectivity, low toxicity and cost, availability and stability, and recoverability and reusability for several runs were among significant advantages of this new catalyst.



**SCHEME 3.57** Nano-CTW/PMA catalyzed oxidation of sulfides to sulfoxides using H<sub>2</sub>O<sub>2</sub>.

Introducing PVMo into clay interlayer template in an acidic suspension with different contents of the heteropoly acid H<sub>4</sub>PMo<sub>11</sub>VO<sub>40</sub> (PVMo) using a sol-gel method, Boudjema's research group [58] synthesized mesoporous silica pillared clay (SPC) species (PVMo-SPC-SG). The characterization results revealed that PVMo was homogeneously dispersed within the encapsulated samples. The encapsulated species demonstrated good catalytic activity in the oxidation of cyclohexene. The PVMo-SPC-SG species with 20% of loading showed better catalytic activity for cyclohexene oxidation in comparison with the 10% counterparts.

Afzalnia and coworkers [59] performed the ultrasound-assisted oxidative desulfurization of liquid fuels using a novel heterogeneous highly dispersed Keggin-type  $\text{H}_3\text{PW}_{12}\text{O}_{40}$ , (HPW) catalyst encapsulated in an amino-functionalized MOF (HPW@TMU-17- $\text{NH}_2$ ). The prepared catalyst exhibited high activity and reusability in the oxidative desulfurization of the model fuel. Ultrasound-assisted oxidative desulfurization (UAOD) is a new method for rapid oxidation of sulfur-containing compounds, which is economic, green and safe, being performed under moderate conditions. Ultrasonic waves could be applied as an effective tool to lower the reaction time and improve the performance of the oxidative desulfurization system. PTA@TMU-17- $\text{NH}_2$  was able to improve the desulfurization of the model oil, and 20 mg of the catalyst, with the O/S molar ratio of 1:1 in the presence of MeCN as extraction solvent, was used. The results demonstrated that 98% conversion was achieved after 15 min in room temperature. Three refractory sulfur-containing compounds (benzothiophene, BT **222**, dibenzothiophene, DBT **223**, and 4,6-dimethyldibenzothiophene, 4,6-DMDBT **224**) were oxidized using hydrogen peroxide as an oxidizing agent. A schematic representation of the UAOD system is shown in Scheme 3.58.



**SCHEME 3.58** Schematic representation of the UAOD system.

Clean fuels with very low sulfur content are desirable due to environmental concerns. Lin et al. [60] employed three water-stable and green metal-organic frameworks with adjustable window diameters, denoted by MOF-808 $\times$ , as solid supports for phosphotungstic acid (HPW). An array of HPW@MOF-808 $\times$  composites was readily synthesized using an encapsulation protocol. With adjustable window diameters and tunable HPW loading amounts, the resultant HPW@MOF-808 $\times$  composites were screened for catalytic oxidative desulfurization with hydrogen peroxide as an oxidant. The authors found that HPW@MOF-808A with 42% loading had the highest catalytic activity and could completely remove the dibenzothiophene in a model fuel with an initial sulfur content of 1000 ppm in 30 min to put far below the acceptable limits for the fuel standards (10 ppm). More probing revealed that the high catalytic activity was attributable to the cooperative catalysis of metal clusters in the host framework and the guest HPW molecules. In addition, the 42% HPW@MOF-808A was readily recoverable and reusable for at least five cycles with negligible loss in activity. Therefore, the 42% HPW@MOF-808A, with features like high activity, eco-sustainability, high stability, and good recyclability, provided a new benchmark for catalytic oxidative desulfurization and a new perspective for ultra-deep desulfurization.

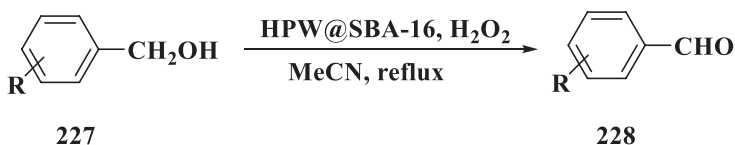
Zhang and others [61] supported heteropoly acid nanoparticles on cesium-modified macroporous SiO<sub>2</sub> with a three-dimensional order (3DOM) and used the composite as a catalyst for the oxidation of methacrolein to methacrylic acid. Hydrothermal treatment and incipient wetness impregnation were employed for the cesium-modification. It was revealed that hydrothermal cesium-modification of 3DOM SiO<sub>2</sub> promoted the dispersion of the supported heteropoly acid showing an average particle size of 5.2 nm, which was much smaller than that on the cesium-modified 3DOM SiO<sub>2</sub> prepared by incipient wetness impregnation (i.e., 17.6 nm). The authors explored the effects of the hydrothermal treatment on the structure and activity of the catalyst. The results revealed that the ion exchange between the cesium ion and the surface silanol groups on the 3DOM SiO<sub>2</sub> was enhanced as the hydrothermal temperature increased. In addition, cesium-modification helped the heteropoly acid preserve its Keggin structure, preventing it from forming MoO<sub>3</sub> so that the MoO<sub>3</sub> phase was decreased and totally disappeared with the hydrothermal temperature increasing from 90°C to 150°C. The effect significantly improved the performance of the supported catalyst.

Li and others [62] obtained a kind of composite catalytic material, i.e., metal-POM@MOF-199@MCM-41 (Metal-PMM), by confining MOF-199 encapsulating metallic Keggin POM into mesoporous MCM-41. The catalyst was used in an oxidative desulfurization process. The catalyst structures were determined by XRD, IR, XPS, N<sub>2</sub> adsorption-desorption, SEM, and TEM. The reaction was extensively enhanced, up to 99.1%, in the presence of the Co-PMM as a catalyst and O<sub>2</sub> as an oxidant. After the reaction was complete, the catalyst could be easily recovered and reused more than five runs without any significant change in its structure due to the strongly fixation of MOF-199 and MCM-41 to



metallic modified Keggin polyoxometalates. The kinetic investigations revealed that the oxidation desulfurization of dibenzothiophene was a pseudo-first-order reaction with an activation energy of 45.6 kJ/mol.

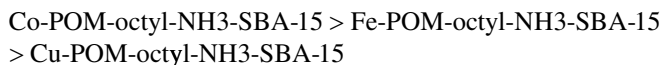
Masteri-Farahani and coworkers [63] encapsulated a Wells-Dawson type 18-tungstophosphoric acid (i.e.,  $H_6P_2W_{18}O_{62}$ ) as a guest inside the nanocages of mesoporous SBA-16 as a host. The pore entrance of the SBA-16 material was modified by silylating reagent to prevent the escape of encapsulated  $H_6P_2W_{18}O_{62}$  (HPW) from the nanocages. A variety of physicochemical techniques such as XRD and transmission electron microscopy were applied to characterize the prepared host-guest system. The results indicated the retention of the mesoporous structure of SBA-16 and good dispersion of the  $H_6P_2W_{18}O_{62}$  into the nanocages of SBA-16. The obtained catalyst demonstrated high activity, stability, and recyclability in the epoxidation of olefins and oxidation of alcohols **227** in the presence of hydrogen peroxide as oxidant (Scheme 3.59).



R= H, 4-NO<sub>2</sub>, 2-NO<sub>2</sub>, 4-OMe, 2-OMe, 4-Cl, 2-Cl, 4-Br

**SCHEME 3.59** Benzylic alcohols oxidation with hydrogen peroxide catalyzed by HPW@SBA-16.

Jin and coauthors [64] synthesized a series of Keggin-type heterogeneous catalysts with heteropoly acids (Co-/Fe-/Cu-POM-octyl NH<sub>3</sub>-SBA-15) via immobilization of a phosphotungstic acid mono-substituted by a transition metal (Co-/Fe-/Cu-POM) on octyl-amino-co-functionalized mesoporous silica SBA-15 (octyl-NH<sub>2</sub>-SBA-15). Analytical results revealed that the Co-/Fe-/Cu-POM units were highly dispersed in mesochannels of SBA-15, and both types of Brønsted and Lewis acid sites existed in Co-/Fe-/Cu-POM-octyl-NH<sub>3</sub>-SBA-15 catalysts. The Co-POM-octyl-NH<sub>3</sub>-SBA-15 catalyst demonstrated excellent catalytic activity in H<sub>2</sub>O<sub>2</sub>-mediated cyclohexene epoxidation with 83.8% of cyclohexene conversion, 92.8% of cyclohexene oxide selectivity, and 98:2 of epoxidation: allylic oxidation selectivity. The order of catalytic activity was as follows:



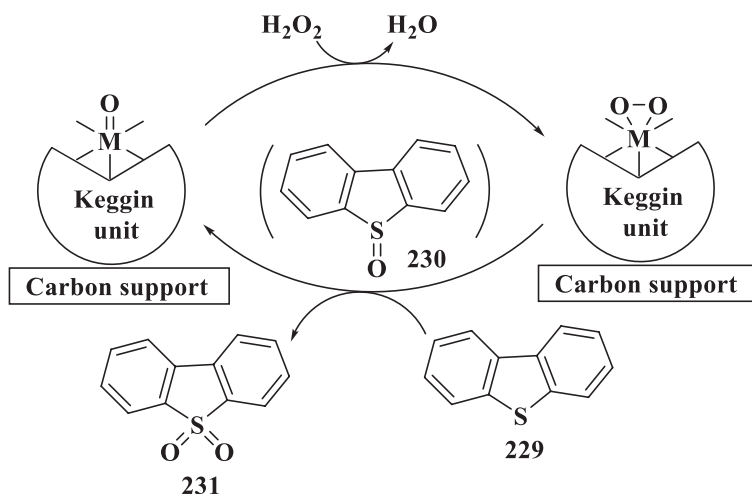
To specify the role of the -octyl moieties during the catalysis, an octyl-free catalyst (Co-POM-NH<sub>3</sub>-SBA-15) was also synthesized. Compared with Co-POM-NH<sub>3</sub>-SBA-15, the Co-POM-octyl-NH<sub>3</sub>-SBA-15 species showed improved catalytic properties (i.e., activity and selectivity) in the epoxidation of

cyclohexene. Strong chemical bonding between the  $-\text{NH}_3^+$  groups anchored on the surface of SBA-15 and heteropolyanions led to the excellent stability of the Co-POM-octyl- $\text{NH}_3$ -SBA-15 catalyst. In addition, it could be reused for six runs without any appreciable loss in activity.

Keggin-type heteropoly acids supported on activated carbon (HPA/C) are active catalysts for oxidative desulfurization (ODS) of diesel fuel under mild conditions in a biphasic system composed of a benzothiophene-containing model diesel fuel (heptane) and aqueous 30% hydrogen peroxide. The catalytic activity of HPA/C was found to decrease in the order of HPA:  $\text{H}_3\text{PMo}_{12}\text{O}_{40} > \text{H}_3\text{PW}_{12}\text{O}_{40} > \text{H}_4\text{SiW}_{12}\text{O}_{40}$ . The most active catalyst,  $\text{H}_3\text{PMo}_{12}\text{O}_{40}/\text{C}$ , exhibited 100% removal of benzothiophenes from model diesel fuel at  $60^\circ\text{C}$ , and could be recovered and reused without loss of activity. This catalyst outperforms other recently reported heterogeneous catalysts for ODS in similar systems. Kinetic and DRIFTS studies provide new insights into the mechanism of ODS reaction on carbon-supported HPAs.

Ghubayra et al. [65] investigated the heterogeneous catalysis of the biphasic oxidative desulfurization of a benzothiophene-containing model diesel fuel (heptane) by aqueous 30% hydrogen peroxide in the presence of Keggin-type heteropoly acids ( $\text{H}_3\text{PMo}_{12}\text{O}_{40}$ ,  $\text{H}_3\text{PW}_{12}\text{O}_{40}$ , and  $\text{H}_4\text{SiW}_{12}\text{O}_{40}$ ) supported on activated carbon (HPA/C) (Scheme 3.60). The catalyst proved to be relatively efficient, showing higher activity for the oxidation of benzothiophenes compared to other recently reported heterogeneous catalysts in similar systems. Strong adsorption of  $\text{H}_3\text{PMo}_{12}\text{O}_{40}$  onto the carbon support stabilized the heteropoly acid structure and prevented the heteropoly acid from leaching.

Hydrogen peroxide is usually used as an oxidizing agent in oxidative desulfurization. However, an excess of hydrogen peroxide would be added into the

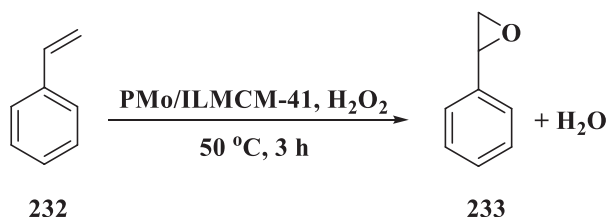


**SCHEME 3.60** Oxidation of DBT by  $\text{H}_2\text{O}_2$  catalyzed by HPA/C (M=MoVI or WVI).

oxidative system to reach a high level of sulfur removal. Xiong et al. [66] immobilized the phosphomolybdic acid on an imidazole-based ionic liquid modified mesoporous SBA-15 (HPMo-IL/SBA-15) to catalyze the mentioned oxidative system. The prepared species combined the merits of  $\text{H}_3\text{PMo}_{12}\text{O}_{40}$  (HPMo) and SBA-15 so that the high special surface area of the SBA-15 could effectively disperse HPMo active species. The results revealed that HPMo could be steadily immobilized on the SBA-15 using an imidazole-based ionic liquid. Meanwhile, after the introduction of imidazole-based ionic liquid, the HPMo-IL/SBA-15 species demonstrated hydrophobic performance. The experiment showed that the hydrophobic catalyst was highly active in oxidative desulfurization. When hydrogen peroxide with a stoichiometric ratio (hydrogen peroxide/sulfur mole ratio being 2) was used, the removal of dibenzothiophene could exceed 90%, at 60°C within 90 min. When hydrogen peroxide was slightly increased (hydrogen peroxide/sulfur mole ratio was increased from 2 to 2.5), the sulfur removal reached 100% within 40 min. Notably, the catalyst was able to adsorb the oxidation product of dibenzothiophene, i.e., dibenzothiophene sulfone. From this point of view, HPMo-IL/SBA-15 served not only as a high-efficiency catalyst but also as an adsorbent.

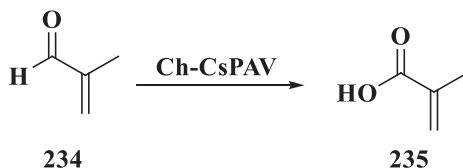
Wang and others [67] selectively oxidized styrene **232** to 1,2-epoxyethylbenzene **233** using hydrogen peroxide as an oxidizing agent (Scheme 3.61). The reaction was catalyzed by phosphomolybdic acid supported on a modified ionic liquid MCM-41. The prepared catalyst was characterized by FT-IR, XRD, and  $\text{N}_2$  adsorption-desorption. The results revealed that the sample retained its mesoporous structure after modification by the ionic liquid and immobilization of phosphomolybdic acid. A maximum activity was observed at phosphomolybdic acid loading of 30% on an ionic liquid modified MCM-41. The reaction parameters such as reaction time, temperature, catalyst amount, and hydrogen peroxide/styrene molar ratio were systematically optimized to afford a maximum conversion of 95.4%. Selectivity of 90.2% for 1,2-epoxyethylbenzene was acquired when the reaction parameters were set to 3 h reaction time, 100 mg catalyst, 50°C, and a hydrogen peroxide/styrene molar ratio of 1.2. The heterogeneous catalyst was easily separated by centrifugation and reused without any considerable deactivation after six runs.

Cao and coworkers [68] prepared a series of Chitin-C $\text{sH}_3\text{PMo}_{11}\text{VO}_{40}$  (Ch-C $\text{sPAV}$ ) hybrids with an easy, one-pot approach. The resulted species were



**SCHEME 3.61** Oxidation of styrene in the presence of PMo/ILMCM-41.

characterized by FT-IR, SEM, XRD, TG/DTA,  $\text{NH}_3$ -TPD, NMR, and XPS. The performance of Ch-CsPAV as a catalyst was studied over the oxidative transformation of methacrolein **234** to methacrylic acid **235** (Scheme 3.62). It was revealed that both acidity and redox property of the precursor (CsPAV) could be adjusted when introducing chitin as a component. In particular, the prepared Ch-CsPAV with uniform microspheres had higher amount of acidic sites, better redox active sites ( $\text{VO}^{2+}$ ), and improved agent ( $\text{NH}_4^+$ ). The result was an improved catalytic performance in the reaction. Under the optimized conditions, higher methacrolein conversion (80%) and methacrylic acid selectivity (94%) were achieved in the presence of Ch-CsPAV. The introduction of chitin into the CsPAV could enhance the acidity of the hybrid compounds due to the formation of  $\text{NH}_4^+$  during the calcination by  $\text{NH}_3$ -TPD analysis. After the calcination, the relative ratio of  $\text{V}^{4+}/\text{V}^{5+}$  and the proportion of double-bonded/terminal oxygen ( $\text{O}_i$ ) was increased upon the introduction of chitin. The higher methacrolein conversion (80%) and methacrylic acid selectivity (94%) for Ch-CsPAV were acquired by comparison with CsPAV. Moreover, the catalyst exhibited good stability.



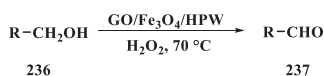
**SCHEME 3.62** Oxidation of MAL to MAA in the presence of the calcined Ch-CsPAV.

In order to resolve the diffusion limitation of zeolite-based catalysts in oxidizing large-size organosulfur compounds in real petroleum feedstock, Vedachalam and others [69] developed a series of oxidative desulfurization (ODS) catalysts based on mesoporous TUD-1 as a support. Different mesoporous oxidation catalysts were formed by substituting titanium in the TUD-1 framework and impregnating a molybdenum heteropoly acid (Keggin) on the TUD-1 support. The mesoporosity of TUD-1 and the presence of Ti(IV) and Mo Keggin units in the prepared catalysts were established based on the results from XRD, XPS, XANES, and BET- $\text{N}_2$ . The performance of the catalysts in oxidative desulfurization was examined using a mild hydrotreated bitumen derived from heavy gas oil feedstock. The heteropoly acid dispersed in the Ti-TUD-1 catalyst was revealed to be most active for desulfurizing the heavy gas oil feedstock due to a strong synergy effect of titanium and molybdenum Keggin ions on catalyzing oxygen transfer from an oxidizing agent to a substrate. Oxidizing agent such as cumene hydroperoxide, hydrogen peroxide, *tert*-butyl hydroperoxide, and molecular oxygen ( $\text{O}_2$ ) were screened. The first two oxidizing agent were found to be better than others and equally efficient. The HPA/Ti-TUD-1 catalyst was suitable for oxidative desulfurization and oxidative denitrogenation

(ODN) both in a batch stirred tank reactor and continuous fixed-bed reactor systems. The use of methanol instead of acetonitrile and dimethylformamide was proved to be more cost-effective for the extraction of the oxidized sulfur and nitrogen compounds of the heavy gas oil.

Gao et al. [70] designed a new type of supported catalyst and prepared it by three different methods with a polyoxometalate ( $\text{H}_8\text{P}_2\text{Mo}_{16}\text{V}_2\text{O}_{62}\cdot\text{mH}_2\text{O}$ ) as an active component, modified MOF-199 as a support. The catalytic performance of all samples was investigated. The conditions were optimized and the reusability was explored. In addition, in order to analyze and confirm the accuracy of the results, the response surface design was applied. The structures of the final products were characterized using several techniques, e.g., elemental analysis, XRD, IR, and SEM. Then, the catalysts were tested for the model fuel desulfurization under certain conditions. The results revealed that the catalyst synthesized by the one-pot method was the best in desulfurization, which in turn proved that the heteropoly acid played a significant role in the desulfurization process. The effects of four main parameters on the rate of desulfurization were also studied to obtain the optimum conditions. The thiophene could be totally removed with the catalyst CNTs@MOF-199- $\text{Mo}_{16}\text{V}_2$  (O) under the optimized conditions. When the catalyst was reused for the ninth run, the desulfurization rate could still reach 85.12%.

Darvishi and coworkers [71] prepared graphene oxide- $\text{Fe}_3\text{O}_4\text{-NH}_3^+$   $\text{H}_2\text{PW}_{12}\text{O}_{40}^-$  magnetic nanocomposite (GO/ $\text{Fe}_3\text{O}_4$ /HPW) by linking amino-functionalized  $\text{Fe}_3\text{O}_4$  nanoparticles ( $\text{Fe}_3\text{O}_4\text{-NH}_2$ ) on the graphene oxide (GO), and then grafting  $\text{H}_3\text{PW}_{12}\text{O}_{40}$  (HPW) on the graphene oxide-magnetite hybrid (GO- $\text{Fe}_3\text{O}_4\text{-NH}_2$ ). The acquired GO/ $\text{Fe}_3\text{O}_4$ /HPW nanocomposite was characterized with FT-IR, TEM, SEM, EDX, TGA-DTA, XRD, AGFM, ICP, and BET. The applied techniques revealed that the graphene oxide layers were prepared and the various stages of preparation of the GO/ $\text{Fe}_3\text{O}_4$ /HPW nanocomposites were successfully completed. The new nanocomposite exhibited excellent activity as a heterogeneous catalyst in the oxidation of alcohols **236** with hydrogen peroxide (Scheme 3.63). The prepared GO/ $\text{Fe}_3\text{O}_4$ /HPW catalyst was more stable. It was recyclable for at least five runs without any significant decrease in its catalytic activity. In this catalytic system, graphene oxide sheets were used as a suitable support as they had appropriate properties such as good chemical stability, high surface area, sufficient thermal and mechanical stability, as well as the presence of favorable functional groups to form covalent bonds with other catalyst components.



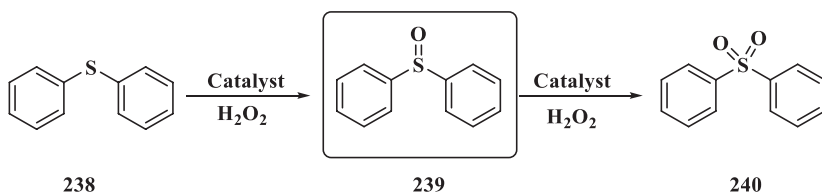
R = Ph, 4-OMeC<sub>6</sub>H<sub>4</sub>, 4-ClC<sub>6</sub>H<sub>4</sub>, 2,4-(Cl)<sub>2</sub>C<sub>6</sub>H<sub>3</sub>, 2-NO<sub>2</sub>C<sub>6</sub>H<sub>4</sub>, 4-NO<sub>2</sub>C<sub>6</sub>H<sub>4</sub>, 2-OHC<sub>6</sub>H<sub>4</sub>, 4-CH<sub>2</sub>OHC<sub>6</sub>H<sub>4</sub>, PhCH<sub>2</sub>, PhCH<sub>2</sub>CH<sub>2</sub>, PhCHCH<sub>3</sub>, PhCHC<sub>2</sub>H<sub>5</sub>

**SCHEME 3.63** The selective oxidation of alcohols with hydrogen peroxide in the presence of GO/ $\text{Fe}_3\text{O}_4$ /HPW.

Huang and coworkers [72] successfully prepared layered double hydroxides (LDHs) modified with sodium dodecyl benzene sulfonate (SDBS) and used them as catalysts in oxidative desulfurization processes. Characterization of the layered double hydroxide samples revealed that modification with sodium dodecyl benzene sulfonate could enhance the hydrophilic and lipophilic properties of the layered double hydroxides due to its amphiphilicity. In comparison with the MgAl-LDH itself, the sodium dodecyl benzene sulfonate modified MgAl-LDH-SDBS samples demonstrated significant differences in surface area, morphology, and pore volume. After immobilizing  $\text{H}_3\text{PW}_{12}\text{O}_{40}$  (HPW), the desulfurization activity was significantly increased in comparison with that of the HPW/MgAl-LDH catalyst. Under the optimized conditions, the desulfurization rate of the catalyst reached 99.81%. In addition, the desulfurization still remained over 95% after 15 runs. This high catalytic activity and recyclability was ascribed to the enhancement of the surface area, hydrophilicity, and oleophilicity of the layered double hydroxides.

Wang and others [73] prepared an effective catalyst for the direct hydroxylation of benzene to phenol using hydrogen peroxide through anchoring  $\text{H}_5\text{PMo}_{10}\text{V}_2\text{O}_{40}$  ( $\text{PMoV}_2$ ) by the hydroxyl groups of titania nanotubes (TNT) via electrostatic interactions between the Keggin unit of  $\text{PMoV}_2$  and the hydroxyl groups. The FT-IR, solid-state  $^{31}\text{P}$  NMR, XRD, X-ray photoelectron spectroscopy (XPS), and thermogravimetric analysis (TGA) results revealed that  $\text{PMoV}_2$  was immobilized on the surface of titania nanotubes via electrostatic interactions. In order to characterize the textural and morphology of the  $\text{PMoV}_2$ /titania nanotubes,  $\text{N}_2$  adsorption-desorption, scanning electronic micrograph (SEM), and transmission electron microscopy (TEM) were employed. The  $\text{PMoV}_2$ /titania nanotubes exhibited excellent catalytic activity in benzene hydroxylation with 27.3% conversion of benzene and 99.1% selectivity toward phenol. The contact angle and adsorption experiments results revealed that the excellent catalytic performance could be ascribed to the confinement effect of titania nanotubes with the nanotube structure and hydrophobic microenvironment that efficiently dispersed  $\text{PMoV}_2$  and concentrated the reactants, while decreasing the intrinsic mass transfer resistance. The anchoring effect of hydroxyl groups stabilized and inhibited the leak of  $\text{PMoV}_2$ , resulting in good recyclability of the catalyst with negligible loss of catalytic efficiency after six runs.

Migliorero's research group [74] synthesized a new niobium-containing phosphomolybdic acid (PNbMo). Using a sol-gel technique, they included the heteropoly acid in silica, alumina, and silica/alumina matrices to use it as a heterogeneous catalyst. The matrices granted stability to the active phase, as well as good textural and morphological properties. PNbMo and the included materials were analyzed by FT-IR,  $^{31}\text{P}$  NMR, UV-vis, TGA, TEM, SEM, XRD,  $\text{N}_2$  physisorption, and potentiometric titration, and tested as a catalyst in the sulfoxidation of diphenyl sulfide **238** in aqueous hydrogen peroxide as an oxidant and ethanol as a solvent at 25°C (Scheme 3.64). The redox activity was compared with that of phosphomolybdic acid and correlated with the edge energy obtained from UV-vis

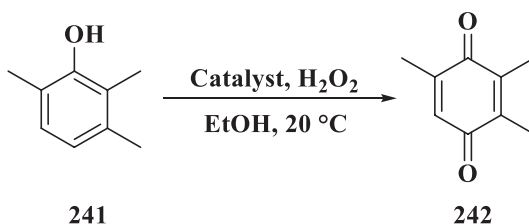


**SCHEME 3.64** Selective oxidation of diphenyl sulfide.

data. The best results in the sulfoxidation of diphenyl sulfide were acquired with PNbMo-SiAl-4:1 (92% conversion and 95% selectivity at 3 h) and with PNbMo-Si (92% conversion and 94% selectivity at 4 h). The reusability of these catalysts was assessed and only a slight decrease in the conversion was observed.

Han et al. [75] prepared several organic/inorganic composite catalysts by modifying  $\text{H}_3\text{PW}_{12}\text{O}_{40}$  with different amino acids such as alanine (Ala), phenylalanine (Phe), and glycine (Gly). The physical, chemical and acidic properties of the  $(\text{MH})_x\text{H}_{3-x}\text{PW}_{12}\text{O}_{40}$  species ( $\text{M}=\text{Phe}, \text{Ala}, \text{and Gly}; x=1-3$ ) were determined by various techniques such as FT-IR, TGA, XRD, XPS, and NMR. The species were used as heterogeneous catalysts in selective oxidation of benzyl alcohol with hydrogen peroxide. Among them,  $[\text{PheH}]\text{H}_2\text{PW}_{12}\text{O}_{40}$  demonstrated the best oxidative activity with an excellent benzyl alcohol conversion of 99.0% and benzaldehyde selectivity of 99.6%. More kinetic examinations and model analysis by response surface methodology revealed that the oxidation of benzyl alcohol with hydrogen peroxide followed a second-order reaction with an activation energy of  $56.7 \text{ kJ}\cdot\text{mol}^{-1}$  under optimal conditions.

Palacio and coworkers [76] synthesized novel catalysts containing phosphomolybdic acid (PMA) and vanadophosphomolybdic acid (VPMA) in a titania matrix by the sol-gel process with different loads of heteropoly acid (i.e., 5%, 15%, and 30% (w/w): 5PMA-TiO<sub>2</sub>, 15PMA-TiO<sub>2</sub>, 30PMA-TiO<sub>2</sub>, 5VPMA-TiO<sub>2</sub>, 15VPMA-TiO<sub>2</sub>, and 30VPMA-TiO<sub>2</sub>). Various techniques, e.g., XRD, DRS, SEM, FT-IR, <sup>31</sup>P MAS-NMR, potentiometric titration with n-butylamine, and N<sub>2</sub> physisorption at  $-196^\circ\text{C}$ , were used to characterize the mentioned species. Then they were used as heterogeneous catalysts in the oxidation of 2,3,6-trimethylphenol **241** to 2,3,5-trimethyl-p-benzoquinone **242**, which is a key intermediate in the synthesis of vitamin E (Scheme 3.65). The catalysts allowed a green synthesis of 2,3,5-trimethyl-p-benzoquinone



**SCHEME 3.65** Oxidation of 2,3,6-trimethylphenol to 2,3,5-trimethyl-p-benzoquinone.



with ethanol as solvent and aqueous hydrogen peroxide as a clean oxidant, at ambient temperature. The conversion of 2,3,6-trimethylphenol reached 90% and 99% for the samples with 15PMA-TiO<sub>2</sub> and 15VPMA-TiO<sub>2</sub>, respectively, after 4 h. The amounts of Mo and V in the reaction medium were determined by ICP-MS, which exhibited a leaching extent of only 17%–18% of molybdenum. However, the extent was 48% for vanadium. Reusability of the catalysts was also evaluated. For 15PMA-TiO<sub>2</sub>, the conversion was preserved in the second run. A homolytic mechanism was proposed for this synthesis, which involved the formation of a peroxometallic species via an HPA-Ti center.

Li et al. [77] tried three different methods to synthesize a new type of inorganic/organic hybrid catalyst (HPMo@MOF@CA) used inoxidative desulfurization by the composition of the heteropoly acid H<sub>3</sub>PMo<sub>6</sub>W<sub>6</sub>O<sub>40</sub>·nH<sub>2</sub>O (HPMo), MOF-199 and cellulose acetate (CA). The structure features of the catalyst were characterized using XRD, IR, XPS, N<sub>2</sub> adsorption-desorption, and SEM. The impregnation method was found to be the best preparation method and considered as a possibility for the catalyst manufacture in industrial application. The best loading of the heteropoly acid and optimized conditions for desulfurization were also explored while the removal efficiency reached 99.23% with O<sub>2</sub> as an oxidizing agent at 40°C within 3 h. The catalyst was easily recoverable and reusable for 10 cycles without any considerable degradation in the desulfurization rate. The authors believed that the HPMo@MOF@CA, as a novel catalyst, was highly active for thiophene, having the potential to be used in industry.

Yuan and others [78] prepared vanadium-substituted polymolybdenum phosphoric acid (PV<sub>x</sub>Mo) supported on mesoporous silica and studied it as a catalyst for the oxidation of glycerol to formic acid in a batch operation. Different synthetic methods for PV<sub>x</sub>Mo supported on mesoporous silica were compared.

The final products were characterized in detail by FT-IR, SEM, XRD, ICP-OES, HR-TEM, XANES, NH<sub>3</sub>-TPD, and N<sub>2</sub> adsorption and desorption to identify the chemical properties and the porous structure of the silica-supported PV<sub>x</sub>Mo species. The strong interactions between PV<sub>x</sub>Mo with the silica skeleton were also explored by the mentioned techniques. The critical properties explained the bifunctionality of the silica-supported PV<sub>x</sub>Mo species as a catalyst for the selective oxidation of glycerol to formic acid (60% conversion and 30% selectivity) with outstanding stability. Vanadium was found to be the key factor in the oxidation process.

Cao et al. [79] synthesized [EMIM]PAV<sub>[X]</sub> (X=Ac, NO<sub>3</sub>, BF<sub>4</sub>) using a simple method with 1-ethyl-3-methyl-imidazolium-based ionic liquids ([EMIM][X], X=Ac, NO<sub>3</sub>, BF<sub>4</sub>) as modifying reagents. The FT-IR, XRD, SEM, H<sub>2</sub>-TPR, TG/DTA, and XPS data revealed that [EMIM]PAV<sub>[Ac]</sub> had uniform rod-like morphology, better redox property, and higher amount of NH<sub>4</sub><sup>+</sup> composite, and consequently provided a high selectivity of 98% in the transformation of methacrolein to methacrylic acid as a catalyst. Theoretical computations suggested that the relatively strong H-bond basicity of C<sub>2</sub>-H in [EMIM]<sub>[Ac]</sub> had a great positive effect on the structure and redox property of [EMIM]PAV<sub>[X]</sub> hybrids.

### 3.5. Photocatalysis

Basically, photocatalysis is the acceleration of a photoreaction in the presence of a catalyst. In catalyzed photolysis, light is absorbed by an adsorbed substrate. In photogenerated catalysis, the photocatalytic activity (PCA) depends on the ability of the catalyst to create electron-hole pairs, which generate free radicals (e.g., hydroxyl radicals:  $\bullet\text{OH}$ ) able to undergo secondary reactions. Its practical application was made possible by the discovery of water electrolysis by means of titanium dioxide ( $\text{TiO}_2$ ).

Hassan and coauthor [80] prepared  $\text{TiO}_2$ - and  $\text{Sn}^{4+}$ -doped  $\text{TiO}_2$  nanoparticles via the surfactant-assisted sol-gel method. Then, using the wet impregnation method,  $\text{H}_3\text{PW}_{12}\text{O}_{40}$  (HPW) was loaded onto Sn- $\text{TiO}_2$  nanoparticles with different HPW contents. The prepared samples were characterized by FT-IR, XRD, TEM, SEM, UV-vis, diffuse reflection (DRS), and photoluminescence (PL) techniques. The surface acidity was studied by potentiometric titration and pyridine was used as a probe molecule to distinguish between Brønsted and Lewis acid sites. The analysis of the XRD patterns indicated that the crystallite size reduced remarkably as the HPW loading increased. TEM and SEM images exhibited irregular particles shape and the amount of HPW on the surface of Sn- $\text{TiO}_2$  increased as the HPW loading increased to 60 wt%. The addition of HPW and  $\text{Sn}^{4+}$  improved the surface acidity and catalytic activity of  $\text{TiO}_2$ . Besides, the addition of  $\text{Sn}^{4+}$  promoted the electron transfer between HPW and  $\text{TiO}_2$  and diminished the recombination of electrons ( $e^-$ ) and holes ( $h^+$ ). The catalytic activity was tested over the synthesis of 7-hydroxy-4-methyl coumarin and 14-phenyl-14H-dibenzo [a,j] xanthene. Both acidity and catalytic activity increased sharply after Sn- $\text{TiO}_2$  was modified by HPW. The sample with 50 wt% of HPW exhibited the highest catalytic activity and acidity.

Pomilla and coworkers [81] functionalized lab-prepared and commercial  $\text{TiO}_2$  samples with a Keggin heteropoly acid, i.e.,  $\text{H}_3\text{PW}_{12}\text{O}_{40}$  (HPW) or with a hydrothermally lab-prepared salt, i.e.,  $\text{K}_7\text{PW}_{11}\text{O}_{39}$  (KPW). All the species were characterized by specific surface area measurements (BET), XRD, Raman, DRS, and SEM. They were used for photocatalytic conversion of glucose in an aqueous suspension. Different reaction extent and distribution of intermediate oxidation products were observed depending on the photocatalyst used. Gluconic acid, erythrose, arabinose, and formic acid were observed as the oxidation products when bare  $\text{TiO}_2$  or HPW/ $\text{TiO}_2$  composites were used. Glucose isomerization to fructose was observed as well. In some cases, traces of glucaric acid and glyceraldehyde were also observed. No reactivity was observed in the presence of HPW alone while KPW induced only isomerization of the glucose.

Yu and others [82] reported direct and selective photocatalytic oxidation of methane into carbon monoxide at ambient conditions. The latter is an important chemical intermediate in manufacture of many chemicals. Composite catalysts consisting of zinc, tungstophosphoric acid and titania exhibited exceptional performance for this reaction, with high carbon monoxide selectivity and quantum

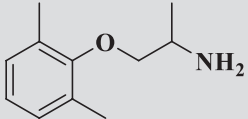
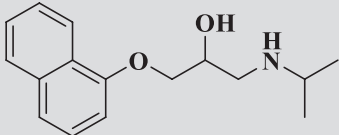
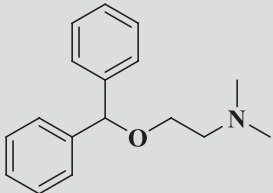
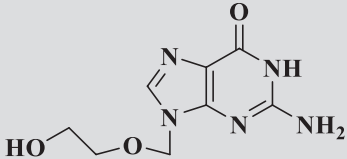
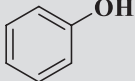
efficiency of 7.1% at 362 nm. X-ray photoelectron and in-situ FT-IR spectroscopy revealed that the catalytic performance could be ascribed to zinc species highly dispersed on tungstophosphoric acid/titania, which followed reduction/oxidation cycles during the reaction in a Mars-van Krevelen sequence. The process took place via the intermediate formation of surface methyl carbonates.

Taghavi and coworkers [83] prepared phosphotungstic acid ( $\text{H}_3\text{PW}_{12}\text{O}_{40}$ ) nanophotocatalysts supported by ZnO and  $\text{TiO}_2$  nanoparticles (within the range of 10–80 nm). They assessed the surface morphology, phase analysis, crystal structure, and surface structure of their nanophotocatalysts ( $\text{ZnO}/\text{H}_3\text{PW}_{12}\text{O}_{40}$ ,  $\text{TiO}_2/\text{H}_3\text{PW}_{12}\text{O}_{40}$ ). In order to explore the photocatalytic activity of the synthesized nanophotocatalysts, the authors selected aniline as an organic pollutant. The results revealed that the degradation efficiency was more than 70% for both nanophotocatalysts in the presence of  $\text{H}_2\text{O}_2$ . In addition, the results from photocatalytic degradation of aniline using synthesized nanophotocatalysts were properly fitted to the Langmuir-Hinshelwood model. The hydroxyl radicals and holes were considered as the species with the most oxidizing ability in degrading aniline using the prepared nanophotocatalysts. In the end, the results demonstrated that the prepared nanophotocatalysts could be regarded as suitable photocatalysts in removing organic pollutant from aqueous solutions.

Tayebee et al. [84] prepared a  $\text{WZnO-NH}_2@/\text{H}_3\text{PW}_{12}\text{O}_{40}$  ( $\text{WZnO}/\text{HPW}$ ) nanocomposite through a simple solution route in water at low temperatures. Then, the UV-vis photocatalytic activity and energy storage ability of the nanocomposite containing ~5 wt% of  $\text{WO}_3$  was determined in the decomposition of methylene blue (MB) in an aqueous solution. Besides, photocatalytic degradation efficiencies of all ingredients of  $\text{WZnO}/\text{HPA}$  were compared and important, interesting mechanistic spot-lights were introduced using a range of scavengers to detect the active oxidizing species in the process. In addition, a range of important polluting drugs were tested under the standard photocatalytic conditions (Table 3.2). Finally, various irradiation sources such as cheap and commercially available LED lamps were also compared in the photodegradation process. In this process,  $\text{WO}_3$  behaved as an absorber of the irradiation energy and ZnO served as a cocatalyst to reduce the electron-hole recombination. The FT-IR results indicated the successful loading of HPW on the surface of  $\text{WZnO-SiO}_2/\text{NH}_2$  without changing its Keggin structure. Furthermore, the XRD pattern of the  $\text{WZnO}$  photocatalyst confirmed no clear change in the crystal structure after being doped with tungsten and  $\text{WO}_3$  uniformly dispersed on ZnO nanoparticles. The XPS results confirmed that Zn existed in the form of  $\text{Zn}^{2+}$  and tungsten in the form of  $\text{W}^{6+}$  in the nanocomposite.

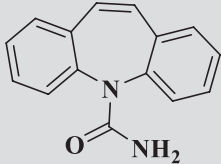
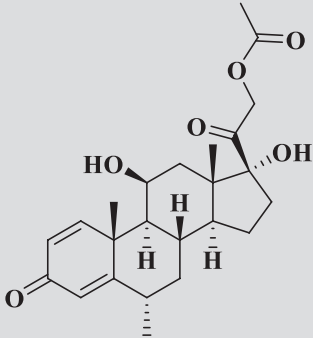
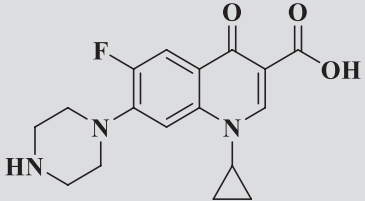
Wang and others [85] prepared a novel heterogeneous photocatalyst  $\text{Ca}_x\text{H}_{4-x}\text{SiW}_{12}\text{O}_{40}/\text{Ca}_2\text{Ta}_2\text{O}_7$  by planting silicotungstic acid on the surface of calcium tantalate. The resulted species were characterized by FT-IR, XRD, SEM, XPS, UV-visible diffuse reflectance spectroscopy (UV-vis), energy-dispersive X-ray spectroscopy (EDS), BET surface area, and Malvern ZEN3690 Particle Analyzer (ZP). The results indicated that  $\text{Ca}_2\text{Ta}_2\text{O}_7$  presented regular

**TABLE 3.2** Photodegradation of some important drugs catalyzed by WZnO/HPA under the standard reaction conditions.

Drug	Structure	Deg. %	Method drug conc.	Major Deg. products
Mexiletine		100	HPLC, 10 μM	2,6-Dimethylphenol
Propranolol		87	HPLC, 10 μM	Naphthalene-1-ol
Diphenhydramine		79	HPLC, 10 μM	Diphenylmethanol, benzophenone
Acyclovir		67	HPLC, 40 μM	Various oxidation products mediated by OH <sup>•</sup>
Phenol		95	HPLC, 50 μM	Hydroquinone, para quinone

*Continued*

**TABLE 3.2** Photodegradation of some important drugs catalyzed by WZnO/HPA under the standard reaction conditions—cont'd

Drug	Structure	Deg. %	Method drug conc.	Major Deg. products
Carbamazepine		88	HPLC, 40 μM	Acridine-9 carboxyaldehyde, acridine
Methylprednisol one		57	HPLC, 10 μM	Oxo-derivatives
Ciprofloxacin		66	HPLC, 10 μM	(2-Aminoethyl)amino derivatives

octahedron morphology with a cubic phase structure, and  $\text{H}_4\text{SiW}_{12}\text{O}_{40}$  uniformly grew on the surface of  $\text{Ca}_2\text{Ta}_2\text{O}_7$  in the form of  $\text{C}_x\text{H}_{4-x}\text{SiW}_{12}\text{O}_{40}$ . The XRD and FT-IR data suggested that primary Keggin structures of  $\text{H}_4\text{SiW}_{12}\text{O}_{40}$  remained intact. The modification of  $\text{H}_4\text{SiW}_{12}\text{O}_{40}$  on  $\text{Ca}_2\text{Ta}_2\text{O}_7$  surface caused an increase in the negative zeta potential and red shifts. The prepared catalyst demonstrated a great improvement in the UV photocatalytic efficiency in the reduction of Cr(VI) ions up to 94.6% under the optimized conditions (the  $\text{Ca}_2\text{Ta}_2\text{O}_7$  to  $\text{H}_4\text{SiW}_{12}\text{O}_{40}$  ratio was 1:2). Besides, the composite exhibited an excellent reusability—this was mainly attributed to the local formation of water-insoluble  $\text{C}_x\text{H}_{4-x}\text{SiW}_{12}\text{O}_{40}$  so that the removal was maintained at 73.8% after five runs.

Fakhri et al. [86] synthesized two new sets of heteropoly acid-based functionalized graphene oxide species, i.e.,  $\text{H}_3\text{PMo}_2\text{W}_{10}\text{O}_{40}$ @ethylene diamine functionalized magnetic graphene oxide ( $\text{Mo}_2\text{W}_{10}$ @EDMG) and  $\text{H}_3\text{PMo}_4\text{W}_8\text{O}_{40}$ @ethylene diamine functionalized magnetic graphene oxide ( $\text{Mo}_4\text{W}_8$ @EDMG), and characterized them by XRD, TEM, and FT-IR techniques. The suitability of the synthesized nanocomposites as inorganic ion exchangers was studied. In order to assess the adsorption efficacy of these nanocomposites, the cerium ion was chosen as the model adsorbate and the influence of initial concentration of metal ion, pH of solution, and temperature on adsorption performance were investigated. The maximum adsorption capacity was found to be 96.15 mg/g and 90.90 at pH 6.0 for 30%  $\text{Mo}_2\text{W}_{10}$ @EDMG and 30%  $\text{Mo}_4\text{W}_8$ @EDMG, respectively.  $\text{Mo}_2\text{W}_{10}$ @EDMG and  $\text{Mo}_4\text{W}_8$ @EDMG were used for photodegradation of methylene blue under visible light irradiation. The photocatalytic results indicated that 20%  $\text{Mo}_4\text{W}_8$ @EDMG acted as an effective photocatalyst with 100% removal efficiency in 50 min irradiation. In addition, the effect of substitution of Mo with W on the adsorption and photocatalytic performances was studied.

Taghavi and coworkers [87] synthesized three nanocomposites of phosphomolybdic acid supported on  $\text{TiO}_2$  and  $\text{ZnO}$  nanoparticles were and characterized using FESEM, FT-IR, and XRD techniques. The photocatalytic activity of the synthesized nanocomposite was examined for aniline as an organic pollutant model. Rather good efficiency of degradation, i.e., above 70%, was accomplished for all nanocomposites in the presence of hydrogen peroxide as an electron scavenger. However, other scavengers negatively affected the efficiency of the process in the order of sodium oxalate > ethanol > methanol. The kinetic studies revealed that the photocatalytic degradation of aniline followed the Langmuir-Hinshelwood model. The results of this study indicated that the hydroxyl radicals and holes played a significant role in the photocatalytic degradation of aniline using synthesized nanocomposites. The results suggested that the synthesized nanocomposites could be favorable photocatalysts in the removal of aniline from aqueous solutions.

Sampurnam et al. [88] prepared a photocatalyst by doping noble metal nanoparticle into  $\text{H}_3\text{PW}_{12}\text{O}_{40}/\text{TiO}_2$  composite using a wet impregnation method. The prepared nanocomposite was characterized by FT-IR, XRD, and UV-vis

techniques. It was found that the photocatalytic activity of the prepared species increased by doping the noble metal silver nanoparticles into the composite. The photocatalytic activity of the catalyst was tested for the degradation of methylene blue dye under the visible light.

Taghavi and others [89] investigated the  $\text{TiO}_2/\text{ZnO}$ -supported phosphomolybdic acid (HPMo) nanoparticles by the impregnation method. In the next step, they analyzed their photocatalytic activity under the UV-LED light and studied the kinetics of aniline degradation as an organic pollutant model. Nanoparticles and the remaining of the Keggin structure in the nanocomposites were characterized by FESEM, FT-IR, and XRD. Heterogenization of phosphomolybdic acid on  $\text{TiO}_2$  and ZnO nanoparticles improved the light absorption intensity and decreased the bandgap of nanocomposites. Furthermore, the photocatalytic degradation of aniline was improved for composite nanoparticles and reached 25.62%, 43.48%, and 38.25% for  $\text{TiO}_2/\text{HPMo}$ ,  $\text{ZnO}/\text{HPMo}$ , and  $\text{TiO}_2/\text{ZnO}/\text{HPMo}$ , respectively. On the whole, the results exhibited a good fit to the Langmuir-Hinshelwood kinetic model.

Marcì and coauthors [90] studied bulk and surface properties of three heteropoly acid clusters ( $\text{H}_3\text{PW}_{12}\text{O}_{40}$ ,  $\text{H}_3\text{PMo}_{12}\text{O}_{40}$ , and  $\text{H}_4\text{SiW}_{12}\text{O}_{40}$ ) supported on  $\text{TiO}_2$  Evonik P25 as well as their application as heterogeneous photocatalysts in two different reactions, i.e., hydration of propene and dehydration of glycerol. The study focused on how the photoreactivity might depend on the type of heteropoly acid but also how the interaction between the support and heteropoly acid might be important. Notably, as far as the dehydration of glycerol was concerned, in contrast to what reported in the literature regarding the thermal catalysis, in our UV irradiated system, the reaction took place at a very low temperature (35°C).

Saghi and coworkers [91] supported spherical  $\alpha\text{-Fe}_2\text{O}_3$  nanoparticles on the surface of 12-tungstosilicic acid (12-TSA.7 $\text{H}_2\text{O}$ ) using two different solid-state dispersion and forced hydrolysis and reflux condensation methods. The photocatalytic activity of the supported  $\alpha\text{-Fe}_2\text{O}_3$  nanoparticles ( $\alpha\text{-Fe}_2\text{O}_3/12\text{-TSA.7H}_2\text{O}$ ) for the degradation of tetracycline in aqueous media was investigated using a UV/ $\text{H}_2\text{O}_2$  process. The results were compared with those of pure  $\alpha\text{-Fe}_2\text{O}_3$  nanoparticles. All species were characterized with FT-IR, EDX, SEM, and XRD. Design of the experiments was done considering four parameters, i.e., pH, the initial concentration of tetracycline, concentration of the catalyst, and hydrogen peroxide concentration at three different levels. The decrease in the concentration of tetracycline was measured using UV-vis at  $\lambda_{\text{max}}=357$  nm. The results of experiments revealed that supporting  $\alpha\text{-Fe}_2\text{O}_3$  nanoparticles on the surface of 12-TSA.7 $\text{H}_2\text{O}$  through solid-state dispersion and forced hydrolysis and reflux condensation methods improved the filtration, recovery, and photocatalytic activity of the nanoparticles. In addition, it was shown that those nanoparticles supported through the solid-state dispersion method had better photocatalytic performance than those supported through forced hydrolysis and reflux condensation methods. A statistical analysis demonstrated that the



maximum degradation of tetracycline (97.39%) was achieved under conditions in which the pH and catalyst concentration parameters were maximum and the initial parameters of tetracycline and hydrogen peroxide concentrations were minimum (pH 8, catalyst concentration = 150 ppm, initial concentration of tetracycline = 30 ppm, hydrogen peroxide concentration = 0.1 ppm). For the photocatalytic degradation reaction, a first-order reaction with  $k = 0.0098 \text{ min}^{-1}$  was observed.

Bertolini and others [92] prepared a series of composite systems based on titania and growing quantities of tungstophosphoric acid ( $\text{H}_3\text{PW}_{12}\text{O}_{40}\text{-TiO}_2$ ). The prepared species were characterized using various techniques such as IR, NMR, UV-vis, photoluminescence, and photoelectron spectroscopies, transmission electron microscopy, XRD, and porosimetry, confirming the leading role of the specific polytungstate species in the enhancement of the activity and selectivity of the tested reaction. The stability and activity of the samples for the photo-oxidation of toluene in gas phase under UV and sunlight irradiations were evaluated using the reaction rate and the photonic efficiency parameters. The radiation field was modeled by solving the radiative transfer equation in a numeric manner. The photoactivity of the composites demonstrated a considerable selectivity toward the transformation of the hydrocarbon into a partially oxidized product, i.e., benzaldehyde. Both the activity and selectivity of the titania were considerably affected by the presence of the tungstophosphoric acid species.

Mohammadghasemi-Samani et al. [93] prepared a new organic hybrid of silicotungstic acid employing an easily available, inexpensive, and nontoxic amine via a simple precipitation method. The hybrid was characterized using FT-IR, elemental analyses, powder XRD, TGA, differential scanning calorimetry, and SEM. Dye adsorption and photocatalytic properties of the prepared water-insoluble hybrid were studied by decolorization of model dyes such as methyl orange and methylene blue and their mixture solutions under ultraviolet, and sunlight irradiations. The effects of various parameters including the initial concentration, pH, hydrogen peroxide, and catalyst dosage, as well as salt adding, were examined on the decolorization of dyes. The results revealed that the hybrid was a good heterogeneous photocatalyst in the degradation of methylene blue, methyl orange, and their mixture, and can be recovered and reused. Methyl orange was removed through ultraviolet and solar photocatalytic degradation via indirect oxidation by OH radicals. Methylene blue was removed via a combination of adsorption and photocatalytic degradation under ultraviolet, visible, and sunlight through direct oxidation by the prepared hybrid. While the visible light was not able to degrade the methyl orange solution alone in the presence of the hybrid, the methyl orange mixed with methylene blue solution was degraded.

Sun and coworkers [94] prepared a new effective hybrid photocatalyst consisting of tungstophosphoric acid (HPW) and acidified carbon nitride. The acidified carbon nitride and HPW were found to interact via hydrogen bonds

to improve the photocatalytic activity of the resulted composite by means of enhanced photogenerated hole electron separation efficiency. The graphitic carbon nitride (g-C<sub>3</sub>N<sub>4</sub>) was treated with a mixture of concentrated nitric acid and sulfuric acid to afford porous acidified carbon nitride (ACN). The composite photocatalyst was then synthesized by self-assembly of ACN and HPW under acidic conditions. The characterization results demonstrated the successful introduction of HPW and effective interaction between HPW and acidified carbon nitride. Photocatalytic degradation experiments showed that HPW could act as a photogenerated electron-trapping agent to provide adsorption sites besides photocatalytic redox reaction sites. In addition, the HPW/ACN system exhibited excellent activity in the degradation of imidacloprid and acetamiprid under the irradiation of visible light ( $\lambda > 400$  nm). The photocatalytic degradation results showed that the degradation rate constant of HPW/ACN ( $0.0058 \text{ min}^{-1}$ ) was 16 times greater than that of ACN ( $3.55 \times 10^{-4} \text{ min}^{-1}$ ) in the photocatalytic degrading imidacloprid. Moreover, the photocatalytic degradation rate constant of HPW/ACN ( $0.0017 \text{ min}^{-1}$ ) was 30 times greater than that of ACN ( $5.64 \times 10^{-5} \text{ min}^{-1}$ ) in degradation of acetamiprid.

Ayati and coauthors [95] deposited gold nanoparticles on the surface of tungstophosphoric acid (HPW) immobilized on TiO<sub>2</sub> nanotubes. Tungstophosphoric acid served as both a highly localized UV-switchable reducing agent and a multifunctional photocatalyst linker molecule. The prepared novel nanocomposite was characterized with FT-IR, XRD, EDX, and TEM, and was found to be highly photocatalytic efficient in the removal of nitrobenzene. The results revealed that by introducing the gold nanoparticles, the photocatalytic performance considerably improved, where the photocatalytic rate of using Au/HPW/TiO<sub>2</sub>-NT nanocomposites was increased compared to that of the TiO<sub>2</sub> nanotubes by 4.1 times. The results showed that the photocatalytic performance changed in order of HPW < TiO<sub>2</sub> < HPW/TiO<sub>2</sub> < Au/HPW/TiO<sub>2</sub>-NT. In the proposed possible mechanism, it was outlined that the bridging layer of the photoactive HPW, with strong electron transferability, between TiO<sub>2</sub> nanotubes and gold nanoparticles, might provide an additional driving force to accelerate the charge transfer between them.

Farhadi et al. [96] prepared a new nanohybrid compound, LaFeO<sub>3</sub>@SiO<sub>2</sub>-NH<sub>2</sub>/HPW, in which tungstophosphoric acid (HPW) was successfully anchored onto the surface of 3-aminopropylsilica modified LaFeO<sub>3</sub>. The resulting nanohybrid compound was characterized using FT-IR, XRD, ICP-MS, FESEM, TEM, EDX, BET, and AFM techniques. The magnetic properties of all synthesized compounds as well as the hybrid compound were measured using a vibrating sample magnetometer (VSM) at ambient temperature. The photocatalytic activity of the hybrid compound was evaluated by degradation of methylene blue in aqueous media under the irradiation of visible light. In comparison with the bare LaFeO<sub>3</sub> and pure HPW, the new hybrid compound demonstrated improved photocatalytic activity under the irradiation of visible light. This improvement could be ascribed to a synergistic effect between LaFeO<sub>3</sub> and HPW.

After the photocatalytic reaction, the hybrid compound could be easily separated from the reaction solution and reused several times without any significant loss of photocatalytic activity.

Using  $\text{H}_3\text{PW}_{12}\text{O}_{40}$  (HPW), melem, and pyromellitic dianhydride as precursors, Meng and others [97] prepared a series of (HPW)-containing polyimide hybrid composites (TPI) via in-situ a solid-state polymerization process. The effect of HPW on the chemical structure, morphology, porosity, and optical and visible-light photocatalytic degradation efficiency of TPI composites were examined by various methods. A comparison of the structures, properties, and photocatalytic activity of the TPI composites and the HPW-PI composites revealed that HPW was able to promote the formation of C–N bond in the five-membered imide rings between amines and anhydrides during the in-situ process of the solid-state condensation. The visible-light ( $\lambda > 400\text{ nm}$ ) photocatalytic degradation efficiency of imidacloprid on TPI composites was also compared with the pristine PI due to the improvement of the in-situ solid-state condensation reaction, photogenerated electron-hole separation efficiency, and visible-light utilization efficiency after the introduction of HPW. The visible-light photocatalytic degradation rate constants  $k$  of 15% TPI composites prepared at  $300^\circ\text{C}$  and 5% TPI composites prepared at  $325^\circ\text{C}$  were 10.33 and 2.42 times greater than that of the corresponding pristine PI, respectively. In comparison with commercial P25, the photocatalytic degradation efficiency of 15% TPI-300 and 5% TPI-325 were 4.58 and 5.13 times greater than that of P25 under the irradiation of visible light.

Yao and coworkers [98] synthesized mesoporous titanium dioxide ( $\text{MTiO}_2$ ) photocatalysts codoped with Fe and  $\text{H}_3\text{PW}_{12}\text{O}_{40}$  by the template method using  $\text{Ti}(\text{OC}_4\text{H}_9)_4$  (tetrabutyl titanate),  $\text{Fe}(\text{NO}_3)_3 \cdot 9\text{H}_2\text{O}$ , and  $\text{H}_3\text{PW}_{12}\text{O}_{40}$  as precursors and Pluronic P123 as a template. The prepared photocatalyst was characterized by XRD,  $\text{N}_2$  adsorption-desorption measurements, SEM, and UV-vis. In addition, the photocatalytic activities of the prepared samples under ultraviolet and visible lights were estimated by measuring the degradation rate of methylene blue (50 mg/L) in aqueous media. The characterizations revealed that the photocatalysts had a homogeneous pore diameter of  $\sim 10\text{ nm}$  with high surface area of  $\sim 150\text{ m}^2/\text{g}$ . The results of the methylene blue photodecomposition demonstrated that the codoped mesoporous  $\text{TiO}_2$  had higher photocatalytic activities than the undoped, and single doped mesoporous  $\text{TiO}_2$  under the irradiations of ultraviolet and visible lights. The codoped  $\text{MTiO}_2$  was found to be activated by visible light and therefore could be used as an efficient catalyst in photo-oxidation reactions. The synergistic effect of iron and  $\text{H}_3\text{PW}_{12}\text{O}_{40}$  codoping had an important role in improving the photocatalytic activity.

Koohi and coworkers [99] impregnated silicotungstic acid (HSiW) on natural minerals such as mordenite (HSiW/Mord), clinoptilolite (HSiW/Clin), bentonite (HSiW/Bent), and kaolinite (HSiW/Kaoln), and evaluated them toward photocatalytic degradation of methylene blue in wastewater. These photocatalysts were characterized by means of XRD, field emission scanning microscopy

(FESEM), FT-IR, and UV-vis diffuse reflectance spectroscopy (UV-vis DRS). The results revealed that HSiW crystallized differently on the above minerals so that HSiW on clinoptilolite had the highest crystallinity and the smallest crystallite size. The FESEM results revealed that the supported HSiW had nanometric spherical particles with uniform and narrow distribution. FT-IR revealed that there was a strong interaction between HSiW and minerals in all photocatalysts and the Keggin structure of HSiW was intact. The UV-vis DRS studies revealed that HSiW/Clin and HSiW/Mord had photoactivity in both visible and ultraviolet regions, while HSiW/Bent and HSiW/Kaoln photocatalysts were active only in the UV region. Moreover, it was found that HSiW/Clin had the lowest bandgap of 3.1 eV among the studied nanophotocatalysts. The HSiW/Clin sample was able to degrade 92% of methylene blue after 90 min of UV irradiations while HSiW/Mord, HSiW/Bent, and HSiW/Kaoln were in the next positions, respectively. Kinetic studies showed that the photocatalytic degradation of methylene blue fitted a pseudo-first order reaction with the highest rate constant belonging to HSiW/Clin. The effect of operation parameters such as initial dye concentration, wastewater pH, photocatalyst loading, and successive cycles of using HSiW/Clin was examined as well. For this catalytic system, a new mechanism was proposed in which the existence of clinoptilolite would lead to extensive dispersion of tungstosilicic acid over the support which enhanced the electron-hole formation. In addition, clinoptilolite trapped an electron on the conduction band of HSiW and prevented from the recombination of the electron-hole.

Marchena et al. [100] prepared immobilized tungstosilicic acid materials (TSA) on zeolites (NH<sub>4</sub>Y and NH<sub>4</sub>ZSM5) by wet impregnation of the zeolite matrix with tungstosilicic acid aqueous solutions. The concentration was varied to achieve the tungstosilicic acid contents of 5%, 10%, 20%, and 30% w/w in the solid. The prepared catalysts were then characterized using techniques such as FT-IR, XRD, SEM, N<sub>2</sub> adsorption-desorption isotherms, and DRS-UV-vis. The results showed that the surface area of the materials decreased when higher amounts of tungstosilicic acid was added due to pore entrance blocking by the anion [SiW<sub>12</sub>O<sub>40</sub>]<sup>4-</sup> in both matrices. The resulting materials were tested over the photodecomposition of the azo dye methyl orange. The results showed that they had suitable properties to be used as a catalyst in the photocatalytic treatment of the wastewater containing dyes, and the photodegradation followed a pseudo-first-order kinetics. Reaction parameters such as catalysts mass, tungstosilicic acid content, reuse, and pH were assessed.

Zhu's research group [101] synthesized ZnS/HPW composites via a green sonochemical process without any surfactant or template. The incorporation of phosphotungstic acid (HPW) was confirmed by FT-IR, TEM-EDS, XRD, and XPS. TEM revealed that ZnS/HPW composites were spherical. The bandgap energy of the ZnS/HPW10 composite was estimated to be 1.13 eV, which demonstrated a significant red-shift in comparison with 2.35 eV for the pure ZnS. Furthermore, as the HPW concentration varied from 0.005 M to 0.020 M, the

red shift became more obvious. Due to the incorporation of HPW, the charge carrier separation and transfer of ZnS were promoted. Under the simulated solar irradiation, the photocatalytic activity examinations also suggested that the ZnS/HPW composites exhibited higher photodegradation rate of Rhodamine B dye in comparison with pure ZnS. In particular, the ZnS/HPW10 composite exhibited the highest photocatalytic efficiency. Notably, the ZnS/HPW10 composite retained its activity for five successive runs.

Moosavifar and others [102] synthesized neat and supported  $H_6P_2W_{18}O_{62}$  into nanocage of  $\beta$ -zeolite via template synthesis method. In addition,  $TiO_2$  was supported on the  $H_6P_2W_{18}O_{62}/\beta$  zeolite by the impregnation method. The gained species were characterized by means of XRD, FT-IR, UV-vis, FESEM, and EDS techniques. In addition, the tungsten and titanium contents of the catalyst were measured. The results showed that the photocatalyst activity were dependent on the pH effect, catalyst loading, and the concentration of methyl orange. The photocatalytic degradation of methyl orange was found to follow a pseudo-first order kinetic and the chemical oxygen demand (COD) test proved the mineralization of methyl orange. Other evidence for the degradation and mineralization of methyl orange was the absence of hydrazine at the end of reaction as one of the photodecolorization products. The catalytic systems were recoverable and usable for four runs without any significant loss of catalytic activity.

Yang and coworkers [103] synthesized  $H_3PW_{12}O_{40}/TiO_2-SiO_2$  by the impregnation method, which considerably improved the catalytic activity under simulated natural light. The properties of the samples were characterized by FT-IR, XRD, SEM, and Zeta potential techniques. Degradation of methyl violet was employed as a test reaction to examine the factors affecting the photodegradation reaction. The results revealed the optimal conditions as follows: initial concentration of methyl violet, 10 mg/L, pH 3.0; catalyst dosage, 2.9 g/L, and light irradiation time 2.5 h. Under these optimized conditions, the degradation rate of methyl violet was 95.4%. The photodegradation for methyl violet could be fitted to a first-order kinetic model, and a possible mechanism was suggested. After being used for five successive runs, the catalyst kept its inherent photocatalytic activity. The photodegradation of methyl orange, methyl red, naphthol green B, and methylene blue was also explored, and the degradation rate of those dyes could reach 81%–100%.

Moosavifar et al. [104] prepared molybdophosphoric acid encapsulated into dealuminated zeolite Y (DAZY) by the template synthesis method. Incorporation of  $TiO_2$  into nanocage of DAZY was conducted by the impregnation method. The obtained photocatalyst (HPA/ $TiO_2$ /DAZY) was characterized by FT-IR, UV-vis, XRD, FESEM, EDS, and ICP techniques. This catalytic system was investigated in the photodegradation of methyl orange. The results exhibited that the photocatalyst activity was dependent on photocatalyst loading and  $TiO_2$ /(HPA/HY) ratio. The photocatalytic activity of the molybdophosphoric acid encapsulated into the zeolite cage was improved with impregnation of  $TiO_2$  into the nanocage of dealuminated Y zeolite, and accordingly complete removal of the methyl orange occurred.

Liu et al. [105] prepared a novel HPW/Bi<sub>2</sub>WO<sub>6</sub> composite photocatalyst by means of an easy, effective approach. The prepared photocatalyst was characterized using various techniques such as IR, XRD, SEM, and photoelectrochemical measurements. The photocatalytic activity of the HPW/Bi<sub>2</sub>WO<sub>6</sub> composite photocatalyst was assessed using a model reaction of the photocatalytic degradation of rhodamine B (RhB) under the visible light. In comparison with pure Bi<sub>2</sub>WO<sub>6</sub>, the HPW/Bi<sub>2</sub>WO<sub>6</sub> photocatalyst demonstrated a considerable enhancement in the photocatalytic degradation of RhB under such conditions. The HPW/Bi<sub>2</sub>WO<sub>6</sub> composite demonstrated high photocatalytic activity with an RhB degradation ratio of 499% within 4 h, which was almost two times greater than that of pure Bi<sub>2</sub>WO<sub>6</sub>. A reaction mechanism was also proposed for the enhanced photocatalytic performance. The introduction of HPW could effectively improve the photocatalytic activity of Bi<sub>2</sub>WO<sub>6</sub> due to an increase in the efficiency of charge separation and restraining the fast electron-hole recombination in Bi<sub>2</sub>WO<sub>6</sub>.

### 3.6. Conclusion

Homogenous catalysts are being replaced by solid (heterogeneous) catalysts because of the drawbacks of homogeneous catalysts to conduct organic transformations such as unwanted saponification, difficulty in separation of the products and/or catalyst recovery. The mentioned problems can be resolved by employing heterogeneous (solid) acid catalysts. In addition, solid acid catalysts are more environmentally friendly than other catalysts applied in organic reactions.

Heteropoly acids have advantages in comparison with other Brønsted acids, including higher acidity strengths, thermal stability, water tolerance, and easy handling. Therefore, they have proven to be relatively efficient catalysts, but there are restrictions such as high polarity and low surface area for using them in catalytic systems. On the other hand, the most attractive feature of the heteropoly acids is that they can be used as homogeneous or heterogeneous catalysts. To resolve such restrictions, heteropoly acids are supported on suitable supports to serve as heterogeneous catalysts. The use of such heterogeneous catalysts makes the processes environmentally friendly owing to the lower effluent generation, easy recovery, and catalyst reuse.

This chapter described various reactions catalyzed by heterogeneous heteropoly acid catalyst, including the syntheses of heterocyclic compounds, multi-component reactions, oxidation reactions, and photocatalytic reactions.

### References

- [1] J.H. Clark, *Solid acids for green chemistry*, *Acc. Chem. Res.* 35 (9) (2002) 791–797.
- [2] I.C. Emeji, *Production and Characterization of Biofuel from Waste Cooking*, 2015.
- [3] M.A. Hanif, S. Nisar, U. Rashid, *Supported solid and heteropoly acid catalysts for production of biodiesel*, *Catal. Rev.* 59 (2) (2017) 165–188.
- [4] I.V. Kozhevnikov, *Catalysis by heteropoly acids and multicomponent polyoxometalates in liquid-phase reactions*, *Chem. Rev.* 98 (1) (1998) 171–198.



- [5] G. Romanelli, J. Autino, G. Baronetti, H. Thomas, A fast and efficient deprotection of aldehydes from acylals using a Wells-Dawson heteropoly acid catalyst ( $H_6P_2W_{18}O_{62} \cdot 24H_2O$ ), *Synth. Commun.* 34 (21) (2004) 3909–3914.
- [6] A. Corma, H. Garcia, Lewis acids: from conventional homogeneous to green homogeneous and heterogeneous catalysis, *Chem. Rev.* 103 (11) (2003) 4307–4366.
- [7] T. Okuhara, N. Mizuno, M. Misono, Catalytic chemistry of heteropoly compounds, *Adv. Catal.* 41 (1996) 113–252.
- [8] S.M. Sadeghzadeh, A heteropoly acid -based ionic liquid immobilized onto  $Fe_3O_4/SiO_2/Salen/Mn$  as an environmentally friendly catalyst for synthesis of cyclic carbonate, *Res. Chem. Intermed.* 42 (3) (2016) 2317–2328.
- [9] M.D. Morales, A. Infantes-Molina, J. Lázaro-Martínez, G.P. Romanelli, L.R. Pizzio, E. Rodríguez-Castellón, Heterogeneous acid catalysts prepared by immobilization of  $H_3P-W_{12}O_{40}$  on silica through impregnation and inclusion, applied to the synthesis of 3H-1, 5-benzodiazepines, *Mol. Catal.* 485 (2020) 110842.
- [10] S.-H. Hao, X.-Y. Zhang, D.-Q. Dong, Z.-L. Wang, Alumina-supported heteropoly acid: an efficient catalyst for the synthesis of azaarene substituted 3-hydroxy-2-oxindole derivatives via C(sp<sup>3</sup>) H bond functionalization, *Chin. Chem. Lett.* 26 (5) (2015) 599–602.
- [11] S. Siddiqui, M.U. Khan, Z.N. Siddiqui, Synthesis, characterization, and application of silica-supported copper-doped phosphotungstic acid in claisen-schmidt condensation, *ACS Sustain. Chem. Eng.* 5 (9) (2017) 7932–7941.
- [12] S. Li, X. Qi, B. Huang, Synthesis of 7-hydroxy-4-methylcoumarin via the Pechmann reaction with PVP-supported phosphotungstic acid catalyst, *Catal. Today* 276 (2016) 139–144.
- [13] S.-L. Xie, Y.-H. Hui, X.-J. Long, C.-C. Wang, Z.-F. Xie, Aza-Michael addition reactions between nitroolefins and benzotriazole catalyzed by MCM-41 immobilized heteropoly acids in water, *Chin. Chem. Lett.* 24 (1) (2013) 28–30.
- [14] S. Habibzadeh, G. Firouzzadeh Pasha, M. Tajbakhsh, N. Amiri Andi, E. Alaei, A novel ternary  $GO@SiO_2-HPW$  nanocomposite as an efficient heterogeneous catalyst for the synthesis of benzazoles in aqueous media, *J. Chin. Chem. Soc.* 66 (8) (2019) 934–944.
- [15] S.M. Sadeghzadeh, A heteropoly acid -based ionic liquid immobilized onto fibrous nanosilica as an efficient catalyst for the synthesis of cyclic carbonate from carbon dioxide and epoxides, *Green Chem.* 17 (5) (2015) 3059–3066.
- [16] E. Rafiee, N. Rahpeima, S. Eavani, Nano scale magnetically recoverable supported heteropoly acid as an efficient catalyst for the synthesis of benzimidazole derivatives in water, *Acta Chim. Slov.* 61 (1) (2014).
- [17] A.M. Escobar, D.M. Ruiz, J.C. Autino, G.P. Romanelli, Single-step synthesis of 4-phenyl and 3, 4-dihydro-4-phenyl coumarins using a recyclable Preyssler heteropoly acid catalyst under solvent-free reaction conditions, *Res. Chem. Intermed.* 41 (12) (2015) 10109–10123.
- [18] J. Xiao, L. Wang, J. Ran, J. Zhao, N. Ma, M. Tao, W. Zhang, Quaternary ammonium functionalized polyacrylonitrile fiber supported phosphotungstic acid as efficient heterogeneous catalyst: hydrophobic tuning of the catalytic microenvironment, *J. Clean. Prod.* 274 (2020) 122473.
- [19] L.-J. Liu, Q.-J. Luan, J. Lu, D.-M. Lv, W.-Z. Duan, X. Wang, S.-W. Gong, 8-Hydroxy-2-methylquinoline-modified  $H_4SiW_{12}O_{40}$ : a reusable heterogeneous catalyst for acetal/ketal formation, *RSC Adv.* 8 (46) (2018) 26180–26187.
- [20] R. Mozafari, F. Heidarzadeh, F. Nikpour,  $MnFe_2O_4$  magnetic nanoparticles modified with chitosan polymeric and phosphotungstic acid as a novel and highly effective green nanocatalyst for regio- and stereoselective synthesis of functionalized oxazolidin-2-ones, *Mater. Sci. Eng. C* 105 (2019) 110109.



- [21] M. Kumaresan, V. Saravanan, P. Sami, M. Swaminathan, A green solid acid catalyst 12-tungstophosphoric acid  $H_3[PW_{12}O_{40}]$  supported on g- $C_3N_4$  for synthesis of quinoxalines, *Res. Chem. Intermed.* 46 (9) (2020) 4193–4209.
- [22] D. Bennardi, M.N. Blanco, L.R. Pizzio, J.C. Autino, G.P. Romanelli, An efficient and green catalytic method for friedländer quinoline synthesis using tungstophosphoric acid included in a polymeric matrix, *Curr. Catal.* 4 (1) (2015) 65–72.
- [23] A. Gharib, N.N. Pesyan, L.V. Fard, M. Roshani, Catalytic synthesis of Dicoumarols using silica-supported Preyssler nanoparticles (SPN),  $H_{14} [NaP_5W_{30}O_{110}]/SiO_2$ , *Am. J. Heterocycl. Chem.* 1 (2) (2015) 21–28.
- [24] V.V. Costa, K.A. da Silva Rocha, R.A. Mesquita, E.F. Kozhevnikova, I.V. Kozhevnikov, E.V. Gusevskaya, Heteropoly acid catalysts for the synthesis of fragrance compounds from bio-renewables: cycloaddition of crotonaldehyde to limonene,  $\alpha$ -Pinene, and  $\beta$ -Pinene, *Chem-CatChem* 5 (10) (2013) 3022–3026.
- [25] S. Takale, S. Manave, K. Phatangare, V. Padalkar, N. Darvatkar, A. Chaskar, Phosphomolybdic acid ( $H_3Mo_{12}O_{40}P$ ) as a reusable heterogeneous catalyst for the synthesis of 5-substituted 1 H-Tetrazoles via [2+ 3] cycloaddition of nitriles and sodium Azide, *Synth. Commun.* 42 (16) (2012) 2375–2381.
- [26] M.-S. Hosseini, M. Masteri-Farahani, Fabrication of new magnetite based sulfonic-phosphotungstic dual-acid catalyst for catalytic acetalization of benzaldehyde with ethylene glycol, *React. Kinet. Mech. Catal.* 130 (2) (2020) 979–991.
- [27] Y.-F. Sun, J.-M. Liu, J. Sun, Y.-T. Huang, J. Lu, M.-M. Li, N. Jin, X.-F. Dai, B. Fan, One-Pot Synthesis of Coumarins Unsubstituted on the Pyranic Nucleus Catalysed by a Wells-Dawson Heteropoly Acid ( $H_6P_2W_{18}O_{62}$ ), 2018.
- [28] K. Khosravi, M. Zendehdel, S. Naserifar, F. Tavakoli, K. Khalaji, A. Asgari, Heteropoly acid/ NaY zeolite as a reusable solid catalyst for highly efficient synthesis of gem-dihydroperoxides and 1, 2, 4, 5-tetraoxanes, *J. Chem. Res.* 40 (12) (2016) 744–749.
- [29] S.M. Sadeghzadeh, A heteropoly acid -based ionic liquid immobilized onto magnetic fibrous nanosilica as robust and recyclable heterogeneous catalysts for the synthesis of tetrahydrodipyrzopolopyridines in water, *RSC Adv.* 6 (79) (2016) 75973–75980.
- [30] S. Zolfagharinia, E. Kolvari, N. Koukabi, A new type of magnetically-recoverable heteropoly acid nanocatalyst supported on zirconia-encapsulated  $Fe_3O_4$  nanoparticles as a stable and strong solid acid for multicomponent reactions, *Catal. Lett.* 147 (6) (2017) 1551–1566.
- [31] S. Sadjadi, M.M. Heravi, M. Malmir, Heteropoly acid @creatin-halloysite clay: an environmentally friendly, reusable and heterogeneous catalyst for the synthesis of benzopyranopyrimidines, *Res. Chem. Intermed.* 43 (11) (2017) 6701–6717.
- [32] S.M. Sadeghzadeh, A heteropoly acid -based ionic liquid immobilized onto  $Fe_3O_4/SiO_2$ /salen/Mn as an environmentally friendly catalyst in a multicomponent reaction, *RSC Adv.* 5 (22) (2015) 17319–17324.
- [33] H. Eshghi, A. Javid, A. Khojastehnezhad, F. Moeinpour, F.F. Bamoharram, M. Bakavoli, M. Mirzaei, Dressler heteropoly acid supported on silica coated  $NiFe_2O_4$  nanoparticles for the catalytic synthesis of bis (dihydropyrimidinone) benzene and 3, 4-dihydropyrimidin-2 (1H)-ones, *Chin. J. Catal.* 36 (3) (2015) 299–307.
- [34] O.M. Portilla-Zuñiga, Á.G. Sathicq, J.J. Martínez, S.A. Fernandes, T.R. Rezende, G.P. Romanelli, Synthesis of Biginelli adducts using a Preyssler heteropoly acid in silica matrix from biomass building block, *Sustain. Chem. Pharm.* 10 (2018) 50–55.
- [35] M. Kumaresan, V. Karthika, K. Selvakumar, P. Sami, Green synthesis of naphtho [2, 3-f] quinolin-13-one and naphtho [2, 3-a] acridin-1 (2H)-one derivatives catalyzed by heteropoly acid supported montmorillonite K-10 clay, *Synth. Commun.* 49 (21) (2019) 2856–2868.

- [36] S. Sadjadi, M.M. Heravi, M. Malmir, B. Masoumi, Heteropoly acid decorated Halloysite Nanoclay: an efficient catalyst for the green synthesis of Spirooxindole derivatives, *Appl. Organomet. Chem.* 32 (3) (2018), e4113.
- [37] M. Ghanbari, S. Moradi, M. Setoodehkah,  $\text{Fe}_3\text{O}_4@\text{SiO}_2@ \text{ADMPT}/\text{H}_6\text{P}_2\text{W}_{18}\text{O}_{62}$ : a novel Wells-Dawson heteropoly acid -based magnetic inorganic-organic nanohybrid material as potent Lewis acid catalyst for the efficient synthesis of 1, 4-dihydropyridines, *Green Chem. Lett. Rev.* 11 (2) (2018) 111–124.
- [38] R. Jahanshahi, B. Akhlaghinia, Heteropoly acid anchored on SBA-15 functionalized with 2-aminoethyl dihydrogen phosphate: a novel and highly efficient catalyst for one-pot, three-component synthesis of trisubstituted 1, 3-thiazoles, *Res. Chem. Intermed.* 44 (4) (2018) 2451–2474.
- [39] K. Selvakumar, T. Shanmugaprabha, M. Kumaresan, P. Sami, One-pot multicomponent synthesis of N, N'-alkylidene bisamides and imidazoles using heteropoly-11-tungsto-1-vanado-phosphoric acid supported on natural clay as catalyst: a green approach, *Synth. Commun.* 47 (22) (2017) 2115–2126.
- [40] S. Pradhan, B. Mishra,  $\text{Cs}_x\text{H}_{3-x}\text{PW}_{12}\text{O}_{40}$  nanoparticles dispersed in the porous network of Zr-pillared  $\alpha$ -zirconium phosphate as efficient heterogeneous catalyst for synthesis of spirooxindoles, *Mol. Catal.* 2018 (446) (2018) 58–71.
- [41] A.J. Sabaghian, B. Laali, A. Khojastehnezhad, Preyssler Heteropoly Acid Supported on Silica Coated  $\text{Ni}_{0.5}\text{Zn}_{0.5}\text{Fe}_2\text{O}_4$  Nanoparticles; Synthesis and Characterization, 2015.
- [42] R. Tayebee, M. Fattahi Abdizadeh, N. Erfaninia, A. Amiri, M. Baghayeri, R.M. Kakhki, B. Maleki, E. Esmaili, Phosphotungstic acid grafted zeolite imidazolate framework as an effective heterogeneous nanocatalyst for the one-pot solvent-free synthesis of 3, 4-dihydropyrimidinones, *Appl. Organomet. Chem.* 33 (8) (2019), e4959.
- [43] S. Sadjadi, M.M. Heravi, V. Zadsirjan, V. Farzaneh, A ternary hybrid system based on combination of mesoporous silica, heteropoly acid and double-layered clay: an efficient catalyst for the synthesis of 2, 4-dihydro-3 H-pyrazol-3-ones and pyranopyrazoles in aqueous medium: studying the effect of the synthetic procedure on the catalytic activity, *Res. Chem. Intermed.* 44 (11) (2018) 6765–6785.
- [44] N.H. Mohtasham, M. Gholizadeh, Nano silica extracted from horsetail plant as a natural silica support for the synthesis of  $\text{H}_3\text{PW}_{12}\text{O}_{40}$  immobilized on aminated magnetic nanoparticles ( $\text{Fe}_3\text{O}_4@\text{SiO}_2\text{-EP-NH-HPA}$ ): a novel and efficient heterogeneous nanocatalyst for the green one-pot synthesis of pyrano [2, 3-c] pyrazole derivatives, *Res. Chem. Intermed.* 46 (6) (2020) 3037–3066.
- [45] A. Jamshidi, B. Maleki, F.M. Zonoz, R. Tayebee, HPA-dendrimer functionalized magnetic nanoparticles ( $\text{Fe}_3\text{O}_4@\text{D-NH}_2\text{-HPA}$ ) as a novel inorganic-organic hybrid and recyclable catalyst for the one-pot synthesis of highly substituted pyran derivatives, *Mater. Chem. Phys.* 209 (2018) 46–59.
- [46] S. Sadjadi, M.M. Heravi, M. Daraie, A novel hybrid catalytic system based on immobilization of phosphomolybdic acid on ionic liquid decorated cyclodextrin-nanosponges: efficient catalyst for the green synthesis of benzochromeno-pyrazole through cascade reaction: triply green, *J. Mol. Liq.* 231 (2017) 98–105.
- [47] M. Ghanbari, N.M. Dastjerdi, S. Ahmadi, S. Moradi, A novel inorganic–organic nanohybrid material SBA-15@triazine/ $\text{H}_3\text{PW}_{10}\text{V}_2\text{O}_{40}$  as efficient catalyst for the one-pot multicomponent synthesis of multisubstituted pyridines, *J. Iran. Chem. Soc.* 15 (5) (2018) 1119–1131.
- [48] F. Ataie, A. Davoodnia, A. Khojastehnezhad, Graphene oxide functionalized organic-inorganic hybrid (GO-Si-NH<sub>2</sub>-PMo): an efficient and green catalyst for the synthesis of tetrahydrobenzo [b] pyran derivatives, *Polycycl. Aromat. Compd.* (2019) 1–14.

- [49] D.S. Aher, K.R. Khillare, L.D. Chavan, S.G. Shankarwar, Quaternary Vanado-Molybdotungstophosphoric acid [ $\text{H}_5\text{PW}_6\text{Mo}_4\text{V}_2\text{O}_{40}$ ] over natural montmorillonite as a heterogeneous catalyst for the synthesis 4H-Pyran and polyhydroquinoline derivatives, *ChemistrySelect* 5 (25) (2020) 7320–7331.
- [50] S. Sadjadi, M.M. Heravi, M. Daraie, Heteropoly acid supported on amine-functionalized halloysite nano clay as an efficient catalyst for the synthesis of pyrazolopyranopyrimidines via four-component domino reaction, *Res. Chem. Intermed.* 43 (4) (2017) 2201–2214.
- [51] A. Ayati, M.M. Heravi, M. Daraie, B. Tanhaei, F.F. Bamoharram, M. Sillanpaa,  $\text{H}_3\text{PMo}_{12}\text{O}_{40}$  immobilized chitosan/ $\text{Fe}_3\text{O}_4$  as a novel efficient, green and recyclable nanocatalyst in the synthesis of pyrano-pyrazole derivatives, *J. Iran. Chem. Soc.* 13 (12) (2016) 2301–2308.
- [52] L.V. Chopda, P.N. Dave, 12-tungstosilicic acid H4 [ $\text{W}_{12}\text{SiO}_{40}$ ] over natural bentonite as a heterogeneous catalyst for the synthesis of 3, 4-dihydropyrimidin-2 (1H)-ones, *Chemistry-Select* 5 (8) (2020) 2395–2400.
- [53] S.M. Sadjadi, M. Heravi, V. Zadsirjan, S.Y.S. Beheshtiha, R.R. Kelishadi, HPA@Methenamine-HNTs: a novel catalyst for promoting one-pot and three-component synthesis of chromenopyrimidine-2, 5-diones and thioxochromenopyrimidin-5-ones in aqueous media, *ChemistrySelect* 3 (43) (2018) 12031–12038.
- [54] R. Tayebee, M. Amini, M. Akbari, A. Aliakbari, A novel inorganic–organic nanohybrid material  $\text{H}_4\text{SiW}_{12}\text{O}_{40}$ /pyridino-MCM-41 as efficient catalyst for the preparation of 1-amidoalkyl-2-naphthols under solvent-free conditions, *Dalton Trans.* 44 (20) (2015) 9596–9609.
- [55] R. Tayebee, M. Amini, S. Pouyamanesh, A. Aliakbari, A new inorganic-organic hybrid material Al-SBA-15-TPI/ $\text{H}_6\text{P}_2\text{W}_{18}\text{O}_{62}$  catalyzed one-pot, three-component synthesis of 2 H-indazolo [2, 1-b] phthalazine-triones, *Dalton Trans.* 44 (12) (2015) 5888–5897.
- [56] L. Rožić, B. Grbić, S. Petrović, N. Radić, L. Damjanović, Z. Vuković, The tungsten heteropoly acid supported on activated bentonites as catalyst for selective oxidation of 2-propanol, *Mater. Chem. Phys.* 167 (2015) 42–48.
- [57] S. Zolfagharinia, E. Kolvari, N. Koukabi, A practical heteropoly acid nanocatalyst supported on nano-sized ceramic for the chemoselective oxidation of sulfides to sulfoxides through an experimental design approach, *Chem. Pap.* 71 (12) (2017) 2505–2520.
- [58] S. Boudjema, A. Choukhou-Braham, R. Bachir, In oxidation of cyclohexene over mesoporous silica pillared clay incorporated with heteropoly acid prepared by sol gel method, *Adv. Mater. Res.* (2015) 71–76. *Trans Tech Publ.*
- [59] A. Afzalnia, A. Mirzaie, A. Nikseresht, T. Musabeygi, Ultrasound-assisted oxidative desulfurization process of liquid fuel by phosphotungstic acid encapsulated in a interpenetrating amine-functionalized Zn(II)-based MOF as catalyst, *Ultrason. Sonochem.* 34 (2017) 713–720.
- [60] Z.-J. Lin, H.-Q. Zheng, J. Chen, W.-E. Zhuang, Y.-X. Lin, J.-W. Su, Y.-B. Huang, R. Cao, Encapsulation of phosphotungstic acid into metal–organic frameworks with tunable window sizes: screening of PTA@ MOF catalysts for efficient oxidative desulfurization, *Inorg. Chem.* 57 (20) (2018) 13009–13019.
- [61] H. Zhang, J. Liu, C. Liu, T. Wang, W. Zhu, High dispersion of heteropoly acid nanoparticles on hydrothermally Cs-modified three-dimensionally ordered macroporous  $\text{SiO}_2$  with excellent selectivity in methacrolein oxidation, *Chin. J. Chem. Eng.* 28 (11) (2020) 2785–2791.
- [62] S.-W. Li, J.-R. Li, Y. Gao, L.-L. Liang, R.-L. Zhang, Zhao, J.-s., Metal modified heteropoly acid incorporated into porous materials for a highly oxidative desulfurization of DBT under molecular oxygen, *Fuel* 197 (2017) 551–561.
- [63] M. Masteri-Farahani, G.R. Najafi, M. Modarres, Taghvai-Nakhjiri, M., Wells-Dawson heteropoly acid encapsulated into the nanocages of SBA-16 as heterogeneous catalyst for the oxidation of olefins and alcohols, *J. Porous. Mater.* 23 (1) (2016) 285–290.

- [64] M. Jin, Q. Niu, Z. Guo, Z. Lv, Epoxidation of cyclohexene with  $H_2O_2$  over efficient water-tolerant heterogeneous catalysts composed of mono-substituted phosphotungstic acid on co-functionalized SBA-15, *Appl. Organomet. Chem.* 33 (9) (2019), e5115.
- [65] R. Ghubayra, C. Nuttall, S. Hodgkiss, M. Craven, E.F. Kozhevnikova, I.V. Kozhevnikov, Oxidative desulfurization of model diesel fuel catalyzed by carbon-supported heteropoly acids, *Appl. Catal. B Environ.* 253 (2019) 309–316.
- [66] J. Xiong, W. Zhu, W. Ding, L. Yang, M. Zhang, W. Jiang, Z. Zhao, H. Li, Hydrophobic mesoporous silica-supported heteropoly acid induced by ionic liquid as a high efficiency catalyst for the oxidative desulfurization of fuel, *RSC Adv.* 5 (22) (2015) 16847–16855.
- [67] B. Wang, J. Zhang, X. Zou, H. Dong, P. Yao, Selective oxidation of styrene to 1, 2-epoxyethylbenzene by hydrogen peroxide over heterogeneous phosphomolybdic acid supported on ionic liquid modified MCM-41, *Chem. Eng. J.* 260 (2015) 172–177.
- [68] Y.-L. Cao, L. Wang, B.-H. Xu, S.-J. Zhang, The chitin/Keggin-type heteropoly acid hybrid microspheres as catalyst for oxidation of methacrolein to methacrylic acid, *Chem. Eng. J.* 334 (2018) 1657–1667.
- [69] S. Vedachalam, P. Boahene, A.K. Dalai, Oxidative desulfurization of heavy gas oil over a Ti-TUD-1-supported Keggin-type molybdenum heteropoly acid, *Energy Fuel* 34 (12) (2020) 15299–15312.
- [70] Y. Gao, Z. Liu, G. Hu, R. Gao, J. Zhao, Design and synthesis heteropoly acid modified mesoporous hybrid material CNTs@ MOF-199 catalyst by different methods for extraction-oxidation desulfurization of model diesel, *Microporous Mesoporous Mater.* 291 (2020) 109702.
- [71] K. Darvishi, K. Amani, M. Rezaei, Preparation, characterization and heterogeneous catalytic applications of GO/Fe<sub>3</sub>O<sub>4</sub>/HPW nanocomposite in chemoselective and green oxidation of alcohols with aqueous H<sub>2</sub>O<sub>2</sub>, *Appl. Organomet. Chem.* 32 (5) (2018), e4323.
- [72] P. Huang, A. Liu, L. Kang, M. Zhu, B. Dai, Heteropoly acid supported on sodium dodecyl benzene sulfonate modified layered double hydroxides as catalysts for oxidative desulfurization, *New J. Chem.* 42 (15) (2018) 12830–12837.
- [73] H. Wang, C. Wang, M. Zhao, Y. Yang, L. Fang, Y. Wang, H<sub>3</sub>PMo<sub>10</sub>V<sub>2</sub>O<sub>40</sub> anchor by OH of the Titania nanotubes: highly efficient heterogeneous catalyst for the direct hydroxylation of benzene, *Chem. Eng. Sci.* 177 (2018) 399–409.
- [74] M.B.C. Migliorero, V. Palermo, G.P. Romanelli, P.G. Vázquez, New niobium heteropoly acid included in a silica/alumina matrix: application in selective sulfoxidation, *Catal. Today* 372 (2020) 89–97.
- [75] X. Han, Y. Kuang, C. Xiong, X. Tang, Q. Chen, C.-T. Hung, L.-L. Liu, S.-B. Liu, Heterogeneous amino acid-based tungstophosphoric acids as efficient and recyclable catalysts for selective oxidation of benzyl alcohol, *Korean J. Chem. Eng.* 34 (7) (2017) 1914–1923.
- [76] M. Palacio, P.I. Villabrille, V. Palermo, G.P. Romanelli, Titania- heteropoly acid composites (TiO<sub>2</sub>-HPA) as catalyst for the green oxidation of trimethylphenol to 2, 3, 5-trimethyl-p-benzoquinone, *J. Sol-Gel Sci. Technol.* (2020) 1–11.
- [77] J. Li, Z. Yang, G. Hu, J. Zhao, Heteropoly acid supported MOF fibers for oxidative desulfurization of fuel, *Chem. Eng. J.* 388 (2020) 124325.
- [78] D.-J. Yuan, J. Yang, A.M. Hengne, Y.-T. Lin, C.-Y. Mou, K.-W. Huang, Mesoporous silica-supported V-substituted heteropoly acid for efficient selective conversion of glycerol to formic acid, *J. Saudi Chem. Soc.* 24 (1) (2020) 1–8.
- [79] Y.-L. Cao, L. Wang, Y.-G. Bai, R.-Y. Yan, B.-H. Xu, Molybdovanadophosphoric heteropoly acid-catalyzed aerobic oxidation of methacrolein: the crucial role of ionic liquid as a modifier, *Catal. Lett.* 150 (6) (2020) 1774–1785.

- [80] S.M. Hassan, A.I. Ahmed, M.A. Mannaa, Surface acidity, catalytic and photocatalytic activities of new type  $H_3PW_{12}O_{40}/Sn-TiO_2$  nanoparticles, *Colloids Surf. A Physicochem. Eng. Asp.* 577 (2019) 147–157.
- [81] F. Pomilla, M. Bellardita, E. Garcia Lopez, G. Marci, L. Palmisano, Photocatalytic conversion of glucose in aqueous suspensions of heteropoly acid- $TiO_2$  composites, in: *FINECAT 2015 Symposium on Heterogeneous Catalysis for Fine Chemicals*, 2015, pp. 67–68.
- [82] X. Yu, V. De Waele, A. Löfberg, V. Ordonsky, A.Y. Khodakov, Selective photocatalytic conversion of methane into carbon monoxide over zinc- heteropoly acid -titania nanocomposites, *Nat. Commun.* 10 (1) (2019) 1–10.
- [83] M. Taghavi, M.H. Ehrampoush, M.T. Ghaneian, M. Tabatabaee, Y. Fakhri, Application of a Keggin-type heteropoly acid on supporting nanoparticles in photocatalytic degradation of organic pollutants in aqueous solutions, *J. Clean. Prod.* 197 (2018) 1447–1453.
- [84] R. Tayebee, E. Esmaili, B. Maleki, A. Khoshniat, M. Chahkandi, N. Mollania, Photodegradation of methylene blue and some emerging pharmaceutical micropollutants with an aqueous suspension of  $WZnO-NH_2@H_3PW_{12}O_{40}$  nanocomposite, *J. Mol. Liq.* 317 (2020) 113928.
- [85] C. Wang, Y. Ma, J. Lang, Z. Chai, G. Li, X. Wang, A novel heterogeneous photocatalyst for Cr(VI) reduction via planting silicotungstic acid on the surface of calcium tantalate, *Mol. Catal.* 455 (2018) 48–56.
- [86] H. Fakhri, A.R. Mahjoub, H. Aghayan, Effective removal of methylene blue and cerium by a novel pair set of heteropoly acids based functionalized graphene oxide: adsorption and photocatalytic study, *Chem. Eng. Res. Des.* 120 (2017) 303–315.
- [87] M. Taghavi, M. Tabatabaee, M.H. Ehrampoush, M.T. Ghaneian, M. Afsharnia, A. Alami, J. Mardaneh, Synthesis, characterization and photocatalytic activity of  $TiO_2/ZnO$ -supported phosphomolybdic acid nanocomposites, *J. Mol. Liq.* 249 (2018) 546–553.
- [88] S. Sampurnam, T. Dhanasekaran, A. Padmanaban, S. Muthamizh, D. Latha, G. Gnanamoorthy, S. Munusamy, V. Narayanan, Synthesis, characterization and heterogeneous photocatalytic activity of  $H_3PW_{12}O_{40}/TiO_2/Ag$  composites, *Mater. Today* 5 (2) (2018) 8808–8811.
- [89] M. Taghavi, M.T. Ghaneian, M.H. Ehrampoush, M. Tabatabaee, M. Afsharnia, A. Alami, J. Mardaneh, Feasibility of applying the LED-UV-induced  $TiO_2/ZnO$ -supported  $H_3 PMo_{12}O_{40}$  nanoparticles in photocatalytic degradation of aniline, *Environ. Monit. Assess.* 190 (4) (2018) 1–10.
- [90] G. Marci, E. García-López, V. Vaiano, G. Sarno, D. Sannino, L. Palmisano, Keggin heteropoly acids supported on  $TiO_2$  used in gas-solid (photo) catalytic propene hydration and in liquid-solid photocatalytic glycerol dehydration, *Catal. Today* 281 (2017) 60–70.
- [91] M. Saghi, K. Mahanpoor, Photocatalytic degradation of tetracycline aqueous solutions by nanospherical  $\alpha-Fe_2O_3$  supported on 12-tungstosilicic acid as catalyst: using full factorial experimental design, *Int. J. Ind. Chem.* 8 (3) (2017) 297–313.
- [92] G.R. Bertolini, L.R. Pizzio, A. Kubacka, M.J. Muñoz-Batista, M. Fernández-García, Composite  $H_3PW_{12}O_{40}/TiO_2$  catalysts for toluene selective photo-oxidation, *Appl. Catal. B Environ.* 225 (2018) 100–109.
- [93] S. Mohammadghasemi-Samani, M. Taghdiri, Facile synthesis of hexamine-silicotungstic acid hybrid and its photocatalytic activity toward degradation of dyes, *Int. J. Environ. Sci. Technol.* 14 (10) (2017) 2093–2108.
- [94] Y. Sun, P. Meng, X. Liu, Self-assembly of tungstophosphoric acid/acidified carbon nitride hybrids with enhanced visible-light-driven photocatalytic activity for the degradation of imidacloprid and acetamiprid, *Appl. Surf. Sci.* 456 (2018) 259–269.

- [95] A. Ayati, B. Tanhaei, F.F. Bamoharram, A. Ahmadpour, P. Maydannik, M. Sillanpää, Photocatalytic degradation of nitrobenzene by gold nanoparticles decorated polyoxometalate immobilized TiO<sub>2</sub> nanotubes, *Sep. Purif. Technol.* 171 (2016) 62–68.
- [96] S. Farhadi, M.M. Amini, F. Mahmoudi, Phosphotungstic acid supported on aminosilica functionalized perovskite-type LaFeO<sub>3</sub> nanoparticles: a novel recyclable and excellent visible-light photocatalyst, *RSC Adv.* 6 (105) (2016) 102984–102996.
- [97] P. Meng, H. Heng, Y. Sun, J. Huang, J. Yang, X. Liu, Positive effects of phosphotungstic acid on the in-situ solid-state polymerization and visible light photocatalytic activity of polyimide-based photocatalyst, *Appl. Catal. B Environ.* 226 (2018) 487–498.
- [98] S. Yao, X. Wang, M. Guo, Z. Shi, Preparation and photocatalytic activity of mesoporous TiO<sub>2</sub> photocatalyst co-doped with Fe and H<sub>3</sub>PW<sub>12</sub>O<sub>40</sub>, *J. Chin. Chem. Soc.* 62 (2) (2015) 163–169.
- [99] S.R. Koochi, S. Allahyari, D. Kahforooshan, N. Rahemi, M. Tasbihi, Natural minerals as support of silicotungstic acid for photocatalytic degradation of methylene blue in wastewater, *J. Inorg. Organomet. Polym. Mater.* 29 (2) (2019) 365–377.
- [100] C.L. Marchena, L. Lericci, S. Renzini, L. Pierella, L. Pizzio, Synthesis and characterization of a novel tungstosilicic acid immobilized on zeolites catalyst for the photodegradation of methyl orange, *Appl. Catal. B Environ.* 188 (2016) 23–30.
- [101] W. Zhu, Enhanced photocatalytic activity of solar light driven ZnS composites incorporated with phosphotungstic acid, *Solid State Sci.* (2020) 106406.
- [102] M. Moosavifar, S. Bagheri, Photocatalytic performance of H<sub>6</sub>P<sub>2</sub>W<sub>18</sub>O<sub>62</sub>/TiO<sub>2</sub> nanocomposite encapsulated into beta zeolite under UV irradiation in the degradation of methyl orange, *Photochem. Photobiol.* 95 (2) (2019) 532–542.
- [103] S.-J. Yang, Y.-L. Xu, W.-P. Gong, Y.-K. Huang, G.-H. Wang, Y. Yang, C.-Q. Feng, Photocatalytic degradation of organic dyes with H<sub>3</sub>PW<sub>12</sub>O<sub>40</sub>/TiO<sub>2</sub>-SiO<sub>2</sub>, *Rare Metals* 35 (10) (2016) 797–803.
- [104] M. Moosavifar, M. Jafarbahmani, Synthesis characterization and investigation of photocatalytic activity of H<sub>3</sub>PMO<sub>12</sub>O<sub>40</sub>/TiO<sub>2</sub>/HY nanocomposite for degradation of methyl orange in aqueous media, *Mod. Chem. Appl.* 5 (205) (2017) 2.
- [105] G. Liu, Y. Zhang, L. Xu, B. Xu, F. Li, A PW<sub>12</sub>/Bi<sub>2</sub>WO<sub>6</sub> composite photocatalyst for enhanced visible light photocatalytic degradation of organic dye pollutants, *New J. Chem.* 43 (8) (2019) 3469–3475.

## Chapter 4

# Applications of heteropoly acids as homogeneous catalysts

### 4.1. Introduction

Development of new and safe materials with catalytic capabilities is an important objective in sustainable chemistry. Generally speaking, catalysts accelerate chemical reactions and enhance yields. Therefore, most organic transformations are attempted under catalytic conditions. Catalysis, as mentioned before, is the process of increasing the rate of a chemical reaction through a different mechanism by using a particular substance as a catalyst. The catalyst is not used up in the reaction and constantly continues to act [1, 2]. Sustainable chemistry, also referred to as green chemistry, is a field of chemistry particularly used in the chemical industry, which focuses on designing reactions and industrial processes to reduce or eliminate the usage and production of hazardous compounds [3]. Green chemistry has many advantages including human health, cleaner air, release of lower amounts of hazardous compounds to the air, and a decrease in consumption of toxic compounds [4].

Acid catalysis is one of the most attractive and prominent fields of catalysis; it has been extensively used in the chemical industry to produce a wide variety of chemical compounds [5–7]. However, traditional mineral acids (sulfuric acid, hydrofluoric acid, etc.) and Lewis acids (aluminum trichloride, boron trifluoride, etc.) are usually corrosive materials with hazardous properties which produce toxic and corrosive wastes [8]. Consequently, during previous decades, much attention was focused on developing green acid catalytic systems including solid acids and acidic ionic liquids [9–18]. In this regard, heteropoly acids and related polyoxometalate compounds have been among the most considerable candidates for both academia and industry because of their structural variety and wide applications in fields such as material chemistry [19–21], energy sciences [22, 23], carbon dioxide chemistry [24–28], pharmaceuticals [29], and catalyzed processes [30–39].

Among solid catalysts, heteropoly acids are excellent candidates due to their exceptional architectures and prominent chemico-physical properties such as strong Brønsted acidity, fast multielectron transfer, high proton mobility, and high solubility in a wide variety of solvents [40, 41].

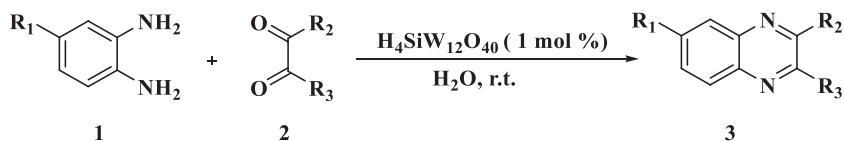


From a technological point of view, heteropoly acids may be appropriately used instead of traditional acid catalysts such as ion exchange resins, mineral acids, or zeolites in both homogeneous and heterogeneous catalytic processes [42–44]. It is important to note that their use in homogeneous systems is not an obstacle to reuse. Heteropoly acids are extensively soluble in polar solvents, but they are not soluble in nonpolar solvents such as hydrocarbons. Therefore, heteropoly acids can be recovered from a polar organic solvent by precipitation using a nonpolar solvent without any neutralization [45–48].

## 4.2. Synthesis of heterocycles

Heterocyclic rings are pervasively present in bioactive compounds and pharmaceutical agents [49–52]. Accordingly, synthetic chemists remain interested in synthesis and functionalization of heterocyclic rings.

Huang and others [53] reported that Keggin-type heteropoly acids had turned out to be reusable efficient catalysts for the synthesis of biologically active derivatives of quinoxaline **3**. The route included the condensation of a 1,2-diamine **1** with a 1,2-dicarbonyl compound **2** in water, resulting in compound **3** in excellent yields (Scheme 4.1). This method afforded a new efficient protocol in view of the small amount of catalyst and wide variety of substrates, as well as easy workup. The inexpensive Keggin-type heteropoly acid  $\text{H}_4\text{SiW}_{12}\text{O}_{40}$  was used and proved to be a reusable, noncorrosive, easy-to-handle, and environmentally friendly catalyst for this synthesis.

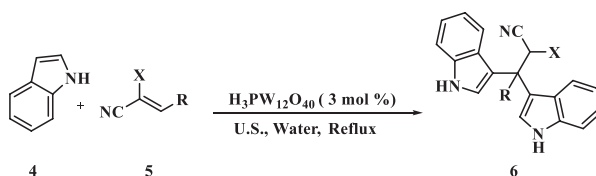


$\text{R}_1 = \text{H, Me, Cl, NO}_2$

$\text{R}_2, \text{R}_3 = \text{C}_6\text{H}_5, 4\text{-MeC}_6\text{H}_4, \text{Me, Furyl}$

**SCHEME 4.1** Synthesis of quinoxaline derivatives catalyzed by a heteropoly acid.

In 2015, Amrollahi and coworkers [54] reported the reaction of indole **4** with electron-deficient alkenes **5** at  $90^\circ\text{C}$  under conventional and ultrasound irradiation conditions, leading to the rapid synthesis of bis(indole) derivatives **6** in satisfactory yields (Scheme 4.2). Notably, the abovementioned reaction was catalyzed by 12-tungstophosphoric acid ( $\text{H}_3\text{PW}_{12}\text{O}_{40}$ ) in aqueous media. The reaction is operationally simple and complies with green chemistry principles by evading toxic catalysts and solvents.



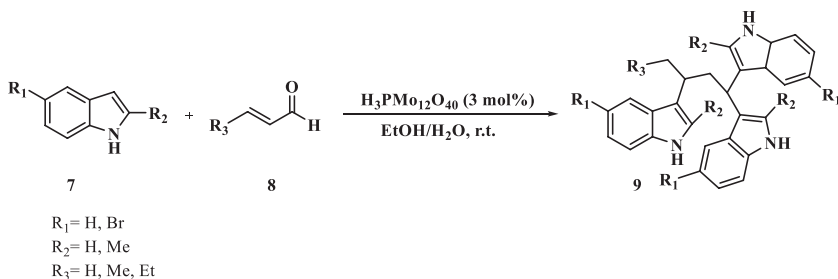
X= CN, CO<sub>2</sub>Me, CO<sub>2</sub>Et

R= C<sub>6</sub>H<sub>5</sub>, 4-NO<sub>2</sub>C<sub>6</sub>H<sub>4</sub>, 2-FC<sub>6</sub>H<sub>4</sub>, 4-FC<sub>6</sub>H<sub>4</sub>, 4-ClC<sub>6</sub>H<sub>4</sub>, 4-MeOC<sub>6</sub>H<sub>4</sub>, 3,4-diMeOC<sub>6</sub>H<sub>3</sub>, 4-HOC<sub>6</sub>H<sub>4</sub>, 4MeC<sub>6</sub>H<sub>4</sub>, 4-iPrC<sub>6</sub>H<sub>4</sub>

**SCHEME 4.2** Synthesis of bis(indole) derivatives in the presence of H<sub>3</sub>PW<sub>12</sub>O<sub>40</sub>.

This reaction is believed to proceed via the Michael reaction of indole using various electron-deficient alkenes. In fact, ultrasound irradiation accelerated this reaction. This strategy also accommodates both electron-releasing and electron-withdrawing substituents in benzaldehydes. In all cases, the reactions proceeded smoothly under reflux and mild conditions to give the respective products in respectable yields. The structures of the products were elucidated by <sup>1</sup>H- and <sup>13</sup>C-NMR, IR spectroscopy and elemental analysis. Under already secured optimal reaction conditions, 2-(pyridylmethylene) malononitriles, or 3-(pyridyl)acrylates as electron-deficient alkenes, were reacted with indole to furnish the corresponding bis(indole) derivatives. The reaction progressed effectively as expected to give the satisfactory yields of the corresponding products.

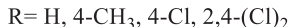
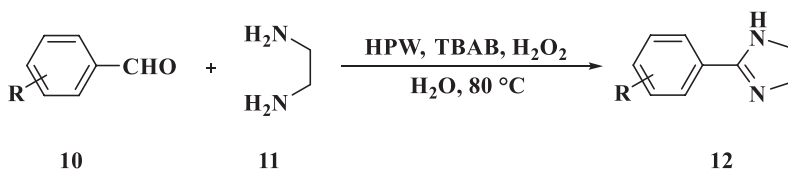
A one-pot green reaction was reported by Zakeri and coworkers [55] for the synthesis of 1,1,3-triheteroaryl compounds **9** from indoles **7** and α,β-unsaturated carbonyl compounds **8** with a heteropoly acid as a reusable catalyst (Scheme 4.3). This procedure afforded the target products in excellent yields (60%–80%). In the presence of a catalytic amount of H<sub>3</sub>PMo<sub>12</sub>O<sub>40</sub> in EtOH/H<sub>2</sub>O, the procedure took a green, mild course. The Keggin heteropoly acid catalyst was reusable for a minimum of four times and mainly remained intact without a notable change in its catalytic activity and chemical structure. Simplicity, recyclability of the catalyst, environmental friendliness, and easy implementation of the reaction indicate the potential of this procedure as a real alternative to the conventional protocol. It is therefore hoped that this eco-efficient, green protocol will be of great value to medicinal and synthetic chemistry.



**SCHEME 4.3** Synthesis of 1,1,3-triheteroaryl derivatives in the presence of H<sub>3</sub>PMo<sub>12</sub>O<sub>40</sub>.

In order to demonstrate the generality of this method, the authors employed a variety of appropriate substrates. Using different  $\alpha$ - and  $\beta$ -enals and indols, the reactions afforded the desired products under optimized reaction conditions. A plethora of 1,1,3-triheteroaryl compounds were produced in satisfactory yields using this procedure.

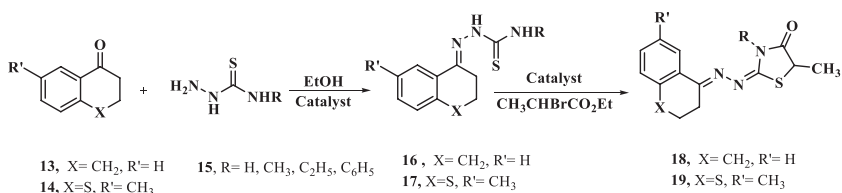
Liu's research group [56] reported an environmentally benign and economical one-pot synthetic method for a wide variety of 2-substituted imidazolines **12** from aromatic aldehydes **10**, ethylenediamine **11**, and hydrogen peroxide as an oxidant in aqueous media. 12-Tungstophosphoric acid (HPW) turned out to accelerate this reaction as it possesses catalytic and oxidative nature (Scheme 4.4). Notably, the efficiency of the transformation was improved upon further combination of tetrabutylammonium bromide (TBAB). The yields of the 2-substituted imidazolines were considerably affected by the nature and position of the substituents on the aromatic ring.



**SCHEME 4.4** Synthesis of 2-substituted imidazolines from aromatic aldehydes and ethylenediamine.

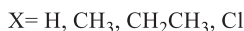
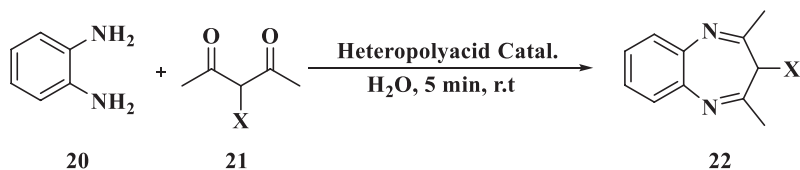
To assess the adaptability of this catalytic system, a number of aromatic aldehydes were examined with ethylenediamine under the identical reaction conditions. Either aldehydes with electron-withdrawing substituents or the ones with electron-releasing substituents smoothly underwent the reaction to afford the corresponding products in satisfactory yields. The important merits of this method were excellent efficiency, as well as availability, use of green solvents, and inexpensive reagents.

Sadou and coworkers [57] described a two-step procedure for the synthesis of thiazolidin-4-ones **18** and **19** from  $\alpha$ -tetralone **13** or thiochroman-4-one **14** in the presence of an acid catalyst.  $\alpha$ -Tetralone **13** or thiochroman-4-one **14** reacted with substituted thiosemicarbazides **15** to produce thiosemicarbazones **16** and **17** in high yields. The reaction was catalyzed by the Keggin-type heteropoly acid (H<sub>4</sub>SiW<sub>12</sub>O<sub>40</sub>·nH<sub>2</sub>O) or AcOH. Then, condensation of compounds **16** and **17** with  $\alpha$ -bromoester catalyzed by the same heteropoly acid or sulfuric acid in ethanol or acetonitrile resulted in the formation of thiazolidin-4-ones **18** and **19** (Scheme 4.5). Catalytic amounts of the heteropoly acid could replace strong acids in the synthesis of heterocyclic compounds. The method afforded easy access to thiazolidin-4-one in relatively short times.

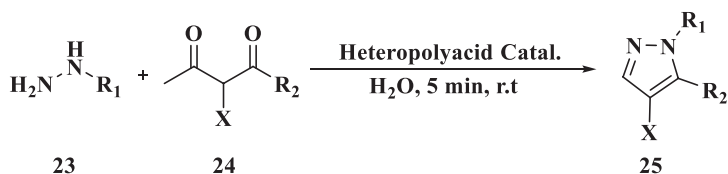


**SCHEME 4.5** Synthesis of thiosemicarbazones and thiazolidine-4-ones.

Gharib and coworkers [58] studied the catalytic efficiency of Preyssler ( $H_{14}[NaP_5W_{30}O_{110}]$ ), Wells-Dawson ( $H_6[P_2W_{18}O_{62}]$ ), and Keggin ( $H_3[PW_{12}O_{40}]$ ) and  $H_4[PMo_{11}VO_{40}]$ , heteropoly acids separately in the synthesis of diazepines **22** and pyrazoles **25** through the condensation of diamines **20**, hydrazines, and hydrazides **23** with different 1,3-diketones **21** and **24** (Schemes 4.6 and 4.7). In all cases, they obtained the best yields using the Preyssler heteropoly acid, i.e.,  $H_{14}[NaP_5W_{30}O_{110}]$ . In this work, the authors studied the synthesis of benzodiazepines with  $H_{14}[NaP_5W_{30}O_{110}]$ ,  $H_6[P_2W_{18}O_{62}]$ , and  $H_4[PMo_{11}VO_{40}]$ . Then, they extended their studies to the synthesis of a variety of diazepines through the condensation of diamines with different 1,3-diketones in aqueous media. For instance, 1,2-phenylenediamine was reacted with many 1,3-diketones to afford diazepines in a single step in excellent yields. The reaction progressed within 5 min at room temperature. The synthesis of pyrazoles and diazepines through condensation of hydrazines, hydrazides, and diamines with different 1,3-diketones in the presence of  $H_{14}[NaP_5W_{30}O_{110}]$  led to eminent results, providing a greener and more efficient approach for the synthesis of pyrazoles and diazepines. The reaction completed in 5 min at ambient temperature and might be useful in rapid drug discovery as pyrazoles and diazepines are pharmaceutically active agents. An inexpensive agent,  $H_{14}[NaP_5W_{30}O_{110}]$  might be used as a recyclable and ecofriendly catalyst. The results also indicated that temperature, reaction time, and solvent types were determining factors. The catalysts used in the homogeneous phase could be recovered and reused without any appreciable loss in their activity and change in structure.



**SCHEME 4.6** Synthesis of benzodiazepines through condensation of diamines with different 1,3-diketones in aqueous media.



$\text{R}_1 = \text{CO}$ -thirnyl,  $\text{CO}$ -furyl,  $\text{C}_6\text{H}_5$ , 4- $\text{ClC}_6\text{H}_4$ ,  $\text{COC}_6\text{H}_5$

$\text{X} = \text{H}$ ,  $\text{CH}_2\text{CH}_3$ ,  $\text{Cl}$

$\text{R}_2 = \text{CH}_3$ ,  $\text{OCH}_2\text{CH}_3$

**SCHEME 4.7** Synthesis of pyrazole using heteropoly acid catalysts in water.

Glycerol is being produced on a large scale as a biodiesel coproduct. Consequently, it has been highly relevant to develop procedures for its conversion to more valuable products. Glycerol ketals are among chemicals proved to be useful as fragrance ingredients, synthetic intermediates, and, more importantly, bio additives for gasoline and diesel. Glycerol ketals have been produced via reactions catalyzed by mineral acids.

Da Silva and coworkers [59] evaluated the catalytic activity of the heteropoly acid  $\text{H}_3\text{PW}_{12}\text{O}_{40}$  in ketalization of glycerol with various ketones in the absence of auxiliary solvents at ambient temperature (Table 4.1). The influences of reaction parameters such as the stoichiometry of the reactants, reaction temperature, and catalyst concentration, as well as the type of the carbonylic reactant, were studied. Regardless of the ketone used,  $\text{H}_3\text{PW}_{12}\text{O}_{40}$  was demonstrated to have far more activity than other Brønsted acid catalysts (e.g., sulfuric acid, *p*-toluene sulfonic acid,  $\text{H}_4\text{SiW}_{12}\text{O}_{40}$  or  $\text{H}_3\text{PMo}_{12}\text{O}_{40}$ ). It also showed higher selectivity for five-membered (1,3-dioxolane) cyclic ketals relative to Brønsted acid catalysts. The heteropoly acid catalyst was recoverable and reusable without losing activity although it was homogeneous.

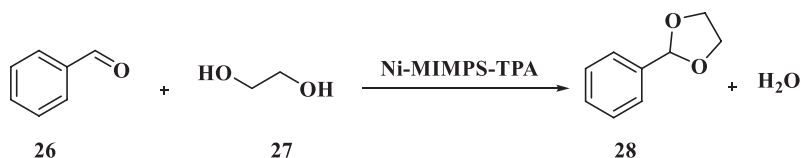
Previously, acid functionalized solid catalytic materials had been used in the solvent-free ketalization of glycerol with propanone to afford solketal (2,2-dimethyl-1,3-dioxolane-4-methanol). However, the reaction mixture was heated to the temperature of propanone reflux. In their work, the authors extended the reaction to other ketones. Aliphatic ketones with carbon chain containing more than five carbon atoms, in contrast to cyclic ketones, were immiscible with glycerol. This made it difficult to determine the conversion extent and provide the corresponding kinetic curves. Cyclohexanone exhibited high reactivity and was totally converted to the related ketal (i.e., 1,4-dioxaspiro [4.5] decane-2-yl) methanol) (Table 4.1). Although conversion was not assessed, the ketals formed in these reactions were soluble and could be detected by GC or GC-MS analyses. In general, regardless of the ketone structure, the reaction was selective.

Han's research group [60] used a series of transition-metal (manganese, iron, cobalt, nickel, and copper) ion-exchanged ionic liquid catalysts based on tungstophosphoric acid (TPA) synthesized by incorporating the metal and

**TABLE 4.1** Effect of ketone nature on solvent-free ketalization of  $H_3PW_{12}O_{40}$ -catalyzed glycerol.

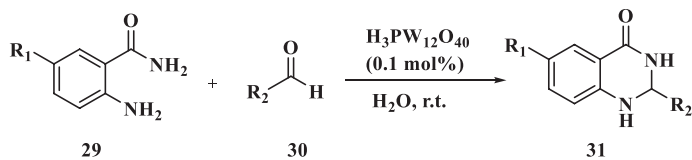
Run	Ketone	Conv.%	Ketal Select.%	Ketal
1	Propanone	90	97	
2	Butanone	74	99	
3	Cyclohexanone	98	99	
4	Cyclopentanone	88	95	
5	4-Methyl-2-pentanone	–	47 45	 (trans)   (cis)
6	2,4-Dimethyl-3-pentanone	–	78	

methylimidazolium propyl sulfobetaine (MIMPS) zwitterionic precursors onto TPA to catalyze the acetalization of benzaldehyde with ethylene glycol **27** (Scheme 4.8). The inorganic/organic composite catalysts prepared in this work proved to be useful for heterogeneous/homogeneous catalysis. These water-soluble M-MIMPS-TPA composite salts not only are strong Brønsted/Lewis acids but also demonstrate an unparalleled self-separation property, which is desirable for separating and recycling the catalyst. The high catalytic activities of these novel M-MIMPS-TPA catalysts observed in acetalization reactions were ascribed to their strong Brønsted/Lewis acidity, and low resistance against mass transport. The Ni[MIMPSH]PW<sub>12</sub>O<sub>40</sub> catalyst exhibited an unusual catalytic performance and durability with benzaldehyde glycol acetal selectivity of 99.0% and a yield of 94.6%, which strongly agreed with the results from response surface methodology. A more detailed kinetic analysis resulted in an activation energy of 34.11 kJ/mol for the acetalization reaction, which surpassed most of the reported catalysts. These eco-friendly and potent catalysts, with beneficial properties for product separation and catalyst recycling, will make catalytic conversions of biomass cost-effective.



**SCHEME 4.8** Preparation of benzaldehyde ethylene glycol acetal via the acid-catalyzed acetalization of benzaldehyde with ethylene glycol.

Zong and coworkers [61] reported that heteropoly acid, H<sub>3</sub>PW<sub>12</sub>O<sub>40</sub> (0.1 mol%) effectively catalyzed the cyclocondensation reaction of anthranilamide **29** with aldehydes **30** in water at room temperature to give the corresponding 2,3-dihydro-4(1*H*)-quinazolinones **31** in satisfactory to excellent yields (Scheme 4.9). Utilizing a small quantity of the catalyst and a simple workup procedure, mild reaction conditions along with clean reaction profiles were established.



R<sub>1</sub> = H, Cl

R<sub>2</sub> = C<sub>6</sub>H<sub>5</sub>, *P*-(CH<sub>3</sub>O)C<sub>6</sub>H<sub>4</sub>, *P*-(CH<sub>3</sub>)C<sub>6</sub>H<sub>4</sub>, 2,3,4,-(CH<sub>3</sub>O)<sub>3</sub>C<sub>6</sub>H<sub>2</sub>, *P*-(Cl)C<sub>6</sub>H<sub>4</sub>, 2,4-(CH<sub>3</sub>O)<sub>2</sub>C<sub>6</sub>H<sub>3</sub>, *P*-(F)C<sub>6</sub>H<sub>4</sub>, *P*-(NO<sub>2</sub>)C<sub>6</sub>H<sub>4</sub>, *O*-(CH<sub>3</sub>O)C<sub>6</sub>H<sub>4</sub>, 2-furyl, 2-thiazolyl,

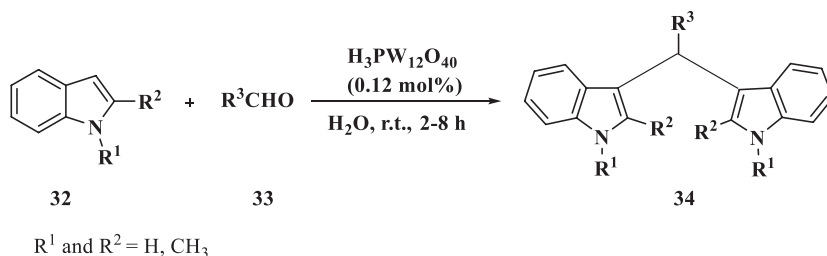
**SCHEME 4.9** Condensation of anthranilamide with aromatic aldehydes catalyzed by a heteropoly acid.



This result attracted the attention of the authors to the reactions of other aldehydes, so that they could build the generality of the process. A series of aldehydes with either electron-releasing or electron-withdrawing groups attaching to the aromatic ring were investigated. As expected, the substituted groups on the aromatic ring had no apparent effect on the yield. On the other hand, upon replacing aromatic aldehydes with aromatic heterocyclic aldehydes, the corresponding products were resulted in excellent yields. However, the steric effects observed for the aldehydes might have played an important role and led to moderate yields of the products. Although the aldehydes and amines had low solubility in water, the cyclocondensation reactions catalyzed by  $\text{H}_3\text{PW}_{12}\text{O}_{40}$  still proceeded effectively at room temperature. The reaction likely took place at the organic phase/aqueous phase interface with water in the heterogeneous system. Vigorous stirring was found to be necessary for these reactions to progress successfully.

Among the other advantages of the procedure were low loading of catalyst, enhanced yields, and clean reactions, which made it a desirable strategy for the synthesis of solid chemicals. In addition, as the procedure has quite an easy workup, it does not require organic solvents. When the products were solid and insoluble in water, the pure products were obtainable directly by filtration and simple washing of the filtrate with water and recrystallization from ethanol or column chromatography.

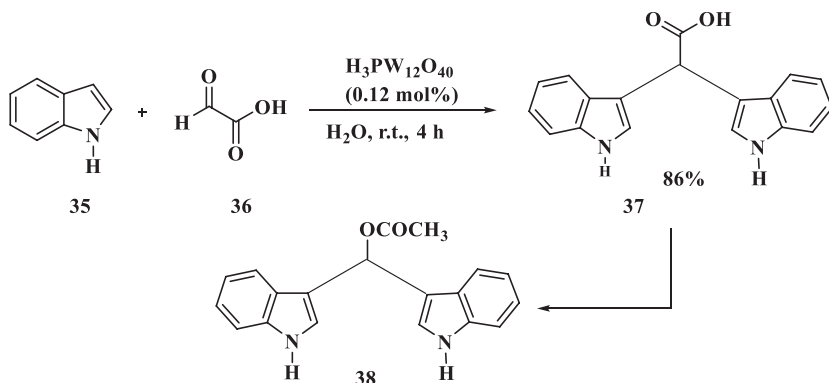
Azizi and coworkers [62] demonstrated that heteropoly acids were able to catalyze the electrophilic substitutions of indole and substituted indoles **32** with various aldehydes and ketones **33** in water to give bis(indolyl) methanes **34** at ambient temperature in very good yields. In addition, the methodology was highly chemoselective for aldehydes (Scheme 4.10). As shown in Table 4.2,  $\text{H}_3\text{PMo}_{12}\text{O}_{40}$  and  $\text{H}_3\text{PW}_{12}\text{O}_{40}$  were found to provide the same results in water and other solvents. The electrophilic reaction of indole **35** was conducted with glyoxylic acid **36** (50% aqueous solution), and the product was obtained in satisfactory yields under the reaction conditions (Scheme 4.11).



**SCHEME 4.10** Electrophilic substitutions of indoles to give a series of bis(indolyl)methanes.

**TABLE 4.2** Effects of different heteropoly acids and solvents on electrophilic substitution of indoles.

Entry	Catalyst (mol%)	Solvent (2 mL)	Yield%	Time (h)
1	None	H <sub>2</sub> O	5	1
2	H <sub>3</sub> PMo <sub>12</sub> O <sub>40</sub> (0.12)	H <sub>2</sub> O	86	1
3	H <sub>3</sub> PW <sub>12</sub> O <sub>40</sub> (0.12)	H <sub>2</sub> O	90	1
4	H <sub>3</sub> PMo <sub>12</sub> O <sub>40</sub> (0.12)	THF	90	6
5	H <sub>3</sub> PW <sub>12</sub> O <sub>40</sub> (0.12)	THF	90	6
6	H <sub>3</sub> PMo <sub>12</sub> O <sub>40</sub> (0.12)	CH <sub>3</sub> CN	85	3
7	H <sub>3</sub> PW <sub>12</sub> O <sub>40</sub> (0.12)	CH <sub>3</sub> CN	90	3
8	H <sub>3</sub> PMo <sub>12</sub> O <sub>40</sub> (0.12)	CH <sub>2</sub> Cl <sub>2</sub>	88	2
9	H <sub>3</sub> PW <sub>12</sub> O <sub>40</sub> (0.12)	CH <sub>2</sub> Cl <sub>2</sub>	90	2
10	H <sub>3</sub> PMo <sub>12</sub> O <sub>40</sub> (0.12)	ClC <sub>2</sub> H <sub>4</sub> Cl	86	2
11	H <sub>3</sub> PW <sub>12</sub> O <sub>40</sub> (0.12)	ClC <sub>2</sub> H <sub>4</sub> Cl	88	2
12	ZnCl <sub>2</sub> (5)	H <sub>2</sub> O	45	1
13	RuCl <sub>3</sub> (1)	H <sub>2</sub> O	48	1
14	H <sub>2</sub> SO <sub>4</sub> (1)	H <sub>2</sub> O	55	1
15	HClO <sub>4</sub> (1)	H <sub>2</sub> O	74	1
16	CeCl <sub>3</sub> ·7H <sub>2</sub> O (5)	H <sub>2</sub> O	58	1
17	WCl <sub>6</sub> (1)	H <sub>2</sub> O	60	1

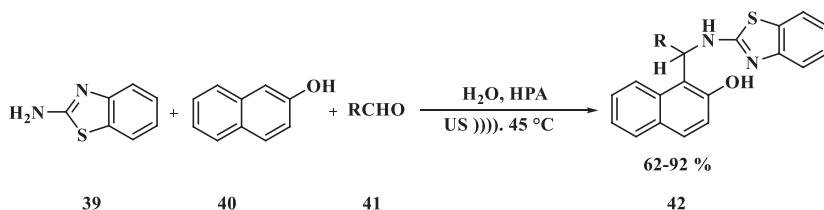


**SCHEME 4.11** Electrophilic reaction of indole with glyoxylic acid.

### 4.3. Multicomponent reactions

Multicomponent reactions (MCRs) are regarded as a powerful, outstanding protocol for the synthesis of a wide variety of organic compounds. Compared with multistep reactions, several new bonds are formed simultaneously in a one-pot manner in such reactions. MCRs have other obvious advantages among which are low number of reaction and purification steps, selectivity, convergence, high atom economy, ease of operation, and synthetic efficiency [63, 64]. The development of multicomponent reactions has indeed resulted in novel and efficient synthetic routes to provide a wide variety of small organic molecules in fields such as modern organic, bio-organic, and medicinal chemistry [65, 66].

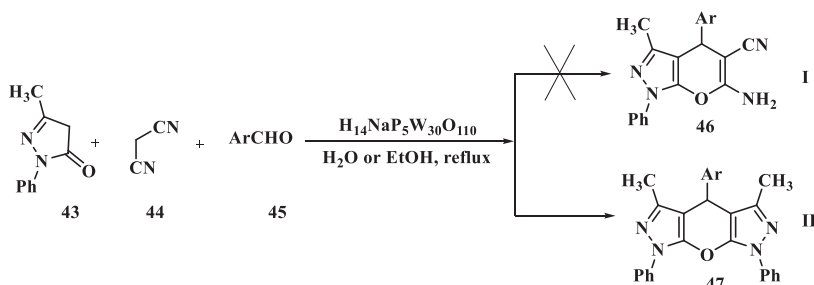
Javanshir et al. [67] reported a one-pot condensation of 2-aminobenzothiazole **39**, 2-naphthol **40**, and appropriate aldehydes **41** catalyzed by a Wells-Dawson type heteropoly in aqueous media that gave the Mannich adducts 2'-aminobenzothiazolomethylnaphthols **42** at 45°C under ultrasound irradiation. The reaction proceeded satisfactorily with both electron-withdrawing and electron-releasing groups to afford a variety of derivatives in yields of 62%–92% (Scheme 4.12).



R = 4-MeC<sub>6</sub>H<sub>4</sub>, 4-OMeC<sub>6</sub>H<sub>4</sub>, C<sub>6</sub>H<sub>5</sub>, 4-ClC<sub>6</sub>H<sub>4</sub>, 2-ClC<sub>6</sub>H<sub>4</sub>, 4-CNC<sub>6</sub>H<sub>4</sub>, 3-NO<sub>2</sub>C<sub>6</sub>H<sub>4</sub>, 4-BrC<sub>6</sub>H<sub>4</sub>, 2-OHC<sub>6</sub>H<sub>4</sub>, 2,4-(Cl)<sub>2</sub>C<sub>6</sub>H<sub>3</sub>, C<sub>6</sub>H<sub>5</sub>-C<sub>2</sub>H<sub>4</sub>, 4-OH, 3-OMeC<sub>6</sub>H<sub>3</sub>, 4-OME, 3-CH<sub>2</sub>OPh-C<sub>6</sub>H<sub>3</sub>, Furyl, Thiophenyl

**SCHEME 4.12** Synthesis of 2-aminobenzothiazolomethylnaphthols.

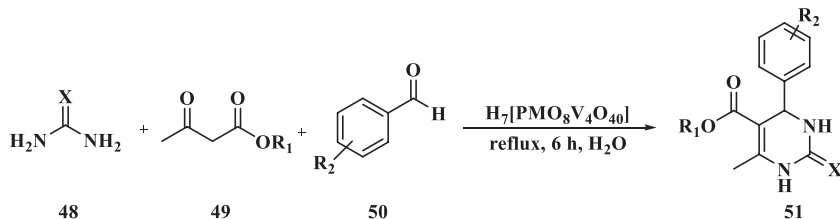
Heravi and others [68] examined the feasibility of using  $H_{14}NaP_5W_{30}O_{110}$  as a catalyst for the three-component synthesis of 1,4-dihydropyran[2,3-*c*] pyrazole derivatives **47** through the condensation of 3-methyl-1-phenyl-1H-pyrazol-5(4H)-one **43**, malononitrile **44** and various aldehydes **45** in water or ethanol under heating (Scheme 4.13). The reaction accommodated a variety of aryl groups with electron-releasing as well as electron-withdrawing substituents. However, diethylmalonate, ethylcyanoacetate, ethylbenzoylacetate, and acetophenone did not react under the mentioned conditions.



Ar = Ph, 3-NO<sub>2</sub>-Ph, 4-NO<sub>2</sub>-Ph, 4-MeO-Ph, 2-Cl-Ph, 4-Cl-Ph, 4-HO-Ph, 4-Me-Ph

**SCHEME 4.13** Synthesis of 1,4-dihydropyran[2,3-*c*] pyrazoles.

Gharib and others [69] reported the utilization of heteropoly acids as catalysts for the synthesis of a wide variety of substituted 3,4-dihydropyrimidin-2(1H)-ones **51** under Biginelli conditions in aqueous media (Scheme 4.14). The best results were obtained when urea (or thiourea) **48**, ethyl acetoacetate **49**, and aldehyde **50** were refluxed for 6 h in the presence of 0.03 mmol of the heteropoly acid as a catalyst and water as a green solvent. This method proved effective with various substituted aromatic aldehydes regardless of the nature of the substituents on the aromatic ring, demonstrating an improvement over the classical Biginelli methodology. However, relatively higher yields were obtained by substituents



X = O, S

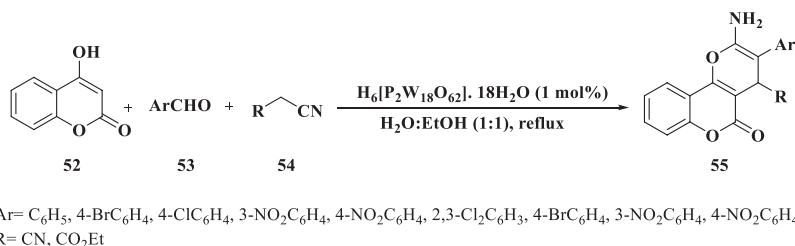
R<sub>1</sub> = H, 4-OMe, 4-NO<sub>2</sub>, 4-Cl

R<sub>2</sub> = C<sub>2</sub>H<sub>5</sub>, CH<sub>3</sub>

**SCHEME 4.14** Synthesis of various substituted 3,4-dihydropyrimidin-2(1H)-ones using heteropoly acid catalyst,  $H_7[PMO_8V_4O_{40}]$  in the presence of water as a green solvent and under reflux conditions.

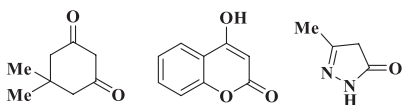
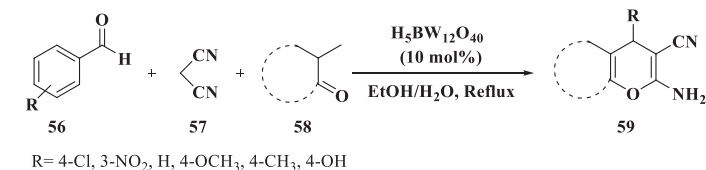
with electron-withdrawing groups. The reaction yields were greater in the presence of water, and the reaction times were generally shorter than those of conventional methods. The series of heteropoly acids  $H_{3+n}PMo_{12-n}V_nO_{40}$  ( $n=1-4$ ) exhibited satisfactory to excellent catalytic activities.

Heravi and coworkers [70] described the three-component synthesis of 2-amino-5-oxodihydropyrano[3,2-*c*]chromene derivatives **55** via the condensation of 4-hydroxycoumarin **52**, aldehydes **53**, and alkylnitriles **54** utilizing catalytic amounts of a heteropoly acid ( $H_6P_2W_{18}O_{62} \cdot 18H_2O$ ) in EtOH/ $H_2O$  under heating conditions (Scheme 4.15). In comparison with  $H_6P_2W_{18}O_{62} \cdot 18H_2O$ , the same reaction catalyzed by  $H_{14}[NaP_5W_{30}O_{110}]$  or  $NH_2SO_3H$  and refluxed in EtOH/ $H_2O$  (50:50) gave lower yields.



**SCHEME 4.15** Synthesis of 2-amino-4-aryl-3-cyano-5-oxo-4H,5H-pyrano-[3,2-*c*] chromenes in EtOH/ $H_2O$  using  $H_6P_2W_{18}O_{62} \cdot 18H_2O$  as a catalyst.

Heravi et al. [71] used a Keggin-type heteropoly acid,  $H_5BW_{12}O_{40}$  (BWA), with a higher negative charge and stronger Brønsted acidity than those of the Si or P analogues as a green, efficient, and reusable catalyst in a three-component procedure that involved the cyclocondensation of a variety of aromatic aldehydes **56**, differently substituted malononitrile **57** with  $\beta$ -dicarbonyl compounds **58** in aqueous ethanol for the easy, clean, and efficient synthesis of 4H-pyrans (**59**) (Scheme 4.16). The reactions were generally completed in short times and the products were obtained in satisfactory to excellent yields. The reaction medium was recyclable and reusable for several times without any loss in efficiency.

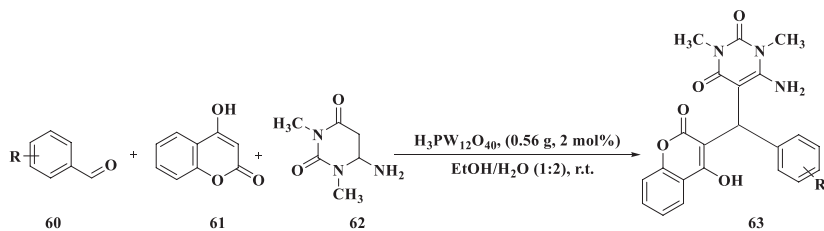


**SCHEME 4.16** Synthesis of 4H-pyran derivatives via one-pot, multicomponent reaction.

Heravi and others [71] revealed for the first time the application of a newly reported heteropoly acid,  $H_3BW_{12}O_{40}$ , serving as a green, efficient, and homogeneous yet reusable catalyst for the diversity-oriented synthesis of 4*H*-pyrans via a one-pot, three-component cyclocondensation reaction of aldehydes, malononitrile, and carbonyl compounds with a reactive  $\alpha$ -methylene group in the presence of BWA refluxed in EtOH/H<sub>2</sub>O. The reaction medium could be recycled and reused several times without any loss in efficiency.

The generality of the method was studied in the reactions of aldehydes with various substituents, containing either electron-releasing or electron-withdrawing functional groups in the *ortho*, *meta*, and *para* positions with malononitrile and either dimedone or 4-hydroxycoumarin or 3-methyl-4*H*pyrazole-5(4*H*)-one optimal reaction conditions under already secured. The desired 4*H*-pyran derivatives were achieved in satisfactory to excellent yields within relatively short times while no by-products were formed. For library validation, the authors also examined 4-hydroxycoumarin and 3-methyl-4*H*-pyrazole-5(4*H*)-one instead of dimedone to achieve the desired products in satisfactory to excellent yields.

Foroughi and coworkers [72] described an easy, highly efficient one-pot and three-component synthesis of derivatives of chromene pyrimidine-2,4-dione from available substrates catalyzed by a heteropoly acid ( $H_3PW_{12}O_{40}$ ). Their protocol included the reaction of diverse aldehydes (**60**), 4-hydroxycoumarin **61**, and 4-amino-1,3-dimethyluracil **62** in EtOH/H<sub>2</sub>O (1:2) at ambient temperature in the presence of  $H_3PW_{12}O_{40}$  as a powerful efficient catalyst to furnish the corresponding chromene pyrimidine-2,4-dione **63** in satisfactory to excellent yields (Scheme 4.17). Simplicity of operation, low cost, environmental eco-friendliness, facile workup and purification, short reaction times, excellent yields of products, green media, and mild reaction conditions were among the advantages of the protocol. The *in vitro* antibacterial activities of the products were obtained against *Staphylococcus aureus* (ATCC 6538) and *Escherichia coli* (ATCC 35218) as Gram-positive and Gram-negative bacteria, respectively, to compare their activities with those of gentamycin and penicillin as references. In order to demonstrate the scope of the designed protocol for the synthesis of chromene-pyrimidine 2,4-dione derivatives, the authors extended the

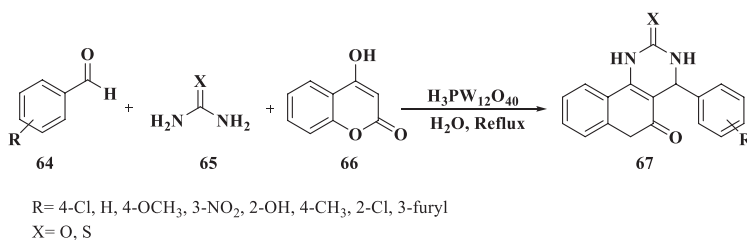


R = H, 4-Cl, 3-Cl, 4-Br, 4-F, 4-Me, 4-OMe, 4-C(CH<sub>3</sub>)<sub>3</sub>, 3-NO<sub>2</sub>, 2-NO<sub>2</sub>, 4-pyridyl

**SCHEME 4.17** Synthesis of the derivatives of chromene pyrimidine-2,4-dione via a one-pot, multicomponent reaction.

optimal reaction conditions for various aromatic and heteroaromatic aldehydes, and concluded that aromatic aldehydes with electron-releasing substituents decreased the yield and reaction rate to a certain degree. However, aromatic aldehydes with electron-withdrawing substituents increased the reaction rate and the yields to some extent.

Heravi and others [73] employed  $H_5BW_{12}O_{40}$ , a Keggin-type heteropoly acid, an effective, eco-friendly, and reusable acid catalyst for highly efficient synthesis of chromenopyrimidine-2,5-diones (O-products) and thioxochromenopyrimidin-5-ones (S-products) **67** via a multicomponent reaction of differently substituted benzaldehydes **64**, urea/thiourea **65**, and 4-hydroxycoumarin **66** refluxed in aqueous media (Scheme 4.18). The heteropoly acid catalyst was recoverable by simple filtration and reusable for three consecutive runs without any considerable decrease in its efficiency. Notably, the structure pattern of this catalyst may serve as a useful model for the design and assembly of functional molecule-based catalysts, particularly in the field of molecular sieve materials. In addition, the thermochemical properties in the synthesis of desired compounds were evaluated using density functional theory calculations.



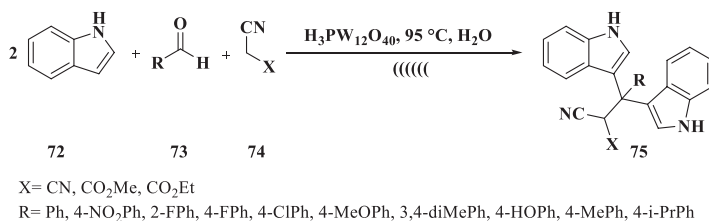
**SCHEME 4.18** Synthesis of chromenopyrimidine-2,5-diones (O-products) and thioxochromenopyrimidin-5-ones (S-products) via a multicomponent reaction in the presence of  $H_5BW_{12}O_{40}$  in water.

The authors also studied the substrate scope under optimal reaction conditions by using various benzaldehydes with electron-releasing and electron-withdrawing groups. They also replaced urea with thiourea. Regardless of the reagent nature, the catalyst efficiently promoted the reactions to afford the corresponding products in excellent yields. Interestingly, urea resulted in the desired products with slightly higher yields. In addition, benzaldehydes bearing electron-withdrawing substituents gave the products in higher yields in comparison with benzaldehydes having electron-releasing substituents.

The authors thus developed a highly efficient and environmentally friendly strategy for the synthesis of chromenopyrimidine-2,5-diones and thioxochromenopyrimidin-5-ones as biologically and pharmaceutically active compounds using BWA as a green, homogeneous, and recyclable catalyst refluxed in water via a multicomponent reaction. Characteristics such as effectiveness, mild conditions, a broad substrate scope, high to excellent yields in



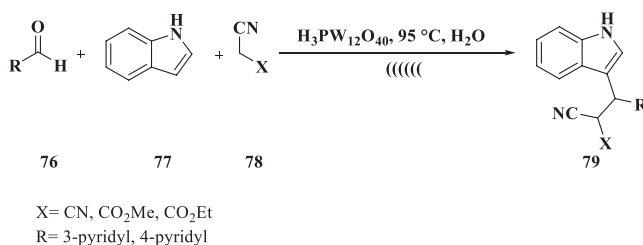




**SCHEME 4.20** Synthesis of bis(indole) derivatives by H<sub>3</sub>PW<sub>12</sub>O<sub>40</sub>.

the easy experimental procedures, short reaction times, and very good yields with green features by avoiding use of toxic solvents and catalysts. Amrollahi et al. also observed that the procedure accommodated both electron-releasing and electron-withdrawing substituents in the benzaldehyde. In all cases, the reactions progressed efficiently under the reflux and mild conditions to furnish the desired products in excellent yields. All the products were characterized by <sup>1</sup>H-, <sup>13</sup>C-NMR and IR spectra and elemental analyses.

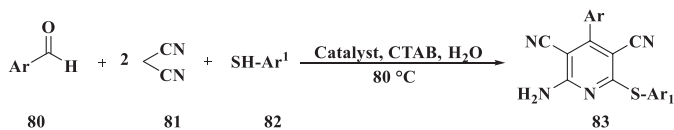
The reaction could be extended to other aldehydes under the optimized conditions. 2- and 3-pyridinecarboxaldehyde **76** were also chosen to react with indole **77** and active methylene compounds **78**. The reaction proceeded smoothly as expected in high yields (Scheme 4.21). However, when the authors wanted to obtain bis(indole) derivatives, only indolyl derivatives **79** were obtained. A probable reason for this result was that the oxidative dehydrogenation of 2-((indolyl)(pyridyl) methylene) malononitriles and 3-(indolyl) (pyridyl) acrylates in the presence of H<sub>3</sub>PW<sub>12</sub>O<sub>40</sub> was less reactive than 2-((aryl)indolyl)methyl malononitriles and 3-(aryl) (indolyl)acrylates, respectively. In order to examine the scope and limitations of this reaction, Amrollahi et al. extended their studies to the reactions of pyrrole, aldehydes, and active methylene compounds in the present of H<sub>3</sub>PW<sub>12</sub>O<sub>40</sub> as a catalyst in water at 90 °C under silent conditions.



**SCHEME 4.21** Synthesis of 2-(pyridyl)(1H-indol-3-yl)(methyl)malononitriles and 3-(indolyl) (pyridyl) acrylates in the presence of H<sub>3</sub>PW<sub>12</sub>O<sub>40</sub>.

Su's research group [76] reported the one-pot synthesis of 2-amino-3,5-dicarbonitrile-6-thiopyridines **83** with benzaldehyde **80**, malononitrile **81**, and thiophenol **82** using tungstophosphoric acid (H<sub>3</sub>PW<sub>12</sub>O<sub>40</sub>) as an effective

and green catalyst in aqueous solutions (Scheme 4.22). The advantages of this method are easy workout, high storage stability, and environmental friendliness.



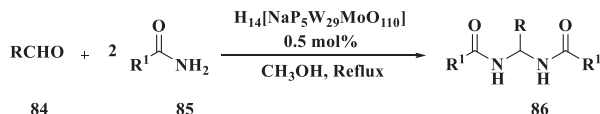
Ar = Ph, 4-Cl-Ph, 4-OH-Ph, 4-NO<sub>2</sub>-Ph, 4-Me-Ph, 4-OMe-Ph, 4-CHO-Ph, 4-OH-3-OMe-Ph, 4-Me-Ph  
 Ar<sup>1</sup> = Ph, 4-NH<sub>2</sub>-Ph

**SCHEME 4.22** Synthesis of 2-amino-3,5-dicarbonitrile-6-thio-pyridines.

The reaction took a long time to complete without surfactants as the reactants were insoluble in water. Therefore, Su et al. used cetyltrimethylammonium bromide (CTAB) as the surfactant since it is able to decrease the surface tension of the aqueous phase and organic phase. The method increased the relative concentration of the reactants.

The reaction could proceed efficiently using 2 mol% of H<sub>3</sub>PW<sub>12</sub>O<sub>40</sub> as a catalyst, 5 mL water as a solvent, CTAB as a surfactant, and a 1:2:1 molar ratio of the reactants (aromatic aldehyde: malononitrile: substituted thiophenol) under 80°C.

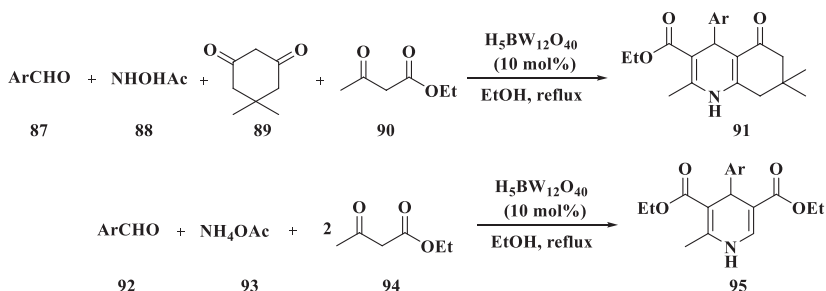
Maleki and coworkers [77] reported that H<sub>14</sub>[NaP<sub>5</sub>W<sub>29</sub>MoO<sub>110</sub>] could serve as an excellent catalyst for an alternative and simple synthesis of symmetrical *N,N'*-alkylidene bis-amide derivatives **86** (Scheme 4.23). A heteropoly acid, the catalyst had several advantages over traditional acid catalysts. It was noncorrosive and environmentally benign, had fewer disposal problems, was thermally stable, and could be removed easily.



R = C<sub>6</sub>H<sub>5</sub>, 4-NO<sub>2</sub>C<sub>6</sub>H<sub>4</sub>, 4-CNC<sub>6</sub>H<sub>4</sub>, 3-NO<sub>2</sub>C<sub>6</sub>H<sub>4</sub>, 2-NO<sub>2</sub>C<sub>6</sub>H<sub>4</sub>, 4-ClC<sub>6</sub>H<sub>4</sub>, 2,4-Cl<sub>2</sub>C<sub>6</sub>H<sub>3</sub>, 3-ClC<sub>6</sub>H<sub>4</sub>, 4-BrC<sub>6</sub>H<sub>4</sub>, 3-BrC<sub>6</sub>H<sub>4</sub>, 2-MeC<sub>6</sub>H<sub>4</sub>, 4-MeC<sub>6</sub>H<sub>4</sub>, 3-PhOC<sub>6</sub>H<sub>4</sub>, H, C<sub>6</sub>H<sub>5</sub>CH=CH  
 R<sup>1</sup> = C<sub>6</sub>H<sub>5</sub>, CH<sub>3</sub>

**SCHEME 4.23** Synthesis of symmetrical *N,N'*-alkylidene bis-amide derivatives.

Momeni and coworkers [78] efficiently synthesized a series of polyhydroquinoline derivatives **91** and **95** via the Hantzsch reaction in very good yields in the presence of a catalytic amount of borotungstic acid (H<sub>3</sub>BW<sub>12</sub>O<sub>40</sub>) and refluxed in EtOH under green and mild reaction conditions (Scheme 4.24). H<sub>3</sub>BW<sub>12</sub>O<sub>40</sub> is a Keggin-type heteropoly acid with a highly negative charge and strong Brønsted acidity. This protocol not only exhibited significant improvements in the rate of reaction and provided higher yields, but also avoided



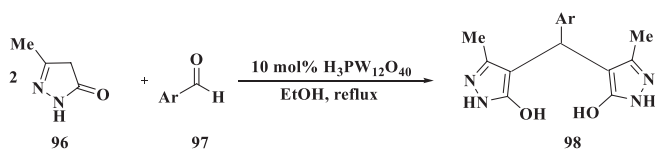
Ar = C<sub>6</sub>H<sub>5</sub>, 4-CH<sub>3</sub>C<sub>6</sub>H<sub>4</sub>, 4-OCH<sub>3</sub>C<sub>6</sub>H<sub>4</sub>, 3-NO<sub>2</sub>C<sub>6</sub>H<sub>4</sub>, 4-NO<sub>2</sub>C<sub>6</sub>H<sub>4</sub>, 4-ClC<sub>6</sub>H<sub>4</sub>, 4-BrC<sub>6</sub>H<sub>4</sub>, 2-OCH<sub>3</sub>C<sub>6</sub>H<sub>4</sub>

**SCHEME 4.24** Symmetrical and unsymmetrical Hantzsch reactions catalyzed by H<sub>5</sub>BW<sub>12</sub>O<sub>40</sub>.

the utilization of hazardous solvents or catalysts. Major features of the protocol were competence, generality, high yields in relatively short times, ease of product isolation, and recyclability of the catalyst. In addition, a comparative mechanistic analysis of the Hantzsch reaction was made based on the structural, thermodynamic, and electronic properties in the reaction course using quantum theory of atoms in molecules (QTAIM) and density functional theory (DFT) approaches.

The authors studied the substrate scopes and limitations of this multicomponent reaction under optimal conditions. A variety of aromatic aldehydes bearing either electron-releasing or electron-withdrawing groups on the aromatic ring, in the *ortho*, *meta*, and *para* positions, afforded related products in very good yields.

Vafae and colleagues [79] described a fast, efficient, and green procedure for the effective synthesis of 4,4'-(arylmethylene)-bis(3-methyl-1H-pyrazol-5-ols) **98** by a one-pot reaction of two equivalents of 3-methyl-1H-pyrazol-5(4H)-one (**96**) with aryl aldehydes **97** efficiently catalyzed by H<sub>3</sub>PW<sub>12</sub>O<sub>40</sub> (Scheme 4.25). The catalyst was relatively available and inexpensive, and could be readily recovered and reused so that appreciable catalytic activity still remained after the tenth run. Compared to the other procedures, they offered several advantages such as short reaction times, excellent yields, and mild reaction conditions and easy workup. Using the abovementioned optimal conditions,

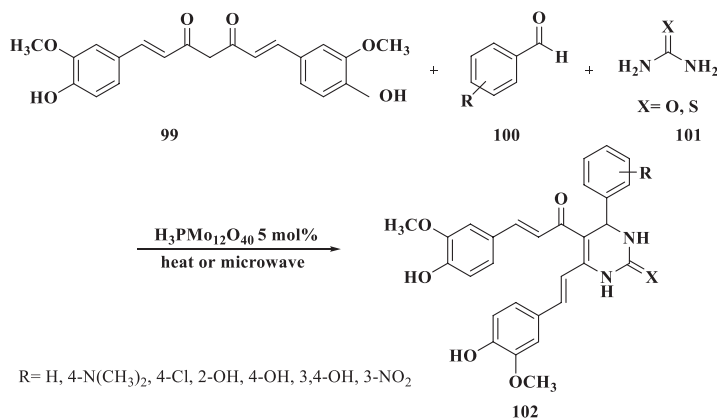


Ar = Ph, 4-ClC<sub>6</sub>H<sub>4</sub>, 3-O<sub>2</sub>NC<sub>6</sub>H<sub>4</sub>, 4-O<sub>2</sub>NC<sub>6</sub>H<sub>4</sub>, 4-HOC<sub>6</sub>H<sub>4</sub>, 4-BrC<sub>6</sub>H<sub>4</sub>, 4-MeC<sub>6</sub>H<sub>4</sub>, 4-MeOC<sub>6</sub>H<sub>4</sub>, 2-pyridyl, 2-thienyl

**SCHEME 4.25** H<sub>3</sub>PW<sub>12</sub>O<sub>40</sub> catalyzed synthesis of 4,4'-(arylmethylene)bis(3-methyl-1H-pyrazol-5-ols).

the scope and efficiency of the procedure were examined for the synthesis of various 4,4'-(arylmethylene)-bis(3-methyl-1H-pyrazol-5-ol)s. All the reactions afforded the corresponding products in excellent yields and tolerated various aromatic aldehydes with either electron-releasing or electron-withdrawing substituents. In addition, heteroaromatic aldehydes afforded a high yield of the related products.

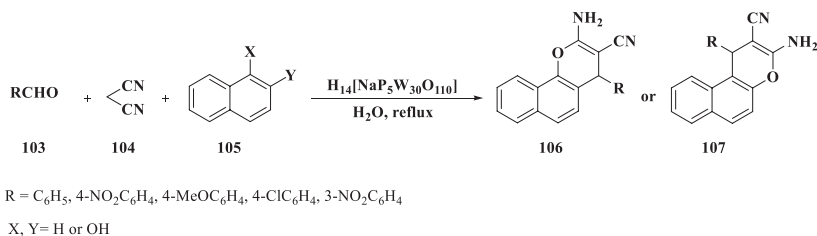
Khaldi-Khellafi et al. [80] used a simple, efficient, and improved Biginelli reaction to synthesize 3,4-dihydropyrimidin-2(1H)-one/thione analogues of curcumin **102** in satisfactory yields by one-pot, multicomponent cyclocondensation of curcumin **99**, substituted aromatic aldehydes **100**, and urea/thiourea **101** substituted aromatic aldehydes in a smaller volume of EtOH catalyzed by a commercially available heteropoly acid of Keggin type,  $H_3PMo_{12}O_{40}$  5 mol%, as a nontoxic and recyclable catalyst under conventional conditions of heating and microwave irradiation (Scheme 4.26). All the synthesized derivatives of curcumin were explored for antioxidant and antimicrobial activities. Biological activity data of the synthesized products demonstrated that most of the derivatives had greater antioxidant and antibacterial activities than curcumin. Geometries of the synthesized products were optimized by the B3LYP method using the 6-31G\* basis set. Curcumin-3,4-dihydropyrimidinones/thiones synthesized from 2-hydroxybenzaldehyde, 4-hydroxy-benzaldehyde, and 3,4-dihydroxybenzaldehyde exhibited a high intensity in UV-visible absorption spectrophotometry. However, the wavelengths were less affected by the nature of substituents on the benzaldehyde. The compound synthesized from 3,4-dihydroxybenzaldehyde and urea exhibited the maximum antioxidant activity, while the antioxidant activity decreased in the compounds synthesized from 2-hydroxybenzaldehyde and others. When the reaction conditions were



**SCHEME 4.26** Synthesis of 3,4-dihydropyrimidinones/thiones of curcumin under conventional reflux or microwave irradiation.

optimized, the authors conducted the three-component cyclocondensation reaction of curcumin and urea/thiourea with a series of aromatic aldehydes under the same conditions in order to investigate the scope of their procedure. The reactions were completed after 6–9 h under conventional reflux and 2–3 min under microwave irradiation to give the corresponding curcumin-DHPMs in satisfactory to excellent yields.

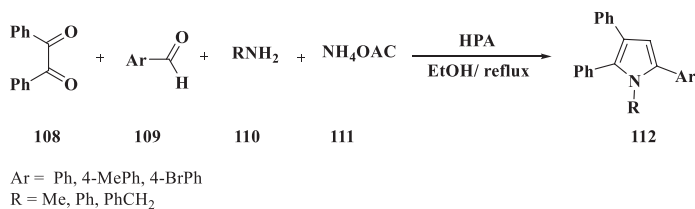
We [81] described an easy, neat, and environmentally friendly protocol for the synthesis of 2-amino-4H-chromenes **106** and **107** utilizing a Preyssler type heteropoly acid, i.e.,  $H_{14}[NaP_5W_{30}O_{110}]$ , as a reusable, green catalyst in water (Scheme 4.27). The products were obtained in high yields. The application range of the protocol was then demonstrated by the reaction of a variety of aldehydes **103** with malononitrile **104** and *a*- or *b*-naphthol **105**. In every case, a satisfactory yield with good selectivity was realized. Notably, the nature of the substituent on the aromatic ring exhibited no evident effect on the conversion as they were gained in high yields with relatively short reaction times.



**SCHEME 4.27** Synthesis of substituted 2-amino-chromenes catalyzed by  $H_{14}[NaP_5W_{30}O_{110}]$ .

The authors concluded that  $H_{14}[NaP_5W_{30}O_{110}]$  could act as an effective catalyst for the synthesis of 2-amino-4H-chromenes as biologically and pharmaceutically active chemicals. The protocol offered a number of advantages, among which were mild reaction conditions, neater reactions, high yields, a simple experimental procedure, and easy workup to make it attractive and useful for the synthesis of the target compounds. Most importantly, water served as a green solvent for the reactions.

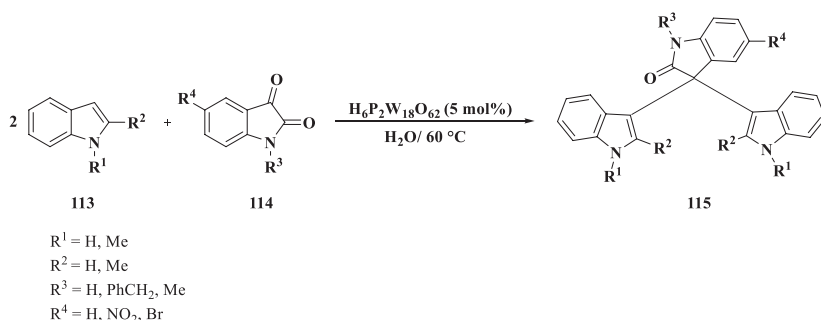
We [82] developed an effective and enhanced methodology for the synthesis of tetrasubstituted imidazoles **112** catalyzed by a Keggin-type heteropoly acid, which included a four-component, one-pot coupling protocol with refluxing in EtOH. Benzyl **108**, benzaldehyde derivatives **109**, primary amines **110**, and ammonium acetate **111** were reacted in a four-component, one-pot condensation protocol in the presence of Keggin heteropoly acids such as  $H_4[SiW_{12}O_{40}]$ ,  $H_3[PW_{12}O_{40}]$ ,  $H_3[PMo_{12}O_{40}]$ ,  $H_4[PMo_{11}VO_{40}]$ , and  $HNa_2[PMo_{12}O_{40}]$  as a catalyst to afford tetrasubstituted imidazoles **112** (Scheme 4.28).



**SCHEME 4.28** Synthesis of tetrasubstituted imidazoles using a catalytic amount of H<sub>4</sub>[PMo<sub>11</sub>VO<sub>40</sub>] with refluxing in EtOH.

The optimized system was used for the synthesis of other imidazole derivatives to establish the generality of this methodology. The methodology was proved to be effective for the preparation of tetrasubstituted imidazoles from both aliphatic and aromatic amines. The catalytic system worked best for aromatic amines. The catalytic efficiency of H<sub>4</sub>[PMo<sub>11</sub>VO<sub>40</sub>] was the highest for the synthesis of 1,2,4,5- tetrasubstituted imidazoles. The catalyst was reusable after a simple workup, with a gradual decrease in its activity. The reaction seemed to be heterogeneously catalyzed. High yields, rather short reaction times, simplicity of operation, and easy workup were among the merits of this protocol.

Alimohammadi and coworkers [83] developed an efficient, enhanced protocol for the synthesis of oxindole and its derivatives **115** through the electrophilic substitution reaction of indoles **113** with isatins **114** catalyzed by a Wells-Dawson tungsten heteropoly acid in water (Scheme 4.29). Very good yields, short reaction times, and easy workup were among the advantages of this protocol.



**SCHEME 4.29** The synthesis of oxindoles via the reaction of isatins with indoles in the presence of H<sub>6</sub>P<sub>2</sub>W<sub>18</sub>O<sub>62</sub> in water.

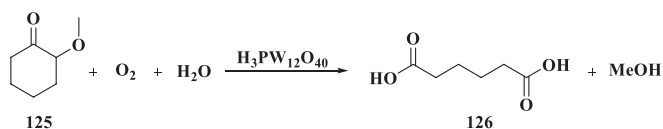
Javid and coworkers [84] reported an easy, one-pot, four-component protocol for the synthesis of tetrasubstituted imidazole derivatives **120** from benzyl **116**, aromatic aldehydes **117**, primary amines **118**, and ammonium acetate **119** catalyzed by a Preyssler-type heteropoly acid (H<sub>14</sub>[NaP<sub>5</sub>W<sub>30</sub>O<sub>110</sub>]) (Scheme 4.30). This protocol was proved to be eco-friendly and convenient, with easy workup and relatively short reaction times. In addition, the products were isolated in very good yields.





instrumental methods (pH-measurements, potentiometry, and titration analysis), and NMR spectroscopy revealed the retainment of their Keggin structure as their oxidation potential increased with the V<sup>V</sup> content. With complete optimization of the reaction conditions, they were able to reach a yield of 92% for DFF using Co<sub>2</sub>H<sub>6</sub>P<sub>3</sub>Mo<sub>18</sub>V<sub>7</sub>O<sub>84</sub> in H<sub>2</sub>O/MIBK within 90 min at 110°C, under atmospheric pressure. The described method of 5-HMF oxidation was based on using efficient soft oxidants that were easily recyclable and reusable for at least five runs without any considerable loss in catalytic activity. The authors synthesized both catalysts of the Keggin type, H<sub>3+x</sub>PMo<sub>12-x</sub>V<sub>x</sub>O<sub>40</sub>, and modified non-Keggin type, H<sub>a</sub>P<sub>z</sub>MoyV<sub>x</sub>O<sub>b</sub>. They also prepared a series of acid salts substituting H<sup>+</sup> ions in heteropoly acids with Na<sup>+</sup> or Co<sup>2+</sup> cations to estimate the effect of the counter cation on their properties and reactivities. The prepared catalysts possessed high oxidative ability and large Brønsted acidity, both of which affected the distribution of the products. It was found that raising the reaction temperature and vanadium content increased the yield of the desired product. In addition, improving the acidity of the catalyst by increasing the vanadium (V) content had the opposite effect arising from the formation of levulinic and formic acids, as well as oligomerization of by-products. The acid salts were demonstrated to have lower acidity than the heteropoly acid solutions, which improved their catalytic efficiency.

Hatakeyama and coworkers [110] investigated the oxidative cleavage of 2-methoxycyclohexanone (2-MCO) **125** to adipic acid **126** and methanol with O<sub>2</sub> in an aqueous solution (Scheme 4.32). It was known that a variety of vanadium compounds and heteropoly acids that were tested as homogeneous catalysts as vanadium compounds, particularly phosphomolybdovanadic acids, were active in various oxidative cleavage reactions with gaseous oxygen. However, the simple vanadium-free phosphotungstic acid (H<sub>3</sub>PW<sub>12</sub>O<sub>40</sub>), which had not been thought to have oxidation catalysis activity using O<sub>2</sub> as the oxidant, proved to be a good catalyst with excellent selectivity toward adipic acid. The carbon-based yield for adipic acid reached 74% (86% in molar basis), which was higher than values gained by vanadium-based catalysts. Reuse tests and <sup>31</sup>P NMR analyses confirmed that the H<sub>3</sub>PW<sub>12</sub>O<sub>40</sub> catalyst retained its stability and reusability. Kinetic investigations and the reaction tests using radical inhibitors revealed that the reaction mechanism was not an auto-oxidation involving free radicals. Rather, the H<sub>3</sub>PW<sub>12</sub>O<sub>40</sub> catalyst first activated the substrate by a single-electron oxidation and then it reacted with O<sub>2</sub>.

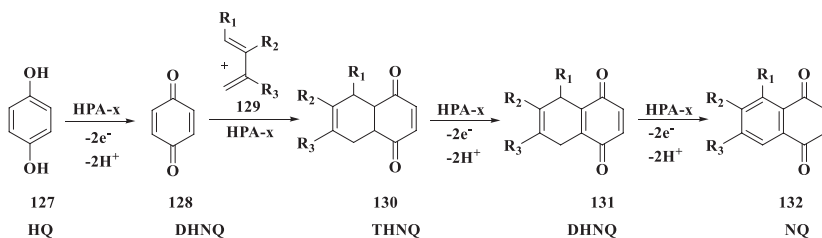


**SCHEME 4.32** Synthesis of adipic acid from 2-methoxycyclohexanone catalyzed by H<sub>3</sub>PW<sub>12</sub>O<sub>40</sub>.

Notably, significant amounts of CO<sub>2</sub> were produced with vanadium-based catalysts owing to the high activity of vanadium as an oxidation catalyst. Moreover, catalyst deactivation was observed for phosphomolybdovanadic acid. However, the H<sub>3</sub>PW<sub>12</sub>O<sub>40</sub> catalyst remained stable during experiments. The produced adipic acid was readily separated from the reaction solution by crystallization. The catalytic system worked well in the oxidative cleavage of  $\alpha$ -hydroxyketones. On the other hand, the selectivity toward the desired acids was lower than that of  $\alpha$ -methoxyketones from oxidation of 1,2-cyclohexanedione. The authors conducted the DFT calculations of the formation energy of radical cation of various molecules, i.e., energy change by a single-electron oxidation. Given the low  $\Delta E$  (+ 694 kJ mol<sup>-1</sup>), the radical cation of the enol form of 2-MCO could be favorably formed. This value was even lower than that of 2,6-di-*tert*-butyl-*p*-cresol (+ 706 kJ mol<sup>-1</sup>), which is a common one-electron reducing agent that works as a radical inhibitor. The calculations confirmed the participation of the radical cation in the oxidation catalysis.

1,4-Naphthoquinones **132** are a group of organic compounds with an important property. The previous methods of their synthesis either gave low yields in multistage procedures or required long reaction times.

However, Gogin et al. [111] proposed a new one-pot procedure for synthesis of 1,4-naphthoquinones from hydroquinone **127** and substituted 1,3-dienes **129** at ambient temperature (Scheme 4.33). They used solutions of the Mo-V-P heteropoly acids HPA-*x* (*x* = 4, 7, 10), e.g., H<sub>7</sub>PMo<sub>8</sub>V<sub>4</sub>O<sub>40</sub>, as a bifunctional (redox and acid) catalyst for the procedure. By studying the effect of some factors on key process parameters, they demonstrated that unsubstituted as well as some alkyl-substituted 1,4-naphthoquinones could be achieved using this method with yields of 50%–80% and 92%–99% purity. Significantly, their method made it possible to simplify the direct synthesis of 1,4-naphthoquinones from hydroquinone compared to the previous methods.



SCHEME 4.33 NQ synthesis from HQ.

It was shown that under these moderate conditions, the presence of a hydrophilic organic solvent, such as 1,4-dioxane, was affected most of all. The authors also demonstrated that it was possible to use their one-pot procedure to synthesize 6,7-dimethylnaphthoquinone with 92% purity and 77% yield.

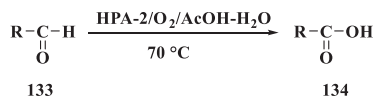
Direct conversion of raw biomass into fine chemicals is interesting both conceptually and practically, and considered a great challenge. In this regard, the oxidation of biomass to formic acid and acetic acid seems to be a promising industrial process.

Lu and coworkers [112] reported the effectiveness of a binary catalyst system consisting of a Keggin-type heteropoly acid  $H_5PV_2Mo_{10}O_{40}$  and sulfuric acid in direct conversion of corn cobs to formic acid and acetic acid using  $O_2$  as an oxidant in aqueous solutions. They investigated the effects of reaction temperature, sulfuric acid concentration, reaction time, and the initial pressure of  $O_2$  on the conversion of corn cobs in detail. Decreasing the pH caused the rapid conversion of corn cobs and the product yields could be enhanced significantly to 42.5% for formic acid and 9.1% for acetic acid after 30 min at 170°C. The decrease in pH could also accelerate the hydrolysis of the corn cobs and promote the activity of  $H_5PV_2Mo_{10}O_{40}$  by using protonation and dissociation reactions. The reaction course exhibited that polysaccharide components (hemicellulose and cellulose) of corn cobs were initially hydrolyzed to monosaccharides and then they were oxidized to formic acid and acetic acid through formation of the intermediates with aldehyde and carboxyl groups. The lignin component of the corn cob was oxidized to products and carbon dioxide through formation of the intermediates with quinone structures. The products, i.e., formic acid and acetic acid, mainly came from polysaccharides, i.e., hemicellulose and cellulose. The catalytic system exhibited good reusability.

The production of carboxylic acids by partial wet oxidation of alkali lignin under high temperatures and pressures has been extensively studied. Demesa and coauthors [113] used two different heteropoly acids, phosphomolybdic acid ( $H_3PMo_{12}O_{40}$ ) and phosphotungstic acid ( $H_3PW_{12}O_{40}$ ), to catalyze the oxidation of lignin under hydrothermal conditions. They investigated factors affecting the total yield of carboxylic acids formed during the partial oxidation of lignin. Formic, acetic, and succinic acids were the major products. Of the two heteropoly acids used as catalysts, phosphomolybdic acid proved to be most promising. The carboxylic acid yields and lignin conversions were up to 45% and 95%, respectively.

It was also found that the relative amount of the catalyst used considerably affects the yields and the lignin conversion rates. The two heteropoly acids exhibited different catalytic behaviors so that the reaction pathway of lignin oxidation seemed to be determined by the type of addenda atom in the heteropoly acid catalyst, with Mo favoring a selective oxidation reaction. The catalyst was easily recoverable for both heteropoly acids, rendering the procedure an environmentally friendly and potentially economical one.

The heteropoly acids  $H_{3+n}[PMo_{12-n}V_nO_{40}]_{aq}$  (denoted as HPA- $n$ ,  $n=2,3,8$ ) are able to catalyze the oxidation of aldehydes **133** to carboxylic acids **134** in the presence of  $O_2$  in high yields (Scheme 4.34). El Amrani and coworkers [114] explored the influence of a variety of parameters such as the precursors, solvents, temperature, or catalyst/substrate ratio on catalytic activity. The process



R = C<sub>7</sub>H<sub>15</sub>, C<sub>4</sub>H<sub>9</sub>, 4-OMeC<sub>6</sub>H<sub>4</sub>, 3-OMeC<sub>6</sub>H<sub>4</sub>, 3,4-(OMe)<sub>2</sub>C<sub>6</sub>H<sub>3</sub>, 4-ClC<sub>6</sub>H<sub>4</sub>, 2-Furyl, C<sub>9</sub>H<sub>17</sub>

**SCHEME 4.34** Oxidation of aldehydes to carboxylic acids by a catalytic system of HPA-2/O<sub>2</sub>/AcOH/H<sub>2</sub>O.

was especially selective for linear and aromatic aldehydes. The oxidation of adipaldehyde using O<sub>2</sub> under moderate conditions, in the presence of HPA-2 as a catalyst, led to the formation of adipic acid along with a considerable amount of other by-products. Thus, they made several modifications to the catalytic systems to enhance their selectivity.

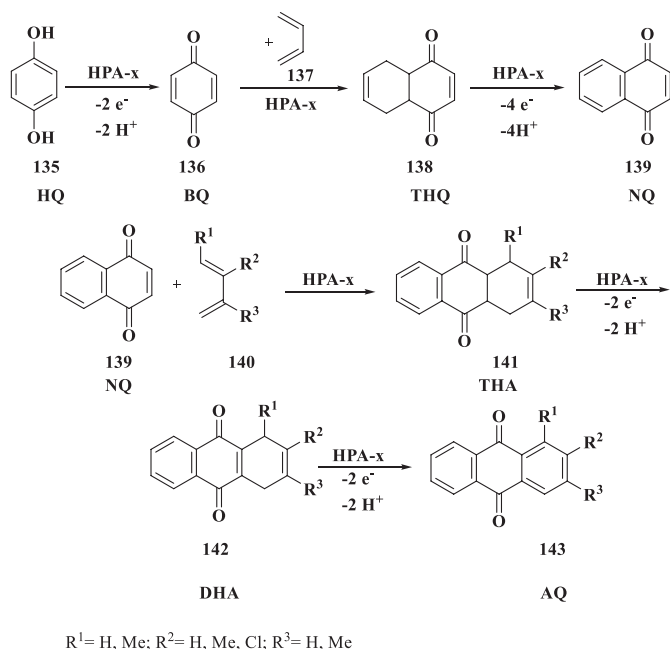
HPA-2 was proved to be highly active in the oxidation of both aliphatic and aromatic aldehydes to the corresponding acids with O<sub>2</sub> in mixtures of AcOH/H<sub>2</sub>O with a volume ratio of 4.5/0.5. The performance observed for linear aldehydes was not affected by the chain length as a complete conversion was obtained for octanal, with a selectivity of 99%. Of the aliphatic aldehydes examined, those with branched carbon chains reacted slower than aldehydes with linear carbon chains. The oxidation of iso-valeraldehyde afforded *iso*-valeric acid as the main product. Under such conditions, benzaldehyde also led to almost a quantitative conversion to benzoic acid with an excellent yield.

On the other hand, the reaction rate of aromatic substrates bearing electron-releasing substituents dramatically decreased to 36% conversion in 48 h. This clearly demonstrated that such strong electron-releasing groups did not favor the oxidation of aldehydes to carboxylic acids, but rather resulted in the formation of the related phenols through the migration of the aromatic group.

Gogin's research group [115] performed a one-pot procedure for the synthesis of anthraquinone and its derivatives **143** by reaction with 1,3-butadienes in the presence of a catalyst, i.e., a solution of Mo-V-P-HPA in water-miscible organic solvents. It was established that anthraquinone could be gained by this procedure with yields up to 90% and product purities of 96%–97% (Scheme 4.35).

In this regard, the condensation of 1,4-naphthoquinone (139) with 1,3-butadiene **140** in solutions of high-vanadium heteropoly acids with the empirical compositions of H<sub>15</sub>P<sub>4</sub>Mo<sub>18</sub>V<sub>7</sub>O<sub>89</sub> and H<sub>17</sub>P<sub>3</sub>Mo<sub>16</sub>V<sub>10</sub>O<sub>89</sub> in the presence of polar organic solvents (acetone, 1,4-dioxane) resulted in the construction of 9,10-anthraquinone **142** in yields of ~70% and purities of up to 97% with a complete conversion of anthraquinone. Under the same conditions, the reactions of anthraquinone with substituted 1,3-butadienes gave substituted anthraquinones in yields of up to 90% and purities of up to 99%.

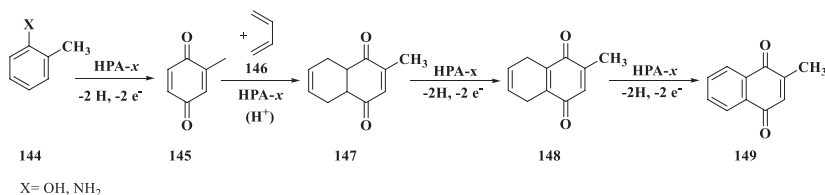
Gogin et al. also demonstrated the feasibility of its reuse in the synthesis of anthraquinone with reproducible results. Their results provided prospects for the improvement of low-waste, one-pot procedures for the synthesis of anthraquinone and its substituted derivatives from 1,3-butadienes and 1,4-naphthoquinone



**SCHEME 4.35** Synthesis of AQ derivatives in the presence of solutions of Mo-V-P-HPA.

in the presence of solutions of Mo-V-P-HPA as effective bifunctional (acidic and oxidative) catalytic systems.

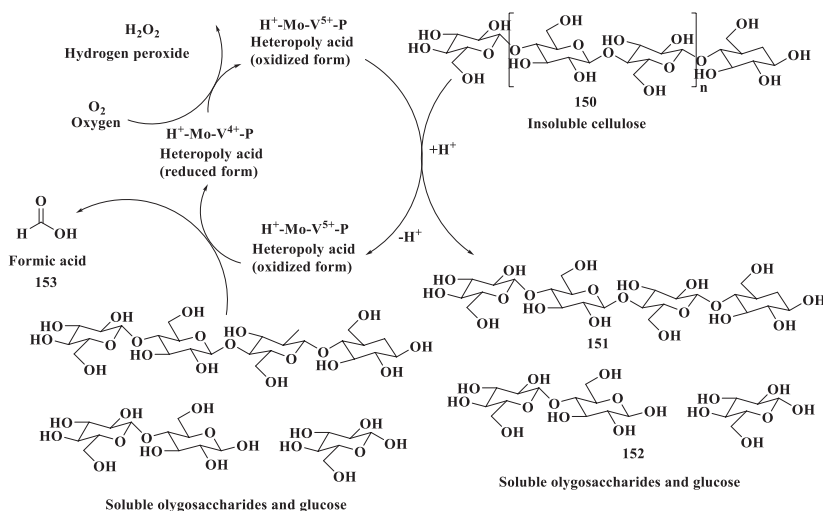
Gogin et al. [116] demonstrated the feasibility of the catalyzed synthesis of vitamin K<sub>3</sub> **149** in the presence of HPA-*x* solutions in one step from *o*-cresol and *o*-toluidine **144** under an atmosphere of 1,3-butadiene **146** (Scheme 4.36). HPA-*x* serves as a bifunctional (acid and oxidative) catalyst. Although the yield of the target product is low (below 33%), the new protocol had its own merits as menadione was synthesized from easily available precursors and a multistep process was performed in one single step. The regeneration of HPA-*x* solutions with O<sub>2</sub> will pave the way for new methods of the synthesis of vitamin K<sub>3</sub> in the



**SCHEME 4.36** One-pot synthesis of menadione in Mo-V-P-HPA-*x* solutions.

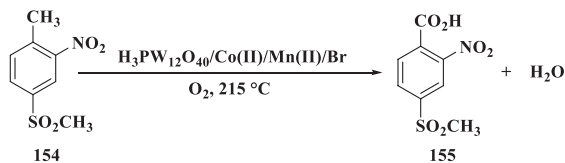
presence of HPA-*x* as a bifunctional catalyst.

Gromov et al. [117] demonstrated that it is possible to synthesize formic acid **153** from cellulose **150** in very good yields (65–66 mol%) via a single-step process of hydrolytic oxidation catalyzed by bifunctional homogeneous Mo-V-P heteropoly acid catalysts (Scheme 4.37). The optimization of the reaction conditions led to a temperature range of 150–160°C and air pressures of 10–20 bar. It turned out that pressure would have no effects on the initial rate of the process, while did have an effect on the target product yield. An increase in the O<sub>2</sub> content of the reaction medium greatly improved the yield of formic acid and helped the catalyst solution regenerate more efficiently. In their quest for the optimal heteropoly acid composition among H<sub>5</sub>PMo<sub>10</sub>V<sub>2</sub>O<sub>40</sub>, Co<sub>0.6</sub>H<sub>3.8</sub>PMo<sub>10</sub>V<sub>2</sub>O<sub>40</sub>, H<sub>11</sub>P<sub>3</sub>Mo<sub>16</sub>V<sub>6</sub>O<sub>76</sub>, and H<sub>17</sub>P<sub>3</sub>Mo<sub>16</sub>V<sub>10</sub>O<sub>89</sub>, the authors observed the highest reaction rate in the presence of heteropoly acid solutions that provided greater acidity for the reaction medium. Therefore, a linear correlation between the reaction rate and the hydronium ion concentration was established. The correlation between the reaction rate or formic acid yields and the vanadium content of the heteropoly acids was found to be linear up to the point that the ratio of glucose units to vanadium was 6:1. Afterward, the correlation was flat. Therefore, Gromov et al. concluded that when choosing a bifunctional catalyst, three criteria should be considered: high acidity, vanadium amounts greater than 1:6 with respect to the glucose units, and the catalyst price. The formic acid gained from vegetable lignocellulosic feed is usable as a hydrogen source or reducing agent for the production of precious raw materials and fuel from vegetable biomass.



**SCHEME 4.37** Hydrolysis/oxidation of cellulose.

Long and coworkers [118] investigated the oxidation of 2-nitro-4-methylsulfonyltoluene **154** to 2-nitro-4-methylsulfonylbenzoic acid **155** in acetic acid in the presence of oxygen catalyzed by a homogeneous catalytic system such as  $\text{H}_3\text{PW}_{12}\text{O}_{40}/\text{Co}/\text{Mn}/\text{Br}$  (Scheme 4.38).



**SCHEME 4.38** Oxidation of 2-nitro-4-methylsulfonyltoluene to 2-nitro-4-methylsulfonylbenzoic acid catalyzed by  $\text{H}_3\text{PW}_{12}\text{O}_{40}/\text{Co}/\text{Mn}/\text{Br}$ .

Based on their experimental results, the authors came to the following specific conclusions for the mentioned catalytic system:

- The oxidation of 2-nitro-4-methylsulfonyltoluene to 2-nitro-4-methylsulfonyl benzoic acid by oxygen in acetic acid is achievable using the homogeneous catalytic system of  $\text{H}_3\text{PW}_{12}\text{O}_{40}/\text{Co}/\text{Mn}/\text{Br}$ .
- Phosphotungstic acid has a critical role in this catalytic system and the catalytic system activity is optimized when the concentration of phosphotungstic acid is 2500 ppm.
- Cobalt (II) has an essential role in this catalytic system. The catalytic system activity is optimized for the production of 2-nitro-4-methylsulfonylbenzoic acid when the concentration of cobalt (II) is 148 ppm.
- The concentration of bromine is an influential factor in the oxidation of 2-nitro-4-methylsulfonyltoluene to 2-nitro-4-methylsulfonylbenzoic acid. The optimal bromine concentration was found to be 1163 ppm.
- The ratio of Mn/Co can highly affect the extent and selectivity of this reaction. The highest yield of the conversion of 2-nitro-4-methylsulfonylbenzoic acid into 2-nitro-4-methylsulfonyltoluene was obtained when the Mn/Co ratio was 2:1.

In addition, Long et al. found that greater oxygen partial pressures and higher temperatures favored the oxidation of 2-nitro-4-methylsulfonyltoluene to production of 2-nitro-4-methylsulfonylbenzoic acid. In order to describe the reaction rate in this catalytic system, a kinetic model was presented.

Lu and others [119] employed one of the most widely used heteropoly acids,  $\text{H}_5\text{PV}_2\text{Mo}_{10}\text{O}_{40}$ , with sulfuric acid as a pH modifier in an aqueous solution to catalyze the oxidation of cellulose. In the catalyzed oxidation of cellulose in the  $\text{H}_5\text{PV}_2\text{Mo}_{10}\text{O}_{40}/\text{sulfuric acid}$  system, it was found that conversion of cellulose could accelerate and enhance the formic acid yield greatly by decreasing the pH. The authors discussed the influence of decreasing the pH on the catalyst,  $\text{H}_5\text{PV}_2\text{Mo}_{10}\text{O}_{40}$ , and the reaction course as well. The results



demonstrated that the hydrolysis rate of cellulose was enhanced and the reactivity of  $H_5PV_2Mo_{10}O_{40}$  improved as the pH decreased.

In addition, adjusting the effects of pH on the catalytic oxidation of cellulose catalyzed by the  $H_5PV_2Mo_{10}O_{40}$ /sulfuric acid system was studied. By decreasing the pH, the hydrolysis rate of cellulose could be accelerated and formic acid yield could be significantly improved to 61% within a reaction time of 5 min. The addition of sulfuric acid had a significant effect on the catalyst and the conversion course. For the catalyst, a decrease in pH could raise the formation of the protonated  $H_5PV_2Mo_{10}O_{40}$  and  $VO_2^+$  via protonation and dissociation. Consequently, the  $H_5PV_2Mo_{10}O_{40}$ /sulfuric acid system had a stronger catalytic effect compared to using only  $H_5PV_2Mo_{10}O_{40}$ . For the conversion course, a decrease in pH improved the initial hydrolysis rate of cellulose to glucose, thus it favored the formic acid production. However, a decrease in pH accelerated the deep hydrolysis of glucose to by-products such as levulinic acid as well. This, in turn, led to a decrease in formic acid selectivity to form more acetic acid.

Reichert et al. [120] found out that under the conditions of water-organic, in situ extraction oxidation of biomass under typical OxFA conditions (363 K, 20 bar of  $O_2$  pressure) catalyzed by polyoxometalates led to considerably higher formic acid yields in comparison with any monophasic reaction protocol reported. The established protocols employed to isolate pure formic acid from the aqueous solutions include liquid-liquid extraction, azeotropic distillation, extraction followed by distillation, reactive extraction, and extractive distillation. When it comes to biomass oxidation catalyzed by polyoxometalates, the formic acid isolation process must deal with the water-soluble, highly acidic heteropoly acid catalyst as well so that efficient catalyst recycling is realized.

While the previous works demonstrated that the selectivity of the formic acid produced from the oxidation of carbohydrates and biomass did not exceed 70%, even with simple substrates, such as glucose or glycerol, the authors demonstrated that formic acid yields of up to 85% from glucose and up to 61% from the challenging substrate of beech wood were achievable. The authors realized that the in situ extraction of the biomass oxidation reaction mixture with long-chain primary alcohols, such as 1-hexanol and 1-heptanol, not only provided a straightforward method for the isolation of formic acid but also limited the pH decrease in the catalytic aqueous phase during formic acid formation. Their results indicated that this collateral effect improved the formic acid selectivity since the applied polyoxometalate catalyst, i.e.,  $H_8PV_5Mo_7O_{40}$  (HPA-5), tended to generate larger amounts of  $CO_2$  at pH values below 1.5.

A precious chemical compound, 2,3-dimethyl-*p*-benzoquinone, has various applications, e.g., as a soft oxidizing and dehydrogenating agent and as a synthon in preparing a variety of complex products including pharmaceutical and biochemical compounds.

Rodikova and coworkers [121] reported that Keggin-type and modified-type aqueous solutions of Mo-V-phosphoric heteropoly acids (Mo-V-P heteropoly acids) of the gross compositions  $H_{3+x}PMo_{12-x}V_xO_{40}$  (HPA-*x*) and

$H_aP_zMo_yV_xO_b$  (HPA- $x'$ ), respectively, with high oxidation potential and ease of regeneration, might serve as effective soft oxidizing agents to obtain such para-quinones from 2,3-dimethylphenol. The synthesized heteropoly acid catalysts having different vanadium contents were characterized by analysis techniques such as  $^{51}\text{V}$ NMR and  $^{31}\text{P}$ NMR spectroscopy, titrimetry, potentiometry, and pH measurement. The authors found that the preferred formation of 2,3-dimethyl-*p*-benzoquinone over the corresponding diphenoquinone in a single-electron oxidation was achieved by successive optimization of the reaction conditions, with the most significant ones being the organic solvent and the molar ratio of vanadium (V) to substrate. With substitution of HPA- $x$  by HPA- $x'$  it was possible to raise the quinone selectivity and reduce the optimal molar ratio of vanadium (V) to substrate. The highest yield for the target quinone (97%) at total conversion of the substrate was gained with the biphasic system of water-benzene at the molar ratio of vanadium (V) to substrate equal to 12. The optimum reaction conditions were determined to be a temperature of 50°C under an inert atmosphere. It turned out that the aqueous HPA-10' solution containing the highest content of  $\text{VO}_2^+$  ions had the most efficiency as a catalyst among the studied heteropoly acids. Regeneration of the catalyst at a separate step allowed the preservation of its activity and selectivity at an initial level for at least 10 runs.

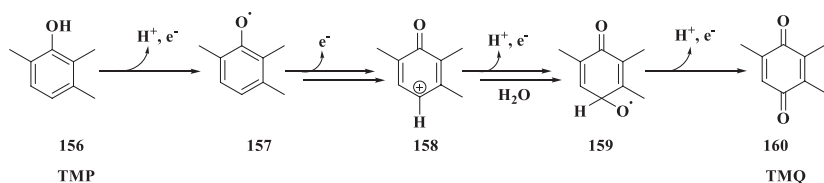
The authors studied how the composition of aqueous Mo-V-P heteropoly acid solutions and their oxidative properties and reaction conditions affected the reaction time and product distribution during the synthesis of 2,3-dimethyl-*p*-benzoquinone through the oxidation of 2,3-dimethylphenol to obtain the maximal quinone selectivity. The main problem that limited the usage of homogeneous catalytic processes was the difficulty in recovering and recycling of the catalyst.

Rodikova and others [122] disclosed the results of their investigations on the reactivity of modified V-containing heteropoly acids  $H_aP_zMo_yV_xO_b$  (HPA- $x'$ ) in the oxidation of 2,6-dimethylphenol. An absolutely valuable and efficient path to the corresponding 2,6-dimethyl-1,4-benzoquinone, the reaction practically avoided the formation of diphenoquinone, which is an interesting compound as a sensitizer and a platform molecule. The total process consisted of two reactions: the oxidation of 2,6-dimethylphenol by  $\text{V}^{\text{V}}\text{O}_2^+ \leftrightarrow \text{V}^{\text{V}}\text{-HPA}$  and the oxidation of the reduced  $\text{V}^{\text{IV}}\text{-HPA} \leftrightarrow \text{V}^{\text{IV}}\text{O}_2^{2+}$  by  $\text{O}_2$  to the initial state. The former process was particularly scrutinized to determine the influence of the reaction parameters on the product distribution. The desired quinone was synthesized in a very high yield (95%) with total conversion substrate affecting the oxidation in a biphasic system of water-trichloroethene at 70°C under an  $\text{N}_2$  atmosphere in the presence of a solution of  $\text{H}_{17}\text{P}_3\text{Mo}_{16}\text{V}_{10}\text{O}_{89}$ . As the vanadium content increased, the selectivity of 2,6-dimethyl-1,4-benzoquinone was enhanced owing to faster electron transfer. The multicycle tests of the catalyst showed its stability against deposition to  $\text{V}_2\text{O}_5 \cdot n\text{H}_2\text{O}$ .

The authors showed that the application of Mo-V-P heteropoly acid catalysts and fine-tuning of the reaction conditions could be utilized as a robust means to govern the product distribution in reactions of phenol oxidation, and transformations of substituted phenols may be channeled into the formation of preferable benzoquinones instead of diphenoquinones and polyphenylene oxides. It was also demonstrated that the yields and compositions of products were dependent on the V<sup>V</sup>-content and solvent nature. The successful generation of the desired product (quinone) and significant reduction of by-products were ascribed to the use of heteropoly acid solutions with high content of vanadium, which in turn increased the content of VO<sub>2</sub><sup>+</sup> ions as well as using polar solvents with electron acceptor properties. In addition, increasing the reaction temperature from 25°C to 70°C and the application of the inert atmosphere raised the selectivity of 2,6-dimethyl-1,4-benzoquinone. The catalyst could be easily recovered and reused.

Rodikova and coworkers [123] discussed the application of a few homogeneous P-Mo-V heteropoly acids with high contents of vanadium and modified gross composition, i.e., H<sub>11</sub>P<sub>3</sub>Mo<sub>18</sub>V<sub>8</sub>O<sub>87</sub> (HPA-8') and H<sub>17</sub>P<sub>3</sub>Mo<sub>16</sub>V<sub>10</sub>O<sub>89</sub> (HPA-10'), in the oxidation of 2,3- and 2,6-dimethylphenols into the corresponding 2,3- and 2,6-dimethyl-1,4-benzoquinones, emphasizing the stability and reusability of the heteropoly acids in these reactions. During the experiments, the authors varied some reaction parameters and studied the properties and states of the HPA-*x*' catalysts before and after the reactions. They demonstrated that the oxidation reactions of 2,3- and 2,6-dimethylphenols into the related 2,3- and 2,6-dimethyl-1,4-benzoquinones catalyzed by heteropoly acid solutions could be effectively conducted with selectivities of up to 95%–97%. The important factors to accelerate the electron transfer and achieve the dominance of para-quinone formation were the application of H<sub>11</sub>P<sub>3</sub>Mo<sub>18</sub>V<sub>8</sub>O<sub>87</sub> and H<sub>17</sub>P<sub>3</sub>Mo<sub>16</sub>V<sub>10</sub>O<sub>89</sub> catalysts with high contents of vanadium and increased content of VO<sub>2</sub><sup>+</sup> oxocations and  $[n_V^V]/[\text{substrate}]$  molar ratio greater than or equal to 12. The dropwise addition of 2,6-dimethylphenols increased para-quinone selectivity owing to an instantaneous decrease in the substrate concentration. The product selectivity and catalyst activity were found to correlate with the initial redox potential of heteropoly acid solutions. The high E values of heteropoly acids before the reaction, obtained by effective regeneration of the catalyst, allowed the preservation of product selectivity. The catalysts were revealed to retain their stability and efficiency even after being reused for at least 20–25 runs. No vanadium-containing deposits were detected in the catalyzed reaction as well as the catalyst regeneration in all cycles. Both catalysts kept their stability and productivity during reactions, rendering them promising candidates for developing efficient catalytic processes for the oxidation of organic compounds.

Rodikova et al. [124] considered various manners for preparing 2,3,5-trimethyl-1,4-benzoquinone (TMQ) **160**, which is an important intermediate in the synthesis of vitamin E, by catalytic oxidation of 2,3,6-trimethylphenol (TMP) **156** (Scheme 4.39). The aqueous solutions of Mo-V phosphoric heteropoly



**SCHEME 4.39** Oxidation of 2,3,6-trimethylphenol (TMP).

acids proved to be promising catalysts for the oxidation of 2,3,6-trimethylphenol with  $\text{O}_2$ . The efficiency of a biphasic procedure that ensured high selectivity for 2,3,5-trimethyl-1,4-benzoquinone (up to 99.5%) and high catalyst activity in the target reaction ( $\approx 600\text{--}800 \text{ gTMQ h}^{-1}$ ) was demonstrated.

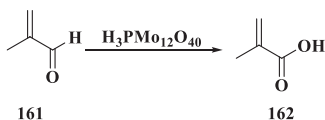
Despite the many catalysts used for this reaction in the literature, the most effective means were based on the use of an excess of  $\text{H}_2\text{O}_2$ . However, the use of oxygen (air) combined with a suitable catalytic system proved to be a better way of conducting this process on an industrial scale from an economic viewpoint. It was shown that aqueous Mo-V-P heteropoly acid solutions as catalysts for the oxidation of 2,3,6-trimethylphenol with oxygen were promising. Different available options for using heteropoly acids in this reaction were analyzed, which were one-step homogeneous acetic acid oxidation of 2,3,6-trimethylphenol and biphasic two-step means. It was confirmed that the acetic-acid means was technologically inefficient. On the other hand, the effectiveness of the biphasic version in the presence of HPA- $x$  solutions was confirmed as it provided almost 100% selectivity for 2,3,5-trimethyl-1,4-benzoquinone, and high performance ( $\approx 280\text{--}470 \text{ gTMQ h}^{-1}$ ) in this reaction was demonstrated. The proposed approach was environmentally friendly with low waste. The catalysts were appropriate for long-term runs, and their regeneration was fast and relatively efficient.

Yang and others [125] proposed a new procedure for the oxidation of lignite to give carboxylic acids. They studied the effects of heteropoly acid concentration, sulfuric acid concentration, reaction temperature, initial pressure of oxygen, and reaction time on the conversion of lignite to carboxylic acids in detail. Their results revealed that the oxidation of lignite in a solution of sulfuric acid and heteropoly acid could afford 56.9 of weight percent of the desired products, which included 33.5 wt% of formic acid, 14.4 wt% of acetic acid, 1.1 wt% oxalic acid, 1.5 wt% of succinic acid, and 6.4 wt% benzene carboxylic acids when the concentrations of heteropoly acid and sulfuric acid were 1.25 wt% and 1.5 wt%, respectively, and the conditions of  $170^\circ\text{C}$ , initial  $\text{O}_2$  pressure of 3 MPa, and the reaction time of 60 min. In addition, the catalyst system exhibited a satisfactory reusability for the procedure. In this catalyzed oxidation, lignite was first converted to water-soluble intermediates. Then the water-soluble intermediates were converted to the desired carboxylic acids. The mechanistic study suggested that sulfuric acid not only promoted the conversion of lignite in the reaction system but also assisted the generation of protonated heteropoly

acid and the active species of  $\text{VO}_2^+$ . The heteropoly acid in the reaction could assist both the depolymerization of lignite and the production of carboxylic acids. In the catalytic process of oxidation with a heteropoly acid, lignite or water soluble intermediates were oxidized by vanadium (V) while the vanadium (V) was concurrently reduced to vanadium (IV). Then, the vanadium (IV) was oxidized to vanadium (V) by oxygen, and a redox cycle was completed. In comparison with alkali-oxygen oxidation of the lignite, the present method avoided the use of large amounts of alkali and acid and the reaction temperature was lower.

Yang and others [126] proposed that polyoxometalates (e.g.,  $\text{H}_3\text{PMo}_{12}\text{O}_{40}$ ) could be a perfect candidate to convert woody biomass directly into precious products (water-soluble carbohydrates and aromatic monomers) under moderate conditions, which are quite different from the harsh operating conditions usually required for such processes. Polyoxometalates could be applied either as a direct oxidation agent or as a catalyst to depolymerize lignin. However, the technical lignin oil yield for this process is rather low. In place of using technical lignin, the authors used an oxidation approach and directly converted native lignocellulose in a mixture of methanol/water using  $\text{H}_3\text{PMo}_{12}\text{O}_{40}$  as a catalyst to afford the precious desired products. In the hardwood, 80% of lignin was depolymerized to low-molecular weight lignin oil (ca. 376 Da) at  $150^\circ\text{C}$  and 1 MPa  $\text{O}_2$  in 2 h. The lignin oil afforded 38.0% aromatic monomers, based on total lignin mass. At the same time, only 9.2% residual solids remained; 83.7% of the hemicellulose in the hardwood was converted to water-soluble carbohydrates.

Yasuda and coworkers [106] investigated the role of steam in selective oxidation of methacrolein **161** with molecular oxygen ( $\text{O}_2$ ) over  $\text{H}_3\text{PMo}_{12}\text{O}_{40}$  as a catalyst (Scheme 4.40). Upon the addition of steam to the feed gas, catalytic activity and selectivity toward methacrylic acid **161** were significantly enhanced fivefold and increased twice, respectively, under the optimal pressure of steam ( $P_{\text{H}_2\text{O}}=0.13$  atm). Kinetic analysis revealed that the addition of steam increased the preexponential factor for the formation of methacrylic acid by 200 times, resulting in a significant increase in the activity. Under the reaction conditions, the steam in the feed gas changed the hydrous state of  $\text{H}_3\text{PMo}_{12}\text{O}_{40}$ , but it had no effect on the redox property, crystalline and molecular structures, or the surface area of the catalyst. In the presence of steam at 573 K, three  $\text{H}_2\text{O}$  per molecule of  $\text{H}_3\text{PMo}_{12}\text{O}_{40}$  were absorbed and hydrated protons like hydronium ion ( $[\text{H}_3\text{O}]^+$ ) were formed in the bulk of  $\text{H}_3\text{PMo}_{12}\text{O}_{40}$ . Methacrolein could be adsorbed on the surface of the hydrous catalyst. However, it was not absorbed on the anhydrous specie at all. These results suggested that the activation of methacrolein readily occurred on the catalyst surface in the presence of steam, resulting in a significant increase in the preexponential factor. Quantum mechanical calculations confirmed the mild activation of methacrolein via the reaction with hydronium ion ( $[\text{H}_3\text{O}]^+$ ) without any transition state.



**SCHEME 4.40** Oxidation of methacrolein over  $\text{H}_3\text{PMo}_{12}\text{O}_{40}$ .

Gromov et al. [127] demonstrated that *Parachlorella kessleri* IC-11 microalga biomass had a high potential of producing biogenic formic acid under air atmosphere and hydrothermal conditions.

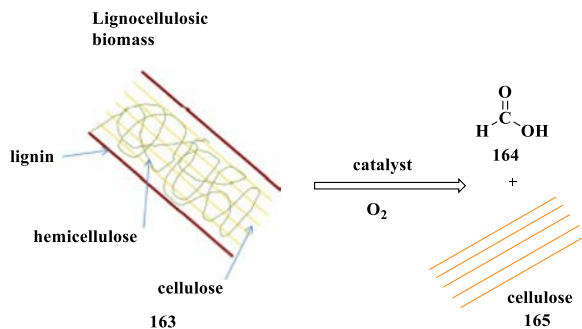
The purpose of the authors was to transform the microalgae biomass to formic acid for the first time in the presence of soluble and solid Mo-V-P heteropoly acid catalysts under an air atmosphere without any additives or cocatalysts, and to compare the effectiveness of homogeneous and heterogeneous approaches.

Homogeneous and heterogeneous approaches were applied and compared in the catalysis of the above process. The authors conducted the experiments in the presence of soluble ( $\text{H}_5\text{PMo}_{10}\text{V}_2\text{O}_{40}$ ) and solid ( $[(\text{C}_4\text{H}_9)_4\text{N}]_{3.5}\text{H}_{0.5}\text{PMo}_{11}\text{VO}_{40}$ ) bifunctional catalysts. The effect of the reaction temperature and catalyst loading on the formation of formic acid was observed. It was evident from the experimental data that transformation of the microalgae biomass to formic acid was restricted by biomass depolymerization as well as hydrolysis processes, but not by the oxidation of intermediates to formic acid. Formic acid was achieved in the presence of  $\text{H}_5\text{PMo}_{10}\text{V}_2\text{O}_{40}$ , with better yields in comparison with  $[(\text{C}_4\text{H}_9)_4\text{N}]_{3.5}\text{H}_{0.5}\text{PMo}_{11}\text{VO}_{40}$ . Yields of 30 wt% and 49 wt% were achieved for the desired product over  $[(\text{C}_4\text{H}_9)_4\text{N}]_{3.5}\text{H}_{0.5}\text{PMo}_{11}\text{VO}_{40}$  and  $\text{H}_5\text{PMo}_{10}\text{V}_2\text{O}_{40}$ , respectively. The solid catalyst ( $[(\text{C}_4\text{H}_9)_4\text{N}]_{3.5}\text{H}_{0.5}\text{PMo}_{11}\text{VO}_{40}$ ) exhibited high stability in at least seven runs of the reaction, while the activity of soluble heteropoly acid diminished in the fifth run.

Therefore, different types of plant and microbial resources were already involved in the oxidation process to formic acid.

Albert and others [128] identified and optimized appropriate polyoxometalate catalysts for the partial oxidation of lignocellulosic biomass **163** (i.e., wood and residues from sugar or paper industries) to give formic acid **164** as well as high-grade cellulose **165** for other processes, e.g., production of bio-ethanol (Scheme 4.41). Homogeneous vanadium precursors such as sodium metavanadate and vanadyl sulfate and Keggin-type polyoxometalates or even other structures like Anderson-, Wells-Dawson-, or Lindqvist type polyoxometalates were evaluated for the desired catalytic performance. The Lindqvist-type polyoxometalate  $\text{K}_5\text{V}_3\text{W}_3\text{O}_{19}$  demonstrated the most favorable activity for the first time in the literature in the selective oxidation of only hemicellulose and lignin to formic acid, while the cellulose fraction remained intact.

The strategy of the authors provided the best value for using clean complex biomass as a substrate without any pretreatment and simply in aqueous media under oxygen pressure.



**SCHEME 4.41** Oxidation of lignocellulosic biomass formic acid and cellulose.

In order to grasp the specific effect of different active species on the stepwise degradation of the carbon-framework, the authors made a comparison of appropriate homogeneous catalysts for the selective depolymerization and oxidation of molecular well-defined substrates. The catalysts were selected based on the results obtained from previous similar studies. Two homogeneous vanadium catalysts as well as a variety of polyoxometalates from four structural categories were selected to make a comparison. An outstanding result from these experiments was the importance of the presence of a minimum of two vanadium atoms in the framework of the catalyst for the production of formic acid under moderate conditions. In addition, the vanadium-substituted Keggin-type polyoxometalates HPA- $n$  ( $n \geq 2$ ) exhibited the highest yields for formic acid. However, it was observed that these structures catalyzed the oxidation of every model substrate, even those for cellulose. Consequently, they could not be utilized for partial biomass conversion. In addition, the water-soluble vanadium precursors  $\text{NaVO}_3$  and  $\text{VOSO}_4$  exhibited similar catalytic performances; therefore, they were not appropriate for the target conversion. Furthermore, the Anderson-type polyoxometalate  $\text{Na}_4\text{Cu}_2\text{V}_8\text{O}_{24}$  was not able to show any catalytic activity under the reaction conditions. On the other hand, the Wells-Dawson type polyoxometalate  $\text{K}_8\text{P}_2\text{V}_2\text{W}_{16}\text{O}_{62}$  proved to be quite favorable, while a slight extent of the undesired conversion of glucose and cellobiose was still observed. The most intriguing result of the performed studies was that partial oxidation of biomass was observed only with the Lindqvist-type catalyst  $\text{K}_5\text{V}_3\text{W}_3\text{O}_{19}$ . The latter seemed to satisfy the need for catalyzed partial oxidation of only lignin and hemicellulose fractions of lignocellulosic biomass under the applied reaction conditions. However, the yields of formic acid were quite low, suggesting a need to optimize the reaction parameters and the utilized equipment for the desired partial conversion.

Albert and others [129] reported the selective catalyzed oxidation of complex, second- and third-generation water-insoluble and wet biomasses to formic acid with efficient recycling of the catalyst. Furthermore, the relevance and



limits of potential contaminants were demonstrated by a variety of experimental approaches. Utilizing a polyoxometalate as a very powerful homogeneous catalyst in an aqueous solution,  $O_2$  as the oxidizing agent, and an acid as solubilizer, conversion of different lignocellulosic and algae feedstock into formic acid and pure carbon dioxide was made possible. The merits of the applied green oxidation system were low reaction temperatures (below  $100^\circ\text{C}$ ) and high selectivity. Moreover, catalyst recycling was successfully conducted for three runs.

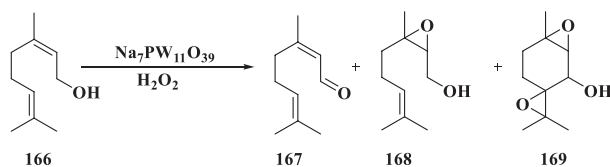
The authors managed to broaden the substrate scope considerably for the reaction by converting a wide variety of substrates such as many complex water-insoluble biogenic feeds and contaminated materials. While food industry waste, sewage sludge, and even railroad tie was found to be effectively converted under the typical reaction conditions of the OxFA process (i.e.,  $90^\circ\text{C}$ , 30 bar  $O_2$ , and 24 h reaction time), an obvious yet undetected limitation thus far was found for the feedstock containing metal ions. Whenever biological feed contaminated with metal ions capable of forming stable water-insoluble complexes with the catalytically active polyoxometalate ions was present in the feedstock, the reactivity of the oxidation system was observed to reduce drastically or almost completely vanish. The supportive role of the TSA additive for depolymerization and solubilization of the second and third generations was dramatically accentuated by comparative oxidation experiments with pomace and cyanobacter. Eventually, with repetitive uses of the applied HPA-2 catalyst and the TSA additive, it was possible to confirm that the applied homogeneous polyoxometalate-based catalytic systems for both conversions of water-soluble (glucose, cellobiose) and water-insoluble (beech and pine wood) substrates were generally recyclable. Only slight losses in the conversion of the biomass and formic acid selectivity were detected over three successive runs using the same catalyst and additive solution, which demonstrated the robustness and practical usability of the studied catalytic system.

Odyakov and others [130] investigated the use of a homogeneous catalysis system, which included a two-component catalyst comprising of an aqueous solution of palladium complexes in a 0.25-M solution of modified (non-Keggin) heteropoly acid with the molecular formula  $H_{12}P_3Mo_{18}V_7O_{85}$  (HPA-7'), in the scale-up of the oxidation of *n*-butylenes to methylethylketone to an industrial level in 2005–2006. The oxidation was performed in a chloride-free aqueous solution of palladium complexes in a modified solution of Mo-V-P heteropoly acid with the molecular formula of  $H_{12}P_3Mo_{18}V_7O_{85}$  (HPA-7'). The method had the advantages that it increased the oxidative capacity in the primary oxidation of *n*- $C_4H_8$  and increased the thermal stability, which allowed quick regeneration of the catalyst with atmospheric oxygen at  $160$ – $170^\circ\text{C}$ . The authors described the preparation of a pilot batch of a total volume of 50 L; the starting materials were vanadium (V) oxide ( $V_2O_5$ ), molybdenum trioxide ( $MoO_3$ ), and phosphoric acid. The important aspect of the process was dissolving vanadium (V) oxide while stirring it in a dilute and cooled solution of  $H_2O_2$ . In this way, vanadium (V) peroxide complexes were formed, which decomposed at elevated



temperatures to give a solution of  $H_6V_{10}O_{28}$  with a concentration of 0.0175 M. A calculated amount of phosphoric acid was then added to the resultant solution to achieve a more stable of  $H_9PV_{14}O_{42}$  solution (0.0125 M). As the  $H_9PV_{14}O_{42}$  solution occupied an enormous volume, it was prepared three times in a reactor with a capacity of 300L. In the main reactor (with a capacity of 500L), molybdenum trioxide was dissolved in water with stirring, while the remaining portion of phosphoric acid was added incrementally. The resulting mixture was then evaporated; all of the previously obtained portions of the dilute  $H_9PV_{14}O_{42}$  solution were gradually introduced. The resultant HPA-7' solution was evaporated to about 100L and filtered twice to separate the slight amount of the precipitate. Once more, the filtrate was evaporated to 50L, and a calculated amount of palladium chloride was added while the solution was being stirred at 70–80°C. In total, 27 batches of the catalyst ( $Pd^+ 0.25 M$  HPA-7') with a total volume of 1350L were obtained. All the equipment of the pilot industrial unit for MEK synthesis was filled with the resulted catalyst.

Vilanculo and others [131] assessed the activity of a wide variety of Keggin heteropoly acid salts in a novel and one-pot synthesis of invaluable chemicals from the oxidation of terpenic alcohols **166** (i.e., an aldehyde **167**, an epoxide **168**, and a diepoxide **169**) using a green oxidizing agent ( $H_2O_2$ ) under moderate conditions (Scheme 4.42). Lacunar Keggin heteropoly acid sodium salts were investigated in this reaction as the goal catalysts. Starting with heteropoly acids  $H_3PMo_{12}O_{40}$ ,  $H_3PW_{12}O_{40}$ , and  $H_4SiW_{12}O_{40}$ , the authors synthesized the lacunar sodium salts (i.e.,  $Na_7PW_{11}O_{39}$ ,  $Na_7PW_{11}O_{39}$ ,  $Na_8SiW_{11}O_{39}$ ) as well as the saturated salt ( $Na_3PW_{12}O_{40}$ ). Every case was examined for oxidation reactions in a homogeneous phase with nerol as a model molecule. It was observed that  $Na_7PW_{11}O_{39}$  had the most selectivity and activity toward the products of the oxidation reactions. All the catalysts were analyzed using FT-IR, TG/DSC, BET, XRD, SEM-EDS technics, and potentiometric titration. The authors assessed the main reaction parameters. Geraniol,  $\beta$ -citronellol,  $\alpha$ -terpineol, and borneol were successfully oxidized as well. Particular attention was paid to the correlation between the composition and properties of a catalyst and its activity.

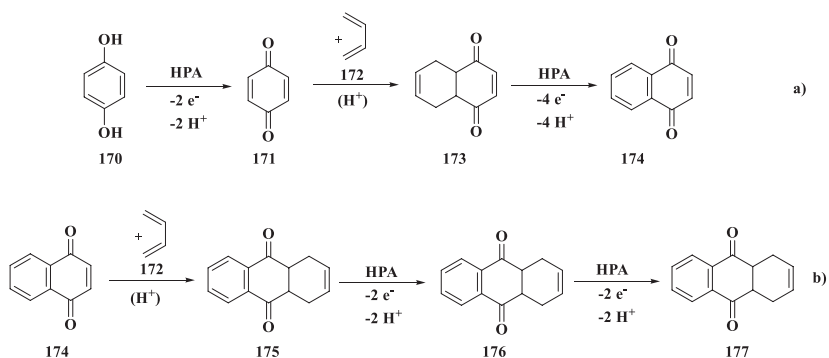


**SCHEME 4.42** Oxidation of terpene alcohols.

The authors explored the oxidation of terpenic alcohols (with nerol as the model molecule) using hydrogen peroxide as an oxidizing agent in acetonitrile solutions. The author successfully extended the reaction scope to other terpenic alcohols.

In this work, the lacunar salt sodium phosphotungstate exhibited more activity than the silicotungstate and phosphomolybdate catalytic systems. The author demonstrated that the presence of a vacancy in the Keggin heteropolyanion had an important role in the activity of the catalyst. The saturated salt ( $\text{Na}_3\text{PW}_{12}\text{O}_{40}$ ) was nearly inactive; the main products in this case were alkyl peroxides. In reactions catalyzed by  $\text{Na}_7\text{PW}_{11}\text{O}_{39}$ , the major product was always nerol epoxide ( $\sim 90\%$ ) with less formation of the aldehyde and diepoxide. The effects of the main reaction parameters were also studied and it was found that the catalyst concentration and the oxidizing agent load had an evident impact on the reaction selectivity. In addition, other terpenic alcohols were subjected to oxidation by  $\text{H}_2\text{O}_2$  in reactions catalyzed by  $\text{Na}_7\text{PW}_{11}\text{O}_{39}$ . While the reactivity of geraniol was similar to that of nerol,  $\alpha$ -terpineol,  $\beta$ -citronellol, and borneol were less reactive.

Zhizhina and coworkers [132] were able to perform condensation of 1,3-butadiene with *para*-quinones and oxidation of the resulting adducts as a one-pot process in the presence of aqueous solutions of molybdenum-vanadium phosphoric heteropoly acids with the general formula  $\text{HaPzMoyVxOb}$  as an acidic catalyst. Having bifunctional catalytic properties, these solutions were both strong Brønsted acids and reversible oxidizing agents. Upon condensation of hydroquinone **170**, 1,4-benzoquinone **171**, or 1,4-naphthoquinone **174** with 1,3-butadiene **172** in a solution of the heteropoly acid, 9,10-anthraquinone **177** was resulted in a mixture with tetrahydro-9,10-anthraquinone **175** and dihydro-9,10-anthraquinone **176** (Scheme 4.43). In this one-pot procedure, which proceeded in the absence of an organic solvent, the heteropoly acid solution was reduced. A slightly soluble mixture of **175**, **176**, and **177** was precipitated and filtered off. The solution of the non-Keggin-type heteropoly acid  $\text{H}_{12}\text{P}_3\text{Mo}_{18}\text{V}_7\text{O}_{85}$  was found to be the most effective in the process. This solution could be rapidly regenerated by  $\text{O}_2$  or air at temperatures of up to  $170^\circ\text{C}$  and reused. The prepared mixture of **175**, **176**, and **177** could be used as a catalyst



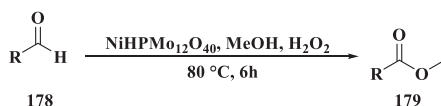
**SCHEME 4.43** The synthesis of 9,10-anthraquinone **177** from hydroquinone **170**, 1,4-benzoquinone **171**, or 1,4-naphthoquinone **174** in the presence of the aqueous solution of a heteropoly acid as a bifunctional catalyst.

for alkaline delignification of wood. The homogeneous bifunctional heteropoly acid catalytic system used in this work was quite stable and proved to be promising for use in similar one-pot processes.

Chepaikin et al. [133] explored the possibility of utilizing heteropoly acids (e.g.,  $\text{H}_5\text{PMo}_{10}\text{V}_2\text{O}_{40}$  and  $\text{H}_7\text{PMo}_8\text{V}_4\text{O}_{40}$ ) as a cocatalyst and compared their efficiencies with those of copper (II) in the oxidation of propane in aqueous acetic acid media in the presence of palladium, rhodium, and platinum compounds upon the action of a carbon dioxide/oxygen mixture.

It was demonstrated that the systems exhibited catalytic activities only when carbon dioxide was introduced as a reducing agent; by switching from copper (II) compounds to heteropoly acids, the activity increased for the platinum catalysts, while it decreased for the palladium and rhodium systems. The contribution of the inner-sphere and outer-sphere mechanism to the activation and oxidation of propane was also determined. The authors realized that the role of heteropoly acids in propane oxidation was similar to that of copper compounds. The use of heteropoly acids as cocatalysts turned out to be promising for designing heterogenized catalytic systems on the basis of inorganic or polymeric porous supports.

Patel and others [134] characterized the Ni salt of phosphomolybdic acid by EDX, UV-vis, TGA, FT-IR, Raman spectroscopy, and XPS in detail. They also evaluated its catalytic activity for the oxidative esterification of benzaldehyde **178** to ester **179** (Scheme 4.44). The reaction was conducted utilizing methanol and hydrogen peroxide under a variety of reaction parameters, e.g., the catalyst and hydrogen peroxide amounts, methanol volume, as well as reaction time and temperature to optimize the conversion and selectivity toward ester. The synthesized catalyst was recycled and reused for up to three cycles. A detailed mechanism was proposed for the reaction based on the UV-visible and Raman spectroscopies. In addition, the activity of the synthesized catalyst toward various aromatic aldehydes was assessed. The authors demonstrated that  $-\text{Cl}$ , as a strong electron-withdrawing group, facilitated the reaction more than  $-\text{Br}$ . Aliphatic aldehydes also underwent the conversion satisfactorily. The achieved results exhibited that the activity of the catalyst with various substrates under mild conditions was quite eminent.



**SCHEME 4.44** Oxidative esterification of benzaldehyde.

The authors came up with the bifunctional catalytic activity of nickel (as a Lewis acid) and molybdenum (with redox property) for the conversion of benzaldehyde to benzoate. Very small amounts of nickel (0.155 mg) could improve

the TON value (mole ratio of the product to the catalyst) from 1731 to 2560. The catalyst was found to be efficient for a few aldehydes, giving selectivities of 77%–89% for the ester with a maximum TON value of 2711. Although the catalyst was homogeneous, it was easily recyclable by a simple method and reusable for several cycles.

Kai and others [135] described the synthesis of several organic/inorganic composite catalysts using ionic liquids and heteropoly acids as precursors. To be more specific, they prepared heteropoly acid/ionic liquid (HPAIL) catalysts via combining an ionic liquid with an  $-\text{SO}_3\text{H}$  functional group of high molecular weight [*N,N*-dimethyl(benzyl)-ammonium propyl sulfobetaine (DMBPS)] and a Keggin-type structure of tungstophosphoric acid ( $\text{H}_3\text{PW}_{12}\text{O}_{40}$ ) with different composition ratios. Using various techniques, the resultant inexpensive, nontoxic, and water-soluble HPAIL catalysts were analyzed and employed for the oxidation of benzyl alcohol with 30% hydrogen peroxide in water. This catalyzed reaction was specifically carried out in a biphasic system. After the reaction was completed, the catalyst was readily recycled from the aqueous phase. The products were separated from the organic phase. The reaction was therefore efficient, safe, and environmentally friendly.

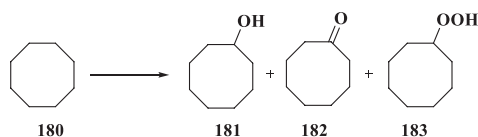
Among the catalysts explored, the [DMBPSH] $\text{H}_2\text{PW}_{12}\text{O}_{40}$  catalyst showed the best catalytic activity, being utilized to obtain the optimal oxidation conditions at a molar ratio of 1:1.7 for benzyl alcohol/hydrogen peroxide, catalyst amount of 5.4 wt%, reaction time of 3.9 h, and 24 ml water, which resulted in a desirable yield of 95.8% for benzoic acid. Based on the kinetic model developed for the reaction, an order of 2.2 and activation energy of 36.18 kJ/mol were deduced.

Karcz and coworkers [136] studied the effect of the polyatomic nature (tungsten or molybdenum) and/or the location of the cobalt dopant within the heteropoly compound structure on the aerobic oxidation of cyclooctane in liquid phase. Their work included both experimental and theoretical aspects. Monosubstituted cobalt-containing compounds, either within a Keggin anion, e.g.,  $\text{TBA}_4\text{HPW}(\text{Mo})_{11}\text{CoO}_{39}$  (TBA=tetrabutylammonium), or in the cationic position, e.g.,  $\text{CoHPW}(\text{Mo})_{12}\text{O}_{40}$ , were synthesized and their identities were confirmed by characterization with FT-IR, XRF, and UV-vis. The oxidation of cyclooctane was performed through an auto-oxidation mechanism. The experimentally observed patterns of the catalytic behavior were dependent on the polyatomic nature (tungsten or molybdenum) and/or the location of the cobalt dopant within the heteropoly compound structure. The molybdenum catalysts were generally found to have more activity than their tungsten counterparts. In addition, the cobalt location within the Keggin structure proved to be more beneficial than its addition as a counter cation. DFT modeling of the cobalt-substituted Keggin anions and free enthalpy computation for the elementary steps of the chain initiation and the chain propagation/branching explained the observed effects.

The higher maximum turnover frequencies and shorter period of induction observed for  $\text{HPMo}_{12}$ , in comparison with those of  $\text{HPW}_{12}$  were ascribed to

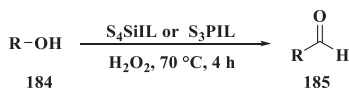
more favorable energetics of the chain initiation and chain propagation steps over the former. The observed effects were tightly related to the higher reducibility of the molybdenum-based heteropoly acid. The decrease in the induction time and augmenting maximum turnover frequencies owing to the addition of cobalt in the form of a compensating cation, which was observed both for 12-tungstophosphate and 12-molybdophosphate salts, was due to the creation of new paths energetically favorable for chain initiation and decomposition of the cyclooctyl-hydroperoxide intermediate. A strong upward shift of HOMO and LUMO with respect to those of the unmodified  $\text{PMo}_{12}$  and  $\text{PW}_{12}$  anions resulted from the insertion of cobalt into the Keggin anion primary structure, which in turn lowered the reducibility of the substituted catalysts. Consequently, incorporation of cobalt into the Keggin anion resulted in two effects, i.e., having a reverse effect on the chain initiation and the chain propagation. Chain initiation via H abstraction from cyclooctane was energetically less favorable because of the lower reducibility of the cobalt-substituted anions. However, the advent of a new path for the formation of radicals via oxygen activation over cobalt sites diminished the induction period. The observed final result was a drastic decrease in the induction period compared to those of the unsubstituted forms, which was even more evident than in the case of cationic cobalt species. According to the computational studies  $\Delta G$  values of the relevant reactions are much lower than for those of other considered chain initiation reactions supported the extraordinary efficient oxygen activation over the cobalt sites incorporated into the Keggin anions. The catalytic effect of adding cobalt on the chain propagation step was observed regardless of the cobalt position. However, its magnitude depended on the cobalt placement. The  $\Delta G$  value of the interaction between the cationic cobalt species and cyclooctyl-hydroperoxide intermediate was therefore similar to those calculated for 12-molybdophosphate anions, explaining the observed increase in the maximum turnover frequencies in comparison with the pure acid catalysts.

As for cobalt-containing heteropoly anions, the negative  $\Delta G$  values indicated that the decomposition of the cyclooctyl-hydroperoxide intermediate over these catalysts probably took place spontaneously, and a very strong catalytic effect could be expected. As a matter of fact, the experimental data demonstrated that for both the W- and the Mo-based catalyst series, the highest maximum turnover frequencies values were observed for the cobalt-substituted heteropoly anions (Scheme 4.45).



**SCHEME 4.45** Reaction products in the aerobic oxidation of cyclooctane.

Li et al. [137] prepared and characterized two novel heteropolyanion-based ionic liquids with long-chain multi-SO<sub>3</sub>H functional groups. As homogeneous catalysts, they exhibited high activities in selective oxidation of alcohols (**184**) with aqueous hydrogen peroxide (35%) under solvent-free conditions without using a phase transfer catalyst (Scheme 4.46). The aldehydes or ketones were produced in good to excellent yields (63%–100%). Benzyl alcohols afforded related benzoic acids in yields of 64%–94%. The two ionic liquids were easily recoverable and reusable for five cycles without any considerable loss in their activities.



R = PhCH<sub>2</sub>, 4-CH<sub>3</sub>C<sub>6</sub>H<sub>4</sub>CH<sub>2</sub>, 4-CH<sub>3</sub>OC<sub>6</sub>H<sub>4</sub>CH<sub>2</sub>, 4-ClC<sub>6</sub>H<sub>4</sub>CH<sub>2</sub>, 4-NO<sub>2</sub>C<sub>6</sub>H<sub>4</sub>CH<sub>2</sub>, cyclohexyl, cyclopentyl, CH<sub>3</sub>(CH<sub>2</sub>)<sub>4</sub>CHCH<sub>3</sub>, C<sub>3</sub>H<sub>11</sub>, PhCHCH<sub>3</sub>, Ph(CH<sub>2</sub>)<sub>2</sub>, (Ph)<sub>2</sub>CH

**SCHEME 4.46** Selective oxidation of alcohols catalyzed by two novel heteropolyanion-based ionic liquids with long-chain multi-SO<sub>3</sub>H functional groups.

Given the efficiency of manganese- and cobalt-based catalysts for the oxidation of cyclohexane, Mouanni and others [138] tried the introduction of these two elements as a counter ion of [PMo<sub>12</sub>O<sub>40</sub>]<sup>3-</sup>. Therefore, they prepared a series of polyoxometalates of the general formula H<sub>3-2(x+y)</sub>Mn<sub>x</sub>Co<sub>y</sub>PMo<sub>12</sub>O<sub>40</sub> (x + y ≤ 3/2 and x, y: 0–1.5) and characterized them by several physicochemical techniques including infrared, scanning electron microscopy/energy dispersive X-ray (SEM/EDX), <sup>31</sup>P NMR, X-ray diffraction, and thermogravimetric analysis. Mouanni et al. used the species as catalysts for the oxidation reaction of cyclohexanone using H<sub>2</sub>O<sub>2</sub> (30%) as an oxidizing agent. The results of the catalytic examinations demonstrated that all examined systems were quite active in the oxidation of cyclohexanone and afforded adipic acid, succinic acid, glutaric acid, hexanoic acid, 6-hydroxyhexanoic acid, 7,7-dimethoxy and heptanoic acids, and 1,1-dimethoxy octane, which were identified by GC-MS. Among these, adipic acid was the major product, using a catalyst/substrate molar ratio of 2.84 × 10<sup>-3</sup> and 20h of reaction. With a composition of HMn<sub>0.25</sub>Co<sub>0.75</sub>, the adipic acid yield attained the maximum (75%). The effects of factors such as the polyoxometalate counter ion, molar ratios of the catalyst to the reactants, and reaction time on the product distribution were examined. The used catalysts were analyzed by <sup>31</sup>P NMR. The catalytic stability of HMn<sub>0.25</sub>Co<sub>0.75</sub>PMo<sub>12</sub>O<sub>40</sub> was investigated in five successive cycles.

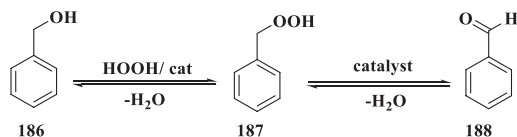
The possible active species for the formation of carboxylic acids from the products formed in the first step could be a peroxo-polyoxometalate species. Application of H<sub>3-2(x+y)</sub>Mn<sub>x</sub>Co<sub>y</sub> as catalysts, and hydrogen peroxide as an oxidizing agent without using any solvent, led to a clean and efficient process and might be an alternative to using toxic, harmful, and corrosive nitric acid.

Coronel and others [139] assessed the catalytic activity of a series of metal-substituted Keggin heteropoly acids ( $M = \text{Cu}^{2+}$ ,  $\text{Co}^{2+}$ ,  $\text{Fe}^{3+}$ ,  $\text{Al}^{3+}$ , and  $\text{Ni}^{2+}$ ) in the oxidation of benzylic alcohol with hydrogen peroxide in liquid phase under phase transfer catalyst-free conditions. The catalysts were synthesized from the lacunar salt derivatives of the Keggin heteropoly acids ( $\text{H}_3\text{PMo}_{12}\text{O}_{40}$ ,  $\text{H}_3\text{PW}_{12}\text{O}_{40}$ , and  $\text{H}_4\text{SiW}_{12}\text{O}_{40}$ ). The resultant catalysts were characterized by BET, XRD, FT-IR, EDS, TG-DSC, and potentiometric titration. The effects of the main reaction variables, i.e., stoichiometry of the reactants, temperature, solvent, and catalyst concentration, were evaluated.

The solvent played a critical role in the completion of the reaction. The authors thoroughly studied the correlation between the nature of heteropoly acid and their catalytic activities. The recovery and reuse of the heteropoly acid catalyst were also evaluated.

Then, the oxidation of benzyl alcohol with hydrogen peroxide was achieved in the presence of metal-substituted phosphotungstate potassium salts as a potent class of catalysts. A series of transition metal cations ( $\text{Cu}^{2+}$ ,  $\text{Co}^{2+}$ ,  $\text{Fe}^{3+}$ , and  $\text{Ni}^{2+}$ ) were incorporated into the vacancy of the lacunar phosphotungstate salts. However, the more selective cation (i.e.,  $\text{Ni}^{2+}$ ) was also incorporated into two more Keggin lacunar salts (i.e., silicotungstate and phosphomolybdate potassium salts). Among the evaluated catalysts,  $\text{K}_5\text{PW}_{11}\text{NiO}_{39}$  exhibited the highest activity and selectivity. This species catalyzed the oxidation of benzyl alcohol in a biphasic system (i.e., toluene/aqueous hydrogen peroxide), chiefly affording benzaldehyde and benzoic acid.

This selective process was found to be a desirable alternative to the solid supported-catalyzed processes as it avoided the time-consuming synthesis of both support and metal catalyst doped-support. The catalyst was successfully recoverable and reusable with no loss of activity (Scheme 4.47).



**SCHEME 4.47** Oxidation of benzyl alcohol with hydrogen peroxide.

Bertleff and coworkers [140] demonstrated a new method for fuel desulfurization—that is, the selective oxidation of the organic sulfur compounds in fuels to water-soluble sulfur compounds to be extracted in situ into an aqueous phase. However, the authors presented a technique that extensively (60%–70%) converted the sulfur compounds in fuel to sulfate using oxygen as an oxidizing agent and an aqueous solution of  $\text{H}_8\text{PV}_5\text{Mo}_7\text{O}_{40}$  (HPA-5) as a catalyst. Other water-soluble desulfurization products were sulfoacetic acid (10%–20%), 2-sulfobenzoic acid, and 2-(sulfoxy) benzoic acid (with both less than 10%). The new desulfurization method was optimized for the removal of



benzothiophene from isoctane to give the best results with a desulfurization degree of 99% at 120°C, under 20 bar oxygen pressure, and 1000rpm of 6h reaction time using a volume water/oil ration of 10:1. The potential advantage of this work from a sustainable viewpoint in refining processes was the fact that oxidative desulfurization could be combined with the aqueous extraction of sulfate in a single operation and water could be used as a green extraction solvent.

Lei and others [141] developed a catalytic system utilizing a Keggin-type phosphomolybdic acid (PMA) and hydrogen peroxide ( $H_2O_2$ ) to degrade 4-chlorophenol. They studied the degradation of 4-chlorophenol as a type of adsorbable organic halide (AOX), and its mechanism. The influence of the reaction conditions, e.g., temperature,  $H_2O_2$  concentration, phosphomolybdic acid concentration, pH, and other reaction parameters, on the oxidative degradation of 4-chlorophenol was studied in a systematic manner. The intermediates of degradation of 4-chlorophenol by a phosphomolybdic acid/hydrogen peroxide system were detected by HRLC-ToF-MS and GC-MS, and accordingly a plausible path was proposed for the degradation of 4-chlorophenol. In addition, the cleavage of 4-chlorophenol indicated that the catalytic system for the oxidation of phosphomolybdic acid/hydrogen peroxide was an efficient method for the removal of halogenated organic pollutants.

Consequently, phosphomolybdic acid/hydrogen peroxide proved to be an effective catalytic oxidation system. Phosphomolybdic acid promoted the activation of hydrogen peroxide to afford free radicals while oxidizing and degrading the organic matter, and phosphomolybdic acid collaborated with free radicals to enhance and accelerate the degradation of the organic matter. 4-chlorophenol was completely oxidizable and degradable in phosphomolybdic acid/hydrogen peroxide homogeneous reactions with no pH restriction. At 90°C, the removal efficiency of 4-chlorophenol reached 100% after 120 min. The rate of AOX removal was found to be 80.19%. The phosphomolybdic acid/hydrogen peroxide catalytic oxidation was able to degrade the organic matter relatively efficiently, not depending on pH with no iron sludge. Therefore, the method proved promising for toxic and difficult wastewater treatment.

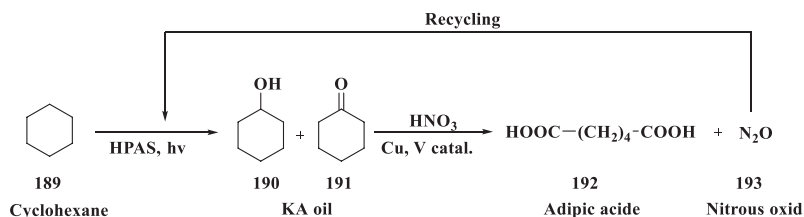
#### 4.5. Photocatalysis

Photocatalysis is an astounding topic in many fields of chemistry, e.g., selective organic synthesis, water treatment, air cleaning, hydrogen production, and manufacture of disinfectants [142–144]. In the last 20 years, green photocatalysts such as polyoxometalates have been extensively introduced and used, and exhibited similarities to semiconductor photocatalysts in their photochemical characteristics and general properties. Among them, Keggin heteropoly acids and their derivatives have been widely used as oxidation and acid catalysts for many industrial applications and numerous organic syntheses [145–150]. In homogeneous catalysis, polyoxometalates have been widely applied in liquid phase owing to their high solubility in polar solvents. Therefore, in photo-assisted



oxidation reactions, they could be activated using ultraviolet light [151, 152]. Polyoxometalates exhibit a high photocatalytic performance, which is due to an electron transfer from the HOMO to the LUMO and this creates a positive charged hole in the HOMO orbital, which has a strong oxidative property [153]. As multielectron redox agents, polyoxometalates have some advantages, which are attributed to the huge number of metal centers existing in the structure of such species [154]. This renders them a strong light absorber in the range of 200–500 nm owing to the O/M ligand-to-metal charge transfer absorption bands [155]. The reduced polyoxometalate may be re-oxidized in the presence of persulfate. Consequently, even when harsh conditions are employed in the absence of organic ligands, the system reliability is preserved [155].

Balaska et al. [156] investigated the synthesis of several Wells-Dawson heteropoly acids and then applied them in homogeneous photocatalytic processes (Scheme 4.48). The efficiency of the photocatalytic process was evaluated by examining the initial concentration of phenol, pH, and catalyst loading. The authors assessed the effects of operational key parameters on phenol photodegradation under ambient conditions and the first-order rate kinetics.



**SCHEME 4.48** Production of adipic acid by photocatalytic oxidation of cyclohexane.

The experimental results revealed that the UV radiation assisted by heteropoly acids as effective acidic catalysts might be efficiently used in degradation of refractory organic compounds like phenol at relatively short times (60 min for  $\text{H}_7\text{P}_2\text{W}_{17}\text{VO}_{62}\cdot 14\text{H}_2\text{O}$  and 90 min for  $\text{H}_5\text{P}_2\text{W}_{12}\text{Mo}_5\text{FeO}_{62}\cdot 10\text{H}_2\text{O}$ ). Clearly, various parameters, particularly pH, irradiation time, and catalyst loading, exerted intense influences on this photodegradation process. The photodegradation of phenol is more effective in acidic media. The optimal pH for the photodegradation was 2 for both heteropoly acids. To describe the photodegradation reaction, a first-order rate expression was used in which the rate constants  $k = 8.56 \times 10^{-2}$  and  $9.94 \times 10^{-2} \text{ min}^{-1}$  were obtained in the optimal conditions for the iron- and vanadium-substituted heteropoly acids, respectively. The total organic carbon (TOC) results revealed that the photocatalysis processes required more time to complete the mineralization of phenol into water and carbon dioxide. The photodegradation study and mineralization test indicated that the tungstate heteropoly acid,  $\text{H}_7\text{P}_2\text{W}_{17}\text{VO}_{62}\cdot 14\text{H}_2\text{O}$ , was the most efficient photocatalyst degradation of phenol.

Developing a moderate process with high efficiency for the utilization of nitrous oxide ( $N_2O$ ) as a green oxidizing agent is of great academic and industrial importance in the synthesis of oxygenated products. She and others [157], for the first time, reported that a series of vanadium-substituted molybdophosphoric acids ( $PMo_{12-n}V_n$ ,  $n=1-3$ ), in the presence of hydrochloric acid in an aqueous solution, could catalyze the oxygenation of cyclohexane (189) by  $N_2O$  (193) in liquid phase (acetonitrile) driven by visible light. The reaction yielded about 26.2% cyclohexane conversion and 90.2% selectivity for cyclohexanol and cyclohexanone (KA oil) under optimal conditions; in addition, a small quantity of chlorination was observed. Among the catalysts explored,  $PMo_{10}V_2$  and particularly  $PMo_9V_3$  exhibited higher activities for this photocatalytic oxygenation in comparison with  $PMo_{11}V$ . In addition, the amount of added water drastically affected this photocatalysis oxygenation, which is assisted by hydrochloric acid. The cyclohexanone selectivity was incessantly and considerably enhanced from 21.8% to 82.7% as the water amount increased from 0 to 0.15 mL. However, the conversion of cyclohexane obviously diminished as the amount of the added water exceeded 0.12 mL. The assisting effect of hydrochloric acid on this photocatalysis reaction was likely because of the fact that the donor-acceptor adduct formed between hydrochloric acid and  $PMo_{12-n}V_n$  could be excited by visible light so that an intra-molecular electron transfer from  $Cl^-$  to  $PMo_{12-n}V_n$  anions became achievable, which in turn resulted in the generation of  $Cl\cdot$  radicals and the reduction of catalysts. As UV-vis spectral and cyclic voltammetric measurements revealed, the subsequent reactions initiated by the  $Cl\cdot$  radicals led to the oxygenation of cyclohexane by  $N_2O$  to KA oil and regeneration of the catalysts.

The new catalytic system had several advantages:

- The photocatalyst and light source used in the proposed system were inexpensive and easily available.
- Using  $N_2O$  as an oxidant was environmentally and economically significant in both its recycling and raising the yield of adipic acid production.
- It involved extremely mild operating conditions, high photocatalytic efficiency, and good selectivity for KA oil (particularly cyclohexanone) under optimized conditions.

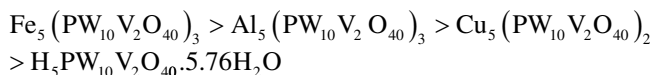
The authors ascribed the reaction performances to the mechanism of cooperation between the excited state of catalyst and that of its reduced form (heteropoly blue). The role of donor-acceptor interactions is important in this catalytic system. In addition, the donor-acceptor interactions between the heteropoly blue and  $N_2O$  may assist the activation of  $N_2O$ .

Yehia and coworkers [158] investigated the photocatalytic oxidation of aromatic aldehydes to their corresponding carboxylic acids in the presence of a Keggin heteropoly acid such as phosphomolybdic acid ( $H_3PMo_{12}O_{40}$ ), silicotungstic acid ( $H_4SiW_{12}O_{40}$ ), and phosphotungstic acid ( $H_3PW_{12}O_{40}$ ). These species were able to catalyze the oxidation of 4-carboxybenzaldehyde and *p*-tolualdehyde in homogeneous reactions. Furthermore, for additional studies,

the authors explored the application of these Keggin catalysts in the presence of persulfate as an oxidizing agent. Their results indicated that in the presence of persulfate ultraviolet light, the most active catalyst was  $\text{H}_3\text{PMo}_{12}\text{O}_{40}$  (80.9% yield) owing to the high oxidative ability of molybdenum. The influence of the catalyst concentration, time, and oxidizing agent load were examined as well. Moreover, the mechanistic aspects of the reaction were discussed.

The easily prepared and inexpensive catalysts showed the way to an alternative technology for other systems and different aromatic and aliphatic aldehydes, as important substances in nanotechnology, and many industrial fields with environmental advantages. Furthermore, easy procedure and experimental setup made this method a valuable addition to the existing methodologies.

Ji and others [159] synthesized the phosphotungstovanadic heteropoly acids with the formula  $\text{H}_5\text{PW}_{10}\text{V}_2\text{O}_{40}\cdot 5.76\text{H}_2\text{O}$ , utilizing the hydrothermal method.  $\text{Fe}_5(\text{PW}_{10}\text{V}_2\text{O}_{40})_3$ ,  $\text{Al}_5(\text{PW}_{10}\text{V}_2\text{O}_{40})_3$ , and  $\text{Cu}_5(\text{PW}_{10}\text{V}_2\text{O}_{40})_2$  were obtained by doping  $\text{H}_5\text{PW}_{10}\text{V}_2\text{O}_{40}\cdot 5.76\text{H}_2\text{O}$  with Fe, Al, and Cu in the molar ratios of 10:6, 10:6, and 10:4, respectively. Then, their activities and mechanisms in the Photo-Fenton reaction were studied. Under irradiation with a mercury lamp, 96% of phenol was degraded in less than 60 min in a solution containing phenol, 50 mg/L;  $\text{Fe}_5(\text{PW}_{10}\text{V}_2\text{O}_{40})_3$ , 2  $\mu\text{mol/L}$ ; and hydrogen peroxide, 4 mmol/L. The activities exhibited by the catalysts were in the following order:



The photocatalytic activities for degradation of phenol over  $\text{Fe}_5(\text{PW}_{10}\text{V}_2\text{O}_{40})_3$  reached 96% within 30 min when hydrogen peroxide was added simultaneously. Notably, the hydrogen peroxide concentration was an essential factor in controlling the phenol degradation rate, due to the balance of the forming and self-scavenging of OH radicals.

Zhu et al. [160] prepared the polyoxometalate,  $\text{K}_6\text{TiW}_{11}\text{O}_{39}\text{Sn}\cdot 7\text{H}_2\text{O}$ . They then assessed  $\text{K}_6\text{TiW}_{11}\text{O}_{39}\text{Sn}\cdot 7\text{H}_2\text{O}$  and  $\text{K}_6\text{ZrW}_{11}\text{O}_{39}\text{Sn}\cdot 12\text{H}_2\text{O}$  for photocatalytic degradation of triarylmethane (brilliant green and acid blue 9), bisazo (C.I. reactive black 5), and monoazo dyestuffs (C.I. reactive red 24, C.I. reactive red 194, and C.I. reactive orange 5) under sunlight in homogeneous aqueous solutions.  $\text{K}_6\text{TiW}_{11}\text{O}_{39}\text{Sn}\cdot 7\text{H}_2\text{O}$  and  $\text{K}_6\text{ZrW}_{11}\text{O}_{39}\text{Sn}\cdot 12\text{H}_2\text{O}$  were effectively and photocatalytically able to decolorize the abovementioned dyestuffs. Mediated by  $\text{K}_6\text{TiW}_{11}\text{O}_{39}\text{Sn}\cdot 7\text{H}_2\text{O}$  and  $\text{K}_6\text{ZrW}_{11}\text{O}_{39}\text{Sn}\cdot 12\text{H}_2\text{O}$ , the photocatalytic degradation of the dyestuffs was found to involve a pseudo-first-order reaction, which was modeled by Langmuir-Hinshelwood-type kinetics. In general, the pseudo first-order rate constants ( $k'$ ) observed for the triarylmethane dyestuffs were greater than those of the azo dyestuffs. Using partial least-square regression, quantitative structure-property relationship models of the  $k'$  values were developed for the dyestuffs. For every optimized model, the cumulative variance of the dependent variable explained by the partial least-square components was

greater than 0.753. This value demonstrated that the model was of good robustness and predictive ability. The authors attempted to establish an ideal model to be used in prediction of the  $k'$  values from the structure and properties of dyestuffs, and draw the main factors influencing  $k'$  from the model. There was indeed a correlation between the  $k'$  values of the dyestuffs and the energies of their LUMO, and the most positive net atomic charge on a sulfur atom of the dyestuffs. The linear correlation coefficients between the predicted and experimental values were all greater than 0.9950.

Yan and coworkers [161] synthesized a series of heteropoly acid salt catalysts by adding various metal ions. Heteropoly acid salts  $(\text{TBA})_4\text{Hx}[\text{PW}_{11}\text{M}(\text{Q})\text{O}_{39}]\cdot n\text{H}_2\text{O}$ , with Keggin-type structure were formed ( $\text{M}=\text{Fe}, \text{Co}, \text{Ni}$ ). A series of changes in the surface of the material after the addition of metal ions could be seen using scanning electron microscopy. The stability of the material was also experimentally designed and the material showed good stability. The synthesized species were successfully subjected to the photocatalytic degradation of organophosphorus compounds followed by *O,O*-diethyl-*S*-(*p*-tolyl) phosphorothioate as a degradation substrate. The catalytic activity of  $(\text{TBA})_4[\text{PW}_{11}\text{Fe}(\text{H}_2\text{O})\text{O}_{39}]\cdot 2\text{H}_2\text{O}$  turned out to be the best among all synthesized species as it completely degraded under visible light within 90 min. The degradation performance was analyzed using ion chromatography by determining the presence of a phosphate ion. To study its degradation mechanism, ammonium oxalate, isopropanol, and benzoquinone were employed to quench holes ( $\text{h}^+$ ), hydroxyl radicals ( $\cdot\text{OH}$ ), and superoxide radicals ( $\cdot\text{O}_2^-$ ). It was concluded that the  $\cdot\text{OH}$  radicals played the most important role in the degradation reaction.

The above conclusions indicated the  $(\text{TBA})_4[\text{PW}_{11}\text{Fe}(\text{H}_2\text{O})\text{O}_{39}]\cdot 2\text{H}_2\text{O}$  could be better applied to the degradation of organophosphorus compounds to decrease the environmental pollution caused by these chemicals, and they could prove promising in solving environmental issues at an industrial level.

Hori and others [162] investigated the decomposition of hydroperfluorocarboxylic acids ( $\text{HC}_n\text{F}_{2n}\text{COOH}$  with  $n=4$  and 6) catalyzed by  $\text{H}_4\text{SiW}_{12}\text{O}_{40}$  in water as a heteropoly acid photocatalyst. Under the irradiation of UV-visible light, and in the presence of  $\text{H}_4\text{SiW}_{12}\text{O}_{40}$ , hydroperfluorocarboxylic acids efficiently decomposed to  $\text{F}^-$  and  $\text{CO}_2$ , at relatively high pH (up to 5.2). At this threshold pH value, the conventional heteropoly acid  $\text{H}_3\text{PW}_{12}\text{O}_{40}$  could not act any more. The decomposition rate constants were 1.8–2.5 times more than those for the corresponding perfluorocarboxylic acids. The decomposition of hydroperfluorocarboxylic acids was initiated by elimination of the  $\omega$ -H atom of the hydroperfluorocarboxylic acids as  $\text{H}^+$ , followed by formation of perfluorodicarboxylic acids.

## 4.6. Conclusion

Due to their unique, remarkable properties in comparison with other Brønsted acids, e.g., higher acidity strengths, thermal stability, water tolerance, and easy handling, heteropoly acids have attracted increasing attention. A wide variety

of organic reactions as well as photocatalytic processes could be catalyzed by this class of catalytic systems with high to excellent efficiency. The advantages of using these catalysts include selectivity, reusability, bifunctional properties, and simplicity of workup. In this chapter, a number of applications of heteropoly acids were discussed. Heteropoly acids could be used as a homogeneous catalyst in many different reactions like oxidation, multicomponent reactions, and synthesis of heterocyclic compounds. Based on the reported results, one can conclude that heteropoly acids are efficient, green, reusable, and inexpensive catalysts, and their use has been increasingly growing. In addition to catalytic applications in organic synthesis, they have intriguing applications in photochemistry.

## References

- [1] Y. Pan, X. Shen, L. Yao, A. Bentalib, Z. Peng, Active sites in heterogeneous catalytic reaction on metal and metal oxide: theory and practice, *Catalysts* 8 (10) (2018) 478.
- [2] C. Descorme, P. Gallezot, C. Geantet, C. George, Heterogeneous catalysis: a key tool toward sustainability, *ChemCatChem* 4 (12) (2012) 1897–1906.
- [3] M.A. Albrecht, C.W. Evans, C.L. Raston, Green chemistry and the health implications of nanoparticles, *Green Chem.* 8 (5) (2006) 417–432.
- [4] T. Kitanosono, K. Masuda, P. Xu, S. Kobayashi, Catalytic organic reactions in water toward sustainable society, *Chem. Rev.* 118 (2) (2018) 679–746.
- [5] Y. Izumi, Hydration/hydrolysis by solid acids, *Catal. Today* 33 (4) (1997) 371–409.
- [6] P. Gupta, S. Paul, Solid acids: green alternatives for acid catalysis, *Catal. Today* 236 (2014) 153–170.
- [7] T. Akiyama, K. Mori, Stronger Brønsted acids: recent progress, *Chem. Rev.* 115 (17) (2015) 9277–9306.
- [8] Y. Gu, F. Wu, J. Yang, Oxidative [3+3] annulation of atropaldehyde acetals with 1, 3-bisnucleophiles: an efficient method of constructing six-membered aromatic rings, including salicylates and carbazoles, *Adv. Synth. Catal.* 360 (14) (2018) 2727–2741.
- [9] F. Su, Y. Guo, Advancements in solid acid catalysts for biodiesel production, *Green Chem.* 16 (6) (2014) 2934–2957.
- [10] M. Hechelski, A. Ghinet, B. Louvel, P. Dufrénoy, B. Rigo, A. Daïch, C. Waterlot, From conventional lewis acids to heterogeneous montmorillonite K10: eco-friendly plant-based catalysts used as green lewis acids, *ChemSusChem* 11 (8) (2018) 1249–1277.
- [11] A. Corma, H. Garcia, Lewis acids: from conventional homogeneous to green homogeneous and heterogeneous catalysis, *Chem. Rev.* 103 (11) (2003) 4307–4366.
- [12] M. Li, F. Wu, Y. Gu, Brønsted acidic ionic liquid catalyzed synthesis of benzo[*a*]carbazole from renewable acetol and 2-phenylindoles in a biphasic system, *Chin. J. Catal.* 40 (2019) 1135–1140.
- [13] A. Taheri, X. Pan, C. Liu, Y. Gu, Brønsted acid ionic liquid as a solvent-conserving catalyst for organic reactions, *ChemSusChem* 7 (8) (2014) 2094–2098.
- [14] C. Miao, H. Zhuang, Y. Wen, F. Han, Q.F. Yang, L. Yang, Z. Li, C. Xia, Efficient thiolation of alcohols catalyzed by long chained acid-functionalized ionic liquids under mild conditions, *Eur. J. Org. Chem.* 2019 (19) (2019) 3012–3021.
- [15] C. Miao, Q. Hou, Y. Wen, F. Han, Z. Li, L. Yang, C.-G. Xia, Long-chained acidic ionic liquids-catalyzed cyclization of 2-substituted aminoaromatics with  $\beta$ -diketones: a metal-free strategy to construct benzoazoles, *ACS Sustain. Chem. Eng.* 7 (14) (2019) 12008–12013.

- [16] A. El-Harairy, B. Lai, L. Vaccaro, M. Li, Y. Gu, A sulfone-containing imidazolium-based Brønsted acid ionic liquid catalyst enables replacing dipolar aprotic solvents with butyl acetate, *Adv. Synth. Catal.* 361 (14) (2019) 3342–3350.
- [17] L. Miao, H. Duan, D. Zhu, Y. Lv, L. Gan, L. Li, M. Liu, Boron “gluing” nitrogen heteroatoms in a prepolymerized ionic liquid-based carbon scaffold for durable supercapacitive activity, *J. Mater. Chem. A* 9 (5) (2021) 2714–2724.
- [18] Q. Zhang, C. Zhang, Y. Sun, Y. Guo, D. Song, Hierarchically porous Brønsted acidic ionic liquid functionalized nitrogen-doped carbons for pyrolysis biofuel upgrading *via* esterification of acetic acid with high boiling point alcohols, *Appl. Catal. A Gen.* 574 (2019) 10–24.
- [19] D.L. Long, R. Tsunashima, L. Cronin, Polyoxometalates: building blocks for functional nanoscale systems, *Angew. Chem. Int. Ed.* 49 (10) (2010) 1736–1758.
- [20] P. Ma, F. Hu, J. Wang, J. Niu, Carboxylate covalently modified polyoxometalates: from synthesis, structural diversity to applications, *Coord. Chem. Rev.* 378 (2019) 281–309.
- [21] Y. Chen, S. Sun, D. Lu, Y. Shi, Y. Yao, Water-soluble supramolecular polymers constructed by macrocycle-based host-guest interactions, *Chin. Chem. Lett.* 30 (1) (2019) 37–43.
- [22] L. Chen, W.-L. Chen, X.-L. Wang, Y.-G. Li, Z.-M. Su, E.-B. Wang, Polyoxometalates in dye-sensitized solar cells, *Chem. Soc. Rev.* 48 (1) (2019) 260–284.
- [23] Y. Ji, J. Hu, J. Biskupek, U. Kaiser, Y.F. Song, C. Streb, Polyoxometalate-based bottom-up fabrication of graphene quantum dot/manganese vanadate composites as lithium ion battery anodes, *Chem Eur J* 23 (65) (2017) 16637–16643.
- [24] Y. Cao, Q. Chen, C. Shen, L. He, Polyoxometalate-based catalysts for CO<sub>2</sub> conversion, *Molecules* 24 (11) (2019) 2069.
- [25] L.M. Sanchez, H.J. Thomas, M.J. Climent, G.P. Romanelli, S. Iborra, Heteropolycompounds as catalysts for biomass product transformations, *Catal. Rev.* 58 (4) (2016) 497–586.
- [26] B. Yu, B. Zou, C.-W. Hu, Recent applications of polyoxometalates in CO<sub>2</sub> capture and transformation, *J. CO<sub>2</sub> Util.* 26 (2018) 314–322.
- [27] Q. Huang, J. Liu, L. Feng, Q. Wang, W. Guan, L.-Z. Dong, L. Zhang, L.-K. Yan, Y.-Q. Lan, H.-C. Zhou, Multielectron transportation of polyoxometalate-grafted metalloporphyrin coordination frameworks for selective CO<sub>2</sub>-to-CH<sub>4</sub> photoconversion, *Natl. Sci. Rev.* 7 (1) (2020) 53–63.
- [28] G. Yang, Y. Liu, K. Li, W. Liu, B. Yu, C. Hu, H<sub>3</sub>PMo<sub>12</sub>O<sub>40</sub>-catalyzed coupling of diarylmethanols with epoxides/diols/aldehydes toward polyaryl-substituted aldehydes, *Chin. Chem. Lett.* (2020).
- [29] I.A. Weinstock, R.E. Schreiber, R. Neumann, Dioxxygen in polyoxometalate mediated reactions, *Chem. Rev.* 118 (5) (2017) 2680–2717.
- [30] Y. Zhang, X. Chen, L. Li, W. Chen, H.N. Miras, Y.-F. Song, Mesoporous polymer loading heteropoly acid catalysts: one-step strategy to manufacture high value-added cellulose acetate propionate, *ACS Sustain. Chem. Eng.* 7 (5) (2019) 4975–4982.
- [31] S.-S. Wang, G.-Y. Yang, Recent advances in polyoxometalate-catalyzed reactions, *Chem. Rev.* 115 (11) (2015) 4893–4962.
- [32] G.-P. Yang, S.-X. Shang, B. Yu, C.-W. Hu, Ce(III)-Containing tungstotellurate(VI) with a sandwich structure: an efficient Lewis acid-base catalyst for the condensation cyclization of 1, 3-diketones with hydrazines/hydrazides or diamines, *Inorganic Chem. Front.* 5 (10) (2018) 2472–2477.
- [33] Q.-W. Song, B. Yu, X.-D. Li, R. Ma, Z.-F. Diao, R.-G. Li, W. Li, L.-N. He, Efficient chemical fixation of CO<sub>2</sub> promoted by a bifunctional Ag<sub>2</sub>WO<sub>4</sub>/Ph<sub>3</sub>P system, *Green Chem.* 16 (3) (2014) 1633–1638.

- [34] C.-X. Guo, B. Yu, J.-N. Xie, L.-N. He, Silver tungstate: a single-component bifunctional catalyst for carboxylation of terminal alkynes with CO<sub>2</sub> in ambient conditions, *Green Chem.* 17 (1) (2015) 474–479.
- [35] H. Yu, J. Wang, Z. Wu, Q. Zhao, D. Dan, S. Han, J. Tang, Y. Wei, Aldehydes as potential acylating reagents for oxidative esterification by inorganic ligand-supported iron catalysis, *Green Chem.* 21 (16) (2019) 4550–4554.
- [36] Z. Wei, S. Ru, Q. Zhao, H. Yu, G. Zhang, Y. Wei, Highly efficient and practical aerobic oxidation of alcohols by inorganic-ligand supported copper catalysis, *Green Chem.* 21 (15) (2019) 4069–4075.
- [37] K. Suzuki, N. Mizuno, K. Yamaguchi, Polyoxometalate photocatalysis for liquid-phase selective organic functional group transformations, *ACS Catal.* 8 (11) (2018) 10809–10825.
- [38] A. Enferadi-Kerenkan, T.-O. Do, S. Kaliaguine, Heterogeneous catalysis by tungsten-based heteropoly compounds, *Catal. Sci. Technol.* 8 (9) (2018) 2257–2284.
- [39] K. Kamata, Design of highly functionalized polyoxometalate-based catalysts, *Bull. Chem. Soc. Jpn.* 88 (8) (2015) 1017–1028.
- [40] N. Narkhede, S. Singh, A. Patel, Recent progress on supported polyoxometalates for biodiesel synthesis *via* esterification and transesterification, *Green Chem.* 17 (1) (2015) 89–107.
- [41] W. Deng, Q. Zhang, Y. Wang, Polyoxometalates as efficient catalysts for transformations of cellulose into platform chemicals, *Dalton Trans.* 41 (33) (2012) 9817–9831.
- [42] E.V. Gusevskaya, Reactions of terpenes catalyzed by heteropoly compounds: valorization of biorenewables, *ChemCatChem* 6 (6) (2014) 1506–1515.
- [43] R.F. Cotta, K.A. da Silva Rocha, E.F. Kozhevnikova, I.V. Kozhevnikov, E.V. Gusevskaya, Heteropoly acid catalysts in upgrading of biorenewables: cycloaddition of aldehydes to monoterpenes in green solvents, *Appl. Catal. B Environ.* 217 (2017) 92–99.
- [44] Y. Kamiya, T. Okuhara, M. Misono, A. Miyaji, K. Tsuji, T. Nakajo, Catalytic chemistry of supported heteropoly acids and their applications as solid acids to industrial processes, *Catal. Surv. Jpn.* 12 (2) (2008) 101.
- [45] K.A. da Silva Rocha, J.L. Hoehne, E.V. Gusevskaya, Phosphotungstic acid as a versatile catalyst for the synthesis of fragrance compounds by  $\alpha$ -pinene oxide isomerization: solvent-induced chemoselectivity, *Chem Eur J* 14 (20) (2008) 6166–6172.
- [46] I. Kozhevnikov, *Catalysts For Fine Chemical Synthesis, Catalysis by Polyoxometalates, Vol. 2*, Wiley, 2002.
- [47] I.V. Kozhevnikov, Catalysis by heteropoly acids and multicomponent polyoxometalates in liquid-phase reactions, *Chem. Rev.* 98 (1) (1998) 171–198.
- [48] M.S.P. Ribeiro, C. de Souza Santos, C.G. Vieira, K.A. da Silva Rocha, Catalytic transformations of (+)-aromadendrene: functionalization and isomerization reactions in the presence of the heteropoly acid catalyst H<sub>3</sub>PW<sub>12</sub>O<sub>40</sub>, *Mol. Catal.* 498 (2020) 111264.
- [49] S.E. Ward, F.P. Harrington, L.J. Gordon, S.C. Hopley, C.M. Scott, J.M. Watson, Discovery of the first potent, selective 5-hydroxytryptamine 1D receptor antagonist, *J. Med. Chem.* 48 (10) (2005) 3478–3480.
- [50] S. Massari, D. Daelemans, M.L. Barreca, A. Knezevich, S. Sabatini, V. Cecchetti, A. Marcellino, C. Pannecouque, O. Tabarrini, 1, 8-Naphthyridone derivative targets the HIV-1 Tat-mediated transcription and potently inhibits the HIV-1 replication, *J. Med. Chem.* 53 (2) (2010) 641–648.
- [51] T. Soneda, H. Takeshita, Y. Kagoshima, Y. Yamamoto, T. Hosokawa, T. Konosu, N. Masuda, T. Uchida, I. Achiwa, J. Kuroyanagi, Preparation of imidazolecarboxamide derivatives as antibacterial agents, *Chem. Abstr.* (2009), 148320.



- [52] R. Murugan, S. Anbazhagan, S.S. Narayanan, Synthesis and in vivo antidiabetic activity of novel dispiropyrrolidines through [3+2] cycloaddition reactions with thiazolidinedione and rhodanine derivatives, *Eur. J. Med. Chem.* 44 (8) (2009) 3272–3279.
- [53] T.K. Huang, L. Shi, R. Wang, X.Z. Guo, X.X. Lu, Keggin type heteropoly acids-catalyzed synthesis of quinoxaline derivatives in water, *Chin. Chem. Lett.* 20 (2) (2009) 161–164.
- [54] S. Rahimi, M.A. Amrollahi, Z. Kheilkordi, An efficient ultrasound-promoted method for the synthesis of bis (indole) derivatives, *C. R. Chim.* 18 (5) (2015) 558–563.
- [55] M. Zakeri, M.M. Nasef, E. Abouzari-Lotf, H. Haghi, Keggin heteropoly acid as a green and recyclable catalyst for one-pot synthesis of 1, 1, 3-triheteroaryl compounds, *Malaysian J. Chem.* 18 (2016).
- [56] S. Liu, W. Li, Y. Pang, H. Xiao, Y. Zhou, X. Wang, Green synthesis of 2-substituted imidazolines using hydrogen peroxide catalyzed by tungstophosphoric acid and tetrabutylammonium bromide in water, *J. Heterocyclic Chem.* 56 (3) (2019) 998–1002.
- [57] N. Sadou, S. Aichouche-Bouzroua, R. Nechak, B. Nedjar-Kolli, V. Morizur, S. Poulain-Martini, E. Dunach, Acid-catalyzed synthesis of thiazolidin-4-ones, *Polycycl. Aromat. Compd.* 38 (4) (2018) 311–321.
- [58] A. Gharib, M. Jahangir, J.W. Scheeren, Catalytic synthesis of pyrazoles and diazepines under green conditions at room temperature using heteropoly acids catalysts, *Synth. Commun.* 43 (3) (2013) 309–325.
- [59] M. Da Silva, A. Julio, F. Dorigetto, Solvent-free heteropoly acid-catalyzed glycerol ketalization at room temperature, *RSC Adv.* 5 (55) (2015) 44499–44506.
- [60] X. Han, K. Ouyang, C. Xiong, X. Tang, Q. Chen, K. Wang, L.-L. Liu, C.-T. Hung, S.-B. Liu, Transition-metal incorporated heteropoly acid-ionic liquid composite catalysts with tunable Brønsted/Lewis acidity for acetalization of benzaldehyde with ethylene glycol, *Appl. Catal. A Gen.* 543 (2017) 115–124.
- [61] Y. Zong, Y. Zhao, W. Luo, X.H. Yu, J.K. Wang, Y. Pan, Highly efficient synthesis of 2, 3-dihydroquinazolin-4 (1H)-ones catalyzed by heteropoly acids in water, *Chin. Chem. Lett.* 21 (7) (2010) 778–781.
- [62] N. Azizi, L. Torkian, M.R. Saidi, Highly efficient synthesis of bis (indolyl) methanes in water, *J. Mol. Catal. A Chem.* 275 (1-2) (2007) 109–112.
- [63] J. Zhu, H. Bienayme, *Reactions Multicomponent*, Wiley-VCH, Weinheim, 2005.
- [64] A. Dömling, I. Ugi, Multicomponent reactions with isocyanides, *Angew. Chem. Int. Ed.* 39 (18) (2000) 3168–3210.
- [65] M.N. Elinson, A.I. Ilovaisky, V.M. Merkulova, P.A. Belyakov, A.O. Chizhov, G.I. Nikishin, Solvent-free cascade reaction: direct multicomponent assembling of 2-amino-4H-chromene scaffold from salicylaldehyde, malononitrile or cyanoacetate and nitroalkanes, *Tetrahedron* 66 (23) (2010) 4043–4048.
- [66] M.G. Dekamin, Z. Mokhtari, Highly efficient and convenient Strecker reaction of carbonyl compounds and amines with TMSCN catalyzed by MCM-41 anchored sulfonic acid as a recoverable catalyst, *Tetrahedron* 68 (3) (2012) 922–930.
- [67] S. Javanshir, A. Ohanian, M.M. Heravi, M. Naimi-Jamal, F.F. Bamoharram, Ultrasound-promoted, rapid, green, one-pot synthesis of 2'-aminobenzothiazolomethylnaphthols *via* a multi-component reaction, catalyzed by heteropoly acid in aqueous media, *J. Saudi Chem. Soc.* 18 (5) (2014) 502–506.
- [68] M. Heravi, A. Ghods, F. Derikvand, K. Bakhtiari, F. Bamoharram, H<sub>14</sub> [NaP<sub>5</sub>W<sub>30</sub>O<sub>110</sub>] catalyzed one-pot three-component synthesis of dihydropyrano [2, 3-c] pyrazole and pyrano [2, 3-d] pyrimidine derivatives, *J. Iran. Chem. Soc.* 7 (3) (2010) 615–620.

- [69] A. Gharib, Catalytic synthesis of 3, 4-dihydropyrimidin-2 (1H)-ones under green conditions and by Keggin type heteropoly acid catalyst  $H_7[PMo_8V_4O_{40}]$ , Gazi Univ. J. Sci. 25 (4) (2012) 823–834.
- [70] M.M. Heravi, B.A. Jani, F. Derikvand, F.F. Bamoharram, H.A. Oskooie, Three component, one-pot synthesis of dihydropyrano [3, 2-c] chromene derivatives in the presence of  $H_6P_2W_{18}O_{62} \cdot 18H_2O$  as a green and recyclable catalyst, Catal. Commun. 10 (3) (2008) 272–275.
- [71] M.M. Heravi, M. Mirzaei, S.Y.S. Beheshtiha, V. Zadsirjan, F. Mashayekh Ameli, M. Bazargan,  $H_5BW_{12}O_{40}$  as a green and efficient homogeneous but recyclable catalyst in the synthesis of 4H-Pyrans *via* multicomponent reaction, Appl. Organomet. Chem. 32 (9) (2018), e4479.
- [72] H.O. Foroughi, M. Kargar, Z. Erjaee, E. Zarenezhad, One-pot three-component reaction for facile and efficient green synthesis of chromene pyrimidine-2, 4-dione derivatives and evaluation of their anti-bacterial activity, Monatsh. Chem. 151 (10) (2020) 1603–1608.
- [73] M.M. Heravi, T. Hosseinejad, M. Tamimi, V. Zadsirjan, M. Mirzaei, 12-Tungstoboric acid ( $H_5BW_{12}O_{40}$ ) as an efficient Lewis acid catalyst for the synthesis of chromenopyrimidine-2, 5-diones and thioxochromenopyrimidin-5-ones: joint experimental and computational study, J. Mol. Struct. 1205 (2020) 127598.
- [74] L.D. Chavan, S.N. Deshmukh, S.G. Shankarwar, A simple and green protocol for the synthesis of 3, 4-dihydropyrimidin-2 (1H)-ones using 11-Molybdo-1-vanado phosphoric acid as a catalyst under ultrasound irradiation, Orbital: Electron. J. Chem. 11 (5) (2019) 314–320.
- [75] M.A. Amrollahi, Z. Kheilkordi,  $H_3PW_{12}O_{40}$ -catalyzed one-pot synthesis of bis (indole) derivatives under silent and ultrasonic irradiation conditions in aqueous media, J. Iran. Chem. Soc. 13 (5) (2016) 925–929.
- [76] M.S. Su, X.J. Ji, B.B. Zhao, M. Tian, J.J. Ma, Phosphotungstic acid catalyzed one-pot synthesis of 2-amino-3, 5-dicarbonitrile-6-thio-pyridines in aqueous media, J. Chem. Soc. Pak. 37 (06) (2015) 1130.
- [77] B. Maleki, F.M. Zonoz, H.A. Akhlaghi, An efficient synthesis of symmetrical N, N'-alkylidene bis-amides catalyzed by a heteropoly acid, Org. Prep. Proced. Int. 47 (5) (2015) 361–367.
- [78] T. Momeni, M.M. Heravi, T. Hosseinejad, M. Mirzaei, V. Zadsirjan,  $H_5BW_{12}O_{40}$ -Catalyzed synthesis of 1, 4-dihydropyridines and polyhydroquinolines *via* Hantzsch reaction: joint experimental and computational studies, J. Mol. Struct. 1199 (2020) 127011.
- [79] A. Vafaee, A. Davoodnia, M. Pordel, A rapid, efficient, and high-yielding synthesis of 4, 4'-(arylmethylene) bis (3-methyl-1H-pyrazol-5-ol) derivatives catalyzed by 12-tungstophosphoric acid ( $H_3PW_{12}O_{40}$ ), Res. Chem. Intermed. 41 (11) (2015) 8343–8354.
- [80] N. Khalidi-Khellafi, M. Makhloufi-Chebli, D. Oukacha-Hikem, S.T. Bouaziz, K.O. Lamara, T. Idir, A. Benazzouz-Touami, F. Dumas, Green synthesis, antioxidant and antibacterial activities of 4-aryl-3, 4-dihydropyrimidinones/thiones derivatives of curcumin. Theoretical calculations and mechanism study, J. Mol. Struct. 1181 (2019) 261–269.
- [81] M.M. Heravi, K. Bakhtiari, V. Zadsirjan, F.F. Bamoharram, O.M. Heravi, Aqua mediated synthesis of substituted 2-amino-4H-chromenes catalyzed by green and reusable Preyssler heteropoly acid, Bioorg. Med. Chem. Lett. 17 (15) (2007) 4262–4265.
- [82] M.M. Heravi, F. Derikvand, F.F. Bamoharram, Highly efficient, four-component one-pot synthesis of tetrasubstituted imidazoles using Keggin-type heteropoly acids as green and reusable catalysts, J. Mol. Catal. A Chem. 263 (1-2) (2007) 112–114.
- [83] K. Alimohammadi, Y. Sarrafi, M. Tajbakhsh,  $H_6P_2W_{18}O_{62}$ : a green and reusable catalyst for the synthesis of 3, 3-diaryloxindole derivatives in water, Monatsh. Chem. 139 (9) (2008) 1037–1039.

- [84] A. Javid, M.M. Heravi, F. Bamoharram, M. Nikpour, One-pot synthesis of tetrasubstituted imidazoles catalyzed by preyssler-type heteropoly acid, *E-J. Chem.* 8 (2011).
- [85] T. Andrushkevich, Heterogeneous catalytic oxidation of acrolein to acrylic acid: mechanism and catalysts, *Catal. Rev.-Sci. Eng.* 35 (2) (1993) 213–259.
- [86] Y. Konishi, K. Sakata, M. Misono, Y. Yoneda, Catalysis by heteropoly compounds: IV. Oxidation of methacrolein to methacrylic acid over 12-molybdophosphoric acid, *J. Catal.* 77 (1) (1982) 169–179.
- [87] M. Misono, K. Sakata, Y. Yoneda, W.Y. Lee, Acid-redox bifunctional properties of heteropoly compounds of molybdenum and tungsten correlated with catalytic activity for oxidation of methacrolein, in: *Studies in Surface Science and Catalysis*, Vol. 7, Elsevier, 1981, pp. 1047–1059.
- [88] L.B. Levy, P.B. DeGroot, Deactivation characteristics of an acrolein oxidation catalyst: I. Kinetics of activity loss, *J. Catal.* 76 (2) (1982) 385–392.
- [89] V. Ernst, Y. Barbaux, P. Courtine, Phosphomolybdic acid ( $H_3PMo_{12}O_{40}$ ) as a catalyst for the vapour-phase oxidative dehydrogenation of isobutyric acid: kinetic parameters of supported and unsupported catalysts. Role of water, *Catal. Today* 1 (1-2) (1987) 167–180.
- [90] C. Marchal-Roch, N. Laronze, R. Villanneau, N. Guillou, A. Tézé, G. Hervé, Effects of  $NH_4^+$ ,  $Cs^+$ , and  $H^+$  counterions of the molybdophosphate anion in the oxidative dehydrogenation of isobutyric acid, *J. Catal.* 190 (1) (2000) 173–181.
- [91] J. Hu, R.C. Burns, The effect of cation type and  $H^+$  on the catalytic activity of the Keggin anion  $[PMo_{12}O_{40}]^{3-}$  in the oxidative dehydrogenation of isobutyraldehyde, *J. Catal.* 195 (2) (2000) 360–375.
- [92] L. Marosi, G. Cox, A. Tenten, H. Hibst, In situ XRD investigations of heteropoly acid catalysts in the methacrolein to methacrylic acid oxidation reaction: structural changes during the activation/deactivation process, *J. Catal.* 194 (1) (2000) 140–145.
- [93] H. Kim, J.C. Jung, S.H. Yeom, K.-Y. Lee, I.K. Song, Preparation of  $H_3PMo_{12}O_{40}$  catalyst immobilized on polystyrene support and its application to the methacrolein oxidation, *J. Mol. Catal. A Chem.* 248 (1-2) (2006) 21–25.
- [94] H. Kim, J.C. Jung, D.R. Park, S.-H. Baeck, I.K. Song, Preparation of  $H_5PMo_{10}V_2O_{40}$  ( $PMo_{10}V_2$ ) catalyst immobilized on nitrogen-containing mesoporous carbon (N-MC) and its application to the methacrolein oxidation, *Appl. Catal. A Gen.* 320 (2007) 159–165.
- [95] N. Ballarini, F. Candiracci, F. Cavani, H. Degrand, J.-L. Dubois, G. Lucarelli, M. Margotti, A. Patinet, A. Pigamo, F. Trifiro, The dispersion of Keggin-type P/Mo polyoxometalates inside silica gel, and the preparation of catalysts for the oxidation of isobutane to methacrolein and methacrylic acid, *Appl. Catal. A Gen.* 325 (2) (2007) 263–269.
- [96] M. Kanno, T. Yasukawa, W. Ninomiya, K. Ooyachi, Y. Kamiya, Catalytic oxidation of methacrolein to methacrylic acid over silica-supported 11-molybdo-1-vanadophosphoric acid with different heteropoly acid loadings, *J. Catal.* 273 (1) (2010) 1–8.
- [97] M. Kanno, Y.-K. Miura, T. Yasukawa, T. Hasegawa, W. Ninomiya, K. Ooyachi, H. Imai, T. Tatsumi, Y. Kamiya, 11-Molybdo-1-vanadophosphoric acid  $H_4PMo_{11}VO_{40}$  supported on ammonia-modified silica as highly active and selective catalyst for oxidation of methacrolein, *Catal. Commun.* 13 (1) (2011) 59–62.
- [98] H. Goldberg, D. Kumar, G.N. Sastry, G. Leitus, R. Neumann, An antimony(V) substituted Keggin heteropoly acid,  $H_4PSbMo_{11}O_{40}$ : why is its catalytic activity in oxidation reactions so different from that of  $H_4PVMo_{11}O_{40}$ ? *J. Mol. Catal. A Chem.* 356 (2012) 152–157.
- [99] F. Jing, B. Katryniok, F. Dumeignil, E. Bordes-Richard, S. Paul, Catalytic selective oxidation of isobutane to methacrylic acid on supported  $(NH_4)_3HPMo_{11}VO_{40}$  catalysts, *J. Catal.* 309 (2014) 121–135.

- [100] L. Zhou, L. Wang, Y. Cao, Y. Diao, R. Yan, S. Zhang, The states and effects of copper in Keggin-type heteropolyoxometalate catalysts on oxidation of methacrolein to methacrylic acid, *Mol. Catal.* 438 (2017) 47–54.
- [101] L. Zhou, L. Wang, Y. Diao, R. Yan, S. Zhang, Cesium salts supported heteropoly acid for oxidation of methacrolein to methacrylic acid, *Mol. Catal.* 433 (2017) 153–161.
- [102] Y.-L. Cao, L. Wang, L.-L. Zhou, G.-J. Zhang, B.-H. Xu, S.-J. Zhang, Cs (NH<sub>4</sub>)<sub>x</sub>H<sub>3-x</sub>PMo<sub>11</sub>VO<sub>40</sub> catalyzed selective oxidation of methacrolein to methacrylic acid: effects of NH<sub>4</sub><sup>+</sup> on the structure and catalytic activity, *Ind. Eng. Chem. Res.* 56 (3) (2017) 653–664.
- [103] Y.-L. Cao, L. Wang, B.-H. Xu, S.-J. Zhang, The Chitin/Keggin-type heteropoly acid hybrid microspheres as catalyst for oxidation of methacrolein to methacrylic acid, *Chem. Eng. J.* 334 (2018) 1657–1667.
- [104] X. Li, J. Zhang, F. Zhou, Y. Wang, X. Yuan, H. Wang, Oxidative desulfurization of dibenzothiophene and diesel by hydrogen peroxide: catalysis of H<sub>3</sub>PMo<sub>12</sub>O<sub>40</sub> immobilized on the ionic liquid modified SiO<sub>2</sub>, *Mol. Catal.* 452 (2018) 93–99.
- [105] L. Zhou, S. Zhang, Z. Li, J. Scott, Z. Zhang, R. Liu, J. Yun, Selective oxidation of methacrolein to methacrylic acid over H<sub>4</sub>PMo<sub>11</sub>VO<sub>40</sub>/C<sub>3</sub>N<sub>4</sub>-SBA-15, *RSC Adv.* 9 (58) (2019) 34065–34075.
- [106] S. Yasuda, J. Hirata, M. Kanno, W. Ninomiya, R. Otomo, Y. Kamiya, The role of steam in selective oxidation of methacrolein over H<sub>3</sub>PMo<sub>12</sub>O<sub>40</sub>, *Appl. Catal. A Gen.* 570 (2019) 164–172.
- [107] S. Yasuda, A. Iwakura, J. Hirata, M. Kanno, W. Ninomiya, R. Otomo, Y. Kamiya, Strong Brønsted acid-modified chromium oxide as an efficient catalyst for the selective oxidation of methacrolein to methacrylic acid, *Catal. Commun.* 125 (2019) 43–47.
- [108] M. Misono, N. Nojiri, Recent progress in catalytic technology in Japan, *Appl. Catal.* 64 (1990) 1–30.
- [109] Y. Rodikova, E. Zhizhina, Catalytic oxidation of 5-hydroxymethylfurfural into 2, 5-diformylfuran using V-containing heteropoly acid catalysts, in: *Reaction Kinetics Mechanisms and Catalysis*, 2020.
- [110] K. Hatakeyama, Y. Nakagawa, M. Tamura, K. Tomishige, Efficient production of adipic acid from 2-methoxycyclohexanone by aerobic oxidation with a phosphotungstic acid catalyst, *Green Chem.* 22 (15) (2020) 4962–4974.
- [111] L.L. Gogin, E.G. Zhizhina, Z.P. Pai, One-pot process of naphthoquinones synthesis from hydroquinone in the presence of solutions of Mo-VP heteropoly acids as bifunctional catalysts, *Modern Res. Catal.* 8 (01) (2019) 1.
- [112] T. Lu, Y. Hou, W. Wu, M. Niu, Y. Wang, Formic acid and acetic acid production from corn cob by catalytic oxidation using O<sub>2</sub>, *Fuel Process. Technol.* 171 (2018) 133–139.
- [113] A.G. Demesa, A. Laari, M. Sillanpää, T. Koironen, Valorization of lignin by partial wet oxidation using sustainable heteropoly acid catalysts, *Molecules* 22 (10) (2017) 1625.
- [114] I. El Amrani, A. Atlamsani, M. Dakkach, M. Rodríguez, I. Romero, S. Amthiou, Efficient and selective oxidation of aldehydes with dioxygen catalysed by vanadium-containing heteropolyanions, *C. R. Chim.* 20 (9-10) (2017) 888–895.
- [115] L. Gogin, E. Zhizhina, Z. Pai, V. Parmon, Prospects of application of Mo-V-phosphoric heteropoly acid solutions as bifunctional catalysts for synthesis of anthraquinones and their substituted derivatives, *Russ. Chem. Bull.* 64 (9) (2015) 2069–2075.
- [116] L. Gogin, E. Zhizhina, Preparation of vitamin K 3 in Mo-V-P heteropoly acid solutions by diene synthesis, *Kinet. Catal.* 61 (2020) 276–282.
- [117] N.V. Gromov, O.P. Taran, I.V. Delidovich, A.V. Pestunov, Y.A. Rodikova, D.A. Yatsenko, E.G. Zhizhina, V.N. Parmon, Hydrolytic oxidation of cellulose to formic acid in the presence of Mo-VP heteropoly acid catalysts, *Catal. Today* 278 (2016) 74–81.

- [118] X.-L. Long, C. Zhang, Y. Zhu, Z.-L. Yang, W.-K. Yuan, Production of NMSBA from the oxidation of NMST with oxygen catalyzed by  $H_3PW_{12}O_{40}/Co/Mn/Br$  homogeneous catalytic system, *Chem. Eng. J.* 286 (2016) 361–368.
- [119] T. Lu, M. Niu, Y. Hou, W. Wu, S. Ren, F. Yang, Catalytic oxidation of cellulose to formic acid in  $H_5PV_2Mo_{10}O_{40}+H_2SO_4$  aqueous solution with molecular oxygen, *Green Chem.* 18 (17) (2016) 4725–4732.
- [120] J. Reichert, B. Brunner, A. Jess, P. Wasserscheid, J. Albert, Biomass oxidation to formic acid in aqueous media using polyoxometalate catalysts-boosting FA selectivity by in-situ extraction, *Energy Environ. Sci.* 8 (10) (2015) 2985–2990.
- [121] Y.A. Rodikova, E.G. Zhizhina, Z.P. Pai, Catalytic way of transforming 2, 3-dimethylphenol to para-quinone with the use of vanadium-containing heteropoly acids, *Appl. Catal. A Gen.* 549 (2018) 216–224.
- [122] Y.A. Rodikova, E.G. Zhizhina, Z.P. Pai, Phosphomolybdovanadic acid catalyzed oxidation of 2, 6-dimethylphenol into para-quinone in a biphasic system, *React. Kinet. Mech. Catal.* 124 (2) (2018) 469–485.
- [123] Y.A. Rodikova, E.G. Zhizhina, Z.P. Pai, Multicycle testing of P-Mo-V heteropoly acid catalysts in oxidation of substituted phenols, *ChemistrySelect* 3 (16) (2018) 4200–4206.
- [124] Y.A. Rodikova, E. Zhizhina, Homogeneous catalysts of redox processes based on heteropoly acid solutions III: developing effective ways for the preparation of 2, 3, 5-trimethyl-1, 4-benzoquinone, *Catal. Ind.* 11 (3) (2019) 179–190.
- [125] F. Yang, Y. Hou, M. Niu, T. Lu, W. Wu, Z. Liu, Catalytic oxidation of lignite to carboxylic acids in aqueous  $H_5PV_2Mo_{10}O_{40}/H_2SO_4$  solution with molecular oxygen, *Energy Fuel* 31 (4) (2017) 3830–3837.
- [126] W. Yang, X. Du, W. Liu, Z. Wang, H. Dai, Y. Deng, Direct valorization of lignocellulosic biomass into value-added chemicals by polyoxometalate catalyzed oxidation under mild conditions, *Ind. Eng. Chem. Res.* 58 (51) (2019) 22996–23004.
- [127] N.V. Gromov, T.B. Medvedeva, K.N. Sorokina, Y.V. Samoylova, Y.A. Rodikova, V.N. Parmon, Direct conversion of microalgae biomass to formic acid under an air atmosphere with soluble and solid Mo-V-P heteropoly acid catalysts, *ACS Sustain. Chem. Eng.* 8 (51) (2020) 18947–18956.
- [128] J. Albert, Selective oxidation of lignocellulosic biomass to formic acid and high-grade cellulose using tailor-made polyoxometalate catalysts, *Faraday Discuss.* 202 (2017) 99–109.
- [129] J. Albert, P. Wasserscheid, Expanding the scope of biogenic substrates for the selective production of formic acid from water-insoluble and wet waste biomass, *Green Chem.* 17 (12) (2015) 5164–5171.
- [130] V. Odyakov, E. Zhizhina, K. Matveev, V. Parmon, Homogeneous catalysts of redox reactions based on heteropoly acid solutions. II. Synthesis of catalyst for pilot industrial production of methylethylketone, *Catal. Ind.* 7 (2) (2015) 111–118.
- [131] C.B. Vilanculo, M.J. Da Silva, Unraveling the role of the lacunar  $Na_7PW_{11}O_{39}$  catalyst in the oxidation of terpene alcohols with hydrogen peroxide at room temperature, *New J. Chem.* 44 (7) (2020) 2813–2820.
- [132] E.G. Zhizhina, V.F. Odyakov, Aqueous solutions of Mo-V-phosphoric heteropoly acids as bifunctional catalysts for preparation of 9, 10-anthraquinone and its hydrogenated derivatives, *ChemCatChem* 4 (9) (2012) 1405–1410.
- [133] E. Chepaikin, G. Menchikova, S. Pomogailo, Homogeneous metal-complex catalyst systems in the partial oxidation of propane with oxygen, *Pet. Chem.* 60 (11) (2020) 1260–1267.
- [134] A. Patel, J. Patel, Nickel salt of phosphomolybdic acid as a bi-functional homogeneous recyclable catalyst for base free transformation of aldehyde into ester, *RSC Adv.* 10 (37) (2020) 22146–22155.

- [135] O. Kai, H. Xiaoxiang, X. Chunhua, T. Xiujuan, C. Qing, Water-soluble heteropoly acid-based ionic liquids as effective catalysts for oxidation of benzyl alcohol in water with hydrogen peroxide, *Green Process. Synth.* 6 (4) (2017) 385–395.
- [136] R. Karcz, P. Niemiec, K. Pamin, J. Poltowicz, J. Kryściak-Czerwenka, B.D. Napruszewska, A. Michalik-Zym, M. Witko, R. Tokarz-Sobieraj, E.M. Serwicka, Effect of cobalt location in Keggin-type heteropoly catalysts on aerobic oxidation of cyclooctane: experimental and theoretical study, *Appl. Catal. A Gen.* 542 (2017) 317–326.
- [137] X. Li, R. Cao, Q. Lin, Selective oxidation of alcohols with H<sub>2</sub>O<sub>2</sub> catalyzed by long chain multi-SO<sub>3</sub>H functionalized heteropolyanion-based ionic liquids under solvent-free conditions, *Catal. Commun.* 69 (2015) 5–10.
- [138] S. Mouanni, T. Mazari, D. Amitouche, S. Benadji, L. Dermeche, C. Roch-Marchal, C. Rabia, Preparation and characterization of H<sub>3-2(x+y)</sub>Mn<sub>x</sub>Co<sub>y</sub>PMo<sub>12</sub>O<sub>40</sub> heteropolysalts. Application to adipic acid green synthesis from cyclohexanone oxidation with hydrogen peroxide, *C. R. Chim.* 22 (4) (2019) 327–336.
- [139] N.C. Coronel, M.J. da Silva, S.O. Ferreira, R.C. da Silva, R. Natalino, K<sub>5</sub>PW<sub>11</sub>NiO<sub>39</sub>-catalyzed oxidation of benzyl alcohol with hydrogen peroxide, *ChemistrySelect* 4 (1) (2019) 302–310.
- [140] B. Bertleff, J. Claußnitzer, W. Korth, P. Wasserscheid, A. Jess, J. Albert, Extraction coupled oxidative desulfurization of fuels to sulfate and water-soluble sulfur compounds using polyoxometalate catalysts and molecular oxygen, *ACS Sustain. Chem. Eng.* 5 (5) (2017) 4110–4118.
- [141] M. Lei, Q. Gao, K. Zhou, P. Gogoi, J. Liu, J. Wang, H. Song, S. Wang, X. Liu, Catalytic degradation and mineralization mechanism of 4-chlorophenol oxidized by phosphomolybdic acid/H<sub>2</sub>O<sub>2</sub>, *Sep. Purif. Technol.* 257 (2020), 117933.
- [142] F.F. Bamoharram, M.M. Heravi, S. Mehdizadeh, Preyssler anion as a green and eco-friendly catalyst for photocatalytic oxidation of aromatic aldehydes, *Synth. React. Inorgan. Metal-Organ. Nano-Metal Chem.* 39 (10) (2009) 746–750.
- [143] A. Mills, S. Le Hunte, An overview of semiconductor photocatalysis, *J. Photochem. Photobiol. A Chem.* 108 (1) (1997) 1–35.
- [144] O. Carp, C.L. Huisman, A. Reller, Photoinduced reactivity of titanium dioxide, *Prog. Solid State Chem.* 32 (1-2) (2004) 33–177.
- [145] C. Tanielian, C. Schweitzer, R. Seghrouchni, M. Esch, R. Mechin, Polyoxometalate sensitization in mechanistic studies of photochemical reactions: the decatungstate anion as a reference sensitizer for photoinduced free radical oxygenations of organic compounds, *Photochem. Photobiol. Sci.* 2 (3) (2003) 297–305.
- [146] T. Yamase, E. Ishikawa, Photochemical self-assembly reaction of β-[Mo<sub>8</sub>O<sub>26</sub>] 4-to mixed-valence cluster [Mo<sub>37</sub>O<sub>112</sub>]<sub>26-</sub> in aqueous media, *Langmuir* 16 (23) (2000) 9023–9030.
- [147] V. Houšková, V. Štengl, S. Bakardjieva, N. Murafa, Photoactive materials prepared by homogeneous hydrolysis with thioacetamide: part 2-TiO<sub>2</sub>/ZnO nanocomposites, *J. Phys. Chem. Solids* 69 (7) (2008) 1623–1631.
- [148] D. Li, Y. Guo, C. Hu, L. Mao, E. Wang, Photocatalytic degradation of aqueous formic acid over the silica composite films based on lacunary Keggin-type polyoxometalates, *Appl. Catal. A Gen.* 235 (1-2) (2002) 11–20.
- [149] A. Mylonas, E. Papaconstantinou, On the mechanism of photocatalytic degradation of chlorinated phenols to CO<sub>2</sub> and HCl by polyoxometalates, *J. Photochem. Photobiol. A Chem.* 94 (1) (1996) 77–82.
- [150] C. Hu, B. Yue, T. Yamase, Photoassisted dehalogenation of organo-chlorine compounds by paratungstate A in aqueous solutions, *Appl. Catal. A Gen.* 194 (2000) 99–107.

- [151] E. Papaconstantinou, Photochemistry of polyoxometallates of molybdenum and tungsten and/or vanadium, *Chem. Soc. Rev.* 18 (1989) 1–31.
- [152] P. Kormali, A. Troupis, T. Triantis, A. Hiskia, E. Papaconstantinou, Photocatalysis by polyoxometallates and  $\text{TiO}_2$ : a comparative study, *Catal. Today* 124 (3–4) (2007) 149–155.
- [153] S. Zhang, L. Chen, H. Liu, W. Guo, Y. Yang, Y. Guo, M. Huo, Design of  $\text{H}_3\text{PW}_{12}\text{O}_{40}/\text{TiO}_2$  and  $\text{Ag}/\text{H}_3\text{PW}_{12}\text{O}_{40}/\text{TiO}_2$  film-coated optical fiber photoreactor for the degradation of aqueous rhodamine B and 4-nitrophenol under simulated sunlight irradiation, *Chem. Eng. J.* 200 (2012) 300–309.
- [154] Y.-F. Song, R. Tsunashima, Recent advances on polyoxometalate-based molecular and composite materials, *Chem. Soc. Rev.* 41 (22) (2012) 7384–7402.
- [155] C. Streb, New trends in polyoxometalate photoredox chemistry: from photosensitisation to water oxidation catalysis, *Dalton Trans.* 41 (6) (2012) 1651–1659.
- [156] A. Balaska, M.E. Samar, A. Grid, Phenol photodegradation process assisted with Wells-Dawson heteropoly acids, *Desalin. Water Treat.* 54 (2) (2015) 382–392.
- [157] J. She, Z. Fu, J. Li, B. Zeng, S. Tang, W. Wu, H. Zhao, D. Yin, S.R. Kirk, Visible light-triggered vanadium-substituted molybdophosphoric acids to catalyze liquid phase oxygenation of cyclohexane to KA oil by nitrous oxide, *Appl. Catal. B Environ.* 182 (2016) 392–404.
- [158] F. Yehia, G. Elkady, A. Mady, E. Elnaggar, A. Hussein, Keggin heteropoly acids as an efficient catalysts for photocatalytic oxidation of aromatic aldehydes, *Al-Azhar Bull. Sci.* 28 (1-A) (2017) 67–74.
- [159] D. Ji, R. Xue, M. Zhou, Y. Zhu, F. Zhang, L. Zang, Preparation and photocatalytic performance of tungstovanadophosphoric heteropoly acid salts, *RSC Adv.* 9 (32) (2019) 18320–18325.
- [160] X. Zhu, F. Sheng, W. Wang, F. Shi, G. Ding, R. Zhang, P. Wang, Polyoxometalates for photocatalytic degradation of aqueous dyestuff solutions and quantitative structure-property relationship study on photolysis rate constants, *Toxicol. Environ. Chem.* 99 (3) (2017) 363–375.
- [161] Y. Yan, X. Wang, M.A. Khan, M. Xia, W. Lei, F. Wang, Synthesis and characterisation of (Fe, Co, Ni)-polyoxometalates to degrade O, O-diethyl-S-(p-tolyl) phosphorothioate under visible light irradiation, *Int. J. Environ. Anal. Chem.* 100 (12) (2020) 1376–1389.
- [162] H. Hori, K. Ishida, N. Inoue, K. Koike, S. Kutsuna, Photocatalytic mineralization of hydroperfluorocarboxylic acids with heteropoly acid  $\text{H}_4\text{SiW}_{12}\text{O}_{40}$  in water, *Chemosphere* 82 (8) (2011) 1129–1134.



## Chapter 5

# Supported heteropoly acids

### 5.1. Introduction

While homogeneous catalysis paved the way for advanced technological processes using heteropoly acids, challenges regarding these reactions including precipitation, aggregation, loss of activity, and separation difficulties resulted in studies in which the use of heteropoly acids as heterogeneous catalysts was explored [1].

In comparison with homogeneous catalysts, separate immobilized catalysts (filtration, centrifuge, magnetic separation, etc.) are always much easier to separate. As a result, reusing the as-prepared catalysts becomes more realistic. In addition, the product separation and purification, and the removal of the catalyst residues are carried out more efficiently, which is particularly important for the catalytic systems that involve toxic metals. Immobilization of the homogeneous heteropoly acid catalysts can ease up the isolation of the surface active species, which in turn prevents the agglomeration of the catalysts and maintains their activity for longer times. Sometimes the support may even interact with the functional groups immobilized on them to promote the overall catalyzed reaction. An immobilized catalyst is readily applied in different reactors, e.g., fixed bed reactors, membrane reactors, etc. In this manner, incorporation of the catalysts into the industrial chemical processes will be easier.

Bulk solid polyoxometalates were initially used as heterogeneous acid and oxidation catalysts. Nevertheless, the approach is often affected by low specific surface areas and the result is a reduction in activity [2]. Thus, later studies included the immobilization of polyoxometalates on high surface area substrates, e.g., porous silica and other metal oxides [2]. More advanced materials like carbon nanostructures [3] and metal-organic frameworks (MOFs) have been investigated as well [4]. Such a strategy may maximize the exposure of the individual heteropoly acid molecules to the reactants. Furthermore, it facilitates the separation via centrifugation or filtration [5]. Heterogeneous supports were used for mechanical stabilization and maximized surface-area in early studies on polyoxometalate immobilization. Nevertheless, more recent studies have been shifting toward added properties caused by the support. They included light-absorption and charge transport in semiconductors (TiO<sub>2</sub>, CdSe, etc.),

electrical conductivity (by metals, carbons, and conductive polymers) as well as specific polyoxometalate binding sites, introduced into MOFs and organo-functionalized supports.

## 5.2. Techniques of immobilization

During the past decade, owing to the challenges related to their precipitation, aggregation, and degradation under operational conditions and in order to extend their application range, many reviews have focused on the specialized aspects of the heterogenization of polyoxometalates. Focusing on recent advances in applications of such catalysts in liquid phase, Zhou and coworkers [5] provided an exhaustive overview of a wide variety of routes for the heterogenization of polyoxometalates. Ji and coworkers [3] summarized developments in POM-nanocarbon composites focusing on (electro) catalysis, energy storage and sensing. Herrmann and coworkers reviewed POM-conductive polymer composites and their applications. Ye et al. [4] provided an overview of the design, synthesis, and catalytic properties of polyoxometalate-based solids including MOFs, polyoxometalate crystals and organic/inorganic polyoxometalate hybrids. Chen and coworkers [6] reviewed the progress of dye-sensitized solar cells containing polyoxometalate. Cherevan and coworkers [7] provided an outlook on emerging areas of academic and technological importance in which supported polyoxometalate systems could promisingly result in new applications.

## 5.3. Synthetic methods for the immobilization of polyoxometalates

In order to deposit polyoxometalates as individual molecules, micro- or nano-structured particles, layers, or bulk materials on heterogeneous substrates, a wide variety of techniques have been developed [3,5,8], as shown in Fig. 5.1. These techniques are briefly introduced in the following sections.

### 5.3.1 Dip-coating

In this classical approach, the necessary heterogeneous substrate is immersed in a solution of the desired heteropoly acid. This methodology is plain, easily scalable, and applicable to almost any combination of polyoxometalates and substrates. Yet it usually suffers from reversible polyoxometalate-binding (leaching), which may result in nonhomogeneous distribution, because of polyoxometalate crystallization during drying. This gives little control over the deposition process.

### 5.3.2 Solvothermal deposition

With this approach, it is often possible to anchor polyoxometalate crystals mechanically and chemically on substrates at elevated temperatures and pressures in a stable manner. The process conditions facilitate polyoxometalate

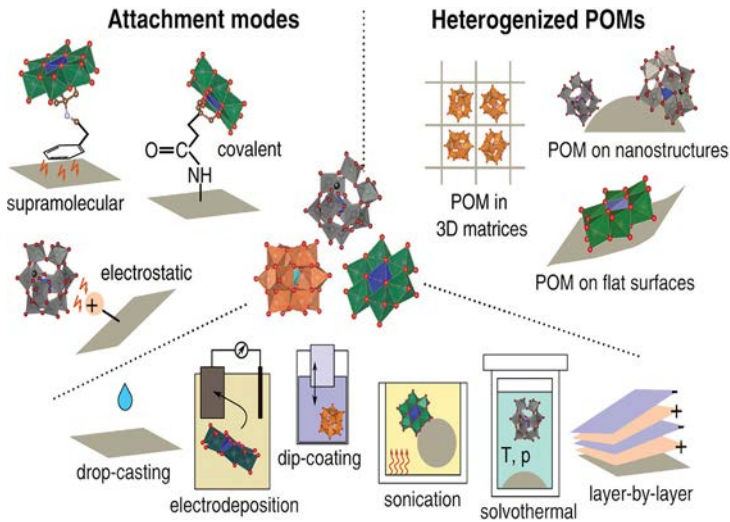


**FIG. 5.1** A schematic of a variety of attachment modes, substrate types, and immobilization strategies, which are usually applied to prepare heterogenized polyoxometalates. A.S. Cherevan, S.P. Nandan, I. Roger, R. Liu, C. Streb, D. Eder, *Polyoxometalates on functional substrates: concepts, synergies, and future perspectives*, *Adv. Sci.* 7 (8) (2020) 1903511–1903533.

crystallization, mostly in highly condensed, insoluble lattices so that leaching and reversible deposition can be resolved. On the other hand, the harsh conditions of the process may lead to structural rearrangements of sensitive polyoxometalates as well. The degradation into solid-state metal oxides is also possible.

### 5.3.3 Sonication deposition

Sonication-driven deposition of heteropoly acids (performed in organic solvents under ambient conditions) has been used as a moderate alternative to solvothermal syntheses in recent studies [9]. Notably, in this method, the size, shape, and surface arrangement of particles are adjustable by varying the sonication parameters. Nonetheless, recent studies have also revealed that under the conditions of the sonication deposition, structurally labile species, particularly vanadates, may undergo structural rearrangements into nanostructured solid-state oxides [10–12].

### 5.3.4 Layer-by-layer assembly

The stepwise deposition of anionic polyoxometalate layers and cationic layers to form well-defined films of high stability with adjustable thickness on heterogeneous substrates is used in this approach. Nevertheless, if thick films are targeted, the approach can be laborious and time-consuming. Furthermore, depending on the conditions under which the films are used, leaching may be an issue.

### 5.3.5 Drop-casting

This method usually employs polyoxometalates (as micro/nanoparticles) dispersed in an appropriate solvent, which is subsequently dropped onto a substrate. The drop-casting method is usually used to alter the surface of an electrode with a polyoxometalate or polyoxometalate composite. For electrocatalysis, a protective layer of Nafion is frequently added on top of the polyoxometalate layer for the protection and stabilization of the electrode [13]. Fast surface-modification of the electrodes is made possible with this method; however, the control that it gives the exact structure and morphology of the composite layer on the electrode is so challengeable and it can negatively affect the electrical contact between the electrode and composite.

### 5.3.6 Electrodeposition

In this method, cyclic voltammetry of a POM-containing homogeneous solution is used to deposit the polyoxometalate (or POM-composites) onto the electrode surface. The method is therefore restricted to conductive substrates for (photo) electrochemical applications. However, it benefits from controlled film growth providing direct electrochemical information on the polyoxometalate deposition process.

### 5.3.7 Entrapment

In this technique, the catalysts are prepared in a manner that they are entrapped inside the cavities of porous materials like zeolites, MCM-41, etc. The dimensions of the polyoxometalates are usually bigger than the size of the cavity mouth so that immobilization techniques prevent the diffusion of the active species out of them. However, catalysts prepared in this manner usually suffer from constraints on the diffusion of reactants and products and restrictions on the interactions between the substrates and active sites, meaning that this technique may not be generally used.

### 5.3.8 Impregnation and drying

Impregnation and drying is a preparation method often used owing to its simple operation and low streams of waste. As the first step, a polyoxometalate solution is contacted with a support. The most commonly used solvent for this technique is water due to the high solubility of polyoxometalates. On the other hand, organic solvents are mainly used for the organ salts of polyoxometalates. In order to avoid premature deposition in bulk solution, concentrations below (super) saturation are necessary.

There are mainly two distinguished impregnation methods, i.e., the pore volume impregnation (PVI) in which an exact amount to fill the pore volume of the support is used and wet impregnation (WI) in which an excess amount of

the solution is employed. The former method is also known as dry impregnation (DI) or incipient wetness impregnation (IWI), since the impregnated material keeps its dry character at macroscopic scales.

## 5.4. Chemical interactions between the polyoxometalate and the support

Basically, three different modes of chemical binding are observed for POM-substrate composites. These modes are briefly described here.

### 5.4.1 Electrostatic anchoring

Electrostatic binding of the anionic polyoxometalates is realized through the introduction of cationic surface charges (e.g., ammonium or pyridinium groups). While the method is quite simple and may be used to anchor a majority of heteropoly acids, it is also liable to leaching so that the stability of the anchoring is dependent upon the strength of the electrostatic interactions, the pH of the solution, solvents, and of course the conditions under which the material will be deployed.

### 5.4.2 Covalent anchoring

In order to form covalent bonds between the heteropoly acid and substrate for stable and persistent anchoring, functionalization of the substrate surface and the heteropoly acid with complementary, typically organic groups is applied. Prominent examples are the imine bonds formed between aldehydes and amines, amide bonds formed utilizing amine and carboxylate functionalization, or 1,3-dipolar cycloadditions by alkyne and azide functionalization (CLICK chemistry) [14]. Although this approach provides stable covalent bonds, it is limited to heteropoly acids, which can be organofunctionalized; in addition, multistep reactions and expert knowledge are necessary to use this approach.

### 5.4.3 Supramolecular anchoring

Supramolecular interactions like hydrogen bonding or  $\pi$ -stacking may be used to anchor heteropoly acid to a substrate. For this purpose, appropriate interactions between both species must be identified and the heteropoly acid has to be functionalized accordingly. A prominent example for this approach is the organofunctionalization of heteropoly acids with aromatic rings (such as pyrene) that enable  $\pi$ -stacking attachment, e.g., to nanostructured carbon substrates [15].

## 5.5. Substrate effects and functional properties

The selection of the appropriate substrate for a heteropoly acid deposition is principally ruled by the target application. Regarding the acid-, base-, or redox

catalysis, particularly in liquid phase, inorganic substrates with large, accessible surface areas, like porous metal oxides and nanostructured carbons, have been used to support heteropoly acids. State-of-the-art materials such as MOFs, ZIFs, COFs, and zeolites have attracted enormous attention as active supports to immobilize polyoxometalate, since they incorporate a distinct porous environment with potentially added catalytic functionalities. However, for the applications in which conductive supports are desired, including electrocatalysis or optoelectronics, conductive polymers, metals or nanocarbons with high electrical conductivity are preferred. This is while for application in which charge separation or light harvesting are the important features, such as photovoltaics and photo(electro)catalysis, semiconducting materials with adjustable bandgaps, electronic structure, and (photo)conductivity have mainly received attention.

Based on the type and the chemistry of a substrate, a variety of synthetic approaches and attachment strategies must be utilized to deposit a certain heteropoly acid on a selected support. Usually, carbon-based and organic/polymeric materials provide a broad range of chemical adjust ability to enable controllable attachment of heteropoly acids and the desired interaction (e.g., supramolecular or covalent). On the contrary, the deposition of a polyoxometalate on an inorganic substrate could benefit from the more hydrophilic characteristic of the latter. For instance, metal oxides have quite similar chemistry; therefore, they may be incorporated with polyoxometalate clusters through direct covalent bonding by forming M–O–M bonds so that no organic linking groups are necessary [16].

However, immobilizing a polyoxometalate ion on a heterogeneous substrate is not only ruled by both the physicochemical properties of the support and their synergistic functions. For instance, in the field of thermal heterogeneous catalysis, workers have demonstrated that the catalytic support type strongly affects the total performance, which is referred to as *metal-support interactions*, or *substrate effect* [17]. Such substrate effects, in their simplest form, stem from both structural and electronic changes caused by strong interactions between the catalyst and support. Prominent examples are polarization effects in which a heterogeneous substrate results in charge density changes within the catalyst as well as the decoration of the metal nanoparticles through mobile molecular substrate species. Both cases drastically influence the catalyst's selectivity and reactivity. The extent and role of synergistic effects in POM-based composites have been studied in some works. However, a few more recent studies have revealed that the changes in polyoxometalate structure and reactivity depend strongly on the type of the substrate and the interaction mode between both components.

As an example, Argitis and coworkers [18] investigated how the redox properties of two immobilized Wells-Dawson ammonium salts, i.e.,  $(\text{NH}_4)_6[\text{P}_2\text{Mo}_{18}\text{O}_{62}]$ ,  $(\text{NH}_4)_6[\text{P}_2\text{W}_{18}\text{O}_{62}]$ , and their corresponding Keggin heteropoly acids  $[\text{H}_3\text{PMo}_{12}\text{O}_{40}]$  and  $[\text{H}_3\text{PW}_{12}\text{O}_{40}]$  are under the influence of the very substrate used. They compared metallic aluminum, dielectric silicon dioxide, and semiconducting ITO substrates and, using UV-vis and XPS techniques,

followed the reduction degree of the polyoxometalates immobilized in this manner. The authors observed spontaneous redox reactions between a polyoxometalate ion and both aluminum and ITO substrates at room temperature and pressure to conclude that the extent of the polyoxometalate reduction depends upon the relative position of its LUMO with respect to the Fermi level of the substrate as well as the presence of ammonium counter ions. However, for the dielectric silicon dioxide substrate, no spontaneous charge transfer was observed, which indicated that deposition of the polyoxometalate on the substrates might be utilized to alter the polyoxometalate redox state with immobilization.

According to the most pertinent examples found in the literature [7], immobilization may influence the structure and reactivity of the heterogenized polyoxometalates from the following aspects:

- the nature and extent of the interactions between the substrate and the polyoxometalate;
- the attachment impact on the electronic properties; and
- the implication on the stability of the polyoxometalate species.

## 5.6. Host/guest interactions in supported polyoxometalate hybrids

The hybrid species prepared by supporting a polyoxometalate onto a metal-organic frameworks or incorporating it into it enjoy unique properties. When the polyoxometalate is encapsulated inside an MOF as a host, the POM-based MOF hybrids may be applied in catalytic systems (e.g., electrocatalysis, organocatalysis, or photocatalysis). While keeping the strong acidity, redox capability, and oxygen-rich surface of heteropoly acids, their drawbacks, i.e., difficult handling, low surface areas, and a high solubility, are resolved in such systems. Owing to their high surface area, high adjustability in terms of the pore size and channels, and long-range ordered structure, MOFs may serve as ideal hosts. In certain cases, MOFs are able to increase the functionality of the hybrids. During the past few decades, a plenty of porous materials, such as silica, zeolites, ion-exchange resin, and activated carbon have been investigated as a support to immobilize a polyoxometalate ion [19–22]. Since the discovery of metal-organic frameworks (MOFs), considerable effort has been made to apply these porous materials as a support for a polyoxometalate. MOFs are inorganic/organic hybrid crystalline materials, which are built from organic linkers and metal ions or clusters via coordination bonds.

Férey and coworkers [23] reported the very first case of a POM@MOF hybrid in 2005. In this original work, a polyoxometalate, i.e.,  $K_7PW_{11}O_{39}$  (with a van der Waals radius of 13.1 Å) was encapsulated into the large cavities of the highly stable chromium-based MOF, i.e., MIL-101, using an impregnation method. Since then, many other thermally and chemically stable MOFs have been used as supports to host polyoxometalates to be applied in catalytic systems



among which are UiO, MIL, NU-1000, ZIF series, and Cu-BTC frameworks. The polyoxometalates encapsulated into MOFs which have been examined most of all are the Keggin  $[XM_{12}O_{40}]n^-$  polyoxometalates and Wells-Dawson  $[X_2M_{18}O_{62}]n^-$  polyoxometalates ( $X=Si, P, V, Bi, \text{etc.}; M=V, Mo, W, \text{etc.}$ ) and their derivatives. These polyoxometalates are very important since their structures and properties are easily varied by eliminating one or more  $MO^{4+}$  units resulting to lacunary polyoxometalates like  $[PW_9O_{34}]^{9-}$ . In addition, sandwich-type polyoxometalates, such as  $[Tb(PW_{11}O_{39})_2]^{11-}$ , can be derived via the substitution of X and/or M by different metals or a combination of two fragments of the Keggin structure.

Encapsulation of polyoxometalates into MOFs as a host matrix provides many advantages. Primarily, their unusually high surface areas and confined cavities/channels allow for a homogeneous distribution of a polyoxometalate in the MOF host. This not only inhibits the agglomeration of polyoxometalates, but also enhances their recyclability and stability while ensuring a fast diffusion of substrates and products. Secondly, the highly regular cavities of MOFs ensure a high selectivity for the substrate; that is to say that only specific substrates/products can reach the active polyoxometalate sites. Thirdly, because of the proper interaction and electron transfer between the MOF and polyoxometalate, usually an increased synergistic catalytic activity is observed. As the fourth feature, the chemical environment of polyoxometalates may be readily adjusted through modification or functionalization of MOFs. APOM@MOF hybrid not only incorporates the interesting properties of polyoxometalates and MOFs, but also permits the resolution of the mentioned drawbacks of polyoxometalates to increase the catalysis performance.

### 5.6.1 Synthesis of POM@MOFs

Thus far, a lot of highly stable MOFs, including UiO, MIL, and ZIF series, as well as NU-1000 and Cu-BTC frameworks, have been applied in the encapsulation of polyoxometalates. Impregnation is among the most commonly used approaches to embed polyoxometalates in MOFs. A simple method is wet impregnation, as most of the polyoxometalates are highly soluble in polar solvents. The activated MOF powder is usually dipped in the polyoxometalate solution to afford the composite. A plenty of POM@MOF hybrids have been prepared through the wet impregnation method among which are POM@ZIF, POM@MIL, and POM@UN-1000. A prominent feature that permits the use of this method is that the polyoxometalate ion size must be smaller than the windows of the MOF. The impregnation approach may not be used for MOFs whose window size is smaller than the polyoxometalate ion size; the examples having this property are UiO, Cu-BTC, and ZIF. Accordingly, for these MOFs, the one-pot synthesis method has been applied to obtain POM@MOF hybrids. This one-pot methodology is also frequently used to prepare POM-encapsulated MOFs in which the anionic form of the heteropoly acid serves as an agent that directs the

structure to ensure the deprotonation of an organic carboxylate ligand. Usually, the synthesis parameters employed to afford the parent MOF are used upon addition of the polyoxometalate to prepare the POM@MOF hybrids. Although this one-pot method can be used to synthesize POM@MOF species, which may not be prepared by impregnation, it can confine the polyoxometalates in the MOF cavities to inhibit from leaching provided that the polyoxometalate ion size is larger than the MOF windows.

Gascon and coworkers [24] synthesized PW@MIL-101 (PW =  $[\text{PW}_{12}\text{O}_{40}]^{3-}$ ) composites using the one-pot, wet impregnation method. When applying the one-pot synthesis under stirring conditions, the authors observed a homogeneous distribution of PW. High loadings of PW in MIL-101 resulted in a drastic decrease in the surface area and pore volume, when the wet impregnation method was used. This reduction in the surface area and pore volume was, however, smaller for the one-pot synthesis method compared with the impregnation method when the same PW loading was used. The authors claimed that in the one-pot synthesis, both the large- and medium-sized cages were occupied, while solely the larger cages were accessible when the impregnation method was used.

Canoni and coworkers [25] compared various synthesis methods utilized to encapsulate polyoxometalates in MIL-100 (Fe). They noticed a good agreement between the experimentally obtained polyoxometalate loading and the theoretical maximum loading for the PMo@MIL-100 (PMo =  $[\text{PMo}_{12}\text{O}_{40}]^{3-}$ ), which was obtained by a one-pot solvothermal synthesis. Additionally, the PMo@MIL-100 obtained solvothermally exhibited a good stability in aqueous media while no polyoxometalate leaching was detected after 2 months.

Using a one-pot, microwave-assisted synthesis, Gascon and coworkers [26] obtained PW@MIL-101-NH<sub>2</sub>(Al) since their attempts to afford MIL-101-NH<sub>2</sub>(Al) containing PW by a solvothermal, one-pot synthesis had proved unsuccessful. However, 1 year later, Bromberg and coworkers [27] explored the encapsulation of polyoxometalates in amino-functionalized NH<sub>2</sub>-MIL-53(Al) and MOFs (NH<sub>2</sub>-MIL-101(Al)) by immobilization. They came to the conclusion that polyoxometalates formed a stable composite through electrostatic interaction with the MOF surface. The thermal stability of the composites PW@NH<sub>2</sub>-MIL-53(Al) and PW@NH<sub>2</sub>-MIL-101(Al) was similar to that of the parent MOFs.

In addition to MIL-101, Cu-BTC (i.e., HKUST-1 or MOF-199) has been used to serve as a host to encapsulate Keggin- or Dawson-type polyoxometalates [28,29]. The larger cavities in Cu-BTC have an inner diameter of 1.3 nm with a pore window of 0.9 nm. This ideally guarantees the stable entrapment of polyoxometalates.

Shuxia Liu et al. [30,31] synthesized a series of Keggin-type polyoxometalates in Cu-BTC, denoted as NENU-*n*, where *n* = 1–10, and formulated as  $[\text{Cu}_2(\text{BTC})_{4/3}(\text{H}_2\text{O})_2]_6[\text{HnXM}_{12}\text{O}_{40}] \cdot (\text{C}_4\text{H}_{12}\text{N})_2$  (X = Si, Ge, P, As, V, Ti;

M=W, Mo). To this end, they used a hydrothermal, one-pot synthesis. The templating effect of the polyoxometalates resulted in highly crystalline composite materials that showed improved thermal stability. Furthermore, since large crystals were formed, it was possible to elucidate the structures using single-crystal X-ray diffraction, which demonstrated that Keggin polyanions were entrapped in larger cuboctahedral cavities (with an inner diameter of 1.3 nm) [31].

In addition to Cu-BTC and MIL-101, isostructural imidazolate frameworks, i.e., ZIF-67 and ZIF-8, have often been applied as the host matrix. The size of sodalite-type cavities in ZIF-8 is about 1.1 nm, but the accessible window of the cavity is quite small (0.34 nm). Keggin-based polyoxometalates have relatively larger particle sizes of up to 1.3–1.4 nm compared with the cavities of ZIF-8. However, they can perfectly fit in their anionic form (1 nm diameter of PW). The one-pot method is therefore an ideal one for entrapping polyoxometalates inside ZIF-8 or ZIF-67 [32]. For example, Malkar and coworkers [33] encapsulated a polyoxometalate in ZIF-8 and used it as an esterification catalyst. In order to functionalize the surface of the ZIF-8 nanoparticles with a Keggin-type PW and gain a core-shell MOF-POM composite, Jeon et al. [34] used an impregnation method. Notably, because of strong interactions, the POM-decorated MOF became insoluble in polar solvents.

Lin et al. formed a POM@MOF molecular catalytic system with a nickel-containing polyoxometalate  $[\text{Ni}_4(\text{H}_2\text{O})_2(\text{PW}_9\text{O}_{34})_2]^{10-}$  (abbreviated as NiP) into an MOF derived from  $[\text{Ir}(\text{ppy})_2(\text{bpy})]^+$  by means of the one-pot synthesis; the MOF was isostructural to UiO-66 with extended ligands. NiP polyoxometalates can be capsulated in the octahedral cages with an inner dimension of 2.2 nm [35]. Other efficient methods have been utilized for the construction of POM-encapsulated MOFs in addition to the widely used one-pot and impregnation method. Zhong and coworkers [36] synthesized NENU-3(PW@HKUST-1) by a liquid-assisted grinding method. By using a two-step synthesis, PW and the Cu salt were first dissolved and evaporated to obtain the copper salt of PW. The  $\text{H}_3\text{BTC}$  ligand was then added in the presence of small amounts of alcohol (MeOH or EtOH) as the grinding liquid. The mixture was ground for 5 min until the color gradually changed to blue. When washed and dried at 60°C for 24 h, the obtained nanocrystalline, NENU-3, exhibited a high crystallinity, and the surface area was a little higher in comparison with NENU-3 obtained in a solvothermal, one-pot synthesis. Li et al. [37] employed an in-situ hot-pressing process to entrap the Keggin-type PW inside an In-based MOF (MFM-300(In)). As illustrated in Fig. 5.2, all the ingredients were ground in the absence of a solvent. Then they were packed with an aluminum foil and heated on a plate at 80°C for only 10 min to afford PW@MFM-300(In) composites. The resulted substances showed a high crystallinity and stability with no PW aggregates observed on the surface of the MOF.

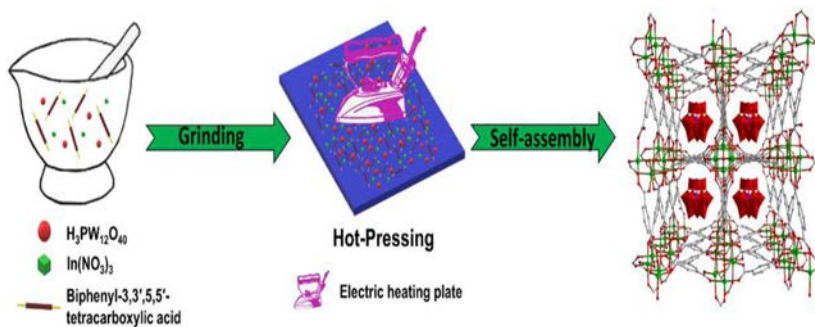


**FIG. 5.2** The hot-pressing process for the synthesis of PW@MFM-300(In). Reprinted from G. Li, K. Zhang, C. Li, R. Gao, Y. Cheng, L. Hou, Y. Wang, *Solvent-free method to encapsulate polyoxometalate into metal-organic frameworks as efficient and recyclable photocatalyst for harmful sulfamethazine degrading in water. Appl. Catal. Environ.* 245 (2019) 753–759. Copyright (2019), with permission from Elsevier.

## 5.6.2 Organocatalysis

### 5.6.2.1 Oxidation reaction

Owing to the presence of acidic sites within MOFs as well as the strong acidity and redox activity of polyoxometalates, POM@MOF hybrid materials are regarded as potential oxidation catalysts. For this reason, some well-known MOFs, including MIL (Cr, Fe, or Al), UiO (Zr), and ZIF series, as well as Cu-BTC and NU-1000 frameworks, are able to encapsulate polyoxometalates to be used in oxidation reactions. Among the different oxidation reactions, oxidative desulfurization and the selective oxidation of alcohols and alkenes are among the most studied reactions using POM@MOF catalysts. Oxidative desulfurization (ODS), as one of the methods that may be promisingly used in the removal sulfur-containing compounds from fuels, is very important from both academic and industrial viewpoints. During the past decade, many Keggin- and sandwich-type polyoxometalates, e.g.,  $[\text{A-PW}_9\text{O}_{34}]^{9-}$  [38],  $[\text{PW}_{11}\text{Zn}(\text{H}_2\text{O})\text{O}_{39}]^{5-}$  [39,40],  $[\text{PW}_{12}\text{O}_{40}]^{3-}$  [41–44],  $[\text{Tb}(\text{PW}_{11}\text{O}_{39})_2]^{11-}$  [45], and  $[\text{Eu}(\text{PW}_{11}\text{O}_{39})_2]^{11-}$  [46], have been encapsulated in MIL (Cr, Fe, or Al) for the ODS reactions by means of  $\text{H}_2\text{O}_2$  as the oxidizing agent. These heterogeneous POM@MIL catalysts could be easily recycled and reused, while showing a higher catalytic activity in comparison with their corresponding homogeneous polyoxometalates. For instance, Balula and coworkers [45] reported that the heterogeneous  $[\text{Tb}(\text{PW}_{11}\text{O}_{39})_2]^{11-}$ @MIL-101 catalyst was able to convert 95% of benzothio-*phene* (BT) at 50°C within 2 h, whereas the homogeneous  $\text{Tb}(\text{PW}_{11})_2$  catalyst afforded a conversion of only 32% under similar conditions.

In addition, Naseri [47] and coworkers noted that the thermal stability of the materials they prepared, i.e.,  $[(\text{OCe}^{\text{IV}}\text{O})_3(\text{PW}_9\text{O}_{34})_2]^{12-}$ @MIL-101 and  $[(\text{HOSn}^{\text{IV}}\text{OH})_3(\text{PW}_9\text{O}_{34})_2]^{12-}$ @MIL-101, was enhanced in comparison

with the single MIL-101(Cr) framework. The thermally stable POM@MOF materials exhibited more than 95% conversion of the diphenyl sulfide after five cycles.

Cao and coworkers [48] studied the effect of the window size within MOFs on the catalytic activity of different POM@MOF materials on ODS reactions. PW was encapsulated into three potent MOFs with different window sizes, i.e., UiO-66 (6 Å), MIL-100(Fe) (8.6 and 5.8 Å), and ZIF-8 (3.4 Å). In comparison with ZIF-8 (9.1%) and UiO-66 (39.1%), PW@MIL-100(Fe) demonstrated the highest activity (92.8%) in the oxidation of 4,6-dimethyldibenzothiophene ( $3.62 \times 6.17 \times 7.86 \text{ \AA}^3$ ). The higher activity observed was ascribed to the large window size of MIL-100(Fe), which allowed for fast diffusion of the substrate into the cavities, which in turn improves the reactivity and recyclability of POM@MOF materials in ODS reactions even more. Amine-functionalized MOFs were used for the encapsulation of polyoxometalates due to strong electrostatic interactions between amine groups and polyoxometalate anions. For example, Cao and coworkers [49] reported the encapsulation of PW into  $\text{NH}_2$ -MIL-101(Cr) and using the resulted catalyst for the ODS reaction. The obtained material gave a full conversion of dibenzothiophene (DBT) at 50°C after 1 h. Interestingly, a series of reusability tests revealed that the conversion of DBT remained unchanged during six successive runs using PW@ $\text{NH}_2$ -MIL-101(Cr) as a catalyst. The observation may be due to strong electrostatic interactions between the amine groups and PW. Another work by Su et al. revealed that the PW@MIL-101(Cr)-diatomite allowed for 98.6% conversion of DBT at 60°C for 2 h after three successive runs being attributed to the high dispersion of polyoxometalates.

In addition to the ODS reactions, selective oxidations of alcohols [50] and alkenes [51–56] were evaluated by means of POM@MIL catalysts. Bo and coworkers synthesized a series of  $\text{H}_{3+x}\text{PMo}_{12-x}\text{V}_x\text{O}_{40}$ @MIL-100(Fe) ( $x=0, 1, 2$ ) materials and their catalytic performance were evaluated in the oxidation of cyclohexene, using hydrogen peroxide as an oxidizing agent.  $\text{H}_4\text{PMo}_{11}\text{VO}_{40}$ @MIL-100(Fe) showed 83% conversion of cyclohexene, with an excellent selectivity toward 2-cyclohexene-1-one (90%) after five consecutive runs. Based on a dual amino-functionalized ionic liquid (DAIL), Abednatanzi et al. [50] developed a novel POM@MIL-101 catalyst. The DAIL was first introduced onto the chromium sites of MIL-101(Cr) with unsaturated coordination sites. Then the Keggin-type PW was immobilized onto the DAIL-modified MIL-101 through an anion exchange. The PW<sub>12</sub>/DAIL/MIL-101 catalyst demonstrated a very high turnover number (TON: 1900) for the selective oxidation of benzyl alcohol toward benzaldehyde at 100°C for 6 h. The catalytic activity of PW/DAIL/MIL-101 was higher in comparison with that of PW<sub>12</sub>/MIL-101 without DAIL functionalities (TON:1400). This observed higher activity was attributed to the presence of remaining free amino groups anchored on the imidazolium moieties of the DAIL, which drastically improved the accessibility of TBHP as an oxidizing agent.

Another instance of MOF, i.e., Cu-BTC, has been utilized to encapsulate polyoxometalates. Sun and coworkers encapsulated six Keggin-type polyoxometalates into Cu-BTC (aka NENU-n, NENU=Northeast Normal University) using a hydrothermal, one-pot method and their crystal structures were determined [31]. Subsequently, various polyoxometalates were encapsulated into the Cu-BTC framework and their catalytic activities were evaluated in ODS reactions [57,58], oxidation of olefins [29,59–61], alcohols [62,63], benzene, and H<sub>2</sub>S [64,65].

Lu and coworkers [63] synthesized a series of composite catalysts, i.e., POM@Cu-BTC (POM=PW, PMO<sub>12-x</sub>V<sub>x</sub>O<sub>40</sub><sup>(3+x)-</sup> (x=0, 1, 2, 3)) to examine their activities for the oxidation of benzyl alcohol to benzaldehyde, with hydrogen peroxide as an oxidizing agent (Fig. 5.3). The V-containing polyoxometalates enhanced the conversion of benzyl alcohol owing to their high redox ability. However, as the vanadium content was increased in the polyoxometalates, overoxidation to benzoic acid led to a lower selectivity toward benzaldehyde. PMO<sub>12</sub>@Cu-BTC demonstrated approximately 75% conversion of benzyl alcohol with a selectivity of ~90% toward benzaldehyde, whereas PMO<sub>9</sub>V<sub>3</sub>@Cu-BTC demonstrated ~98% conversion of benzyl alcohol with a selectivity of ~65% using the same reaction conditions. Simply put, the product distribution was adjustable by tuning the redox capability of the polyoxometalates. Notably, in several works, a synergistic effect was observed between Cu-BTC and the polyoxometalate [64–66].

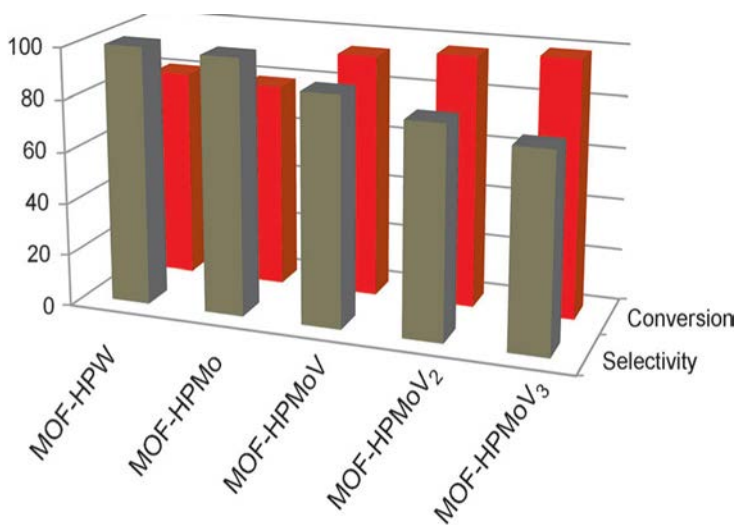


**FIG. 5.3** Oxidation of benzyl alcohol catalyzed by a variety of POM@MOF-199. Reprinted with permission from J. Zhu, M.-N. Shen, X.-J. Zhao, P.-C. Wang, M. Lu, Polyoxometalate-based metal-organic frameworks as catalysts for the selective oxidation of alcohols in micellar systems. *ChemPlusChem* 79(6) (2014) 872–878. Copyright (2014), John Wiley.



Yu and coworkers [67] utilized UiO-bpy (bpy=2,2'-bipyridine-5,5'-dicarboxylic acid) for the encapsulation of polyoxomolybdic cobalt (CoPMA). The bpy sites on the UiO-bpy framework supplied an added interaction with the polyoxometalate in comparison with the UiO-67 robbed of its bpy moieties. The catalytic activities of CoPMA@UiO-bpy and CoPMA@UiO-67 were evaluated over the oxidation of styrene, using oxygen gas as an oxidizing agent. The CoPMA@UiO-bpy showed the highest catalytic performance, with 80% conversion of styrene and 59% selectivity toward styrene epoxide.

Another zirconium-based MOF, NU-1000, with large hexagonal (31 Å) and smaller triangular (12 Å) channels, was used to support polyoxometalate ions such as  $[PW_{12}O_{40}]^{3-}$  and  $[PMo_{10}V_2O_{40}]^{5-}$  [68–70]. For instance, Farha and coworkers [68] prepared PW@NU-1000 through an impregnation method for the oxidation reaction of 2-chloroethyl ethyl sulfide (CEES) using hydrogen peroxide as an oxidizing agent. The authors showed that the most probable location for PW clusters is inside the small triangular channels; this was further established using powder X-ray diffraction, scanning transmission electron microscopy, and difference envelope density analysis. The PW@NU-1000 showed a higher conversion of CEES (98% after 20 min) in comparison with the intact NU-1000 (77% after 90 min) and homogeneous polyoxometalate (98% after 90 min).

In addition to the well-known MOFs, many other POM@MOF hybrid materials, such as  $[Co(BBPTZ)_3][HPMo_{12}O_{40}]\cdot 24H_2O$  and  $[Cu_6^I(trz)_6(PW_{12}O_{40})_2]$ , were prepared and utilized for ODS [71], oxidation of alkylbenzenes [72], aryl alkenes [73,74], and alcohols [75].

In addition to using polyoxometalates entrapped inside the cavities of MOFs, some polyoxometalates have been used to cover the surface of MOFs to achieve core/shell structured hybrid materials for the oxidation reactions [34,76]. For instance, PW was loaded onto the surface of ZIF-8 to afford a core/shell catalyst for the oxidation of benzyl alcohol. Interestingly, strong formation of O–N bonds between PW and the imidazole group of the ZIF-8 was detected by means of X-ray absorption near-edge structure and X-ray photoelectron spectroscopy techniques. Therefore, the ZIF-8@PW material was not soluble in hydrophilic solvents. The ZIF-8@PW material converted benzyl alcohol (more than 95%), with a selectivity of 90% toward benzaldehyde, outperforming the activity of pure PW (51%) and ZIF-8 (30%).

### 5.6.2.2 Condensation reaction

POM@MOF has proven useful in a range of condensation reactions, which are used for producing value-added cyclic organic compounds. Recently, Malkar et al. [77] compared the catalytic activity of three different catalysts, i.e., 20%-Cs-DTP-K10, 18%-DTP@ZIF-8, and  $Al_{0.66}$ -DTP@ZIF-8 (DTP = dodecatungstophosphate), for the aldol condensation 5-hydroxymethylfurfural (Fig. 5.4). It has been demonstrated that the substitution of heteropoly acids



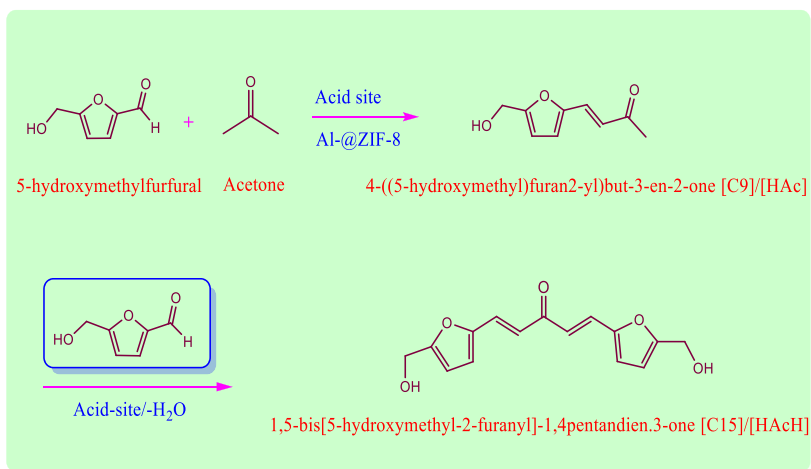


**FIG. 5.4** Aldol condensation of 5-hydroxymethylfurfural with acetone over Al-DTP@ZIF-8. Reproduced with permission from R.S. Malkar, H. Daly, C. Hardacre, G.D. Yadav, Aldol condensation of 5-hydroxymethylfurfural to fuel precursor over novel aluminum exchanged-DTP@ZIF-8. *ACS Sustain. Chem. Eng.* 7(19) (2019) 16215–16224. Copyright (2019), American Chemical Society.

protons with metal ions raises the mobility of protons, which in turn improves the acidity. In the  $\text{NH}_3$ -TPD analysis, Cs-DTP-K10 exhibits the highest acidity ( $1.51 \text{ mmol g}^{-1}$ ), while of acidic sites for DTP@ZIF-8 and Al-DTP@ZIF-8 are 0.44 and  $0.54 \text{ mmol g}^{-1}$ , respectively. Cs-DTP-K10, with the highest acidity, exhibited the highest activity for the aldol condensation of HMF and acetone for the selective production of the desired C<sub>9</sub> product (71.6% after 6 h of reaction); however, the selectivity was only 43.1%. Even though the total number of the acidic sites in the case of the Al-DTP@ZIF-8 catalyst was much lower, a conversion of 63.1% was observed after 6 h of reaction, which was comparable to the former value. It is noteworthy that the Al-DTP@ZIF-8 catalyst demonstrated a much higher selectivity ( $\sim 92\%$ ) toward the C<sub>9</sub> product in comparison with the C<sub>15</sub> one. The lowest rate of conversion was accomplished in the case of the lowest acidic species, i.e., 18% -DTP@ZIF-8. However, a high selectivity was observed toward the C<sub>9</sub> product. This higher selectivity toward the C<sub>9</sub> product indicated the shape selectivity provided by the small pore diameter of ZIF-8 that allows for prevention from the C<sub>15</sub> adduct production.

In a different work [78], PW@MIL-101(Cr) composites were prepared through a direct hydrothermal process or a modifying postsynthesis route. The acidic sites within MIL-101 and PW@MIL-101(Cr) are desirable in the catalysis of the Baeyer condensation of 2-naphthol and benzaldehyde, in a three-

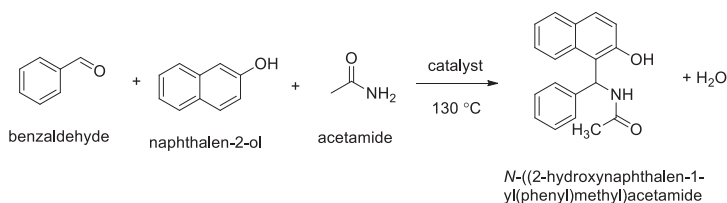


**FIG. 5.5** Condensation reaction of 2-naphthol, benzaldehyde, and acetamide. Reprinted with permission from L. Bromberg, Y. Diao, H. Wu, S.A. Speakman, T.A. Hatton, *Chromium(III) terephthalate metal organic framework (MIL-101): HF-free synthesis, structure, polyoxometalate composites, and catalytic properties*. *Chem. Mater.* 24(9) (2012) 1664–1675. Copyright (2012), American Chemical Society.

component condensation of benzaldehyde, 2-naphthol, and acetamide; the process is illustrated in Fig. 5.5.

Formation of 1-amidoalkyl-2-naphthol was achieved at 130°C using microwave heating for 5 min with a high yield of ~95%.

Moreover, PW clusters were evenly encapsulated in the cavities of MIL-101 serving as a heterogeneous catalyst for the self-condensation of cyclic ketones with high selectivity [79]. As illustrated in Fig. 5.6, depending on the active sites in the applied catalysts, the self-condensation of cyclopentanone can afford three products. With PW as a catalyst, a conversion of ~78% to trindane as the main product was obtained after 24 h. However, PW@MIL-101 showed a substantially higher selectivity (more than 98%) toward the mono-condensed component (i.e., 2-cyclopentylidenecyclopentanone) as

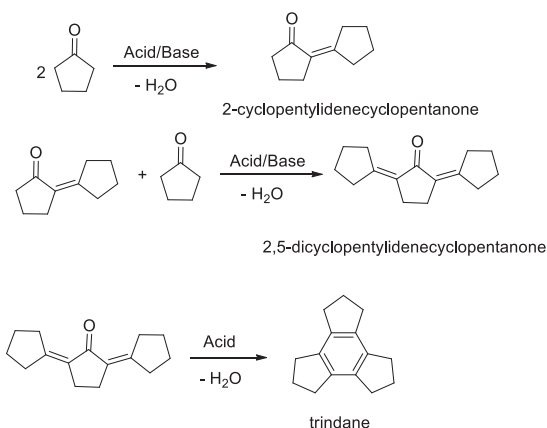


**FIG. 5.6** Cyclopentanone self-condensation reaction. Adapted with permission from Q. Deng, G. Nie, L. Pan, J.-J. Zou, X. Zhang, L. Wang, *Highly selective self-condensation of cyclic ketones using MOF-encapsulating phosphotungstic acid for renewable high-density fuel*. *Green Chem.* 17(8) (2015) 4473–4481. Copyright (2015), Royal Society of Chemistry.

the desired product; this was because of the feasibility of shape-selective catalysis.

### 5.6.2.3 Esterification reaction

MOFs modified with polyoxometalates can be utilized as effective catalysts for a wide variety of esterification reactions. Xie and coworkers [80] examined the catalyzed one-pot transesterification of acidic vegetable oil over a functionalized UiO-66-2COOH with a Keggin-type polyoxometalate, i.e., AILs/POM/UiO-66-2COOH (AIL=sulfonated acidic ionic liquid). The whole process is depicted in Fig. 5.7. The synthesized catalyst exhibited synergic merits owing to the introduction of AIL as Brønsted acid sites. The fact that both Lewis acid sites and Brønsted acid sites of ionic liquids were present in the polyoxometalate accelerated the catalytic reaction for green production of biodiesel. It was revealed by the control experiments that all of the utilized polyoxometalates ( $\text{PW}_{12}\text{O}_{40}^{3-}$ ,  $\text{SiW}_{12}\text{O}_{40}^{4-}$ , and  $\text{PMo}_{12}\text{O}_{40}^{3-}$ , abbreviated as PW, SiW, PMo, respectively) were capable of catalyzing the conversion of soybean oil to biodiesel with a high efficiency (~100% conversion). Notably, AILs/POM/UiO-66-2COOH catalysts can incorporate the advantages of AILs, polyoxometalates, and porous MOFs,

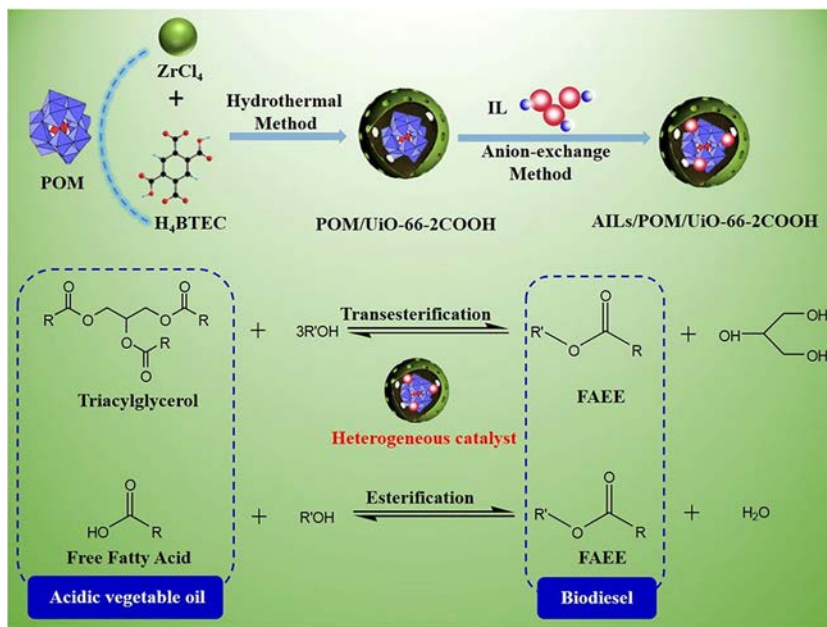


**FIG. 5.7** (A) Synthesis of the AILs/HPW/UiO-66-2COOH catalyst, and (B) one-pot transesterification-esterification of acidic vegetable oils. Reprinted from W. Xie, F. Wan, Immobilization of polyoxometalate-based sulfonated ionic liquids on UiO-66-2COOH metal-organic frameworks for biodiesel production via one-pot transesterification-esterification of acidic vegetable oils. *Chem. Eng. J.* 365 (2019) 40–50. Copyright (2019), with Elsevier.

thus providing the highest catalytic efficiency in the mentioned reaction (more than 90% conversion). In addition, the high extent of interaction between the AILs and polyoxometalates prevented leaching of active ingredients into the reaction media, which in turn led to an insignificant decrease in the catalytic conversion of oil to biodiesel after five successive runs of the catalyzed reaction.

Liu and coworkers reported an efficient procedure for designing NENU-3a with different crystal morphologies (octahedral and cubic) consisting of a Cu-BTC skeleton and encapsulated tungstophosphoric acid catalyst [81]. The NENU-3a with cubic crystals was able to accelerate the conversion of long-chain (C12–C22) fatty acids into their corresponding monoalkyl esters (with more than 90% yield) in comparison with the octahedral counterpart (less than 22% yield). Furthermore, the cubic NENU-3a catalyst was quite potent and reusable for five runs while its structure and catalytic activity was virtually preserved.

Zhu and coworkers [82] investigated the selective esterification of glycerol catalyzed by a MOF-supported polyoxometalate. The catalytic activity of the POM@Cu-BTC catalyst they obtained was compared with that of the metal oxide-supported polyoxometalates as reference. Given that when using POM@metaloxide, there was no pore limitation impact, the glycerol conversion stopped at the acid stage without any more reaction and it could be freely released from the reaction site (Fig. 5.8). Nevertheless, when applying the POM@Cu-BTC catalyst, diffusion of the acid product within the MOF pores was re-

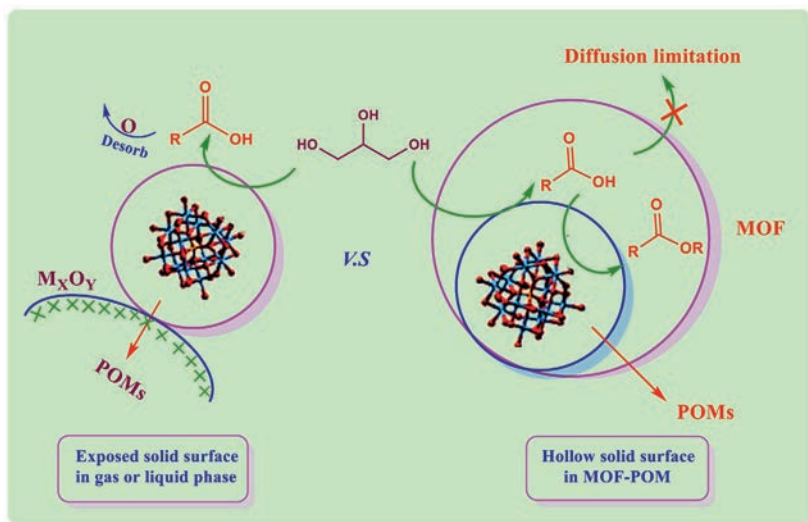


**FIG. 5.8** Restricted transformation of glycerol on MOF-polyoxometalates due to diffusion. Reprinted with permission from J. Zhu, P.-C. Wang, M. Lu, Study on the one-pot oxidative esterification of glycerol with MOF supported polyoxometalates as catalyst. *Cat. Sci. Technol.* 5(6) (2015) 3383–3393. Copyright (2015), Royal Society of Chemistry.

stricted and acid product underwent further reaction to afford the corresponding ester compound.

#### 5.6.2.4 Other organic transformations

HPW was examined in the hydrolysis of ethyl acetate in excess water. Formulated as NENU-3a, the catalyst caused almost a complete conversion (more than 95%) after about 7 h, which proved totally better than most inorganic solid acids and similar to organic solid acids. Moreover, with the activity reported per unit of acid, NENU-3a was three to seven times more active than sulfuric acid, HPW, Amberlyst-15, and nafion-H.

Furthermore, water was not observed to deactivate the acid sites and for at least 15 runs, leaching of the polyoxometalate was not noted. The same group reported using polyoxometalates as templates to construct new hybrid compounds, for which the properties of the polyoxometalate could be adapted to a definite application [83–85]. One of these definite applications was adsorption followed by hydrolysis of dimethyl methylphosphonate (a nerve gas) to methyl alcohol, for which the conversion was enhanced to 93% when the temperature was increased to 50°C [83].

Hupp and coworkers [86] studied the application of a zirconium-based MOF, i.e., NU-1000, loaded with HPW in the catalyzed reaction of oxylene isomerization/disproportionation at 250°C (see Fig. 5.9). No activity was observed at low loadings of polyoxometalate (0.3 to 0.7 polyoxometalate per  $Zr_6$  node), which was attributed to the breakdown of the polyoxometalate and/or the MOF structure due to the activation or at the start of the reaction. Nevertheless, when the loading was extremely

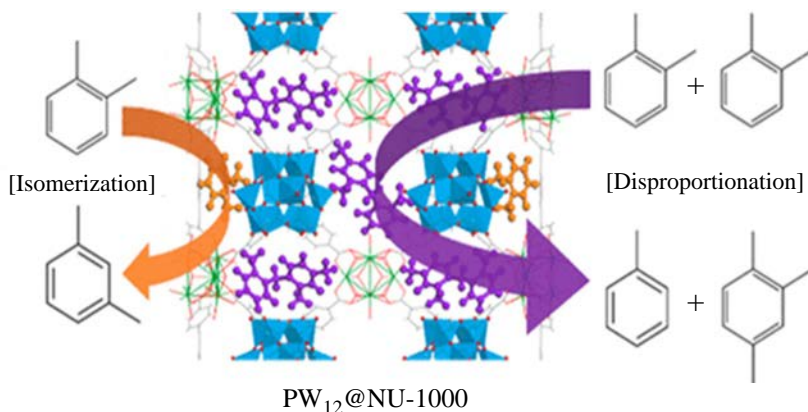


**FIG. 5.9** Tungstophosphoric acid encapsulated in NU-1000 to be used in the aggressive isomerization of hydrocarbon. Reprinted with permission from S. Ahn, S.L. Nauert, C.T. Buru, M. Rimoldi, H. Choi, N.M. Schweitzer, J.T. Hupp, O.K. Farha, J.M. Notestein, Pushing the limits on metal-organic frameworks as a catalyst support: NU-1000 supported tungsten catalysts for *o*-xylene isomerization and disproportionation. *J. Am. Chem. Soc.* 140(27) (2018) 8535–8543. Copyright (2018), American Chemistry Society.

increased so that one Keggin unit per unit cell of NU-1000 was obtained, the hybrid catalyst showed an initial reactivity in the examined C–C skeletal rearrangement reaction, which was even higher than that of the reference  $\text{WO}_x\text{-ZrO}_2$  catalyst.

In a study [87], a mesoporous MOF, i.e., COK-15, was investigated in the alcoholysis of styrene oxide (Fig. 5.10); this reaction was characterized by low selectivity. The COK-15 catalyst not only demonstrated a significant activity (100% conversion), but also accomplished 100% selectivity for 2-methoxy-2-phenylethanol after 3 h at 40°C. In comparison, the microporous Cu-BTC and POM@Cu-BTC only exhibited 2% and 40% conversion, respectively. The authors attributed this good performance of the COK-15 to the mesoporous feature that enabled an efficient mass transport. In addition, the catalyst was recyclable for at least four cycles, with insignificant loss of selectivity and activity.

The Mn-POM@MIL-100 (30 wt% loaded) was assessed for its catalytic efficiency in the reduction of p-nitrophenol to p-aminophenol by means of  $\text{NaBH}_4$  [88]. While both compounds individually showed no catalytic activity, the composite demonstrated an excellent performance, even comparable with those of the catalysts containing noble metals. The authors attributed the high observed catalytic activity to the fact that the Mn-POM facilitated the electron transfer from  $\text{BH}_4^-$  to the  $\text{Fe}^{3+}$  Lewis acid sites of the MOF, since they thought that the MIL-100 alone was not able to accept electrons directly from  $\text{BH}_4^-$ .

In addition, Shul and coworker [34] observed a distinct acid-base synergy when exploring the core-shell structured heteropoly acid-functionalized ZIF-8 in the production of biodiesel via the transesterification of rapeseed oil with methanol. More than 95% of the rapeseed oil was converted to biodiesel be-

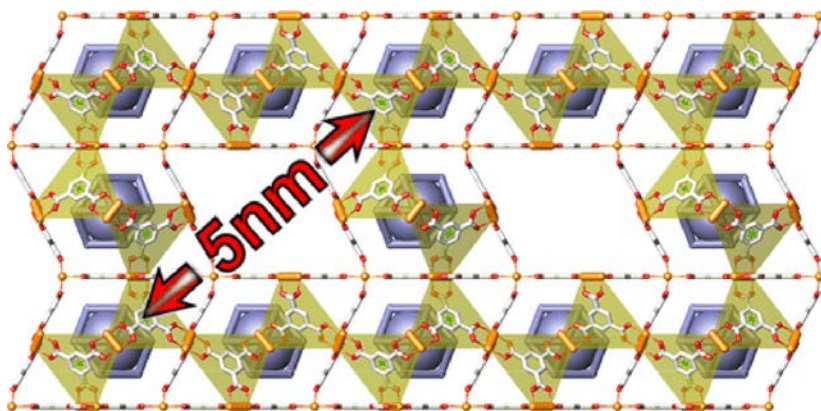


**FIG. 5.10** A copper benzene tricarboxylate metal organic framework, COK-15, with a wide permanent mesoporous characteristic stabilized by Keggin polyoxometalate ions for the methanolysis of styrene oxide. Adapted with permission from L.H. Wee, C. Wiktor, S. Turner, W. Vanderlinden, N. Janssens, S.R. Bajpe, K. Houthoofd, G. Van Tendeloo, S. De Feyter, C.E.A. Kirschhock, J.A. Martens, Copper benzene tricarboxylate metal-organic framework with wide permanent mesopores stabilized by Keggin polyoxometalate ions. *J. Am. Chem. Soc.* 134(26) (2012) 10911–10919. Copyright (2012), American Chemistry Society.



cause of simultaneous basicity of the imidazolate groups on the MOF and the presence of the acid functionalities of the polyoxometalate.

### 5.6.3 Electrocatalysis

In addition to the application of POM@MOF hybrids in organocatalysis systems, polyoxometalates demonstrate intriguing electrocatalytic properties since they can go through fast, reversible multielectron transfers [89]. In this setting, polyoxometalates have revealed great potential in the electrochemical oxygen evolution reaction (OER) as homogenous catalysts [90]. Although remarkable progress has been made in this field, not many reports may be found on the encapsulation of polyoxometalates in the cavities of MOFs for the electrocatalytic oxidation of water. This may be attributed to the fact that the MOFs mostly have a low electrical conductivity while being highly hydrophobic. Das et al. [91,92] reported the very first case of the encapsulation of an unsubstituted Keggin polyoxometalate within an MOF to be utilized in the electrocatalytic oxidation of water. A one-pot synthesis was conducted to insert the  $[\text{CoW}_{12}\text{O}_{40}]^{6-}$  anion in the size matching cavity of ZIF-8. The POM@MOF catalyst showed excellent stability, since only a very slight drop in the catalytic current was detected after 1000 catalytic runs and no leaching of the cobalt-based species was noted. Zhang and coworkers [93] successfully coated ZIF-67 with  $\text{H}_3\text{PW}_{12}\text{O}_{40}$ . The unique yolk/shell structure of the ZIF-67@HPW catalyst enabled a fast charge transfer as well as high electrical conductivity giving rise to a substantial reduction of the overpotential.

Moreover, in these examples of oxygen evolution reaction (OER), polyoxometalates have demonstrated a great potential in the second half reaction for water-splitting, i.e., the hydrogen evolution reaction [94]. Nevertheless, to resolve their weak points, especially the limited stability of polyoxometalates in the highly acidic pH for, which is required for hydrogen evolution reaction, Zhang and coworkers [95,96] encapsulated polyoxometalates in metal-organic nanotubes (MONTs), which could be regarded as a special type of MOF. The best POM@MONTs electrocatalyst exhibited an overpotential of 131 mV (at a current density of  $10 \text{ mA cm}^{-2}$ ), far better than other POM-based MOFs (exhibiting overpotentials above 200 mV) [97].

### 5.6.4 Photocatalysis

In view of the exceptionally large-scale application of solar energy, the POM@MOF species have proven especially attractive for their utilization in the photocatalytic reactions driven by the visible light. In recent years, they have been particularly used as a catalyst for proton reduction. In this field, in et al. [35,98] reported the integration of the two necessary components, i.e., a photosensitizer,  $[\text{Ru}(\text{bpy})_3]^{2+}$  or  $[\text{Ir}(\text{ppy})_2(\text{bpy})]^+$ , and a hydrogen evolution catalyst, into a zirconium-based MOF to conduct the proton reduction. Using a prefunctionalized  $[\text{Ir}(\text{ppy})_2(\text{bpy})]^+$ -derived dicarboxylate ligand, a nickel-based anionic polyoxometalate was embedded into the highly cationic MOF [35]. For the hierarchically organized POM@MOF assembly, a TON value of 1476 was recorded



which allowed facile electron transfer owing to the proximity of the  $\text{Ni}_4\text{P}_2$  to multiple photosensitizers in  $\text{Ni}_4\text{P}_2\text{@MOF}$ .

Li and coworkers [99] synthesized the first water-soluble supramolecular MOF, i.e., SMOF-1, via a self-assembly process from the hex armed  $[\text{Ru}(\text{bpy})_3]^{2+}$ -based precursor and cucurbit uril (CB). The resulted polycationic SMOF-1 displayed a weak gas adsorption ability. However, it could receive the bulky redox active anion  $[\text{P}_2\text{W}_{18}\text{O}_{62}]^{6-}$ . The resulting WD-POM@SMOF-1 produced hydrogen approximately four times more than that of its heterogeneous counterpart. The authors believed this high activity was due to a unique encapsulation pattern in which each cavity hosted one guest. Such a pattern allowed:

- (i) quick diffusion and close contact of the hydronium and methanol molecules; and
- (ii) easy electron transfer from the excited  $[\text{Ru}(\text{bpy})_3]^{2+}$  to the WD-POM.

Dolbecq and coworkers reported the first photoactive POM@MOF catalyst free of noble metals [100]. A cobalt-based polyoxometalate with redox activity was embedded in a light-harvesting porphyrinic MOF, designated by MOF-545, for oxidation of water by the visible light as illustrated in Fig. 5.11; simply put, the catalyst and the photosensitizer were both incorporated into the same porous substance. The evolution of the oxygen gas

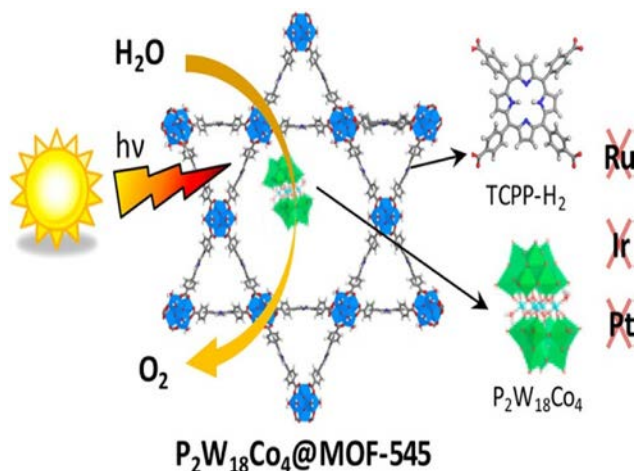


**FIG. 5.11** A POM@MOF catalyst completely free from noble metals for the photocatalytic oxidation of water. Reprinted with permission from G. Paille, M. Gomez-Mingot, C. Roch-Marchal, B. Lassalle-Kaiser, P. Mialane, M. Fontecave, C. Mellot-Draznieks, A. Dolbecq, A fully noble metal-free photosystem based on cobalt-polyoxometalates immobilized in a porphyrinic metal-organic framework for water oxidation. *J. Am. Chem. Soc.* 140(10) (2018) 3613–3618. Copyright (2018), American Chemistry Society.

started when the system was exposed to light and increased linearly with time until a steady state was reached after the catalysis was continued for 1 h. The authors asserted that the unparalleled activity of this *three-in-one* photo-active catalyst resulted from:

- (i) the immobilization of the porphyrin ligand in the MOF, which raised its oxidizing power; and
- (ii) the entrapment of the Co-POM within the pores of MOF-545, which led to an increase in the stabilization the polyoxometalate catalytic sites.

In a novel study by Niu and coworkers [101], the integration of a photosensitizer, electron donor, and acceptor into one single framework was realized. In order to synthesize this zinc-based framework, a photosensitizer compound, *N,N'*-di(4-pyridyl)-1,4,5,8-naphthalenetetracarboxydiimide (DPNDI), was used as the organic ligand; pyrrolidine-2-yl-imidazole and the  $[\text{BW}_{12}\text{O}_{40}]^{5-}$  anion were used as the electron donor and electron acceptor, respectively (Fig. 5.12). The obtained Zn-DPNDI-PYI catalyst was tested over the oxidative coupling reaction of benzyl amine and displayed a conversion of 99% after 16h. This great activity was resulted from the successive photo-induced electron transfer (con PET) processes; however, it was also assigned to a long-lived charge separated state.

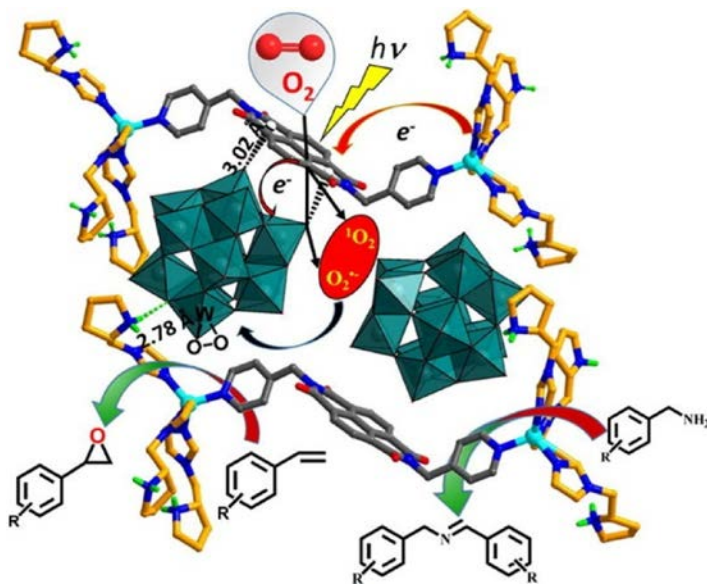


**FIG. 5.12** Zn-DPNDI-PYI as a photocatalyst for the coupling reaction of primary amines and oxidation of olefins by means of air under visible light. Reprinted from J.C. He, Q.X. Han, J. Li, Z.L. Shi, X.Y. Shi, J.Y. Niu, Ternary supramolecular system for photocatalytic oxidation with air by consecutive photo-induced electron transfer processes. *J. Catal.* 376 (2019) 161–167. Copyright (2019), with permission from Elsevier.

## 5.7. Polyoxometalate hybrids covalently immobilized onto mesoporous supports

### 5.7.1 Polymer-supported polyoxometalates catalysts

Polymeric substances, particularly organic polymers, have been extensively examined owing to their adjustable and abundant structures, functionality, and easy operation [102]. Polymers have proven appropriate as supports for heterogeneous catalysts, due to advantages such as easy production and low weight. In addition, the organic frameworks of polymers allow them to be compatible with organic substrates. Consequently, during the past decade, the synthesis of polyoxometalates/polymer hybrid substances or polymer-supported polyoxometalates catalysts has been of great interest [103]. Leng and Wang worked thoroughly on polyoxometalate-based hybrids for a variety of catalytic reactions, including esterifications [104], epoxidation of alkenes mediated by hydrogen peroxide [105,106], oxidation of alcohols [107,108], and hydroxylation of benzene [109]. The synthesis of the catalysts was achieved by the anion exchange of different organic groups' functionalized polymers or ionic copolymers with heteropoly acids of Keggin type. The was able to synthesize a polyoxometalate-based cross-linked ionic copolymer via the anion exchange of a novel ionic copolymer with a Keggin heteropoly acid and containing amino groups and designed for a specific task (Fig. 5.13) [105]. The afforded hybrid catalyst was tested over the liquid-solid heterogeneous epoxidation of alkenes with aqueous hydrogen peroxide. Promising results were observed as the supported system displayed a conversion of 98.5% for the cyclooctene with 100% selectivity. The values were higher in comparison with the polyoxometalate alone, exhibiting the effectiveness of the hybrid substance.

Porosity significantly affects the interactions between the catalyst and the surface, the mass transfer efficiency, and the substrate accessibility [110].

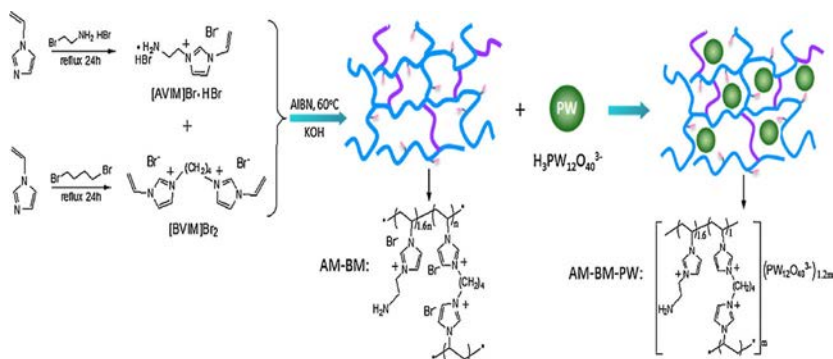


FIG. 5.13 Synthesis of the ionic hybrid AB-BM-POM. Reprinted from Y. Leng, W. Zhang, J. Wang, P. Jiang, A novel heteropolyanion-based amino-containing cross-linked ionic copolymer catalyst for epoxidation of alkenes with H<sub>2</sub>O<sub>2</sub>. *Appl. Catal. A. Gen.* 445-446 (2012) 306–311. Copyright (2012), with permission from Elsevier.

Based on these factors, plenty of mesoporous polymers have been synthesized and utilized as a support for a heterogeneous catalyst. Additionally, many approaches have been proposed for the examination of the porosity effects of the polymeric supports on the reactions catalyzed by polyoxometalates.

Ryoo and coworkers [111] prepared an ordered mesoporous polymer. After the prepared polymers were functionalized with ammonium groups, the Ishi-Venturello polyperoxotungstate anion,  $[\text{PO}_4\{\text{WO}(\text{O}_2)_2\}_4]^{3-}$ , was immobilized by introducing it as a counter ion to the ammonium group. The hybrid material was observed to have good catalytic performance in the epoxidation of olefins in liquid phase, by means of an aqueous solution of hydrogen peroxide as an oxidizing agent. Easy filtration and reuse of the catalyst with no considerable loss of activity were among the other characteristics of the process.

As a final instance, Xiao and coworker [112] synthesized a hybrid catalyst in which the polyoxometalate ion was covalently grafted on a polymer surface. Covalent immobilization was accomplished via the surface reaction of two polyoxometalate clusters modified azido-organically with functionalized groups on the channel surface of the macroporous resin. The prepared catalyst displayed high activity and selectivity for the oxidation of tetrahydrothiophene. The approach had the advantage that the catalyst was reusable many times.

### 5.7.2 Polyoxometalate catalysts supported on mesoporous transition metal oxide

As the materials science and synthetic technology develops, various mesoporous transition metal oxide materials, such as zirconium dioxide, chromium (III) oxide, and iron (III) oxide, have been designed and used as catalyst supports. They are regarded as ideal supports owing to adjustable chemical composition, inert framework which is resistant against the corrosion of the guest materials, porous structure, as well as the ability to establish strong host/guest interactions for higher catalytic performance. Consequently, many efforts have been made to immobilize the active sites of a polyoxometalate on a mesoporous transition metal oxide to synthesize an anchored homogeneous catalysts. In order to synthesize new hybrid catalysts, Armatas et al. [113] utilized phosphomolybdic acid (HPMo) in combination with nanocrystalline zirconium dioxide or with nanocomposite mesoporous frameworks of  $\text{Cr}_2\text{O}_3$ . For the  $\text{ZrO}_2$  case, the synthesis was conducted via a sol-gel copolymerization route assisted by a surfactant, and different HPMo loadings were examined for the synthesized species. Various characterization techniques revealed that HPMo maintained its Keggin structure inside the mesoporous frameworks. These species were applied in the oxidation of alkenes by means of hydrogen peroxide as an oxidizing agent demonstrating an extraordinary stability. For the  $\text{Cr}_2\text{O}_3$  case, the same Keggin-type heteropoly acid was utilized with  $\text{Cr}_2\text{O}_3$  to prepare well-ordered mesoporous frameworks. The hexagonal mesoporous SBA-15 was utilized as

a hard template. Again, the hybrid species were applied in oxidation reactions, specifically in the oxidation of 1-phenylethanol with hydrogen peroxide as an oxidizing agent [114].

Skliri and coworkers [115] synthesized ordered mesoporous composite catalysts containing nano crystalline tetragonal zirconium dioxide and tungstophosphoric acid (HPW) and silicotungstic (HSiW) acid via a copolymerization route assisted by a surfactant. The authors showed that the inclusion of HPW and HSiW clusters in the mesoporous framework efficiently affected the catalytic activity of these materials. Although  $ZrO_2$  and heteropoly acids alone exhibited little catalytic activity, the  $ZrO_2$ -HPW and  $ZrO_2$ -HSiW heterostructures displayed surprisingly high activity in the oxidation of 1,1-diphenyl-2-methylpropene by means of hydrogen peroxide under mild conditions. In addition, Guo and coworkers [116–118] synthesized an array of mesoporous HPW/ $ZrO_2$ -Si(Et/Ph)Si and HPW/ $ZrO_2$ -Si(*pH*)Si hybrid catalysts using a template-assisted, one-pot, sol-gel condensation-hydrothermal treatment route. The first catalyst was used as a green solid acid catalyst in the transesterification of inexpensive oil from *Eruca Sativa Gars* with methanol to afford methyl esters of fatty acids under atmosphere refluxing. The synthesized catalyst demonstrated higher catalytic activity in comparison with alkyl-free HPW- $ZrO_2$  [116]. Su et al. [117] utilized the prepared catalysts for the esterification of levulinic acid with a variety of alcohols under moderate conditions owing to their pore morphologies, acidity, and textural properties.

### 5.7.3 Polyoxometalate catalysts supported on zeolites

Zeolites may be utilized as a support for the synthesis of novel hybrid catalysts. Many types of processes can be accomplished with zeolites used as supports in the heterogenization of polyoxometalates. In most cases, heteropoly acids are impregnated onto the surface of zeolites or encapsulated within the pores. Wang and coworkers [119] supported HPW on dealuminated ultra-stable Y zeolite (DUSY) by an impregnation method. Then its physicochemical properties were characterized. The HPW catalyst supported on DUSY showed a high catalytic activity for the acetalization of ethylacetoacetate in liquid phase with ethylene glycol as a synthesis route to fructose. Nevertheless, continuous leaching of the heteropoly acids into the reaction medium resulted in poor catalytic stability.

In addition, Mukai and coworkers [120] used a Y-type zeolite for the encapsulation of HPMo as a catalyst for the esterification of acetic acid with ethanol. The authors studied the influence of the Si/Al ratio in the zeolite on the amount of HPMo encapsulation. They came to the conclusion that HPMo could be formed within the super cavities of the support when the number of aluminum atoms per unit cell was approximately in the range of 4–20. As soon as the number exceeded this range, it was probable that the support was destroyed during the synthesis of the catalyst as the durability in acidic solutions was low for supports with high contents of aluminum. Besides, the encapsulation of HPMo using supports with very low aluminum contents was a difficult process.

The same team [121] examined the effect of other parameters, such as the temperature and the solvent nature, on the amount of heteropoly acid inclusion as well as the stability of the resulted engaged catalyst. It was revealed that by tuning the reaction temperature, the stability of the resulted engaged catalyst could be improved. It was also established that adding *t*-butyl alcohol to the solution of the catalyst synthesis resulted in an active and stable engaged catalyst, even at low temperatures.

Jarrahi et al. [122] prepared novel nanohybrid material, i.e.,  $H_6P_2W_{18}O_{62}/$ nanoclinoptilolite, to utilize it as a reusable, efficient catalyst in the mild, one-pot condensation of an array of acetophenones. These zeolites contained open tetrahedral cavities that provide a system of channels; the sizes of such channels are determined by the silicon content. The cages are formed with a network of 8- and 10-membered rings.

#### 5.7.4 Mesoporous silica-based heteropoly acid catalysts

Mesoporous silica species are characterized by a variety of excellent textural parameters, e.g., great surface areas and pore volumes, a narrow distribution of pore sizes, as well as special quantum size effects [123,124]. Moreover, the synthesis and modification of mesoporous silica is readily adjustable in a continuous wide arrangement. Therefore, mesoporous silica materials, particularly high-ordered mesoporous silicas [124], have been extensively applied as supports for the immobilization of polyoxometalates in the heterogeneous catalysis reactions.

There are a variety of strategies, including impregnation, ion exchange, sol-gel techniques, and covalent grafting, to synthesize mesoporous silica catalytic species loaded with heteropoly acids.

One can divide the immobilization of polyoxometalates onto the surface of mesoporous silica into three different groups. The first group includes no vacant heteropoly acids bound to the silica supports via the protonation of the hydroxyl groups on the surface and through the interaction of the resulted  $\equiv SiOH_2^+$  species with the external oxygen atoms on the heteropoly acids. In the second group, the polyoxometalate anchoring inside the channels of mesoporous substances functionalized by positive alkylammonium or imidazolium groups are concerned. Eventually, the third group deals with polyoxometalates covalently grafted on the surface.

##### 5.7.4.1 Immobilizing heteropoly acids onto mesoporous silica by means of electrostatic interactions

There are numerous cases of heteropoly acids immobilized onto mesoporous. Here, several representative examples will be given for the purpose of illustration.

Kaur et al. [125] and Kozhevnikova et al. [126] synthesized silica-supported heteropoly acid catalysts by impregnation of Aerosil 300 silica with aqueous solution of HPW. The first group tested the catalytic activity of their acquired



species over the Friedel-Crafts acylation while the second group tested theirs on the Fries rearrangement of aryl esters.

In the course of the reaction, even using nonpolar solvents, e.g., dodecane, HPW leached from the silica support. The catalyst could, however, be separated by filtration and washing with dichloroethane, and reused, although with a decrease in activity.

Yadav et al. [127] supported HPW on hexagonal mesoporous silica. The afforded catalyst was observed to be quite active and stable without any deactivation in green route for the synthesis of acetoveratrone.

Blasco and coworkers [128] used supported the same heteropoly acid (HPA) on three different carriers: a commercial silica, an amorphous aluminosilicate (MSA) of a high surface area and an all silica-mesoporous MCM-41. Their catalytic properties were assessed for the alkylation of 2-butene with isobutene. The high surface area of the MCM-41 and MSA displayed higher acid dispersions in comparison with silica; however, HPW/SiO<sub>2</sub> exhibited the highest activity and selectivity toward trimethylpentane, and the highest stability. The authors demonstrated that the heteropoly acid activity was directly dependent on its interaction with the functional group on the support. Therefore, in the PW/MSA samples, in which the heteropoly acid and the surface sites of the aluminosilicate interacted strongly, a lower catalytic activity was predicted. In the PW/MCM-41 samples, limited blockage of the monodimensional pores on MCM-41 reduced the availability of the Brønsted acid sites of the heteropoly acid included inside the pores to the reactants. To resolve this pore blockage, a MCM-41 sample with larger pore diameters could be used. Chen et al. [129] compared the catalytic and structural properties of SBA-15 and MCM-41 as supports for HPW. The results demonstrated that the mesoporous substances maintained the typical hexagonal mesoporous as a support for HPW. It was revealed that the heteropoly acid displayed a higher degree of dispersion within MCM-41 than SBA-15 and other mesoporous molecular sieves. Furthermore, the synthesized materials were observed to be the effective catalysts for the environmentally benign synthesis of benzoic acid. HPA/MCM-41 in particular displayed the best catalytic properties, due to appropriate structural and textural characteristics.

Popa and coworkers [130] synthesized an array of HPA-mesoporous silica composites from NiHPMo<sub>12</sub>O<sub>40</sub> by supporting it on SBA-15 mesoporous silica in active phase with different concentrations. By impregnating a Ni<sup>2+</sup> salt on mesoporous silica, the thermal stability of the Keggin structure was raised compared with its parent bulk heteropoly acid. In fact, the total acidities of the strong and weak acidic sites of NiHPMo<sub>12</sub>O<sub>40</sub>/SBA-15 composites were evidently increased compared with the bulk Ni salt.

#### 5.7.4.2 *Polyoxometalates noncovalently immobilized onto mesoporous materials functionalized with Alkylammonium/imidazolium groups*

Recently, anchoring inside the channels of mesoporous materials or at the surface of oxide nanoparticles functionalized with positive alkylammonium or imidazolium



groups has been used more than before. These electrostatic interactions, though they strengthen the POM-support link, do not thoroughly prevent the leaching of the supported active phase, especially for catalytic processes that take place in usual polar solvents or in ionic liquids. Several examples of such case will be presented.

As the very first workers, Kera et al. prepared a series of catalysts by depositing a heteropoly acid on silica gel utilizing their ion-exchange properties modified by an agent with an amino group. Indeed, the amounts of the heteropoly acid adsorbed and/or deposited increased in proportion with the modification extent.

Amini and coworkers [131] immobilized HPW and  $H_{14}[NaP_5W_{30}O_{110}]$  on the inner surface of mesoporous MCM-41, silica gel and fume silica using chemical bonding to aminosilane groups. Of the functionalized silica species, MCM-41 exhibited the largest amine/silica and the least heteropoly acid/silica ratios. The species were characterized by different methods including IR spectroscopy, low-angle XRD, and BET surface area analysis.

Yamanaka and coworkers [132] designed and prepared catalysts consisting of a heteropoly acid and organ grafted mesoporous silica. The resulted species were used over the ester hydrolysis in water with extraordinary catalytic activity. The authors demonstrated that the nanostructure due to mesoporous silica raised the availability of the active sites to the aqueous reaction mixture in spite of being surrounded by hydrophobic moieties.

Richards et al. [133] formulated a hybrid catalyst consisting of tetrairon(III)-substituted polytungstates immobilized on SBA-15-modified by 3-aminopropyltriethoxysilane. The synthesized material demonstrated excellent catalytic performance for the solvent-free oxidation of long-chain n-alkanes using air as an oxidizing agent under ambient conditions via a classical free-radical chain autoxidation mechanism. In addition, the anchored catalyst was recyclable for several runs without losing catalytic activity. Nomiya et al. [134] proposed a new methodology for grafting polyoxometalates with transition metal substitutes onto a modified silica surface. A Keggin-type, V<sup>V</sup>-substituted polyoxomolybdate, i.e.,  $[PMo_{11}V^VO_{40}]^{4-}$  (PMoV), was electrostatically anchored to a modified silica surface with a cationic ammonium moiety. The resulted PMoV-grafted silica material displayed higher activities in comparison with those of homogeneous PMoV reactions for the oxidation of a variety of alcohols under oxygen gas (1 atm) in the presence of isobutyraldehyde (IBA).

Fraissard and coworkers [135] devised a protocol for the preparation of acid onium salts of Keggin heteropoly acids through an ion exchange process on the amorphous silica functionalized with pyridinium and alkyl imidazolium cations (SiO<sub>2</sub>-Q). The interaction between the heteropoly acid and the surface-grafted cations provided the acid salts of the heteropoly acid with the Keggin structure intact.

### 5.7.5 Covalent grafting of polyoxometalates onto mesoporous materials

There exist a few examples in which polyoxometalates are covalently bound to an oxide support. This covalent linking may be accomplished by two

different methods. In the first approach, polyoxometalates with transition-metal substitutes are attached onto the surface by means of coordination of the transition-metal centers of the polyoxometalates with the nitrogen atoms of porous materials with alkylamine substitutes. As an example, this method has been followed with  $[M(H_2O)PW_{11}O_{39}]^{5-}$  ( $M=Co^{II}, Ni^{II}$ ) (Fig. 5.14). A study by Stein et al. [136] was among the very first ones revealing a covalent linkage between the polyoxometalate with transition-metal substitutes and mesoporous silica. Polyoxometalate with transition-metal substitutes of the type  $[M^{II}(H_2O)PW_{11}O_{39}]^{5-}$  ( $M=Co, Zn$ ) and  $[SiW_9O_{37}\{Co^{II}(H_2O)\}_3]^{10-}$  has been chemically anchored to modified macroporous (400 nm pores), mesoporous (2.8 nm pores), and amorphous silica surfaces. The availability of the open coordination sites to such clusters of polyoxometalates with transition-metal substitutes enabled them to be chemically anchored to the surfaces of the functionalized supports. The catalytic activity of each supported cluster was tested over the epoxidation of cyclohexene to cyclohexene oxide in the presence of isobutyraldehyde. More examples are described in [138,139].

Yet, many questions remain regarding the strength of the link between the transition metal cations and the surface in the course of the catalytic process, while these cations play the role of active centers as well. The second method is related to the direct grafting of a Keggin-type, mono-, or divacant polyoxometalate on the surface of the ordered porous silica through organosilane moieties. In that case, polyoxometalates are incorporated either by a postsynthesis route or by copolymerization with silicon precursors. Following the second approach, Stein and coworkers [137] prepared three-dimensionally ordered macroporous (3DOM) silica species functionalized with the direct synthesis of highly dispersed polyoxometalate clusters. Lacunary clusters of  $\gamma$ -decatingstosilicate were entrapped inside the wall structures of macroporous silica through the

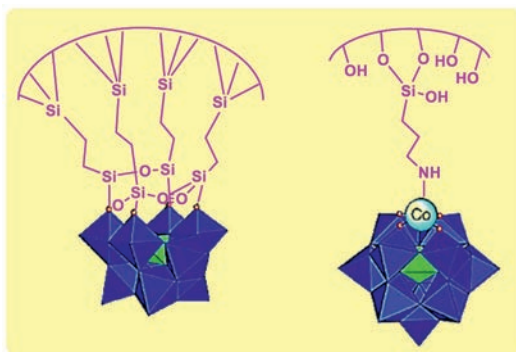


**FIG. 5.14** A schematic of the covalent linking of polyoxometalates via grafting organosilanes onto the silica or direct coordination of polyoxometalate with transition-metal substitutes and organically modified supports [136,137]. ACS publication.

reaction of the clusters in an acidic solution with tetraethoxysilane, with or without adding the polyfunctional linking group 1,2-bis(triethoxysilyl)ethane. Afterward, condensation around polystyrene colloidal crystals was effected. The porous hybrid species were produced upon the removal of the polystyrene template by extraction with a tetrahydrofuran/acetone solution. The prepared species were observed to show catalytic activity over the epoxidation of cyclooctene with an anhydrous hydrogen peroxide/*t*-BuOH solution at ambient temperature. Yang and coworkers [139] prepared new polyoxometalate (POM)-grafting mesoporous hybrid silicas,  $XW_{11}/MHS$  ( $X=P, Si$ ) and  $TBAPW_{11}Si_2/MHS$  through cocondensation and postsynthesis routes utilizing the Keggin-type monovacant  $XW_{11}$  or a Si-substituted compound, i.e.,  $TBAPW_{11}Si_2$ , as precursors for the polyoxometalates in the presence of block copolymer P123 ( $EO_{20}PO_{70}EO_{20}$ ) under acidic conditions [140,141]. These species, particularly the cocondensed samples, displayed reversible and stable photochromic properties under ultraviolet irradiation even though no additional organic component was supplied as an electron donor. Nevertheless, in both cases the authors have mentioned the cleavage of some links between the polyoxometalate and the surface because of the rather weak {Si–O–W} bonds, even after mild heating of the materials (45°C). Moreover, no more nucleophilic oxygen atoms were available for metal substitution due to the implementation of the binding strategy.

## References

- [1] J. Siqueira Mancilha Nogueira, J.P. Alves Silva, S.I. Mussatto, L. Melo Carneiro, Synthesis and application of heterogeneous catalysts based on heteropolyacids for 5-hydroxymethylfurfural production from glucose, *Energies* 13 (3) (2020) 655.
- [2] I.V. Kozhevnikov, Catalysis by heteropoly acids and multicomponent polyoxometalates in liquid-phase reactions, *Chem. Rev.* 98 (1) (1998) 171–198.
- [3] Y. Ji, L. Huang, J. Hu, C. Streb, Y.-F. Song, Polyoxometalate-functionalized nanocarbon materials for energy conversion, energy storage and sensor systems, *Energy Environ. Sci.* 8 (3) (2015) 776–789.
- [4] J.-J. Ye, C.-D. Wu, Immobilization of polyoxometalates in crystalline solids for highly efficient heterogeneous catalysis, *Dalton Trans.* 45 (25) (2016) 10101–10112.
- [5] Y. Zhou, G. Chen, Z. Long, J. Wang, Recent advances in polyoxometalate-based heterogeneous catalytic materials for liquid-phase organic transformations, *RSC Adv.* 4 (79) (2014) 42092–42113.
- [6] L. Chen, W.-L. Chen, X.-L. Wang, Y.-G. Li, Z.-M. Su, E.-B. Wang, Polyoxometalates in dye-sensitized solar cells, *Chem. Soc. Rev.* 48 (1) (2019) 260–284.
- [7] A.S. Cherevan, S.P. Nandan, I. Roger, R. Liu, C. Streb, D. Eder, Polyoxometalates on functional substrates: concepts, synergies, and future perspectives, *Adv. Sci.* 7 (8) (2020) 1903511–1903533.
- [8] M. Ammam, Polyoxometalates: formation, structures, principal properties, main deposition methods and application in sensing, *J. Mater. Chem. A* 1 (21) (2013) 6291–6312.
- [9] J. Hu, Y. Ji, W. Chen, C. Streb, Y.-F. Song, “Wiring” redox-active polyoxometalates to carbon nanotubes using a sonication-driven periodic functionalization strategy, *Energy Environ. Sci.* 9 (3) (2016) 1095–1101.

- [10] Y. Ji, J. Hu, J. Biskupek, U. Kaiser, Y.F. Song, C. Streb, Polyoxometalate-based bottom-up fabrication of graphene quantum dot/manganese vanadate composites as lithium ion battery anodes, *Chem. A Eur. J.* 23 (65) (2017) 16637–16643.
- [11] B. Schwarz, J. Forster, M.H. Anjass, S. Daboss, C. Kranz, C. Streb, From molecular to colloidal manganese vanadium oxides for water oxidation catalysis, *Chem. Commun.* 53 (84) (2017) 11576–11579.
- [12] X. Xing, R. Liu, K. Cao, U. Kaiser, G. Zhang, C. Streb, Manganese vanadium oxide–N-doped reduced graphene oxide composites as oxygen reduction and oxygen evolution electrocatalysts, *ACS Appl. Mater. Interfaces* 10 (51) (2018) 44511–44517.
- [13] S. Zhang, O. Oms, L. Hao, R. Liu, M. Wang, Y. Zhang, H.Y. He, A. Dolbecq, J. Marrot, B. Keita, L. Zhi, P. Mialane, B. Li, G. Zhang, High oxygen reduction reaction performances of cathode materials combining polyoxometalates, coordination complexes, and carbonaceous supports, *ACS Appl. Mater. Interfaces* 9 (44) (2017) 38486–38498.
- [14] A. Proust, B. Matt, R. Villanneau, G. Guillemot, P. Gouzerh, G. Izzet, Functionalization and post-functionalization: a step towards polyoxometalate-based materials, *Chem. Soc. Rev.* 41 (22) (2012) 7605–7622.
- [15] L. Huang, J. Hu, Y. Ji, C. Streb, Y.-F. Song, Pyrene-Anderson-modified CNTs as anode materials for lithium-ion batteries, *Chem. A Eur. J.* 21 (51) (2015) 18799–18804.
- [16] M. Raula, G. Gan Or, M. Saganovich, O. Zeiri, Y. Wang, M.R. Chierotti, R. Gobetto, I.A. Weinstock, Polyoxometalate complexes of anatase-titanium dioxide cores in water, *Angew. Chem. Int. Ed.* 54 (42) (2015) 12416–12421.
- [17] S.J. Tauster, S.C. Fung, R.L. Garten, Strong metal-support interactions. Group 8 noble metals supported on titanium dioxide, *J. Am. Chem. Soc.* 100 (1) (1978) 170–175.
- [18] A.M. Douvas, D. Tsikritzis, C. Tselios, A. Haider, A.S. Mougharbel, U. Kortz, A. Hiskia, A.G. Coutsolelos, L.C. Palilis, M. Vasilopoulou, S. Kennou, P. Argitis, Multi-electron reduction of Wells–Dawson polyoxometalate films onto metallic, semiconducting and dielectric substrates, *Phys. Chem. Chem. Phys.* 21 (1) (2019) 427–437.
- [19] A. Misra, K. Kozma, C. Streb, M. Nyman, Beyond charge balance: counter-cations in polyoxometalate chemistry, *Angew. Chem. Int. Ed.* 59 (2) (2020) 596–612.
- [20] D.X. Liu, D.T. Zou, H.L. Zhu, J.Y. Zhang, Mesoporous metal-organic frameworks: synthetic strategies and emerging applications, *Small* 14 (37) (2018) 1801454–1801493.
- [21] B. Huang, D.H. Yang, B.H. Han, Application of polyoxometalate derivatives in rechargeable batteries, *J. Mater. Chem. A* 8 (9) (2020) 4593–4628.
- [22] L. Zhai, H. Li, Polyoxometalate-polymer hybrid materials as proton exchange membranes for fuel cell applications, *Molecules (Basel, Switzerland)* 24 (19) (2019) 3425–3444.
- [23] G. Férey, C. Mellot-Draznieks, C. Serre, F. Millange, J. Dutour, S. Surble, I. Margiolaki, A chromium terephthalate-based solid with unusually large pore volumes and surface area, *Science* 309 (5743) (2005) 2040–2042.
- [24] J. Juan-Alcañiz, E.V. Ramos-Fernandez, U. Lafont, J. Gascon, F. Kapteijn, Building MOF bottles around phosphotungstic acid ships: one-pot synthesis of bi-functional polyoxometalate-MIL-101 catalysts, *J. Catal.* 269 (1) (2010) 229–241.
- [25] R. Canioni, C. Roch-Marchal, F. Sécheresse, P. Horcajada, C. Serre, M. Hardi-Dan, G. Férey, J.-M. Grenèche, F. Lefebvre, J.-S. Chang, Y.-Q. Hwang, O. Lebedev, S. Turnerf, G.V. Tendeloo, Stable polyoxometalate insertion within the mesoporous metal organic framework MIL-100(Fe), *J. Mater. Chem. A* 21 (4) (2011) 1226–1233.
- [26] E.V. Ramos-Fernandez, C. Pieters, B. Van der Linden, J. Juan-Alcañiz, P. Serra-Crespo, M.W.G.M. Verhoeven, H. Niemantsverdriet, J. Gascon, F. Kapteijn, Highly dispersed

- platinum in metal organic framework NH<sub>2</sub>-MIL-101(Al) containing phosphotungstic acid—characterization and catalytic performance, *J. Catal.* 289 (2012) 42–52.
- [27] L. Bromberg, X. Su, T.A. Hatton, Heteropolyacid-functionalized aluminum 2-aminoterephthalate metal-organic frameworks as reactive aldehyde sorbents and catalysts, *ACS Appl. Mater. Interfaces* 5 (12) (2013) 5468–5477.
- [28] S.R. Bajpe, C.E. Kirschhock, A. Aerts, E. Breynaert, G. Absillis, T.N. Parac-Vogt, L. Giebel, J.A. Martens, Direct observation of molecular-level template action leading to self-assembly of a porous framework, *Chemistry* 16 (13) (2010) 3926–3932.
- [29] X. Liu, J. Luo, T. Sun, S. Yang, A simple approach to the preparation of H<sub>6</sub>P<sub>2</sub>W<sub>18</sub>O<sub>62</sub>/Cu<sub>3</sub>(BTC)<sub>2</sub> (BTC = 1,3,5-benzenetricarboxylate) and its catalytic performance in the synthesis of acetals/ketals, *React. Kinet. Mech. Catal.* 116 (1) (2015) 159–171.
- [30] S.-M. Liu, Z. Zhang, X. Li, H. Jia, M. Ren, S. Liu, Ti-substituted Keggin-type polyoxotungstate as proton and electron reservoir encaged into metal-organic framework for carbon dioxide photoreduction, *Adv. Mater. Interfaces* 5 (21) (2018) 1801062–1801069.
- [31] C.Y. Sun, S.X. Liu, D.D. Liang, K.Z. Shao, Y.H. Ren, Z.M. Su, Highly stable crystalline catalysts based on a microporous metal-organic framework and polyoxometalates, *J. Am. Chem. Soc.* 131 (5) (2009) 1883–1888.
- [32] Z. Huang, Z. Yang, M.Z. Hussain, B. Chen, Q. Jia, Y. Zhu, Y. Xia, Polyoxometalates@zeoliticimidazole-framework derived bimetallic tungsten-cobalt sulfide/porous carbon nanocomposites as efficient bifunctional electrocatalysts for hydrogen and oxygen evolution, *Electrochim. Acta* 330 (2020) 135335–135373.
- [33] R.S. Malkar, H. Daly, C. Hardacre, G.D. Yadav, Novelty of iron-exchanged heteropolyacid encapsulated inside ZIF-8 as an active and superior catalyst in the esterification of furfuryl alcohol and acetic acid, *React. Chem. Eng.* 4 (10) (2019) 1790–1802.
- [34] Y. Jeon, W.S. Chi, J. Hwang, D.H. Kim, J.H. Kim, Y.G. Shul, Core-shell nanostructured heteropoly acid-functionalized metal-organic frameworks: bifunctional heterogeneous catalyst for efficient biodiesel production, *Appl. Catal. Environ.* 242 (2019) 51–59.
- [35] X.J. Kong, Z. Lin, Z.-M. Zhang, T. Zhang, W. Lin, Hierarchical integration of photosensitizing metal-organic frameworks and nickel-containing polyoxometalates for efficient visible-light-driven hydrogen evolution, *Angew. Chem. Int. Ed.* 128 (22) (2016) 6521–6526.
- [36] X. Zhong, Y. Lu, F. Luo, Y. Liu, X. Li, S. Liu, A nanocrystalline POM@MOFs catalyst for the degradation of phenol: effective cooperative catalysis by metal nodes and polyoxometalate guests, *Eur. J. Chem.* 24 (12) (2018) 3045–3051.
- [37] G. Li, K. Zhang, C. Li, R. Gao, Y. Cheng, L. Hou, Y. Wang, Solvent-free method to encapsulate polyoxometalate into metal-organic frameworks as efficient and recyclable photocatalyst for harmful sulfamethazine degrading in water, *Appl. Catal. Environ.* 245 (2019) 753–759.
- [38] C.M. Granadeiro, A.D.S. Barbosa, S. Ribeiro, I.C.M.S. Santos, B. De Castro, L. Cunha-Silva, S.S. Balula, Oxidative catalytic versatility of a trivacant polyoxotungstate incorporated into MIL-101(Cr), *Cat. Sci. Technol.* 4 (5) (2014) 1416–1425.
- [39] D. Julião, A.C. Gomes, M. Pillinger, L. Cunha-Silva, B. De Castro, I.S. Gonçalves, S.S. Balula, Desulfurization of model diesel by extraction/oxidation using a zinc-substituted polyoxometalate as catalyst under homogeneous and heterogeneous (MIL-101(Cr) encapsulated) conditions, *Fuel Process. Technol.* 131 (2015) 78–86.
- [40] D. Julião, A.C. Gomes, M. Pillinger, R. Valença, J.C. Ribeiro, B. De Castro, I.S. Gonçalves, L. Cunha Silva, S.S. Balula, Zinc-substituted polyoxotungstate@amino-MIL-101(Al)—an efficient catalyst for the sustainable desulfurization of model and real diesels, *Eur. J. Inorg. Chem.* 2016 (32) (2016) 5114–5122.

- [41] S. Ribeiro, A.D.S. Barbosa, A.C. Gomes, M. Pillinger, I.S. Gonçalves, L. Cunha-Silva, S.S. Balula, Catalytic oxidative desulfurization systems based on Keggin phosphotungstate and metal-organic framework MIL-101, *Fuel Process. Technol.* 116 (2013) 350–357.
- [42] X.F. Hu, Y.K. Lu, F.N. Dai, C.G. Liu, Y.Q. Liu, Host-guest synthesis and encapsulation of phosphotungstic acid in MIL-101 via “bottle around ship”: an effective catalyst for oxidative desulfurization, *Microporous Mesoporous Mater.* 170 (2013) 36–44.
- [43] R. Fazaeli, H. Aliyan, M. Masoudinia, Z. Heidari, Building MOF bottles (MIL-101 family as heterogeneous single-site catalysts) around  $H_3PW_{12}O_{40}$  ships: an efficient catalyst for selective oxidation of sulfides to sulfoxides and sulfones, *J. Mater. Chem. Eng.* 2 (2) (2014) 46–55.
- [44] M. Sun, W.-C. Chen, L. Zhao, X.-L. Wang, Z.-M. Su, A PTA@MIL-101(Cr)-diatomite composite as catalyst for efficient oxidative desulfurization, *Inorg. Chem. Commun.* 87 (2018) 30–35.
- [45] S. Ribeiro, C.M. Granadeiro, P. Silva, F.A. Almeida Paz, F.F. De Biani, L. Cunha-Silva, S.S. Balula, An efficient oxidative desulfurization process using terbium-polyoxometalate@MIL-101(Cr), *Cat. Sci. Technol.* 3 (9) (2013) 2404–2414.
- [46] C.M. Granadeiro, L.S. Nogueira, D. Julião, F. Mirante, D. Ananias, S.S. Balula, L. Cunha-Silva, Influence of a porous MOF support on the catalytic performance of Eu-polyoxometalate based materials: desulfurization of a model diesel, *Cat. Sci. Technol.* 6 (5) (2016) 1515–1522.
- [47] E. Naseri, R. Khoshnavazi, Sandwich type polyoxometalates encapsulated into the mesoporous material: synthesis, characterization and catalytic application in the selective oxidation of sulfides, *RSC Adv.* 8 (49) (2018) 28249–28260.
- [48] X.-S. Wang, L. Li, J. Liang, Y.-B. Huang, R. Cao, Boosting oxidative desulfurization of model and real gasoline over phosphotungstic acid encapsulated in metal-organic frameworks: the window size matters, *ChemCatChem* 9 (6) (2016) 971–979.
- [49] X.S. Wang, Y.B. Huang, Z.J. Lin, R. Cao, Phosphotungstic acid encapsulated in the mesocages of amine-functionalized metal-organic frameworks for catalytic oxidative desulfurization, *Dalton Trans.* 43 (31) (2014) 11950–11958.
- [50] S. Abednatanzi, K. Leus, P.G. Derakhshandeh, F. Nahra, K. De Keukeleere, K. Van Hecke, I. Van Driessche, A. Abbasi, S.P. Nolan, P.V. Der Voort, POM@IL-MOFs –inclusion of polyoxometalates in ionic liquid modified MOFs to produce recyclable oxidation catalysts, *Cat. Sci. Technol.* 7 (7) (2017) 1478–1487.
- [51] X.-L. Ni, J. Liu, Y.-Y. Liu, K. Leus, H. Depauw, A.-J. Wang, P. Van Der Voort, J. Zhang, Y.-K. Hu, Synthesis, characterization and catalytic performance of Mo based metal-organic frameworks in the epoxidation of propylene by cumene hydroperoxide, *Chin. Chem. Lett.* 28 (5) (2017) 1057–1061.
- [52] N.V. Maksimchuk, M.N. Timofeeva, M.S. Melgunov, A.N. Shmakov, Y.A. Chesalov, D.N. Dybtsev, V.P. Fedin, O.A. Kholdeeva, Heterogeneous selective oxidation catalysts based on coordination polymer MIL-101 and transition metal-substituted polyoxometalates, *J. Catal.* 257 (2) (2008) 315–323.
- [53] Z. Saedi, S. Tangestaninejad, M. Moghadam, V. Mirkhani, I. Mohammadpoor-Baltork, The effect of encapsulated Zn-POM on the catalytic activity of MIL-101 in the oxidation of alkenes with hydrogen peroxide, *J. Coord. Chem.* 65 (3) (2012) 463–473.
- [54] N.V. Maksimchuk, K.A. Kovalenko, S.S. Arzumanov, Y.A. Chesalov, M.S. Melgunov, A.G. Stepanov, V.P. Fedin, O.A. Kholdeeva, Hybrid polyoxotungstate/MIL-101 materials: synthesis, characterization, and catalysis of  $H_2O_2$ -based alkene epoxidation, *Inorg. Chem.* 49 (6) (2010) 2920–2930.
- [55] S.S. Balula, C.M. Granadeiro, A.D.S. Barbosa, I.C.M.S. Santos, L. Cunha-Silva, Multifunctional catalyst based on sandwich-type polyoxotungstate and MIL-101 for liquid phase oxidations, *Catal. Today* 210 (2013) 142–148.

- [56] J. Tong, W. Wang, L. Su, Q. Li, F. Liu, W. Ma, Z. Lei, L. Bo, Highly selective oxidation of cyclohexene to 2-cyclohexene-1-one over polyoxometalate/metal-organic framework hybrids with greatly improved performances, *Cat. Sci. Technol.* 7 (1) (2017) 222–230.
- [57] J.-W. Ding, R. Wang, A new green system of HPW@MOFs catalyzed desulfurization using O<sub>2</sub> as oxidant, *Chin. Chem. Lett.* 27 (5) (2016) 655–658.
- [58] E. Rafiee, N. Nobakht, Keggin type heteropoly acid, encapsulated in metal-organic framework: a heterogeneous and recyclable nanocatalyst for selective oxidation of sulfides and deep desulfurization of model fuels, *J. Mol. Catal. A Chem.* 398 (2015) 17–25.
- [59] X.L. Yang, L.M. Qiao, W.L. Dai, One-pot synthesis of a hierarchical microporous-mesoporous phosphotungstic acid-HKUST-1 catalyst and its application in the selective oxidation of cyclopentene to glutaraldehyde, *Chin. J. Catal.* 36 (11) (2015) 1875–1885.
- [60] S. Wang, Y. Liu, Z. Zhang, X. Li, H. Tian, T. Yan, X. Zhang, S. Liu, X. Sun, L. Xu, F. Luo, S. Liu, One-step template-free fabrication of ultrathin mixed-valence polyoxovanadate-incorporated metal organic framework nanosheets for highly efficient selective oxidation catalysis in air, *ACS Appl. Mater. Interfaces* 11 (13) (2019) 12786–12796.
- [61] F. Ke, F. Guo, J. Yu, Y.Q. Yang, Y. He, L.Z. Chang, X.C. Wan, Highly site-selective epoxidation of polyene catalyzed by metal-organic frameworks assisted by polyoxometalate, *J. Inorg. Organomet. Polym. Mater.* 27 (2017) 843–849.
- [62] A.K. Babahydari, R. Fareghi-Alamdari, S.M. Hafshejani, H.A. Rudbari, M.R. Farsani, Heterogeneous oxidation of alcohols with hydrogen peroxide catalyzed by polyoxometalate metal-organic framework, *J. Iran. Chem. Soc.* 13 (2016) 1463–1470.
- [63] J. Zhu, M.-N. Shen, X.-J. Zhao, P.-C. Wang, M. Lu, Polyoxometalate-based metal-organic frameworks as catalysts for the selective oxidation of alcohols in micellar systems, *ChemPlusChem* 79 (6) (2014) 872–878.
- [64] J. Song, Z. Luo, D.K. Britt, H. Furukawa, O.M. Yaghi, K.I. Hardcastle, C.L. Hill, A multiunit catalyst with synergistic stability and reactivity: a polyoxometalate-metal organic framework for aerobic decontamination, *J. Am. Chem. Soc.* 133 (42) (2011) 16839–16846.
- [65] H. Yang, J. Li, L.Y. Wang, W. Dai, Y. Lv, S. Gao, Exceptional activity for direct synthesis of phenol from benzene over PMoV@MOF with O<sub>2</sub>, *Cat. Com.* 35 (2013) 101–104.
- [66] H.R. Tian, Y.W. Liu, Z. Zhang, S.M. Liu, T.Y. Dang, X.H. Li, X.W. Sun, Y. Lu, S.X. Liu, A multicenter synergistic polyoxometalate-based metal-organic framework for one-step selective oxidative cleavage of β-O-4 lignin model compounds, *Green Chem.* 22 (1) (2020) 248–255.
- [67] X. Song, D. Hu, X. Yang, H. Zhang, W. Zhang, J. Li, M. Jia, J. Yu, Polyoxomolybdic cobalt encapsulated within Zr-based metal-organic frameworks as efficient heterogeneous catalysts for olefins epoxidation, *ACS Sustain. Chem. Eng.* 7 (3) (2019) 3624–3631.
- [68] C.T. Buru, M.C. Wasson, O.K. Farha, H<sub>3</sub>PV<sub>2</sub>Mo<sub>10</sub>O<sub>40</sub> polyoxometalate encapsulated in NU-1000 metal-organic framework for aerobic oxidation of a mustard gas simulant, *ACS Appl. Nano. Mater.* 3 (1) (2019) 658–664.
- [69] C.T. Buru, A.E. Platero-Prats, D.G. Chica, M.G. Kanatzidis, K.W. Chapman, O.K. Farha, Thermally induced migration of a polyoxometalate within a metal-organic framework and its catalytic effects, *J. Mater. Chem. A* 6 (17) (2018) 7389–7394.
- [70] C.T. Buru, P. Li, B.L. Mehdi, A. Dohnalkova, A.E. Platero-Prats, N.D. Browning, K.W. Chapman, J.T. Hupp, O.K. Farha, Adsorption of a catalytically accessible polyoxometalate in a mesoporous channel-type metal-organic framework, *Chem. Mater.* 29 (12) (2017) 5174–5181.
- [71] X.L. Hao, Y.Y. Ma, H.Y. Zang, Y.H. Wang, Y.G. Li, E.B. Wang, A polyoxometalate-encapsulating cationic metal-organic framework as a heterogeneous catalyst for desulfurization, *Eur. J. Chem.* 21 (9) (2015) 3778–3784.



- [72] D.D. Li, X.Y. Ma, Q.Z. Wang, P.T. Ma, J.Y. Niu, J.P. Wang, Copper-containing polyoxometalate-based metal-organic frameworks as highly efficient heterogeneous catalysts toward selective oxidation of alkylbenzenes, *Inorg. Chem.* 58 (23) (2019) 15832–15840.
- [73] Y.Y. Ma, H.Y. Peng, J.N. Liu, Y.H. Wang, X.L. Hao, X.J. Feng, S.U. Khan, H.Q. Tan, Y.G. Li, Polyoxometalate-based metal-organic frameworks for selective oxidation of aryl alkenes to aldehydes, *Inorg. Chem.* 57 (7) (2018) 4109–4116.
- [74] S. Roy, V. Vemuri, S. Maiti, K.S. Manoj, U. Subbarao, S.C. Peter, Two Keggin-based isostructural POMOF hybrids: synthesis, crystal structure, and catalytic properties, *Inorg. Chem.* 57 (19) (2018) 12078–12092.
- [75] D.D. Li, Q.F. Xu, Y.G. Li, Y.T. Qiu, P.T. Ma, J.Y. Niu, J.P. Wang, A stable polyoxometalate-based metal-organic framework as highly efficient heterogeneous catalyst for oxidation of alcohols, *Inorg. Chem.* 58 (8) (2019) 4945–4953.
- [76] M. Ghahramaninezhad, F. Pakdel, M. Niknam Shahrak, Boosting oxidative desulfurization of model fuel by POM-grafting ZIF-8 as a novel and efficient catalyst, *Polyhedron* 170 (2019) 364–372.
- [77] R.S. Malkar, H. Daly, C. Hardacre, G.D. Yadav, Aldol condensation of 5-hydroxymethylfurfural to fuel precursor over novel aluminum exchanged-DTP@ZIF-8, *ACS Sustain. Chem. Eng.* 7 (19) (2019) 16215–16224.
- [78] L. Bromberg, Y. Diao, H. Wu, S.A. Speakman, T.A. Hatton, Chromium(III) terephthalate metal organic framework (MIL-101): HF-free synthesis, structure, polyoxometalate composites, and catalytic properties, *Chem. Mater.* 24 (9) (2012) 1664–1675.
- [79] Q. Deng, G. Nie, L. Pan, J.-J. Zou, X. Zhang, L. Wang, Highly selective self-condensation of cyclic ketones using MOF-encapsulating phosphotungstic acid for renewable high-density fuel, *Green Chem.* 17 (8) (2015) 4473–4481.
- [80] W. Xie, F. Wan, Immobilization of polyoxometalate-based sulfonated ionic liquids on UiO-66-2COOH metal-organic frameworks for biodiesel production via one-pot transesterification-esterification of acidic vegetable oils, *Chem. Eng. J.* 365 (2019) 40–50.
- [81] Y.W. Liu, S.M. Liu, D.F. He, N. Li, Y.J. Ji, Z.P. Zheng, F. Luo, S.X. Liu, Z. Shi, C.W. Hu, Crystal facets make a profound difference in polyoxometalate-containing metal-organic frameworks as catalysts for biodiesel production, *J. Am. Chem. Soc.* 137 (39) (2015) 12697–12703.
- [82] J. Zhu, P.-C. Wang, M. Lu, Study on the one-pot oxidative esterification of glycerol with MOF supported polyoxometalates as catalyst, *Cat. Sci. Technol.* 5 (6) (2015) 3383–3393.
- [83] F.J. Ma, S.X. Liu, C.Y. Sun, D.D. Liang, G.J. Ren, F. Wei, Y.G. Chen, Z.M. Su, A sodalite-type porous metal-organic framework with polyoxometalate templates: adsorption and decomposition of dimethyl methylphosphonate, *J. Am. Chem. Soc.* 133 (12) (2011) 4178–4181.
- [84] F.J. Ma, S.X. Liu, G.J. Ren, D.D. Liang, S. Sha, A hybrid compound based on porous metal-organic frameworks and polyoxometalates: NO adsorption and decomposition, *Inorg. Chem. Commun.* 22 (2012) 174–177.
- [85] D.D. Liang, S.X. Liu, F.J. Ma, F. Wei, Y.G. Chen, A crystalline catalyst based on a porous metal-organic framework and 12-tungstosilicic acid: particle size control by hydrothermal synthesis for the formation of dimethyl ether, *Adv. Synth. Catal.* 353 (5) (2011) 733–742.
- [86] S. Ahn, S.L. Nauert, C.T. Buru, M. Rimoldi, H. Choi, N.M. Schweitzer, J.T. Hupp, O.K. Farha, J.M. Notestein, Pushing the limits on metal-organic frameworks as a catalyst support: NU-1000 supported tungsten catalysts for o-xylene isomerization and disproportionation, *J. Am. Chem. Soc.* 140 (27) (2018) 8535–8543.
- [87] L.H. Wee, C. Wiktor, S. Turner, W. Vanderlinden, N. Janssens, S.R. Bajpe, K. Houthoofd, G. Van Tendeloo, S. De Feyter, C.E.A. Kirschhock, J.A. Martens, Copper benzene tricarboxylate

- metal-organic framework with wide permanent mesopores stabilized by Keggin polyoxometallate ions, *J. Am. Chem. Soc.* 134 (26) (2012) 10911–10919.
- [88] W.A. Shah, L. Noureen, M.A. Nadeem, P. Kogerler, Encapsulation of Keggin-type manganesepolyoxomolybdates in MIL-100 (Fe) for efficient reduction of p-nitrophenol, *J. Solid State Chem.* 268 (2018) 75–82.
- [89] D.D. Gao, I. Trentin, L. Schwiedrzik, L. Gonzalez, C. Streb, The reactivity and stability of polyoxometalate water oxidation electrocatalysts, *Molecules (Basel, Switzerland)* 25 (1) (2020) 157–176.
- [90] V.S. Kalimuthu, R. Attias, Y. Tsur, Electrochemical impedance spectra of RuO<sub>2</sub> during oxygen evolution reaction studied by the distribution function of relaxation times, *Electrochem. Commun.* 110 (2020) 106641.
- [91] S. Mukhopadhyay, J. Debgupta, C. Singh, A. Kar, S.K. Das, A Keggin polyoxometalate shows water oxidation activity at neutral pH: POM@ZIF-8, an efficient and robust electrocatalyst, *Angew. Chem. Int. Ed.* 57 (7) (2018) 1918–1923.
- [92] Q.L. Li, L. Zhang, Y.X. Xu, Q. Li, H. Xue, H. Pang, Smart yolk/Shell ZIF-67@POM hybrids as efficient electrocatalysts for the oxygen evolution reaction, *ACS Sustain. Chem. Eng.* 7 (5) (2019) 5027–5033.
- [93] S. Mukhopadhyay, O. Basu, A. Kar, S.K. Das, Efficient electrocatalytic water oxidation by Fe(salen)-MOF composite: effect of modified microenvironment, *Inorg. Chem.* 59 (1) (2020) 472–483.
- [94] B. Rausch, M.D. Symes, G. Chisholm, L. Cronin, Decoupled catalytic hydrogen evolution from a molecular metal oxide redox mediator in water splitting, *Science* 345 (6202) (2014) 1326–1330.
- [95] S.B. Li, L. Zhang, Y.Q. Lan, K.P. O'Halloran, H.Y. Ma, H.J. Pang, Polyoxometalate-encapsulated twenty-nuclear silver-tetrazole nanocage frameworks as highly active electrocatalysts for the hydrogen evolution reaction, *Chem. Commun.* 54 (2018) 1964–1967.
- [96] L. Zhang, S.B.B. Li, C.J. Gomez-Garcia, H.Y. Ma, C.J. Zhang, H.J. Pang, B.N. Li, Two novel polyoxometalate-encapsulated metal-organic nanotube frameworks as stable and highly efficient electrocatalysts for hydrogen evolution reaction, *ACS Appl. Mater. Interfaces* 10 (37) (2018) 31498–31504.
- [97] J.S. Qin, D.Y. Du, W. Guan, X.J. Bo, Y.F. Li, L.P. Guo, Z.M. Su, Y.Y. Wang, Y.Q. Lan, H.C. Zhou, Ultrastable polymolybdate-based metal organic frameworks as highly active electrocatalysts for hydrogen generation from water, *J. Am. Chem. Soc.* 137 (22) (2015) 7169–7177.
- [98] Z.M. Zhang, T. Zhang, C. Wang, Z. Lin, L.S. Long, W. Lin, Photosensitizing metal-organic framework enabling visible-light-driven proton reduction by a Wells-Dawson-type polyoxometalate, *J. Am. Chem. Soc.* 137 (9) (2015) 3197–3200.
- [99] J. Tian, Z.-Y. Xu, D.-W. Zhang, H. Wang, S.-H. Xie, D.-W. Xu, Y.-H. Ren, H. Wang, Y. Liu, Z.-T. Li, Supramolecular metal-organic frameworks that display high homogeneous and heterogeneous photocatalytic activity for H<sub>2</sub> production, *Nat. Commun.* 7 (2016) 11580–11589.
- [100] G. Paille, M. Gomez-Mingot, C. Roch-Marchal, B. Lassalle-Kaiser, P. Mialane, M. Fontecave, C. Mellot-Draznieks, A. Dolbecq, A fully noble metal-free photosystem based on cobalt-polyoxometalates immobilized in a porphyrinic metal-organic framework for water oxidation, *J. Am. Chem. Soc.* 140 (10) (2018) 3613–3618.
- [101] J.C. He, Q.X. Han, J. Li, Z.L. Shi, X.Y. Shi, J.Y. Niu, Ternary supramolecular system for photocatalytic oxidation with air by consecutive photo-induced electron transfer processes, *J. Catal.* 376 (2019) 161–167.
- [102] D. Wu, F. Xu, B. Sun, R. Fu, H. He, K. Matyjaszewski, Design and preparation of porous polymers, *Chem. Rev.* 112 (7) (2012) 3959–4015.

- [103] W. Qi, L. Wu, Polyoxometalate/polymer hybrid materials: fabrication and properties, *Polym. Int.* 58 (11) (2009) 1217–1225.
- [104] Y. Leng, P. Jiang, J. Wang, A novel Brønsted acidic heteropolyanion-based polymeric hybrid catalyst for esterification, *Cat. Com.* 25 (2012) 41–44.
- [105] Y. Leng, W. Zhang, J. Wang, P. Jiang, A novel heteropolyanion-based amino-containing cross-linked ionic copolymer catalyst for epoxidation of alkenes with  $\text{H}_2\text{O}_2$ , *Appl. Catal. A. Gen.* 445–446 (2012) 306–311.
- [106] Y. Leng, J. Wu, P. Jiang, J. Wang, Amphiphilic phosphotungstate-paired ionic copolymer as a highly efficient catalyst for triphase epoxidation of alkenes with  $\text{H}_2\text{O}_2$ , *Cat. Sci. Technol.* 4 (5) (2014) 1293.
- [107] Y. Leng, J. Liu, P. Jiang, J. Wang, Heteropolyanion-based polymeric hybrids: highly efficient and recyclable catalysts for oxidation of alcohols with  $\text{H}_2\text{O}_2$ , *RSC Adv.* 2 (31) (2012) 11653–11656.
- [108] Y. Leng, J. Wang, P. Jiang, Amino-containing cross-linked ionic copolymer- anchored heteropoly acid for solvent-free oxidation of benzyl alcohol with  $\text{H}_2\text{O}_2$ , *Cat. Com.* 27 (2012) 101–104.
- [109] Y. Leng, J. Liu, P. Jiang, J. Wang, Carboxylic acid-functionalized phosphovanadomolybdate-paired ionic polymer as a green heterogeneous catalyst for hydroxylation of benzene, *Cat. Com.* 40 (2013) 84–87.
- [110] S. Doherty, J.G. Knight, J.R. Ellison, D. Weekes, R.W. Harrington, C. Hardacre, H. Man- yar, An efficient recyclable peroxometalate-based polymer-immobilised ionic liquid phase (PIILP) catalyst for hydrogen peroxide-mediated oxidation, *Green Chem.* 14 (4) (2012) 925–929.
- [111] S.P. Maradur, C. Jo, D.-H. Choi, K. Kim, R. Ryoo, Mesoporous polymeric support retaining high catalytic activity of polyoxotungstate for liquid-phase olefin epoxidation using  $\text{H}_2\text{O}_2$ , *ChemCatChem* 3 (9) (2011) 1435–1438.
- [112] Y. Xiao, D. Chen, N. Ma, Z. Hou, M. Hu, C. Wang, W. Wang, Covalent immobilization of a polyoxometalate in a porous polymer matrix: a heterogeneous catalyst towards sustainability, *RSC Adv.* 3 (44) (2013) 21544–21551.
- [113] G.S. Armatas, G. Bilis, M. Louloudi, Highly ordered mesoporous zirconia-polyoxometalate nanocomposite materials for catalytic oxidation of alkenes, *J. Mater. Chem.* 21 (9) (2011) 2997–3005.
- [114] I. Tamiolakis, I.N. Lykakis, A.P. Katsoulidis, M. Stratakis, G.S. Armatas, Mesoporous  $\text{Cr}_2\text{O}_3$ - phosphomolybdic acid solid solution frameworks with high catalytic activity, *Chem. Mater.* 23 (18) (2011) 4204–4211.
- [115] E. Skliri, I.N. Lykakis, G.S. Armatas, Heteropolytungstic acids incorporated in an ordered mesoporous zirconia framework as efficient oxidation catalysts, *RSC Adv.* 4 (16) (2014) 8402–8409.
- [116] F. Su, L. Ma, Y. Guo, W. Li, Preparation of ethane-bridged organosilica group and Keggin type heteropoly acid co-functionalized  $\text{ZrO}_2$  hybrid catalyst for biodiesel synthesis from *Eruca Sativa* gars oil, *Cat. Sci. Technol.* 2 (11) (2012) 2367–2374.
- [117] F. Su, Q. Wu, D. Song, X. Zhang, M. Wang, Y. Guo, Pore morphology-controlled preparation of  $\text{ZrO}_2$ -based hybrid catalysts functionalized by both organosilica moieties and Keggin-type heteropoly acid for the synthesis of Levulinate esters, *J. Mater. Chem. A* 1 (42) (2013) 13209–13221.
- [118] F. Su, L. Ma, D. Song, X. Zhang, Y. Guo, Design of a highly ordered mesoporous  $\text{H}_3\text{P}-\text{W}_{12}\text{O}_{40}/\text{ZrO}_2-\text{Si}(\text{Ph})\text{Si}$  hybrid catalyst for methyl levulinate synthesis, *Green Chem.* 15 (4) (2013) 885–890.

- [119] F. Zhang, C. Yuan, J. Wang, Y. Kong, H. Zhu, C. Wang, Synthesis of Fructose over dealuminated USY supported heteropoly acid and its salt catalysts, *J. Mol. Catal. A Chem.* 247 (1–2) (2006) 130–137.
- [120] S. Mukai, L. Lin, T. Masuda, K. Hashimoto, Key factors for the encapsulation of Keggin-type heteropoly acids in the Supercages of Y-type zeolite, *Chem. Eng. Sci.* 56 (3) (2001) 799–804.
- [121] S.R. Mukai, M. Shimoda, L. Lin, H. Tamon, T. Masuda, Improvement of the preparation method of “ship-in-the-bottle” type 12-molybdophosphoric acid encaged Y-type zeolite catalysts, *Appl. Catal. A. Gen.* 256 (1–2) (2003) 107–113.
- [122] R. Tayebee, M. Jarrahi,  $H_6P_2W_{18}O_{62}$ /nanoclinoptilolite as an efficient nanohybrid catalyst in the cyclotrimerization of aryl methyl ketones under solvent-free conditions, *RSC Adv.* 5 (15) (2015) 21206–21214.
- [123] F. Hoffmann, M. Cornelius, J. Morell, M. Fröba, Silica-based mesoporous organic–inorganic hybrid materials, *Angew. Chem. Int. Ed.* 45 (20) (2006) 3216–3251.
- [124] U. Díaz, D. Brunel, A. Corma, Catalysis using multifunctional organosiliceous hybrid materials, *Chem. Soc. Rev.* 42 (9) (2013) 4083.
- [125] J. Kaur, K. Griffin, B. Harrison, I.V. Kozhevnikov, Friedel–Crafts acylation catalysed by heteropoly acids, *J. Catal.* 208 (2) (2002) 448–455.
- [126] E.F. Kozhevnikova, E. Rafiee, I.V. Kozhevnikov, Fries rearrangement of aryl esters catalysed by heteropoly acid: catalyst regeneration and reuse, *Appl. Catal. A. Gen.* 260 (1) (2004) 25–34.
- [127] G.D. Yadav, H.G. Manyar, Novelty of synthesis of acetoveratrone using heteropoly acid supported on hexagonal mesoporous silica, *Microporous Mesoporous Mater.* 63 (1–3) (2003) 85–96.
- [128] T. Blasco, A. Corma, A. Martínez, P. Martínez-Escolano, Supported heteropolyacid (HPW) catalysts for the continuous alkylation of isobutane with 2-Butene: the benefit of using MCM-41 with larger pore diameters, *J. Catal.* 177 (1998) 306–313.
- [129] Y. Chen, Y. Cao, G.-P. Zheng, B.-B. Dong, X.-C. Zheng, Comparative study on the structural and catalytic properties of mesoporous hexagonal silica anchored with  $H_3PW_{12}O_{40}$ : green synthesis of benzoic acid from benzaldehyde, *Adv. Powder Technol.* 25 (4) (2014) 1351–1356.
- [130] A. Popa, V. Sasca, D. Bajuk-Bogdanović, I. Holclajtner-Antunović, Acidic nickel salts of Keggin type heteropolyacids supported on SBA-15 mesoporous silica, *J. Porous. Mater.* 23 (1) (2016) 211–223.
- [131] A. Tarlani, M. Abedini, A. Nemati, M. Khabaz, M.M. Amini, Immobilization of Keggin and Preyssler tungsten heteropolyacids on various functionalized silica, *J. Colloid Interface Sci.* 303 (1) (2006) 32–38.
- [132] K. Inumaru, T. Ishihara, Y. Kamiya, T. Okuhara, S. Yamanaka, Water-tolerant, highly active solid acid catalysts composed of the Keggin-type polyoxometalate  $H_3PW_{12}O_{40}$  immobilized in hydrophobic nanospaces of organomodified mesoporous silica, *Angew. Chem. Int. Ed.* 46 (40) (2007) 7625–7628.
- [133] L. Chen, K. Zhu, L.-H. Bi, A. Suchopar, M. Reicke, G. Mathys, H. Jaensch, U. Kortz, R.M. Richards, Solvent-free aerobic oxidation of N-alkane by Iron(III)-substituted polyoxotungstates immobilized on SBA-15, *Inorg. Chem.* 46 (21) (2007) 8457–8459.
- [134] C.N. Kato, A. Tanabe, S. Negishi, K. Goto, K. Nomiya, An efficient  $PMo_{11}V^VO_{40}^{4-}$ /silica material having cationic ammonium moiety: synthesis, characterization, and catalytic performance for oxidation of alcohols with dioxygen, *Chem. Lett.* 34 (2) (2005) 238–239.
- [135] T.V. Kovalchuk, H. Sfihi, V.N. Zaitsev, J. Fraissard, Preparation and characterization of catalysts based on onium silica-immobilized Keggin acids, *Catal. Today* 169 (1) (2010) 138–149.

- [136] B.J.S. Johnson, A. Stein, Surface modification of mesoporous, macroporous, and amorphous silica with catalytically active polyoxometalate clusters, *Inorg. Chem.* 40 (4) (2001) 801–808.
- [137] R.C. Schroden, C.F. Blanford, B.J. Melde, B.J.S. Johnson, A. Stein, Direct synthesis of ordered macroporous silica materials functionalized with polyoxometalate clusters, *Chem. Mater.* 13 (3) (2001) 1074–1081.
- [138] Y. Guo, C. Hu, Heterogeneous photocatalysis by solid polyoxometalates, *J. Mol. Catal. A Chem.* 262 (1–2) (2007) 136–148.
- [139] Y. Yang, Y. Guo, C. Hu, Y. Wang, E. Wang, Preparation of surface modifications of mesoporous Titania with monosubstituted Keggin units and their catalytic performance for organochlorine pesticide and dyes under UV irradiation, *Appl. Catal. A. Gen.* 273 (1–2) (2004) 201–210.
- [140] R. Zhang, C.A. Yang, Novel polyoxometalate-functionalized mesoporous hybrid silica: synthesis and characterization, *J. Mater. Chem.* 18 (23) (2008) 2691–2703.
- [141] X. Luo, C. Yang, Photochromic ordered mesoporous hybrid materials based on covalently grafted polyoxometalates, *Phys. Chem. Chem. Phys.* 13 (17) (2011) 7892–7902.

## Chapter 6

# Applications of heteropoly acids in industry

### 6.1. Introduction

Green catalytic processes as well as catalytic processes for greener products play key roles in green chemistry [1,2]. However, since green chemistry takes the whole life cycle of a product into account, the priority of research and development could not be determined unless the greenness of the product or process for the whole system is assessed. Therefore, it is necessary to establish the concept of greenness or a *green index*, which is usable without much difficulty. It should be noted that this is not an easy task. In order to assess the greenness in a quantitative manner, or the extent to which the undesirable environmental impact is reduced, the following factors should be considered:

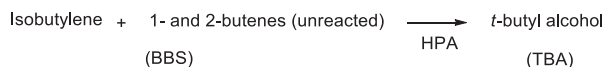
- (1) resource consumption;
- (2) energy consumption;
- (3) distasteful effects on humans;
- (4) undesirable effects on eco-systems; and.
- (5) safety (physical, chemical, and biological) in addition to efficiency.

Thus, for conducting the chemical reactions in large-scale production [1], the principles suggested for green chemistry should be practically considered. The most important one is selection of green and eco-friendly catalyst. In this regard, heteropoly acids are considered as promising candidates. Several successful examples have already shown that heteropoly acids are actually applied as green catalysts in different industries. In addition, since they have been used as active solid acid catalysts offering unique reaction fields such as pseudoliquid, i.e., catalytically active solid solvent, they are expected to find more sustainable applications in future. It is worthy of mention that in spite of their great properties and merits, heteropoly acids show some limitations in industrial applications due to their low surface area, usually less than  $10\text{m}^2/\text{g}$ , difficulty of handling, and high solubility in many solvents that lowers their recyclability. Therefore, different methods have been tried to immobilize such homogeneous catalysts on various supports to transform them into heterogeneous ones and resolve the abovementioned serious drawbacks [3].

### 6.1.1 Successful industrial applications of heteropoly acid catalysts and their greenness

There are already many large-scale industrial processes in which heteropoly acid catalysts are utilized [4–6]. Two examples are presented highlighting their characteristic features and greenness aspects. Both instances show that heteropoly acid catalysts can affect highly efficient and green synthetic processes not only as solid catalysts but also as soluble biphasic catalysts.

(a) *Hydration of isobutylene*. This process furnishes the starting material (*t*-butyl alcohol or a mixture of isobutylene and water) for the oxidation of isobutylene to methacrylic acid in two steps. The process proceeds by separating selectively isobutylene from BB spent (BBS) of naphtha cracking, which contains isobutylene, ~50%, and 1- and 2-butenes, ~50%. The 1-butene and 2-butene left after the reaction (BBSS) are used as raw materials, e.g., for linear low density polyethylene (LLDPE) (Scheme 6.1).



SCHEME 6.1 The hydration of isobutylene.

The excellent activity and selectivity of heteropoly acid catalysts are realized when their concentrations are more than 50 w/w%. The high activity observed is attributed to the strong acidity, increased solubility of butenes, as well as the formation of a complex with the carbocation intermediate. The high selectivity is because of the preferred coordination of the heteropoly anion with isobutylene [7]. The established process is comparable with competing processes in which H<sub>2</sub>SO<sub>4</sub> and ion-exchange resins are used as catalysts.

Depicted in Fig. 6.1 is the flowchart of the process industrialized by Asahi Chemical Company. An under-pressure mixture of butenes is counter-currently put in contact with 50 w/w% or more concentrated aqueous solution of heteropolymolybdate below 83°C to give *tert*-butyl alcohol with a yield of 90%–100%. The reactions of 1-butene and 2-butene are quite low. In the biphasic liquid, *tert*-butyl alcohol is chiefly present in the aqueous catalyst solution, which is readily separable by a decanter. After removing the small amount of butenes, it is distilled under reduced pressure. Then, *tert*-butyl alcohol is collected from the top of the distillation column, while the bottom is directly recycled back to the reactor. Although the product, *tert*-butyl alcohol, contains about 15 w/w% water, it can be directly fed to the subsequent oxidation process which requires steam as well.

The described process is a simple, one-step process. Water, butenes, and the catalyst are the only used components. The catalyst, which is not corrosive, is directly recycled after a simple separation. It is remarkable that the heteropoly



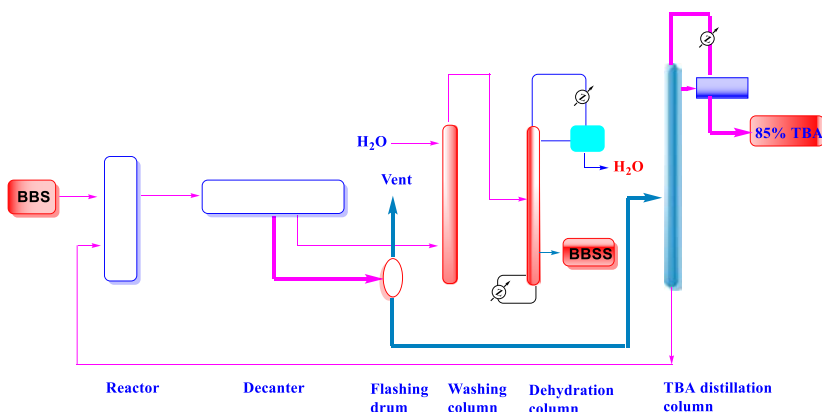


**FIG. 6.1** Flowchart of the process for selective hydration of a mixture of isobutylene, 1- and 2-butene (Asahi Chemical Company).

acids catalyst has a life cycle of more than 10 years. The plant investment was about one half and the utility consumption was around 60% of that of the sulfuric acid process. In the sulfuric acid process, extraction and decomposition of the sulfuric ester is required. In addition, sulfuric acid is extremely corrosive. On the other hand, the ion-exchange resin process requires a mixture of water and acetic acid as the solvent to enhance the contact of the reactants with catalyst. The corrosion problem caused by acetic acid may therefore be inevitable, and the hydrolysis of butyl acetate is an unavoidable coproduct.

Regarding the by-products, the heteropoly acid process proceeds quite selectively; the oligomer of isobutylene is formed less than 0.1% and the conversion of n-butene takes place less than 0.05%. In comparison, the values for the sulfuric acid process are 4%–8% and 0.4%–0.8%, respectively. Thus, the latter needs laborious treatment of wastes. Therefore, because of the high selectivity, simple separation, and involvement of only reactants and catalyst, the heteropoly acid process is a neat, noncorrosive, closed (no waste), energy- and resource-saving, compact system, which may be regarded as a highly green process.

(b) *Polymerization of tetrahydrofuran.* This reaction serves as a ring-opening polymerization process to convert tetrahydrofuran to polyoxytetramethyleneglycol, which has applications in the manufacture of elastics fiber and elastomers. The reaction proceeds with efficiency and selectivity (narrower molecular weight distribution) also in a biphasic liquid system (tetrahydrofuran and catalyst phases). Over a definite range of the molar ratio of water, tetrahydrofuran, and heteropoly acid, the reaction proceeds in a biphasic system, giving the desired catalytic activity. The product is recovered from the tetrahydrofuran phase, and the catalyst phase is recycled repeatedly. It was supposed that the proper solubility of the product in the tetrahydrofuran phase controlled the molecular weight providing a narrower distribution of

the molecular weight [8]. The flowchart of the process also industrialized by Asahi Chemical Company is essentially the same as that for the *tert*-butyl alcohol process illustrated in Fig. 6.1, but even simpler. The separation step is very simple. The catalyst, unreacted tetrahydrofuran, containing water, and a small amount of by-product (tetrahydrofuran oligomers) may be recycled to the reactor without any purification, as they are indeed the ingredients of the reaction system. The heteropoly acid process is therefore a simple closed system without producing waste. These features are in contrast with preceding processes utilizing super acids like fluorosulfuric acid as a catalyst or a combination of acetic acid and perchloric acid. In the latter, case the catalysts are not totally reused, and the waste treatments as well as further treatment of the product are inevitable. The plant investment and cost of utility consumption for the heteropoly acid process were evaluated to be less than one half of the preceding processes.

This is another good instance of green processes utilizing heteropoly acids as a soluble acid catalyst.

Due to the importance of heteropoly acids as solid acids in organic chemistry and industrial, in this chapter we try to highlight the applications of heteropoly acids in chemical (e.g., desulfurization), pharmaceutical, food industries, biomass, and removal of pollutant.

## 6.2. Applications of heteropoly acids in the chemical industry

In recent decades, desulfurization of gasoline has received increasing attention, chiefly for environmental reasons. The growing strict regulations restricting sulfur contents in the gasoline produced by fluid catalytic cracking (FCC) drastically demand developing novel refining techniques [9]. Responsible for 85%–95% of the total sulfur emission, mostly in the form of SO<sub>x</sub>, FCC gasoline has the largest contribution to the sulfur pollution. To resolve this, one feasible approach is hydrodesulfurization (HDS) [10]. On the other hand, hydrogenation is an energy-consuming process decreasing the octane number and the quality of gasoline [11,12].

Lately, new non-HDS approaches for production of clean, low-sulfur fuels have been studied to eliminate organic sulfur from petroleum fractions. One of these approaches is olefinic alkylation of thiophenic sulfur (OATS), first developed by British Petroleum in 1999. It is an intriguing way to resolve the problem without reducing the octane number and consuming a plenty of energy [13]. In this approach, acidic catalysis is employed for the alkylation of thiophene and its derivatives in the presence of olefines in gasoline in order to modify the b.p. of thiophene and its derivatives. In this way, heavier thiophenic derivatives may be eliminated from gasoline by distillation to realize the goal of desulfurization [14,15].

Thiophene and its derivatives are alkylated with olefin through the formation of a carbocation, for which an acid catalyst is necessary [16]. Among such

catalysts, heteropoly acids are increasingly favored by researchers and receiving more attention as green solid acid catalysts owing to their very strong Brønsted acidity, unique pseudoliquid phase and multifunctionality [17].

Arias et al. [18] reported that silica-supported heteropoly acids were the best catalysts among the acidic catalysts of zeolites (H $\beta$ , USY, and MCM-22), silica-supported phosphoric acid, and silica-supported 12-phosphotungstic (HPW) and 12-silicotungstic (HSiW) acids for the alkylation of 3-methylthiophene with 2-methyl-2-butene.

To study the FCC gasoline desulfurization, the authors chose the supported Keggin-type H<sub>3</sub>PW<sub>12</sub>O<sub>40</sub> (HPW). Providing a larger surface area and improving the accessibility of active sites, the supported HPW presented a means to eliminate the feature of water-soluble low surface area of bulk HPW. Different types of supports have been reported for this purpose, among which notably are SiO<sub>2</sub> [19], ZrO<sub>2</sub> [20], and aluminophosphate molecular sieves [21]. Due to aspects such as small size and superparamagnetism, catalysts supported by magnetic nanoparticles could be employed in a magnetic fluidized bed reactor (MSFBR) and suspension catalytic distillation (SCD), in which fine catalyst particles were mixed in the liquid so that sufficient contact with the reactants is provided. Additionally, catalysts in these reactors are easily separated in an external magnetic field [22–24].

In 2014, Zili and coworkers [25] demonstrated that the alkylation of sulfur compounds with olefins was an attractive way to achieve high levels of sulfur removal by raising the boiling point of sulfur-containing chemicals to facilitate their separation from lighter fractions by distillation. A number of superparamagnetic supported catalysts, used for alkylation of thiophene with 1-octene, were synthesized by loading HPW onto commercially available nanoparticles,  $\gamma$ -Fe<sub>2</sub>O<sub>3</sub> using the wet impregnation method.  $\gamma$ -Fe<sub>2</sub>O<sub>3</sub> nanoparticles with high magnetization were chosen as a magnetic support. The catalytic activity of HPW supported on  $\gamma$ -Fe<sub>2</sub>O<sub>3</sub> (HPW/ $\gamma$ -Fe<sub>2</sub>O<sub>3</sub>) fully optimized in respect with the alkylation of thiophene with 1-octene as model compounds of an FCC feed was reported. Physicochemical characterizations demonstrated that  $\gamma$ -Fe<sub>2</sub>O<sub>3</sub> could be accommodated to immobilize and disperse HPW. In addition, the species with 40% loading of the HPW catalyst was found to be the proper catalyst for olefinic alkylation of thiophenic sulfur (OATS) being separable in an external magnetic field with high magnetization of 26.1 A m<sup>2</sup>/kg and a mesoporous structure with a specific surface area of 35.9 m<sup>2</sup>/g. The catalytic activity was studied in the alkylation of thiophene with 1-octene to reveal that the conversion of thiophene was up to 46% at 160°C within 3 h. The 40% HPW/ $\gamma$ -Fe<sub>2</sub>O<sub>3</sub> catalyst was reusable for six runs without any appreciable loss of activity, being able to keep its property of superparamagnetism.

The production of energy has been growingly entangled in environmental issues. Fossil fuels account for more than 82% of the world's energy supply [26,27]. In addition, petroleum, with a plethora of hydrocarbons of different small molecular weights and large organic compounds, provides half of the fossil

oil [28]. Unfortunately, petroleum-based fuels contain various molecular forms of sulfur with huge negative effects on industry and environmental sustainability. Furthermore, during combustion, the formed  $\text{SO}_x$  had a major role in air pollution, causing acid rain and destroying after-treatment devices [29,30]. These hazards have increased stringent restrictions for fuels to contain the least possible sulfur level. Therefore, the desulfurization equipment used in S-containing compounds, mainly for dibenzothiophene (DBT) and its derivatives have to be renovated [31,32]. However, they are hard to remove by the conventional process, hydrodesulfurization (HDS), due to the severe temperature and pressure conditions, high levels of hydrogen consumption, and longer times [33]. Therefore, finding supplementary and/or alternative cost-effective, energy-efficient technologies for the purpose of desulfurization are in much demand [34].

Oxidative desulfurization (ODS) may be a good, promising choice under mild operation conditions ( $< 100^\circ\text{C}$ ) with no hydrogen requirement under low cost [35]. In the ODS process, the  $\text{O}_2$  gas used as an oxidizing agent is the most satisfactory regarding environmental and economic concerns [36,37]. Employing graphene oxide and  $\text{HNO}_3$  modified carbon black as adsorbents, Zhang [38] reported a highly effective oxidative-adsorption desulfurization process with  $\text{O}_2$ . This method achieved a prominent desulfurization effect on sulfur compounds. Jiang [39] used a sort of reverse micellar catalyst in the oxidation of DBT to sulfone using  $\text{O}_2$ . The direct oxidation rate of sulfur level from 500 ppm to 1.0 ppm was received, chiefly at ambient temperature and pressure. During the ODS process, choosing not only the oxidizing agent, but also the catalyst, was important. While extensively applied in many fields, heteropoly acids have limited industrial uses for their low surface area, usually less than  $10\text{ m}^2/\text{g}$ , and are difficult to handle [40]. Therefore, different methods have been tested to immobilize homogeneous catalysts on various supports to give heterogeneous catalysts [41].

Rafiee [42] reported  $\gamma\text{-Fe}_2\text{O}_3$  nanoparticles encapsulated in silica incorporated with  $\text{H}_{3+n}\text{PMo}_{12-n}\text{VnO}_{40}$  for the deep extractive desulfurization to yield a high DBT conversion rate from a model fuel. Qianghua Qiu and coworkers [43] precipitated phosphomolybdic acid (HPMo) on mesoporous silica to study them in the oxidative desulfurization process. Owing to their well physicochemical properties, chiefly for their low volatility and tenability, ionic liquids are regarded as promising alternative solvents for desulfurization. In addition, such green solvents make the most important contribution to the extraction of the oxidized products [44,45]. Replacing cations in polyoxometalates by ionic liquids as catalysts is extensively used in the ODS process [46,47]. Ali Abdalla and coworkers [48] prepared highly ordered mesoporous materials such as  $(\text{Bu}_4\text{N})_4\text{H}_3(\text{PW}_{11}\text{O}_{39})/\text{MCM-41}$  with different loadings of  $(\text{Bu}_4\text{N})_4\text{H}_3(\text{PW}_{11}\text{O}_{39})$  by impregnation methods. Under the application of ODS, 97.2% of the sulfur was removed. Benefiting the large lipophilic hydrocarbon moiety of the quaternary ammonium salt, the catalysts could be distributed in oil, favoring faster reaction rates and less mass transfer resistance.

Zhao et al. [49] examined catalysts with polyoxometalates modified by one N atom, two N atoms, and cyclic N type of quaternary ammonium salt ionic liquid (S-POM, D-POM, and C-POM, respectively) to accomplish the advantages of heteropoly acids and ionic liquids. The authors focused on the catalytic performance on the polyoxometalates modified by ionic liquids. In addition, different types of ionic liquids were compared to obtain the best catalytic performance on the industrial scale. The relative heterogeneous catalysts system for oxidative desulfurization was obtained from simple one-pot hydrothermal reaction and modified heteropoly acids in the pores of MCM-41 after the MOF-199 template self-assembly (S/D/C-POM@MOF@MCM-41). Results revealed that the S/D/C-POM active species could be successfully immobilized into the mesoporous materials without any change in their Keggin structures. The C-POM demonstrated excellent performance for oxide sulfuration and under optimal conditions, the DBT removal rate could reach 100% in 90 min and the catalyst was reusable for more than 10 runs with almost no significant reduction in its activity. Testing the method on the real diesel oxidative desulfurization revealed that almost all the sulfur compounds could be completely removed.

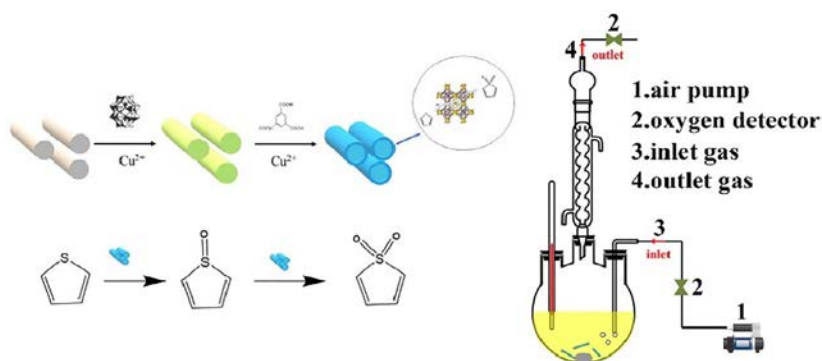
In order to solve the problem of heteropoly acids with low solubility in organic solvents, catalysts with supported heteropoly acids are widely prepared in which the support could increase their catalytic activity and recovery rate [50]. Common supports such as carbon materials [51,52], MOFs [53,54], and metal oxides [55] share features like high surface area and high thermal stability. Much effort has been devoted to the modification and functionalization of the abovementioned supports [56] or combinations of them [57] to better immobilize the heteropoly acids and achieve the highest catalytic property. MOF-199 is a porous support of high surface area as well as high thermal and chemical stability. Owing to their porosity, MOFs can be employed to promote the applications in the field of catalyst under ODS [58]. In addition, it was proved that the catalytic activity could perform better when heteropoly acid was encapsulated in MOF-199 [59]. Under the conditions of 1.0 g/L catalyst, 150 min, 60°C, and 500 rpm in the lab environment, sulfur conversion efficiency reached 100%. However, powder catalysts were found to be inappropriate for the real industrial settings. In those settings, it was highly expensive to filter and recover the powder catalysts. When the powder was compressed into tablets for economic considerations in the industry, the advantage of high surface area of the catalyst was lowered and its catalytic ability was largely restricted. To produce catalysts fitting into the needs in the real industry, the author tried three different methods—hydrothermal, impregnation, and impregnation-hydrothermal—to design a series of catalysts through immobilizing the heteropoly acid and MOF-199 on cellulose acetate.

The model oil was prepared by transferring 0.663 mL of thiophene into a 250-mL volumetric flask and diluting with n-octane to volume and mixing. The sulfur content in the model oil was 1000 ppm. The oxidative reactions were conducted in a 100-mL three-neck flask connected to a pump to feed oxygen,

a magnetic stirrer, and a reflux condenser. The flask contained 50 mL of the model oil (containing 0.133 mL thiophene and 49.867 mL n-octane), as shown in Scheme 6.2. Before the experiments, the catalysts were dried under vacuum pressure at 50°C overnight. From the test sample, 0.2 mL was collected from n-octane solution every 30 min and analyzed by gas chromatography to calculate the sulfur removal efficiency calculated by the following equation.

$$\eta = (C_0 - C) / C_0$$

where  $C_0$  and  $C$  are the initial and final concentration of S-compounds in the oil phase at initial and final reaction time ( $t$ ), respectively.



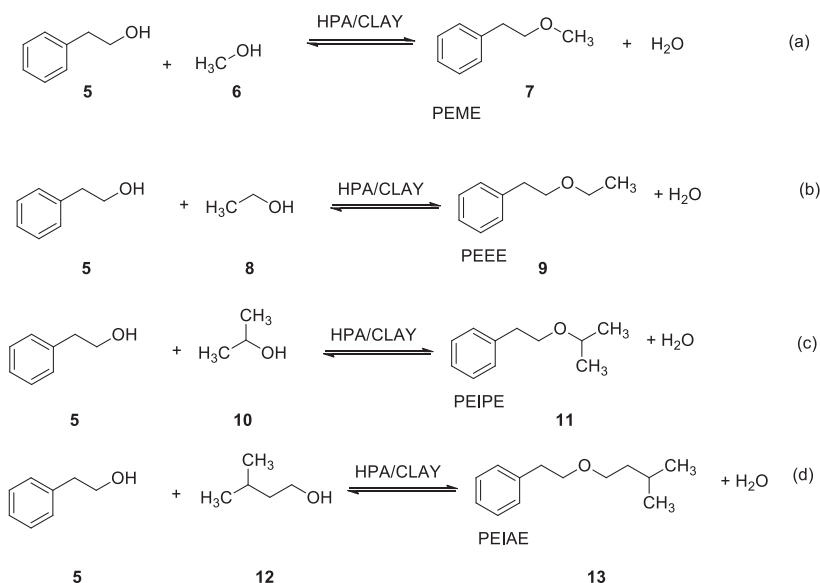
**SCHEME 6.2** Preparation of catalysts and setup of oxidative desulfurization.

The best heteropoly acid loading and optimal conditions for desulfurization were also investigated, while the removal efficiency reached 99.23% with  $O_2$  as an oxidizing agent at 40°C after 3 h. The authors believed that HPA@MOF@CA, as a novel catalyst, had a high catalytic activity for thiophene and could be considered as a potential in industry. Consequently, in comparison with the previous powder catalysts, this type of catalyst could be better suited to real industrial needs [60].

An interesting group of oxygenated compounds in the perfume and flavor industry consists of ethers, acetals, ketals, and hemiacetals. Substituted phenyl and phenethyl ethers have eminent characteristics and they could be typically prepared by the Williamson synthesis on a laboratory scale, which works best for primary halides while it is least successful for tertiary halides. Water, dimethyl formamide, acetone, or even alcohols may be employed as solvents. Alkyl phenethyl ethers like phenethyl methyl ether (PEME), phenethyl isopropyl ether (PEIPE), phenethyl ethyl ether (PEEE), phenethyl isoamyl ether (PEIAE), and ethyl-ortho-methoxy benzyl ether (EOMBE) are important perfumery ingredients, whereas methyl-*tert*-butyl-ether (MTBE), ethyl-*tert*-butylether (ETBE), and *tert*-amyl-methyl ether (TAME) are

important oxygenates in reformulated gasoline meeting strict environmental antipollution measures.

The main raw material for preparation of ether in this study was phenethyl alcohol, also known as rose oil. It was synthesized via the Friedel-Crafts reaction of benzene with ethylene oxide, using stoichiometrically excessive amounts of aluminum chloride. This route was not a clean one and a better and cleaner process was via epoxidation of styrene and direct hydrogenation of styrene oxide to phenethyl alcohol. The epoxidation route was generic and substances like methyl styrene, *p*-isobutyl styrene, etc. could be used. The reaction equations for acid catalyzed etherification reactions are given in Scheme 6.3.



**SCHEME 6.3** Reaction scheme for acid catalyzed etherification reactions.

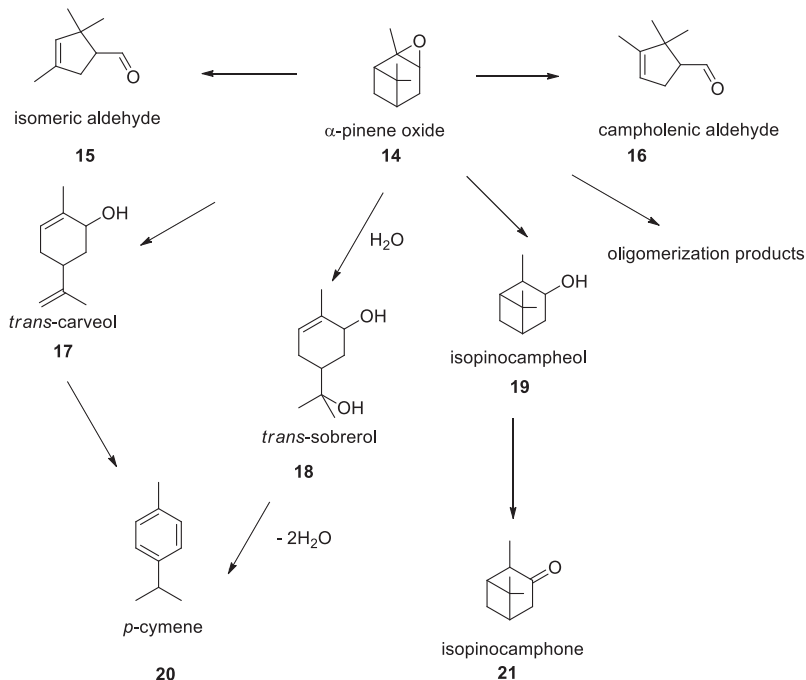
Bokade and coworkers [61] reported the *O*-alkylation reaction of phenethyl alcohol with alkanols like methanol, ethanol, isopropanol, and isoamyl alcohol, in the presence of tungstophosphoric acid, supported on K10 (montmorillonite) to achieve selective formation of PEME, PEEE, PEIPE, and PEIAE, respectively. The initial reaction rate of phenethyl alcohol with different alkanols was found to be independent of the concentration of the alkanol for an initial phenethyl alcohol concentration of  $1.465 \times 10^{-3} \text{ gmol/cm}^3$ . Despite the fact that different initial concentrations of alkanols were chosen, the reaction time was also independent of the concentration of alkanols.

Abundant, natural monoterpenes and their epoxides are important precursors in the flavor and fragrance industry [62,63].  $\alpha$ -Pinene is extensively used in the production of synthetic substitutes for natural aromas. Rearrangements



of  $\alpha$ -pinene oxide can lead to campholenic aldehyde **16** and *trans*-carveol **17**, which are the constituents of the East Indian sandalwood and Valencia orange essence oils, respectively. Ampholenic aldehyde and *trans*-carveol are both expensive ingredients in the flavor industry used as intermediates in the manufacture of sandalwood-like fragrances [64]. The acid-catalyzed isomerization of  $\alpha$ -pinene oxide, which is a very reactive substrate, can lead to various products. More than 200 compounds have been found at temperatures above 100°C [65].

Gusevskaya et al. reported that homogeneous and silica-supported heteropoly acid catalysts were efficient for the hydration/acetoxylation of monoterpenes [66], cyclization of citronellal [67], Friedel-Crafts acylation [68], and Fries rearrangement of aryl esters [69]. Solid heteropoly acids were the active catalysts for isomerization reactions as well [70]. In their work, they described the application of silica-supported  $H_3PW_{12}O_{40}$ , the strongest heteropoly acid in the Keggin series [71], as a solid Brønsted acid catalyst for the isomerization of  $\alpha$ -pinene oxide in the liquid phase with an emphasis on the optimization of catalyst performance to accomplish high selectivity toward the desired products, i.e., campholenic aldehyde and *trans*-carveol (Scheme 6.4). The authors directed their efforts to achieve high selectivity to a more valuable product, i.e., campholenic aldehyde **16**. The formation of *trans*-scarveol **17** and other *para*-menthenic compounds was also expected in the presence of HPW as a Brønsted

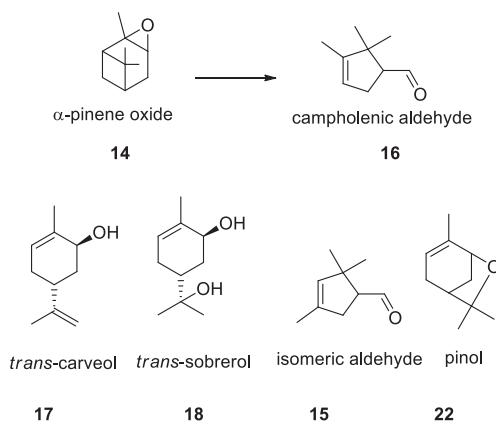


**SCHEME 6.4** The reactions of  $\alpha$ -pinene oxide.

acid catalyst. The acidity of HPW supported on silica was measured by calorimetric techniques using ammonia and pyridine adsorption [72]. The results revealed that HPW/SiO<sub>2</sub> was also a strong Brønsted acid. The silica-supported HPW was found to be a quite effective and environmentally benign solid acid catalyst for the isomerization of  $\alpha$ -pinene oxide **14** in liquid phase. The reaction was performed in cyclohexane solutions at 15–40°C to afford campholenic aldehyde **16** and *trans*-carveol **17** as the main products with total yields of up to 98% and 70% selectivity toward the more valuable product **16** [73].

Terpenic compounds are natural products derived from essential oils of a variety of plants and flowers at relatively low costs [74,75]. For instance,  $\alpha$ -pinene is the major component of the turpentine oil, which is obtained from coniferous trees. It is also available as a by-product in the paper industry.  $\alpha$ -Pinene provides  $\alpha$ -pinene oxide upon epoxidation, which in acidic media it can be transformed into valuable products with many industrial applications [64,76]. The isomerization of  $\alpha$ -pinene oxide is among of the most prominent reactions in the fragrance industry. In this regard, the development of processes with high selectivity toward specific products has always been a challenge owing to high reactivity of  $\alpha$ -pinene oxide in the presence of acids. Gusevskaya et al. reported the isomerization of  $\alpha$ -pinene oxide in the presence of Cs<sub>2.5</sub>H<sub>0.5</sub>PW<sub>12</sub>O<sub>40</sub> (CsPW) as a solid acid catalyst. The reactions were conducted in various solvents affording *trans*-carveol, *trans*-sobreol, and pinol each with a yield of 60%–80%, which exceeded yields reported previously. The CsPW catalyst was recoverable and reusable without any loss in its activity and selectivity.

Acid-catalyzed transformation of  $\alpha$ -pinene oxide **14** may result in many products, e.g., campholenic aldehyde **16**, *trans*-carveol **17**, *trans*-sobreol **18**, and pinol **22** (Scheme 6.5), as well as isopinocamphehol, *p*-cymene, and isopinocampheone. Unlike the most of the studies, in which campholenic aldehyde was the major target and other products were usually detected in low yields,

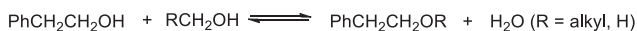


**SCHEME 6.5** Products of the acid-catalyzed transformations of  $\alpha$ -pinene oxide.

this work focused on the development of heterogeneous catalytic systems for the synthesis of *para*-menthene compounds **17** and **18** from  $\alpha$ -pinene oxide. In their previous studies [77,78], the authors proposed that the chemoselectivity of the  $\alpha$ -pinene oxide rearrangements in acidic solutions could be tuned by solvent and that polar solvents such as acetone would favor the formation of *para*-menthene products. Acetone is ranked as an environmentally friendly solvent [79], as it is biodegradable. Additionally, the low boiling point of acetone allows easy solvent recovery during the separation of the reaction products [80].

Yadav et al. [81] found that tungstophosphoric acid supported on K10—a montmorillonite clay—is a very efficient and novel catalyst compared to several other catalysts in the etherification of phenethyl alcohol with a variety of alkanols. The reactions were 100% selective toward the formation of the ethers with significant application in the perfume industry. The experimental data revealed that the chemisorption of.

onto the catalytic site would control the overall rate of the reaction for every etherification reaction with methanol, ethanol, isopropanol, and isopentanol (Scheme 6.6). A mechanism of Eiley-Rideal type was in operation. The basic reaction was as follows.

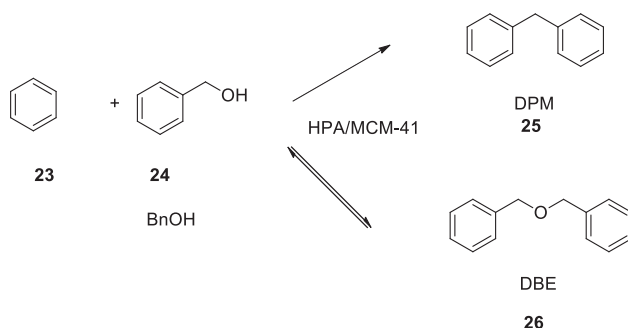


**SCHEME 6.6** The etherification of phenethyl alcohol.

Five catalysts, i.e., HPA, HPA/C, HPA/K10 clay, K10 clay, and Indion 830, were examined. The HPA loading on the support was 20% w/w. The typical catalyst loading in the reaction mixture was 10% w/w of the entire mass of the reaction mixture (0.08725 g/cm<sup>3</sup> of the liquid phase). The reactions were carried out at 70°C. Each run was typically conducted for 5 h.

The Friedel-Crafts alkylation and acylation reactions are conducted using alkyl/acyl halides as alkylating/acylating agents and Lewis acid catalysts (e.g., AlCl<sub>3</sub>) or Brønsted acids (e.g., sulfuric acid) as a catalyst. Among Brønsted acids, heteropoly acids have been widely investigated for many organic transformations and industrial applications owing to their strong acidity [82–87]. Due to low surface area and difficulties with recycling heteropoly acids, Sugi and coworkers [88] examined the catalytic applications of mesoporous silica-supported heteropoly acids, i.e., HPA/MCM-41, HPA/FSM-16, and HPA/SBA-15, for the Friedel-Crafts benzylation of aromatic compounds with benzyl alcohols (Scheme 6.7). Heteropoly acids such as HPW, H<sub>3</sub>PMo<sub>12</sub>O<sub>40</sub> (HPMo) and H<sub>4</sub>SiW<sub>12</sub>O<sub>40</sub> (HSiW) were supported on mesoporous silica, e.g., MCM-41, FSM-16, and SBA-15 by an impregnation method to improve the catalytic activity of the mentioned solid acids through dispersing them on supports with a high surface area. The supported solid catalysts were employed in the benzylation of benzene and substituted aromatic compounds with benzyl alcohol. The immobilization improved the catalytic activities and HPW supported on

MCM-41 demonstrated the best activity for benzylation among the heteropoly acids, although formation of dibenzyl ether through the dehydration of benzyl alcohol occurred as well. The mesoporous architecture of the silica improved the activity of benzylation due to the high dispersion of HPW on supports with high surface areas. However, no steric restrictions by the pores of mesoporous silica were observed. The catalysts used in this study preserved their catalytic activity for five successive runs. The rate of benzylation of substituted benzenes and benzylating agents was affected by the electronic nature of the substituent. The formation of the polybenzylated products was under the influence of the reactivity of diphenylmethane products.



**SCHEME 6.7** The rate of benzylation of substituted benzenes.

Phenol, as one of the most important basic chemicals, is commercially produced by the cumene process in the chemical industry. There are three main pathways for the one-step hydroxylation of benzene to phenol, which is increasingly attracting attention. Benzene can be selectively oxidized to phenol in gas phase over zeolite catalysts such as Fe-ZSM-5 using  $N_2O$  as an oxidizing agent [89,90]. However,  $N_2O$  is not readily available. In addition, used zeolite-based catalyst is easily deactivated due to coke formation [90]. The gas-phase oxidation of benzene can also produce phenol using hydrogen peroxide formed in situ from the reaction of oxygen with hydrogen gas in a Pd-based composite membrane reactor. However, its low selectivity for phenol and the difficulties with scaling up the membrane reactor prevents the process from being industrialized [91,92].

Given the abovementioned problems, various heterogeneous catalysts have been used in the hydroxylation of benzene to phenol by hydrogen peroxide [93,94]. Thus, the used catalysts have not been able to have a reasonable activity as well as high selectivity toward phenol since the results are the rather low yield of phenol. Pleasingly, vanadium containing heteropoly acids have been proven to be effective catalysts for the hydroxylation of benzene to phenol [95–97].

Zhang and coworkers [98] prepared and characterized a variety of catalysts, including the heteropoly acid  $H_4PMo_{11}VO_{40}$ , its cesium salts, and modified

inorganic/organic dual (hybrid). The prepared catalysts were used in the hydroxylation of benzene to phenol by hydrogen peroxide as an oxidizing agent. The inorganic/organic modified dual  $\text{Cs}_{2.5}(\text{MIMPS})_{1.5}\text{PMo}_{11}\text{VO}_{40}$  was provided by partially exchanging  $\text{Cs}^+$  with protons in  $\text{H}_4\text{PMo}_{11}\text{VO}_{40}$ , followed by the immobilization of 3-(1-methylimidazolium-3-yl)propane-1-sulfonate (MIMPS), which resulted in a liquid-solid biphasic catalysis system in the hydroxylation. It actually exhibited the best catalytic performance in terms of reusability and activity in the conversion of benzene to phenol. The high reusability of  $\text{Cs}_{2.5}(\text{MIMPS})_{1.5}\text{PMo}_{11}\text{VO}_{40}$  in the heterogeneous hydroxylation might be due to its high resistance in leaching of the bulk heteropoly acid into the reaction medium. The minor enhancement in the catalytic activity for the catalyst was due to the acid sites available from MIMPS, which was beneficial to the hydroxylation. The organic segment acted as a dynamic trap to enhance the probability of an interaction between the substrate and the catalytic center improving their catalytic activity and selectivity. On the other hand, the inorganic segment (e.g.,  $\text{Cs}^+$ ) could significantly adjust the crystalline nature and high lattice energy of heteropoly acids due to strong ionic interactions [99,100]. Consequently, water-soluble pure heteropoly acids could be transformed into insoluble salts in polar media via inorganic modification to facilitate their recovery.

In general, alcohol dehydration reactions take place by heating the alcohol with a strongly acidic compound like sulfuric acid, potassium bisulfate, or phosphoric acid as a catalyst. In addition, other Brønsted acids and some Lewis acids have been used as catalysts as well [101]. Among the advantages of using Keggin-type heteropoly acids, the greater catalytic activity can be mentioned since they are stronger acids, and milder experimental conditions are required and lower proportions of side reactions are possible [83]. Another advantage is that no toxic waste is produced during the process thus helping to incorporate clean technologies and reduce environmental concerns. Moreover, the presence of heteropoly anions as conjugated bases accelerates the reactions quite efficiently. This is unlike the case of conventional protic acids, in which the counter anion is not involved in the activation of the reactants [102].

Baba and Ono [103] have investigated the dehydration of 1,4-butanediol, both in aqueous solutions and in dioxane, using a heteropoly acid as a catalyst. They found that the reaction was completed 70 times faster in the latter solvent and attributed this behavior to the inhibitory effect exerted by water.

The dehydration of alcohols of low molecular weight using heteropoly acids as a catalyst has been extensively studied [104,105] by Misono and coworkers [106,107], who reported the results obtained in the dehydration of ethanol.

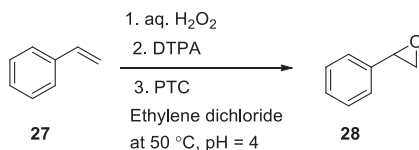
To carry out heterogeneous reactions in liquid phase, the heteropoly acids were supported on a carrier, in order to ensure high dispersion. A measure of the acid strength of the supported heteropoly acids can be obtained by determination of the catalytic activity in the dehydration of isopropanol in vapor phase. Vázquez et al. [108] have studied the behavior of diverse catalysts based

on heteropoly acids supported onto silica, titania, or alumina. They observed that such catalysts would present specific conversions higher than those of bulk acids. Accordingly, the authors prepared and characterized the catalysts and examined the min dehydration reactions. In particular, the catalytic behavior of molybdophosphoric acid (MoPA) and tungstophosphoric acid (WPA) supported on silica after washing with the solvent used as the reaction medium was studied in the industrial dehydration of 1,2-diphenylethanol, 1-3,4-di-methoxyphenyl-2-phenylethanol, and cholesterol.

Blanco and coauthors [109] prepared catalysts based on Keggin-type heteropoly acids supported on silica to use them in dehydration of alcohols in liquid phase. Both HPMo and HPW were found with their primary Keggin structures intact. Blanco et al. obtained a process for the direct dehydration of cholesterol. They found that the catalysts were quite active and selective, while allowing easy separation from the reaction medium. The same catalysts were employed for several cycles without considerable loss of catalytic activity. After the reaction and upon recovery, they showed physicochemical properties similar to those of the original catalysts.

An important intermediate in chemical industries is styrene oxide which can be produced by epoxidation of styrene. Yadav et al. [110] reported the epoxidation of styrene to styrene oxide using a synergism of heteropoly acids and phase-transfer catalysts via Ishii-Venturello epoxidation. Several methods are used in preparation of epoxides, starting from olefins, R-halocarbonyls, carbonyls, epichlorohydrin, and substituted hydroxyl compounds [111–113]. Epoxidation with commercially available peroxyacids such as peroxybenzoic acid, peroxyacetic acid, *m*-chloroperoxybenzoic acid, peroxyfluoroacetic acid, and *m*-nitroperoxybenzoic acid is a method often used for laboratory preparations.

Heteropoly acids such as tungstophosphoric acid and molybdophosphoric acid are usually employed not only for the oxidation of organic substrates but also to catalyze reactions as they possess the dual characteristics of oxidizing ability and strong acidity. In general, using a heteropoly acid for the oxidation of olefins with hydrogen peroxide produces *trans* glycols owing to the subsequent cleavage of the oxirane ring of the reacting epoxide as a result of the electrophilic attack of strong acid. However, with a phase transfer catalyst, the epoxides are easily formed under milder reaction conditions. Since the concentration and partitioning of the epoxidizing species were functions of the heteroatom in the heteropoly acid, the effect of the type of heteropoly acid on the epoxidation of styrene was studied as well. The efficacy of different heteropoly acid catalysts was evaluated at 50°C under similar conditions in the absence of any mass transfer resistance. The catalysts used were namely, HPW, HPMo, and tungstosilicic acid (HSiW). The result revealed that HPW was the best heteropoly acid, affording very high conversions. The concentration of the epoxidizing species in the organic phase was also dependent on the concentration of quaternary cation  $Q^+$  (Scheme 6.8).



**SCHEME 6.8** The epoxidation reaction.

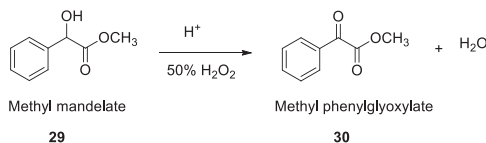
With two carbonyl groups, methyl phenylglyoxylate is a chemical used as an important intermediate in the fine chemical industry. R-Dicarbonyl compounds are synthesized via the oxidation of R-hydroxycarbonyl precursors. Because of the sensitivity of the R-dicarbonyl compounds, particular reagents and reaction conditions are necessary to inhibit side reactions accompanying the oxidation of R-hydroxycarbonyls [114]. Several methods have been developed to accomplish this transformation, but most of them have disadvantages such as using corrosive acids or toxic metallic compounds, which produce undesirable waste materials. There are a number of methods available for the oxidation of  $\alpha$ -hydroxyl compounds using oxidizing agents like bromosuccinimide [115], *N*-bromoacetamide [116], trichloroisocyanuric acid [117], *N*-bromobenzene sulphonamide [118], *N*-chlorobenzene sulphonamide [119], 1-chlorobenzotriazole [120], *N*-bromosaccharin [121], bromate [122], and *N*-bromophthalimide [123]. The oxidation process has also been reported with catalytic amounts of vanadyl chloride ( $\text{VOCl}_3$ ) in acetonitrile under an oxygen atmosphere [124]. Methyl phenylglyoxylate was synthesized via ozonolysis of 1-bromophenylacetylene, and then reaction with potassium iodide [125], while the oxidation step was enhanced [126] by treating trimethylsilylphenylacetylenes with osmium tetroxide and *tert*-butyl hydroperoxide in methanol to afford methyl phenylglyoxylate.

Yadav and coworkers [127] developed a novel nanocatalyst using HPW partially substituted with cesium and supporting it on acid activated clay. Nanoparticles of 20% w/w  $\text{Cs}_{2.5}\text{H}_{0.5}\text{PW}_{12}\text{O}_{40}$  were therefore created in the pore network of acid treated K10 clay (designated as Cs-HPW/K10) and applied for a series of acid-catalyzed reactions [128,129].

Methyl mandelate was oxidized to afford methyl phenylglyoxylate, with 85% selectivity, using  $\text{H}_2\text{O}_2$  in the presence of the novel catalyst, i.e., 20% w/w  $\text{Cs}_{2.5}\text{H}_{0.5}\text{PW}_{12}\text{O}_{40}$ /K10 catalyst, which was reusable. The workup was easy.  $\text{H}_2\text{O}_2$  is an excellent nucleophile with the structure  $-\text{O}-\text{O}-\text{H}$ . Therefore, it is also a superb reactant for the preparation of a hydroxylperoxide in the presence of catalytic amounts of an acid like Cs-HPW/K10 which can be used as a proton source to go through an  $\text{S}_{\text{N}}1$  displacement, which involves a carbonium ion intermediate. In addition, the C-H bond is ruptured by losing a hydrogen atom as a proton to give the methyl phenylglyoxylate. This supports the mechanism proposed by Kwart and Francis [130] for the oxidation of secondary alcohols involving the rupture of a C-H bond. It is already reported in the literature that mandelic acid [131] reacts about six times faster than its methyl ester. The slower oxidation of the ester in comparison with mandelic acid could be



accounted for as the  $-\text{COOH}$  group has a stronger  $-I$  effect than the  $-\text{COOMe}$  group. The formation of mandelic acid might be attributed to the fact that the ester-acid equilibrium is sensitive to the amount of water present in the reaction at any time and the ester might be hydrolyzed to the acid. This mandelic acid goes through further degradation to give benzaldehyde and is decarbonized by losing a proton, as illustrated in Scheme 6.9.  $\text{H}^+$  represents the Cs-HPW/K10 catalyst.

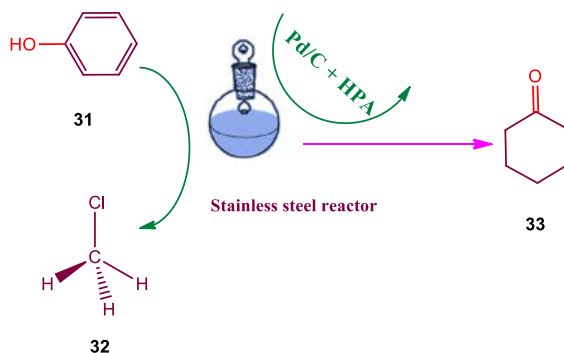


**SCHEME 6.9** Oxidation of methyl mandelate to methyl phenylglyoxylate.

Cyclohexanone is a key intermediate in the synthesis of caprolactam and adipic acid, which are, in turn, the main ingredients for the manufacture of Nylon 6, Nylon 66, and polyamide resins [132–134]. The industrial processes for cyclohexanone production are oxidation of cyclohexane [135] and hydrogenation of phenol [136]. In comparison with the hydrogenation of phenol, the oxidation of cyclohexane has more drawbacks as it requires higher temperatures and pressures, while generating several undesirable by-products. In the hydrogenation of phenol, cyclohexanone is usually produced through a one- or two-step process [137]. Phenol hydrogenation in the gas phase normally requires high temperatures (150–300°C) along with generation of carbonaceous deposits in the course of the reaction, which results in the deactivation of the supported catalyst. On the other hand, a liquid-phase process reduces the cost and saves energy, since hydrogenation is performed at relatively low temperatures.

Joshi et al. had reported that molybdophosphoric acid-catalyzed would transfer the hydrogenation of nitroaromatics with excellent catalytic performance into a homogeneous phase [138]. Cobalt-containing catalysts modified with Keggin-type heteropoly acid salts were demonstrated to enhance the selectivity on hydrogenation of crotonaldehyde [139]. The one-pot transformation of (+)-citronellal into menthol over a  $\text{Pd-H}_3\text{PW}_{12}\text{O}_{40}/\text{SiO}_2$  catalyst yielded 92% of menthol with 100% conversion of citronellal and 85% stereoselectivity of the desired (–)-menthol [140]. The catalyst modified with a heteropoly acid exhibited better catalytic performance for the hydrogenation. Consequently, Liu et al. [141] studied the hydrogenation of phenol using the bifunctional catalyst  $\text{Pd/C-HPA}$  in the liquid phase.

Hydrogenation/oxidation of phenol **31** to cyclohexanone **33** was achieved within 3 h under 80°C and 1.0 MPa hydrogen pressure in the presence of the composite catalytic system of  $\text{Pd/C-heteropoly acid}$  in dichloromethane **32** with 100% conversion of phenol and 93.6% selectivity toward cyclohexanone. It has



**SCHEME 6.10** Hydrogenation/oxidation of phenol.

been found that the effect of Pd/C with a heteropoly acid would improve the catalytic performance of the composite catalytic system (Scheme 6.10).

The heteropoly acids can be used in multiphase reactants as a phase transfer catalyst. In addition, Liu and coworkers [142] achieved both excellent conversion and selectivity in the hydrogenation of furfural and cinnamic aldehyde using modified heteropoly acid salt as catalysts.

Preparation of a gasoline cut with a high octane number is possible through the alkylation of isobutane with *n*-butene. Industrially, only anhydrous hydrofluoric acid and concentrated sulfuric acid are applied as catalysts [143–145]. However, the expected increase in alkylation capacity in the future is relatively low because restrictions imposed on the use of highly corrosive and contaminating acids as industrial catalysts.

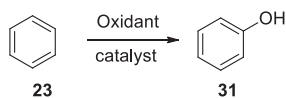
Recently, reactivity of cesium salts of HSiW and HPW in the alkylation of isobutane with 2-butene have been studied [146,147]. Wu and coworkers [148] reported the use of catalysts containing heteropoly acids supported on different silica and mesoporous molecular sieves prepared by impregnation and sol-gel methods, respectively. They investigated the behavior of their catalysts in fixed-bed alkylation of isobutane with butene. The activity, selectivity, and stability of the supported-HPA catalysts could be correlated with the surface acidity of the catalysts, the structure of the supports, and the time on stream. In the fixed-bed reactor, the acidity of the heteropoly acid was beneficial to the formation of dimerization products ( $C_8$ ); in particular, the pore size of supports was found to be an important factor affecting the activity and product distribution of the catalysts. Opposite to the traditional solid-acid catalysts, the supported-HPA catalysts had excellent stability for alkylation, allowing for the supported catalysts to replace the liquid-acid catalysts currently used in industry.

Jiang and coworkers [149] directly hydroxylated benzene to phenol [150] and investigated the reaction as a promising route for the production of phenol. Various oxidants have been used in the direct hydroxylation of benzene to phenol including nitrous oxide [151,152], hydrogen peroxide [153], and molecular oxygen [154,155], as well as a mixture of oxygen and hydrogen.

Molecular sieves, particularly those with mesopores, have been widely studied in heterogeneous catalysis due to their large surface area, large pore volume, uniform pore size, and well-ordered structure. Selective oxidation of organic compounds with  $\text{H}_2\text{O}_2$  as an oxidizing agent and molecular sieve catalysts is an attractive, high-potential area in the development of environmentally benign technologies. Two industrial applications (phenol hydroxylation and cyclohexanone ammoxidation) were demonstrated on an industrial scale employing a titanium silicalite-1 (TS-1) catalyst [156]. Active catalysts were synthesized by incorporation of transition metals such as titanium, vanadium, iron, cobalt, nickel, and copper into the framework of mesoporous materials [157]. Some of active species like metal ions or metal oxides could be directly supported on such materials to provide effective catalysts applied in the hydroxylation of benzene [158,159].

However, the production of phenol in a selective manner with high yields is still a challenge as phenol exhibits more reactivity toward oxidation in comparison with benzene. Achieving high selectivity using molecular oxygen is difficult owing to the high reaction temperatures and overoxidation arising from the more active catalysts used for activating oxygen. Among the oxidizing agents,  $\text{H}_2\text{O}_2$  has evident advantages since it generates water as the only by-product. A variety of catalysts have been designed and used for the direct hydroxylation of benzene with  $\text{H}_2\text{O}_2$  as an oxidizing agent. Heteropoly acids supported on molecular sieves are widely used as homogeneous and heterogeneous catalysts for some of their typical properties, such as Brønsted acidity, capability to catalyze redox reactions as well as high solubility in water and organic solvents. Heteropoly acids based on the Keggin structure are thermally stable, strongly acidic with oxidizing abilities [71].

A Keggin-type V-substituted molybdophosphoric acid ( $\text{H}_5\text{PMo}_{10}\text{V}_2\text{O}_{40}\cdot n\text{H}_2\text{O}$ ) supported on the amine-functionalized SBA-15 was assessed in direct hydroxylation of benzene to phenol in the liquid phase [160]. The supported catalyst demonstrated good stability with negligible leaching of the heteropoly acid from the support during the reaction, which was due to strong acid-base interactions between the heteropoly anions and amine groups on the surface. Twenty percent conversion of benzene and 95% selectivity to phenol was accomplished in acetonitrile at  $60^\circ\text{C}$  after 6 h. The vanadium species was found to be the active site in this reaction. In the hydroxylation of benzene, the amount of  $\text{H}_2\text{O}_2$  consumed by self-decomposition was much more than hydroxylation, which led to the very low selectivity observed in the conversion of hydrogen peroxide (Scheme 6.11) [160].



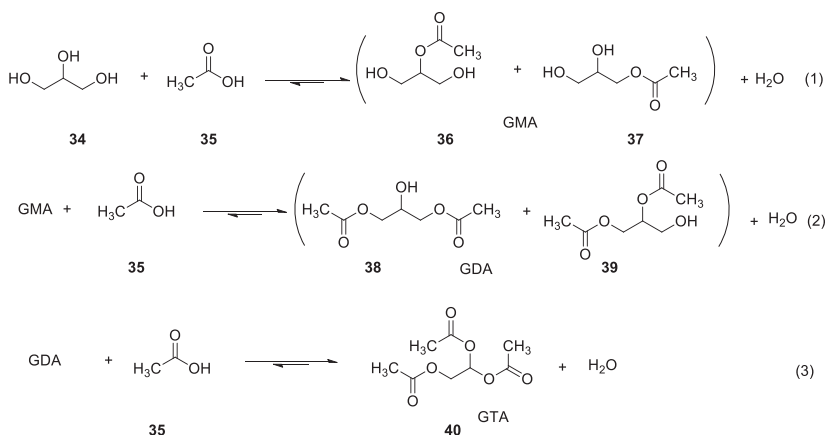
Oxidant:  $\text{O}_2$ ,  $\text{O}_2$  + reducing agent,  $\text{N}_2\text{O}$ , or  $\text{H}_2\text{O}_2$  etc.

**SCHEME 6.11** The direct hydroxylation of benzene to phenol using different oxidants.

A large number of solid catalysts have been synthesized in nano sizes or created as nanomaterials inside a porous matrix. A plenty of inorganic oxides, mixed oxides, e.g., alumina, silica, zirconia, titania, zeolites, and clays, have been used as both supports and catalysts [161–163] to fulfil the green chemistry requirements. Among them, clays have resurfaced as solid acids. Clays were the original fluid catalytic cracking (FCC) catalysts, but they were replaced by silica-alumina, which were thermally more stable in the 1940s. Then, in the 1960s, zeolites of different hue were used as they were most profitable. Clay structures collapse at high temperatures and must be somehow stabilized. The thermal stability and pore size issues were resolved via pillaring of the clays, which resulted in a wide variety of new applications. Natural clays are acid treated or ion-exchanged to be used as solid acids, with their acidity and pore structure being dependent on the treatment method [164,165]. As another important class of catalysts, heteropoly acids possess both redox and acid properties [166,167]. Yadav and coworkers [168] investigated different aspects of green processes with benign solid acid catalysts, having direct industrial applications in refineries, pharmaceuticals, petrochemicals, dyestuff, rubber chemicals, agrochemicals, perfumery, and flavor chemicals. Clays, heteropoly acids supported on clays, sulfated zirconia, and ion exchange resins have been evaluated in several processes [166,167].

Glycerol (GL) is the primary by-product of biodiesel production. Around 10% of the global glycerol production is the result of transesterification of vegetable oils with methanol [169]. Given the growing demand for biodiesel fuels like fatty acid methyl ester via transesterification of triglyceride, an excessive amount of glycerol is accumulated unavoidably [170]. Glycerol is an edible, nontoxic, and biodegradable viscous liquid that can readily be oxidized, reduced, halogenated, etherified, or esterified to obtain alternative valuable chemicals [171–173]. Among the various derivatives produced from glycerol, glycerol acetates as a product of acetylation of glycerol with acetic acid is a practical option.

As shown in [Scheme 6.12](#), acetylation of glycerol with acetic acid typically consists of three correlated steps, which are consecutive formations of glycerol monoacetate, glycerol diacetate, and glycerol triacetate in the presence of excessive water. An esterification reaction may generally be accelerated by acid catalysts in homogeneous media, e.g., over hydrofluoric acid, sulfuric acid, p-toluenesulfonic acid, or acidic ionic liquids [174,175]. However, such mineral acid catalysts usually have environmental and economic issues. In order to resolve these problems, heterogeneous catalysts like zeolites [176], surface-functionalized mesoporous silicas [177], ion-exchange resins [178], niobium/zirconium [179], as well as supported heteropoly acids [180,181] have been investigated.



**SCHEME 6.12** Acetylation of glycerol with acetic acid.

Liu et al. [182] synthesized a series of homogeneous catalysts consisting of pyridinium propyl sulfobetaine (PPS), HPW, and acetic acid (HOAc) and utilized for catalytic acetylation of glycerol. Their acid properties were characterized by  $^{31}\text{P}$ NMR of trimethylphosphine oxide as the probe molecule, the factors affecting acidic strength, PPS/HPW, HPW/GL, and HOAc/GL ratios as well as the reaction temperatures on catalytic performances during the acetylation reaction were investigated. Tending to segregate from glycerol acetate products and form distinct biphasic liquid layers spontaneously after the reaction, these water-tolerable catalysts (PPS-HPW-HOAc) was found to be highly effective and durable for the acetylation reaction under continuous operation conditions. Usually, a complete conversion of glycerol may be achievable with a very good selectivity of 86%–99% toward glycerol triacetate. Besides, the unique self-separation biphasic features of the catalyst system assists in facile product separation and catalyst recycle, rendering the acetylation process feasible at an industrial level. However, notable decrease in activity was commonly observed for the heteropoly acids salt during esterification. Therefore, catalyst degradation and recyclability are still regarded as challenging and demanding issues.

Monoethylene glycol is an industrial chemical compound applied in the manufacture of polyester resins and fibers and antifreeze agents. While global antifreeze agent demand is steady, demand for polyester is experiencing an annual increase of 10%. The demand for ethylene, the raw material used to make monoethylene glycol, is outpacing supply, resulting in price increases for this chemical.

Direct synthesis of monoethylene glycol from syngas is possible but it requires pressures between 1300 and 7000 atm, temperatures above 200°C, while giving very low yields [183,184].

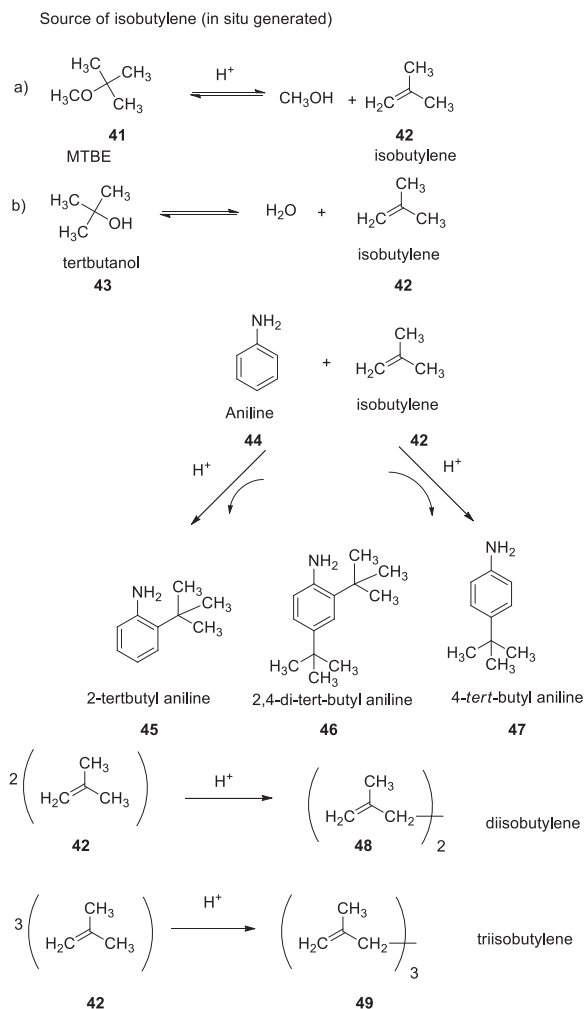
Bell and others [185] studied the manufacture of monoethylene glycol from methanol and its derivatives, e.g., formaldehyde. The process is potentially attractive, because the carbon needed for it can be derived from syngas, which is a cheaper carbon source compared to ethylene derived from petroleum. The authors reported formaldehyde carbonylation using methyl formate as the source of carbon monoxide. They used silicotungstic acid and other heteropoly acids as catalysts. Methyl glycolate and methyl methoxyacetate, which are both precursors to ethylene glycol, were formed together with dimethoxymethane and dimethyl ether, as the primary by-products. Different factors, i.e., formaldehyde source, reaction temperature, time, and catalyst were studied. Methoxymethanol, paraformaldehyde, 1,3,5-trioxane, and dimethoxymethane were studied as sources of formaldehyde. The highest yields for methyl glycolate and methyl methoxyacetate were gained with 1,3,5-trioxane as a formaldehyde source. Carbon monoxide release from methyl formate was slow and limited the rate of carbonylation. Among the heteropoly acids studied, silicotungstic acid gave rise to the highest yields of methyl glycolate and methyl methoxyacetate, while with methanesulfonic acid the products were not achieved with similar acid loading. The difference between the efficiency of heteropoly acids and methanesulfonic acid was attributed to the role of the heteropoly anion, a soft base, which is stabilizing the reactive intermediates involved in the carbonylation of formaldehyde.

Aniline is used as a building block for the manufacture of several products in chemical industries. Aromatic amines with alkyl groups on the ring have various applications in chemical synthesis. They were used as intermediates for substituted isocyanates, herbicidal compositions, dyestuffs, and textile auxiliary agents. Typically, Friedel-Crafts alkylation of aromatics is performed using highly corrosive homogeneous Lewis acids, e.g.,  $\text{AlCl}_3$ ,  $\text{AlBr}_3$ ,  $\text{ZnCl}_2$ ,  $\text{FeCl}_3$ ,  $\text{TiCl}_4$ , and strong Brønsted acids such as sulfuric acid and phosphoric acid with various alkylating agents [186].

Among alkylated anilines, *tert*-butylanilines are used in pharmaceuticals, pesticides, plastics, additives, and dyes. They are prepared by reacting aniline with pure isobutylene or  $\text{C}_4$  fraction from naphtha crackers containing isobutylene in presence of a liquid acid as a catalyst. Alkylation of aniline is an acid catalyzed consecutive reaction. In the first step, *N*-alkylaniline is formed, which is further dialkylated to di-alkylaniline under suitable conditions.

Because of problems such as unavailability, difficulty of transportation and handling of isobutylene, especially when used in low-tonnage, fine chemical manufacture to produce *tert*-butyl derivatives, generation of isobutylene in situ has advantages. Cracking of methyl *tert*-butyl ether and dehydration of *tert*-butanol are attractive means for this purpose. *Tert*-Butanol is available as a by-product in the Arco process for the propylene oxide. Methyl *tert*-butyl ether is a good source for the generation of pure isobutylene. The coproduct of this process, i.e., methanol, can be recovered and reused. However, the in situ dehydration of *tert*-butanol gives water as a coproduct in the alkylation reaction and

therefore, in comparison with methyl *tert*-butyl ether as an alkylating agent, different yields of the alkylated product are expected [187,188]. Yadav et al. [189] studied several solid acids, most of which were heteropoly acids supported on various clays, and found them to be novel catalysts [190] exhibiting excellent activity as a catalyst compared to other solid acids employed in the alkylation and etherification reactions that involve isobutylene [191]. They assessed the novel catalysts with both methyl *tert*-butyl ether and *tert*-butanol as alkylating agents under autogenous pressure in a pressure reactor (Scheme 6.13). The 20% (w/w) tungstophosphoric acid on K10 montmorillonite clay (HPW/K10)

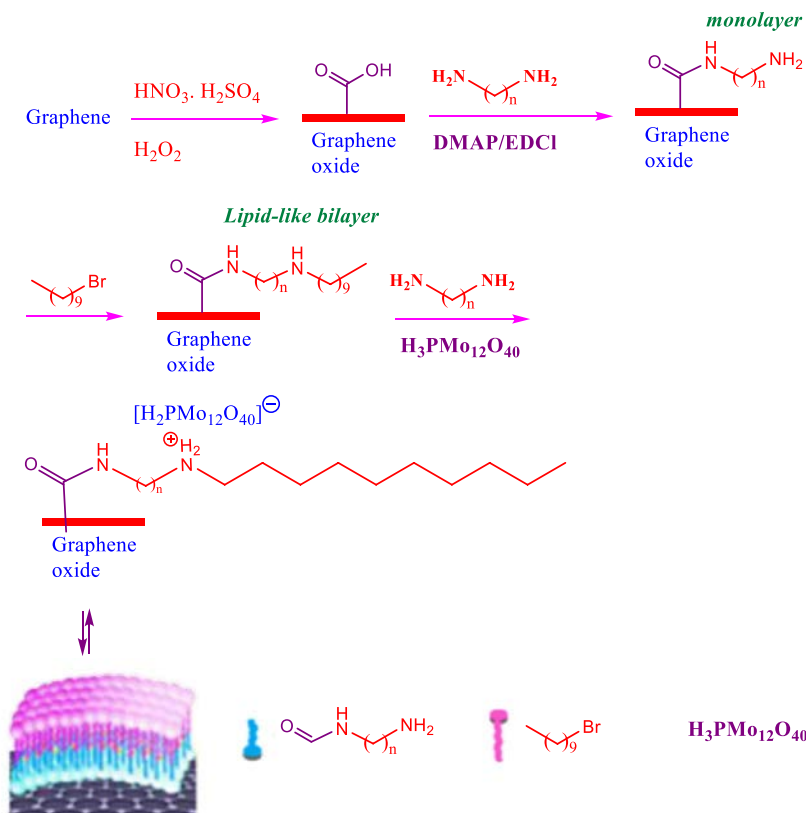


**SCHEME 6.13** Product distribution of acid catalyzed alkylation of aniline with generated in situ isobutylene.



was observed to have the highest activity for the alkylation of aniline with both methyl *tert*-butyl ether and *tert*-butanol. Only C-alkylated products were gained. The yields of mono-alkylated products were more than 84% with a selectivity of 53% to 2-*tert*-butylaniline with methyl *tert*-butyl ether at 175°C. *tert*-Butanol solely afforded mono-alkylated products at 150°C with equal distribution of the isomers. Effects of various parameters on rates and selectivities were discussed. In the presence of HPW/K10, C-alkylated products were formed exclusively. A reaction mechanism is also described with a kinetic model.

Graphene, which indeed a one-atom-thick planar sheet of carbon atoms connected through  $sp^2$ - $sp^2$  bonds, demonstrates a large specific surface area (theoretically 2630 m<sup>2</sup>/g for single-layer graphene) [192], extraordinary electron transport abilities [193], as well as excellent electrical and thermal conductivities [194]. Due to these properties, graphene materials exhibit high adsorption ability toward substrates to accelerate the reactions in catalysis. Consequently, graphene materials, particularly chemically modified graphene oxide (GO), serve as an ideal platform used for anchoring a variety of active sites [195]. The synergistic effect between the active sites and graphene oxide can promote the reactivity. Wanga et al. [196] reported a novel, two-step methodology for functionalization of graphene oxide (GO) with heteropoly acids and the catalytic activity of the obtained species in the conversion of glycerol to lactic acid. The covalent bonding of a  $-\text{NH}-(\text{CH}_2)_2-\text{NH}_2^+-\text{CH}_2(\text{CH}_2)_8\text{CH}_3$  lipid-like bilayer to the graphene oxide surface was followed by embedding of heteropoly acids to afford HPMo@lipid(*n*)/GO, where *n* is the length of the diamine carbon chain (*n*=2, 4, 6, 8, 10). The lipid bilayer tightly surrounds the heteropoly acid via electrostatic interactions with the protonated amine groups. As a result, the heteropoly acid became highly resistant to environmental changes and leaching from graphene oxide. The hydrophobic properties of the lipid bilayer as well as the hydrophilic property of the heteropoly acid and graphene oxide were readily adjustable by the length of the alkyl chain, and the redox potential was varied by the distance between the heteropoly acid and graphene oxide. The species exhibited excellent catalytic performance in the glycerol cascade conversion to lactic acid so that HPMo@lipid(4)/GO achieved the highest reported efficiency with a yield of 90% at 97% conversion under mild conditions (1 M glycerol, 60°C, 3.5 h, 10 bar O<sub>2</sub>). This high efficiency was attributed to the combination of a number of parameters such as suitable redox potential, balanced hydrophobic and hydrophilic properties, and a capillary-like reactor formed by the wall of the lipid bilayer, which enhanced the adsorption of O<sub>2</sub> and glycerol around the catalytic active sites. HPMo@lipid(4)/GO works organic solvent-free conditions and in the absence of base, with high concentration of glycerol (9.2% (w/w)), in the presence of methanol and other impurities formed during the biodiesel production. The crude glycerol gives almost 87% yield. No structural changes or heteropoly acid leaching from graphene oxide took place in the course of reaction, with recyclability of up to 15 runs (Scheme 6.14).



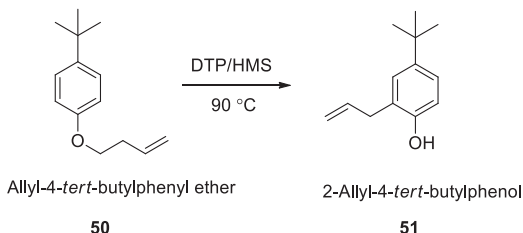
**SCHEME 6.14** Synthetic methodology for the assemblage of HPMo@lipid(*n*)/GO hybrid catalyst materials.

### 6.3. Applications of heteropoly acids in pharmaceuticals

The Claisen rearrangement reactions are among the most powerful means for the formation of carbon-carbon bonds in the art of organic synthesis [197]. This reaction may be used in the synthesis of *o*-allyl phenols, which are precursors to a wide variety of natural products moieties e.g., chromones and coumarones [198–200]. A series of novel catalysts with extraordinary acidities such as Lewis acids ( $\text{BCl}_3$ ,  $\text{BF}_3$ ,  $\text{BBr}_3$ ,  $\text{AlCl}_3$ ,  $\text{SnCl}_4$ ,  $\text{ZnCl}_2$ ,  $\text{TiCl}_4$ ,  $\text{AgBF}_4$ , etc.), Brønsted acids (trifluoroacetic acid, sulfuric acid, etc.), bases, and transition metal complexes (Rh (I) and Pt(0)) have been studied for their effectiveness in Claisen rearrangement [201]. The Claisen rearrangement of allyl-4-*tert*-butylphenyl ether to 2-allyl-4-*tert*-butylphenol is a commercially important reaction since the latter is used as a cross linking agent in polymers, antioxidant, reactive diluent in

UV-curable coating composition, as well as an intermediate in preparation of drugs for the treatment of heart ischemia. It is also used in perfumes, flavors, and especially the formulation of products such as soaps, air fresheners, and detergents, and in cosmetic materials.

Yadav and coworkers in 2005 achieved [202] the Claisen rearrangement of allyl-4-*tert*-butylphenyl ether to 2-allyl-4-*tert*-butylphenol with 100% selectivity in an efficient, economically feasible, and green route using solid acid catalysts such as acid sulfated zirconia, treated clays, and 20% (w/w) tungstophosphoric acid/hexagonal mesoporous silica (HPW/HMS). Among them, HPW/HMS was observed to perform the best. The catalyst was totally reusable without any loss in activity, and was 100% selective toward 2-allyl-4-*tert*-butylphenol. Based on the experimental data, a suitable mathematical model was proposed to describe the reaction kinetics (Scheme 6.15).

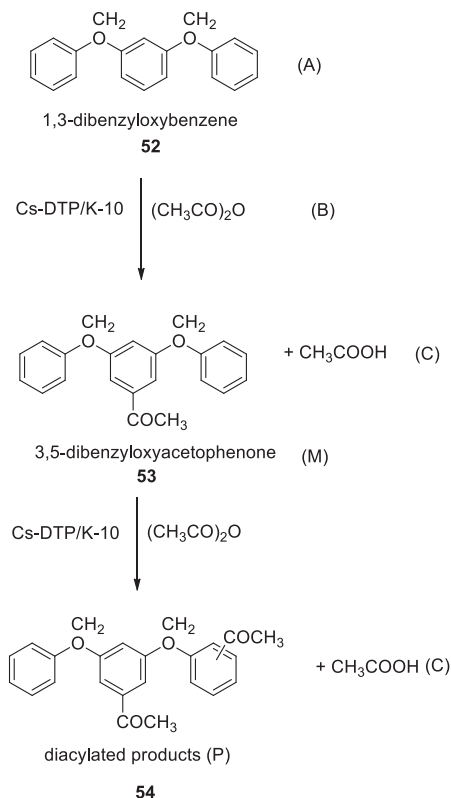


**SCHEME 6.15** Claisen rearrangement.

The catalyst forms an acylium ion intermediate from the interaction of acylating agent with acid. The acid catalysts conventionally used in Friedel-Crafts acylation are homogeneous catalysts such as Lewis acids ( $\text{AlCl}_3$ ,  $\text{FeCl}_3$ ,  $\text{ZnCl}_2$ ,  $\text{TiCl}_4$ ,  $\text{ZrCl}_4$ ) and Brønsted acids (polyphosphoric acids, HF) [203].

Heteropoly acids supported on hexagonal mesoporous silica (HMS) have been found to be highly active catalysts for Friedel-Crafts acylation [204]. On the other hand, ion exchange resins deactivate the catalyst in the acylation of diphenyl oxide and thioanisole [205,206].

Yadav and coworkers [207] acylated 1,3-dibenzyloxybenzene with acetic anhydride using several solid super acids to obtain 3,5-dibenzyloxyacetophenone, which is a critical intermediate in the production of drugs for the treatment of various diseases and disorders. They studied the activities of 20% (w/w)  $\text{Cs}_{2.5}\text{H}_{0.5}\text{PW}_{12}\text{O}_{40}/\text{K10}$  clay, UDCaT-5, sulfated zirconia, Amberlyst-36, and Indion-130. Among them, 20% (w/w)  $\text{Cs}_{2.5}\text{H}_{0.5}\text{PW}_{12}\text{O}_{40}/\text{K10}$  clay demonstrated the highest selectivity. The authors systematically studied the reaction to understand the reaction mechanism and catalyst functioning with  $\text{Cs}_{2.5}\text{H}_{0.5}\text{PW}_{12}\text{O}_{40}/\text{K10}$ . The catalyst gradually deactivated over repeated use. The adsorption of reactants and products from pure component solutions and mixtures was also investigated. The acquired experimental data were used to develop a model in which the observed deactivation was taken into account. The model fitted the experimental data quite well (Scheme 6.16).



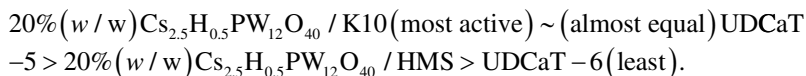
**SCHEME 6.16** Acylation of 1,3-dibenzyloxybenzene (A) with acetic anhydride (B) leading to monoacylated product (M) and coproduct acetic acid (C). Subsequent diacylation leads to formation of by-products (P). Both C and P show deactivating effect.

Fries rearrangement of phenyl benzoate has been catalyzed using various solid acids. Although the use of zeolites in Fries rearrangement appears to be promising [208–210], the selectivity and reactivity of zeolites must be enhanced and rapid deactivation of the catalysts has to be resolved so that they are apt for industrial applications. Olah et al. [211] tested Nafion-H to catalyze the Fries rearrangement of phenyl benzoate while Kozhevnikova et al. [212] used cesium salts of substituted heteropoly acids. The high temperature and high mole ratio required for this reaction along with low selectivity and long reaction time have rendered it highly energy-intensive and uneconomical.

A novel methodology to minimize the waste in this type of reaction should be the esterification and Fries rearrangement with the same catalyst capable of regeneration in a one-pot operation in the absence of solvent. Such a strategy was adopted and the reaction between phenol and benzoic acid was studied using an array solid acid catalysts. Yadav and coworkers [213] reported the results of the direct, clean Fries reaction together with the effects of different

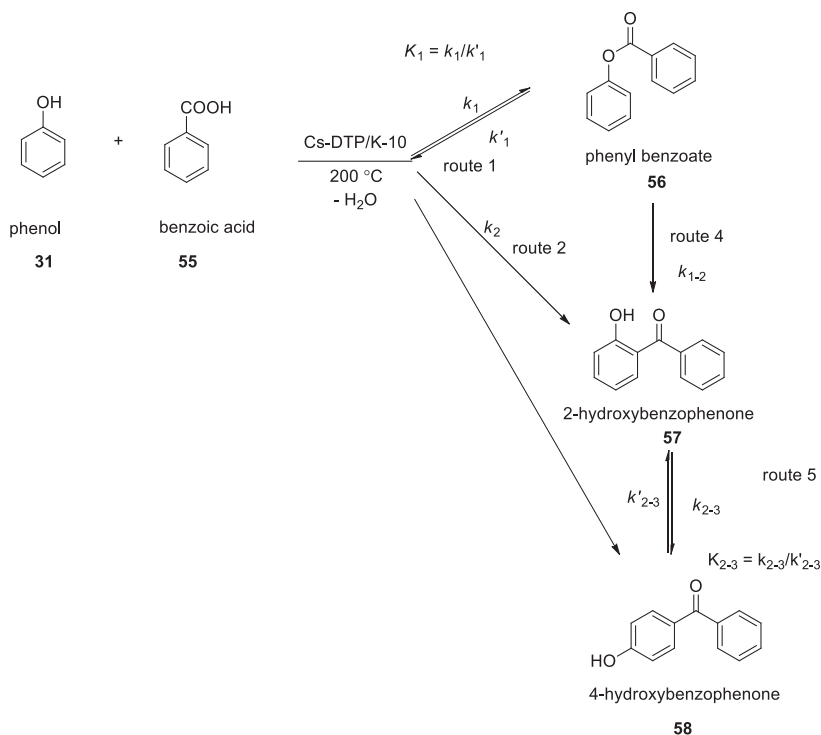
parameters on product profile to provide an insight into the reaction mechanism. They also studied the direct Fries rearrangement of phenyl benzoate to throw light on the reaction pathway.

Hydroxybenzophenones are important starting materials in manufacture of fine chemical and pharmaceutical industries. The esterification of phenol with benzoic acid, and Fries rearrangement of the product to hydroxybenzophenones in a one-pot operation in liquid phase was investigated with several catalysts in the absence of any solvent. Cesium substituted tungstophosphoric acid supported on K10 clay ( $\text{Cs}_{2.5}\text{H}_{0.5}\text{PW}_{12}\text{O}_{40}/\text{K10}$ ) was observed to be the most active catalyst with the most selectivity toward 4-hydroxybenzophenone in comparison with the others. The order of activity was as follows:



The reaction of benzoic acid **55** and phenol **33** in the mole ratio of 7:1, using  $0.05 \text{ g/cm}^3$   $\text{Cs}_{2.5}\text{H}_{0.5}\text{PW}_{12}\text{O}_{40}/\text{K10}$  at  $200^\circ\text{C}$  was studied, which gives a selectivity of 32.5% for the formation of 4-hydroxybenzophenone **58**. The effects of different reaction parameters on the reaction rate and selectivity were studied. In addition, the direct Fries rearrangement of phenyl benzoate was investigated at  $200^\circ\text{C}$  in chlorobenzene as a solvent with a catalyst loading of  $0.05 \text{ g/cm}^3$  which afforded 60% for phenyl benzoate **56** after 3 h. The selectivities for 2-hydroxybenzophenone **57** and 4-hydroxybenzophenone **58** were 4% and 12%, respectively. Unreacted phenol and benzoic acids were still the chief by-products. This suggested a reverse reaction was still predominant, as illustrated in [Scheme 6.17](#). Therefore, direct acylation via routes 2 and 3 contributed substantially in comparison with Fries rearrangement and the one-pot synthesis of 4-hydroxybenzophenone **58** from phenol and benzoic acid was most favorable.

Among heteropoly acids, the ones with the Preyssler structure are green catalysts in view of corrosion, safety, waste quantity, and easy separability. Heteropoly acids with 14 acidic protons are efficient solid super acid catalysts with unique hydrolytic stability (pH 0–12) [214,215]. During recent years, synthesis and characterization of catalysts of lower dimensions have been among the most interesting research topics due to the unique properties provided by nanoparticles along with their new characteristic and potential applications in different fields [216]. As the particle size is diminished, the relative number of surface atoms and consequently the activity increases. In their attempts to utilize heteropoly acids as catalysts in organic synthesis, Nazari and others [217] reported that the Preyssler-type heteropoly acid,  $\text{H}_{14}[\text{NaP}_5\text{W}_{30}\text{O}_{110}]$ , exhibited strong catalytic characterization [218]. In view of the extraordinary properties of nanoparticles, the authors decided to immobilize  $\text{H}_{14}[\text{NaP}_5\text{W}_{30}\text{O}_{110}]$  into the  $\text{SiO}_2$  nanoparticles and examine



**SCHEME 6.17** Product profile for esterification and Fries rearrangement.

the catalytic behavior of the novel catalyst. Acetyl salicylic acid is commonly known by its trade name, aspirin. The synthesis of acetyl salicylic acid is indeed an esterification reaction. Salicylic acid is treated with acetic anhydride, and as a result, the hydroxyl group on salicylic acid is converted into an acetyl group. Catalytic amounts of sulfuric acid (or phosphoric acid) are almost always used. Both acids are strongly corrosive and care must be taken in handling them. The authors carried the esterification of salicylic acid with acetic anhydride in the presence of  $H_{14}[NaP_5W_{30}O_{110}]$  alone and  $H_{14}[NaP_5W_{30}O_{110}]$  supported onto silica nanoparticles. The best results were obtained with the heteropoly acid supported onto silica nanoparticles. The catalyst was totally recyclable and reusable.

Acid-catalyzed alkoxylation of terpenes is an important synthesis route to valuable terpenic ethers with a myriad of applications in perfumery and pharmaceutical industry [219]. For example, camphene is converted to alkyl isobornyl ether; it is used in formulation of cosmetic and perfumes; it is also used in the commercial production of camphor. The reaction is usually conducted in the presence of homogeneous catalysts, such as sulfuric acid and silicotungstic acid [220].

Using heteropoly acids as efficient catalysts has the drawback of low surface area (1–10 m<sup>2</sup>/g). In addition, the separation problem from reaction mixtures and low stability at relatively high temperatures are among their other disadvantages. To resolve these problems, Castanheiro et al. [221] immobilized heteropoly acids on silica-occluded. The resultant silica-included tungstophosphoric acid (HPW-Ssg) proved to be an efficient, environmentally benign heterogeneous catalyst for the alkoxylation of camphene compared with its more valuable alkyl isobornyl ethers in liquid phase. The alkoxylation of camphene with C1–C4 alcohols (methanol, ethanol, 1-propanol, 2-propanol, 1-butanol, and 2-butanol) to alkyl isobornyl ether in the presence of HPW-Ssg (4.2% w/w) at 60–80°C was examined. Different linear and branched alcohols were compared based on their activity toward the alkoxylation of camphene. The catalytic activity was decreased as the number of carbon atoms in the chain alcohol increased. This could be attributed to steric hindrance and diffusion limitations inside the porous system of the catalyst. The HPW-Ssg catalyst exhibited high selectivity toward the alkyl isobornyl ether. The effects of different parameters, such as initial concentration of camphene, catalyst loading, and temperature, were investigated to optimize the ethoxylation of camphene. The catalytic stability of HPW-Ssg in the ethoxylation of camphene was investigated by performing successive batch runs over the same catalyst sample and under the same conditions. After the third run, the catalytic activity did not decline. The catalyst was recovered and reused without any considerable leaching of HPW. The catalytic activity of HPW-Ssg was compared with that of tungstophosphoric acid immobilized on silica by the impregnation method (HPW-Sim). The activity of HPW-Ssg was found to be higher than that of the HPW-Sim catalyst. After reaction, the HPW-Sim sample lost 20% of its heteropoly acid content.

Microcrystalline cellulose (MCC) could be derived from biomass resources [222]. It is a type of odorless, white, water-insoluble fine powder or particle material [223]. Natural cellulose is generally hydrolyzed to hydrocellulose by acid. Then it undergoes posttreatment, i.e., grinding and screening, to obtain MCC for different applications [224].

Several methods have been reported for the preparation of MCC like the traditional acid hydrolysis [225], ionic liquids [226], enzymolysis technology [227], or combinations of these [228]. The acidic hydrolysis has also been catalyzed by heteropoly acids among which the classic tungstophosphoric acid H<sub>3</sub>PW<sub>12</sub>O<sub>40</sub> (HPW) was found to have the highest acid strength in comparison with H<sub>4</sub>SiW<sub>12</sub>O<sub>40</sub> and mineral acids such as perchloric, sulfuric, or hydrochloric acids [229]. In view of these advantages, HPW has received considerable attention for cellulose hydrolysis. Under mild conditions (200°C in 0.5 h), cellulose can be transformed into methyl glucosides in methanol in a yield of 73% by HPW; tungstophosphoric acid also provides the highest turnover number among many acid catalysts examined such as phosphoric, sulfuric, nitric, or hydro-



chloric acids [230]. Tian et al. reported that a significant high yield of glucose (50.5%) and selectivity (more than 90%) was accomplished using HPW for cellulose hydrolysis at 180°C for 2 h with a mass ratio of cellulose/HPW equal to 0.42 [231].

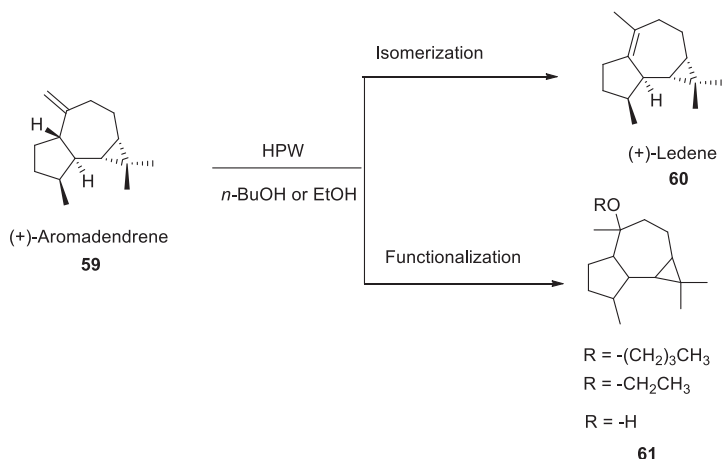
The cellulose molecular chains are composed of crystalline and amorphous regions [232]. To obtain MCC, it is necessary to protect such crystalline regions while selectively promoting the hydrolysis of the amorphous regions. Dandan Qiang and coworkers [233] thoroughly explored HPW for the selective hydrolysis of cellulose for the preparation of MCC. A variety of reaction parameters, such as acid concentration, reaction time, temperature, and solid-liquid ratio were optimized. Rod-like MCC was gained with a high yield of 93.62% at 90°C for 2 h with 58% (w/w) of the HPW catalyst and a solid:liquid ratio of 1:40. In addition, higher crystallinity and narrower particle diameter distribution (76.37%, 13.77–26.17  $\mu\text{m}$ ) were observed in comparison with the raw material (56.47%, 32.41–49.74  $\mu\text{m}$ ). In addition, HPW could easily be extracted and recycled with diethyl ether for four cycles with no significant effect on the quality of the produced MCC. The protection of the crystalline region while selectively hydrolyzing the amorphous region of cellulose as much as possible with HPW was of great significance. Owing to the strong Brønsted acid sites as well as the highest activity in solid heteropoly acids, the use of effective homogeneous HPW may provide a green and sustainable means for selective conversion of fiber resources into chemicals in the future.

The naturally occurring sesquiterpene (+)-aromadendrene belongs to the hydroazulene family of terpenes. It is the main constituent of the essential oil of *Eucalyptus globulus* [234,235].

Superacids such as fluorosulfuric acid are used in the isomerization of (+)-aromadendrene at temperatures higher than 100°C [236]. The functionalization of (+)-aromadendrene has been reported as well. Alcohols and ethers can be obtained using zeolites and formic acid [237]. Using ethanol as a nucleophile [238], the alcohols (–)-epiglobulol and (–)-globulol may be produced by the treatment of (+)-aromadendrene with acids. To obtain oxygenated compounds from this substrate, enzymes have been utilized [239].

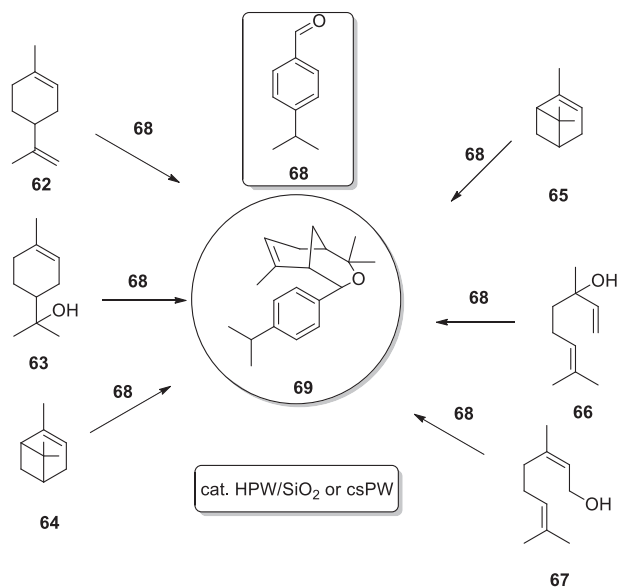
Rocha and coworkers [240] reported the use of the heteropoly acid HPW as a homogeneous catalyst for the transformation of **59** to **60** and **61** through isomerization and functionalization, respectively. The reactions were conducted using alcohols as solvents. The result was the formation of products after functionalization and isomerization of the carbon chain of compound **59**. Transformations of (+)-aromadendrene **59** were performed in the presence of the HPW, which, in principle, can be recovered from polar solutions by precipitation with the use of a nonpolar solvent. In solutions of n-butanol and ethanol, (+)-ledene **60** was formed due to the isomerization of the double bond

in the carbon chain of the substrate. By nucleophilic addition of the alcohol molecule to the exocyclic double bond of **59**, an ether was produced. In the ethanol solution, beside the formation of (+)-ledene **60** and the ether derived from ethanol, a product was also formed by the addition of a water molecule to the (+)-aromadendrene double bond to afford **61** derivatives. The products, alone or mixed, exhibited interesting pharmacological properties with the potential for commercial applications (Scheme 6.18).



**SCHEME 6.18** Transformations of (+)-aromadendrene (**59**) catalyzed by HPW.

*Reactions of terpenes with cuminaldehyde.* Cuminaldehyde **68** is a monoterpene found in a variety of essential oils. Owing to its persistent pleasant odor, cuminaldehyde is commercially produced and used in perfumes and cosmetics [241]. Oxygenated diterpenic compounds with interesting fragrance properties and/or biological activity may result from the addition of cuminaldehyde **68** to other monoterpenes. The reaction between the latter and limonene **62** (it is a colorless liquid aliphatic hydrocarbon classified as a cyclic monoterpene, and is the major component in the oil of citrus fruit peels) was achieved in the presence of HPW/SiO<sub>2</sub> and CsPW catalysts in various solvents. In the experiments conducted in the absence of a catalyst, limonene **62** was virtually stable under the reaction conditions. The chief product of the reaction was compound **69**; its structure was identified by MS and NMR. The selectivity for **69** was drastically influenced by the reaction time and other reaction parameters. In addition to **69**, isomeric *para*-menthene terpenes were formed from limonene under acidic conditions (chiefly terpinolene,  $\alpha$ -terpinene, and  $\gamma$ -terpinene; see Scheme 6.19). With a pleasant woody smell, the isolated ether **69** was a new compound with commercial applications [242].



**SCHEME 6.19** Cycloaddition of limonene (**62**),  $\alpha$ -terpineol (**63**),  $\alpha$ -pinene (**64**),  $\beta$ -pinene (**65**), linalool (**66**), and nerol (**67**) to cuminaldehyde (**68**) in the presence of HPW/SiO<sub>2</sub> or CsPW.

#### 6.4. Applications of Heteropoly acids in the food industry

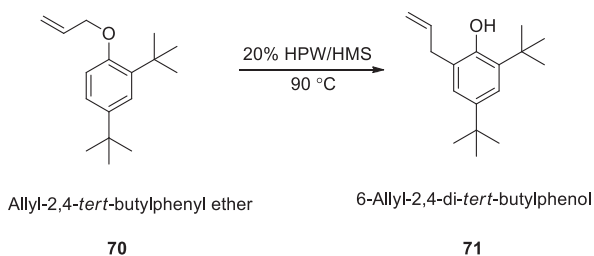
Dietary phytosterols including phytostanols are believed to effectively lower the absorption of cholesterol. Typically, 0.5–3.0 g/day of plant sterols lowers the cholesterol absorption by 30–80% which in turn may result in a decrease of 10%–15% in LDL cholesterol [243,244]. Phytosterols are nontoxic natural products and inexpensive by-products of food processing. Although potentially attractive, their usefulness has been restricted by their lower solubility in both water and oil phases, higher melting point, and their chalky taste. Should they be used broadly as a food additive, phytosterols must also be conveniently incorporated into food, without the adverse organoleptic effects. Therefore, a number of ways have been suggested to increase the solubility or bioavailability of phytosterols [245,246]. It has been demonstrated that phytosteryl esters are much more soluble than the free phytosterols in the oil phase. Therefore, using phytosteryl esters in oil has been proposed in order to lower cholesterol absorption [247].

There are a variety of methods for the production of phytosteryl esters. The typical operation is a transesterification reaction of phytosterols and methyl esters of edible oil in the presence of sodium methylate as a catalyst. However, the acyl profile of phytosteryl esters is difficult to control since it depends on

the array of fatty acids used in the oil employed in the reaction. In addition, the disposed sodium methylate, as a strongly corrosive chemical, may potentially pollute the environment. Heteropoly acid is a strong solid acid with high catalytical activity and lower corrosiveness; it is often used as catalyst for esterification reactions in the food and chemical industries [248]. In order to develop a green method for the production of phytosteryl esters from phytosterols and fatty acids in high yields, and low cost on a large scale, Meng and coworkers [249] investigated the feasibility of replacing sodium methylate by a heteropoly acid salt. For this purpose, they evaluated four different heteropoly acids, tungstosilicic acid, tungstophosphoric acid, molybdosilicic acid, and molybdophosphoric acid, to determine the best catalyst and optimize the reaction conditions for the esterification reaction between various fatty acids and phytosterols. The results revealed that tungstosilicic acid was more selective toward butyric acid and caprylic acid than toward lauric, palmitic, and oleic acids. However, in terms of the selectivity of tungstosilicic acid catalyst toward stearic, oleic, linoleic, and alpha-linolenic acids, all with C<sub>18</sub> chains, in the esterification reaction there was no significant discrimination. Phytosteryl ester higher than 90% was yielded when the esterification reaction was carried out at 150°C, with phytosterols and fatty acids in a molar ratio of 1:1.5, and catalyzed by 0.2% of tungstosilicic acid in silica gel. The catalyst recovery results revealed that the immobilized tungstosilicic acid would not considerably lose its activity after six consecutive runs. Therefore, the immobilized tungstosilicic acid could be replaced with sodium methylate to synthesize phytosteryl esters with fatty acids and phytosterols as the starting materials on an industrial scale.

The Claisen rearrangement of 6-allyl-2,4-di-*tert*-butylphenylether **70** to 6-allyl-2,4-di-*tert*-butylphenol **71** is an industrially valuable reaction. 6-Allyl-2,4-di-*tert*-butylphenol is used as antioxidant, cross linking agent in polymers as well as a reactive diluent in UV-curable coating composition. In addition, it is used in perfumes, flavors, and especially in the formulation of products such as detergents, soaps, air fresheners, and cosmetics. Various solid acids have been used for the Claisen the above mentioned rearrangement including Al-MCM-41 [250], H-FAU and H-MOR [251,252],  $\beta$ -zeolite [253], mesoporous silica [254], and bentonite [255] specifically for allyl phenyl ether as the reactant. Yadav and coworkers [256] accomplished the Claisen rearrangement of 6-allyl-2,4-di-*tert*-butylphenyl ether **70** to 6-allyl-2,4-di-*tert*-butylphenol **71** using different solid acid catalysts such as K10 clay, sulfated zirconia, 20% w/w tungstophosphoric acid (HPW)/hexagonal mesoporous silica (HMS), and 20% (w/w) HPW/K10. The 20% (w/w) HPW/HMS was observed to be quite active and stable without any significant deactivation with 100% atom economy toward preparation of 6-allyl-2,4-di-*tert*-butylphenol **71**. The authors systemically investigated the effect of various operating parameters. They concluded that the high interaction level of a heteropoly acid with the support which have determined both acid structure and mobility. The Claisen

rearrangement of 6-allyl-2,4-*tert*-butylphenyl ether catalyzed by HPW is illustrated in Scheme 6.20.

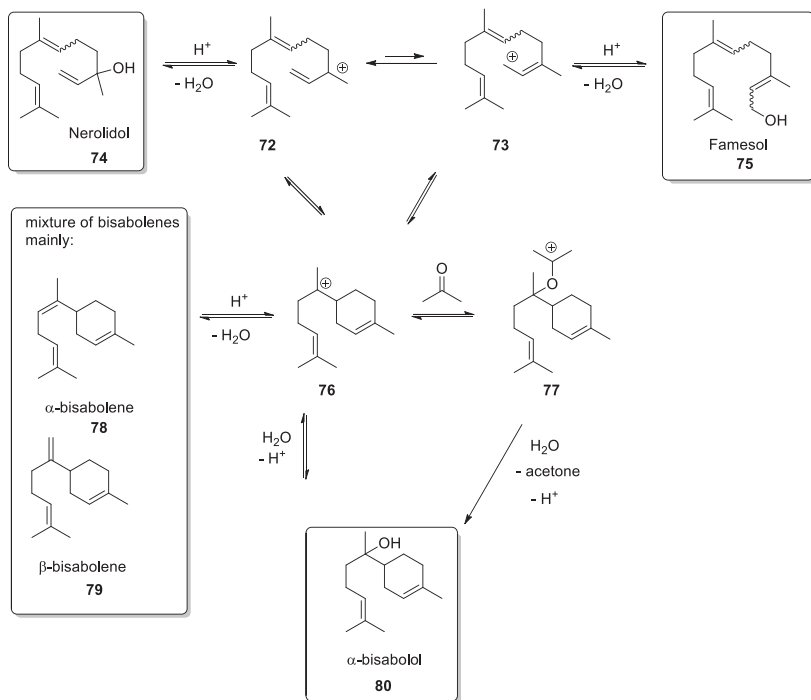


**SCHEME 6.20** Claisen rearrangement of allyl-2,4-*tert*-butylphenyl ether.

With a pleasant floral-sweet odor,  $\alpha$ -bisabolol **80** is a monocyclic sesquiterpene alcohol. It is a major component of the essential oils of chamomile (*Matricaria chamomilla*), candeia (*Eremanthus erythropappus*), and sage (*Salvia runcinata*) oils (up to 50%, 85%, and 90% contents, respectively) [257–260].  $\alpha$ -Bisabolol **80**, also known as levomenol, has exhibited a strong therapeutic potential owing to its antiinflammatory, antibiotic, skin-soothing, analgesic gastro-protective, and antioxidant properties [257–262]. Nerolidol **74** and farnesol **75** are acyclic sesquiterpene allylic alcohols, which are industrially available. Both compounds have a delicate sweet floral odor with extensive applications as fragrance and food flavor ingredients [241]. Farnesol **75** and nerolidol **74** are found in essential oils of various plants and flowers, e.g., neroli, lemon grass, and jasmine oils. They are also commercially produced from acetone and acetylene [241].

Gusevskaya et al. [263] reported the application of HPW, the strongest heteropoly acid in the Keggin series, as a homogeneous catalyst for the isomerization of nerolidol **74** and farnesol **75** in order to obtain  $\alpha$ -bisabolol **80**. HPW proved to be an active and environmentally friendly homogeneous catalyst for the synthesis of  $\alpha$ -bisabolol, an expensive and highly in-demand ingredient for the fragrance, cosmetic and pharmaceutical industries starting from more abundant sesquiterpene alcohols that can be derived from biomass. The nature of the solvent has remarkable effects on the reaction pathways and selectivity. In acetone solutions,  $\alpha$ -bisabolol **80** can be obtained in 60%–70% GC yields from farnesol **75** in 55%–60% GC yields and from nerolidol **74** with complete substrate conversions, which are probably the best results reported for these reactions thus far. The  $\alpha$ -bisabolol **80** that was also synthesized by this method contained no farnesol **75**, a potentially allergenic compound and commercially used  $\alpha$ -bisabolol must be totally free of farnesol. This advantage is particularly important since the separation of  $\alpha$ -bisabolol and farnesol by means of distillation is a troublesome task. The catalyst exhibited high turnover numbers and operated under nearly mild ambient conditions. The results from

the isomerization of nerolidol **74** in acetone solutions containing HPW were provided. The reaction gave  $\alpha$ -bisabolol with a selectivity of up to 66% along with traces of farnesol **75**, which usually disappeared when the conversion of nerolidol **74** was complete (Scheme 6.21). The rest of the substrate was mainly converted into bisabolenes ( $\alpha$ -bisabolene **78** and  $\beta$ -bisabolene **79**), which are formally the products of  $\alpha$ -bisabolol dehydration. The oligomerization that often complicates the reactions with terpenic compounds under acidic conditions did not occur significantly.



SCHEME 6.21 Acid-catalyzed transformations of farnesol and nerolidol.

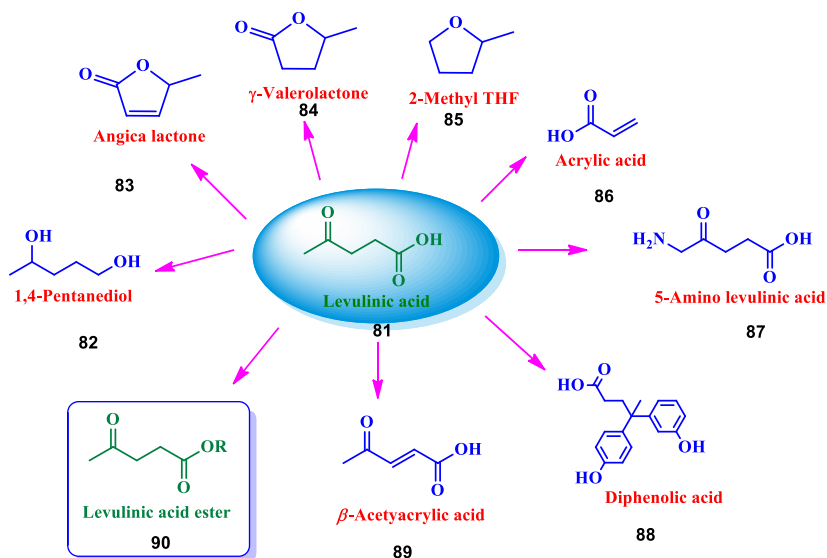
## 6.5. Applications of Heteropoly acids in biomass

Biomass resources are regarded as a good choice for raw material supply in the production of high value products owing to their low cost, accessibility, sufficiency, and, most importantly, renewability [264]. Many industries are focusing on the production of chemicals and other products from biomass such as lactic acid, levulinic acid, formic acid, biodiesel, and cellulose derivatives.

The manufacture of biodiesel from waste lipid feedstock and acidic nonedible oil has the problem of forming soaps in conventional transesterification processes. A solution to this drawback is the esterification in which super acid homogenous catalysts are used. On the other hand, dangerous effluents

are generated by such catalysts. To resolve this, Molina and coworkers [265] utilized heterogeneous acid catalysts such as heteropoly acid supported on activated carbon. Because of its high surface area, the activated carbon paved the way for the high dispersion of the active phase. The authors focused on the esterification of oleic acid over tungstophosphoric acid (HPW) supported on activated carbon derived from passion fruit biomass (ACP), which was prepared by chemical activation using zinc chloride. The composites (HPW/ACP) were prepared to contain 10%–30% w/w of HPW by two procedures, i.e., aqueous impregnation method and incipient moisture. The results revealed that the activated carbon from the passion fruit seed residue provided a high surface area ( $465\text{ m}^2/\text{g}$ ) and the HPW impregnation method on activated carbon was a definitive factor on the catalyst performance. SEM, XPS, NMR, and  $\text{N}_2$  adsorption-desorption results revealed that in the catalyst acquired by aqueous impregnation (HPW/ACP), surface area was reduced to  $50\text{ m}^2/\text{g}$ ; HPW was quite dispersed in the internal pores of the ACP support and provided superior acidity. The initial moisture impregnation (HPW/IACP) formed HPW particles on the external surface of the support. However, because of little interaction among them, a surface area of  $90\text{ m}^2/\text{g}$  resulted. The best result for the esterification of oleic acid with methanol was 86.4% conversion with the catalyst  $\text{HPW}_{30}/\text{ACP}$ , at  $100^\circ\text{C}$ , after 2 h. The leaching of HPW active phase after the reaction was as low as  $\sim 1.0\%$ – $2.6\%$ .

Levulinic acid is among the most important chemicals derived from biomass [266]. Some of useful compounds that can be synthesized from levulinic acid are illustrated in Scheme 6.22. Therefore, how to synthesize levulinic acid and



**SCHEME 6.22** Chemical compounds of great value that could be obtained from alkyl levulinates.



different by-products from biomass derivatives is being studied. Among these derivatives, the alkyl levulinates, particularly n-butyl levulinate, are very important, since they currently have many applications, such as in fragrance manufacture or an additive in gasoline and biodiesel [267]. A majority of the current industrial processes for the manufacture of levulinic acid and alkyl levulinates use phosphoric or sulfuric acids as a catalyst in each step [268], which are of course harmful to health and the environment due to their toxicity. In order to resolve these problems, Pizzio and coworkers [269] synthesized a magnetic catalyst based on Keggin-type heteropoly acids immobilized on mesoporous silica-coated magnetite particles having a core shell structure. The catalyst activity was examined over the esterification of levulinic acid with n-butanol. The reaction kinetics was investigated by systematically varying all reaction parameters, e.g., catalyst loading, stirring speed, reactant molar ratio, and temperature. In addition, the reaction was observed to be free from any external mass transfer and intra-particle diffusion limitations, being kinetically controlled by nature. The experimental data fitted to a second-order kinetic equation. In addition, the experimental activation energy of 17 kcal/mol was found for the reaction. The reaction was conducted in the absence of a solvent, which helped put it in the green chemistry category. In addition, the resulting catalyst could be used repeatedly without any considerable decrease in activity.

Conversion of cellulose in biomass is complicated by the fact that it is insoluble in water as well as in most organic solvents. In addition, cellulose is quite resistant to many manners of chemical and biological transformations [270,271].

From an industrial point of view, novel concepts in the field of biomass-to-energy conversion must fulfil the following three criteria:

- (a) low specific investment cost even at small plants as big plants requires transport of biomass over long distances;
- (b) low operation costs; and
- (c) manufacture of a valuable product or a mixture of product.

Indeed, many of the methodologies developed to convert the lignocellulosic biomass to energy carrier molecules such as hydrogen, syngas, methane, or ethanol do not fulfil all of the above criteria. While gasification of biomass requires high temperatures and laborious efforts for gas purification [272,273], supercritical reforming has the problem of high investment necessary to provide corrosion-resistant equipment [274,275]. On the other hand, aqueous reforming has been observed to be restricted to a small array of biogenic substrates and is usually operated in low concentrations. Even under such conditions, the reaction is still characterized by the formation of undesired solid carbohydrate polymers as dead-end products [276]. In addition, the fermentative processes responsible for the conversion of biomass to ethanol or methane are usually restricted to carbohydrate substrates which directly or indirectly compete with the food industry.

Guldi and others [277] synthesized different Keggin-type polyoxometalates and characterized them to identify the optimized homogeneous catalysts for the selective oxidation of biomass to formic acid with oxygen gas as an oxidizing agent and *p*-toluenesulfonic acid as an additive. Employing the optimized polyoxometalate catalyst system  $H_8[PV_5Mo_7O_{40}]$  (HPA-5), a total yield of 60% for formic acid (with respect to carbon in the biogenic feedstock) could be achieved for glucose within 8 h and for cellulose within 24 h. The characteristics of the transformation were its mild reaction temperature, excellent selectivity toward formic acid in the liquid product phase, and its applicability to an array of biogenic raw materials including complex biogenic mixtures and nonedible biopolymers.

Not many processes for the direct conversion of biomass raw materials into valuable chemicals have been successful in practice. Formic acid and acetic acid are both important chemicals in high demand in the chemical, agricultural, and pharmaceutical industries.

Han and coworkers [278] managed to convert the raw biomass materials directly into fine chemical compounds of great value from both economic and ecological perspectives. They reported that a Keggin-type V-substituted phosphomolybdic acid catalyst, i.e.,  $H_4PVMo_{11}O_{40}$ , was capable of converting various substrates derived from biomass to formic acid and acetic acid with high selectivity in an aqueous media and oxygen atmosphere. Under optimized reaction conditions, the heteropoly acid  $H_4PVMo_{11}O_{40}$  gave an extraordinary high yield for formic acid (67.8%) from cellulose, which far exceeded the values gained by former catalytic systems. The study revealed that due to their strong acidities, heteropoly acids were generally efficient catalysts for the conversion of biomass, while the composition of the metal addenda atoms in the catalysts crucially affected the reaction pathway and the product selectivity.

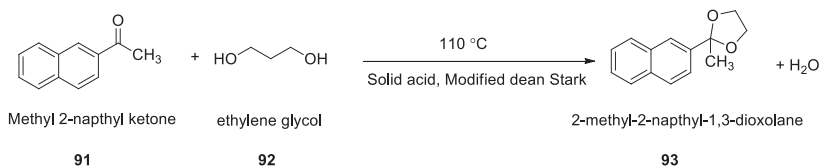
Defunctionalization of biomass and then converting it into various platform molecules is a totally desirable means in the development of sustainable chemical industry. Such feedstock may be generated through the synthesis of syngas (Fischer-Tropsch method), fermentation, and extraction of biomass. Among these routes sugars, 5-hydroxymethylfurfural, glycerol, butanol, ethanol, ethylene glycol, etc. are promising feedstock to make a variety of value-added chemicals. However, acetals and ketals are extensively used in fragrance and flavor industries, due to the type of *notes* they create, while some of these compounds are used as oxygenated fuel additives. Therefore, glycerol and other glycols may be converted into more valuable commodities via acetalization and ketalization, which are acid catalyzed processes. The common method for the synthesis of acetals and ketals of glycerol or other glycols is the reaction with aldehyde or ketone catalyzed by an acid [279,280].

Acetals and ketals of glycerol provide invaluable components for the formulation of diesel, gasoline, and biodiesel fuels. Such oxygenated compounds, when incorporated into standard diesel fuel, will result in emissions with significant reduction in particulate matter, carbon monoxide, hydrocarbons, and

unregulated aldehydes [281,282]. Likewise, these compounds may serve as cold flow improvers in biodiesel and also reduce its viscosity [281]. This issue is very important because of the growing demand for novel additives especially for biodiesel, which are nontoxic, biodegradable and renewable. Acetals and ketals as additives to biodiesel enhance its viscosity and help it meet the conventional requirements of flash point and oxidation stability [283]. The propylene glycol acetal of methyl naphthyl ketone is a flavoring material with orange blossom note, whose synthesis involves the acetalization of the methyl naphthyl ketone with propylene glycol [279].

The industrial process for the synthesis of acetals is catalyzed by strong acids, e.g., *p*-toluenesulfonic acid. The acetalization of ethylene glycol with methyl 2-naphthyl ketone to afford 2-methyl-2-naphthyl-1,3-dioxolane is commercially important and it has the orange blossom fragrance.

Yadav et al. [284] catalyzed the synthesis of 2-methyl-2-naphthyl-1,3-dioxolane by acetalization of ethylene glycol with methyl 2-naphthyl ketone with several heterogeneous solid acid catalysts containing 20% (w/w) Cs<sub>2.5</sub>H<sub>0.5</sub>PW<sub>12</sub>O<sub>40</sub>/K10 (Cs-HPW/K10), UDCaT-4, UDCaT-5, and K10 clay. Among the mentioned species, 20% (w/w) Cs-HPW/K10 catalyst was observed to be the most efficient catalyst, affording 87% conversion of methyl 2-naphthylketone with 100% selectivity toward 2-methyl-2-naphthyl-1,3-dioxolane. Several parameters affecting the reaction were studied and optimized. The optimized reaction conditions were 110°C, molar ratio of methyl 2-naphthyl ketone to ethylene glycol 1:2, catalyst loading of 0.02 g/cm<sup>3</sup>, agitation speed of 800 rpm, and time 3 h (Scheme 6.23).

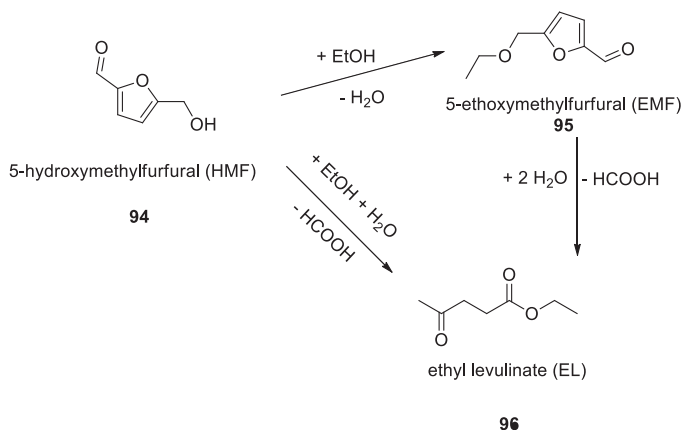


**SCHEME 6.23** Acetalization of ethylene glycol with methyl 2-naphthyl ketone.

Among the different chemicals derived from biomass, 5-hydroxymethylfurfural of central importance, as it is convertible into high-quality fuels and totally value chemicals like  $\gamma$ -valerolactone, levulinic acid, ethyl levulinate, 2,5-dimethylfuran, 5-ethoxymethylfurfural, etc. owing to its specific structure with two functional groups united with a furan ring [285–288].

In the past decade, an array of acidic catalysts have been prepared for the synthesis of 5-ethoxymethylfurfural or ethyl levulinate. For example, Lanzafame and coworkers [289] studied the etherification of 5-hydroxymethylfurfural with EtOH over a series of mesoporous silica catalysts and compared the results with the behavior of Brønsted acids such as sulfuric acid and Amberlyst-15 resin. Although heteropoly acids are also extensively applied for the conversion of

biomass into biofuels [290], phosphomolybdic acid hydrate (HPMo) used as a catalyst in this reaction has rarely been reported. Chen and others [291] reported the conversion of 5-hydroxymethylfurfural into 5-ethoxymethylfurfural and ethyl levulinate using MOFs-based polyoxometalate [Cu-BTC][HPM] (NENU-5) as a catalyst. The homogeneous distribution of HPMo in the pores of Cu-BTC caused the composite combine the properties of catalytic activity of HPMo and the insolubility, large surface and hierarchical pores of Cu-BTC. The catalyst exhibited reusability and catalytic activity with 55% yield for 5-ethoxymethylfurfural and 11% yield of ethyl levulinate (Scheme 6.24).



**SCHEME 6.24** Conversion of 5-hydroxymethylfurfural into 5-ethoxymethylfurfural and ethyl levulinate in EtOH.

Arantes and coworkers [292] synthesized heteropoly salts containing different numbers of vanadium atoms ( $\text{K}_4[\text{PVW}_{11}\text{O}_{40}]\text{-KPWV}_1$  and  $\text{K}_6[\text{PV}_3\text{W}_9\text{O}_{40}]\text{-KPWV}_3$ ) from the heteropoly acid HPW, and used them as catalysts in the hydrolysis of cellulose to change the redox properties and verify if the clusters of catalysts were involved in reaction mechanism. According to the conducted experiments, the catalysts were all observed to be active in the hydrolysis. The best results were obtained when HPW was used. This suggested that the redox properties were not of much influence on the depolymerization of cellulose and the hydrolysis mechanism were attributed to acidic properties of the media. The main products afforded by the reactions were glucose and 5-hydroxymethylfurfural, which are of great interest in the chemical industry.

Many terpenic compounds derived from essential oils are extensively utilized in the pharmaceutical, fragrance, and cosmetic industries [293,294]. In addition, they may be transformed into more valuable products providing abundant feedstock of renewable biomass-based substrates for chemical industries [293–298]. Heteropoly acids, due to their special properties, provide a desirable, green alternative to conventional acid catalysts, i.e., mineral acids, ion-exchange resins, clays, and zeolites [299,300]. Gusevskaya et al. [242]

described the cycloaddition of monoterpenes with a set of aldehydes in the presence of HPW supported on silica and bulk CsPW ( $\text{Cs}_{2.5}\text{H}_{0.5}\text{PW}_{12}\text{O}_{40}$ ) as heterogeneous catalysts. In addition to conventional 1,2-dichloroethane, the reactions were conducted in nontoxic biodegradable green organic solvents, e.g., diethylcarbonate and dimethylcarbonate, as well as 2-methyltetrahydrofuran derived from biomass. The monoterpenes and monoterpene alcohols used as substrates were limonene,  $\alpha$ -terpineol,  $\alpha$ -pinene,  $\beta$ -pinene, linalool, and nerol. Biomass-derived cuminaldehyde and *trans*-cinnamaldehyde, available from essential oils of eucalyptus and cinnamon, respectively, as the aldehydes were used along with crotonaldehyde and benzaldehyde.

Acidic cesium salt of tungstophosphoric acid,  $\text{Cs}_{2.5}\text{H}_{0.5}\text{PW}_{12}\text{O}_{40}$ , is an excellent solid acid catalyst suitable for cycloadditions of biomass-based, easily available from essential oils monoterpene compounds, such as limonene,  $\alpha$ -terpineol,  $\alpha$ -pinene,  $\beta$ -pinene, and nerol, with aldehydes, including benzaldehyde, crotonaldehyde as well as biomass-derived cuminaldehyde and *trans*-cinnamaldehyde in liquid phase. The reactions afford oxabicyclo[3.3.1]nonene compounds with potential applications in fragrance and pharmaceutical industries with satisfactory to excellent yields. The process is green and may be conducted in the biomass-derived solvent 2-methyltetrahydrofuran and eco-friendly, environmentally benign organic solvents like dimethylcarbonate and diethylcarbonate under moderate conditions with low catalyst loadings free of leaching problems. The solid CsPW catalyst could be easily separated from the reaction media, and low-boiling solvents could be removed by distillation. HPW supported on silica also demonstrated good performance.

A sustainable and renewable carbon source for the production of chemicals via catalyzed or biotechnological processes, lignocellulosic biomass is regarded as one of the most promising alternatives to petroleum [301]. One of the chemicals derived from lignocellulosic biomass is lactic acid, which is an important, valuable chemical with various applications in various fields such as the food industry, pharmaceuticals, and plastics. Recently, this chemical has gained even more attention as a precursor for the synthesis of bio-based chemicals, e.g., acrylic acid, 2,3-pentanedione, and acetaldehyde. The existing industrial process for the synthesis of lactic acid is based on enzymatic fermentation of carbohydrates (such as sucrose), which as a sensitive process (in terms of feed quality/purity), requires rigorous adjustment of the reaction conditions and gives rise to a significant amount of waste. Lactic acid may be synthesized from glucose via a catalyst of noticeable Lewis acidity or following a retro-aldol reaction pathway, which is favored under basic conditions. However, glucose itself is produced from the hydrolysis of cellulose, which requires Brønsted acidity. Given the development of a one-pot catalyzed process for the synthesis of lactic acid from cellulose, Triantafyllidis and coworkers [302] investigated the influence of oxides ( $\text{SiO}_2$ ,  $\text{SiO}_2\text{-Al}_2\text{O}_3$ ,  $\text{Nb}_2\text{O}_5$ ,  $\text{Nb}_2\text{O}_5\text{-SiO}_2$ ,  $\text{Nb}_2\text{O}_5\text{-Al}_2\text{O}_3$ ), heteropoly acids (HSiW, HPW), and heteropoly acids supported on the oxides as bifunctional catalysts with varying ratios of Lewis to Brønsted acid sites

on the conversion of cellulose into lactic acid. The experimental data revealed that the acidity type would play an important role in the reaction pathway and accordingly in the product distribution. Amongst the supported catalysts tested, TSA/SiO<sub>2</sub>-Al<sub>2</sub>O<sub>3</sub> with the highest Lewis to Brønsted acidity ratio led to the highest lactic acid selectivity (38.4%) and yield (23.5%), at 61.2% cellulose conversion. For this catalyst, the effect of reaction conditions, catalyst concentration, cellulose crystallinity and the presence of other biomass components (hemicellulose and lignin) was further evaluated. The stability and reusability of HSiW/SiO<sub>2</sub>-Al<sub>2</sub>O<sub>3</sub> were established for at least three reaction cycles, while the reaction route for the cellulose conversion was verified via a power law kinetic modeling scheme.

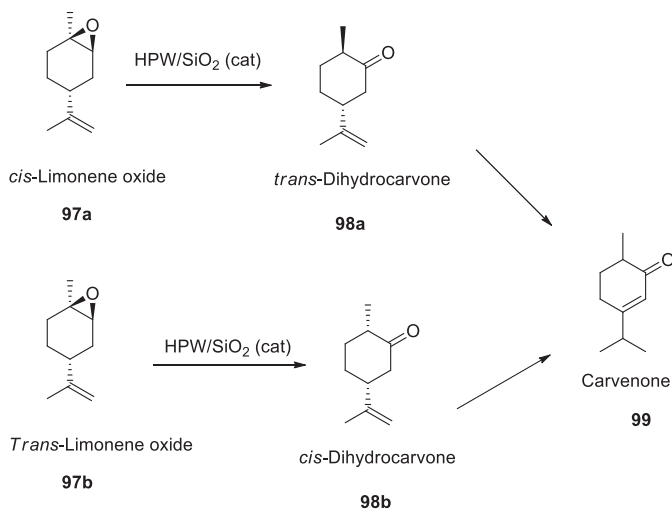
As the most plentiful class of natural products, terpenes are available at a relatively low cost from essential oils. In addition to direct applications in flavor and fragrance industry [241], terpenic compounds can be chemically converted into various valuable products [296,297]. Acid catalyzed reactions are extensively employed for this purpose; however, many of these processes still involve mineral acids as homogeneous catalysts and/or toxic solvents as reaction media.

Heteropoly acid catalysts have been successfully applied in various reactions of terpenes [300]. For instance, Gusevskaya and coworkers [303] reported the isomerization [304,305] and etherification/esterification [306,307] of terpenes over the heteropoly acid catalysts and their coupling with aldehydes [308].

Limonene oxide, which can be synthesized from citric essential oils as well as the epoxidation of limonene, is one of the most widespread terpenic compounds. Through acidic catalysis, limonene oxide may be converted into a variety of valuable products for flavor and fragrance industry, such as carveol, exocarveol, dihydrocarvone, and carvenone [309]. In most cases, satisfactory selectivities were achieved only for *para*-menthenic allylic alcohols like carveol and exocarveol [310–313].

The authors reported the isomerization of limonene oxide over silica-supported HPW in green solvents, i.e., dimethylcarbonate and diethylcarbonate. As low-toxin and biodegradable solvents, dimethylcarbonate and diethylcarbonate are highly recommended compared to ethanol and water [314–316]. The authors realized that the reaction can be directed to either dihydrocarvone or carvenone in these solvents merely by changing the reaction temperature. Additionally, kinetic separation of *trans*-limonene oxide and stereoselective synthesis of *trans*-dihydrocarvone were made possible by full control of the reaction parameters. The more reactive *cis*-limonene oxide was selectively transformed into the *trans*-dihydrocarvone, which is highly valuable, while *trans*-limonene oxide practically remained intact. The *trans*-limonene oxide is particularly used for the production of special biodegradable polymers such as polycarbonates and polyesters [317–319]. Commercial limonene oxide is a mixture of *cis* and *trans* isomers (which are hard to separate by physical means).

The isomerization of limonene oxide over the HPW/SiO<sub>2</sub> catalyst is illustrated in Scheme 6.25. When the catalyst was not present or in the presence



**SCHEME 6.25** Chief products of limonene oxide isomerization over HPW/SiO<sub>2</sub>.

of pure silica, the substrate conversion did not occur at all in blank reactions in any of the solvents used. The structures of reaction products were identified as dihydrocarvone, carvenone, 1-methyl-3-isopropenyl-cyclopentyl-1-carboxaldehyde, and limonene-1,2-diol. Importantly, HPW is not soluble in dimethylcarbonate and diethylcarbonate (unlike 1,4-dioxane); this means that the reaction could proceed under truly heterogeneous conditions. The selectivity for carvenone formation was observed to be strongly dependent on the reaction temperature.

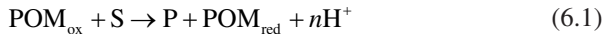
## 6.6. Applications of heteropoly acids in removal of pollutants

The deposition of solid waste generated by various industries that pollutes water, air, and soil is one of the main environmental issues. Green chemistry dictates that the elimination or reduction of hazardous waste and substances must be considered in every chemical/industrial process [320,321]. Great developments have been achieved regarding the application of heteropoly acids in this area, and a few examples will be addressed in this section.

While aerobic processes are usually employed to treat both domestic and industrial wastewaters, it has often been shown that they are not able to totally treat all xenobiotic, harmful organic compounds. The textile preparation, dyeing, and finishing industry is among the industrial sectors that produce large volumes of wastewater with a complex composition made of refractory colors, chemical oxygen demand (COD), total dissolved solids (TDS), temperature, and high pH [322].



Dyes must exhibit a high extent of biochemical, chemical, and photolytic stability so that they fulfil the permanence requirements posed by both consumers and retailers. Consequently, they are not easily degraded under usual aerobic conditions governing biological treatment plants [323,324]. Of the myriad dyes presently in use and listed in the Color Index, about two-thirds are unmetallized azo and metal complexed azo dyes, a majority of which are utilized as acid dyes with applications in wool and nylon fibers (2,3). In addition, it is known that acid dyes resist traditional physicochemical processes (coagulation, activated carbon adsorption, microfiltration etc.) due to their relatively low molecular weight (~ 1000 g/mol) and high water solubility (10 g/L) [325]. Recently, novel treatment catalysts, chiefly in the form of transition-metal salts or oxides, and heteropoly acids, have been designed and introduced to enhance the chemical oxidation of such dyes [326]. In particular, and interestingly, heteropoly acids and their salts have been used as oxidation catalysts since many of them may serve as mild oxidizing agents [327]. Their unique physicochemical, structural properties can be determined and adjusted at nano-dimensions. They have been applied as environmental catalysts for the degradation of several organic priority pollutants [328–330]. Oxidation reactions catalyzed by heteropoly acids are envisioned as a mainly two-stage redox cycle, in which first an interaction takes place between the organic substrate (S) (the electron donor) and the oxidized form of the polyoxometalate (POM<sub>ox</sub>), leading to products (P) and reduced form of the catalyst (POM<sub>red</sub>). The latter stage is also believed to be the rate-determining step throughout the polyoxometalate-catalyzed aerobic oxidation [71]:



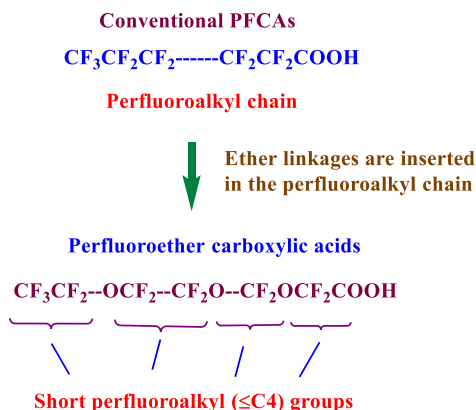
After that, the catalytic cycle is completed by reoxidation of the reduced catalyst, preferably by a molecular oxygen [71]:



*Treatment for Acid Dye Wastewater.* Idil Arslan-Alaton [331] utilized tungstosilicic acid (H<sub>4</sub>SiW<sub>12</sub>O<sub>40</sub>) as a photochemical and wet air oxidation catalyst for the treatment of aqueous Acid Orange 7. Acid Orange 7 (also known as Orange II) was selected as a well-studied, refractory, and representative textile azo dye [332–335]. The catalytic effect of SiW<sub>12</sub>O<sub>40</sub><sup>-4</sup> on wet air oxidation and photochemical treatment of Acid Orange 7 was investigated to obtain an insight into the differences between the reaction kinetics of uncatalyzed oxidation and catalyzed by SiW<sub>12</sub>O<sub>40</sub><sup>-4</sup>. In the wet air oxidation experiments of Acid Orange 7 catalyzed by polyoxometalate ions, an organic (isopropanol; IsOH) and inorganic (bromide in the form of KBr) OH<sup>•</sup> scavenger was also added to probe the possible involvement of OH<sup>•</sup>.

Recently, perfluorocarboxylic acids (PFCAs) like perfluorooctanoic acid (C<sub>7</sub>F<sub>15</sub>COOH, PFOA) have received a great deal of attention since they are

contaminants ubiquitously present in the environment [336–338]. These compounds have been extensively used as products or materials for surfactants. For instance, they are used as emulsifying agents in manufacture of fluoropolymers, surface treatment agents for electronic materials, and additives for paintings and waxes, because of their high thermal and chemical stability, high surface active effect, and high transparency [337]. Perfluoroether carboxylic acids are among important alternatives to PFCA-based surfactants [339,340]. In these molecules, ether linkages are incorporated into the perfluoroalkyl chain of PFCAs so that the molecules include only short perfluoroalkyl ( $\leq C4$ ) groups (Scheme 6.26).



**SCHEME 6.26** PFCAs and perfluoroether carboxylic acids.

These chemicals are more likely to decompose easier than PFCAs, because of the presence of ether linkages. However, the decomposition of perfluoroether carboxylic acids has not been reported. Conventional techniques for organic pollutants in water, e.g., treatment with Fenton's reagent ( $\text{Fe}^{2+} + \text{H}_2\text{O}_2$ ) [341] and irradiation with UV-vis light in the presence of hydrogen peroxide [342], can only slightly decompose PFCAs, since the reactivity of OH radicals with PFCAs in water is not very high [343,344]. Water-soluble heteropolyacids have proved to be attractive photocatalysts for the decomposition of PFCAs and related chemicals owing to their multielectron capability and high stability under highly acidic conditions [328,345]. The oxidation potential of  $[\text{PW}_{12}\text{O}_{40}]^{3-}$  is estimated to be more positive than that of titanium(IV) oxide ( $\text{TiO}_2$ ) [346]. The produced fluoride ions have substantial treatment processes: addition of a calcium salt leads to the formation of  $\text{CaF}_2$ , which is harmless to the environment, a raw material for hydrofluoric acid, the global demand for which is increasing. Development of a system for the decomposition of fluorochemicals is important since such systems not only reduce the environmental impact of these chemicals but also provide a means for the recycling of a fluorine resource.



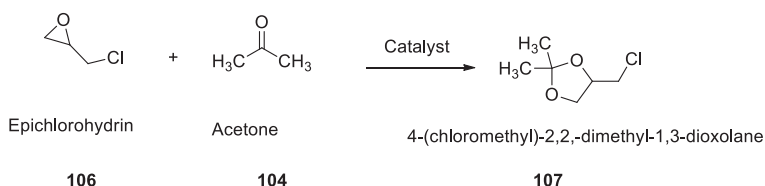
is purified and oxidized with oxygen to give cumene hydroperoxide; then, in the third step, this is isolated and decomposed with sulfuric acid to afford phenol with equimolar quantities of acetone. Using an excess of benzene in Step I is necessary (to avoid dialkylation) and much of this must be recovered and reused. As a chief product, the peroxide generated in step II is an explosive. Therefore, conversion of the cumene is restricted to  $\sim 25\%$  so that the concentration of cumene hydroperoxide is kept low. This is the most hazardous step, and several accidents have been reported [349]. Step II produces around 35% (w/w) cumene hydroperoxide, which is then concentrated to 80% (w/w) in order to produce phenol and acetone. The manufacture and/or concentration of cumene hydroperoxide has inherent process hazards leading to runaway situations and explosions [349]. Then the unreacted cumene must be recovered and reused; in Step III, there are other by-products which need to be controlled [350,351]. Various Brønsted and Lewis acids are used to decompose cumene hydroperoxide in a temperature range of 0–75°C to yield phenol and acetone with some dicumyl peroxide. However, sulfuric acid is still preferred as it secures high yields of phenol. Dicumyl peroxide, in turn, is converted into a mixture of R-methyl styrene, phenol, and acetone [352,353]. The catalyst strength as well as reaction temperature substantially affects the selectivity of the products during the decomposition of cumene hydroperoxide [354,355]. Decomposition of cumene hydroperoxide to acetone and phenol has been investigated by numerous research groups, with various catalysts such as metals, clays, and resins.

Yadav and coworkers [356] engineered a novel technique for the synthesis of bisphenol-A from cumene hydroperoxide and phenol in a single-pot reaction using 20% (w/w) HPW supported on acidic clay (K10) at 100°C, wherein cumene hydroperoxide produced in cumene itself and was used along with phenol to make bisphenol-A. The process was atom economical, producing water as a coproduct. Compared to the traditional route of synthesizing bisphenol-A from phenol and acetone, the yield was improved by 58% and selectivity toward bisphenol-A was improved by 33%. Besides, the reaction mass efficiency was enhanced by 28% and the environmental impact factor was decreased by 25%. In addition to preserving the atom economy, the hazard due to the concentration and handling of cumene hydroperoxide was eliminated. In the current process, cumene hydroperoxide produced from cumene was used as such without any separation.

In recent years, bioglycerol has been converted into more valuable chemicals as a result of several characteristics of glycerol arising from its unique availability, structure, properties, and renewability. Biodiesel production gives rise to 10% (w/w) glycerol as a coproduct, rendering it available in huge amounts [357]. A few reaction pathways for the selective catalytic conversion of bioglycerol into commercially useful chemicals are oxidation, dehydration, hydrogenation (hydrogenolysis), pyrolysis and gasification, thermal reduction into syngas, steam reforming, transesterification, oligomerization, etherification, polymerization, chlorination, acetalization, and carbonylation [358].

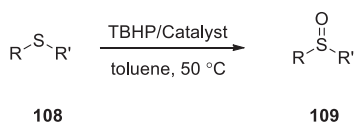
Epichlorohydrin may be synthesized from bioglycerol via green chlorination routes. It is therefore a source of further valorization. Chloromethyl-1,3-dioxolane and its derivatives have important applications as pharmaceutical intermediates, which are obtained through the cycloaddition of epichlorohydrin with a ketone. Chloromethyl-1,3-dioxolane derivatives are used as plasticizers, tranquilizers, and potential monomers for polymerization and polycondensation. They are also important intermediates in the synthesis of a new class of adrenoceptor antagonists [359–361]. These chemicals are often used as protecting groups for 1,2-diols, aldehydes, and ketones in the synthesis of natural product. Several types of Brønsted and Lewis acid catalysts like  $\text{TiCl}_4$ ,  $\text{SnCl}_4$ ,  $\text{RuCl}_3$ ,  $\text{BF}_3\text{-OEt}_2$ , anhydrous  $\text{CuSO}_4$ ,  $\text{TiO}(\text{TFA})_2$ ,  $\text{TiCl}_3$  (OTf), and methyl rhenium trioxide have been utilized in the synthesis of 1,3-dioxolane derivatives [362–364]. The synthesis of 1,3-dioxolanes from epoxides and carbonyl compounds with various solid acid catalysts, e.g., zeolites (ZSM-5, Y, and ultrastabilized HUSY), bentonite clay, and K10 montmorillonite, has been achieved and found to provide satisfactory results [365,366]. These catalytic systems are awash with oligomerization and polymerization. Amrute et al. [367] overcame these problems using 10%  $\text{MoO}_3$  supported on  $\text{SiO}_2$  as a reusable catalyst. However, the reaction required high catalyst loadings and longer reaction times.

Yadav et al. [368] successfully incorporated  $\text{Cs}_{2.5}\text{H}_{0.5}\text{PW}_{12}\text{O}_{40}$  (Cs-HPW) onto the K10 clay via in situ generation of the salt in the K10 clay [369,370]. They investigated the cycloaddition of epichlorohydrin with acetone using 20% (w/w) Cs-HPW supported on K10 clay. Different catalysts such as K10 clay, HPW-20%/K10 clay, Cs-HPW-20%/K10 clay, and Cs-HPW-20%/HMS were synthesized, and their efficiencies were studied. Cs-HPW-20%/K10 clay was found to be highly active. The catalyst was characterized by different methods, e.g., XRD, FTIR, SEM, and  $\text{NH}_3$ -TPD. A temperature of  $70^\circ\text{C}$  and mole ratio of epichlorohydrin to acetone equal to 1:8 was observed to afford the best results. The reaction was 100% atom economical and green. The catalyst was reusable. A kinetic model for the cycloaddition was developed. The reaction mechanism was found to be of the Langmuir-Hinshelwood-Hougen-Watson (LHHW) type, with very weak adsorption of both reactants in the absence of any diffusion resistance. The activation energy of the reaction was 15.77 kcal/mol (Scheme 6.28).



**SCHEME 6.28** Cycloaddition of epichlorohydrin with acetone.

Sathicq and coworkers [371] gathered different residues from a variety of wastes to prepare mixed compounds and used them as catalyst supports. Such wastes included sand and concrete from the building industry, used tires, and nonreturnable glass bottles. The prepared supports were impregnated with molybdophosphoric acid and characterized by various techniques such as potentiometric titration, SEM-EDS, optical microscopy, and textural property analyses. The bifunctional properties of the new catalysts were assessed in two relevant transformations under green conditions, i.e., the selective oxidation of sulfides to sulfoxides with a green oxidizing agent like *tert*-butyl hydroperoxide (Scheme 6.29). As a specific objective, the efficiency of recyclable materials was analyzed as well.



**SCHEME 6.29** Selective oxidation of sulfides to sulfoxides using a *tert*-butyl peroxide/catalyst system.

## 6.7. Miscellaneous applications of heteropoly acids

So far, methyl *tert*-butyl ether (MTBE) has been the most widely used octane booster additive for automotive fuels. Its use has extensively allowed the elimination of tetraethyl lead as the antiknocking component of gasoline. The annual world production of methyl *tert*-butyl ether is as high as about 30 million tons. However, because of objections from an environmental viewpoint, the tendency appeared recently to limit or even totally eliminate its application. Synthesis of methyl *tert*-butyl ether via the electrophilic addition of methanol to isobutylene or etherification of methanol/*tert*-butyl alcohol mixture needs catalysts with strong Brønsted acidity. Therefore, the zeolite acid catalysts [372–374], modified zeolites [375–377], and silicates [378] have been widely studied in the synthesis of methyl *tert*-butyl ether in gas phase. Another group of catalysts that have attracted the interest are heteropoly acids, which are considered among the strongest inorganic acids. Bieláński and coworkers in 2003 investigated the physicochemical aspects of the methyl *tert*-butyl ether synthesis in gas phase over tungstosilicic acid ( $\text{H}_4\text{SiW}_{12}\text{O}_{40}$ ) as a catalyst. They studied the interaction of both substrates, i.e., methanol and isobutylene, and the product, i.e., methyl *tert*-butyl ether, with the crystalline tungstosilicic acid using FT-IR and calorimetric measurements. With kinetic measurements they managed to propose a mechanism for the catalyzed reaction. The mechanism suggested that the resulting reaction order was positive at the initial state of the catalytic process (low bulk concentration of methanol and high concentration of loose protons), and would become negative at the steady state. A set of kinetic equations were proposed to describe all the processes. For the preparation of tungstosilicic

acid-supported catalysts, a series of oxide supports, i.e.,  $\text{TiO}_2$ ,  $\text{SiO}_2$ ,  $\text{SiO}_2\text{-Al}_2\text{O}_3$ ,  $\gamma\text{-Al}_2\text{O}_3$ , and  $\text{AlPO}_4$ , with increasing basicity was used. It has been demonstrated that the activity decreased with the increasing basicity as a result of strong bonding protons by the surface of the support [379].

Biodiesel has been extensively researched in the world because of its renewability, nontoxicity, cleanness, and biodegradability. Raw materials of biodiesel are extensively produced by transesterification of soybean oil, palm oil, colza oil, animal fat, and waste cooking oil [380–385].

The cesium salt of tungstophosphoric acid, i.e.,  $\text{Cs}_{2.5}\text{H}_{0.5}\text{PW}_{12}\text{O}_{40}$  (CsPW) is a super solid acid with intact Keggin structure. More specifically, it is widely used as a heterogeneous catalyst for its high acid value, strong Brønsted acidity, thermal stability, and catalytic activity, and solubilization in water and organic solvent [386]. CsPW, as a green and economically practical solid heteropoly acid catalyst [387], is readily separable by filtration; thus it could help avoid the problems with liquid strong acids (e.g., sulfuric acid) or strong bases (e.g., KOH), equipment corrosion and acidic or alkali wastewater [388–390]. Therefore, CsPW may be a favorable candidate as an excellent catalyst for industrial production processes of biodiesel. Zou and coworkers [391] studied the transesterification of waste cooking oil. The CsPW protected by cucurbit[7]uril (CsPW-CB[7]) was prepared as a highly effective catalyst for the direct production of biodiesel using the transesterification of waste cooking oil. The prepared CsPW-CB[7] was characterized by XRD and FT-IR techniques. In addition, to optimize the operating parameters affecting the conversion rate, response surface methodology was used. Under the optimized experimental conditions, i.e., 2% (w/w) of the catalyst, methanol/oil molar ratio of 11:1, reaction time of 150 min and temperature of 70°C, a maximum conversion rate of 95.1% was reached. Assuming a pseudofirst order for the reaction, the activation energy was calculated to be 36.0 kJ/mol, which indicates that the reaction is easy to conduct. The results demonstrated that the CsPW-CB[7] catalyst could exhibit good catalytic efficiency and its excellent potential application in biodiesel production.

The biodiesel product was also analyzed by a GC/MS spectrometer, and the quality of the biodiesel product was compared with ASTM D6751 and GB/T25199–2010 standards.

$$AV = 56.1V \times C_{\text{KOH}} / M$$

$$C = \frac{AV_i - AV_f}{AV_i} \times 100\%$$

where  $AV$  is the acid value in mg KOH/g,  $V$  is the consumption volume of potassium hydroxide solution in mL,  $C_{\text{KOH}}$  is the concentration of potassium hydroxide in mol/L,  $M$  is the mass of samples, g,  $C$  is the conversion rate of the waste cooking oil in percent, and  $AV_i$  and  $AV_f$  are the acid values of the initial waste cooking oil and the final biodiesel product in mg/g, respectively.



Conventional industrial biodiesel processes occur using homogeneous alkaline catalysts [392]. However, a limitation to alkali catalyzed reactions is their sensitivity to both free fatty acids and water [393,394].

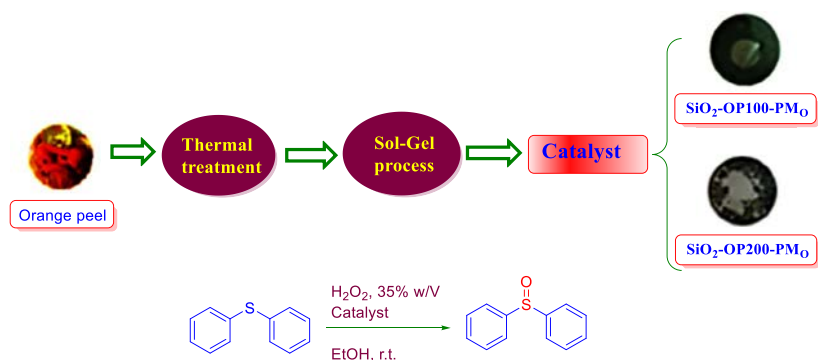
Cyclodextrins are cyclic oligosaccharides with six to eight glucose units linked by 1,4- $\alpha$ -glucosidic bonds demonstrating a donut-shaped ring structure [395]. Due to the specific architectural conformation of the hydrophilic exterior shell and hydrophobic interior cavity, cyclodextrins can accommodate organic and inorganic molecules of proper size in their cavity to give host/guest inclusion complexes by hydrophobicity, particular steric effects, and a variety of interactions including dipole-dipole interactions, electrostatic forces, van der Waals forces, dispersive forces, and hydrogen bonding [396]. In a previous work [397], it was demonstrated that a bridged cyclodextrins dimer was able to form a stable host/guest inclusion complex with the heteropoly acid  $H_9[P_2Mo_{15}V_3O_{62}]$ . Zou and coworkers [387] prepared the inclusion complex of  $Cs_{2.5}H_{0.5}PW_{12}O_{40}$  with bridged bis-cyclodextrin (CsPW/B) as a very efficient catalyst to be used in the direct production of biodiesel via the transesterification of waste cooking oil. Under the optimized experimental conditions, i.e., methanol/oil molar ratio of 9:1, 3% (w/w) of the catalyst, temperature of 65°C, and reaction time of 180 min, up to 94.2% of the waste cooking oil was converted. The physical properties of the biodiesel sample met the requirement of the ASTM D6751 standards. The novel CsPW/B catalyst used for the transesterification could result in 96.9% fatty acid methyl esters and 86.5% of the biodiesel product could act as an ideal substitute for diesel fuel, indicating its excellent potential application in the production of biodiesel.

Acid-catalyzed esterification is usually conducted in the liquid phase using mineral acid catalysts, e.g., sulfuric, hydrochloric, hydrofluoric, and phosphoric acids, which of course cause corrosion in the reactors and also environmental problems [398].

In order to avoid the usual problems with heteropoly acids as a catalyst, Pires and coworkers [399] attempted to support them on an appropriated solid as a way to prevent leaching of the acid into the reagent solution and maintain the advantages of the heterogeneously catalyzed reaction. For this purpose, they used the widely available kaolin waste generated by kaolin industries together with the waste produced during the distillation process used in the deodorization of palm oil. They reported the esterification of the distillate (DDPO) with ethanol for the production of ester over a line of catalysts containing 20%–40% of HPW supported on kaolin in the waste. The reaction was also performed over MCM-48, MCM-41, and SBA-15 molecular sieves modified with 20% HPW. EtOH was chosen because of its renewability, abundance, and low toxicity in comparison with methanol and other alcohols. The surface acidities were measured by titration. The catalytic performance of the catalysts in the esterification of the waste generated during the deodorization processes of palm oil were studied. The results showed that the materials had great potential in the promotion of heterogeneous acid-catalyzed organic transformations.

The orange juice industry generates a huge amount of citrus waste, which is almost half the weight of the used fresh fruit. It is composed of peel, seeds, pulp, and leaves, annually amounting to 15 million tons [400,401]. In some juice industries, the liquid is removed from the residue, and the dry solid is sold to cosmetic industries or used as cattle feed. At any rate, the treatment of citrus waste may represent a huge additional cost, and the disposal in open dumps is a traditional option some industries choose.

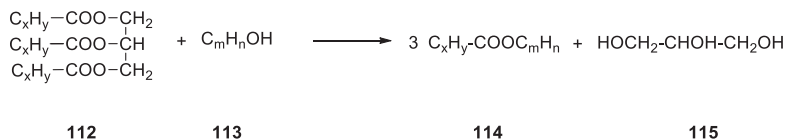
With respect to their application as redox catalysts, Belén et al. [402] used heteropoly acids and with hydrogen peroxide—an eco-friendly oxidizing agent due to its oxygen content, low cost, and the fact that water is the only by-product of the reaction—in the selective oxidation of anilines, alcohols, phenols, naphthols, and sulfides [403–405]. However, due to usual problems with heteropoly acids as a catalyst, the reactions were studied using heteropoly acids supported on conventional oxides [406] or their pyridine salts [407] to convert them to heterogeneous catalysts. Of the various methods used to convert bulk heteropoly acids to heterogeneous catalysts, their inclusion in a silica matrix during the sol-gel process has been one of the best strategies [408]. However, the selective conversion of sulfides to sulfoxides is very important both in the industry and in basic research [409,410], particularly due to their therapeutic properties [411]. The author used the orange waste as a source for charcoal, and its incorporation into a silica matrix that could serve as a support for heteropoly acids. The prepared solids were tested as heterogeneous catalysts over the selective oxidation of diphenyl sulfide to diphenyl sulfoxide in a greener process utilizing aqueous hydrogen peroxide as an oxidizing agent and ethanol as a solvent, at ambient temperature (Scheme 6.30). We expect that this strategy could be used for the valorization of citrus waste generated by the juice industry.



**SCHEME 6.30** Selective oxidation of diphenyl sulfide.

Ethyl or methyl ester of a long chain fatty acid may be synthesized from vegetable oil via the transesterification reaction shown in the equation below, in which a fat (triglyceride of fatty acid) and a small alcohol (methanol or ethanol)

are reacted to afford a monoester of fatty acid and glycerin. For instance,  $x=17$ ,  $y=33$ ,  $m=2$  and  $n=5$  correspond to the reaction between triolein (the main component of palm oil) and ethanol to afford ethyl oleate (Scheme 6.31).



**SCHEME 6.31** The transesterification reaction.

Biodiesel has its own disadvantages in the conventional production process. A homogeneous base such as potassium hydroxide has been used for the transesterification [412]. When the reaction is complete, the catalyst is dissolved into the product liquid, usually neutralized by an acid and then treated as waste. Because of the posttreatment necessary for the waste solution with hazard base and acid, the process is expensive. In addition, there is the corrosion of equipment. It is difficult to utilize glycerin efficiently since it is contained in the waste aqueous solution and therefore it must be combusted during the posttreatment.

Under supercritical conditions (high pressure and temperature), the transesterification proceeds in the absence of any catalyst [413]. The noncatalytic reaction does not suffer from the above disadvantages, but to achieve the supercritical conditions the energy consumption and cost for operation and equipment are increased.

Therefore, using solid (heterogeneous) catalysts is favorable for this reaction. As solid base catalysts, pure and modified CaO [414,415], alkaline zeolite [416], and alkali-modified alumina [417,418] have demonstrated high activities for this reaction. In general, efficient reaction rates are obtained at temperatures as low as 60°C, while the liquid phase reaction can be conducted under atmospheric pressure since the reaction temperature is lower than the boiling point of alcohol. However, avoiding the dissolution of these base catalysts seems difficult, especially when the raw materials are contaminated with a small amount of free fatty acids and/or water; fatty acids are usually contained in natural fat and waste frying oil, while water is usually contained in crude alcohol. The problem results in the irreversible loss of the catalyst and the product is contaminated with inorganic residues.

Therefore, a process consisting of two steps is suggested. Before the reactor is filled with the solid base catalyst, a solid acid catalyst is applied to remove the fatty acids by the esterification of the fatty acid with the alcohol. The process uses the insolubility of the solid acid in an acidic medium. Many solid acids like sulfated mesoporous oxide [419], sulfonated carbon [420], and zeolite [421] exhibit activities for the esterification. The feasibility of this process has been investigated on a pilot scale [419]. Complexity of equipment and operation still remain problems for this two-step process.

Considering the cons and pros given above, a highly active solid acid catalyst which can achieve a practical reaction rate of the transesterification (but not the esterification) at temperatures as low as 100°C is favorable. In this regard, Katada and coworkers [422] reported that a heteropoly acid-derived solid acid catalyst, i.e.,  $H_4PNbW_{11}O_{40}/WO_3-Nb_2O_5$  calcined at 500°C (HPNbW/WNb), exhibited a higher catalytic activity for transesterification between triolein and ethanol into ethyl oleate in comparison with the activities of conventional solid acid catalysts. The HPNbW/W-Nb was insoluble in the reaction mixture, while heteropoly acids like  $H_4PNbW_{11}O_{40}$  and  $H_3PW_{12}O_{40}$  that exhibit high activities were dissolved in the reaction mixture. The activity of the catalyst was sensitive to the temperature of calcination so that temperatures around 500°C led to catalysts with the highest activity. The reaction rate was found to be maximal at 10%–30% of the ethanol/triolein molar ratio.

A wide variety of catalysts, in both homogeneous and heterogeneous phase, may be utilized to accelerate the transesterification and esterification reactions from renewable raw materials such as vegetable oils, animal fats, or free fatty acids. Among these, different catalysts can be found (e.g., basic, acid, or even enzymatic catalysts). Basic homogeneous catalysis is currently the most widely used reaching conversions close to 100% at 80°C and reaction times less than 3 h. However, minimizing the presence of water and free fatty acid in the raw materials is necessary since secondary reactions (e.g., soap formation) may take place between the catalysts and free fatty acids [423]. Such reactions result in the deactivation of the catalysts, a decrease in conversion, and an increase in the purification costs [424,425]. For this reason, using vegetable oils or animal fats with free fatty acid contents lower than 0.5% (w/w) is necessary. This necessitates the use of high purity raw materials such as virgin oils, which raises the final cost of the produced biodiesel. It is estimated that 60%–75% of the final cost of biodiesel production may be ascribed to the refining process of the raw material used. By using recycled materials (e.g., waste cooking oils), the cost would be extremely reduced. However, the free fatty acid content in these materials is higher than 10% (w/w). A possible way to resolve this problem might be designing a two-step process [426,427]; in the first step, the free fatty acids are esterified using an acid catalyst. Then in the second step, a transesterification by means of a basic catalysis is conducted. Strong Brønsted acids, such as  $H_2SO_4$ , HCl, or orthophosphoric acid, are usually used as catalysts. In this regard, heteropoly acids may be used as solid acids. In order to use heteropoly acids as heterogeneous acidic catalysts, they should be supported on porous materials [428–430]. Alcañiz-Monge et al. [431] prepared different catalysts by supporting heteropoly acids on activated carbon fibers for the esterification of palmitic acid. The influence of the catalyst (heteropoly acid) and the support on the catalytic activity have been analyzed. The results revealed that an appropriate combination of both was required to accomplish the most suitable catalysts. As of the heteropoly acids, phosphomolybdic acid appeared to be the most suitable appropriate taking into account its lowest leaching. Regarding the support,

the ones with optimum microporosity, wide enough to permit the entrance and exit of the reagents and products but not too wide to allow the leaching of the catalyst, proved to work best. In addition, the decrease in the catalytic activity and its recovery after several runs were analyzed.

The emission of harmful gases is among the crucial problems when using internal combustion engines [432–436]. Many studies have been carried out globally to reduce gas emissions while maintaining the performance of the engine. Modern cars require high-octane fuels with antiknock properties characterized by motor octane numbers to function well 92, 95, and 98. Elaboration and implementation of processes for the synthesis of environmentally friendly additives to automotive fuels are priorities for the development of the petrochemical industry.

Among the well-known applied high-octane additives, alkyl *tert*-butyl ethers have the most usage. The alkyl *tert*-butyl ethers synthesized by the reaction of isobutylene with aliphatic alcohols in the presence of heterogeneous acid catalysts [437–441]. Sassykova et al. [442] attempted to develop a synthesis technology for a number of promising tertiary esters with the carbon atoms numbers between 6 and 8, i.e., ethyl *tert*-butyl, isobutyl-*tert*-butyl, and isopropyl-*tert*-amyl. To prepare the ethers, the process of interaction of isobutylene with aliphatic alcohols over an acid catalyst was conducted. The synthesis of the additives was effected according to two schemes. As a catalyst, standard gel sulfocationites and catalysts were prepared based on the heteropoly acid/aluminum oxide and heteropoly acid/natural zeolite were tested. The selectivity of the synthesis of alkyl *tert*-butyl ethers on the heteropoly acid catalysts was found to increase with the number of carbon atoms in alcohol. With the amount of gasoline additives varying from 1% to 12%, it was demonstrated that the synthesized additives would allow the octane number to be increased, by up to 20 points in some cases. The obtained results exhibited a good acceptance of the studied base gasoline to the components of the prepared composite additives.

## References

- [1] P.T. Anastas, J.C. Warner, *Green Chemistry; Theory and Practice*, Oxford Univ. Press, 1998.
- [2] J.H. Clark, *Green Chem.* 1 (1999) 1.
- [3] M. Misono, I. Ono, G. Koyano, A. Aoshima, *Pure Appl. Chem.* 72 (2000) 1305.
- [4] M. Misono, *Catal. Rev. Sci. Eng.* 29 (1987) 269. 30, (1987) 339.
- [5] T. Okuhara, N. Mizuno, M. Misono, *Adv. Catal.* 41 (1996) 113. N. Mizuno, M. Misono, *Chem. Rev.* 98 (1998) 199.
- [6] M. Misono, N. Nojiri, *Appl. Catal.* 64 (1990) 1.
- [7] A. Aoshima, *Shokubai* 29 (1987) 378. A. Aoshima, S. Yamamatsu, T. Yamaguchi, *Nippon Kagaku Kaishi* 233 (1990).
- [8] A. Aoshima, S. Tonomura, S. Yamamatsu, *Polym. Adv. Technol.* 2 (1990) 127.
- [9] V. Belliere, C. Lorentz, C. Geantet, Y. Yoshimura, D. Laurenti, M. Vrinat, *Appl. Catal. Environ.* 64 (2006) 254.
- [10] T. Takatsuka, S. Inoue, Y. Wada, *Catal. Today* 39 (1997) 69.

- [11] L. Jaimes, M. Badillo, H. de Lasa, *Fuel* 90 (2011) 2016.
- [12] J.M. Martinez-Magadan, R. Oviedo-Roa, P. Garcia, R. Martinez-Palou, *Fuel Process. Technol.* 97 (2012) 24.
- [13] G.A. Huff, O.S. Owen, B.D. Alexander, D.N. Rundell, W.J. Reagan, J.S. Yoo, U.S. Patent 5863419, 1999.
- [14] S. Brunet, D. Mey, G. Perot, C. Bouchy, F. Diehl, *Appl. Catal. A. Gen.* 278 (2005) 143.
- [15] Z.K. Zhang, H. Jiang, S.L. Liu, Q.X. Wang, L.Y. Xu, *Chin. J. Catal.* 27 (2006) 309.
- [16] V. Belliere, C. Geantet, M. Vrinat, Y. Ben-Taarit, Y. Yoshimura, *Energy Fuel* 18 (2004) 1806.
- [17] I.V. Kozhevnikov, *J. Mol. Catal. A Chem.* 262 (2007) 86.
- [18] M. Arias, D. Laurenti, V. Belliere, C. Geantet, M. Vrinat, Y. Yoshimura, *Appl. Catal. A. Gen.* 348 (2008) 142.
- [19] Y. Kamiya, Y. Ooka, C. Obara, R. Ohnishi, T. Fujita, Y. Kurata, K. Tsuji, T. Nakajyo, T. Okuhara, *J. Mol. Catal. A Chem.* 262 (2007) 77.
- [20] A. Angelis, S. Amarilli, D. Berti, L. Montanari, C. Perego, *J. Mol. Catal. A Chem.* 146 (1999) 37.
- [21] K.U. Nandhini, B. Arabindoo, M. Palanichamy, V. Murugesan, *J. Mol. Catal. A Chem.* 223 (2004) 201.
- [22] C. Webb, H.K. Kang, G. Moffat, R.A. Williams, A.M. Estevez, J. Cuellar, E. Jaraiz, M.A. Galan, *Chem. Eng. J.* 61 (1996) 241.
- [23] W. Li, B.N. Zong, X.F. Meng, X.K.M. Zhang, J.L. Zhang, *Chin. J. Chem. Eng.* 14 (2006) 734.
- [24] D.L. Zhang, Y.J. Zhang, J.L. Zhang, X.F. Li, L.X. Lu, X.K. Meng, X.H. Mu, *Chin. J. Chem. Eng.* 14 (2006) 532.
- [25] X.U. Cuixia, Y.A.N.G. Kedi, L.I.U. Zili, Q.I.N. Zuzeng, H.E. Wei, D.A.I. Qianwen, J. Zhang, F. Zhang, *Chin. J. Chem. Eng.* 22 (2014) 305.
- [26] X. Ren, G. Miao, Z. Xiao, F. Ye, Z. Li, H. Wang, J. Xiao, *Fuel* 174 (2016) 118.
- [27] S. Ren, J. Li, B. Feng, Y. Wang, W. Zhang, G. Wen, Z. Zhang, B. Shen, *Catal. Today* 263 (2016) 136.
- [28] D. Nicholas, G.T.N. Mcnamara, T. Erin, T. Masko, A. Jacqueline, C. Urban, B. Hicks, *J. Catal.* 305 (2013) 217.
- [29] H. Yang, B. Jiang, Y. Sun, L. Zhang, Z. Sun, J. Wang, X. Tantai, *Chem. Eng. J.* 317 (2017) 32.
- [30] M. Tang, L. Zhou, M. Du, Z. Lu, X.D. Wen, X. Li, H. Ge, *Cat. Com.* 61 (2015) 37.
- [31] L. Qin, Y. Zheng, D. Li, Y. Zhou, L. Zhang, Z. Zuhra, *Fuel* 181 (2016) 827.
- [32] P. Wu, W. Zhu, B. Dai, Y. Chao, C. Li, H. Li, M. Zhang, W. Jiang, H. Li, *Chem. Eng. J.* 301 (2016) 123.
- [33] J. Ge, Y. Zhou, Y. Yang, M. Xue, *Ind. Eng. Chem. Res.* 50 (2011) 13686.
- [34] M.A. Dinamarca, A. Rojas, P. Baeza, G. Espinoza, C. Ibacache-Quiroga, J. Ojeda, *Fuel* 116 (2014) 237.
- [35] J. Xiao, L. Wu, Y. Wu, B. Liu, L. Dai, Z. Li, Q. Xia, H. Xi, *Appl. Energy* 113 (2014) 78.
- [36] K.M. Dooley, D. Liu, A.M. Madrid, F.C. Knopf, *Appl. Catal. A. Gen.* 468 (2013) 143.
- [37] S.W. Li, R.M. Gao, R.L. Zhang, J.S. Zhao, *Fuel* 184 (2016) 18.
- [38] Y. Zhang, R. Wang, *Diamond Relat. Mater.* 73 (2016) 23.
- [39] C. Jiang, J. Wang, S. Wang, H.Y. Guan, X. Wang, M. Huo, *Appl. Catal. B Environ.* 106 (2011) 343.
- [40] K. Leng, Y. Sun, X. Zhang, M. Yu, W. Xu, *Fuel* 174 (2016) 9.
- [41] M.A. Rezvani, M. Oveisi, M.A.N. Asli, *J. Mol. Catal. A Chem.* 410 (2015) 121.
- [42] E. Rafiee, S. Rezaei, *J. Taiwan Inst. Chem. Eng.* 61 (2016) 174.
- [43] J. Qiu, G. Wang, Y. Zhang, D. Zeng, Y. Chen, *Fuel* 147 (2015) 195.
- [44] R. Zhao, J. Wang, D. Zhang, Y. Sun, B. Han, N. Tang, N. Wang, K. Li, *Appl. Catal. A. Gen.* 532 (2017) 26.

- [45] H. Zhao, G.A. Baker, Q. Zhang, *Fuel* 189 (2017) 334.
- [46] W. Jiang, D. Zheng, S. Xun, Y. Qin, Q. Lu, W. Zhu, H. Li, *Fuel* 190 (2017) 1.
- [47] A. Afzalnia, A. Mirzaie, A. Nikseresht, T. Musabeygi, *Ultrason. Sonochem.* 34 (2017) 713.
- [48] Z.E.A. Abdalla, B. Li, A. Tufail, *Colloids Surf. A* 341 (2009) 86.
- [49] S.W. Li, R.M. Gao, J.S. Zhao, *ACS Sustain. Chem. Eng.* 6 (2018) 15858.
- [50] F. Mirante, N. Gomes, L.C. Branco, S.L. Cunha, P.L. Almeida, M. Pillinger, S. Gago, C.M. Granadeiro, S.S. Balula, *Microporous Mesoporous Mater.* 275 (2019) 163.
- [51] W. Zhu, B. Dai, P. Wu, Y. Chao, J. Xiong, S. Xun, et al., *ACS Sustain. Chem. Eng.* 3 (2015) 186.
- [52] R. Wang, F. Yu, G. Zhang, H. Zhao, *Catal. Today* 150 (2010) 37.
- [53] C.M. Granadeiro, P. Silva, V.K. Saini, F.A.A. Paz, J. Pires, S.L. Cunha-Silva, S.S. Balula, *Catal. Today* 218–219 (2013) 35.
- [54] S. Ribeiro, C.M. Granadeiro, P. Silva, F.A. Almeida Paz, F.F. de Biani, L. Cunha-Silva, et al., *Cat. Sci. Technol.* 3 (2013) 2404.
- [55] Z. Zhang, F. Zhang, Q. Zhu, W. Zhao, B. Ma, Y. Ding, J. *Colloid Interface Sci.* 360 (2011) 189.
- [56] X.S. Wang, Y.B. Huang, Z.J. Lin, R. Cao, *Dalton Trans.* 43 (2014) 11950.
- [57] X.M. Yan, P. Mei, L. Xiong, L. Gao, Q. Yang, L. Gong, *Cat. Sci. Technol.* 3 (2013) 1985.
- [58] D. Julião, A.C. Gomes, M. Pillinger, S.L. Cunha, B. de Castro, I.S. Gonc, S.S. Balula, *Fuel Process. Technol.* 131 (2015) 78.
- [59] Y.L. Peng, J. Liu, H.F. Zhang, D. Luo, D. Li, *Inorg. Chem. Front.* 5 (2018) 1563.
- [60] J. Li, Z. Yang, G. Hu, J. Zhao, *Chem. Eng. J.* 388 (2020) 124325.
- [61] V.V. Bokade, *Chem. Eng. Res. Des.* 79 (2001) 625.
- [62] D.H. Pybus, C.S. Sell (Eds.), *The Chemistry of Fragrances*, RSC Paperbacks, Cambridge, 1999.
- [63] K. Bauer, D. Garbe, H. Surburg, *Common Fragrance and Flavor. Materials: Preparation, Properties and Uses*, Wiley, New York, 1997.
- [64] G. Orloff, B. Winter, C. Fehr, in: P.M. Muller, D. Lamparsky (Eds.), *Perfumes, Art, Science & Technology*, Elsevier, New York, 1991, p. 287.
- [65] W.F. Hölderich, J. Röseler, G. Heitmann, A.T. Liebens, *Catal. Today* 37 (1997) 353.
- [66] P.A. Robles-Dutenhefner, K.A. da Silva, M.R.H. Siddiqui, I.V. Kozhevnikov, E.V. Gusevskaya, *J. Mol. Catal. A* 175 (2001) 33.
- [67] K.A. da Silva, P.A. Robles-Dutenhefner, E.M.B. Sousa, E.F. Kozhevnikova, I.V. Kozhevnikov, E.V. Gusevskaya, *Cat. Com.* 5 (2004) 425.
- [68] J. Kaur, K. Griffin, B. Harrison, I.V. Kozhevnikov, *J. Catal.* 208 (2002) 448.
- [69] E.F. Kozhevnikova, E.G. Derouane, I.V. Kozhevnikov, *Chem. Commun.* (2002) 1178.
- [70] I.V. Kozhevnikov, *Catalysts for Fine Chemicals, Catalysis by Polyoxometalates*, vol. 2, Wiley, Chichester, 2002.
- [71] I.V. Kozhevnikov, *Chem. Rev.* 98 (1998) 171.
- [72] E.F. Kozhevnikova, I.V. Kozhevnikov, *J. Catal.* 224 (2004) 164.
- [73] K.A. da Silva Rocha, I.V. Kozhevnikov, E.V. Gusevskaya, *Appl. Catal. A Gen.* 294 (2005) 106.
- [74] A.K. Pandey, P. Singh, N.N. Tripathi, *Asian Pac. J. Trop. Biomed.* 4 (2014) 682.
- [75] N.B. de Oliveira, *Quim Nova* 28 (2005) S79.
- [76] W.B. Motherwell, M.J. Bingham, J. Pothier, Y. Six, *Tetrahedron* 60 (2004) 3231.
- [77] K.A. da Silva Rocha, J.L. Hoehne, E.V. Gusevskaya, *Chem. A Eur. J.* 14 (2008) 6166.
- [78] V.V. Costa, K.A. da Silva Rocha, L.F. Sousa, P.A. Robles-Dutenhefner, E.V. Gusevskaya, *J. Mol. Catal. A* 345 (2011) 69.
- [79] D. Prat, J. Hayler, A. Wells, *Green Chem.* 16 (2014) 4546.
- [80] C.J. Ribeiro, M.M. Pereira, E.F. Kozhevnikova, I.V. Kozhevnikov, E.V. Gusevskaya, K.A. da Silva Rocha, *Catal. Today* 344 (2020) 166.



- [81] G.D. Yadav, V.V. Bokade, *Appl. Catal. A. Gen.* 147 (1996) 299.
- [82] K.-Y. Lee, M. Misono, in: G. Ertl, H. Knözinger, J.W. Weitkamp (Eds.), *Handbook of Heterogeneous Catalysis*, Vol. 1, Wiley-VCH, Weinheim, 1997, pp. 118–131.
- [83] I.V. Kozhevnikov, *Catal. Rev. Sci. Eng.* 37 (1995) 311.
- [84] I.V. Kozhevnikov, *Appl. Catal.*, A 256 (2003) 3.
- [85] N. Mizuno, M. Misono, *Curr. Opin. Solid State Mater. Sci.* 2 (2007) 84.
- [86] J.D. Burrington, J.R. Johnson, J.K. Pudelski, *Top. Catal.* 23 (2003) 175.
- [87] L.R. Pizzio, P.G. Vázquez, C.V. Cáceres, M.N. Blanco, *Appl. Catal.*, A 256 (2003) 125.
- [88] G. Kamalakar, K. Komura, Y. Kubota, Y. Sugi, *J. Chem. Technol. Biotechnol.* 81 (2006) 981.
- [89] I. Yuranov, D.A. Bulushev, A. Renken, L. Kiwi-Minsker, *J. Catal.* 227 (2004) 138.
- [90] F.M. Zhang, X. Chen, J. Zhuang, Q. Xiao, Y.J. Zhong, W.D. Zhu, *Cat. Sci. Technol.* 1 (2011) 1250.
- [91] S. Niwa, M. Eswaramoorthy, J. Nair, A. Raj, N. Itoh, H. Shoji, T. Namba, F. Mizukami, *Science* 295 (2002) 105.
- [92] N. Itoh, S. Niwa, F. Mizukami, T. Inoue, A. Igarashi, T. Namba, *Cat. Com.* 4 (2003) 243.
- [93] K. Lemke, H. Ehrich, U. Lohse, H. Berndt, K. Jähnisch, *Appl. Catal. A. Gen.* 243 (2003) 41.
- [94] M. Stöckmann, F. Konietzki, J.U. Notheis, J. Voss, W. Keune, W.F. Maier, *Appl. Catal. A. Gen.* 208 (2001) 343.
- [95] N.K.K. Raj, S.S. Deshpande, R.H. Ingle, T. Raja, P. Manikandan, *Catal. Lett.* 98 (2004) 217.
- [96] H.Q. Ge, Y. Leng, C.J. Zhou, J. Wang, *Catal. Lett.* 124 (2008) 324.
- [97] J. Zhang, Y. Tang, G.Y. Li, C.W. Hu, *Appl. Catal. A. Gen.* 278 (2005) 251.
- [98] L. Jing, F. Zhang, Y. Zhong, W. Zhu, *Chin. J. Chem. Eng.* 22 (2014) 1220.
- [99] A. Nisar, Y. Lu, J. Zhuang, X. Wang, *Angew. Chem. Int. Ed.* 50 (2011) 3187.
- [100] C. Li, Z.X. Jiang, J.B. Gao, Y.X. Yang, S.J. Wang, F.P. Tian, F.X. Sun, X.P. Sun, P.L. Ying, C.R. Han, Ultra-deep desulfurization of diesel, *Chem. A Eur. J.* 10 (2004) 2277.
- [101] D. Barton, W.D. Ollis, *Comprehensive Organic Chemistry*, Vol. 1, Pergamon Press, England, 1979, p. 641.
- [102] Y. Izumi, K. Urabe, M. Onaka, *Zeolite, Clay and Heteropolyacid in Organic Reactions*, Kodansha, Tokyo, 1992, p. 99.
- [103] T. Baba, Y. Ono, *J. Mol. Catal.* 37 (1986) 317.
- [104] T. Okuhara, A. Kasai, N. Hayakawa, Y. Yoneda, M. Misono, *J. Catal.* 83 (1983) 121.
- [105] K. Takahashi, T. Okuhara, M. Misono, *Chem. Lett.* (1985) 841.
- [106] M. Misono, T. Okuhara, T. Ichiki, T. Aria, Y. Kanda, *J. Am. Chem. Soc.* 109 (1987) 5355.
- [107] K.Y. Lee, Y. Kaneda, N. Mizuno, M. Misono, S. Nakata, S. Asaoka, *Chem. Lett.* (1988) 1175.
- [108] P.G. Vázquez, L.R. Pizzio, M.N. Blanco, C.V. Cáceres, *Actas 16th Simposio Iberoamericano de Catálisis, Cartagena de Indias, Colombia, Septiembre de*, Vol. 3, 1998, p. 2123.
- [109] P. Vázquez, L. Pizzio, C. Cáceres, M. Blanco, H. Thomas, E. Alesso, L. Finkielstein, B. Lantano, G. Moltrasio, J. Aguirre, *J. Mol. Catal. A Chem.* 161 (2000) 223.
- [110] G.D. Yadav, A.A. Pujari, *Org. Process Res. Dev.* 4 (2000) 88.
- [111] D. Swern, *Organic Peroxides*, Vol. II, Wiley-Interscience Inc, New York, 1972, p. 265.
- [112] D. Swern, *Chem. Rev.* 45 (1949) 1.
- [113] S.G. Wilkinson, *Int. Rev. Sci., Org. Chem. Ser.* 2 (1975) 111.
- [114] K.P.C. Vollhardt, N.E. Schore, *Organic Chemistry*, second ed., Freeman, New York, 1994, pp. 924–929.
- [115] N. Venkatasubramanian, R. Natarajan, *Indian J. Chem.* 13 (1975) 261.
- [116] M.I. Bishnoi, S.G. Negi, K.K. Banerji, *Indian J. Chem.* 25A (1986) 660.
- [117] P.S. Radhakrishnamurty, N.K. Rath, R.K. Panda, *Indian J. Chem.* 27A (1988) 963.
- [118] A. Mathur, V. Sharma, K.K. Banerji, *Indian J. Chem.* 27A (1988) 123.
- [119] A. Mathur, V. Sharma, K.K. Banerji, *Indian J. Chem.* 20B (1981) 529.

- [120] P. Kuselan, N. Venkatasubramanian, *Indian J. Chem.* 22A (1983) 100.
- [121] K. Vijayamohan, P.R. Rao, E.V. Sundaram, *Proc. Natl. Acad. Sci., India, Sect. A* 58A (1988) 49.
- [122] C.S. Reddy, T. Vijaya Kumar, *Indian J. Chem.* 34A (1995) 871.
- [123] V. Thiagarajan, S. Ramakrishnan, *Indian J. Chem.* 37A (1998) 443.
- [124] (a) J. Muzart, *Synth. Commun.* 19 (1989) 2061.  
(b) J. Muzart, O. Piva, *Tetrahedron Lett.* 29 (1988) 2321.
- [125] S. Cacchi, L. Caglioti, P. Zappelli, *J. Org. Chem.* 20 (1973) 3653.
- [126] P.C.B. Page, S. Rosenthal, *Tetrahedron Lett.* 17 (1986) 1947.
- [127] G.D. Yadav, R.D. Bhagat, *Org. Process Res. Dev.* 8 (2004) 879.
- [128] G.D. Yadav, N.S. Asthana, V.S. Kamble, *Appl. Catal., A* 240 (2003) 53.
- [129] G.D. Yadav, N.S. Asthana, *Appl. Catal., A* 244 (2003) 341.
- [130] H. Kwart, P.S. Francis, *J. Am. Chem. Soc.* 81 (1959) 2116.
- [131] I.P. Dominic, J. Rocek, *J. Am. Chem. Soc.* 101 (1979) 6311.
- [132] S. Hu, G. Yang, J. Hong, Y. Liu, R. Chen, *Appl. Surf. Sci.* 435 (2018) 649.
- [133] J. He, X.H. Lu, Y. Shen, R. Jing, R.F. Nie, D. Zhou, Q.H. Xia, *Mol. Catal.* 440 (2017) 87.
- [134] Y. Zhang, J. Zhou, J. Si, *RSC Adv.* 7 (2017) 54779.
- [135] Q. Guo, S.G. Mo, P.X. Liu, W.D. Zheng, R.X. Qin, C.F. Xu, Y.Q. Wu, B.H. Wu, N.F. Zheng, *Sci. China* 60 (2017) 1444.
- [136] C.H. Li, H.L. Chen, M.S. Yang, U.S. Patent 20180072646, 2018.
- [137] Z. Qu, S. Hu, H. Jiang, Y. Liu, J. Huang, W. Xing, R.Z. Chen, *Ind. Eng. Chem. Res.* 56 (2017) 1755.
- [138] S.L. Wang, R.Z. Tang, Y.Z. Zhang, T. Chen, G.Y. Wang, *Chem. Eng. Sci.* 138 (2015) 93.
- [139] I.K. Song, M.A. Barteau, *J. Mol. Catal. A* 212 (2004) 229.
- [140] K.A. da Silva Rocha, P.A. Robles-Dutenhefner, E.M. Sousa, E.F. Kozhevnikova, I.V. Kozhevnikov, E.V. Gusevskaya, *Appl. Catal., A* 317 (2007) 171.
- [141] B.J. Liu, L.H. Lu, B.C. Wang, T.X. Cai, I. Katsuyoshi, *Appl. Catal., A* 171 (1998) 117.
- [142] S. Liu, J. Han, Q. Wu, B. Bian, L. Li, S. Yu, J. Song, C. Zhang, A. Ragauskas, *J. Catal. Lett.* 149 (2019) 2383.
- [143] J.H. Gary, G.E. Handwerk, *Petroleum Refining, Technology and Economics*, Dekker, New York, 1994, p. 231. chapter 11.
- [144] L.F. Albright, A.R. Goldsby (Eds.), *Industrial and Laboratory Alkylations*, ACS Symposium Series, vol. 55, Am. Chem. Soc, Washington, DC, 1971.
- [145] M.A. Paul, F.A. Long, *Chem. Rev.* 57 (1957) 1.
- [146] M.A. Asensi, A. Corma, A. Martinez, C. Martinez, *Preprints, Div. of Petrol Chem, Am. Chem. Soc.* 41 (1996) 692.
- [147] N. Essayem, S. Kieger, G. Coudurier, J.C. Vadrine, *Stud. Surf. Sci. Catal.* 101 (A) (1996) 591.
- [148] W. Chu, Z. Zhao, W. Sun, X. Ye, Y. Wu, *Catal. Lett.* 55 (1998) 57.
- [149] T. Jiang, W. Wang, B. Han, *New J. Chem.* 37 (2013) 1654.
- [150] P.T. Tanev, M. Chibwe, T.J. Pinnavaia, *Nature* 368 (1994) 321.
- [151] I. Yuranov, D.A. Bulushev, A. Renken, L. Kiwi-Minsker, *Appl. Catal. A* 319 (2007) 128.
- [152] Y. Li, Z. Feng, R.A. Santen, E.J.M. Hensen, C. Li, *J. Catal.* 255 (2008) 190.
- [153] B. Guo, L.F. Zhu, X.K. Hu, Q. Zhang, D.M. Tong, G.Y. Li, C.W. Hu, *Cat. Sci. Technol.* 1 (2011) 1060.
- [154] Y.Y. Gu, X.H. Zhao, G.R. Zhang, H.M. Ding, Y.K. Shan, *Appl. Catal., A* 328 (2007) 150.
- [155] T. Miyahara, H. Kanzaki, R. Hamada, S. Kuroiwa, S. Nishiyama, S. Tsuruya, *J. Mol. Catal. A Chem.* 176 (2001) 141.
- [156] C. Perego, A. Carati, P. Ingallina, M.A. Mantegazza, G. Bellussi, *Appl. Catal., A* 221 (2001) 63.

- [157] C.W. Lee, W.J. Lee, Y.K. Park, S.E. Park, *Catal. Today* 61 (2000) 137.
- [158] K.M. Parida, D. Rath, *Appl. Catal., A* 321 (2007) 101.
- [159] S.V. Sirotnin, I.F. Moskovskaya, *Pet. Chem.* 49 (2009) 99.
- [160] A.N. Kharat, S. Moosavikia, B.T. Jahromi, A. Badiei, *J. Mol. Catal. A Chem.* 348 (2011) 14.
- [161] R.A. Sheldon, H. van Bekkum (Eds.), *Fine Chemicals through Heterogeneous Catalysis*, Wiley, Weinheim, 2001. Toronto.
- [162] E.G. Deroune, G. Crehan, C.J. Dillon, D. Bethell, H. He, S.B.D. Hamid, *J. Catal.* 194 (2000) 410.
- [163] G.D. Yadav, J.J. Nair, *Microporous Mesoporous Mater.* 33 (1999) 1.
- [164] S.R. Chitnis, M.M. Sharma, *React. Funct. Polym.* 33 (1997) 93.
- [165] I. Tkac, P. Komadel, D. Muller, *Clay Miner.* 29 (1991) 101.
- [166] Y. Izumi, K. Urabe, M. Onaka, *Zeolites, Clays and Heteropoly Acids*, VCH Publishers Inc, London, 1992.
- [167] T. Okuhara, T. Nakato, *Catal. Surv. Jpn.* 2 (1998) 31.
- [168] G.D. Yadav, *Catal. Surv. Asia* 9 (2005) 117–137.
- [169] Y. Zheng, X. Chen, Y. Shen, *Chem. Rev.* 108 (2008) 5253.
- [170] E. Lotero, Y. Liu, D.E. Lopez, K. Suwannakarn, D.A. Bruce, J.G. Goodwin Jr., *Ind. Eng. Chem. Res.* 44 (2005) 5353.
- [171] J. Hettwer, H. Oldenburg, E. Flaschel, *J. Mol. Catal. B* 215 (2002) 19.
- [172] K. Wang, M.C. Hawley, S.J. DeAthos, *Ind. Eng. Chem. Res.* 42 (2003) 2913.
- [173] F. Frusteri, F. Arena, G. Bonura, C. Cannilla, L. Spadaro, O. Di Blasi, *Appl. Catal., A* 367 (2009) 77.
- [174] J. Gui, X. Cong, D. Liu, X. Zhang, Z. Sun, *Cat. Com.* 5 (2004) 473.
- [175] D.C. Forbes, K.J. Weaver, *J. Mol. Catal. A Chem.* 214 (2004) 129.
- [176] V.L.C. Goncalves, B.P. Pinto, J.C. Silva, C.J.A. Mota, *Catal. Today* 133 (2008) 673.
- [177] M. Trejda, K. Stawicka, M. Ziolk, *Appl Catal B* 103 (2011) 404.
- [178] K. Klepacova, D. Mravec, M. Bajus, *Appl. Catal., A* 294 (2005) 141.
- [179] P. Lauriol-Garbey, G. Postole, S. Loridant, A. Auroux, V. Belliere-Baca, P. Rey, J. Millet, *Appl Catal B* 106 (2011) 94.
- [180] P. Ferreira, I.M. Fonseca, A.M. Ramos, J. Vital, J.E. Castanheiro, *Cat. Com.* 10 (2009) 481.
- [181] Z. Yuan, S. Xia, P. Chen, Z. Hou, X. Zheng, *Energy Fuel* 25 (2008) 3186.
- [182] M.Y. Huang, X.X. Han, C.T. Hung, J.C. Lin, P.H. Wu, J.C. Wu, S.B. Liu, *J. Catal.* 320 (2014) 42–51.
- [183] R.L. Pruett, W.E. Walker, U.S. Patent 3,957,857, 1976.
- [184] D.R. Fahey, *J. Am. Chem. Soc.* 103 (1981) 136.
- [185] F.E. Celik, H. Lawrence, A.T. Bell, *J. Mol. Catal. A Chem.* 288 (2008) 87.
- [186] G.A. Olah (Ed.), *Friedel–Crafts and Related Reactions*, vol. I–IV, Wiley, New York, 1973.
- [187] G.D. Yadav, A.A. Pujari, A.V. Joshi, *Green Chem.* 1 (1999) 269.
- [188] G.D. Yadav, N.S. Doshi, *Appl. Catal. A Gen.* 236 (2002) 129.
- [189] G.D. Yadav, N.S. Doshi, *J. Mol. Catal. A Chem.* 194 (2003) 195.
- [190] G.D. Yadav, N. Kirthivasan, *J. Chem. Soc. Chem. Commun.* (1995) 203.
- [191] G.D. Yadav, N. Kirthivasan, *Appl. Catal., A* 154 (1997) 29.
- [192] (a) K. Geim, K.S. Novoselov, *Nat. Mater.* 6 (2007) 183.  
(b) M.D. Stoller, S. Park, Y.W. Zhu, J. An, R.S. Ruoff, *Nano Lett.* 8 (2008) 3498.  
(c) S. Park, R.S. Ruoff, *Nat. Nanotechnol.* 4 (2009) 217.
- [193] (a) K.S. Novoselov, A.K. Geim, S.V. Morozov, D. Jiang, M.I. Katsnelson, I.V. Grigorieva, S.V. Dubonos, A.A. Firsov, *Nature* 438 (2005) 197.  
(b) Y.B. Zhang, Y.W. Tan, H.L. Stormer, P. Kim, *Nature* 438 (2005) 201.

- (c) K.S. Novoselov, Z. Jiang, Y. Zhang, S.V. Morozov, H.L. Stormer, U. Zeitler, J.C. Maan, G.S. Boebinger, P. Kim, A.K. Geim, *Science* 315 (2007) 1379.
- [194] (a) A.A. Balandin, S. Ghosh, W.Z. Bao, I. Calizo, D. Teweldebrhan, F. Miao, C.N. Lau, *Nano Lett.* 8 (2008) 902.  
(b) K.I. Bolotin, K.J. Sikes, Z. Jiang, M. Klima, G. Fudenberg, J. Hone, P. Kim, H.L. Stormer, *Solid State Commun.* 146 (2008) 351.
- [195] S. Zhu, J. Wang, W. Fan, *Cat. Sci. Technol.* 5 (2015) 3845.
- [196] M. Tao, N. Sun, Y. Li, T. Tong, M. Wielicako, S. Wang, X. Wang, *J. Mater. Chem. A* 5 (2017) 8325.
- [197] S.J. Rhoads, N.R. Raulins, *Organic Reactions*, vol. 22, Wiley, New York, 1974.
- [198] P. Wipf, B.M. Trost, *Comprehensive Organic Synthesis*, vol. 5, Pergamon Press, Oxford, 1991, p. 827.
- [199] R. Martin, *Org. Prep. Proced. Int.* 24 (1992) 369.
- [200] D. Cagniant, *Adv. Heterocycl. Chem.* 18 (1975) 358.
- [201] R.P. Lutz, *Chem. Rev.* 84 (1984) 205.
- [202] G.D. Yadav, S.V. Lande, *Org. Process Res. Dev.* 9 (2005) 547–554.
- [203] H. Hattori, *Heterogeneous Catalysis and Fine Chemicals III*, Elsevier, Amsterdam, 1993.
- [204] G.D. Yadav, H.G. Manyar, *Microporous Mesoporous Mater.* 63 (2003) 85.
- [205] G.D. Yadav, S.P. Nalawade, *Chem. Eng. Sci.* 58 (2003) 2573.
- [206] G.D. Yadav, R.D. Bhagat, *J. Mol. Catal. A Chem.* 235 (2005) 98.
- [207] G.D. Yadav, O.V. Badure, *Appl. Catal. A. Gen.* 348 (2008) 16–25.
- [208] A. Vogt, H.W. Kouwenhoven, R. Prins, *Appl. Catal. A. Gen.* 123 (1995) 37.
- [209] A.J. Hoefnagel, H. Van Bekkum, *Appl. Catal. A. Gen.* 97 (1993) 87.
- [210] H. Wang, Y. Zou, *Catal. Lett.* 86 (4) (2003) 163.
- [211] G.A. Olah, M. Arvanaghi, V.V. Krishnamurthy, *J. Org. Chem.* 48 (1983) 3359.
- [212] E.F. Kozhevnikova, J. Quartararo, I.V. Kozhevnikov, *Appl. Catal. A. Gen.* 245 (2003) 69.
- [213] G.D. Yadav, G. George, *J. Mol. Catal. A Chem.* 292 (2008) 54.
- [214] F.F. Bamoharram, M.M. Heravi, M. Roshani, M. Jahangir, A. Gharib, *Appl. Catal. A Gen.* 302 (2006) 42.
- [215] M.M. Heravi, F.F. Bamoharram, G. Rajabzadeh, N. Seifi, M. Khatami, *J. Mol. Catal. A Chem.* 259 (2006) 213.
- [216] C.R. Gorla, N.W. Emanetoglu, S. Liang, W.E. Mayo, Y. Lu, M. Wraback, H. Shen, *J. Appl. Phys.* 85 (1999) 259.
- [217] H. Nazari, A. Ahmadpour, F.F. Bamoharram, M.M. Heravi, N. Eslami, *E-J. Chem.* 9 (2012) 272.
- [218] M.M. Heravi, S. Sadjadi, S. Sadjadi, H.A. Oskooie, R.H. Shoar, F.F. Bamoharram, *S. Afr. J. Chem.* 62 (2009) 1.
- [219] D. Whittaker, A.A. Newman (Eds.), *Chemistry of Terpenes and Terpenoids*, Academic Press, London, 1972, p. 11.
- [220] A.B. Radbil, M.V. Kulikov, T.N. Sokolova, V.R. Kartashov, B.A. Zolin, B.A. Radbil, *Chem. Nat. Compd.* 35 (1999) 524.
- [221] M. Caiado, A. Machado, R.N. Santos, I. Matos, I.M. Fonseca, A.M. Ramos, J. Vital, A.A. Valente, J.E. Castanheiro, *Appl. Catal. A. Gen.* 451 (2013) 36.
- [222] M. El-Sakhawy, M.L. Hassan, *Carbohydr. Polym.* 67 (2007) 1.
- [223] D. Wang, S.B. Shang, Z.Q. Song, M.K. Lee, *J. Ind. Eng. Chem.* 16 (2010) 152.
- [224] S.B. Abd Hamid, Z.Z. Chowdhury, M.Z. Karim, *Bioresources* 9 (2014) 7403.
- [225] R.D. Kalita, Y. Nath, M.E. Ochubiojo, A.K. Buragohain, *Colloids Surf. B. Biointerfaces* 108 (2013) 85.
- [226] F.R. Tao, H.L. Song, L.J. Chou, *ChemSusChem* 3 (2010) 1298.
- [227] D. Ciolacu, *J. Optoelectron, Adv. Mater.* 9 (2007) 1033.

- [228] Y.J. Tang, X.C. Shen, J.H. Zhang, D.L. Guo, F.G. Kong, N. Zhang, *Carbohydr. Polym.* 125 (2015) 360.
- [229] X.T. Li, Y.J. Jiang, L.L. Wang, L.Q. Meng, W. Wang, X.D. Mu, *RSC Adv.* 2 (2012) 6921.
- [230] W.P. Deng, M. Liu, Q.H. Zhang, X.S. Tan, Y. Wang, *Chem. Commun.* 46 (2010) 2668.
- [231] J. Tian, J.H. Wang, S. Zhao, C.Y. Jiang, X. Zhang, X.H. Wang, *Cellul.* 17 (2010) 587.
- [232] J.B. Li, D.D. Qiang, M.Y. Zhang, H.J. Xiu, X.R. Zhang, *Carbohydr. Polym.* 129 (2015) 44.
- [233] D. Qiang, M. Zhang, J. Li, H. Xiu, Q. Liu, *Cellul.* 23 (2016) 1199.
- [234] J. Carreras, M. Livendahl, P.R. McGonigal, A.M. Echavarren, *Angew. Chem. Int. Ed.* 53 (2014) 4896.
- [235] F.J. Moreno-Dorado, Y.M.A.W. Lamers, G. Mironov, J.B.P.A. Wijnberg, A. De Groot, *Tetrahedron* 59 (2003) 7743.
- [236] M.P. Polovinka, A.A. Shal, D.V. Korchagina, Y.V. Gatilov, V.V. Shcherbukhin, V.A. Barkhash, *Pergamon* 37 (1996) 2631.
- [237] A. Murakami, *Nippon Nogeikagaku Kaishi* 69 (1995) 23.
- [238] H.J.M. Gijsen, K. Kanai, G.A. Stork, J.B.P.A. Wijnberg, R.V.A. Orru, C.G.J.M. Seelen, S.M. van der Kerk, A. de Groot, *Tetrahedron* 46 (1990) 7237.
- [239] R. Guillermo, J.R. Hanson, A. Truneh, *J. Chem. Res. Synop.* (1997) 28.
- [240] M.S.P. Ribeiro, C. de Souza Santos, C.G. Vieira, K.A. da Silva Rocha, *Mol. Catal.* 498 (2020) 111264.
- [241] E. Breitmaier, *Terpenes, Flavors, Fragrances, Pharmaca, Pheromones*, Wiley-VCH, Weinheim, 2006.
- [242] R.F. Cottaa, K.A. da Silva Rochab, E.F. Kozhevnikovac, I.V. Kozhevnikovc, E.V. Gusevs-kayaa, *Appl Catal B* 217 (2017) 92.
- [243] T.A. Miettinen, T.E. Strandberg, H. Gylling, *Arterioscler. Thromb. Vasc. Biol.* 20 (2000) 1340.
- [244] A.F. Vuorio, H. Gylling, H. Turtola, K. Kontula, P. Ketonen, T.A. Miettinen, *Arterioscler. Thromb. Vasc. Biol.* 20 (2000) 500.
- [245] A. Akashe, M. Miller, U.S. Patent 6,267,963, 2001.
- [246] A. Akashe, M. Miller, U.S. Patent 6,274,574, 2001.
- [247] F.H. Mattson, R.A. Volpenhein, B.A. Erickson, *J. Nutr.* 107 (1977) 1139.
- [248] A. Fujita, E. Kadowaki, T. Higashi, H. Uchida, U.S. Patent 20040152 915, 2004.
- [249] X. Meng, P. Sun, Q. Pan, Z. Shi, K. Yang, R. He, *Eur. J. Lipid Sci. Technol.* 108 (2006) 13.
- [250] N.T. Mathew, S. Khaire, S. Mayadevi, R. Jha, S. Sivasanker, *J. Catal.* 229 (2005) 105.
- [251] J.A. Elings, R.S. Downing, R.A. Sheldon, *Stud. Surf. Sci. Catal.* 94 (1995) 487.
- [252] R.A. Sheldon, J.A. Elings, S.K. Lee, H.E.B. Lempers, R.S. Downing, *J. Mol. Catal. A Chem.* 134 (1998) 129.
- [253] S.G. Wagholikar, S. Mayadevi, S.P. Mirajkar, S. Sivasanker, in: E. van Steen, L. Callanan, M. Claeys, C.T. O'Connor (Eds.), *Proceedings of the 14th International Zeolite Conference*, Cape Town, 2004, p. 2731.
- [254] I. Sucholeiki, M.R. Pavia, C.T. Kresge, S.B. Me Cullen, A. Malek, S. Schram, *Mol. Divers* 3 (1998) 151. *C.A.* 129 (1999) 202736.
- [255] R. Cruz-Almanza, F. Perez-Flores, L. Brena, E. Tapia, R. Ojeda, A.J. Fuentes, *Heterocycl. Chem.* 32 (1995) 219.
- [256] G.D. Yadav, S.V. Lande, *J. Mol. Catal. A Chem.* 243 (2006) 31.
- [257] M.R. Gomes-Carneiro, D.M.M. Dias, A.C.A.X. De-Oliveira, F.J.R. Paumgarten, *Mutat. Res.* 585 (2005) 105.
- [258] A. Pauli, *Int. J. Aromather.* 16 (2006) 21.
- [259] S.P. Bhatia, D. McGinty, C.S. Letizia, A.M. Api, *Food Chem. Toxicol.* 46 (2008) S72.
- [260] G.P.P. Kamatou, A.M. Viljoen, *J. Am. Oil Chem. Soc.* 87 (2010) 1.

- [261] T. Seki, T. Kokuryo, Y. Yokoyama, H. Suzuki, K. Itatsu, A. Nakagawa, T. Mizutani, T. Miyake, M. Uno, K. Yamauchi, M. Nagino, *Cancer Sci.* 102 (2011) 2199.
- [262] A.K. Maurya, M. Singh, V. Dubey, S. Srivastava, S. Luqman, D.U. Bawankule, *Curr. Pharm. Biotechnol.* 15 (2014) 173.
- [263] A.L. de Meireles, M. dos Santos Costa, K.A. da Silva Rocha, E.V. Gusevskaya, *Appl. Catal. A. Gen.* 502 (2015) 271.
- [264] S.J.L. Ribeiro, Y. Messadeq, *Carbohydr. Polym.* 73 (2008) 74.
- [265] R.P. de Almeida, R.C.G. Acirole, A. Infantes-Molina, E. Rodríguez-Castellón, J.G.A. Pacheco, I.D.C.L. Barros, *J. Clean. Prod.* 282 (2021) 124477.
- [266] J.J. Bozell, G.R. Petersen, *Green Chem.* 12 (2010) 539.
- [267] A. Démolis, N. Essayem, F. Rataboul, *ACS Sustain. Chem. Eng.* 2 (2014) 1338.
- [268] K. Yan, C. Jarvis, J. Gu, Y. Yan, *Energy Rev.* 5 (2015) 986.
- [269] A.M. Escobar, M.N. Blanco, J.J. Martínez, J.A. Cubillos, G.P. Romanelli, L.R. Pizzio, *J. Nanomater.* 2019 (2019) 1.
- [270] P. Dhepe, A. Fukuoka, *ChemSusChem* 1 (2008) 969.
- [271] C. Tuck, E. Pérez, I. Horváth, R. Sheldon, M. Poliakoff, *Science* 337 (2012) 695.
- [272] L. Wang, C.L. Weller, D.D. Jones, M.A. Hanna, *Biomass Bioenergy* 32 (2008) 573.
- [273] M.M. Yung, W.S. Jablonski, K.A. Magrini-Bair, *Energy Fuel* 23 (2009) 1874.
- [274] A.A. Petersen, F. Vogel, R.P. Lachance, M. Froling, J.M. Antal, J.W. Tester, *Energ. Environ. Sci.* 1 (2008) 32.
- [275] L.J. Guo, Y.J. Lu, X.M. Zhang, C.M. Ji, Y. Guan, A.X. Pei, *Catal. Today* 129 (2007) 275.
- [276] R.R. Davda, J.W. Shabaker, B.W. Huber, R.D. Cortright, J.A. Dumesic, *Appl Catal B* 56 (2005) 171.
- [277] J. Albert, D. Lüders, A. Bösmann, D.M. Guldi, P. Wasserscheid, *Green Chem.* 16 (2014) 226.
- [278] J. Zhang, M. Sun, X. Liu, Y. Han, *Catal. Today* 233 (2014) 77.
- [279] R. Suffis, L.B. Morton, K. Ishida, K. Sawano, A.G. Van Loveren, N. Tetsuo, C.B. Green, G.A. Reitz, R.K.L. Kang, T. Sato, U.S. Patent 5, 626,852, 1997.
- [280] G.A. Burdock, *Fenarolis Handbook of Flavor Ingredients*, vol. 2, CRC, New York, 1995, p. 152.
- [281] J. Delgado, EP Patent 1331260, 2002.
- [282] B. Delfort, I. Durand, A. Jaecker, T. Lacomme, X. Montagne, F. Paille, U.S. Patent 0163949, 2003.
- [283] E. Garcia, M. Laca, E. Perez, A. Garrido, J. Peinado, *Energy Fuel* 22 (2008) 4274.
- [284] G.D. Yadav, S.O. Katole, *Catal. Today* 237 (2014) 125.
- [285] Y. Roman-Leshkov, C.J. Barrett, Z.Y. Liu, J.A. Dumesic, *Nature* 447 (2007) 982.
- [286] L. Deng, J. Li, D.M. Lai, Y. Fu, Q.X. Guo, *Angew. Chem. Int. Ed.* 48 (2009) 6529.
- [287] J.Q. Bond, D.M. Alonso, D. Wang, R.M. West, J.A. Dumesic, *Science* 327 (2010) 1110.
- [288] I.T. Horvath, H. Mehdi, V. Fabos, L. Boda, L.T. Mika, *Green Chem.* 10 (2008) 238.
- [289] P. Lanzafame, D.M. Temi, S. Perathoner, *Catal. Today* 175 (2011) 435.
- [290] W. Deng, Q. Zhang, Y. Wang, *Dalton Trans.* 41 (2012) 9817.
- [291] Z. Wang, Q. Chen, *Green Chem.* 18 (2016) 5884.
- [292] A.C.C. Arantes, A.C.S.D. Oliveira, W.M.D.S. Borges, M.L. Bianchi, E.C.D. Resende, *Matéria (Rio de Janeiro)* 22 (2017).
- [293] C. Sell, C. Sell (Eds.), *The Chemistry of Fragrances: From Perfumer to Consumer*, second ed., vol. 2, RSC Publishing, Dorset, UK, 2006, pp. 52–88.
- [294] K. Bauer, D. Garbe, H. Surburg, *Common Fragrance and Flavour Materials. Preparation, Properties and Uses*, VCH Verlagsgesellschaft, 1990.
- [295] J.L.F. Monteiro, C.O. Veloso, *Top. Catal.* 27 (2004) 169.
- [296] E.V. Gusevskaya, J. Jiménez-Pinto, A. Börner, *ChemCatChem* 6 (2014) 382.
- [297] A. Behr, A.J. Vorholt, K.A. Ostrowski, T. Seidensticker, *Green Chem.* 16 (2014) 982.

- [298] A. Behr, L. Johnen, *ChemSusChem* 2 (2009) 1072.
- [299] Y. Kamiya, T. Okuhara, M. Misono, A. Miyaji, K. Tsuji, T. Nakajo, *Catal. Surv. Jpn.* 12 (2008) 101.
- [300] E.V. Gusevskaya, *ChemCatChem* 6 (2014) 1506.
- [301] P. Gallezot, *Chem. Soc. Rev.* 41 (2012) 1538.
- [302] A.A. Marianou, C.C. Michailof, D. Ipsakis, K. Triantafyllidis, A.A. Lappas, *Green Chem.* 21 (2019) 6161.
- [303] R.F. Cotta, R.A. Martins, M.M. Pereira, K.A. da Silva Rocha, E.F. Kozhevnikova, I.V. Kozhevnikov, E.V. Gusevskaya, *Appl. Catal. A. Gen.* 584 (2019) 117173.
- [304] V.V. Costa, K.A. da Silva Rocha, I.V. Kozhevnikov, E.F. Kozhevnikova, E.V. Gusevskaya, *Cat. Sci. Technol.* 3 (2013) 244.
- [305] K.A. da Silva Rocha, P.A. Robles-Dutenhefner, I.V. Kozhevnikov, E.V. Gusevskaya, *Appl. Catal., A* 352 (2009) 188.
- [306] A.L.P. de Meireles, M. dos Santos Costa, K.A. da Silva Rocha, E.F. Kozhevnikova, I.V. Kozhevnikov, E.V. Gusevskaya, *ChemCatChem* 6 (2014) 2706.
- [307] K.A. da Silva Rocha, N.V.S. Rodrigues, I.V. Kozhevnikov, E.V. Gusevskaya, *Appl. Catal., A* 374 (2010) 87.
- [308] V.V. Costa, K.A. da Silva Rocha, R.A. Mesquita, E.F. Kozhevnikova, I.V. Kozhevnikov, E.V. Gusevskaya, *ChemCatChem* 5 (2013) 3022.
- [309] R.L. Setine, G.L. Parks, G.L.K. Hunter, *J. Org. Chem.* 29 (1964) 616.
- [310] E.H. Eschinasi, *Isr. J. Chem.* 6 (1968) 713.
- [311] K. Arata, K. Tanabe, *Chem. Lett.* (1976) 321.
- [312] J. Jayasree, C.S. Narayanan, *Res. Chem. Intermed.* 23 (1997) 169.
- [313] C. Raptis, H. Garcia, M. Stratakis, *Angew. Chem. Int. Ed.* 48 (2009) 3133.
- [314] C.M. Alder, J.D. Hayler, R.K. Henderson, A.M. Redman, L. Shukla, L.E. Shuster, H.F. Sneddon, *Green Chem.* 18 (2016) 3879.
- [315] D. Prat, A. Wells, J. Hayler, H. Sneddon, C.R. McElroy, S. Abou-Shehada, P.J. Dunn, *Green Chem.* 18 (2016) 288.
- [316] B. Schöffner, F. Schöffner, S.P. Verevkin, A. Börner, *Chem. Rev.* 110 (2010) 4554.
- [317] C.M. Byrne, S.D. Allen, E.B. Lobkovsky, G.W. Coates, *J. Am. Chem. Soc.* 126 (2004) 11404.
- [318] O. Hauenstein, M. Reiter, S. Agarwal, B. Rieger, A. Greiner, *Green Chem.* 81 (2016) 760.
- [319] R.C. Jeske, A.M. DiCiccio, G.W. Coates, *J. Am. Chem. Soc.* 129 (2007) 11330.
- [320] P.T. Anastas, M.M. Kirchhoff, *Acc. Chem. Res.* 35 (2002) 686.
- [321] J. Clark, D. Macquarrie, (Eds.), *Handbook of Green Chemistry and Technology*, Blackwell Science, United Kingdom, 2002, p. 1.
- [322] J.R. Easton, The dye maker's view, in: P. Cooper (Ed.), *Colour in Dyehouse Effluent*, Alden Press, Oxford, 1995, pp. 9–21.
- [323] A. Reife, D. Betowski, H.S. Freeman, *Dyes, environmental*, in: R.A. Meyers (Ed.), *Environmental Analysis and Remediation*, John Wiley & Sons, Inc., New York, 1998, pp. 1442–1465.
- [324] R. Ganesh, G.D. Boardman, D. Michelsen, *Water Res.* 28 (1994) 1367.
- [325] Y.M. Slokar, A.M. Le Marechal, *Dyes Pigments* 37 (1998) 335.
- [326] S.J. Masten, S.H.R. Davies, Use of ozone and other strong oxidants for hazardous waste management, in: J.O. Nriagen, M.S. Simmons (Eds.), *Environmental Oxidants*, John Wiley and Sons, New York, 1994.
- [327] T.P. Pope, A. Muller, *Angew. Chem. Int. Ed. Engl.* 30 (1991) 34.
- [328] T. Okuhara, N. Mizuno, M. Misono, *Adv. Catal.* 41 (1996) 113.
- [329] D.E. Katsoulis, *Chem. Rev.* 98 (1998) 359.



- [330] I.A. Weinstock, Homogenous-phase electron transfer reactions of POM, *Chem. Rev.* 98 (1998) 113.
- [331] I. Arslan-Alaton, *J. Environ. Sci. Health A* 38 (2003) 1615.
- [332] K. Vinodgopal, D.E. Wynkoop, P.V. Kamat, *Environ. Sci. Technol.* 30 (1996) 1660.
- [333] I. Arslan, I.A. Balcioglu, *Dyes Pigments* 43 (1999) 95.
- [334] I. Arslan, I.A. Balcioglu, D.W. Bahnemnn, *Dyes Pigments* 47 (2000) 207.
- [335] I. Arslan, I.A. Balcioglu, T.J. Tuhkanen, *Environ. Sci. Health A35* (2000) 775.
- [336] J.P. Giesy, K. Kannan, *Environ. Sci. Technol.* 36 (2002) 146A.
- [337] M.M. Schultz, D.F. Barofsky, J.A. Field, *Environ. Eng. Sci.* 20 (2003) 487.
- [338] M. Houde, J.W. Martin, R.J. Letcher, K.R. Solomon, D.C.G. Muir, *Environ. Sci. Technol.* 40 (2006) 3463.
- [339] H. Funaki, R. Seki, K. Oharu, Asahi Glass Company, United States Patent Application 2, 007,011,791,5 A1, 2007.
- [340] K. Hintzer, H. Kasper, A.R. Maurer, W. Schwertfeger, T. Zipplies, 3M Innovative Properties Company, United States Patent Application 20070015866 A1, 2007.
- [341] H. Moriwaki, Y. Takagi, M. Tanaka, K. Tsuruho, K. Okitsu, Y. Maeda, *Environ. Sci. Technol.* 39 (2005) 3388.
- [342] H. Hori, E. Hayakawa, H. Einaga, S. Kutsuna, K. Koike, T. Ibusuki, H. Kitagawa, R. Arakawa, *Environ. Sci. Technol.* 38 (2004) 6118.
- [343] P. Maruthamuthu, S. Padmaja, R.E. Huie, *Int. J. Chem. Kinet.* 27 (1995) 605.
- [344] P. Theron, P. Pichat, C. Guillard, C. Petrier, T. Chopin, *Phys. Chem. Chem. Phys.* 1 (1999) 4663.
- [345] E. Papaconstantinou, *Chem. Soc. Rev.* 18 (1989) 1.
- [346] A. Hiskia, A. Mylonas, E. Papaconstantinou, *Chem. Soc. Rev.* 30 (2001) 62.
- [347] H. Hori, A. Yamamoto, K. Koike, S. Kutsuna, M. Murayama, A. Yoshimoto, R. Arakawa, *Appl. Catal. B82* (2008) 58.
- [348] Ullmann's Encyclopedia of Industrial Chemistry, Wiley-VCH Verlag GmbH, Weinheim, Germany, 2002.
- [349] (a) K.M. Luo, J.G. Chang, S.H. Lin, C.T. Chang, T.F. Yeh, K.H. Hu, C.S. Kao, *J. Loss Prev. Process Ind.* 14 (2001) 229.  
 (b) Y.W. Wang, C.M. Shu, Y.S. Duh, C.S. Kao, *Ind. Eng. Chem. Res.* 40 (2001) 1125.
- [350] H. Hock, S. Lang, *Chem. Ber.* 77B (1944) 257.
- [351] A.S. Lyavinets, *Russ. J. Gen. Chem.* 70 (2000) 563.
- [352] D.H.R. Barton, N.C. Delanghe, *Tetrahedron Lett.* 38 (1997) 6351.
- [353] J. Vodnar, P. Fejes, K. Varga, F. Berger, *Appl. Catal., A* 122 (1995) 33.
- [354] M. Weber, U. Tanger, W. Kleinloh, PCT Int. Appl. WO 0130732, (2001), *Chem. Abstr.*, 134, 2001, p. 341824.
- [355] R. Selvin, G.R. Rajarajeswari, L.S. Roselin, V. Sadasivam, B. Sivasankar, K. Rengaraj, *Appl. Catal. A* 219 (2001) 125.
- [356] G.D. Yadav, S.S. Salgaonkar, *Org. Process Res. Dev.* 13 (2009) 501–509.
- [357] (a) M. Pagliaro, R. Ciriminna, H. Kimura, M. Rossi, G. Della Pina, *Angew. Chem. Int. Ed.* 46 (2007) 4440.  
 (b) F. Jerome, Y. Pouilloux, J. Barrault, *ChemSusChem* 1 (2008) 586.
- [358] a G.D. Yadav, P.A. Chandan, N. Gopalan, *Clean Techn. Environ. Policy* 14 (2012) 85.  
 b G.D. Yadav, P.A. Chandan, D.P. Tekale, *Ind. Eng. Chem. Res.* 51 (2012) 1549.
- [359] A.A.H. Abdel-Rahman, A.S.H. El-Etrawy, E.S.A. Abdel-Megied, I.F. Zeid, E.S.H. Ashry, *Nucleosides Nucleotides Nucleic Acids* 27 (2008) 1257.

- [360] L. Brasili, C. Sorbi, S. Franchini, M. Manicardi, P. Angeli, G. Marucci, A. Leonardi, E. Poggesi, *J. Med. Chem.* 46 (2003) 1504.
- [361] M. Okaoda, K. Mita, *Macromol. Chem.* 176 (1975) 859.
- [362] N. Iranpoor, F. Kazeim, *Synth. Commun.* 28 (1998) 3189.
- [363] N. Iranpoor, B. Zeynizadeh, *J. Chem. Res. Synop.* (1998) 466.
- [364] Z. Zhu, J.H. Espenson, *Organometallics* 16 (1997) 3658.
- [365] A. Cabrera, D. Vazquez, L. Velasco, R. Miranda, M. Salmon, J.L. Arias, *J. Mol. Catal.* 75 (1992) 101.
- [366] I. Bucsi, A. Meleg, A. Molnar, M. Bartok, *J. Mol. Catal. A Chem.* 168 (2001) 47.
- [367] A.P. Amrute, S. Sahoo, A. Bordoloi, Y.K. Hwang, J. Hwang, S.B. Halligudi, *Cat. Com.* 10 (2009) 1404.
- [368] G.D. Yadav, P.S. Surve, *Ind. Eng. Chem. Res.* 52 (2013) 6129.
- [369] G.D. Yadav, S.A.R.K. Deshmukh, N.S. Asthana, *Ind. Eng. Chem. Res.* 44 (2005) 7969.
- [370] G.D. Yadav, P. Kumar, *Appl. Catal., A* 286 (2005) 61.
- [371] V. Palermo, K. Igal, M.B.C. Migliorero, A.G. Sathicq, N. Quaranta, P.G. Vazquez, G.P. Romanelli, *Waste Biomass Valoriz.* 8 (2017) 69.
- [372] K. Eguchi, T. Tokiai, H. Arai, *Appl. Catal.* 34 (1987) 275.
- [373] S.Z. Pien, W.J. Hatcher, *Chem. Eng. Commun.* 93 (1990) 257.
- [374] A. Kogelbauer, A.A. Nikopoulos, J.G. Goodwin Jr., G. Marcelin, *J. Catal.* 152 (1995) 122.
- [375] A. Kogelbauer, A.A. Nikopoulos, J.G. Goodwin Jr., G. Marcelin, *Stud. Surf. Sci. Catal.* 84 (1994) 1685.
- [376] A.A. Nikopoulos, A. Kogelbauer, J.G. Goodwin Jr., G. Marcelin, *Appl. Catal. A Gen.* 119 (1994) 69.
- [377] F. Colignon, M. Mariani, S. Mareno, M. Remy, G. Poncelet, *J. Catal.* 166 (1997) 53.
- [378] K.H. Chang, G.J. Kim, W.S. Ahn, *Ind. Eng. Chem. Res.* 31 (1992) 125.
- [379] A. Bielański, A. Lubanska, J. Pozniczek, A. Micek-Ilnicka, *Appl. Catal. A Gen.* 256 (2003) 153–171.
- [380] W. Xie, L. Zhao, *Energ. Conver. Manage.* 76 (2013) 55.
- [381] M. Balcan, F.C. Mihăilescu, D.F. Anghel, I.C. Văcăreșteanu, L. Aricov, E.L. Vasilescu, *Fuel* 117 (2014) 251.
- [382] T. Maneerung, S. Kawi, C. Wang, *Energ. Conver. Manage.* 92 (2015) 234.
- [383] G.G. Muciño, R. Romero, A. Ramírez, S.L. Martínez, R. Baeza-Jiménez, R. Natividad, *Fuel* 138 (2014) 143.
- [384] T. Saba, J. Estephane, B. El Khoury, M. El Khoury, M. Khazma, H. El Zakhem, S. Aouad, *Renew. Energy* 90 (2016) 301.
- [385] M.W. Azeem, M.A. Hanif, J.N. Al-Sabahi, A.A. Khan, S. Naz, A. Ijaz, *Renew. Energy* 86 (2016) 124.
- [386] A. Alsalmé, E.F. Kozhevnikova, I.V. Kozhevnikov, *Appl. Catal. A Gen.* 349 (2008) 170.
- [387] C. Zou, P. Zhao, L. Shi, S. Huang, P. Luo, *Bioresour. Technol.* 146 (2013) 785.
- [388] T. Mathimani, L. Uma, D. Prabaharan, *Renew. Energy* 81 (2015) 523.
- [389] M. Ehsan, M.T.H. Chowdhury, *Proced. Eng.* 105 (2015) 638.
- [390] P. Zhang, Y. Liu, M. Fan, P. Jiang, *Renew. Energy* 86 (2016) 99.
- [391] L. Li, C. Zou, L. Zhou, L. Lin, *Renew. Energy* 107 (2017) 14–22.
- [392] Z. Wen, X. Yu, S.T. Tu, J. Yan, E. Dahlquist, *Bioresour. Technol.* 101 (2010) 9570.
- [393] S. Gan, H.K. Ng, C.W. Ooi, N.O. Motala, M.A.F. Ismail, *Technology* 101 (2010) 7338.
- [394] W.Y. Shi, J.X. Li, B.Q. He, F. Yan, Z.Y. Cui, K.W. Wu, L.G. Lin, X.M. Qian, Y. Cheng, *Technology* 139 (2013) 316.
- [395] C. Zou, P. Zhao, J. Ge, Y. Lei, P. Luo, *Carbohydr. Polym.* 87 (2012) 607.

- [396] H.N. Xiao, N. Cezar, J. Colloid Interface Sci. 283 (2005) 406.
- [397] C. Zou, P. Zhao, J. Ge, Y. Qin, P. Luo, Fuel 104 (2013) 635.
- [398] H. Liu, N. Xue, L. Peng, X. Guo, W. Ding, Y. Chen, Cat. Com. 10 (2009) 1734.
- [399] L.H. Pires, A.N. de Oliveira, O.V. Monteiro Jr., R.S. Angélica, C.E. da Costa, J.R. Zamian, L.A. do Nascimento, G.N.R. Filho, Appl. Catal. B160–161 (2014) 122.
- [400] K. Rezzadori, S. Benedetti, E.R. Amante, Food Bioprod. Process. 90 (2012) 606.
- [401] S. Djilas, J. Canadanovic-Brunet, G. Cetkovic, Chem. Ind. Chem. Eng. Q. 15 (2009) 191.
- [402] M.B.C. Migliorero, V. Palermo, P.G. Vázquez, G.P. Romanelli, J. Renew. Mater. 5 (2017) 167.
- [403] P. Tundo, G.P. Romanelli, P.G. Vazquez, A. Loris, F. Arico, Synlett 7 (2008) 967.
- [404] V. Palermo, G.P. Romanelli, P.G. Vazquez, J. Mol. Catal. A Chem. 373 (2013) 142.
- [405] G.P. Romanelli, P.I. Villabrille, G.G. Vazquez, C.V. Caceres, P. Tundo, Lett. Org. Chem. 5 (2008) 332.
- [406] V. Palermo, G.P. Romanelli, P.G. Vazquez, Phosphorus Sulfur Silicon Relat. Elem. 184 (2009) 3258.
- [407] V. Palermo, P.I. Villabrille, P.G. Vazquez, C.V. Caceres, P. Tundo, G.P. Romanelli, J. Chem. Sci. 125 (2013) 1375.
- [408] V. Palermo, A.G. Sathicq, T. Constantieux, J. Rodriguez, P. Vazquez, G. Romanelli, Catal. Lett. 145 (2015) 1022.
- [409] M.C. Carreno, Chem. Rev. 95 (1995) 1717.
- [410] I. Fernandez, N. Khiar, Chem. Rev. 103 (2003) 3651.
- [411] I. Ahmad, Int J Pharm Pharm Sci 7 (2015) 19.
- [412] R.O. Feuge, A.T. Gros, J. Am. Oil Chem. Soc. 26 (1949) 97.
- [413] S. Saka, D. Kusdiana, Fuel 80 (2001) 225.
- [414] G.R. Peterson, W.P. Scarrah, J. Am. Oil Chem. Soc. 61 (1984) 1593.
- [415] M. Kouzu, M. Umemoto, T. Kasuno, M. Tajika, Y. Aihara, Y. Sugimoto, J. Hidaka, J. Jpn. Inst. Energy 85 (2006) 135.
- [416] G.J. Suppes, M.A. Dasari, E.J. Duskocil, P.J. Mankidy, M.J. Goff, Appl. Catal. A. Gen. 257 (2004) 213.
- [417] H.-J. Kim, B.-S. Kang, M.-J. Kim, Y.M. Park, D.-K. Kim, J.-S. Lee, K.-Y. Lee, Catal. Today 93-95 (2004) 315.
- [418] T. Ebiura, T. Echizen, A. Ishikawa, K. Murai, T. Baba, Appl. Catal. A. Gen. 283 (2005) 111.
- [419] I.K. Mbaraka, D.R. Radu, V.S.Y. Lin, B.H. Shanks, J. Catal. 219 (2003) 329.
- [420] M. Toda, A. Takagaki, M. Okamura, J.N. Kondo, S. Hayashi, K. Domen, M. Hara, Nature 438 (2005) 178.
- [421] K.-H. Chung, D.-R. Chang, B.-G. Park, Bioresour. Technol. 99 (2008) 7438.
- [422] N. Katada, T. Hatanaka, M. Ota, K. Yamada, K. Okumura, M. Niwa, Appl. Catal. A. Gen. 363 (2009) 164.
- [423] M. Canacki, Bioresour. Technol. 98 (2007) 183.
- [424] N.A. Zafiroopoulos, H.L. Ngo, T.A. Foglia, E.T. Samulski, W. Lin, Chem. Commun. (2007) 3670.
- [425] A.A. Apostoloukou, I.K. Kookos, C. Marazioti, K.C. Angelopoulos, Fuel Process. Technol. 90 (2009) 1023.
- [426] M. Canacki, J.V. Gerpen, Trans. Am. Soc. Agric. Eng. 44 (2001) 1429.
- [427] J.M. Marchetti, V.U. Miguel, A.F. Errazu, Fuel 86 (2007) 906.
- [428] J.B. Moffat (Ed.), Metal–Oxygen Clusters: The Surface and Catalytic Properties of Heteropoly Oxometalates, Kluwer Academic/Plenum Publishers, New York, 2001.
- [429] R.A. Sheldon, R.S. Downing, Appl. Catal., A 189 (1999) 163.

- [430] J. Alcañiz-Monge, G. Trautwein, S. Parres-Esclapez, J.A. Maciá-Agullo, *Microporous Mesoporous Mater.* 115 (2008) 440.
- [431] J. Alcañiz-Monge, G. Trautwein, J.P. Marco-Lozar, *Appl. Catal. A. Gen.* 468 (2013) 432.
- [432] S.A. Petukhov, L.S. Kurmanova, M.P. Erzamaev, *News of the National Academy of Sciences of the Republic of Kazakhstan, Series of Geology and Technical Sciences*, 434, 2019, p. 79.
- [433] K. Bhaskar, S. Sendilvelan, L.R. Sassykova, *News of the National Academy of Sciences of the Republic of Kazakhstan, Series of Geology and Technical Sciences*, 428, 2018, p. 6.
- [434] S.P. Srivastava, J. Hancsók, *Fuels and Fuel-Additives*, John Wiley & Sons, Inc, 2014, pp. 11–47.
- [435] L. Sassykova, A. Nalibayeva, *J. Chem. Technol. Metall.* 53 (2018) 289.
- [436] L.R. Sassykova, A. Ussenov, A.T. Massenova, S.A. Gil'mundinov, K.S. Rakhmetova, V.N. Bunin, Z.T. Basheva, M.K. Kalykberdiyev, *Int. J. Chem. Sci.* 14 (2016) 206.
- [437] E.L. Krasnykh, S.V. Levanova, S. Ya, I.N.K. Karaseva, R.M. Varushchenko, A.I. Druzhinina, L.L. Pashchenko, *Pet. Chem* 45 (2005) 92.
- [438] T. Nambaya Charyulu, P. Naveenchandran, E. Raja, R.N. Babu, *Rasayan J. Chem.* 13 (2020) 876.
- [439] L.R. Sassykova, A.M. Nalibayeva, S.A. Gil'mundinov, *Bulg. Chem. Commun.* 49 (2017) 583.
- [440] D.F. Grishin, N.D. Zinina, *Russ. J. Appl. Chem.* 88 (2015) 1106.
- [441] M. Umar, A.R. Saleemi, S. Qaiser, *Cat. Com.* 9 (2008) 721.
- [442] L.R. Sassykova, K.A. Kadirbekov, N.K. Zhakirova, A.S. Zhumakanova, S. Sendilvelan, T.S. Abildin, A.A. Batyrbayeva, R.N. Azhigulova, O.I. Ponomarenko, R.G. Ryskaliyeva, *Rasayan J. Chem.* 13 (2020) 2085.

# Index

Note: Page numbers followed by *f* indicate figures, *t* indicate tables, and *s* indicate schemes.

## A

Acetals, 343–344  
Acid catalysis, 205  
Acid-catalyzed benzaldehyde acetalization, 153–154, 154s  
Acid-catalyzed esterification, 356  
Acid catalyzed etherification reactions, 313, 313s  
Acidified carbon nitride (ACN), 191–192  
Acid Orange 7, 349  
Active sites, 19  
Addenda nuclei, 80, 116–117  
Adipic acid, 228, 228s, 251, 251s  
Alcohols  
    oxidation, 181, 181s  
    selective oxidation, 248, 248s  
Aldehydes, peroxidation of, 154–155, 155s  
4,4'-Alkylmethylenebis(3-methyl-5-pyrazolones), 165–166, 166s  
Alkyl *tert*-butyl ethers, 360  
Allyl-2,4-*tert*-butylphenyl ether, Claisen rearrangement of, 338–339, 339s  
2-Amino-4-aryl-3-cyano-5-oxo-4H,5H-pyrano-[3,2-*c*] chromenes, 217, 217s  
2-Aminobenzothiazolomethylnaphthols, 215, 215s  
2-Amino-3-cyanopyridine derivatives, 168–169, 168s  
2-Amino-3,5-dicarbonitrile-6-thio-pyridines, 221–222, 222s  
Anderson-Evans structure, 77–79, 77f  
Aniline, 326  
9,10-Anthraquinone, 244–245, 244s  
Anthraquinone derivatives, 231, 232s  
Aromadendrene, 335–336, 336s  
4,4'-(Arylmethylene)bis(3-methyl-1H-pyrazol-5-ols), 223–224, 223s  
Autocatalytic reactions, 3

## B

Benzaldehyde ethylene glycol acetal, 210–212, 212s  
Benzaldehyde, oxidative esterification of, 245, 245s

Benzazoles, 146, 146s  
Benzene to phenol hydroxylation, 182  
Benzochromenopyrazole derivatives, 168, 168s  
Benzodiazepines, 209, 209s  
Benzopyranopyrimidines, 157, 157s  
5-Benzoyl-4-phenyloxazolidin-2-one derivatives, 149, 151s  
Benzyl alcohol, oxidation of, 249, 249s  
Benzylic alcohol oxidation, 177, 177s, 183  
Bi-functional catalysis, 16  
Biodiesel, 340–341, 355, 358  
Bioglycerol, 352  
Biomass, 340–348  
Bis (dihydropyrimidinone)benzene, 158, 159s  
Bis(indole) derivatives, 206, 207s, 220–221, 221s  
Bis(indolyl)methanes, 213, 213s  
Bisphenol-A, 351–352, 351s  
Bulk solid polyoxometalates, 265–266  
Bulk-type I catalysis, 24  
Bulk-type II catalysis, 25

## C

Catalysis, 205  
    classification, 7–9  
    definition, 1  
    history, 3–5  
CAT-12 catalyzed synthesis, 147–148, 148s  
Cellulose, 342  
    hydrolysis/oxidation of, 233, 233s  
Cesium-modified 3DOM SiO<sub>2</sub>, 176  
Cesium salt of tungstophosphoric acid (CsPW), 355  
Chemical industry, 308–328  
Chemical interactions, 269  
Chemisorption, 26–27  
Chromene pyrimidine-2,4-dione, 218–219, 218s  
Chromenopyrimidine-2,5-dione, 171–172, 172s, 219, 219s  
Citrus waste, 357

Claisen rearrangement reactions, 322, 329–330, 330s  
 Clays, 324  
 Condensation reaction, 278–280  
 Copper benzene tricarboxylate metal organic framework, 284, 284f  
 Covalent anchoring, 269  
 Cuminaldehyde, 336, 337s  
 Cyclic carbonate synthesis, 142–143, 142s, 146–147, 146s  
 Cyclic voltammetry (CV), 120, 120f  
 Cyclodextrins, 356  
 Cyclohexanone, 321–322  
 Cyclohexene oxidation, 174  
 Cyclooctane, aerobic oxidation of, 247, 247s

## D

DBT oxidation, 178, 178s  
 Dealuminated ultra-stable Y zeolite (DUSY), 290  
 Dexter-Silverton structure, 79, 79f  
 1,4-DHP derivatives, synthesis of, 161–162, 161s  
 2,5-Diformylfuran (DFF), 227–228, 227s  
 1,4-Dihydropyrano[2,3-c] pyrazoles, 216, 216s  
 3,4-Dihydropyrimidin-2(1H)-ones, 156–158, 156s, 159s, 216–217, 216s, 220, 220s  
 Dihydropyrimidinones synthesis, 159, 159s  
 3,4-Dihydropyrimidinones/thiones, 224–225, 224s  
 Dihydropyrimidone synthesis, 171, 171s  
 2,3-Dihydro-4(1H)-quinazolinones, 212, 212s  
 Dip-coating, 266  
 Diphenyl sulfide  
 oxidation, 182–183, 183s  
 selective oxidation, 357, 357s  
 Dissociation constants, 104–107  
 Drop-casting, 268  
 Drugs, photodegradation of, 186, 187–188t  
 Drying, 268–269  
 Dyes, 349  
 Dynamic light scattering (DLS), 119

## E

Electrocatalysis, 22  
 Electrodeposition, 268  
 Electronic spectroscopy, 115–116  
 Electrospray-ionization mass-spectrometry (ESI-MS), 118  
 Electrostatic anchoring, 172–173, 182, 269  
 Entrapment, 268

Epichlorohydrin, 353  
 Epoxidation reaction, 319, 320s  
 Esterification reaction, 281–282  
 5-Ethoxymethylfurfural and ethyl levulinate, 344–345, 345s  
 Ethyl acetoacetate, three-component condensation of, 165, 165s  
 Extended X-ray absorption fine structure (EXAFS), 119

## F

Farnesol, 339–340  
 Food industry, 337–340  
 Formic acid, 343  
 Free fatty acids, 359–360  
 Friedel-Crafts alkylation, 316–317  
 Fries rearrangement reactions, 331–332, 333s

## G

Gasoline, 308  
 Glycerol, acetylation of, 324, 325s  
 Graphene oxide (GO), 169, 169s  
 Green catalysts, 305  
 Green chemistry, 205  
 Green processes, 12–17  
 Ground-state delocalization (GSD), 97–98

## H

Hammett acidity, 107–109  
 Hantzsch reactions, 222–223, 223s  
 Heterocycles  
 synthesis, 142–155, 206–213  
 Heterogeneous catalysis, 22–25  
 Heteropoly acids (HPAs), 67–69  
 acidic properties, 101–109  
 dissociation constants, 104–107  
 Hammett acidity, 107–109, 108t  
 in solution, 103–104  
 Anderson-Evans structure, 77–79  
 applications  
 biomass, 340–348  
 chemical industry, 308–328  
 food industry, 337–340  
 pharmaceuticals, 329–336  
 removal of pollutants, 348–354  
 basic properties, 109–113  
 catalytic activity, types of, 17–19  
 catalytic properties  
 active sites, 19  
 stability, 19–20  
 characterization, 113–120

- classification, 69–89
  - Dexter-Silverton structure, 79
  - electrocatalysis, 22
  - electrochemical properties, 98–101, 99–100r
  - electronic spectroscopy, 115–116
  - green processes, 12–17
  - heterogeneous catalysis, 22–25
  - Keggin structure, 70–73
  - mass-spectrometry, 118
  - noble metals, 16
  - nomenclature, 69
  - nuclear magnetic resonance (NMR)
    - Addenda nuclei, 116–117
  - overview, 141–142
  - photocatalysis, 21–22
  - potentiometry, 114–115
  - Preyssler structure, 86–89
  - properties, 89–109
  - redox properties, 96–101
  - small angle X-ray scattering, 118–119
  - solubility, 89–94
    - in organic solvents, 94
    - in water, 91–94
  - stability, 94–96
    - in solution, 94–96
    - thermal stability, 96
  - vibrational spectroscopy, 115–116
  - Wells-Dawson structure, 74–77
  - Heteropoly anions, 11
  - Heteropoly blues, 97–98
  - Homogeneous catalysis, 265
  - Horsetail (*Equisetum arvense*), 166–167
  - Host/guest interactions, 271–287
  - HPAs. *See* Heteropoly acids (HPAs)
  - HPMo@lipid(*n*)/GO hybrid catalyst materials, 328, 329s
  - HPW/Bi<sub>2</sub>WO<sub>6</sub> composite photocatalyst, 196
  - 4*H*-pyran derivatives, 217, 217s
  - Hydrodesulfurization (HDS), 308
  - Hydrogen peroxide (H<sub>2</sub>O<sub>2</sub>), 178–179, 178s, 182
  - Hydroperfluorocarboxylic acids,
    - decomposition of, 254
  - Hydroxybenzophenones, 332
  - 4-Hydroxycoumarine, 157, 157s
  - 7-Hydroxy-4-methylcoumarin, 145, 145s
- I**
- Immobilization, 266
    - nano polyoxometalates, 27–28
    - polyoxometalates
      - carbon-based materials, 40–43
      - titanium dioxide, 37–40
    - synthetic methods, 266–269
    - techniques, 266
  - Impregnation method, 144, 195, 268–269
  - Isobutylene, hydration of, 306, 306s
  - Isopolyanions, 11
- K**
- Kaolin waste, 356
  - Keggin-type heterogeneous catalysts, 177
  - Keggin-type heteropoly acids, 70–73, 71t, 178, 206
  - Ketalization, of carbonyl compounds, 148–149, 150–151t
  - Ketals, 343–344
- L**
- Langmuir-Hinshelwood-type kinetics, 253–254
  - Layer-by-layer assembly, 267
  - Layer-by-layer (LbL) deposition, 28–30
  - Layered double hydroxides (LDHs), 182
  - Levulinic acid, 341–342
  - Lignocellulosic biomass, 346–347
  - Limonene oxide, 347–348, 348s
- M**
- Mass-spectrometry (MS), 118
  - Menadione, 232, 232s
  - Mesoporous silica (MESOSI), 143
  - Mesoporous silica-based heteropoly acid catalysts, 291–293
  - Metal-organic frameworks (MOFs), 271
  - Metal-support interactions. *See* Substrate effects
  - Methacrolein, oxidation of, 239, 240s
  - Methanol oxidation, 32–33
  - Methyl glycolate, 326
  - Methyl methoxyacetate, 326
  - 2-Methyl-2-naphthyl-1,3-dioxolane, 344
  - Methyl phenylglyoxylate, 320–321, 321s
  - Methyl *tert*-butyl ether (MTBE), 354–355
  - Microcrystalline cellulose (MCC), 334–335
  - Mixed oxides, 10
  - MNPs-HPW catalyst, 142–143, 142s
  - MOF-199, 311
  - Molecular sieves, 10, 323
  - Monoethylene glycol, 325
  - Multicomponent reactions (MCRs), 155–173, 215–227
- N**
- Nanocatalysis, 5–7
  - Nano-ceramic tile wastes, 174



- Nanomaterials, 36
- Nano polyoxometalates, 26–43
- applications, 30–36
  - chemisorption, 26–27
  - immobilization, 27–28
  - layer-by-layer (LbL) deposition, 28–30
- Naphtho[2,3-*a*] acridin-1(2H)-one, 160, 160s
- Naphtho[2,3-*f*] quinolin-13-one derivatives, 160, 160s
- 1,4-Naphthoquinones, 229, 229s
- Nerolidol, 339–340
- 2-Nitro-4-methylsulfonylbenzoic acid, 234, 234s
- Nitrous oxide (N<sub>2</sub>O), 252
- N,N'*-Alkylidene bisamides, 162, 163s
- Noble metals, 16
- Nuclear magnetic resonance (NMR), 116–118
- O**
- Octyl-free catalyst, 177–178
- Orange juice industry, 357
- Organic/inorganic materials, 10, 43–48
- Organocatalysis, 275–284
- Oxidation reactions, 173–184, 227–250, 275–278
- alcohol, 181, 181s
  - benzylic alcohols, 177, 177s, 183
  - cyclohexene, 174
  - DBT, 178, 178s
  - diphenyl sulfide, 182–183, 183s
  - MAL to MAA, 179–180, 180s
  - 2-propanol, 174
  - styrene, 179, 179s
  - sulfides to sulfoxides, 174, 174s
  - 2,3,6-trimethylphenol to 2,3,5-trimethyl-p-benzoquinone, 183–184, 183s
- Oxidative desulfurization (ODS), 180–181, 310
- Oxindoles, 226, 226s
- Oxygen reduction, 33–36
- P**
- Perfluorocarboxylic acids (PFCAs), 349–350, 350s
- Perfluoroether carboxylic acids, 349–351, 350s
- Pharmaceuticals, 329–336
- Phenethyl alcohol, etherification of, 316, 316s
- Phenol, 317, 351–352, 351s
- Phenoxy pyrazolyl chalcones, 144–145, 144s
- 4-Phenylcoumarins, 147, 148s
- 4-Phenyl-3,4-dihydro-4-phenylcoumarins, 147, 148s
- Phosphomolybdcid (PNbMo), 153, 153s, 168, 182–183
- Phosphotungstic acid (H<sub>3</sub>PW<sub>12</sub>O<sub>40</sub>) nanophotocatalysts, 186
- Phosphotungstovanadic heteropoly acids, 253
- Photocatalysis, 21–22, 185–196, 250–254
- Photocatalytic oxidation, 185–186
- Photodegradation, of drugs, 186, 187–188t
- Phthalhydrazide-triones, 173, 173s
- Phytosterols, 337–338
- $\alpha$ -Pinene, 313–315
- Polyhydroquinolines, 164–165, 165s, 169–170, 170s
- Polymer-supported polyoxometalates catalysts, 288–289
- Polyoxometalates (POMs), 10–11, 181
- applications, 64–66, 65t
  - bulk-type I catalysis, 24
  - bulk-type II catalysis, 25
  - historical backgrounds, 61–62
  - host/guest interactions, 271–287
  - immobilization
    - carbon-based materials, 40–43
    - synthetic methods, 266–269
    - titanium dioxide, 37–40
  - mesoporous supports
    - chemical interactions, 269
    - covalent grafting, 293–295
    - polymers, 288–289
    - silica, 291–293
    - transition metal oxide, 289–290
    - zeolites, 290–291
  - molecular structures, 110f
  - morphological shapes, 48–49
  - nanocomposites, 26–30
  - organic/inorganic hybrid, 43–48
  - properties, 64t
  - structures, 66–67
  - substrate effects, 269–271
  - surface-type catalysis, 24
  - survey on, 62–64
- Polyoxymethyleneglycol (PTMG), 16–17
- POM@MOFs, 272–274
- Potentiometry, 114–115
- Preyssler structure, 86–89, 87f, 332–333
- 2-Propanol oxidation, 174
- Pseudoliquid phase catalysis, 15
- bulk-type I, 24
  - bulk-type II, 25

Pyranol[2,3-*c*] pyrazole synthesis, 166–167, 167s  
 Pyranopyrazole, 165–166, 166s  
 Pyranopyrazole derivatives, 171, 171s  
 Pyrazole, 209, 210s  
 Pyrazolopyranopyrimidines synthesis, 170–171, 170s  
 2-(Pyridyl)(1H-indol-3-yl)(methyl) malononitriles, 221, 221s

## Q

Quinoline derivatives, 151, 152s  
 Quinoxaline derivatives, 149–151, 152s, 206, 206s

## R

Reduced polyoxometalate, 11  
 Removal of pollutants, 348–354

## S

Salicylaldehydes, 157, 158s  
 Silica-included tungstophosphoric acid (HPW-Ssg), 334  
 Silica-supported, copper-doped phosphotungstic acid (CuPTA/SiO<sub>2</sub>), 144–145, 144s  
 Silica-supported, copper-doped phosphotungstic acid (CuPTA/SiO<sub>2</sub>) catalyst, 144–145, 144s  
 Silica-supported Preyssler nanoparticles (SPN), 152, 152s  
 Small angle X-ray scattering (SAXS), 118–119  
 Sodium dodecyl benzene sulfonate (SDBS), 182  
 Sol-gel method, 174, 182–183  
 Solid acid catalysts, 10–12  
 Solid-solid phase catalysis, 16  
 Solubility, 89–94  
   in organic solvents, 94  
   in water, 91–94  
 Solvothermal deposition, 266–267  
 Sonication deposition, 267  
 Spriooxindoles, 164, 164s  
 Stability, 94–96  
   in solution, 94–96  
   thermal stability, 96  
 Styrene oxidation, 179, 179s  
 Styrene oxide, 319  
 Substituted 2-amino-chromenes, 225, 225s

5-Substituted 1H-tetrazoles, 153, 153s  
 Substrate effects, 269–271  
 Sulfides, selective oxidation of, 354, 354s  
 Supported polyoxometalate hybrids, 271–287  
 Supramolecular anchoring, 269  
 Supramolecular self-assembly, 48–49  
 Surface-type catalysis, 24  
 Surfactant-assisted sol-gel method, 185  
 Sustainable chemistry. *See* Green chemistry  
 Symmetrical N,N'-alkylidene bis-amide derivatives, 222, 222s

## T

Terpene alcohols, oxidation of, 243, 243s  
 Terpenic compounds, 315  
 Tetrahydrobenzo[*b*]pyran derivatives, 169–170, 169–170s  
 Tetrahydrodipyrzolo pyridines, 155–156, 156s  
 Tetrahydrofuran, 307–308  
 Tetrasubstituted imidazoles, 225, 226s  
 1,2,4,5-Tetrasubstituted imidazoles, 162, 163s, 226, 227s  
 Thermal analysis, 173–174  
 Thermal stability, 96  
 Thermogravimetric analysis (TGA), 119  
 Thiazolidine-4-ones, 208, 209s  
 Thiazoloquinolines, 157–158, 158s  
 Thiosemicarbazones, 208, 209s  
 Thioxochromenopyrimidin-5-ones, 171–172, 172s, 219, 219s  
 Titanium dioxide-supported polyoxometalates, 37–40  
*Trans*-carveol, 314–316, 314–315s  
 Transesterification reaction, 357–358, 358s  
 Transition metal oxide supported polyoxometalates catalysts, 289–290  
 Transition metal substituted polyoxometalates (TMSPOMs), 62  
 Transition metal substituted sandwich-type polyoxometalate, 82–85  
*Trans*-sobreol, 315–316, 315s  
 1,1,3-Triheteroaryl derivatives, 207, 207s  
 2,3,6-Trimethylphenol, oxidation of, 237–238, 238s  
 2,4,5-Trisubstituted imidazoles, 162, 163s  
 Trisubstituted 1,3-thiazoles, 162, 162s  
 Tungsten heteropoly acids (HPW), 173–174, 176  
 Tungstophosphoric acid, 143, 192  
 2-substituted imidazolines, 208, 208s

## U

- Ultrasonic irradiation, 157, 157–158s
  - benzopyranopyrimidine synthesis, 157, 157–158s
  - three-component reaction catalysis, 160, 160s
- Ultrasound-assisted oxidative desulfurization (UAOD), 175, 175s
- Urea, three-component condensation, 165, 165s

## V

- Vibrational spectroscopy, 115–116
- V-substituted molybdophosphoric acid, 323

## W

- Water oxidation, 30–32
- Water-tolerant solid acid catalysts, 15
- Wells-Dawson heteropoly acids, 74–77, 74f, 251
- Wet impregnation method, 189–190, 194

## Z

- Zeolites, 10, 290–291
- ZnS/HPW composites, 194–195
- Z-POMOFs, 47–48